

EMERGING INFECTIOUS DISEASES[®]



Zoonotic Infections

December 2017



Bindu Viswanathan (b. 1971), *A Timeless Symbiosis*, 2017. Acrylic on canvas, with small mirror embellishments, 22 in × 28 in/56 cm × 71 cm. Digital image courtesy of the artist.

EMERGING INFECTIOUS DISEASES®

EDITOR-IN-CHIEF

D. Peter Drotman

Associate Editors

Paul Arguin, Atlanta, Georgia, USA
 Charles Ben Beard, Fort Collins, Colorado, USA
 Ermias Belay, Atlanta, Georgia, USA
 David Bell, Atlanta, Georgia, USA
 Sharon Bloom, Atlanta, GA, USA
 Mary Brandt, Atlanta, Georgia, USA
 Corrie Brown, Athens, Georgia, USA
 Charles Calisher, Fort Collins, Colorado, USA
 Michel Drancourt, Marseille, France
 Paul V. Effler, Perth, Australia
 Anthony Fiore, Atlanta, Georgia, USA
 David Freedman, Birmingham, Alabama, USA
 Peter Gerner-Smidt, Atlanta, Georgia, USA
 Stephen Hadler, Atlanta, Georgia, USA
 Matthew Kuehnert, Atlanta, Georgia, USA
 Nina Marano, Atlanta, Georgia, USA
 Martin I. Meltzer, Atlanta, Georgia, USA
 David Morens, Bethesda, Maryland, USA
 J. Glenn Morris, Gainesville, Florida, USA
 Patrice Nordmann, Fribourg, Switzerland
 Didier Raoult, Marseille, France
 Pierre Rollin, Atlanta, Georgia, USA
 Frank Sorvillo, Los Angeles, California, USA
 David Walker, Galveston, Texas, USA

Senior Associate Editor, Emeritus

Brian W.J. Mahy, Bury St. Edmunds, Suffolk, UK

Managing Editor

Byron Breedlove, Atlanta, Georgia, USA

Copy Editors Kristina Clark, Dana Dolan, Karen Foster,
 Thomas Gryczan, Jean Michaels Jones, Michelle Moran, Shannon
 O'Connor, Jude Rutledge, P. Lynne Stockton, Deborah Wenger

Production Thomas Ehemann, William Hale, Barbara Segal,
 Reginald Tucker

Editorial Assistants Kristine Phillips, Susan Richardson

Communications/Social Media Sarah Logan Gregory

Founding Editor

Joseph E. McDade, Rome, Georgia, USA

Emerging Infectious Diseases is published monthly by the Centers for Disease Control and Prevention, 1600 Clifton Road, Mailstop D61, Atlanta, GA 30329-4027, USA. Telephone 404-639-1960, fax 404-639-1954, email eideditor@cdc.gov.

The conclusions, findings, and opinions expressed by authors contributing to this journal do not necessarily reflect the official position of the U.S. Department of Health and Human Services, the Public Health Service, the Centers for Disease Control and Prevention, or the authors' affiliated institutions. Use of trade names is for identification only and does not imply endorsement by any of the groups named above.

All material published in Emerging Infectious Diseases is in the public domain and may be used and reprinted without special permission; proper citation, however, is required.

EDITORIAL BOARD

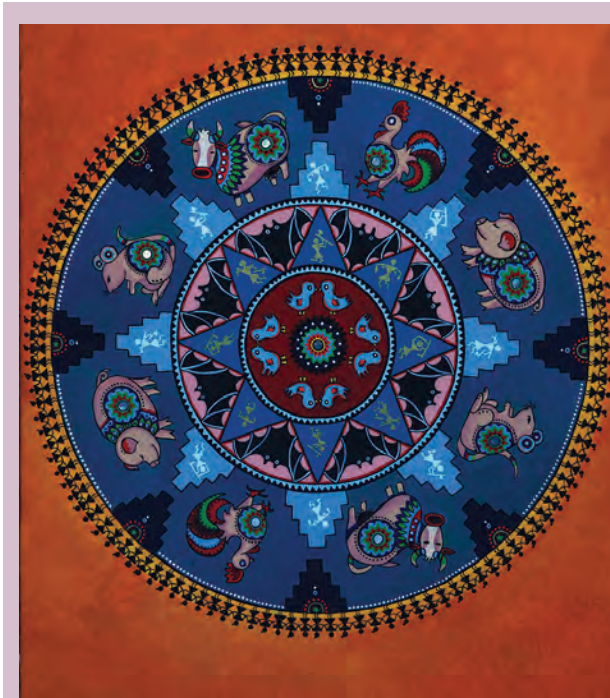
Timothy Barrett, Atlanta, Georgia, USA
 Barry J. Beaty, Fort Collins, Colorado, USA
 Martin J. Blaser, New York, New York, USA
 Richard Bradbury, Atlanta, Georgia, USA
 Christopher Braden, Atlanta, Georgia, USA
 Arturo Casadevall, New York, New York, USA
 Kenneth C. Castro, Atlanta, Georgia, USA
 Benjamin J. Cowling, Hong Kong, China
 Vincent Deubel, Shanghai, China
 Isaac Chun-Hai Fung, Statesboro, Georgia, USA
 Kathleen Gensheimer, College Park, Maryland, USA
 Duane J. Gubler, Singapore
 Richard L. Guerrant, Charlottesville, Virginia, USA
 Scott Halstead, Arlington, Virginia, USA
 Katrina Hedberg, Portland, Oregon, USA
 David L. Heymann, London, UK
 Keith Klugman, Seattle, Washington, USA
 Takeshi Kurata, Tokyo, Japan
 S.K. Lam, Kuala Lumpur, Malaysia
 Stuart Levy, Boston, Massachusetts, USA
 John S. MacKenzie, Perth, Australia
 John E. McGowan, Jr., Atlanta, Georgia, USA
 Jennifer H. McQuiston, Atlanta, Georgia, USA
 Tom Marrie, Halifax, Nova Scotia, Canada
 Nkuchia M. M'ikanatha, Harrisburg, Pennsylvania, USA
 Frederick A. Murphy, Bethesda, Maryland, USA
 Barbara E. Murray, Houston, Texas, USA
 Stephen M. Ostroff, Silver Spring, Maryland, USA
 Marguerite Pappaioanou, Seattle, Washington, USA
 Johann D. Pitout, Calgary, Alberta, Canada
 Ann Powers, Fort Collins, Colorado, USA
 Mario Raviglione, Geneva, Switzerland
 David Relman, Palo Alto, California, USA
 Guenael R. Rodier, Geneva, Switzerland
 Connie Schmaljohn, Frederick, Maryland, USA
 Tom Schwan, Hamilton, Montana, USA
 Ira Schwartz, Valhalla, New York, USA
 Bonnie Smoak, Bethesda, Maryland, USA
 Rosemary Soave, New York, New York, USA
 P. Frederick Sparling, Chapel Hill, North Carolina, USA
 Robert Swanepoel, Pretoria, South Africa
 Phillip Tarr, St. Louis, Missouri, USA
 John Ward, Atlanta, Georgia, USA
 J. Todd Weber, Atlanta, Georgia, USA
 Jeffrey Scott Weese, Guelph, Ontario, Canada
 Mary E. Wilson, Cambridge, Massachusetts, USA

Use of trade names is for identification only and does not imply endorsement by the Public Health Service or by the U.S. Department of Health and Human Services.

EMERGING INFECTIOUS DISEASES is a registered service mark of the U.S. Department of Health & Human Services (HHS).

∞ Emerging Infectious Diseases is printed on acid-free paper that meets the requirements of ANSI/NISO 239.48-1992 (Permanence of Paper)

EMERGING INFECTIOUS DISEASES®



On the Cover

Bindu Viswanathan, (b. 1971), *A Timeless Symbiosis*, 2017.

Acrylic on canvas, with small mirror embellishments, 22 in x 28 in/56 cm x 71 cm. Digital image courtesy of the artist.

About the Cover p. 2124

Multiple Reassorted Viruses as Cause of a Highly Pathogenic Avian Influenza A(H5N8) Virus Epidemic, the Netherlands, 2016

N. Beerens et al. 1966



Related material available online:
http://wwwnc.cdc.gov/eid/article/23/12/17-1062_article

Experimental Infection of Common Eider Ducklings with Wellfleet Bay Virus, a Newly Characterized Orthomyxovirus

V. Shearn-Bochsler et al. 1974

Medscape
EDUCATION
ACTIVITY



Group B *Streptococcus* Infections Caused by Improper Sourcing and Handling of Fish for Raw Consumption, Singapore, 2015–2016

M.L. Chau et al. 1982

Policies and guidelines regarding sale of ready-to-eat raw fish dishes have been updated.



Related material available online:
http://wwwnc.cdc.gov/eid/article/23/12/17-0596_article

Distribution of Usutu Virus in Germany and its Effect on Breeding Bird Populations

R. Lühken et al. 1991



Related material available online:
http://wwwnc.cdc.gov/eid/article/23/12/17-1257_article

Outbreaks of Neuroinvasive Astrovirus Associated with Encephalomyelitis, Weakness, and Paralysis among Weaned Pigs, Hungary

Á. Boros et al. 1999



Related material available online:
http://wwwnc.cdc.gov/eid/article/23/12/17-0804_article

Characterization of *Streptococcus pyogenes* from Animal Clinical Specimens, Spain

A.I. Vela et al. 2011

Synopses

Fatal Outbreak in Tonkean Macaques Caused by Possibly Novel Orthopoxvirus, Italy, January 2015

G. Cardeti et al. 1941

Spread of Canine Influenza A(H3N2) Virus, United States

I.E.H. Voorhees et al. 1950



Related material available online:
http://wwwnc.cdc.gov/eid/article/23/12/17-0246_article

Research

Evolutionary Context of Non-Sorbitol-Fermenting Shiga Toxin-Producing *Escherichia coli* O55:H7

K. Schutz et al. 1958



Related material available online:
http://wwwnc.cdc.gov/eid/article/23/12/17-0628_article



Bourbon Virus in Field-Collected Ticks, Missouri, USA
H.M. Savage et al. **2017**

High Rate of MCR-1–Producing *Escherichia coli* and *Klebsiella pneumoniae* among Pigs, Portugal
N. Kieffer et al. **2023**

Etymologia

Taenia saginata
R. Henry **2029**

Historical Review

History of *Taenia saginata* Tapeworms in Northern Russia
S.V. Konyaev et al. **2030**

 Related material available online:
http://wwwnc.cdc.gov/eid/article/23/12/16-2101_article

Dispatches

Outbreak of Yellow Fever among Nonhuman Primates, Espirito Santo, Brazil, 2017
N.C.C. de A. Fernandes et al. **2038**

 Related material available online:
http://wwwnc.cdc.gov/eid/article/23/12/17-0685_article

***Mycobacterium ulcerans* DNA in Bandicoot Excreta in Buruli Ulcer–Endemic Area, Northern Queensland, Australia**
K. Röltgen et al. **2042**

Avian Influenza A(H7N2) Virus in a Human Exposed to Sick Cats, New York, USA, 2016
A. Marinova-Petkova et al. **2046**

Deaths among Wild Birds During
 Related material available online:
http://wwwnc.cdc.gov/eid/article/23/12/17-0798_article

Highly Pathogenic Avian Influenza A(H5N8) Virus Outbreak, the Netherlands
E. Kleyheeg et al. **2050**

 Related material available online:
http://wwwnc.cdc.gov/eid/article/23/12/17-1086_article

Pathogenic *Elizabethkingia miricola* Infection in Cultured Black-Spotted Frogs, China, 2016
R. Hu et al. **2055**

 Related material available online:
http://wwwnc.cdc.gov/eid/article/23/12/17-0942_article

West Nile Virus Lineage 2 in Horses and Other Animals with Neurologic Disease, South Africa, 2008–2015
M. Venter et al. **2060**

 Related material available online:
http://wwwnc.cdc.gov/eid/article/23/12/16-2078_article

Tick-Borne Encephalitis in Sheep, Romania
J. Salat et al. **2065**

 Related material available online:
http://wwwnc.cdc.gov/eid/article/23/12/17-0166_article



 **Newly Recognized Pediatric Cases of Typhus Group Rickettsiosis, Houston, Texas, USA**

T. Erickson et al. **2068**
Analysis of medical records identified 36 cases since 2011.

Identification of *Dermacentor reticulatus* Ticks Carrying *Rickettsia raoultii* on Migrating Jackal, Denmark
K. Klitgaard et al. **2072**

Investigation of Acute Flaccid Paralysis Reported with La Crosse Virus Infection, Ohio, USA, 2008–2014
M.J. Hennessey et al. **2075**

Phylogenetic Characterization of Crimean-Congo Hemorrhagic Fever Virus, Spain
E.R. de Arellano et al. **2078**

Lack of Secondary Transmission of Ebola Virus from Healthcare Worker to 238 Contacts, United Kingdom, December 2014
P. Crook et al. **2081**

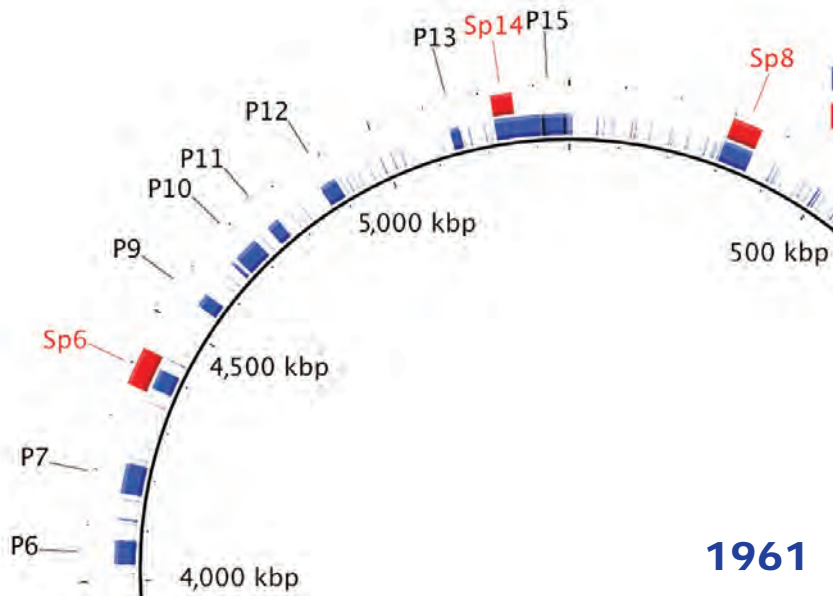
Diagnostic Accuracy of Parameters for Zika and Dengue Virus Infections, Singapore
H.J. Ho et al. **2085**

 Related material available online:
http://wwwnc.cdc.gov/eid/article/23/12/16-1224_article

Research Letters

New Avian Hepadnavirus in Palaeognathous Bird, Germany
W.K. Jo et al. **2089**

 Related material available online:
http://wwwnc.cdc.gov/eid/article/23/12/16-1634_article



Acute Myopericarditis Associated with Tickborne *Rickettsia sibirica mongolitimonae*

P. Revilla-Martí et al. 2091

Enteropathogenic *Escherichia coli* O80:H2 in Young Calves with Diarrhea, Belgium

D.Thiry et al. 2093

Incentives for Bushmeat Consumption and Importation among West African Immigrants, Minnesota, USA

E. Walz et al. 2095

 Related material available online:
http://wwwnc.cdc.gov/eid/article/23/12/17-0563_article

Porcine Astrovirus Type 3 in Central Nervous System of Swine with Polioencephalomyelitis

B. Arruda et al. 2097

 Related material available online:
http://wwwnc.cdc.gov/eid/article/23/12/17-0703_article

Avian Influenza A(H7N9) Viruses Co-circulating among Chickens, Southern China

N. Wang et al. 2100

 Related material available online:
http://wwwnc.cdc.gov/eid/article/23/12/17-0782_article

Rabies and Distemper Outbreaks in Smallest Ethiopian Wolf Population

J. Marino et al. 2102

High Abundance and Genetic Variability of Atypical Porcine Pestivirus in Pigs from Europe and Asia

A. Postel et al. 2104

 Related material available online:
http://wwwnc.cdc.gov/eid/article/23/12/17-0951_article

Human Case of *Streptococcus suis* Disease, Ontario, Canada

J. Gomez-Torres et al. 2107



Moku Virus in Invasive Asian Hornets, Belgium, 2016

M. Garigliany et al. 2109

 Related material available online:
http://wwwnc.cdc.gov/eid/article/23/12/17-1080_article

***Angiostrongylus cantonensis* DNA in Cerebrospinal Fluid of Persons with Eosinophilic Meningitis, Laos**

D.K.Y. Ming et al. 2112

Tool for Eliminating Dog-Mediated Human Rabies through Mass Dog Vaccination Campaigns

E.A. Undurraga et al. 2114

 Related material available online:
http://wwwnc.cdc.gov/eid/article/23/12/17-1148_article

Unexpected Infection with *Armillifer* Parasites

I. Potters et al. 2116

Influenza A(H9N2) Virus, Burkina Faso

B. Zecchin et al. 2118

 Related material available online:
http://wwwnc.cdc.gov/eid/article/23/12/17-1294_article

Detection of Zika Virus in April 2013 Patient Samples, Rio de Janeiro, Brazil

S.R.L. Passos et al. 2120

Letter

Wildlife as Source of Human *Escherichia coli* O157 infection

B. Crook, H. Senior 2122

EMERGING INFECTIOUS DISEASES®

December 2017



Books and Media

The Next Pandemic: On the Front Lines Against Humankind's Gravest Dangers

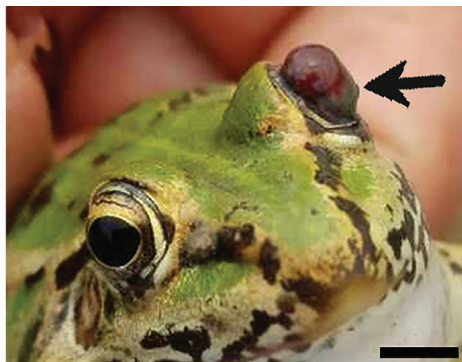
W.P. Hanage 2123

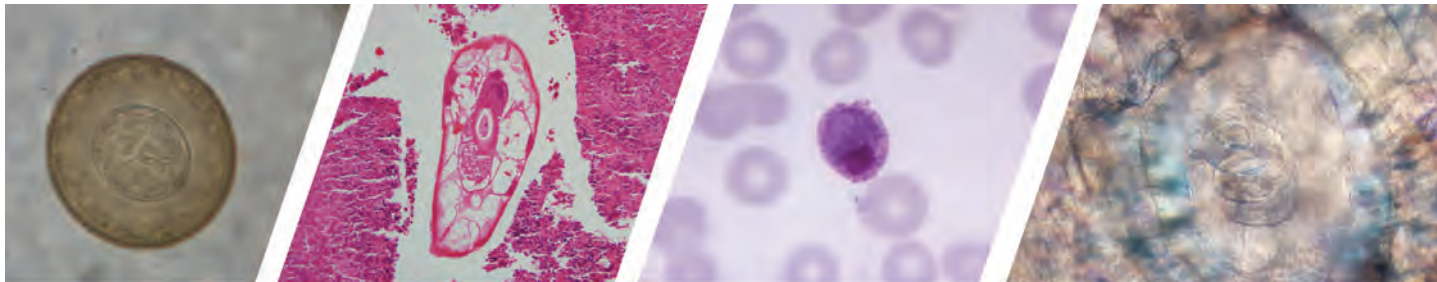
About the Cover

Everything within a Circle Is One Thing

B. Breedlove 2124

Reviewer Appreciation 2126





Diagnostic Assistance and Training in Laboratory Identification of Parasites

A free service of CDC available to laboratorians, pathologists, and other health professionals in the United States and abroad



Diagnosis from photographs of worms, histological sections, fecal, blood, and other specimen types



Expert diagnostic review



Formal diagnostic laboratory report



Submission of samples via secure file share

Visit the DPDx website for information on laboratory diagnosis, geographic distribution, clinical features, parasite life cycles, and training via Monthly Case Studies of parasitic diseases.

www.cdc.gov/dpdx
dpdx@cdc.gov



U.S. Department of Health and Human Services
Centers for Disease Control and Prevention

Fatal Outbreak in Tonkean Macaques Caused by Possibly Novel Orthopoxvirus, Italy, January 2015¹

Giusy Cardeti,² Cesare Ernesto Maria Gruber,² Claudia Eleni, Fabrizio Carletti, Concetta Castilletti, Giuseppe Manna, Francesca Rosone, Emanuela Giombini, Marina Selleri, Daniele Lapa, Vincenzo Puro, Antonino Di Caro, Raniero Lorenzetti, Maria Teresa Scicluna, Goffredo Grifoni, Annapaola Rizzoli, Valentina Tagliapietra, Lorenzo De Marco, Maria Rosaria Capobianchi, Gian Luca Autorino

In January 2015, during a 3-week period, 12 captive Tonkean macaques at a sanctuary in Italy died. An orthopoxvirus infection was suspected because of negative-staining electron microscopy results. The diagnosis was confirmed by histology, virus isolation, and molecular analysis performed on different organs from all animals. An epidemiologic investigation was unable to define the infection source in the surrounding area. Trapped rodents were negative by virologic testing, but specific IgG was detected in 27.27% of small rodents and 14.28% of rats. An attenuated live vaccine was administered to the susceptible monkey population, and no adverse reactions were observed; a detectable humoral immune response was induced in most of the vaccinated animals. We performed molecular characterization of the orthopoxvirus isolate by next-generation sequencing. According to the phylogenetic analysis of the 9 conserved genes, the virus could be part of a novel clade, lying between cowpox and ectromelia viruses.

Genus *Orthopoxvirus* virions are brick-shaped and replicate in the cytoplasm of eukaryotic cells (1). Some orthopoxviruses have limited host ranges; for example, ectromelia virus (ECTV) has only been described infecting captive colonies of laboratory mice (2,3). Other orthopoxviruses can infect multiple animal species; for example, cowpox virus (CPXV) has been observed on multiple occasions to spill over from its natural reservoir (presumably

small wild rodents) to a wide variety of accidental hosts, including humans (4). The 3 orthopoxviruses raccoonpox, skunkpox, and volepox viruses are recognized as endemic in North America and are referred to as New World orthopoxviruses (5). The 6 orthopoxviruses variola virus, vaccinia virus (VACV), camelpox virus, monkeypox virus, ECTV, and CPXV are recognized as originating from the Eurasian continent and are referred to as Old World orthopoxviruses (6). Phylogenetic analyses have determined that CPXV is composed of multiple paraphyletic clades: VACV-like clade; variola virus-like clade; and CPXV clades 1, 2, and 3 (4,7). Moreover, analyses of 2 novel orthopoxviruses discovered in the country of Georgia (8) and the US state of Alaska (9) indicated they represented lineages distantly related from all previously known Old World and New World orthopoxviruses.

In Europe, western Russia, and northern and central Asia, CPXV is endemic, and in Europe, the numbers of reports are increasing (10). Many studies have explored the variable pathogenic potential of CPXV, observing that virulence and the clinical manifestations of a given strain are often correlated with the affected host species (4). In particular, exotic animals from zoos and circuses are reported to be highly susceptible to CPXV infections (11–15).

Among nonhuman primates (NHPs), orthopoxvirus infections have been reported in New World monkeys (16), Barbary macaques (13), squirrel monkeys (17), and tamarins (14), but these infections have not been described in the Tonkean macaque (*Macaca tonkeana*). The Tonkean macaque, belonging to the *Cercopithecidae* family, is found in 4 protected areas in central Sulawesi (18); a few social groups live in 4 rescue centers in Europe,

Author affiliations: Istituto Zooprofilattico Sperimentale del Lazio e della Toscana M. Aleandri, Rome, Italy (G. Cardeti, C. Eleni, G. Manna, F. Rosone, R. Lorenzetti, M.T. Scicluna, G. Grifoni, G.L. Autorino); L. Spallanzani National Institute of Infectious Diseases, Rome (C.E.M. Gruber, F. Carletti, C. Castilletti, E. Giombini, M. Selleri, D. Lapa, V. Puro, A. Di Caro, M.R. Capobianchi); Fondazione Edmund Mach di San Michele all'Adige, Trento, Italy (A. Rizzoli, V. Tagliapietra); Parco Faunistico Piano dell'Abatino, Poggio San Lorenzo, Italy (L. De Marco)

¹Preliminary results from this study were presented at the Xth International Congress of the European Society for Veterinary Virology; August 31–September 3, 2015; Montpellier, France.

²These first authors were co–principal investigators who contributed equally to this article.

DOI: <https://doi.org/10.3201/eid2312.162098>

including in Italy, and in central America. Because of the limited number of these animals in sanctuaries, they are infrequently observed infected with orthopoxviruses, and thus, little information has been published regarding their disease signs and symptoms.

A few cases of orthopoxvirus infection have been reported in Italy. In southern Italy, orthopoxvirus infections with CPXV have been described in domestic ruminants (19). At a farm in the region of Lazio, Italy, a CPXV outbreak occurred involving 7 llamas, which were suspected to have been infected via infected mice that were introduced to feed the birds of prey at the farm (20). Zoonotic infections caused by 2 almost identical orthopoxvirus isolates occurred in 2005 and 2007 in 2 veterinarians from northeastern Italy who acquired the infections during 2 separate incidents from 2 different infected cats (21). Although definitive taxonomic assignment of these orthopoxviruses was not conclusive, hemagglutinin (HA) and *crmB* sequence analyses suggested possible segregation of these virus isolates from other previously described orthopoxvirus strains.

We describe a severe orthopoxvirus epidemic that occurred in 2015 in a social group of Tonkean macaques housed in a sanctuary for wild and exotic animals in a wooded area in central Italy, where 146 NHPs and 240 other wild and domestic mammals were maintained. To prevent other cases in NHPs, we undertook an immunization protocol and conducted epidemiologic investigations to detect orthopoxvirus carriers. We also performed taxonomic characterization to determine its relatedness to other orthopoxviruses.

Methods

The colony of Tonkean macaques was introduced to the sanctuary in 2007 from the Strasbourg Primate Centre of Strasbourg University (Strasbourg, France); the original stock had been imported into France from Indonesia in 1972. The colony housed in the center at the time of the outbreak comprised 54 animals housed in 4 wide enclosures separated from each other at different distances.

In January 2015, twelve of the 18 Tonkean macaques housed in an enclosure located in the northern part of the natural reserve died within a 3-week period. The social group housed in the affected enclosure included both male and female animals, 1–20 years of age. Two macaques died within 48 hours after disease onset with severe respiratory syndrome. In the following weeks, 13 animals from the same enclosure displayed signs of depression, nausea, respiratory distress, and neurologic disease, and in several animals, skin and mucosa lesions developed (Figure 1). Ten of these 13 macaques died within 15 days after the appearance of signs and symptoms; 2 of 13 recovered after 6 and 8 days; and the remaining animal, an adult male, recovered but experienced long-lasting effects from the infection. This macaque had severe lesions limited to the

right side of the face and the eye. In April, when this animal underwent surgery for eye ablation, oral and rectal swabs and a peripheral blood sample were acquired to detect virus and perform serologic studies.

The remaining 3 macaques in the same enclosure were constantly symptomless. Three days after the beginning of the outbreak, 2 of these macaques were immediately isolated in a separate area, and the third, a 1-year-old, was left with the mother, which recovered from the illness. None of the other 9 NHP species, wild ruminants, wild boars, donkeys, raccoons, cats, or dogs hosted in the sanctuary showed any clinical signs related to orthopoxvirus infection in the following 12-month observation period.

At postmortem examination, major organs and skin lesions were collected from all dead Tonkean macaques and processed for routine histologic (hematoxylin and eosin) staining. Virus detection by negative-staining electron microscopy (EM) was conducted with skin lesion samples from 10 animals (22). We extracted nucleic acid from homogenates of skin and lungs taken from 4 of the macaques and performed a molecular diagnostics investigation by using orthopoxvirus-specific PCR assays. We performed an orthopoxvirus-specific SYBR Green (ThermoFisher Scientific, Waltham, MA, USA) real-time PCR targeting *crmB* (23), and to confirm the first result, we tested all samples with an additional endpoint PCR targeting the orthopoxvirus HA gene. We tested 1 tissue sample for the genes encoding acidophilic-type inclusion body (ATI) protein, chemokine-binding protein (K2R), 602-kDa protein, and 14-kDa fusion protein (A27L).

Using tissue homogenates of the skin and tongue mucosa, brain, lungs, liver, spleen, heart, mesenteric lymph nodes, and intestines of the 12 dead animals (a total of 70 samples), we conducted an additional SYBR Green real-time PCR to confirm the presence of orthopoxvirus in all affected animals (Table 1). We performed virus culture by



Figure 1. Crater-shaped skin lesions at inguinal region of Tonkean macaque (*Macaca tonkeana*) housed at animal sanctuary, Italy, January 2015.

Table 1. Virologic examination of samples collected from 12 dead Tonkean macaques, Italy, January 2015*

Method	Skin	Tongue mucosa	Brain	Lungs	Liver	Spleen	Myocardium	Lymph node	Intestine	Total
Negative-staining EM	10/10	1/1	NA	NA	NA	NA	NA	NA	0/12	11/23
SYBR Green real-time PCR	10/10	1/1	3/3	12/12	10/12	12/12	3/3	5/5	3/12	59/70
Cell culture	3/3	1/1	3/3	3/3	2/2	2/2	3/3	NA	0/3	17/20

*Values are no. positive/no. total. EM, electron microscopy; NA, not analyzed.

taking tissue homogenates from up to 3 dead animals and inoculating them on Vero cells (CCL-81; American Tissue Culture Collection, Manassas, VA, USA). We sequenced the whole genome of the virus isolate by using the metagenomic approach with the Ion Torrent Personal Genome Machine platform for next generation sequencing (ThermoFisher Scientific, Waltham, MA, USA). In brief, we grew the virus to passage 4 (titer $1 \times 10^{6.9}$ 50% tissue culture infectious dose/mL) and concentrated it by ultracentrifugation. Then, we extracted pellet-associated DNA with E-Gel SizeSelect Agarose Gels (ThermoFisher Scientific) and quantified with Qubit dsDNA HS Assay Kit (ThermoFisher Scientific). We prepared DNA libraries with the Ion Xpress Plus gDNA Fragment Library Kit (ThermoFisher Scientific). We filtered sequence reads with the VirFind tool (<http://virfind.org/j/>) and de novo assembled sequences with Newbler version 2.5.3 (454 Life Sciences, Branford, CT, USA). We aligned the 5 major contigs (length 13,743–108,913 nt) to CPXV-Germany1998–2 (GenBank accession no. HQ420897.1) with MAUVE software (24) and concatenated the sequences. Inverted terminal repeats were excluded from the genome reconstruction.

We conducted epidemiologic investigations to examine virus transmission between working personnel and other animal species maintained in the reserve and to identify possible orthopoxvirus carriers (13). During February 2015–April 2016, the following animals in the same sanctuary died without specific symptoms: 9 NHPs, 2 foxes, and 1 cat. We conducted a virologic investigation for

orthopoxvirus infection with the lungs, livers, spleens, and intestines of these dead animals.

After the outbreak, we initiated a 1-year rodent control program inside and in proximity to the enclosures. We captured 11 live mice (4 *Apodemus flavicollis* and 7 *Microtus* spp.) and 93 dead wild gray rats (*Rattus rattus*) by using multicapture live traps (Ugglan Special Mouse Trap 2; Grahnab, Hillerstorp, Sweden) (25) and electromechanical equipment. Lungs, liver, spleen, and small intestines of these animals were stored at -80°C until virologic analysis.

The sanctuary owner reported that 1 Japanese macaque (*M. fuscata*) had similar skin lesions (Figure 2) in 2003, and at that time, infection with a herpes zoster virus had been ruled out. This animal was still alive and was sampled for serologic investigations at the time of the 2015 outbreak.

We performed a serologic investigation with blood samples (stored at -20°C after collection) taken from 30 various mammals (Table 2) and 62 NHPs (Table 3) housed at the sanctuary, as well as 11 mice and 56 dead rats. Detection of orthopoxvirus antibodies from NHPs and small rodents was performed by indirect immunofluorescence antibody (IFA) assay with homemade slides that were seeded with Vero-E6 cells and infected with the smallpox vaccine virus Lancy-Vaxina (21). To detect orthopoxvirus-specific antibodies in other mammals, we used a virus neutralization assay (20). We also conducted an epidemiologic and serologic investigation with the sanctuary staff (N = 11; group included veterinarians, researchers, and maintenance personnel) by performing a site visit and interviews and collecting blood samples.



Figure 2. Crater-shaped skin lesions on face of Japanese macaque (*Macaca fuscata*), Italy, 2003.

Results

At necropsy, the 2 animals that died within 48 hours after symptom onset showed severe lung congestion (Figure

Table 2. Serologic analysis of serum samples collected from various mammal species housed at animal sanctuary, Italy, January 2015

Species	Virus neutralization test, no. positive/no. total	Antibody titer*
Wolf	0/1	Negative
Llama	0/8	Negative
Roe deer	0/1	Negative
Mouflon	0/1	Negative
Goat	0/4	Negative
Badger	0/1	Negative
Donkey	0/2	Negative
Cat	0/12	Negative
Total	0/30	

*Threshold dilution was 1:4.

Table 3. Serologic analysis of serum samples from nonhuman primate species housed at animal sanctuary, Italy, January 2015*

Species	IFA IgM test, no.		IFA IgG test, no.	
	positive/no. total (%)	IgM titer†	positive/no. total (%)	IgG titer, † range
Tonkean macaque (<i>Macaca tonkeana</i>)	0/30	Negative	8/30	1:40–1: 640
Cynomolgus macaque (<i>M. fascicularis</i>)	0/11	Negative	3/11	1:20–1:160
Barbary macaque (<i>M. sylvanus</i>)	2/12	1:20	2/12	1:20
Rhesus macaque (<i>M. mulatta</i>)	0/1	Negative	1/1	1:80
Japanese macaque (<i>M. fuscata</i>)	0/2	Negative	2/2	1:80
Tufted capuchin (<i>Sapajus apella</i>)	0/4	Negative	2/4	1:20
Grivet (<i>Cercopithecus aethiops</i>)	0/1	Negative	0/1	Negative
Hamadryas baboon (<i>Papio hamadryas</i>)	0/1	Negative	0/1	Negative
Total	2/62 (3.22)		18/62 (29.03)	

*IFA, immunofluorescence antibody.

†Threshold dilution was 1:20.

3, panel A) and hepatosplenomegaly. The 10 animals that died 5–15 days after onset of clinical signs had erythematous papular and pustular lesions on the face, in the oral cavity, on the tongue mucosa (Figure 3, panel B), and at the inguinal region. All cutaneous lesions were characterized by focal epidermal necrosis and early vesiculation with eosinophilic intracytoplasmic inclusion bodies in enlarged degenerated cells (Figure 4, panel A). The liver showed scattered foci of necrosis and moderate steatosis. Foci of necrosis at the lymphoid follicles and histiocytosis associated with hemorrhages were observed in the spleen and at the lymph nodes. In some cases, mild interstitial pneumonia was associated with focal necrosis of bronchial epithelium.

Negative-staining EM revealed the presence of brick-shaped particles morphologically consistent with orthopoxvirus in the skin lesions of 10 dead macaques (Figure 4, panel B). Vero cell cultures inoculated with skin lesion materials from infected monkeys showed the previously described cytopathic effect (20) 3 days after inoculation. A viable transmissible agent, which we named orthopoxvirus Abatino, was consistently isolated and confirmed to be an orthopoxvirus by negative-staining EM.

Confirming the negative-staining EM results, SYBR Green real-time PCR detected an orthopoxvirus genome in all organs from the 12 dead macaques (Table 1); the melting temperature of the amplicons ($80.8^{\circ}\text{C} \pm 1^{\circ}\text{C}$; Figure 4, panel C) was identical for all tested samples and consistent with that of orthopoxvirus genomes (23). The presence of the HA sequence in tissues confirmed infection with an orthopoxvirus and ruled out the presence of monkeypox.

Oral and rectal swabs collected 3 months after the epidemic from the recovered male macaque were negative by all virologic analyses. Retrospective examination of the sanctuary records of the past 2 years excluded the possibility of introduction of this orthopoxvirus through contacts with other mammal species maintained in captivity.

All tissue samples from the 104 small rodents trapped during February 2015–June 2016 were negative for orthopoxvirus by PCR. The animals that died in the sanctuary after the epidemic were negative for orthopoxvirus by all virologic tests performed.

The Japanese macaque that had orthopoxvirus-like skin lesions in 2003 showed an orthopoxvirus-specific IgG (but not IgM) titer of 1:80 by IFA assay. The IFA assay showed orthopoxvirus-specific IgG in 8 (14.28%) of 56 rats and in 3 (27.27%) *Apodemus flavicollis* mice of 11 small rodents (mice and voles). Orthopoxvirus-specific IgM was never detected (Table 4).

Among the NHPs outside of the affected enclosure, we detected orthopoxvirus IgG in 18 NHPs, 6 of which were asymptomatic Tonkean macaques maintained in an enclosure near the affected one. Orthopoxvirus IgM was detected at low titer only in 2 Barbary macaques that never showed clinical signs of orthopoxvirus infection (Table 3).

Animal Vaccination

To prevent further infections, 96 NHPs of 8 species (*M. tonkeana*, *M. fascicularis*, *M. sylvanus*, *M. fuscata*, *M. mulatta*, *Sapajus apella*, *Chlorocebus aethiops*, and *Papio hamadryas*) were vaccinated during October–December

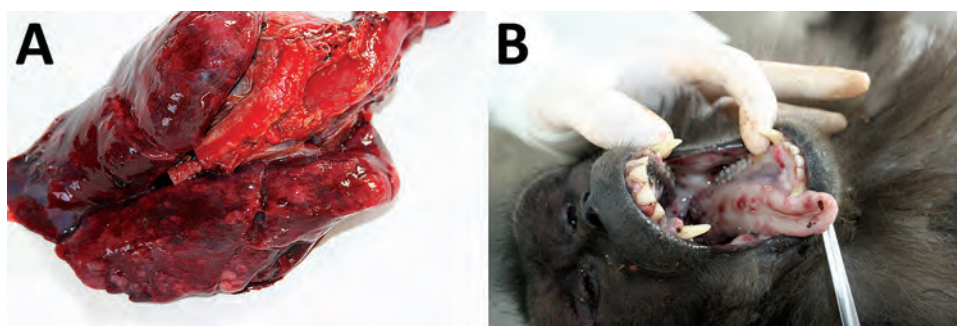


Figure 3. Results from necropsy of Tonkean macaque (*Macaca tonkeana*) from animal sanctuary, Italy, January 2015, showing severe congestion in the lungs (A) and erythematous papules and pustular lesions on the buccal and tongue mucosae (B).

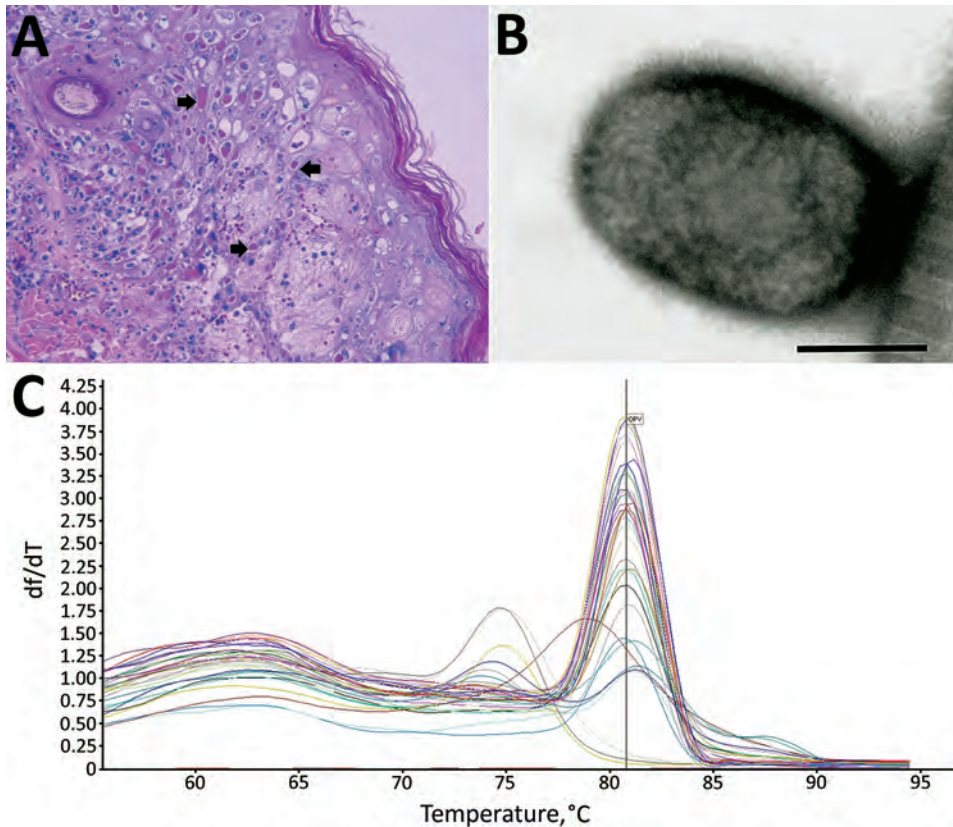


Figure 4. Results from necropsy of Tonkean macaque (*Macaca tonkeana*) from animal sanctuary, Italy, January 2015. A) Hematoxylin and eosin stain of cutaneous lesion. Focal epidermal necrosis, acanthosis ballooning degeneration, and acantholysis of keratinocytes were observed. Staining shows early vesiculation with eosinophilic intracytoplasmic inclusion bodies (arrows) in enlarged degenerated cells. Original magnification $\times 20$. B) Electron micrograph of skin lesion sample showing negatively stained brick-shaped viral particle of $\approx 160\text{--}220$ nm, consistent with orthopoxvirus. Scale bar = 100 nm. C) SYBR Green (ThermoFisher Scientific, Waltham, MA, USA) real-time PCR melting curve of all tested samples. The y-axis shows the ratio of the change in fluorescence over the change in temperature. The average melting temperature ($80.8^{\circ}\text{C} \pm 1^{\circ}\text{C}$) was consistent with that for the orthopoxvirus genome.

2015. Each animal received 2 doses of modified vaccinia virus Ankara (MVA) vaccine (Bavarian Nordic, Kvistgaard, Denmark) given 1 month apart, according to the producer’s immunization protocol. To assess possible vaccine-related adverse reactions, we monitored the NHPs for up to 10 days after dose administration and did not observe lesions at the vaccine inoculation site or general symptoms.

The immune responses to the vaccine were evaluated in a group of 10 animals (4 *M. tonkeana*, 5 *M. fascicularis*, and 1 *M. sylvanus*). Seven animals were negative for antibodies before vaccination, and 3 had a barely detectable baseline IgG titer. After vaccination, all monkeys showed a 2–5-fold increase of IgG titer. IgM were observed in the serum of 4 animals at or near the minimum threshold dilution (1:20) on the day of vaccine booster administration (Table 5). We did not detect viable virus or viral DNA shedding.

Molecular Characterization of Virus Isolate

After the positive results of the first diagnostic molecular analysis, we performed additional genus-specific PCRs targeting HA, ATI, K2R, 602 kDa, and A27L with samples to better characterize the virus (26,27). We compared the complete nucleotide sequences of most amplicons with all orthopoxvirus full-genome sequences available in GenBank by using blastx+ version 2.2.28 (<http://www.ncbi.nlm.nih.gov/books/NBK279690>). The HA gene sequence was closely related to that of CPXV-Germany_1998_2 (GenBank accession no. HQ420897), with a 96% identity. K2R and 602-kDa protein gene sequences were closely related to those of ECTV-Moscow (GenBank accession no. AF012825), with a 96% identity for K2R (96% of gene sequence compared) and a 99% identity for 602-kDa protein. The A27L gene was closely related to those of

Table 4. Immunofluorescence antibody testing of serum samples from small wild rodents trapped at animal sanctuary, Italy, January 2015

Species	IgM		IgG	
	No. positive/no. total (%)	Titer*	No. positive/no. total (%)	Titer*
Gray rat (<i>Rattus rattus</i>)	0/56 (0)	Negative	1/56 4/56 3/56	1:20 1:40 1:80
Total	0/56 (0)		8/56 (14.28)	
Voles (<i>Microtus</i> spp.)	0/7	Negative	0/7	Negative
Yellow-necked mouse (<i>Apodemus flavicollis</i>)	0/4	Negative	3/4	1:40
Total	0/11 (0)		3/11 (27.27)	

Table 5. Immunofluorescence antibody testing of vaccinated nonhuman primates after outbreak at animal sanctuary, Italy, January 2015*

Species	No. animals	IgM, T0/T30/T90	IgG, T0/T30/T90	No. (%) with IgG increase
Tonkean macaque (<i>Macaca tonkeana</i>)	4	Neg/1:20/neg Neg/neg/neg Neg/neg/neg Neg/neg/neg	Neg/1:20/1:320 Neg/1:20/1:80 Neg/neg/1:80 Neg/neg/1:40	4 (100)
Cynomolgus macaque (<i>M. fascicularis</i>)	5	Neg/1:20/1:20 Neg/1:80/1:80 Neg/neg/neg Neg/1:20/1:20 Neg/neg/neg	1:20/1:320/1:320 1:20/1:80/1:80 Neg/1:20/1:80 Neg/1:20/1:80 Neg/1:80/1:160	5 (100)
Barbary macaque (<i>M. sylvanus</i>)	1	Neg/neg/neg	1:20/1:20/1:80	1 (100)

*Threshold dilution for antibody titers was 1:20. Neg, negative; T0, first immunization; T30, booster dose administration; T90, blood collection 60 d after T30.

ECTV-Naval and CPXV-Finland, with a 98% identity with both strains. Finally, the ATI gene sequence was most closely related to that of the cowpox virus CPXV-Norway1994-MAN (GenBank no. HQ420899.1), with a 98% identity.

Because of the discordant identity scores obtained with the preliminary molecular analyses, we sequenced the whole genome of the virus isolate by using next-generation sequencing. The sequence obtained was 202,990-nt long with a median coverage of 507 (range 28–817) nt. We identified 10 complete coding sequences and corrected insertions and deletions manually.

The first coding sequence identified was the HA gene, which had a median coverage of 485 (range 255–586) nt (GenBank accession no. KY100116). We used this gene to check the sequence identity with PCR results and to compare the homology with all available orthopoxvirus strains. Orthopoxvirus Abatino shared 99% nucleotide identity and 98% amino acid identity with ECTV-Moscow and 96% nucleotide identity and 94% amino acid identity with CPXV-Germany1998–2. Furthermore, we observed that Abatino had HA identity scores of 97% for the nucleotide sequence and 96% for the amino acid sequence with FelinePoxITA1 (GenBank accession no. EF612709.1), an orthopoxvirus isolate previously obtained in 2007 from a zoonotic case in northeastern Italy that does not have a definitive taxonomic assignment (21).

Because phylogenetic relationships based on HA are not considered reliable for assigning orthopoxvirus taxonomic relationships (7), we performed a more detailed analysis. Following a previously established pipeline (28,29), we performed core-genome selection, identity clustering, and phylogenetic reconstruction. Using blastx+, we identified the coding sequences of 9 conserved poxvirus genes (D1R, E6R, D5R, E9L, A7L, A10L, J6R, H4L, and A24R; VACV strain Copenhagen nomenclature; GenBank accession nos. KY100107–KY100115) uniformly distributed along the central region of the genome. The median coverage of the selected genes was 528 (range 80–743) nt. We aligned the concatenated sequences with homologous genes from available whole-sequence orthopoxvirus strains (4–7,9) by using MUSCLE version 3.8.31 (30).

The identity score matrix (Figure 5) identified the 11 orthopoxvirus clusters described in previous reports (4,9). The identity score of orthopoxvirus Abatino with other orthopoxviruses ranged 93.26%–98.16%; the viruses with the highest identity scores to Abatino (98.14%, 98.15%, and 98.16%) were the 3 available ECTV sequences.

Using the Bayesian Markov chain Monte Carlo model (31) and the maximum-likelihood model (32), we performed a phylogenetic analysis including a representative genome for each orthopoxvirus clade (Figure 6). The position of orthopoxvirus Abatino was consistent with the results of the identity heat map.

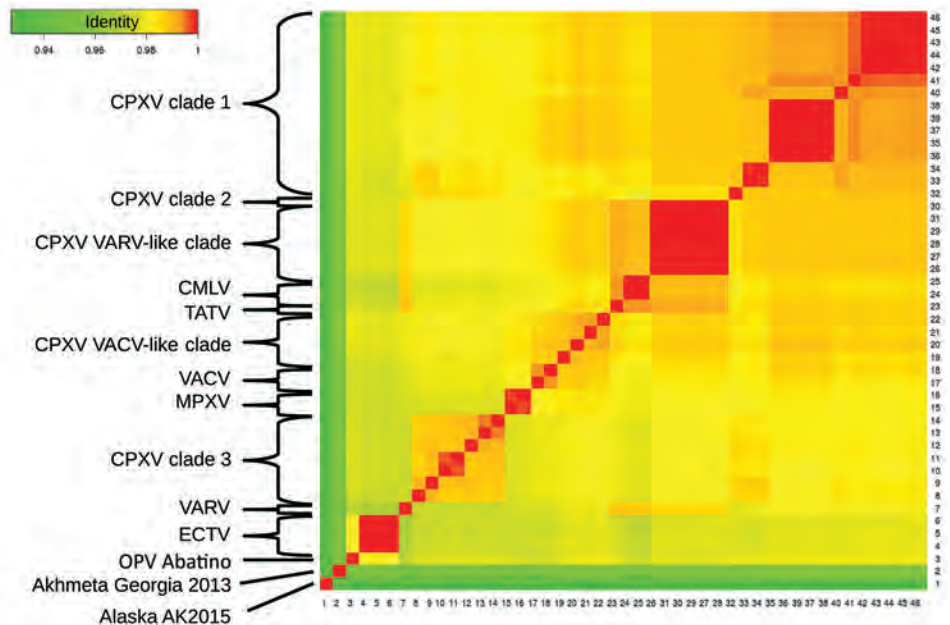
Discussion

This epidemic indicated that Tonkean macaques are highly susceptible to infection with the isolated orthopoxvirus strain and might develop severe, fatal disease. Pathologic findings observed in dead animals were similar to those described in New World monkeys (16). Viable virus and viral DNA were detected not only in the cutaneous tissue and oral mucosa but also in many different organs, such as the liver and heart. Unfortunately, we could not detect viable virus in the intestinal tissues, and therefore, we cannot hypothesize regarding the possibility of viral transmission through feces among living animals.

The severe disease was limited to a single Tonkean macaque social group, and the results of SYBR Green PCR suggested the involvement of the same viral agent, even if not all isolates were genetically characterized. The high IgG titers in 6 macaques from the neighboring enclosure, however, indicated they became infected during the outbreak. Orthopoxvirus IgM and IgG detected in some NHPs in other enclosures support the hypothesis that the virus circulated in the natural reserve, but no orthopoxvirus symptoms were observed in these animals, and no viral DNA or viable virus was isolated from them. Also, no other mammals hosted in the sanctuary appeared to have been exposed to the virus.

The illness observed years before in the Japanese macaque that had orthopoxvirus-specific IgG suggests the possibility that an orthopoxvirus could have been circulating in

Figure 5. Identity between OPV Abatino, obtained from skin lesion of Tonkean macaque during outbreak at animal sanctuary, Italy, January 2015, and available OPV genomes on the basis of 9 concatenated conserved genes: A7L, A10L, A24R, D1R, D5R, H4L, E6R, E9L, and J6R. Red indicates more similarity, green less similarity. Sequences shown (GenBank accession nos.): 1) OPV Tena Dona AK2015 (KX914668–76); 2) OPV GCP2013 Akhmeta (KM046934–42); 4–6) ECTV-Moscow (AF012825.2), ECTV-Naval (KJ563295.1), ECTV-VR-1431 (JQ410350.1); 7) VARV-Bangladesh-1975 (L22579.1); 8–14) CPXV-HumLue09–1 (KC813494.1), CPXV-Germany1990–2 (HQ420896.1), CPXV-Francy2001-Nancy (HQ420894.1), CPXV-MarLei07–1 (KC813499.1), CPXV-Norway1994-MAN (HQ420899.1), CPXV-UK2000-K2984



(HQ420900.1), CPXV-BrightonRed (AF482758.2); 15–16) MPXV-Congo2003–358 (DQ011154.1), MPXV-Liberia-1970–184 (DQ011156.1); 17–18) VACV-IOC-B141 (KT184690.1), VACV-Lister (KX061501.1); 19–22) CPXV-Austria1999 (HQ407377.1), CPXV-HumLit08–1 (KC813493.1), CPXV-GRI90 (X94355.2), CPXV-Finland2000 (HQ420893.1); 23) TATV-Dahomey-1968 (DQ437594.1); 24–25) CMLV-0408151v (KP768318.1), CMLV-M96 (AF438165.1); 26–31) CPXV-HumGra07–1 (KC813510.1), CPXV-RatKre08–2 (KC813505.1), CPXV-RatGer09–1 (KC813503.1), CPXV-RatAac09–1 (KC813501.1), CPXV-HumAac09–1 (KC813508.1), CPXV-HumKre08–1 (KC813512.1); 32) CPXV-Germany1998–2 (HQ420897.1); and 33–46) CPXV-Germany1980-EP4 (HQ420895.1), CPXV-HumPad07–1 (KC813496.1), CPXV-HumLan08–1 (KC813492.1), CPXV-RatHei09–1 (KC813504.1), CPXV-MonKre08–4 (KC813500.1), CPXV-JagKre08–1 (KC813497.1), CPXV-JagKre08–2 (KC813498.1), CPXV-Germany2002-MKY (HQ420898.1), CPXV-HumGri07–1 (KC813511.1), CPXV-HumMag07–1 (KC813495.1), CPXV-CatBer07–1 (KC813502.1), CPXV-HumBer07–1 (KC813509.1), CPXV-CatPox07–1 (KC813506.1), CPXV-BeaBer04–1 (KC813491.1). CMLV, camelpox virus; CPXV, cowpox virus; ECTV, ectromelia virus; MPXV, monkeypox virus; OPV, orthopoxvirus; TATV, taterapox virus; VACV, vaccinia virus; VARV, variola virus.

the area since at least 2003, although no evidence was available to indicate whether that remote episode was caused by the same virus strain identified in the 2015 outbreak. Serologic evidence of orthopoxvirus infection in mice and rats confirms that mice and rats are susceptible to orthopoxviruses but does not definitively prove that they were infected with the virus responsible for the outbreak or establish their role as reservoirs, as has been described for rodents with other orthopoxvirus strains in previous studies (10,13).

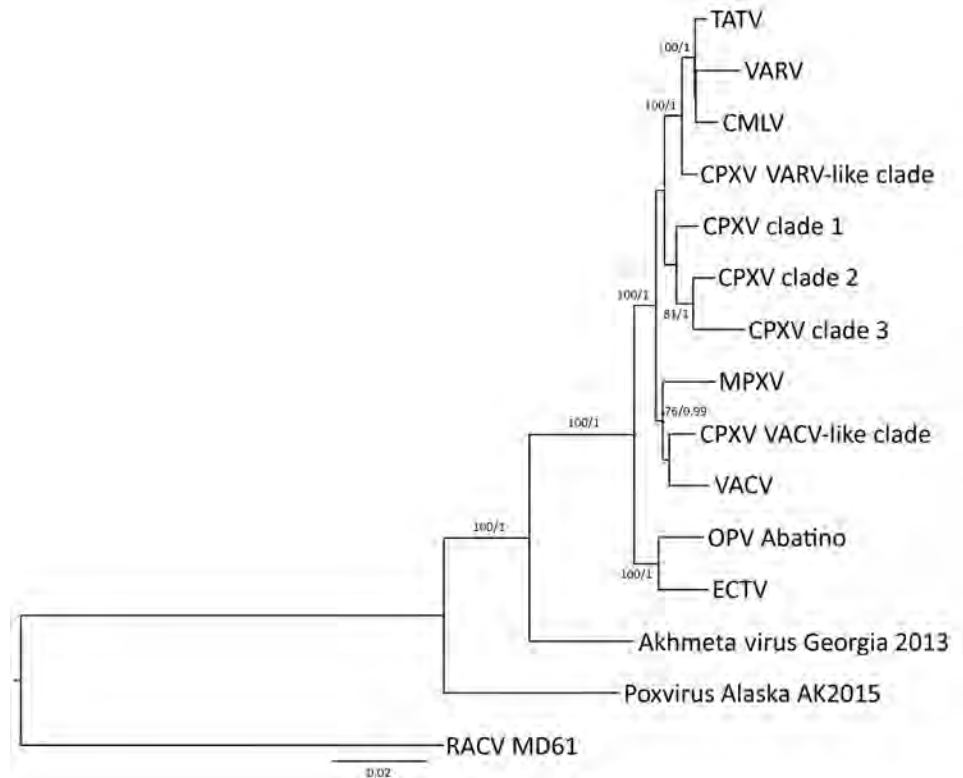
The preliminary characterization of the isolated orthopoxvirus strain that was based on HA similarity analysis suggested that orthopoxvirus Abatino might be related to ECTV, CPXV clade 3, and a previous orthopoxvirus isolate that caused 2 zoonotic infections in northeastern Italy in 2005 and 2007 (21). On the other hand, the extended molecular characterization that was based on 9 conserved orthopoxvirus genes suggested that orthopoxvirus Abatino is in a distinct position with respect to all 11 orthopoxvirus clades, being more related to ECTV than to all other orthopoxvirus clades. ECTV occasionally infects laboratory mice populations (2) and is suspected to naturally spread among wild rodents, although ECTV has never been

isolated from these animals (3). Host range differences between all previously described ECTVs and orthopoxvirus Abatino strongly suggest that Abatino does not belong to the ECTV lineage. We hypothesize that orthopoxvirus Abatino might be part of a novel, paraphyletic ECTV-like clade. A recombination event that affected the host range could also be considered as a possible origin for this virus, but a more extensive characterization is necessary.

MVA vaccine follow-up showed a detectable humoral immune response. Data on the antibody classes elicited by live-modified VACV administration in humans and NHPs are scarce or unavailable (33). However, the observations of Silva-Fernandes et al. (34) describing outbreaks in humans together with our data in vaccinated monkeys suggest that orthopoxvirus infections induce a limited IgM response. On the other hand, the low antibody titers detected could have been caused by a poor sensitivity of the IFA test adopted. Finally, the MVA vaccine was safe in the monkey populations vaccinated; we observed no adverse reactions.

The serologic surveillance conducted among sanctuary staff workers showed 1 staff member who did not previously receive orthopoxvirus vaccine and had close contacts with the

Figure 6. Phylogenetic analysis of OPV Abatino obtained from skin lesion of Tonkean macaque during outbreak at animal sanctuary, Italy, January 2015. Nine conserved genes (GenBank accession nos. KY100107–KY100115) obtained with next-generation sequencing were concatenated and aligned with the homologous concatenated sequences from representative OPV strains (GenBank accession no.): TATV-Dahomey-1968 (DQ437594.1), VARV-Bangladesh-1975 (L22579.1), CMLV-M96 (AF438165.1), CPXV-HumAac09-1 (KC813508.1), CPXV-Germany2002-MKY (HQ420898.1), CPXV-Germany1998-2 (HQ420897.1), CPXV-MarLei07-1 (KC813499.1), MPXV-Congo2003-358 (DQ011154.1), CPXV-Finland2000 (HQ420893.1), VACV-Lister (KX061501.1), ECTV-Moscow (AF012825.2), OPV GCP2013 Akhmeta (KM046934-42), and OPV Tena Dona AK2015 (KX914668-76). New World strain RACV-MD19 (GenBank accession no. FJ807746-54) was added to the analysis as an outgroup. We generated multiple alignments with MUSCLE version 3.8.31 (30) and built the phylogenetic tree by using the Bayesian Markov chain Monte Carlo model with MRBAYES version 3.2.5 (31) using the general time-reversible plus gamma model with 1 million generations, retaining a minimum of 10,000 posterior probabilities, and maximum-likelihood model RAXML version 8.1.24 (32) using the general time-reversible plus gamma with 1,000 pseudoreplicates. Numbers represent the reliability of the nodes with the minimum probability of 75% and minimum bootstrap value of 75. Scale bar indicates nucleotide substitutions per site. CMLV, camelpox virus; CPXV, cowpox virus; ECTV, ectromelia virus; MPXV, monkeypox virus; OPV, orthopoxvirus; RACV, raccoonpox virus; TATV, taterapox virus; VACV, vaccinia virus; VARV, variola virus.



affected Tonkean macaque group seroconverted without clinical signs, suggestive of an asymptomatic infection. However, alternative explanations for this seroconversion (e.g., previous exposure to a closely related virus) could not be ruled out.

This study might be considered alarming because orthopoxvirus vaccination has been discontinued globally since the late 1970s, which has resulted in the reduction of protective immunity over time not only against smallpox virus but also against a variety of other orthopoxviruses, raising the chances of orthopoxvirus infections occurring in humans. Orthopoxvirus infection in humans is not a notifiable disease in Italy, and because virologic diagnosis relies on specialized laboratories, orthopoxvirus infection is often not included among the differential diagnosis. Increased public awareness and linkage between human and veterinary health authorities is necessary to improve public health measures for the control of zoonotic orthopoxviruses.

Acknowledgments

We thank Heidi C. Hauffe for her contribution to the epidemiologic investigations, Antonio De Marco and Laura Toti

for their hospitality at the sanctuary, and Cristian Alimonti for his work preparing figures.

This study was supported by the Italian Ministry of Health grant IZSLT 03/13 RC; the European Union Seventh Framework Programme grant no. 278433 (PREDEMICS); the European Union's Horizon 2020 research and innovation program European Virus Archive goes Global under grant agreement no. 653316; and the European-funded Joint Action Consumers, Health, Agriculture and Food Executive Agency no. 677066 (EMERGE).

Dr. Cardeti is a part of the veterinary staff and head of the Laboratory of Electron Microscopy and Special Virology at the Istituto Zooprofilattico Sperimentale del Lazio e della Toscana M. Aleandri in central Italy. Her research interests are controlling animal infectious diseases and zoonoses, including those involving reptiles, bees, and fish. Dr. Gruber is a member of the bioinformatics unit of the Laboratory of Virology at the National Institute for Infectious Diseases Lazzaro Spallanzani in Rome, Italy. His research interests are developing and applying algorithms to genetically characterize novel and emerging viruses, especially those increasing in pathogenesis.

References

1. McFadden G. Poxvirus tropism. *Nat Rev Microbiol*. 2005;3: 201–13. <http://dx.doi.org/10.1038/nrmicro1099>
2. Fenner F. Mousepox (infectious ectromelia): past, present, and future. *Lab Anim Sci*. 1981;31:553–9.
3. Esteban DJ, Buller RM. Ectromelia virus: the causative agent of mousepox. *J Gen Virol*. 2005;86:2645–59. <http://dx.doi.org/10.1099/vir.0.81090-0>
4. Hoffmann D, Franke A, Jenckel M, Tamošiūnaitė A, Schluckebier J, Granzow H, et al. Out of the reservoir: phenotypic and genotypic characterization of a novel cowpox virus isolated from a common vole. *J Virol*. 2015;89:10959–69. <http://dx.doi.org/10.1128/JVI.01195-15>
5. Smithson C, Tang N, Sammons S, Frace M, Batra D, Li Y, et al. The genomes of three North American orthopoxviruses. *Virus Genes*. 2017;53:21–34. <http://dx.doi.org/10.1007/s11262-016-1388-9>
6. Carroll DS, Emerson GL, Li Y, Sammons S, Olson V, Frace M, et al. Chasing Jenner’s vaccine: revisiting cowpox virus classification. *PLoS One*. 2011;6:e23086. <http://dx.doi.org/10.1371/journal.pone.0023086>
7. Dabrowski PW, Radonić A, Kurth A, Nitsche A. Genome-wide comparison of cowpox viruses reveals a new clade related to variola virus. *PLoS One*. 2013;8:e79953. <http://dx.doi.org/10.1371/journal.pone.0079953>
8. Vora NM, Li Y, Geleishvili M, Emerson GL, Khmaladze E, Maghlakelidze G, et al. Human infection with a zoonotic orthopoxvirus in the country of Georgia. *N Engl J Med*. 2015;372:1223–30. <http://dx.doi.org/10.1056/NEJMoa1407647>
9. Springer YP, Hsu CH, Werle ZR, Olson LE, Cooper MP, Castrodale LJ, et al. Novel orthopoxvirus infection in an Alaska resident. *Clin Infect Dis*. 2017;64:1737–41. <http://dx.doi.org/10.1093/cid/cix219>
10. Chantrey J, Meyer H, Baxby D, Begon M, Bown KJ, Hazel SM, et al. Cowpox: reservoir hosts and geographic range. *Epidemiol Infect*. 1999;122:455–60. <http://dx.doi.org/10.1017/S0950268899002423>
11. Kurth A, Wibbelt G, Gerber HP, Petschaelis A, Pauli G, Nitsche A. Rat-to-elephant-to-human transmission of cowpox virus. *Emerg Infect Dis*. 2008;14:670–1. <http://dx.doi.org/10.3201/eid1404.070817>
12. Schmiedeknecht G, Eickmann M, Köhler K, Herden CE, Kolesnikova L, Förster C, et al. Fatal cowpox virus infection in captive banded mongooses (*Mungos mungo*). *Vet Pathol*. 2010;47:547–52. <http://dx.doi.org/10.1177/0300985810363703>
13. Martina BEE, van Doornum G, Dorrestein GM, Niesters HGM, Stittelaar KJ, Wolters MABI, et al. Cowpox virus transmission from rats to monkeys, the Netherlands. *Emerg Infect Dis*. 2006;12:1005–7. <http://dx.doi.org/10.3201/eid1206.051513>
14. Kalthoff D, Bock WI, Hühn F, Beer M, Hoffmann B. Fatal cowpox virus infection in cotton-top tamarins (*Saguinus oedipus*) in Germany. *Vector Borne Zoonotic Dis*. 2014;14:303–5. <http://dx.doi.org/10.1089/vbz.2013.1442>
15. Kurth A, Straube M, Kuczka A, Dunsche AJ, Meyer H, Nitsche A. Cowpox virus outbreak in banded mongooses (*Mungos mungo*) and jaguarundi (*Herpailurus yagouaroundi*) with a time-delayed infection to humans. *PLoS One*. 2009;4:e6883. <http://dx.doi.org/10.1371/journal.pone.0006883>
16. Mätz-Rensing K, Ellerbrok H, Ehlers B, Pauli G, Floto A, Alex M, et al. Fatal poxvirus outbreak in a colony of New World monkeys. *Vet Pathol*. 2006;43:212–8. <http://dx.doi.org/10.1354/vp.43-2-212>
17. Girling SJ, Pizzi R, Cox A, Beard PM. Fatal cowpox virus infection in two squirrel monkeys (*Saimiri sciureus*). *Vet Rec*. 2011;169:156. <http://dx.doi.org/10.1136/vr.d4005>
18. iNaturalist.org. Tonkean macaque. (*Macaca tonkeana*) [cited 2017 May 5]. <http://www.inaturalist.org/taxa/43453-Macaca-tonkeana>
19. Scagliarini A, Casà G, Trentin B, Gallina L, Savini F, Morent M, et al. Evidence of zoonotic *Poxviridae* coinfections in clinically diagnosed papillomas using a newly developed mini-array test. *J Vet Diagn Invest*. 2016;28:59–64. <http://dx.doi.org/10.1177/1040638715614604>
20. Cardeti G, Brozzi A, Eleni C, Polici N, D’Alterio G, Carletti F, et al. Cowpox virus in llama, Italy. *Emerg Infect Dis*. 2011;17:1513–5. <http://doi.org/10.3201/eid1708.101912>
21. Carletti F, Bordini L, Castilletti C, Di Caro A, Falasca L, Gioia C, et al. Cat-to-human orthopoxvirus transmission, northeastern Italy. *Emerg Infect Dis*. 2009;15:499–500. <http://dx.doi.org/10.3201/eid1503.080813>
22. Biel SS, Gelderblom HR. Electron microscopy of viruses. In: Cann AJ, editor. *Virus culture—a practical approach*. New York: Oxford University Press; 1999. p. 11–47.
23. Carletti F, Di Caro A, Calcaterra S, Grolla A, Czub M, Ippolito G, et al. Rapid, differential diagnosis of orthopox- and herpesviruses based upon real-time PCR product melting temperature and restriction enzyme analysis of amplicons. *J Virol Methods*. 2005;129:97–100. <http://dx.doi.org/10.1016/j.jviromet.2005.05.020>
24. Darling AE, Mau B, Perna NT. progressiveMauve: multiple genome alignment with gene gain, loss and rearrangement. *PLoS One*. 2010;5:e11147. <http://dx.doi.org/10.1371/journal.pone.0011147>
25. Tagliapietra V, Rosà R, Hauffe HC, Laakkonen J, Voutilainen L, Vapalahti O, et al. Spatial and temporal dynamics of lymphocytic choriomeningitis virus in wild rodents, northern Italy. *Emerg Infect Dis*. 2009;15:1019–25. <http://dx.doi.org/10.3201/eid1507.01524>
26. Meyer H, Ropp SL, Esposito JJ. Gene for A-type inclusion body protein is useful for a polymerase chain reaction assay to differentiate orthopoxviruses. *J Virol Methods*. 1997;64:217–21. [http://dx.doi.org/10.1016/S0166-0934\(96\)02155-6](http://dx.doi.org/10.1016/S0166-0934(96)02155-6)
27. Ryabinin VA, Shundrin LA, Kostina EB, Laassri M, Chizhikov V, Shchelkunov SN, et al. Microarray assay for detection and discrimination of orthopoxvirus species. *J Med Virol*. 2006;78:1325–40. <http://dx.doi.org/10.1002/jmv.20698>
28. Emerson GL, Li Y, Frace MA, Olsen-Rasmussen MA, Khristova ML, Govil D, et al. The phylogenetics and ecology of the orthopoxviruses endemic to North America. *PLoS One*. 2009;4:e7666. <http://dx.doi.org/10.1371/journal.pone.0007666>
29. Lakis NS, Li Y, Abraham JL, Upton C, Blair DC, Smith S, et al. Novel poxvirus infection in an immune suppressed patient. *Clin Infect Dis*. 2015;61:1543–8. <http://dx.doi.org/10.1093/cid/civ643>
30. Edgar RC. MUSCLE: multiple sequence alignment with high accuracy and high throughput. *Nucleic Acids Res*. 2004;32:1792–7. <http://dx.doi.org/10.1093/nar/gkh340>
31. Huelsenbeck JP, Ronquist F. MRBAYES: Bayesian inference of phylogenetic trees. *Bioinformatics*. 2001;17:754–5. <http://dx.doi.org/10.1093/bioinformatics/17.8.754>
32. Stamatakis A. RAXML version 8: a tool for phylogenetic analysis and post-analysis of large phylogenies. *Bioinformatics*. 2014;30:1312–3. <http://dx.doi.org/10.1093/bioinformatics/btu033>
33. Product leaflet for IMVANEX. Annex I. Summary of product characteristics. Kvistgaard, Denmark: Bavarian Nordic A/S; 2013 [cited Sep 2016]. http://www.ema.europa.eu/docs/en_GB/document_library/EPAR_-_Product_Information/human/002596/WC500147896.pdf
34. Silva-Fernandes AT, Travassos CE, Ferreira JM, Abrahão JS, Rocha ES, Viana-Ferreira F, et al. Natural human infections with vaccinia virus during bovine vaccinia outbreaks. *J Clin Virol*. 2009;44:308–13. <http://dx.doi.org/10.1016/j.jcv.2009.01.007>

Address for correspondence: Giusy Cardeti, Biotechnology Department, Istituto Zooprofilattico Sperimentale del Lazio e della Toscana M. Aleandri, Via Appia Nuova 1411, 00178 Rome, Italy; email: giusy.cardeti@izslt.it

Spread of Canine Influenza A(H3N2) Virus, United States

Ian E.H. Voorhees, Amy L. Glaser, Kathy Toohey-Kurth, Sandra Newbury, Benjamin D. Dalziel, Edward J. Dubovi, Keith Poulsen, Christian Leutenegger, Katriina J.E. Willgert, Laura Brisbane-Cohen, Jill Richardson-Lopez, Edward C. Holmes, Colin R. Parrish

A canine influenza A(H3N2) virus emerged in the United States in February–March 2015, causing respiratory disease in dogs. The virus had previously been circulating among dogs in Asia, where it originated through the transfer of an avian-origin influenza virus around 2005 and continues to circulate. Sequence analysis suggests the US outbreak was initiated by a single introduction, in Chicago, of an H3N2 canine influenza virus circulating among dogs in South Korea in 2015. Despite local control measures, the virus has continued circulating among dogs in and around Chicago and has spread to several other areas of the country, particularly Georgia and North Carolina, although these secondary outbreaks appear to have ended within a few months. Some genetic variation has accumulated among the US viruses, with the appearance of regional-temporal lineages. The potential for interspecies transmission and zoonotic events involving this newly emerged influenza A virus is currently unknown.

Influenza A viruses (IAVs) periodically spill over to cause single infections or outbreaks in new host animals. In many cases, these events begin with the transfer of a virus from an avian reservoir host to mammals or domestic poultry, whereas other events result from the transfer of a virus infecting mammals into a new mammalian host. Here we describe the epidemic of an avian-origin canine influenza A(H3N2) virus (H3N2 CIV) in the United States that began by late February 2015 with an outbreak of respiratory disease in dogs in Chicago, Illinois, and nearby areas. Since this time, the virus has circulated

Author affiliations: Cornell University, Ithaca, New York, USA (I.E.H. Voorhees, A.L. Glaser, E.J. Dubovi, K.J.E. Willgert, L. Brisbane-Cohen, C.R. Parrish); University of Wisconsin, Madison, Wisconsin, USA (K. Toohey-Kurth, S. Newbury, K. Poulsen); Oregon State University, Corvallis, Oregon, USA (B.D. Dalziel); IDEXX Laboratories, West Sacramento, California, USA (C. Leutenegger); Royal Veterinary College, London, UK (K.J.E. Willgert); Merck Animal Health, Madison, New Jersey, USA (J. Richardson-Lopez); University of Sydney, Sydney, New South Wales, Australia (E.C. Holmes)

DOI: <https://doi.org/10.3201/eid2312.170246>

continuously among dogs in these areas and has caused sporadic outbreaks nationwide.

H3N2 CIV belongs to the family *Orthomyxoviridae*, genus *Influenza virus A*. Currently, 18 hemagglutinin (HA) and 11 neuraminidase (NA) subtypes are known to exist. In addition to their reservoir hosts among waterfowl and seabirds, IAVs have infected several other animals in nature to cause epidemics of disease, including repeated outbreaks among humans, swine, horses, terrestrial and domesticated birds, marine mammals, and, more recently, cats and dogs (1,2). Dogs were not thought to sustain natural IAV infections before the recognition of H3N8 CIV in 2004.

The H3N8 CIV subtype was first detected in 2004 among racing greyhounds in Florida (3) and was later shown by serologic testing to have emerged in dogs around 1999 (4) through the transfer of an H3N8 equine influenza virus from the Florida clade 1 sublineage of equine influenza virus (5). Despite maintaining a relatively low basic reproductive number (R_0) of ≈ 1.0 in the general dog population, H3N8 CIV caused outbreaks in many regions of the United States soon after it emerged (6). Interconnected networks of dense susceptible host populations found in dog shelters and kennels probably enabled the long-term maintenance of the virus (6,7). In recent years, however, this virus has been confined to a small area in the northeastern United States (6). The reasons for the recent limited circulation of the H3N8 CIV have not been defined, but probably include the apparent inability of the virus to evolve increased transmissibility in the general dog population, increased use of vaccinations in dogs in shelters and kennels, and intensification of control measures in shelters where infections are occurring.

The precise time and place of origin of the H3N2 CIV is still not clear. The virus was first reported in South Korea in 2007, although a virus circulating among dogs in China in 2006 was subsequently reported and sequenced (8). Although that virus (A/canine/Guangdong/1/2006 [H3N2]) remains the earliest known H3N2 CIV, serologic evidence shows that H3N2 CIVs were present in South Korea by 2005 (9). This timeline agrees with that determined by analysis of sequenced H3N2 CIV isolates from Asia, which points to a single common ancestral virus present

in dogs during 1999–2006 (95% highest posterior density) (10). Although the timing of the initial H3N2 CIV emergence in dogs is well-supported by serologic surveys and sequence data, the events surrounding the initial emergence are largely unknown. In Asia, the virus appears to be most widespread among dogs in kennels and in meat dog farms and markets (11,12). Given that live poultry markets in Asia have been identified as a major source of IAVs that spill over to infect new hosts (13), close physical contact between birds and dogs in these host-dense environments might have facilitated the emergence of the virus in dogs.

H3N2 CIV Disease, Host Range, and Zoonotic Potential

Similar to H3N8 CIV infections, H3N2 CIV infections in dogs are associated with mild upper respiratory tract disease, including frequent coughing and fever, although infection of the lungs and more severe disease and death occur on occasion and are probably associated with mixed infections by other viruses or bacteria (14). Although CIV epidemics pose a clear threat to canine health, the risks to other animals and humans are largely unknown. Unlike H3N8 CIV, H3N2 CIV appears to have a relatively broad host range, infecting ferrets, guinea pigs, and cats after experimental challenge (15,16). Nevertheless, experimental inoculation of strains of H3N2 CIV from South Korea and the United States (17) into swine resulted in poor replication, suggesting that sustained transmission of the virus after a canine–swine transfer is unlikely, despite swine being a common host of other H3N2 IAVs. Natural spill-over of the virus from dogs to cats has been documented in South Korea and the United States, but those outbreaks were largely confined to the shelter populations where they emerged, and the viruses do not appear to undergo prolonged transmission in household cats, despite high levels of viral shedding (18,19).

To our knowledge, no transfers of either CIV subtype to humans have been documented. However, human pandemic IAVs, including the H1N1 (both seasonal and the 2009 pandemic) (20) and the H3N2 (21) subtypes, appear able to occasionally infect dogs based on results of serologic testing or isolation of the virus. Although none of these infections is known to have resulted in major onward transmission among dogs, this might provide the opportunity for human IAVs to reassort with CIVs through natural co-infections in dogs. In 2010, a novel H3N1 CIV resulting from the reassortment of an H3N2 CIV (HA segment) and pandemic H1N1/09 virus (the other 7 genomic segments) was isolated in a dog from South Korea (22), and in 2012 an H3N2 carrying only the pandemic H1N1/09 matrix segment was isolated from a dog in South Korea (23,24). In 2015, a novel reassortant H3N2 CIV containing the polymerase acidic (PA) genomic segment from an

H9N2 pandemic avian IAV was also isolated from a dog in South Korea (25). Additionally, dogs and humans express a similar diversity of sialic acid variants and linkages, which have been demonstrated to be important determinants of IAV infection and host range (26), including N-acetylneuraminic acid and both the α 2–3 and α 2–6 linkages (27,28). Given these key biologic and physiologic features and the close contact that exists between human and dog populations, the potential for dogs to act as virus “mixing vessels” or as sources of zoonotic infections by IAVs should not be overlooked.

The US H3N2 CIV Outbreak

The H3N2 CIV outbreak likely started in February 2015 and spread rapidly through dog training classes, animal shelters, boarding kennels, and veterinary clinics in the Chicago area by early March, at which time initial reports of an unusual respiratory disease in dogs were received (K. Toohey-Kurth and S. Newbury, pers. comm.). We identified clinical samples from infected dogs as IAV-positive in mid-March 2015 by using a type A influenza-specific PCR for the conserved viral matrix segment sequences (29) and an amplification protocol approved for use by the National Animal Health Laboratories (Ames, IA, USA). We identified the virus as the H3N2 subtype on April 10, 2015, by using Sanger sequencing of partial HA and matrix genomic segments (performed at Cornell University, Ithaca, NY, USA) and partial NA genomic segments (performed at University of Wisconsin, Madison, WI, USA) that had been amplified as previously described (29). Sequences searched in the nucleotide database using blastn (<http://blast.ncbi.nlm.nih.gov/Blast.cgi>) (30) had the highest identity to H3N2 viruses from South Korea. The identification of the virus as the H3N2 subtype and its relation to H3N2 CIV in Asia was announced on April 12 (31), and a probable origin in South Korea of the US H3N2 CIV outbreak was confirmed by whole-genome sequencing performed at the National Veterinary Service Laboratories (Ames, IA, USA) on strain A/canine/Illinois/12191/2015, in which all 8 genome segments (GenBank accession nos. KT002533–40) showed highest similarity to H3N2 CIV in South Korea.

During the last weeks of March and into April 2015, H3N2 CIV was detected in many animal shelters in Chicago and in the neighboring areas of Illinois, Indiana, and Wisconsin but was absent from other regions of the United States (Figure 1). The virus spread through affected regions with a wavelike introduction and with case numbers growing rapidly over periods of 2–4 days after introduction into new dog populations (Figures 1, 2). The infection presented as a mild to moderate respiratory disease, often with a characteristic honking cough, with some progression to pneumonia but, generally, with few or no deaths. Some

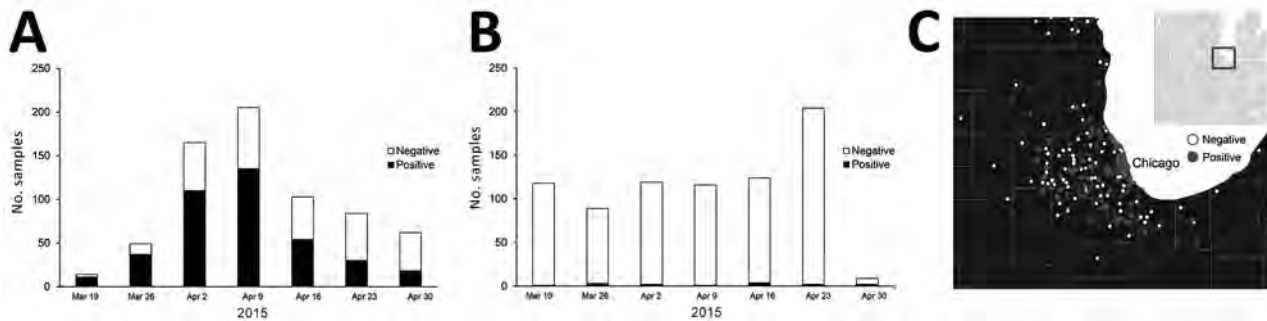


Figure 1. Incidence of canine influenza A(H3N2) virus RNA–positive dogs in the Chicago, Illinois, area, USA, March 14–April 27, 2015. A) Weekly testing summary of samples collected within Illinois. B) Weekly testing summary of samples collected in all other states. C) Presence of virus in the Midwest region, by US postal code.

dogs, particularly those in animal shelters, were coinfecting with other respiratory pathogens, including canine pneumovirus, canine parainfluenza virus, and canine respiratory coronavirus (32). Analyzing the viral loads in shelter dogs during the outbreak showed that the virus peaked in the swabs 2–3 days after the probable time of infection and that in some cases low levels of RNA along with low levels of infectious virus could be detected 2–3 weeks later (33) (Table 1), suggesting that prolonged isolation of infected dogs would be necessary to completely prevent transmission. The highest RNA levels detected by real-time reverse transcription PCR were found in nasal swab specimens collected 2–4 days after infection, with lower levels found in other tissues (Table 2) (32).

Within a few months after its introduction into the Chicago-area dog population, the disease ended in some shelters or kennels, probably because all the resident dogs had become immune. This hypothesis is supported by intensive sampling of the dogs in some shelters, which showed that once the virus entered a closed population of susceptible dogs, most or all dogs would be infected within a few days

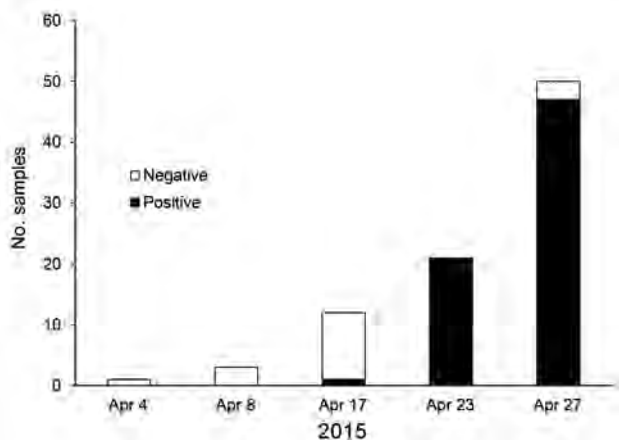


Figure 2. Spread of canine influenza A(H3N2) virus in an animal shelter in the Chicago, Illinois, area, USA, April 2015. The first virus-positive result was obtained on April 17; by April 23, the virus had infected all dogs tested.

(Figure 2), thereafter producing a high level of immunologic resistance in that population.

By May 2015, H3N2 CIV infections were being detected outside of the midwestern United States, and within a year of its introduction, the virus caused substantial outbreaks of disease in several eastern and southeastern states (Table 3, Figure 3). Smaller outbreaks also occurred in Colorado, California, and Washington State, indicating that national spread of the virus occurred. However, none of these secondary outbreaks was sustained or widespread.

Viral RNA Extraction, Full-Genome Sequencing, and Sequence Analysis

We extracted viral RNA by using the QIAamp Viral RNA Kit (QIAGEN, Valencia, CA, USA) from original clinical sample material obtained from IDEXX Laboratories (West Sacramento, CA, USA) or from the New York State Animal Health and Diagnostic Laboratory at Cornell University (Ithaca, NY, USA), and we adapted to CIV an IAV multisegment real-time reverse transcription PCR amplification approach (34). We used amplified genomes to prepare sequencing libraries, which we sequenced on the Illumina MiSeq platform (Illumina, San Diego, CA, USA) with 150 nt paired-end reads, and assembled reads de novo as described in Mena et al. (34). We generated 12 CIV full-genome sequences for this study, all of which were submitted to GenBank and assigned accession numbers (online Technical Appendix, <https://wwwnc.cdc.gov/EID/article/23/12/17-0246-Techapp1.pdf>). We obtained additional H3N2 CIV genomes from the National Center for Biotechnology Information Influenza Virus Resource (<http://www.ncbi.nlm.nih.gov/genomes/FLU/Database/nph-select.cgi?go = database>).

We performed consensus sequence editing, alignment, and phylogenetic analyses by using Geneious 9.0.5 and various modules contained in that package (35). We trimmed each gene segment to contain only its major open reading frame and aligned the segments by using MAFFT

Table 1. Persistence of virus or viral RNA in dogs in 2 separate Chicago-area animal shelters that were infected with canine influenza A(H3N2) virus, United States, April 2015*

Shelter and no. days	C _t value, by dog no.									
	1	2	3	4	5	6	7	8	9	10
Shelter 1										
1	20.8†	34.7	Neg	29.1	Neg	16.7†	19.0†	34.5	25.2†	25.1†
13	39.3	38.1	31.3	35.1	33.9	31.4	31.9	Neg	29.6	37.3
14	Neg	Neg	32.1	Neg	32	35.3	35.4	38.1	32.3	Neg
15	Neg	Neg	36.2	37.1†	Neg	39.1	Neg	Neg	38.5	Neg
17	Neg	Neg	37.2	Neg	Neg	31.1	Neg	Neg	Neg	Neg
19	Neg	NT	Neg	Neg	Neg	Neg	Neg	Neg	Neg	Neg
20	Neg	NT	Neg	NT	Neg	Neg	Neg	38.2	37.9	37.8†
22	Neg	NT	Neg	NT	Neg	Neg	36.5	39.2	Neg	Neg
24	Neg	NT	Neg	NT	Neg	39.3	Neg	Neg	Neg	37.3
29	Neg	NT	Neg	NT	Neg	Neg	Neg	Neg	Neg	Neg
31	Neg	NT	Neg	NT	Neg	Neg	Neg	Neg	Neg	Neg
	1	2	3	4	5	6	7	8	9	10
Shelter 2										
1	Neg	37.4	25.1	37.9	26	29.5†				
5	NT	NT	22.7	24.6†	NT	NT				
6	24.6†	23.7†	NT	NT	NT	NT				
10	36.2	39.5	NT	NT	NT	NT				
11	NT	NT	NT	NT	37.1	NT				
15	NT	NT	38.6†	35.9	38.2†	36				
19	NT	NT	Neg	NT	NT	NT				
20	37.3	37.2	NT	NT	NT	NT				
23	NT	NT	Neg	NT	NT	NT			Neg	
24	Neg	Neg	NT	NT	NT	NT			NT	
28	Neg	Neg	NT	NT	NT	NT			NT	

*Data from Newbury et al. (33) Table 1, used with permission. Data shown as rRT-PCR C_t values. Values ≤36 are considered positive results (black cells), and values ≥37 but <40 are considered weak positive results (dark gray cells). Light gray cells indicate negative rRT-PCR assay results for influenza A virus shedding. C_t, cycle threshold; Neg, negative; NT, not tested; rRT-PCR, real-time reverse transcription PCR.

†Samples for which virus was successfully isolated.

7.222 (36). We then analyzed the segments separately or concatenated with all other genome segment sequences from the same virus. In 39 of the genomes analyzed, we excluded individual segment phylogenies (Figure 4, panel A) and segments from incomplete genomes and intersubtype reassortant viruses. For concatenated full-genome phylogenies (Figure 4, panel B), we excluded intersubtype and intrasubtype reassortant viruses, for a total of 32 genomes analyzed. Total sequence alignment lengths were as follows: polymerase basic 2, 2,277 nt; polymerase basic 1, 2,268–2,271 nt; PA, 2,148 nt; HA, 1,698 nt; nucleocapsid protein, 1,494 nt; NA, 1,407–1,413 nt; matrix 1, 756 nt; and nonstructural 1, 690 nt. Concatenation of the 8 segments yielded a total consensus alignment length of 12,741–12,747 nt. We determined phylogenetic relationships among the sequences by using the maximum-likelihood method available in PhyML (37), employing a general time-reversible substitution model, gamma-distributed rate variation among sites, and bootstrap resampling (1,000×). We rooted all trees with the earliest and most basal H3N2 CIV isolate available (A/canine/Guangdong/1/2006 [H3N2]).

Evolutionary Analysis

As observed previously (10), our phylogenetic analysis suggests that H3N2 CIV originated in dogs by the direct

transfer of an avian virus in late 2005 or early 2006, with the first virus isolated being in southern China; this virus spread rapidly between different regions of China, to or from South Korea, and to Thailand (no complete full genomes from Thailand are available in the database). Although a single ancestral virus is thought to have given rise to all H3N2 CIVs (10), a directly comparable avian virus sequence is not available in the database. However, individual genome segment phylogenies of H3N2 CIV point toward multiple ancestors of the original IAV

Table 2. Results of the rRT-PCR analysis of a necropsied dog in a Chicago-area animal shelter that died after being infected with canine influenza A(H3N2) virus, United States, February 2015*

Type of specimen	C _t value
Nasal swab	20.0
Oral swab	34.3
Tracheal swab	36.4
Bronchial swab	28.1
Cranial lung	31.8
Tracheobronchial lymph node	39.6
Liver	Neg
Pancreas	Neg
Ileum	Neg
Kidney	Neg

*Data from Watson et al. (32), used with permission. Data shown as rRT-PCR C_t values. Values ≤36 are considered positive results (black cells), and values ≥37 but <40 are considered weak positive results (dark gray cells). Light gray cells indicate negative rRT-PCR assay results for influenza A virus shedding. C_t, cycle threshold; Neg, negative; rRT-PCR, real-time reverse transcription PCR.

that gave rise to the canine virus, with lineage sequences from the Americas being observed in the PA segment and lineages from Eurasia being observed in all other segments. Once established in dogs, a handful of hetero- and homo-subtypic reassortment events occurred among the H3N2 CIVs in Asia (10). In contrast, our analysis shows that all US H3N2 CIV genome segments exhibit

approximately the same tree topology (Figure 4, panel A), suggesting that no large-scale viral reassortment has occurred since its introduction, a conclusion also supported by analysis using the Recombination Detection Program (38) (data not shown). Phylogenetic analysis of the concatenated full-genome sequences of viruses from the US epidemic show that a single virus from South Korea was introduced into the Chicago area and that the descendants of that virus continue to circulate in that area and have been dispersed widely across the United States (Figures 1 and 2). The PA, HA, and NA segment phylogenies did not distinguish US viruses from those most recently isolated from South Korea (Figure 4, panel A), confirming the close relationship to the viruses from South Korea and also suggesting that the viral transfer occurred shortly before the virus was recognized in the United States. Despite the short timescale of H3N2 CIV evolution in the United States, some geographic structuring might be present in the data, as indicated by distinct and statistically supported clades (bootstrap proportion >98). For example, a 2015 clade consisting of viruses from Florida, North Carolina, and Georgia probably represents a single introduction of virus to the southeastern United States and a subsequent regional outbreak (Figure 4, panel B).

The US H3N2 CIV and closely related viruses in South Korea show some changes in the sequence adjacent to the receptor binding and antigenic sites of the HA segment. Most notably, a single Gly146Ser amino acid substitution in the HA globular head antigenic site is present in all the US H3N2 CIVs and the most recent CIV in Korea. Because the United States contains a large and naive new host population, with low levels of H3N8 and H3N2 CIV infection or vaccination in most places, it is probably not under selection from antibody immunity during this initial disease emergence, except perhaps among kennel and shelter dogs in the Chicago area.

The exact route of introduction of H3N2 CIV into the United States is unknown. However, whereas an infected dog might shed virus for up to 3 weeks, virus probably remains infectious on fomites for only 12–48 hours. Thus, similar to other IAVs, close host–host contact or direct aerosol exchange is probably the most effective and common route of H3N2 CIV transmission. This hypothesis would suggest that the virus was brought to the United States by infected dogs. Such dogs might have arrived in the United States after being rescued from live animal markets or meat dog farms in South Korea, where the reported overall seroprevalence of H3N2 CIV is ≈19%, with individual dog farms having seroprevalences of up to 100% (11). Hundreds of dogs rescued from meat markets in South Korea have been rehomed in the United States since the beginning of 2015 (39),

Table 3. Results of rRT-PCR tests for canine influenza A(H3N2) virus RNA in specimens collected from dogs, by state, United States, February 2015–March 2016*

State/district	Test result	
	Positive	Negative
Alabama	16	355
Alaska	0	22
Arizona	0	223
Arkansas	0	21
California	11	1,601
Colorado	4	137
Connecticut	0	136
Delaware	0	17
District of Columbia	0	5
Florida	1	432
Georgia	559	1,143
Hawaii	0	27
Idaho	1	80
Illinois	820	1,055
Indiana	14	108
Iowa	1	75
Kansas	0	60
Kentucky	5	51
Louisiana	0	132
Maine	1	132
Maryland	3	133
Massachusetts	2	191
Michigan	6	333
Minnesota	5	302
Mississippi	0	39
Missouri	1	115
Montana	2	20
Nebraska	0	27
Nevada	0	39
New Hampshire	0	49
New Jersey	28	175
New Mexico	0	26
New York	3	667
North Carolina	33	475
North Dakota	0	6
Ohio	87	425
Oklahoma	0	18
Oregon	0	84
Pennsylvania	28	1,050
Rhode Island	0	37
South Carolina	2	137
South Dakota	7	14
Tennessee	1	115
Texas	13	833
Utah	0	121
Vermont	0	45
Virginia	0	232
Washington	2	181
West Virginia	1	16
Wisconsin	15	498
Wyoming	0	13
International or unknown	21	609
Total	1,693	12,837

*rRT-PCR, real-time reverse transcription PCR.

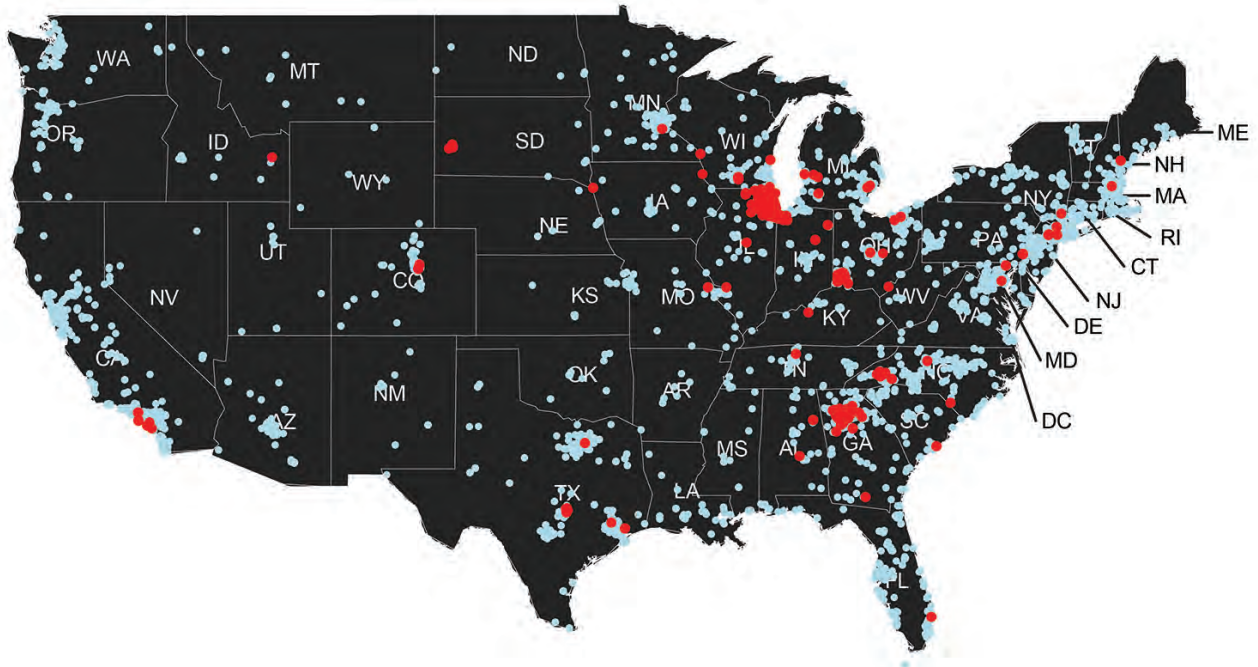


Figure 3. Distribution of clinical samples testing positive (red dots) and negative (blue dots) for canine influenza A(H3N2) virus RNA, United States, March–December 2015.

although no direct link between any of these dogs and the appearance of H3N2 CIV in the United States has been established.

Likewise, the spread of H3N2 CIV within the United States presumably resulted from movement of infected dogs, rather than from transported fomites, probably through the networks involved in rescuing and rehoming dogs, which would connect the host populations in US dog kennels and shelters. These epidemiologic characteristics resemble those of H3N8 CIV and suggest that control, prevention, and even eradication of the virus in dogs is feasible by controlling the transfer of dogs from infected areas. In addition, with effective inactivated vaccines currently available (40) and the possibility of a live-attenuated vaccine (41), targeted vaccination of dog populations at high risk will aid in the control of the US H3N2 CIV epidemic. Further monitoring, epidemiologic analysis, and evolutionary studies of H3N2 CIV in the United States will help determine whether these viruses pose a threat to human health and will answer basic questions regarding how IAVs invade and infect new hosts.

Acknowledgments

We thank Wendy Weichert for providing expert technical support and Jayeeta Duttah and Divya Kriti for performing deep-sequencing and sequence read assembly.

This study was supported by National Institutes of Health grant no. R01 GM080533 to C.R.P. and E.C.H.; the National Science

Foundation (grant no. DGE-1650441 to I.E.H.V.); and the Center of Research in Influenza Pathogenesis, a National Institute of Allergies and Infectious Diseases–funded Center of Excellence in Influenza Research and Surveillance (contract no. HHSN272201400008C to C.R.P.). E.C.H. is supported by a National Health and Medical Research Council Australia Fellowship (grant no. GNT1037231).

Mr. Voorhees is a National Science Foundation Graduate Research Fellowship Program Fellow and graduate student in the Department of Microbiology and Immunology at Cornell University. His primary research interest is the evolution of emerging viruses.

References

1. Yoon S-W, Webby RJ, Webster RG. Evolution and ecology of influenza A viruses. In: Compans RW, Oldstone MBA, editors. *Influenza pathogenesis and control*, volume I [cited 2017 Jan 25]. http://link.springer.com/chapter/10.1007/82_2014_396
2. Parrish CR, Murcia PR, Holmes EC. Influenza virus reservoirs and intermediate hosts: dogs, horses, and new possibilities for influenza virus exposure of humans. *J Virol*. 2015;89:2990–4. <http://dx.doi.org/10.1128/JVI.03146-14>
3. Crawford PC, Dubovi EJ, Castleman WL, Stephenson I, Gibbs EPJ, Chen L, et al. Transmission of equine influenza virus to dogs. *Science*. 2005;310:482–5. <http://dx.doi.org/10.1126/science.1117950>
4. Anderson TC, Bromfield CR, Crawford PC, Dodds WJ, Gibbs EPJ, Hernandez JA. Serological evidence of H3N8 canine influenza-like virus circulation in USA dogs prior to 2004. *Vet J*. 2012;191:312–6. <http://dx.doi.org/10.1016/j.tvjl.2011.11.010>
5. Rivailler P, Perry IA, Jang Y, Davis CT, Chen L-M, Dubovi EJ, et al. Evolution of canine and equine influenza (H3N8) viruses

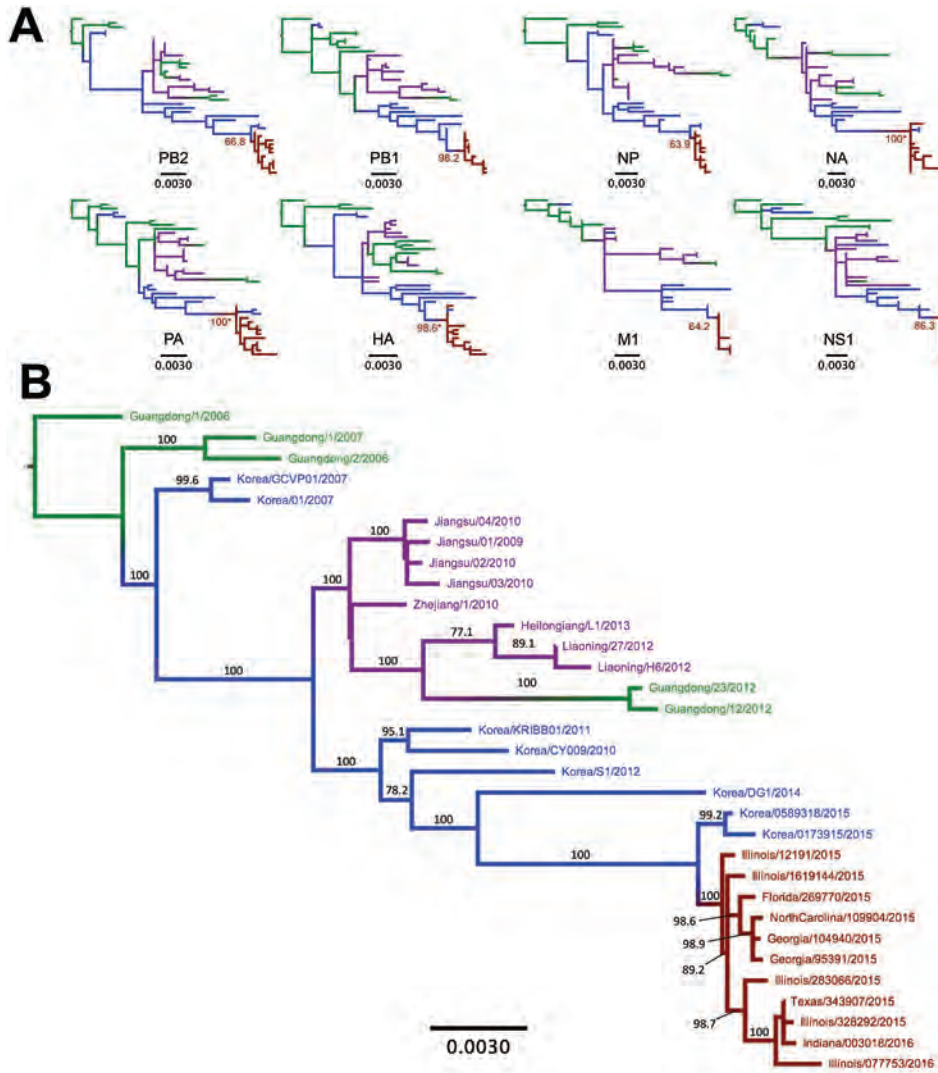


Figure 4. Phylogenetic trees of canine influenza A(H3N2) virus (H3N2 CIV) sequences showing the initial emergence of the virus in southern China (green branches), its appearance in northern and eastern China (magenta branches) and South Korea (blue branches), and its introduction into the United States (red branches). A) Individual genome segment sequences. Red branch numbers indicate bootstrap proportion of US H3N2 CIV clade. Asterisks indicate polyphyletic clades containing US strains and most recent strains from South Korea. B) Concatenated segment phylogenies of all available complete nonreassortant H3N2 CIV genomes. Branch number indicates bootstrap proportions >75. All branch lengths are proportional to the number of nucleotide substitutions per site. All trees rooted by using sequences from the earliest isolated H3N2 CIV. Scale bars indicate nucleotide substitutions per site. HA, hemagglutinin; M1, matrix 1; NA, neuraminidase; NP, nucleocapsid protein; NS1, nonstructural 1; PA, polymerase acidic; PB1, polymerase basic 1; PB2, polymerase basic 2.

co-circulating between 2005 and 2008. *Virology*. 2010;408:71–9. <http://dx.doi.org/10.1016/j.virol.2010.08.022>

6. Dalziel BD, Huang K, Geoghegan JL, Arinaminpathy N, Dubovi EJ, Grenfell BT, et al. Contact heterogeneity, rather than transmission efficiency, limits the emergence and spread of canine influenza virus. *PLoS Pathog*. 2014;10:e1004455. <http://dx.doi.org/10.1371/journal.ppat.1004455>
7. Pecoraro HL, Bennett S, Huyvaert KP, Spindel ME, Landolt GA. Epidemiology and ecology of H3N8 canine influenza viruses in US shelter dogs. *J Vet Intern Med*. 2014;28:311–8. <http://dx.doi.org/10.1111/jvim.12301>
8. Li S, Shi Z, Jiao P, Zhang G, Zhong Z, Tian W, et al. Avian-origin H3N2 canine influenza A viruses in Southern China. *Infect Genet Evol*. 2010;10:1286–8. <http://dx.doi.org/10.1016/j.meegid.2010.08.010>
9. Lee Y-N, Lee D-H, Lee H-J, Park J-K, Yuk S-S, Sung H-J, et al. Evidence of H3N2 canine influenza virus infection before 2007. *Vet Rec*. 2012;171:477. <http://dx.doi.org/10.1136/vr.100718>
10. Zhu H, Hughes J, Murcia PR. Origins and evolutionary dynamics of H3N2 canine influenza virus. *J Virol*. 2015;89:5406–18. <http://dx.doi.org/10.1128/JVI.03395-14>
11. Lee C, Song D, Kang B, Kang D, Yoo J, Jung K, et al. A serological survey of avian origin canine H3N2 influenza virus in dogs in Korea. *Vet Microbiol*. 2009;137:359–62. <http://dx.doi.org/10.1016/j.vetmic.2009.01.019>
12. Su S, Li H-T, Zhao F-R, Chen J-D, Xie JX, Chen Z-M, et al. Avian-origin H3N2 canine influenza virus circulating in farmed dogs in Guangdong, China. *Infect Genet Evol*. 2013;14:444–9. <http://dx.doi.org/10.1016/j.meegid.2012.11.018>
13. Wan X-F, Dong L, Lan Y, Long L-P, Xu C, Zou S, et al. Indications that live poultry markets are a major source of human H5N1 influenza virus infection in China. *J Virol*. 2011;85:13432–8. <http://dx.doi.org/10.1128/JVI.05266-11>
14. Dubovi EJ, Njaa BL. Canine influenza. *Vet Clin North Am Small Anim Pract*. 2008;38:827–35, viii. <http://dx.doi.org/10.1016/j.cvsm.2008.03.004>
15. Lee Y-N, Lee D-H, Park J-K, Yuk S-S, Kwon J-H, Nahm S-S, et al. Experimental infection and natural contact exposure of ferrets with canine influenza virus (H3N2). *J Gen Virol*. 2013;94:293–7. <http://dx.doi.org/10.1099/vir.0.042473-0>
16. Lyoo K-S, Kim J-K, Kang B, Moon H, Kim J, Song M, et al. Comparative analysis of virulence of a novel, avian-origin H3N2 canine influenza virus in various host species. *Virus Res*. 2015;195:135–40. <http://dx.doi.org/10.1016/j.virusres.2014.08.020>
17. Abente EJ, Anderson TK, Rajao DS, Swenson S, Gauger PC, Vincent AL. The avian-origin H3N2 canine influenza virus that

- recently emerged in the United States has limited replication in swine. *Influenza Other Respi Viruses*. 2016;10:429–32. <http://dx.doi.org/10.1111/irv.12395>
18. Jeoung H-Y, Lim S-I, Shin B-H, Lim J-A, Song J-Y, Song D-S, et al. A novel canine influenza H3N2 virus isolated from cats in an animal shelter. *Vet Microbiol*. 2013;165:281–6. <http://dx.doi.org/10.1016/j.vetmic.2013.03.021>
 19. Song DS, An DJ, Moon HJ, Yeom MJ, Jeong HY, Jeong WS, et al. Interspecies transmission of the canine influenza H3N2 virus to domestic cats in South Korea, 2010. *J Gen Virol*. 2011;92:2350–5. <http://dx.doi.org/10.1099/vir.0.033522-0>
 20. Lin D, Sun S, Du L, Ma J, Fan L, Pu J, et al. Natural and experimental infection of dogs with pandemic H1N1/2009 influenza virus. *J Gen Virol*. 2012;93:119–23. <http://dx.doi.org/10.1099/vir.0.037358-0>
 21. Chang CP, New AE, Taylor JF, Chiang HS. Influenza virus isolations from dogs during a human epidemic in Taiwan. *Int J Zoonoses*. 1976;3:61–4.
 22. Song D, Moon H-J, An D-J, Jeoung H-Y, Kim H, Yeom M-J, et al. A novel reassortant canine H3N1 influenza virus between pandemic H1N1 and canine H3N2 influenza viruses in Korea. *J Gen Virol*. 2012;93:551–4. <http://dx.doi.org/10.1099/vir.0.037739-0>
 23. Hong M, Na W, Yeom M, Park N, Moon H, Kang B-K, et al. Complete genome sequences of H3N2 canine influenza virus with the matrix gene from the pandemic A/H1N1 virus. *Genome Announc*. 2014;2:e01010-4. <http://dx.doi.org/10.1128/genomeA.01010-14>
 24. Moon H, Hong M, Kim JK, Seon B, Na W, Park SJ, et al. H3N2 canine influenza virus with the matrix gene from the pandemic A/H1N1 virus: infection dynamics in dogs and ferrets. *Epidemiol Infect*. 2015;143:772–80. <http://dx.doi.org/10.1017/S0950268814001617>
 25. Lee IH, Le TB, Kim HS, Seo SH. Isolation of a novel H3N2 influenza virus containing a gene of H9N2 avian influenza in a dog in South Korea in 2015. *Virus Genes*. 2016;52:142–5. <http://dx.doi.org/10.1007/s11262-015-1272-z>
 26. Suzuki Y, Ito T, Suzuki T, Holland RE Jr, Chambers TM, Kiso M, et al. Sialic acid species as a determinant of the host range of influenza A viruses. *J Virol*. 2000;74:11825–31. <http://dx.doi.org/10.1128/JVI.74.24.11825-11831.2000>
 27. Ning Z-Y, Wu X-T, Cheng Y-F, Qi W-B, An Y-F, Wang H, et al. Tissue distribution of sialic acid-linked influenza virus receptors in beagle dogs. *J Vet Sci*. 2012;13:219–22. <http://dx.doi.org/10.4142/jvs.2012.13.3.219>
 28. Löffling J, Lyi SM, Parrish CR, Varki A. Canine and feline parvoviruses preferentially recognize the non-human cell surface sialic acid N-glycolylneuraminic acid. *Virology*. 2013;440:89–96. <http://dx.doi.org/10.1016/j.virol.2013.02.009>
 29. Senne DA, Panigrahy B, Kawaoka Y, Pearson JE, Süß J, Lipkind M, et al. Survey of the hemagglutinin (HA) cleavage site sequence of H5 and H7 avian influenza viruses: amino acid sequence at the HA cleavage site as a marker of pathogenicity potential. *Avian Dis*. 1996;40:425–37. <http://dx.doi.org/10.2307/1592241>
 30. NCBI Resource Coordinators. Database resources of the National Center for Biotechnology Information. *Nucleic Acids Res*. 2016;44(D1):D7–19. <http://dx.doi.org/10.1093/nar/gkv1290>
 31. Schwartz J. Midwest canine influenza outbreak caused by new strain of virus [cited 2016 Jul 27]. <http://mediarelations.cornell.edu/2015/04/12/midwest-canine-influenza-outbreak-caused-by-new-strain-of-virus>
 32. Watson CE, Bell C, Toohey-Kurth K. H3N2 canine influenza virus infection in a dog. *Vet Pathol*. 2017;54:527–30. <http://dx.doi.org/10.1177/0300985816681411>
 33. Newbury S, Godhardt-Cooper J, Poulsen KP, Cigel F, Balanoff L, Toohey-Kurth K. Prolonged intermittent virus shedding during an outbreak of canine influenza A H3N2 virus infection in dogs in three Chicago area shelters: 16 cases (March to May 2015). *J Am Vet Med Assoc*. 2016;248:1022–6. <http://dx.doi.org/10.2460/javma.248.9.1022>
 34. Mena I, Nelson MI, Quezada-Monroy F, Dutta J, Cortes-Fernández R, Lara-Puente JH, et al. Origins of the 2009 H1N1 influenza pandemic in swine in Mexico. *eLife*. 2016;5:e16777. <http://dx.doi.org/10.7554/eLife.16777>
 35. Kearse M, Moir R, Wilson A, Stones-Havas S, Cheung M, Sturrock S, et al. Geneious Basic: an integrated and extendable desktop software platform for the organization and analysis of sequence data. *Bioinformatics*. 2012;28:1647–9. <http://dx.doi.org/10.1093/bioinformatics/bts199>
 36. Katoh K, Misawa K, Kuma K, Miyata T. MAFFT: a novel method for rapid multiple sequence alignment based on fast Fourier transform. *Nucleic Acids Res*. 2002;30:3059–66. <http://dx.doi.org/10.1093/nar/gkf436>
 37. Guindon S, Gascuel O, Rannala B. A simple, fast, and accurate algorithm to estimate large phylogenies by maximum likelihood. *Syst Biol*. 2003;52:696–704. <http://dx.doi.org/10.1080/10635150390235520>
 38. Martin DP, Murrell B, Golden M, Khoosal A, Muhire B. RDP4: detection and analysis of recombination patterns in virus genomes. *Virus Evol*. 2015;1:vev003. PMID: 27774277
 39. A Humane Nation. 200 more dogs saved from the butcher in South Korea [cited 2017 Jan 26]. <http://blog.humanesociety.org/wayne/2017/01/200-dogs-saved-butcher-south-korea.html>
 40. Cureton DK, Scott-Garrard M, Parker DS, House A, Veal E, Aitcheson T, et al. An inactivated H3N2 canine influenza virus (CIV) vaccine aids in the prevention of clinical disease and virus shedding in dogs challenged with virulent H3N2 CIV. *Int J Appl Res Vet Med*. 2016;14:128–34.
 41. Rodriguez L, Nogales A, Reilly EC, Topham DJ, Murcia PR, Parrish CR, et al. A live-attenuated influenza vaccine for H3N2 canine influenza virus. *Virology*. 2017;504:96–106. <http://dx.doi.org/10.1016/j.virol.2017.01.020>

Address for correspondence: Colin R. Parrish, Baker Institute for Animal Health, College of Veterinary Medicine, Cornell University, Ithaca, NY 14853, USA; email: crp3@cornell.edu

Evolutionary Context of Non–Sorbitol-Fermenting Shiga Toxin–Producing *Escherichia coli* O55:H7

Kyle Schutz, Lauren A. Cowley, Sharif Shaaban, Anne Carroll, Eleanor McNamara, David L. Gally, Gauri Godbole, Claire Jenkins, Timothy J. Dallman

In July 2014, an outbreak of Shiga toxin–producing *Escherichia coli* (STEC) O55:H7 in England involved 31 patients, 13 (42%) of whom had hemolytic uremic syndrome. Isolates were sequenced, and the sequences were compared with publicly available sequences of *E. coli* O55:H7 and O157:H7. A core-genome phylogeny of the evolutionary history of the STEC O55:H7 outbreak strain revealed that the most parsimonious model was a progenitor enteropathogenic O55:H7 sorbitol-fermenting strain, lysogenized by a Shiga toxin (Stx) 2a–encoding phage, followed by loss of the ability to ferment sorbitol because of a non-sense mutation in *srlA*. The parallel, convergent evolutionary histories of STEC O157:H7 and STEC O55:H7 may indicate a common driver in the evolutionary process. Because emergence of STEC O157:H7 as a clinically significant pathogen was associated with acquisition of the Stx2a-encoding phage, the emergence of STEC O55:H7 harboring the *stx2a* gene is of public health concern.

The first outbreak of Shiga toxin–producing *Escherichia coli* (STEC) O55:H7 in the United Kingdom occurred in the county of Dorset, England, in July 2014 (1). Ultimately, 31 cases were linked to the outbreak, and 13 (42%) of those patients had hemolytic uremic syndrome (HUS). Of the 13 with HUS, 8 (66%) had neurologic complications and 11 (90%) required prolonged treatment for kidney replacement. After enhanced epidemiologic surveillance and analysis of the patients' food, exposure, and travel histories, the only epidemiologic link identified was living in or having close links to Dorset County. Extensive microbiological investigations included testing of the environment, nondomestic animals, and household pets. Although no causal link was established, whole-genome sequencing and

epidemiologic analyses were indicative of a local endemic zoonotic source (1).

Previous studies postulated that the common STEC O157:H7 clone evolved from enteropathogenic *E. coli* (EPEC) serotype O55:H7 (2,3). Evolutionary models predict the stepwise acquisition of a Shiga toxin (Stx)–encoding bacteriophage in the EPEC O55:H7 progenitor strain, followed by the substitution of the *rfb* locus encoding the somatic O55 antigen with that encoding the O157 antigen, the acquisition of the pO157 plasmid, loss of the ability to ferment sorbitol, and loss of the ability to produce β -glucuronidase (3–6). Analyses from more recent studies have indicated that the Stx-encoding phage is an unstable evolutionary marker, with frequent acquisition and loss occurring in STEC O55:H7 and all 3 lineages of STEC O157 throughout their evolutionary history (7,8).

STEC O157:H7 has multiple genetic and phenotypic features that contribute to its pathogenicity or are used for detection and identification. The primary virulence factor defining the STEC group is production of Stx1, Stx2, or both. The genes encoding the toxins, *stx1* and *stx2*, are harbored on lambdoid prophage and are the targets of commercial and in-house diagnostic PCR assays (9). Both toxins can be divided into several subtypes, Stx1a–1d and Stx2a–2g (10). The locus of enterocyte effacement (LEE) is a 35-kb pathogenicity island encoding a type III secretion system (T3SS) responsible for the attaching and effacing phenotype that facilitates successful colonization of the human gut (11). The inability to ferment sorbitol or to produce β -glucuronidase differentiates STEC O157 from \approx 90% of other gastrointestinal bacteria (5,12). These characteristics, along with resistance to tellurite, facilitate the detection and identification of STEC O157:H7 on selective media. The pO157 plasmid encodes multiple putative virulence factors, including enterohemolysin (*ehxA*) and an adhesin (*toxB*) (13).

The STEC O55:H7 Dorset outbreak strain shared certain characteristics with the STEC O157:H7 clone. Initial PCRs detected the presence of *stx2* and the intimin gene

Author affiliations: Public Health England Colindale, London, UK (K. Schutz, L.A. Cowley, G. Godbole, C. Jenkins, T.J. Dallman); The University of Edinburgh, Midlothian, UK (S. Shaaban, D.L. Gally); Cherry Orchard Hospital, Dublin, Ireland (A. Carroll, E. McNamara)

DOI: <https://doi.org/10.3201/eid2312.170628>

eae, a marker for *E. coli* attaching and effacing phenotype; non-sorbitol-fermenting colonies of STEC O55 were identified after culture on sorbitol MacConkey agar (1,9). However, unlike the STEC O157 clone, the STEC O55 Dorset outbreak strain exhibited β -glucuronidase activity and was sensitive to tellurite. Laboratory records held at the Gastrointestinal Bacterial Reference Unit of Public Health England showed that this highly pathogenic strain had not previously been isolated from humans or animals in the United Kingdom. Our goal with this study was to identify the genetic determinants responsible for the phenotypic characteristics of the STEC O55:H7 Dorset outbreak strain and to explore the strain's evolutionary history.

Materials and Methods

Bacterial Strains

We studied 26 isolates of STEC O55:H7 from the outbreak, 10 isolates of STEC O55:H7 from Ireland, and 79 isolates selected to represent of the broad phylogeny of STEC O157:H7 (online Technical Appendix Table, <https://wwwnc.cdc.gov/EID/article/23/12/17-0628-Techapp1.pdf>). From public databases, we retrieved 10 genome sequences for *E. coli* O55:H7 and 2 for STEC O157:H7 (6,7,14,15) (Table 1).

Whole-Genome Sequencing, Assembly, and Alignment

We sequenced all isolates by using an Illumina paired-end (100-bp) protocol (<https://www.illumina.com>) and assembled them by using SPAdes Genome Assembler version 3.1.1 (18). The assemblies were annotated by using Prokka version 1.0.1 (19). We used the MinION (<https://nanoporetech.com/products/minion>) nanopore platform to sequence an isolate from the outbreak, designated 122262. A hybrid Illumina/MinION de novo assembly of 122262 constructed by using SPAdes yielded 15 contigs with the largest contig spanning the first 2.4 mbp. We aligned published reference genomes against the outbreak reference strain 122262 by using Mauve (20).

Genome, Plasmid, and Bacteriophage Comparisons

We retrieved from GenBank published nucleotide sequences of key virulence genes associated with toxicity, host-cell adhesion, and metabolic activity and concatenated in FASTA (<http://www.ebi.ac.uk/Tools/sss/fasta/>) file format. To determine the presence and absence of the gene panel, we performed a blastn (21) comparison against the extracted coding sequences of 122262. Significant hits were defined as those with a nucleotide identity of $\geq 90\%$ over at least 90% of the query sequence. Truncated sequences were defined as matches with $< 90\%$ coverage. We uploaded assembled data from the strains in FASTA file format to the PHAGE Search Tool (PHAST) web server for prophage identification (22). Prophage region detection, prophage annotation, and circular genomic views from PHAST results were used along blast ring image generator (BRIG) plots (23) to isolate the prophage regions of 122262 and nucleotide homologies to the prophages in the Sakai reference genome (16). BRIG was used to visually compare the similarities between the Sakai and outbreak strain prophages. We compared prophage regions of 122262 with those extracted and analyzed by Shaaban et al. (17) by using the pipeline and strains presented in their study.

Phylogenetic Analyses

Short reads were quality trimmed (24) and mapped to the STEC O157:H7 Sakai reference genome (GenBank accession no. BA000007) by using Burrows-Wheeler aligner-maximal exact matching (25). We sorted and indexed the sequence alignment map output from the Burrows-Wheeler aligner to produce a binary alignment map by using SAMtools (25). GATK2 (26) was used to create a variant call format file from each of the B binary alignment maps, which were further parsed to extract only single-nucleotide polymorphism (SNP) positions that were of high quality (mapping quality > 30 , coverage of reads that passed quality metrics > 10 , variant ratio > 0.9). We used pseudosequences of polymorphic positions to create maximum-likelihood trees by using RAxML (27). FASTQ (<https://www.ncbi.nlm.nih.gov/pmc/>

Table 1. *Escherichia coli* O55:H7 genome sequences retrieved from publicly available databases*

Name	Accession no.	Serotype	STX	SOR	GUD	Reference
USDA 5905	SRS702210	O55	–	+	+	(7)
3256-97-1	AEUA01000000	O55	–	+	+	(7)
RM12579-1	CP003109	O55	–	+	+	(7)
CB9615	NC_013941	O55	–	+	+	(10)
ZH-1141	Pending	O55:H7	–	+	+	(14)
2013C-4465	GCA_001644745.1	O55	Stx1a	+	+	(15)
Sakai		O157:H7	Stx1a and 2a	–	–	(16)
155	CP018237	O157:H7	Stx2a	–	–	(17)
TL-000142	ERR180875	O55	–	+	+	This study
SRR3578942	SRR3578942	O55:H7	Stx2d	+	+	This study
TL-000132	ERR197199	O55	–	+	+	This study
3041-1_85	ERR197201	O55	–	+	+	This study
100446	ERR178176	O55:H7	–	+	+	This study

*GUD, β -glucuronidase; SOR, sorbitol; Stx, Shiga toxin; –, negative; +, positive.

articles/PMC2847217/) sequences were deposited in the National Center for Biotechnology Information Short Read Archive under the BioProject PRJNA248042.

Results

General Genomic Features

STEC O55:H7 strain 122262 had a 5,364,131-bp chromosome and a 67,247-bp single plasmid of replicon type FIB-15. Use of *blastn* to compare the extracted plasmid sequence from 122262 with publicly available plasmid sequences belonging to CB9615, 2013C-4465, and Sakai indicated that the plasmid of 122262 was 99% identical to pO55 CB9615 over its complete length. Unlike pO157 in STEC O157:H7, the O55:H7 plasmids did not encode toxin B (*toxB*) or the enterohemolysin operon (*ehxABCD*). The *E. coli* O55:H7 strains 122262, CB9615, and 2013C-4465 did, however, encode a remote *toxB* homologue *efal/lifA* on the chromosome that has 29% nt identity (97% coverage) with pO157 *toxB*. The LEE was inserted into the chromosome of strain 122262 at *tRNA-selC*, the most common insertion site in a range of pathogenic *E. coli* chromosomal backgrounds (28). Antimicrobial drug resistance determinants included *aadA-1b* encoding resistance to streptomycin and *dfrA-1* encoding resistance to trimethoprim.

Prophage Composition of 122262

PHAST identified 15 prophage interruptions in 122262, of which 5 were homologous in nucleotide identity to Sp2, Sp3, Sp6, Sp8, and Sp14 found in Sakai (16) (Table 2; Figure 1). Unique genetic content and position was found for 9 putative prophages (Figure 1). In addition, a Stx2a-encoding phage was identified at the Stx-associated bacteriophage insertion site *yecE* in strain 122262. In Sakai, the Stx1a (Sp15) and Stx2a (Sp5) encoding phages are inserted at *wrba* and *yehV*, respectively. However, *yecE* is a known Stx-associated

bacteriophage insertion site in strains of STEC O157:H7 encoding *stx2a* belonging to lineage Ic (29).

Long-read sequencing of 122262 facilitated comparison of the sequence of the Stx2a-encoding phage with other publicly available sequences of Stx2a-encoding phage. Shaaban et al. (17) compared prophage sequences for 14 strains of STEC O157:H7, including 8 Stx2a-encoding phages. Of the 8 Stx2a phages described in that study, 7 were closely related despite being found in globally distributed strains from different lineages. The sequence of the Stx2a-encoding phage from the outbreak strain, 122262, showed most similarity (>98% nt identity and >94% sequence coverage over the complete phage) with an outlier Stx2a-encoding phage designated 155, found in a subset of isolates of STEC O157 phage type 32 in lineage 1c, geographically associated with the island of Ireland (17,29) (Figure 2). The main difference between the 2 prophages was an insertion sequence element, a common source of prophage variation (Figure 2).

Sorbitol-Negative Phenotype of 122262

Like the common STEC O157:H7 clone, the STEC O55:H7 outbreak strain described in this study was characterized by its inability to ferment sorbitol. *srlA* and *srlE* encode components of a glucitol/sorbitol-specific phosphotransferase system. In STEC O157:H7, the sorbitol-negative phenotype was thought to have resulted from frameshifts in *srlA* and *srlE*, as observed in Sakai and EDL933 (5). SNP analysis of STEC O55:H7 122262 in our study revealed a non-sense mutation in *srlA* causing truncation of the last 29 aa, which was likely to reduce expression or produce a nonfunctional product. The sorbitol-negative phenotype, although a characteristic of STEC O157:H7, is rare in *E. coli* O55:H7 and has been described for only 1 other strain (RM12506, also referred to as BB2 and C523-03; genome not publicly available) (7,30).

Table 2. Location of prophages in Shiga toxin-producing *Escherichia coli* O55:H7 isolate 122262 from outbreak in Dorset County, England, July 2014, and related Sakai reference prophage*

Prophage in 122262	Location	Related Sakai phage	Identity, %
P1	298714–355267	Sp8	96
P2	2728769–2738381	NP	NA
P3	2958215–2992979	Sp3	98
P4	3119806–3151485	NP	NA
P5	3702030–3736837	Sp5	99
P6	4031314–4075190	NP	NA
P7	4166735–4223146	NP	NA
P8	4361295–4432383	Sp6	97
P9	4549353–4575262	NP	NA
P10	4662955–4712352	NP	NA
P11	4744636–4768829	NP	NA
P12	4868835–4901248	NP	NA
P13	5136256–5154117	NP	NA
P14	5221278–5261127	Sp14	98
P15	5287889–5361495	NP	NA
Stx-encoding phage	3607500–3655000	NP	NA

*NA, not applicable; NP, not present; Stx, Shiga toxin.

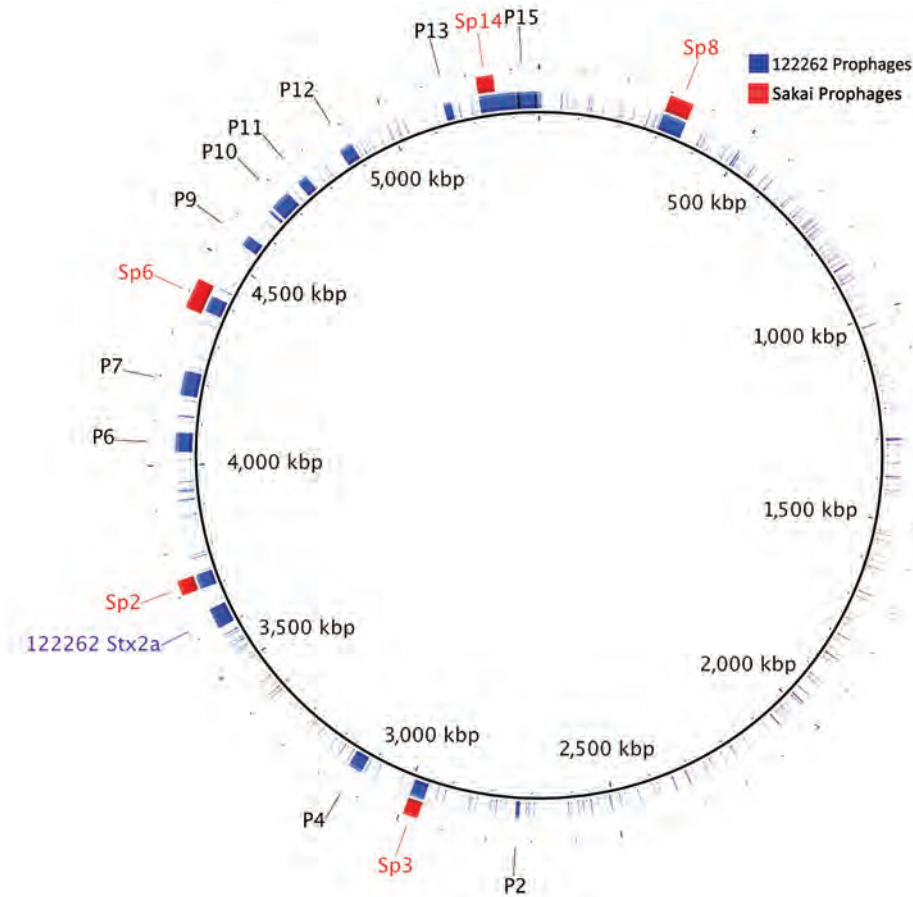


Figure 1. BLAST ring image generator (BRIG) plot generated from BLAST+ (21) comparisons of Shiga toxin-producing *Escherichia coli* (STEC) O55:H7 122262 prophages and homologous STEC O157:H7 Sakai prophages. STEC O55:H7 122262 chromosome is set as the reference genome, and the 122262 prophages (P1–P15) comprise the first ring. The homologous STEC O157:H7 Sakai prophages (Sp2, Sp3, Sp6, Sp8, and Sp14) identified in the BLAST analysis were added to the image according to their known locations (Table 2). Putative prophage sequence data were retrieved content from PHAge Search Tool (22) and plotted in BRIG.

β-Glucuronidase and Tellurite Phenotypes of 122262

β-glucuronidase is an inducible enzyme encoded by *uidA* and produced by ≈90% of pathogenic and nonpathogenic *E. coli*. The common STEC O157:H7 clone is a rare exception. The *uidA* loss of function mechanism in STEC O157:H7 was elucidated by Monday et al. (31) and included 2 frame-shift mutations. The STEC O55:H7 outbreak strain 122262 had a β-glucuronidase-positive phenotype, and analysis of the genome by using MAUVE (20) did not identify any disruptive mutations in *uidA*. No β-glucuronidase-negative strains of *E. coli* O55:H7 have been described. Furthermore, the STEC O55 Dorset outbreak strain 122262 did not contain the *ter* cluster and was phenotypically sensitive to tellurite. As a consequence, it did not propagate when inoculated onto cefixime and tellurite sorbitol MacConkey agar and was not detected by routine culture methods used at the local hospital diagnostic microbiology laboratories in the United Kingdom (<https://www.gov.uk/government/publications/smi-b-30-investigation-of-faecal-specimens-for-enteric-pathogens>).

Phylogenetic Analyses

To investigate the evolutionary history of the STEC O55 Dorset outbreak strain, we constructed a core genome

phylogeny (Figure 3). The analysis divided the sequences of the isolates in this study according to serotype; all isolates of *E. coli* O55:H7 clustered together on a separate branch of the tree, and all isolates of STEC O157:H7 clustered together on the branch below, regardless of sorbitol/β-glucuronidase phenotype or the presence of *stx* (Figure 3). The phylogenetic analysis of *E. coli* O55:H7 indicated that incorporation of the *Stx*-encoding prophage has occurred on multiple occasions within the EPEC O55:H7 background, with independent acquisition of *stx1* (15), *stx2d*, and *stx2a* into EPEC O55:H7. Likewise, multiple acquisition and loss events involving *stx1*, *stx2c*, *stx2a*, and less commonly *stx2d* have been described for STEC O157:H7 (12,32).

As noted by McFarland et al. (1), the outbreak strain was closely related to STEC O55:H7 *stx2a* isolates identified in Ireland during 2013–2014 (Figure 3). These 6 isolates from Ireland were <5 SNPs from the Dorset outbreak strain, indicating that the isolates from Ireland and Dorset County shared a common source (8). The outbreak strain had lost the ability to ferment sorbitol, which appears to be a recent adaptation with all ancestral O55:H7, including those isolated in Ireland in 2012 retaining the ability to ferment sorbitol. A similar relationship exists between the sorbitol-positive and

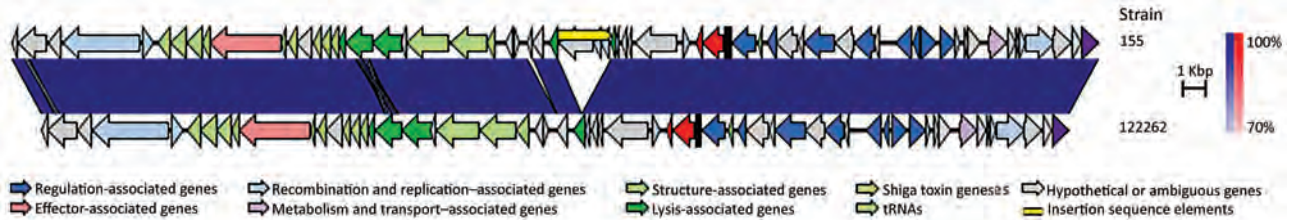


Figure 2. The sequence of the Stx2a-encoding phage from the July 2014 Dorset County, England, outbreak strain of Shiga toxin-producing *Escherichia coli* O55:H7, designated 122262, showed >98% nt identity with an outlier Stx2a-encoding phage designated 155, found in a subset of isolates of Shiga toxin-producing *Escherichia coli* O157 geographically associated with the island of Ireland. The main difference between the 2 prophages was an insertion sequence element.

sorbitol-negative STEC O157:H7 phenotypes; the sorbitol-negative phenotype is a more recent adaptation from the sorbitol-positive progenitor strain (Figure 3) (3,5).

The most parsimonious model of evolution of the STEC O55:H7 Dorset outbreak strain was a progenitor EPEC O55:H7 sorbitol-fermenting strain lysogenized by an Stx2a-encoding phage and subsequent loss of the ability to ferment sorbitol. This stepwise model of evolution seems to mirror that seen in the common STEC O157:H7 clone; the acquisition of the STEC pathotype preceded phenotypic modulation.

Discussion

In the United Kingdom, STEC is regarded as a substantial threat to public health, and enhanced surveillance systems are in place (32). In England, HUS developed in $\approx 5\%$ of symptomatic STEC O157:H7 patients (33), notably less than the 42% of patients in whom HUS developed during the STEC O55:H7 outbreak described in this study. The Dorset outbreak strain was closely related to the common STEC O157:H7 clone and shared several characteristics, most notably the presence of phage-encoded *stx2a*. Stx2a is associated with more severe symptoms, including the development of HUS, and it is probably the key virulence factor causing the high proportion of HUS cases in this outbreak (10). Of additional concern was the inability to detect the outbreak strain at the local hospital level by using the standard microbiology investigation method, cefixime and tellurite sorbitol MacConkey agar, because of this strain's sensitivity to tellurite.

A previously published stepwise evolutionary model showed the acquisition of *stx2* by a strain of EPEC O55:H7, resulting in emergence of a strain of STEC O55:H7, which was β -glucuronidase positive and sorbitol positive, closely related but ancestral to STEC O157:H7, which was β -glucuronidase positive and sorbitol positive (34). The loss of the sorbitol-positive phenotype in STEC O157:H7 was followed by the loss of β -glucuronidase expression, resulting in the common STEC O157 sorbitol-negative β -glucuronidase-negative clone. The evolutionary history of the Dorset outbreak strain begins with the EPEC

O55:H7 progenitor strain described previously (6) (Figure 3). Subsequent acquisition of an Stx2a-encoding phage was confirmed by detection of STEC O55:H7 β -glucuronidase-positive sorbitol-positive isolates in Ireland in 2012 (Figure 3). The loss of the sorbitol-positive phenotype mirrored the genetic events proposed to have occurred in the evolution of STEC O157, albeit by an alternative mechanism.

The parallel, convergent evolutionary history of STEC O157:H7 and STEC O55:H7 may indicate a common driver in the evolutionary process. Adaptation to a new niche may be accompanied by modification of gene expression because genes no longer required for, or incompatible with, the variation in lifestyle are selectively inactivated by point mutation, insertion, or deletion (35). Loss of the sorbitol-positive phenotype may coincide with the successful colonization of a new animal host or the ability to transmit more effectively between animal hosts without the need to survive in the environment for long periods (28,36).

The detection of the STEC O55:H7 sorbitol-negative strain in patients in Ireland before the outbreak in Dorset led to speculation that ruminants (most likely cattle or sheep) on the island of Ireland were the source of the outbreak strain (1). Transmission between Ireland and Dorset may have occurred via movement of persons, livestock, or a secondary vector such as migratory birds (37). The finding that the Stx2a-encoding phage has a high level of similarity to Stx2a-encoding phage found in a previously described sublineage of STEC O157 PT32 geographically linked to Ireland may provide further evidence of the origin of this strain (17,29). Phages from STEC O157 may be exchanged with other phages from serotypes of *E. coli* in the gut of the ruminant host or in the environment. Analysis and comparison of phage sequences to provide clues regarding the origin of a strain of STEC is a novel approach to outbreak investigation; additional studies are required to evaluate the utility of the approach. Further work will be hampered by the lack of available sequences of the Stx-encoding phage and the difficulties with assembling the sequences because of the inability of short-read sequencing to resolve the large number of repetitive and paralogous features characteristic of the prophage.

The STEC O55:H7 Dorset outbreak strain described in this study shared characteristics with the common STEC O157:H7 clone, specifically the acquisition of an Stx2a-encoding phage and the sorbitol-negative phenotype. Key differences between the 2 strains include the *rfb* gene cluster, plasmid content, β -glucuronidase phenotype, and the absence of the *ter* gene cluster in the STEC O55:H7 outbreak strain. Despite these differences, this study provides evidence of parallel, convergent evolution of STEC O157:H7 and STEC O55:H7, involving multiple acquisitions of Stx-encoding phages and loss of the ability to ferment sorbitol. Previous studies have shown a clear association with STEC harboring *stx2a* and progression to HUS (10). Acquisition of the Stx2a-encoding phage seems to explain the emergence of STEC O157:H7 as a clinically significant pathogen; in contrast to the acquisition of *stx2c*, evidence suggests that after Stx2a-encoding phage is integrated in a population, it tends to be maintained and may be associated with higher excretions levels in cattle (29,36). As such, the emergence of STEC O55:H7 harboring *stx2a* is of public health concern.

Acknowledgments

We acknowledge all members of the Outbreak Control Team, especially Noeleen McFarland, Amy Mikhail, and Sooria Balasegaram.

This work was supported by the National Institute for Health Research Health Protection Research Unit in Gastrointestinal Infections. D.L.G., T.J.D., and S.S. were supported by a Food Standards Scotland/Food Standards Agency study grant (FS101055).

Mr. Schutz is a recent graduate of the London School of Hygiene and Tropical Medicine and the Royal Veterinary College in London. His research interests include emerging zoonoses and host adaptation.

References

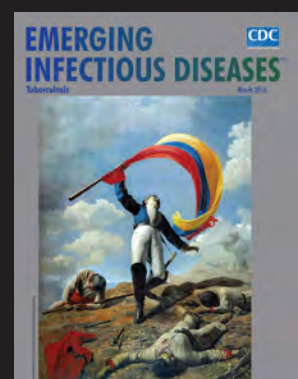
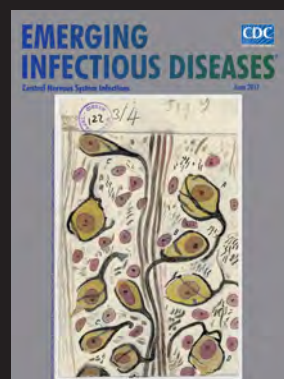
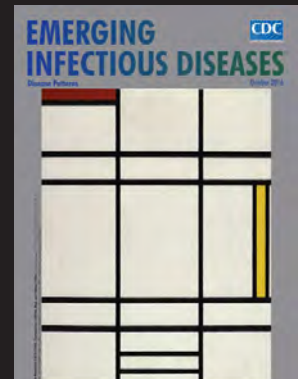
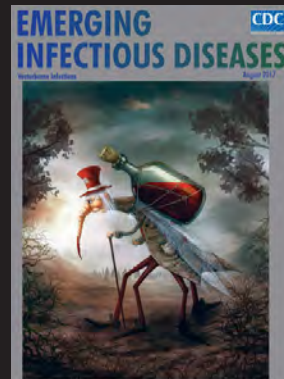
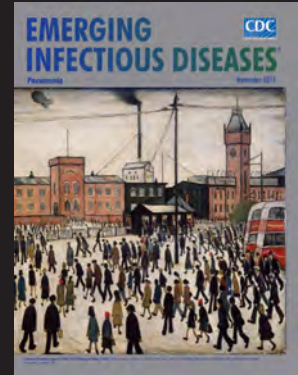
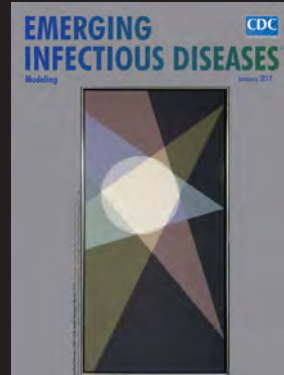
- McFarland N, Bundle N, Jenkins C, Godbole G, Mikhail A, Dallman T, et al. Recurrent seasonal outbreak of an emerging serotype of Shiga-toxin producing *Escherichia coli* (STEC O55:H7 stx 2a) in the South West of England, July 2014–September 2015. *Euro Surveill*. 2017;22:30610. 10.2807/1560-7917.ES.2017.22.36.30610
- Whittam TS, Wolfe ML, Wachsmuth IK, Orskov F, Orskov I, Wilson RA. Clonal relationships among *Escherichia coli* strains that cause hemorrhagic colitis and infantile diarrhea. *Infect Immun*. 1993;61:1619–29.
- Feng P, Lampel KA, Karch H, Whittam TS. Genotypic and phenotypic changes in the emergence of *Escherichia coli* O157:H7. *J Infect Dis*. 1998;177:1750–3. <http://dx.doi.org/10.1086/517438>
- Iguchi A, Ooka T, Ogura Y, Asadulghani, Nakayama K, Frankel G, et al. Genomic comparison of the O-antigen biosynthesis gene clusters of *Escherichia coli* O55 strains belonging to three distinct lineages. *Microbiology*. 2008;154:559–70. <http://dx.doi.org/10.1099/mic.0.2007/013334-0>
- Wick LM, Qi W, Lacher DW, Whittam TS. Evolution of genomic content in the stepwise emergence of *Escherichia coli* O157:H7. *J Bacteriol*. 2005;187:1783–91. <http://dx.doi.org/10.1128/JB.187.5.1783-1791.2005>
- Zhou Z, Li X, Liu B, Beutin L, Xu J, Ren Y, et al. Derivation of *Escherichia coli* O157:H7 from its O55:H7 precursor. *PLoS One*. 2010;5:e8700. <http://dx.doi.org/10.1371/journal.pone.0008700>
- Kyle JL, Cummings CA, Parker CT, Quiñones B, Vatta P, Newton E, et al. *Escherichia coli* serotype O55:H7 diversity supports parallel acquisition of bacteriophage at Shiga toxin phage insertion sites during evolution of the O157:H7 lineage. *J Bacteriol*. 2012;194:1885–96. <http://dx.doi.org/10.1128/JB.00120-12>
- Dallman TJ, Byrne L, Ashton PM, Cowley LA, Perry NT, Adak G, et al. Whole-genome sequencing for national surveillance of Shiga toxin-producing *Escherichia coli* O157. *Clin Infect Dis*. 2015;61:305–12. <http://dx.doi.org/10.1093/cid/civ318>
- Jenkins C, Lawson AJ, Cheasty T, Willshaw GA. Assessment of a real-time PCR for the detection and characterization of verocytotoxigenic *Escherichia coli*. *J Med Microbiol*. 2012;61:1082–5. <http://dx.doi.org/10.1099/jmm.0.041517-0>
- Persson S, Olsen KE, Ethelberg S, Scheutz F. Subtyping method for *Escherichia coli* Shiga toxin (verocytotoxin) 2 variants and correlations to clinical manifestations. *J Clin Microbiol*. 2007;45:2020–4. <http://dx.doi.org/10.1128/JCM.02591-06>
- Stevens MP, Frankel GM. The locus of enterocyte effacement and associated virulence factors of enterohemorrhagic *Escherichia coli*. *Microbiol Spectr*. 2014;2:EHEC-0007–2013. <http://dx.doi.org/10.1128/microbiolspec.EHEC-0007-2013>
- Feng P, Lampel KA. Genetic analysis of uidA expression in enterohaemorrhagic *Escherichia coli* serotype O157:H7. *Microbiology*. 1994;140:2101–7. <http://dx.doi.org/10.1099/13500872-140-8-2101>
- Lim JY, Yoon J, Hovde CJ. A brief overview of *Escherichia coli* O157:H7 and its plasmid O157. *J Microbiol Biotechnol*. 2010;20:5–14.
- Mainda G, Lupolova N, Sikakwa L, Bessell PR, Muma JB, Hoyle DV, et al. Phylogenomic approaches to determine the zoonotic potential of Shiga toxin-producing *Escherichia coli* (STEC) isolated from Zambian dairy cattle. *Sci Rep*. 2016;6:26589. <http://dx.doi.org/10.1038/srep26589>
- Lindsey RL, Rowe L, Garcia-Toledo L, Loparev V, Knipe K, Stripling D, et al. High-quality draft genome sequences for five non-o157 Shiga toxin-producing *Escherichia coli* strains generated with PacBio sequencing and optical maps. *Genome Announc*. 2016;4:e00626–16. <http://dx.doi.org/10.1128/genomeA.00626-16>
- Hayashi T, Makino K, Ohnishi M, Kurokawa K, Ishii K, Yokoyama K, et al. Complete genome sequence of enterohemorrhagic *Escherichia coli* O157:H7 and genomic comparison with a laboratory strain K-12. *DNA Res*. 2001;8:11–22. <http://dx.doi.org/10.1093/dnares/8.1.11>
- Shaaban S, Cowley LA, McAteer SP, Jenkins C, Dallman TJ, Bono JL, et al. Evolution of a zoonotic pathogen: investigating prophage diversity in enterohaemorrhagic *Escherichia coli* O157 by long-read sequencing. *Microb Genom*. 2016;2:e000096.
- Bankevich A, Nurk S, Antipov D, Gurevich AA, Dvorkin M, Kulikov AS, et al. SPAdes: a new genome assembly algorithm and its applications to single-cell sequencing. *J Comput Biol*. 2012;19:455–77. <http://dx.doi.org/10.1089/cmb.2012.0021>
- Seemann T. Prokka: rapid prokaryotic genome annotation. *Bioinformatics*. 2014;30:2068–9. <http://dx.doi.org/10.1093/bioinformatics/btu153>
- Darling AE, Mau B, Perna NT. progressiveMauve: multiple genome alignment with gene gain, loss and rearrangement. *PLoS One*. 2010;5:e11147. <http://dx.doi.org/10.1371/journal.pone.0011147>
- Altschul SF, Gish W, Miller W, Myers EW, Lipman DJ. Basic local alignment search tool. *J Mol Biol*. 1990;215:403–10. [http://dx.doi.org/10.1016/S0022-2836\(05\)80360-2](http://dx.doi.org/10.1016/S0022-2836(05)80360-2)

22. Zhou Y, Liang Y, Lynch KH, Dennis JJ, Wishart DS. PHAST: a fast phage search tool. *Nucleic Acids Res.* 2011;39:W347–52.
23. Alikhan NF, Petty NK, Ben Zakour NL, Beatson SA. BLAST ring image generator (BRIG): simple prokaryote genome comparisons. *BMC Genomics.* 2011;12:402. <http://dx.doi.org/10.1186/1471-2164-12-402>
24. Bolger AM, Lohse M, Usadel B. Trimmomatic: a flexible trimmer for Illumina sequence data. *Bioinformatics.* 2014;30:2114–20. <http://dx.doi.org/10.1093/bioinformatics/btu170>
25. Li H, Durbin R. Fast and accurate long-read alignment with Burrows-Wheeler transform. *Bioinformatics.* 2010;26:589–95. <http://dx.doi.org/10.1093/bioinformatics/btp698>
26. McKenna A, Hanna M, Banks E, Sivachenko A, Cibulskis K, Kernysky A, et al. The Genome Analysis Toolkit: a MapReduce framework for analyzing next-generation DNA sequencing data. *Genome Res.* 2010;20:1297–303. <http://dx.doi.org/10.1101/gr.107524.110>
27. Stamatakis A. RAxML version 8: a tool for phylogenetic analysis and post-analysis of large phylogenies. *Bioinformatics.* 2014;30:1312–3. <http://dx.doi.org/10.1093/bioinformatics/btu033>
28. Ingle DJ, Tauschek M, Edwards DJ, Hocking DM, Pickard DJ, Azzopardi KI, et al. Evolution of atypical enteropathogenic *E. coli* by repeated acquisition of LEE pathogenicity island variants. *Nat Microbiol.* 2016;1:15010. <http://dx.doi.org/10.1038/nmicrobiol.2015.10>
29. Dallman TJ, Ashton PM, Byrne L, Perry NT, Petrovska L, Ellis R, et al. Applying phylogenomics to understand the emergence of Shiga-toxin-producing *Escherichia coli* O157:H7 strains causing severe human disease in the UK. *Microb Genom.* 2015;1:e000029. <http://dx.doi.org/10.1099/mgen.0.000029>
30. Feng PC, Jinneman K, Scheutz F, Monday SR. Specificity of PCR and serological assays in the detection of *Escherichia coli* Shiga toxin subtypes. *Appl Environ Microbiol.* 2011;77:6699–702. <http://dx.doi.org/10.1128/AEM.00370-11>
31. Monday SR, Whittam TS, Feng PC. Genetic and evolutionary analysis of mutations in the *gusA* gene that cause the absence of beta-glucuronidase activity in *Escherichia coli* O157:H7. *J Infect Dis.* 2001;184:918–21. <http://dx.doi.org/10.1086/323154>
32. Sánchez S, Llorente MT, Herrera-León L, Ramiro R, Nebreda S, Remacha MA, et al. Mucus-activatable Shiga toxin genotype stx2d in *Escherichia coli* O157:H7. *Emerg Infect Dis.* 2017;23:1431–3. <http://dx.doi.org/10.3201/eid2308.170570>
33. Byrne L, Jenkins C, Launders N, Elson R, Adak GK. The epidemiology, microbiology and clinical impact of Shiga toxin-producing *Escherichia coli* in England, 2009–2012. *Epidemiol Infect.* 2015;143:3475–87. <http://dx.doi.org/10.1017/S0950268815000746>
34. Feng PC, Monday SR, Lacher DW, Allison L, Siitonen A, Keys C, et al. Genetic diversity among clonal lineages within *Escherichia coli* O157:H7 stepwise evolutionary model. *Emerg Infect Dis.* 2007;13:1701–6. <http://dx.doi.org/10.3201/eid1311.070381>
35. Maurelli AT. Black holes, antivirulence genes, and gene inactivation in the evolution of bacterial pathogens. *FEMS Microbiol Lett.* 2007;267:1–8. <http://dx.doi.org/10.1111/j.1574-6968.2006.00526.x>
36. Matthews L, Reeve R, Gally DL, Low JC, Woolhouse ME, McAteer SP, et al. Predicting the public health benefit of vaccinating cattle against *Escherichia coli* O157. *Proc Natl Acad Sci U S A.* 2013;110:16265–70. <http://dx.doi.org/10.1073/pnas.1304978110>
37. See comment in PubMed Commons below Persad AK, LeJeune JT. Animal reservoirs of Shiga toxin-producing *Escherichia coli*. *Microbiol Spectr.* 2014;2:EHEC-0027–2014.

Address for correspondence: Claire Jenkins, Gastrointestinal Bacteria Reference Unit, Public Health England, 61 Colindale Ave, NW9 5HT, UK; email: claire.jenkins@phe.gov.uk

EID Podcast: Emerging Infectious Diseases Cover Art

Byron Breedlove, managing editor of the journal, elaborates on aesthetic considerations and historical factors, as well as the complexities of obtaining artwork for *Emerging Infectious Diseases*.



Visit our website to listen:

**EMERGING
INFECTIOUS DISEASES**

<https://www.2c.cdc.gov/podcasts/player.asp?f=8646224>

Multiple Reassorted Viruses as Cause of Highly Pathogenic Avian Influenza A(H5N8) Virus Epidemic, the Netherlands, 2016

Nancy Beerens, Rene Heutink, Saskia A. Bergervoet, Frank Harders, Alex Bossers, Guus Koch

In 2016, an epidemic of highly pathogenic avian influenza A virus subtype H5N8 in the Netherlands caused mass deaths among wild birds, and several commercial poultry farms and captive bird holdings were affected. We performed complete genome sequencing to study the relationship between the wild bird and poultry viruses. Phylogenetic analysis showed that the viruses are related to H5 clade 2.3.4.4 viruses detected in Russia in May 2016 but contained novel polymerase basic 2 and nucleoprotein gene segments and 2 different variants of the polymerase acidic segment. Molecular dating suggests that the reassortment events most likely occurred in wild birds in Russia or Mongolia. Furthermore, 2 genetically distinct H5N5 reassortant viruses were detected in wild birds in the Netherlands. Our study provides evidence for fast and continuing reassortment of H5 clade 2.3.4.4 viruses, which might lead to rapid changes in virus characteristics, such as pathogenicity, infectivity, transmission, and zoonotic potential.

Highly pathogenic avian influenza (HPAI) A virus subtype H5N8 was detected in wild birds found dead at Uvs-Nuur Lake at the border between Russia and Mongolia in May 2016. This discovery was considered an early warning for the potential spread of the virus by autumn migration of wild birds. On October 27, 2016, public health authorities in Hungary reported detection of HPAI H5N8 virus in a wild swan. Since then, H5N8 has been detected in many countries in Africa and Eurasia, including the Netherlands.

These reports constitute the fourth time intercontinental spread of an H5 HPAI virus has been observed. The gene segment encoding for the hemagglutinin (HA) surface protein of these viruses is a descendant of HPAI H5N1 virus (A/Goose/Guangdong/1/1996), first detected in China in 1996 (1). In wild birds, H5N1 virus was first reported in 2002 in Hong Kong and was most likely caused by spillover from infected poultry (2). In 2005, H5N1 virus was spread from Asia through Siberia to Europe, the Middle

East, and Africa within a few months by migratory wild birds (3,4). In 2010, H5N1 virus was found in many countries in Asia and some in Europe (5).

In 2014, HPAI H5N8 virus spread from Asia to Europe and North America (6,7), and 5 poultry holdings were infected in the Netherlands (8,9). In the Netherlands, the introduction of H5N8 in 2016 resulted in mass deaths among wild birds, and several commercial poultry holdings and captive birds were infected. The 2016 H5N8 virus appeared more pathogenic than the viruses in the earlier H5 HPAI epidemics, given that mass deaths of wild birds were never observed before. A recent study (10) showed that the H5N8 viruses identified in Russia in 2016 are reassortants, carrying 3 gene segments (HA, neuraminidase [NA], and nonstructural protein [NS]) originating from H5 clade 2.3.4.4 viruses circulating in eastern Asia. The other 5 gene segments (polymerase basic 1 and 2 [PB1 and PB2], polymerase acidic [PA], nucleoprotein [NP], and matrix protein [MP]) were found previously in low pathogenicity avian influenza (LPAI) viruses identified in Mongolia, China, and Vietnam.

In this study, we analyzed the genetic relationship between HPAI H5N8 viruses isolated from wild birds, commercial poultry, and captive birds in the Netherlands in 2016. Median-joining network analysis suggested that multiple separate introductions of the H5N8 virus occurred during the epidemic. Phylogenetic analysis showed that the virus evolved from the H5N8 viruses detected in Russia in 2016 by obtaining novel PB2, PA, and NP gene segments. Two different PA reassorted H5N8 viruses were introduced in the Netherlands, and we detected 2 distinct H5N5 viruses in wild birds. We performed molecular dating to estimate the timing of the reassortment events.

Materials and Methods

Virus Detection and Subtyping

We extracted influenza virus RNA from tracheal or cloacal swabs from dead wild birds by using MagNa Pure 96 (Roche, Basel, Switzerland). For commercial poultry

Author affiliation: Wageningen Bioveterinary Research, Lelystad, the Netherlands

DOI: <https://doi.org/10.3201/eid2312.171062>

farms, we used pools of 5 samples from clinically affected animals. We tested samples by using a matrix-gene real-time PCR, which detects all avian influenza virus subtypes, as described previously (9). We subtyped positive samples by using an H5-specific real-time PCR as recommended by the European Union reference laboratory (11). We determined the sequence of the HA cleavage site and the N subtype by using Sanger sequencing (9).

Complete Genome Sequencing and Analysis

We purified influenza virus RNA by using the High Pure Viral RNA kit (Roche), amplified the RNA by using universal 8-segment primers, and then directly sequenced the RNA, as described previously (12). We sequenced purified amplicons at high coverage (average >1,000/nt position) using the Nextera XT DNA Library Preparation kit (Illumina, San Diego, CA, USA) and MiSeq paired-end 150-bp sequencing (Illumina). We mapped the reads by using the ViralProfiler-Workflow, an extension of the CLC Genomics Workbench (QIAGEN, Hilden, Germany). We generated consensus sequences by using a reference-based method. For generation of a defined set of influenza reference sequences, we clustered all complete genome sequences of Eurasia isolates in the GISAID EpiFlu database (<https://www.gisaid.org>) (years 2000–2016) per segment at 85% identity by using the CD-HIT-EST algorithm (13). We selected cluster representatives for each gene segment to generate a reference set. We first mapped reads to this reference set, and subsequently remapped them to the selected reference sequence. Finally, we extracted the consensus sequence of the complete virus genome. The ViralProfiler-Workflow also assigns the HA cleavage site and coding region of the proteins. We submitted sequences generated in this study to the GISAID database (online Technical Appendix 1 Table 1, <https://wwwnc.cdc.gov/EID/article/23/12/17-1062-Techapp1.xlsx>).

Phylogenetic Analysis

We performed phylogenetic analysis of the complete genome sequences for each genome segment separately. We generated alignments with the closest related viruses obtained from the GISAID database (online Technical Appendix 1 Table 2) by using Muscle in MEGA6 (14). We performed molecular phylogenetic analysis by using the neighbor-joining method. We modeled the rate variation among sites with gamma distribution (shape parameter = 1) and used 1,000 bootstrap replicates to estimate branch support.

We manually concatenated the 8 gene segment alignments to generate a single alignment, which we used to construct phylogenetic networks by applying the median-joining method implemented in NETWORK as described (15). This model-free method uses a parsimony approach,

based on pairwise differences, to connect each sequence to its closest neighbor. It allows creation of internal nodes (median vectors), which could be interpreted as unsampled or extinct ancestral genotypes to link the existing genotypes in the most parsimonious way.

Molecular Dating

For each gene segment alignment, the simplest evolutionary model fitting the dataset was the Hasegawa–Kishino–Yano model with gamma distributed rates (16). We estimated nucleotide substitution rates by using Bayesian Markov chain Monte Carlo methods (17) until all parameters converged (chain lengths of 30 million delivered estimated sample sizes >500). We performed the analysis by using BEAST version 1.8.4 software (18) and strict or relaxed uncorrelated molecular clocks that we calibrated by using the sample isolation dates. We treated all gene segments separately to identify reassortants. We sampled the 30 million generations every 3,000 generations. We constructed a maximum clade credibility tree to summarize all 10,000 trees after removing the initial 10% burn-in by using TreeAnnotator (17). We visualized time-scaled phylogenetic trees by using FigTree version 1.4.2 (19) and further annotated the trees by using iTOL version 3.5.3 (20).

Results

Detection of HPAI H5N8 in Wild Birds and Poultry

The 2016 H5N8 epidemic in the Netherlands started with occurrence of hundreds of dead tufted ducks (*Aythya fuligula*) around a lake near Monnickendam, in the central part of the country. These tufted ducks tested positive for H5N8 on November 10, 2016. Sequencing of the HA gene showed the polybasic amino acid sequence PLREKRRKR*GLF in the cleavage site, confirming its high pathogenicity. As the epidemic continued, wild birds around several lakes and water-rich areas in the central part of the country, and later also in the northern part, were infected. We plotted the geographic locations where the HPAI H5N8 virus was detected (Figure 1, panel A). Tufted ducks were the most affected bird species in November and Eurasian wigeons (*Anas penelope*) in December (21). However, many species of wild birds became infected, including diving and dabbling ducks as well as mute swans, grebes, gulls, and buzzards (21). An HPAI virus of subtype H5N5 was detected in 2 birds, a tufted duck found dead near Monnickendam, and a mute swan near Groningen.

The first introduction of H5N8 into a commercial poultry holding with Peking ducks was detected on November 25, in the municipality of Biddinghuizen. The farm was located in the central part of the country, a few kilometers from the lake where dead H5N8-positive wild birds were detected earlier. Severe clinical signs, such as lethargy,

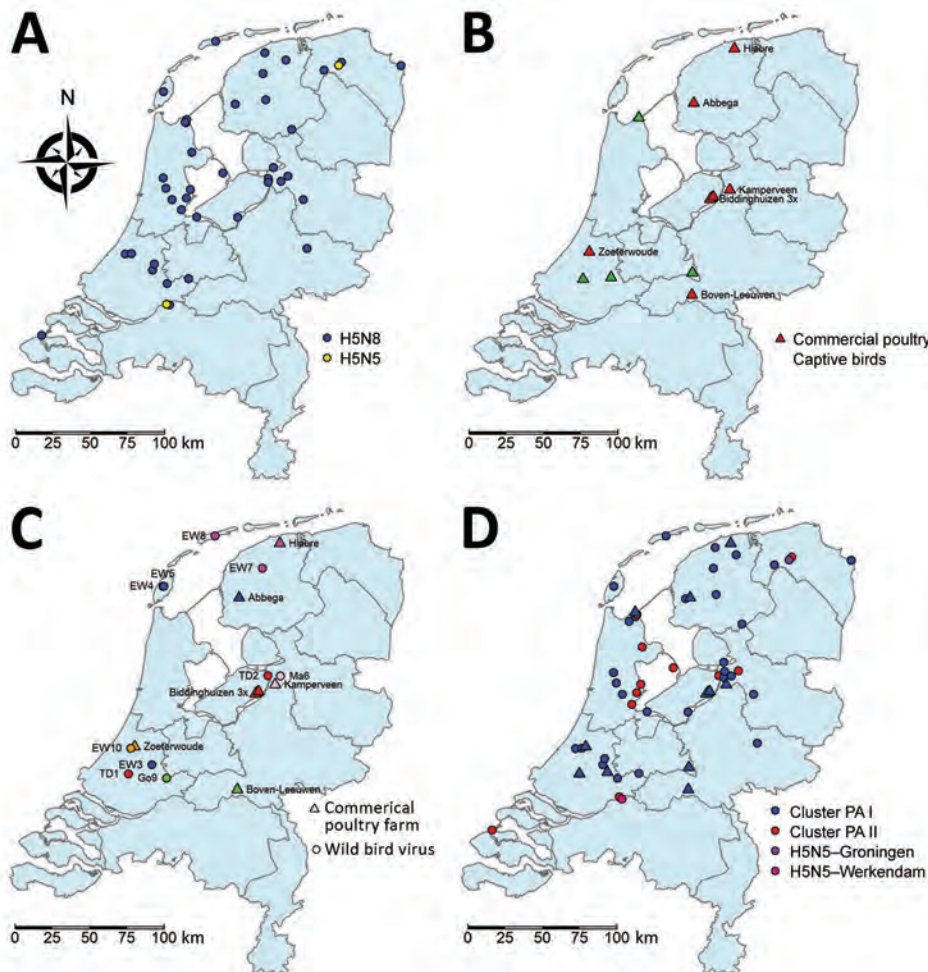


Figure 1. Geographic distribution of wild and captive birds and commercial poultry infected with highly pathogenic avian influenza A virus, the Netherlands, 2016. A) Location of dead wild birds infected with highly pathogenic avian influenza A virus subtypes H5N8 and H5N5; B) location of commercial poultry farms and captive birds infected with H5N8; C) location of H5N8-affected commercial poultry farms and wild bird viruses; colors indicate closest identities between farms and viruses (wild bird virus isolates used for this analysis are numbered 1–10; online Technical Appendix 1 Table 2, <https://wwwnc.cdc.gov/EID/article/23/12/17-1062-Techapp1.xlsx>); D) location of H5N8 viruses with gene segment PA I and PA II for commercial poultry farms and captive bird holdings and wild birds. Also shown are the H5N5 viruses isolated in Groningen and Werkendam. EW, Eurasian wigeon; Go, gray goose; Ma, mallard; PA, polymerase acidic; TD, tufted duck.

neurologic symptoms, and sudden death, were observed at the farm. Samples from the ducks tested positive by PCR, and the HPAI cleavage site (PLREKRRKR*GLF) was confirmed by sequencing. Several days later, samples from 2 other duck farms located within a distance of 3 km tested positive for H5N8. After these initial outbreaks, 5 other poultry holdings were affected in the central and northern parts of the country: 4 farms with laying hens, in Abbega, Boven-Leeuwen, Hiaure, and Zoeterwoude; and 1 duck farm, in Kamperveen. In addition, 4 introductions into captive birds were detected (1 black swan, 2 ducks, and 1 chicken). We noted the geographic locations of the infected commercial farms and captive bird holdings (Figure 1, panel B). All farms, with the exception of Boven-Leeuwen, were located in water-rich areas where dead H5N8-positive wild birds were found.

Genetic Differences between Wild Bird and Poultry H5N8 Viruses

We performed deep sequencing to determine the complete genome sequence of 44 wild bird viruses, the viruses

from 8 commercial poultry farms, and viruses from 4 captive birds in the Netherlands in 2016. We studied the genetic relationship between these viruses by median-joining network analysis, which showed that the viruses divide into 3 major clusters (online Technical Appendix 2 Figure 1, <https://wwwnc.cdc.gov/EID/article/23/12/17-1062-Techapp2.pdf>). Cluster A contained mainly Eurasian wigeons, whereas various wild bird species were found in clusters B and C (online Technical Appendix 2 Figure 1). The viruses detected at the commercial poultry farms and in captive birds were located in clusters A and B, with the exception of those from Abbega. The network analysis showed no correlation between virus cluster and the geographic location of the virus. These results suggest that at least 3 separate introductions of the H5N8 virus occurred in the Netherlands, after which the virus likely spread to different parts of the country. In addition to the major clusters, we detected multiple separate viruses and small clusters, which suggests that more independent introductions of the H5N8 virus have occurred during the epidemic.

To analyze the genetic relationship between H5N8 viruses detected at commercial poultry farms and in wild birds, we identified the most identical wild bird virus for each farm (online Technical Appendix 1 Table 2) and performed median-joining network analysis (Figure 2). The geographic locations of the poultry farms and the dead wild birds infected with the most related virus are shown (Figure 1, panel C). Epidemiologic investigation of the affected farms revealed no dangerous contacts. However, the 3 infected farms in Biddinghuizen were detected within a period of 7 days and are located within 3 km of one another. The median-joining network (Figure 2) showed that the complete genome sequence of the viruses from the farms in Biddinghuizen are highly similar, containing at most 5 nt changes. This fact indicates that the farms were either infected by direct transmission between farms or by separate introduction of virus from the same outside source. The viruses detected at the other 5 farms differed between 14 and 59 nt and are likely the result of separate introductions from wild birds (Figure 2). Closely related wild bird viruses with 5–9 nt changes were identified near the farms in Biddinghuizen, Hiaure, Kamperveen, and Zoeterwoude at 3–20 km distance. For the farm in Boven-Leeuwen, the closest related wild bird virus was found at a distance of 48 km and contained 16 nt differences. For the farm in Abbega, the most similar wild bird virus contained 56 nt changes and was found at a distance of 52 km. We did not identify a more closely related virus, suggesting that the variation of wild bird viruses introduced into the Netherlands was larger than revealed in this study.

The comparison of wild bird and poultry sequences identified no specific mutations related to adaptation of the virus to poultry. Finally, the consensus sequence of the 2016 H5N8 virus was compared with the consensus sequence of the virus detected in the Netherlands in

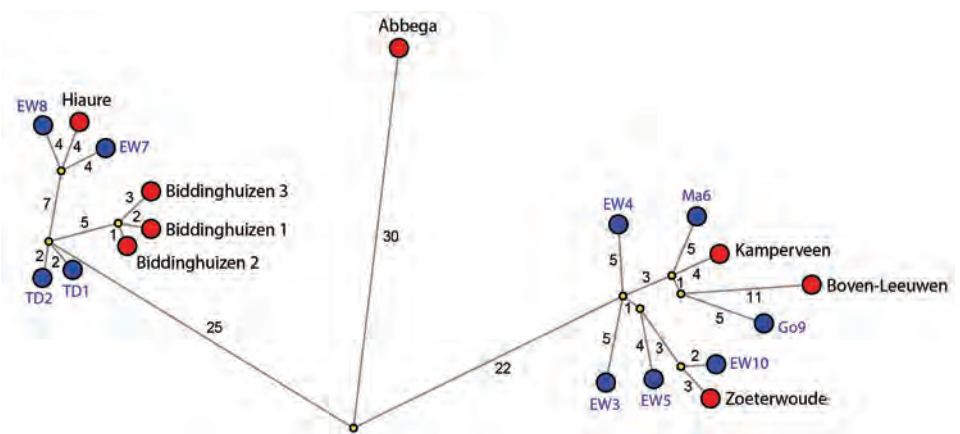
2014, when 5 commercial poultry holdings were infected (results not shown). This analysis identified 97 nt differences, resulting in 18 aa changes in the HA gene segment between the consensus sequences of these viruses. In addition, we found 56 nt (14 aa) differences in the NA segment. In the 6 internal segments, we found a total of 142 aa differences in the open reading frames. The numerous genetic differences between the viruses indicate that the H5N8 virus found in the Netherlands in 2016 results from a new introduction and therefore is not from continuous circulation of the 2014 virus.

Phylogenetic Analysis of the H5N8 Viruses

To study the origin of the H5N8 viruses found in the Netherlands in 2016, we performed a detailed phylogenetic analysis for all gene segments individually (online Technical Appendix 2 Figure 2). This analysis confirms the differences between the 2014 and 2016 H5N8 viruses, which are found separate clusters. The closest relatives of the 2016 viruses in the Netherlands are the Russia–Mongolia H5N8 clade 2.3.4.4 viruses that were first detected in May 2016 in dead wild birds near Uvs-Nuur Lake. However, we identified several reassortments, which we have represented schematically (Figure 3). Five of the gene segments (PB 1, HA, NA, MP, and NS) are highly similar to the Russia–Mongolia viruses. However, the closest relatives of PB2 in the GISAID database are LPAI viruses found in Bangladesh and Russia (online Technical Appendix 1 Table 1). The closest relatives of the NP gene segment are found in LPAI viruses in the Netherlands and the Republic of Georgia. An LPAI H7N9 virus detected in a commercial chicken holding in the Netherlands in June 2016 also carried a closely related NP segment.

Phylogenetic analysis of the PA gene segment showed that the 2016 H5N8 viruses in the Netherlands divert into

Figure 2. Median-joining network showing the genetic relationship between highly pathogenic avian influenza A viruses subtype H5N8 isolated from commercial poultry farms (red circles) and the most identical wild bird viruses (blue circles) found in the Netherlands, 2016. Predicted median vectors are shown in yellow. The length of the line represents the genetic distance, and the number of nucleotide changes is indicated. Wild bird virus isolates used for this analysis are numbered 1–10 (online Technical Appendix 1 Table 2, <https://wwwnc.cdc.gov/EID/article/23/12/17-1062-Techapp1.xlsx>). GISAID EpiFlu database (<https://www.gisaid.org>) accession numbers are shown in online Technical Appendix 1 Table 1. EW, Eurasian wigeon; Go, gray goose; Ma, mallard; TD, tufted duck.



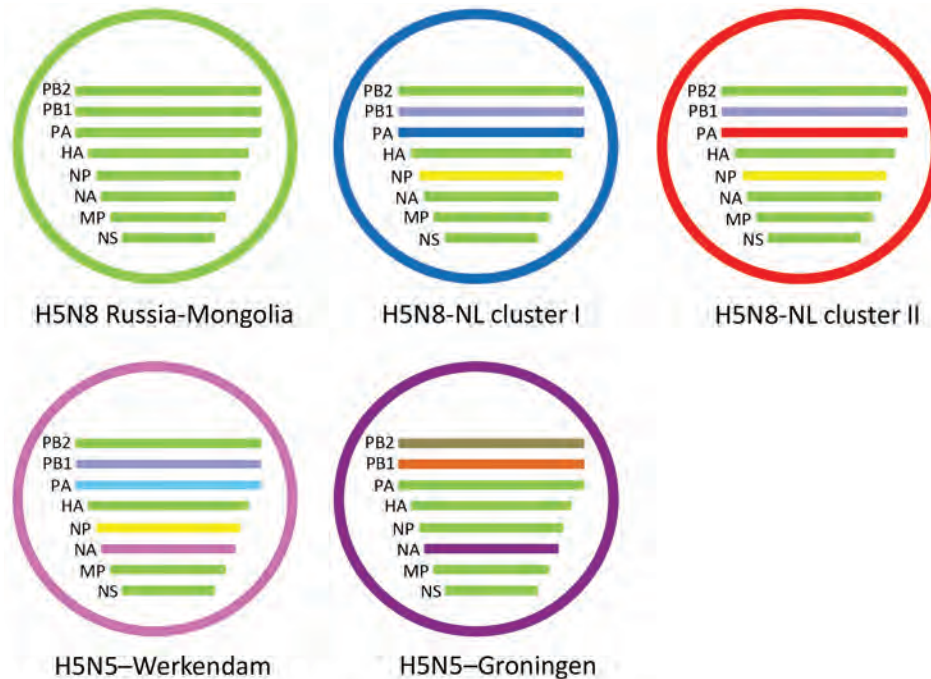


Figure 3. Schematic representation of the reassortant highly pathogenic avian influenza A virus subtypes H5N8 and H5N5 detected in the Netherlands, 2016. The Russia-Mongolia ancestor is shown in green. NL clusters 1 (blue) and 2 (red) viruses obtained novel PB2 and NP gene segments and 2 different PA segments. Two genetically distinct H5N5 viruses were detected, 1 in a tufted duck in Werkendam (pink) and 1 in a mute swan near Groningen (purple). HA, hemagglutinin; MP, matrix protein; NA, neuraminidase; NL, Netherlands; NP, nucleoprotein; NS, nonstructural protein; PA, polymerase acidic; PB1, polymerase basic 1; PB2, polymerase basic 2.

2 separate clusters, designated PA I and PA II. Different subtypes of LPAI viruses found in Russia and Asia were identified as closest relatives for the 2 PA clusters (online Technical Appendix 1 Table 3). Most of the viruses found in wild birds and all viruses detected in commercial poultry and captive birds are in cluster PA I. Cluster PA II contains 12 viruses isolated from various wild bird species and is represented by cluster C in the network analysis (online Technical Appendix 2 Figure 1). These findings show that no correlation exists between PA cluster and bird species or geographic location (online Technical Appendix 2 Figure 1 panels A and B; Figure 1, panel D). The viruses in the Netherlands evolved from the Russia–Mongolia H5N8 viruses by obtaining novel PB2 and NP segments and 2 variants of the PA segment. These results demonstrate that the H5N8 HPAI epidemic in the Netherlands is caused by 2 distinct reassorted viruses.

Phylogenetic Analysis of Two H5N5 Viruses

Two HPAI H5N5 viruses were identified in dead wild birds in the Netherlands. For the tufted duck isolate (t_dk/NL-Werkendam/16014159–001/2016) PB1, PB2, HA, NP, MP, and NS are closely related to the H5N8 viruses detected in the Netherlands in 2016. The closest relatives of NA in the GISAID database are LPAI N5 viruses found in the Netherlands, Europe, and Asia in previous years (online Technical Appendix 1 Table 3; online Technical Appendix 2 Figure 1). For the PA segment, this H5N5 virus does not fall in either cluster PA I or PA II. The closest relatives of PA are LPAI viruses found in the Netherlands and Asia during 2012–2014. For the mute swan

isolate (m-swan/NL-Groningen/16015825–001/2016), all genome segments are highly similar to an H5N5 virus identified in feces of a wild bird in Kamchatka, Russia, in October 2016. Phylogenetic analysis of the HA, PA, NP, MP, and NS segments shows that this H5N5 virus clusters with the Russia–Mongolia H5N8 viruses and not with the H5N8 2016 viruses in the Netherlands. The closest relatives of NA in the GISAID database are LPAI N5 viruses found in Asia in previous years. A similar N5 segment was also found in H5N5 viruses detected in Croatia, Italy, and Poland during the H5N8 epidemic in 2016–2017. The PB2 and PB1 segments cluster with various LPAI viruses detected earlier in Russia, Mongolia, and Europe. The mute swan virus thus is a direct descendant of a reassorted H5N5 virus from Russia, given that it was also previously detected in Kamchatka. We have depicted the genetic constitution of the 2 H5N5 viruses (Figure 3). These results indicate that 2 genetically distinct H5N5 viruses have been found in the Netherlands.

Molecular Dating of H5N8 Reassortment Events

To estimate the timing of the reassortment events that led to the emergence of the H5N8 viruses in the Netherlands, we performed molecular dating (online Technical Appendix 2 Figure 3). We estimated the time of most recent common ancestor for all gene segments by using a relaxed molecular clock (Table). A schematic representation of the time-scaled phylogenetic tree for the HA, PB2, NP, and PA segments is shown (Figure 4). The H5N8 viruses in 2016 diverted from the 2014 viruses in April 2012 (Figure 4, panel A [node 1]), from the Russia–Mongolia

Table. tMRCA of 8 gene segments of highly pathogenic avian influenza A virus subtype H5N8 in the Netherlands, determined by using a relaxed clock, with 95% HPD and posterior values*

Gene segment and node†	tMRCA	95% HPD interval		Posterior
		Begin	End	
Polymerase basic 2				
1	2005 Jul 21	1999 Apr 21	2011 Aug 2	1.00000
2	2015 Apr 13	2014 Aug 19	2015 Dec 23	1.00000
3	2016 Jul 2	2016 Apr 29	2016 Sep 6	1.00000
Polymerase basic 1				
1	2009 Feb 23	2006 Jun 27	2011 Feb 16	1.00000
2	2015 Dec 15	2015 Sep 12	2016 Mar 11	1.00000
3	2016 Aug 18	2016 Jul 3	2016 Sep 29	0.99610
Polymerase acidic				
1	2003 Jan 23	1998 Jun 20	2006 Nov 20	1.00000
2	2007 May 19	2005 Mar 31	2009 Jun 15	0.99070
3	2010 Jul 6	2009 Jul 20	2011 May 2	1.00000
4	2016 Apr 26	2016 Jan 10	2016 Jul 26	1.00000
5	2016 Aug 25	2016 Jun 23	2016 Oct 17	1.00000
Hemagglutinin				
1	2012 Apr 6	2010 Nov 14	2013 Jul 4	1.00000
2	2016 Mar 11	2016 Jan 15	2016 Apr 30	0.99420
3	2016 Aug 23	2016 Apr 8	2016 Aug 15	0.99989
Nucleoprotein				
1	2012 Jun 6	2010 Aug 16	2013 Aug 30	1.00000
2	2015 Apr 15	2014 Sep 11	2015 Dec 5	1.00000
3	2016 Aug 20	2016 Jun 28	2016 Oct 12	1.00000
Neuraminidase (N8)				
1	2011 Sep 5	2002 Nov 5	2013 Dec 24	1.00000
2	2016 Apr 14	2016 Mar 3	2016 May 14	0.91980
3	2016 Aug 31	2016 Jul 18	2016 Oct 8	0.76560
Matrix protein				
1	2011 Aug 29	2008 Sep 21	2013 Aug 21	1.00000
2	2015 Dec 9	2015 Jul 30	2016 Mar 16	1.00000
3	2016 Sep 9	2016 Jul 25	2016 Oct 16	0.97360
Nonstructural protein				
1	2010 May 17	2007 Jan 4	2012 Dec 7	1.00000
2	2015 Dec 9	2015 Jul 30	2016 Mar 18	1.00000
3	2016 Aug 23	2016 Jul 6	2016 Oct 2	0.99630
Neuraminidase (N5)				
A	1989 May 28	1983 Apr 24	1994 Apr 30	0.43740
B	2014 Apr 1	2012 Nov 27	2015 Apr 5	1.00000
C	2015 Jan 4	2013 Aug 11	2016 Jan 18	1.00000
D	2005 Sep 15	2004 Feb 13	2006 Nov 28	1.00000

*HPD, highest posterior density; tMRCA, calculated time of most recent common ancestor.

†Nodes of the time-scaled phylogenetic tree are shown in Figure 4 and online Technical Appendix 2 Figure 3 (<https://wwwnc.cdc.gov/EID/article/23/12/17-1062-Techapp2.pdf>).

H5N8 viruses in March 2016 (node 2), and we estimated the common ancestor of the viruses in the Netherlands to have occurred in August 2016 (node 3). Similar results were obtained for the PB 1, NA, MP, and NS gene segments (Table; online Technical Appendix 2 Figure 3). The PB2 segment was transferred from LPAI viruses in June 2016 (Figure 4, panel B [node 3]) and the NP segment in August 2016 (Figure 4, panel C [node 3]). Two different PA segments were detected in H5N8 viruses in the Netherlands. The viruses in cluster PA I obtained the PA segment from LPAI viruses in April 2016 (Figure 4, panel D [node 4]) and in cluster PA II in August 2016 (Figure 4, panel D [node 5]). We also performed calculations by using a strict molecular clock, with similar outcomes (results not shown). Thus, the H5N8 viruses in the Netherlands were generated by multiple reassortment events

with LPAI viruses, a process that was likely completed in August 2016. Because the H5N8 virus was introduced in the Netherlands in November 2016, this analysis suggests that the reassortment events took place in wild birds in Russia-Mongolia. Molecular dating for H5N5 shows that the common ancestor of the mute swan isolate and the Kamchatka isolate already circulated in January 2015. The N5 gene segments of the tufted duck and mute swan isolate diverged in 1989 (node A). Multiple reassorted viruses thus were introduced in the Netherlands by the autumn migration of wild birds from their breeding grounds in Russia-Mongolia.

Discussion

The introduction of the HPAI H5N8 virus in the Netherlands in 2016 resulted in the death of many wild birds, and

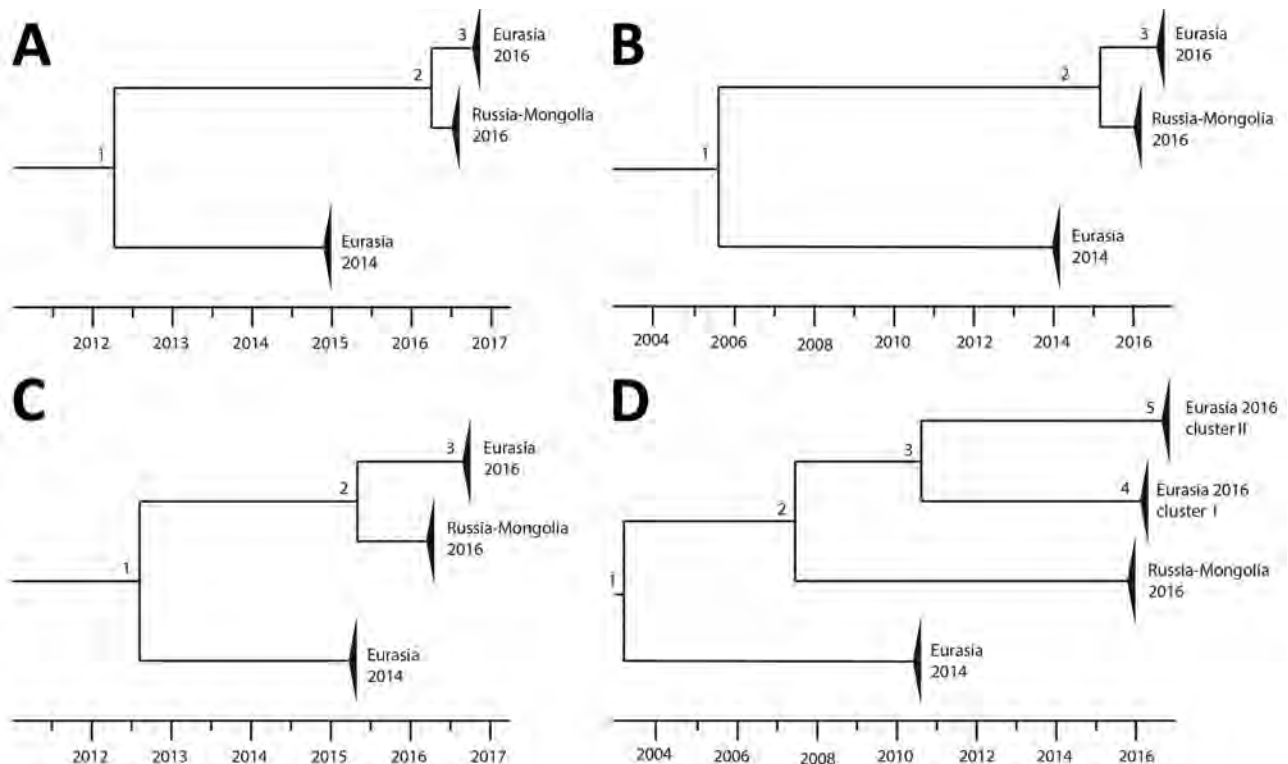


Figure 4. Schematic representation of the molecular dating analysis of highly pathogenic avian influenza A virus subtypes H5N8 and H5N5 detected in the Netherlands, 2016. Time-scaled phylogenetic trees are shown for 4 gene segments: A) hemagglutinin; B) polymerase basic 2; C) nucleoprotein; and D) polymerase acidic. For each of the numbered nodes, calculated time of most recent common ancestor, 95% highest posterior density interval, and posterior are listed in the Table.

several commercial poultry and captive bird holdings were affected. We performed genetic analysis to study the relationship between wild bird and poultry viruses. Median-joining network analysis suggested that multiple separate introductions of the H5N8 virus occurred in the Netherlands. This analysis also demonstrated that the viruses on 5 infected farms were not closely related (Figure 2). On the 3 farms in Biddinghuizen, highly similar viruses were identified, which might have resulted from either farm-to-farm spread or separate introductions from the same source. For most poultry farms, a dead wild bird infected with a related virus was found near the farm. We observed numerous genetic differences between the H5N8 viruses introduced in the Netherlands in 2016 versus 2014, indicating the 2016 epidemic was caused by a new introduction and not by continuous circulation of the 2014 virus.

Phylogenetic analysis showed that the H5N8 viruses introduced in the Netherlands in 2016 are novel reassortants of the Russia–Mongolia H5 clade 2.3.4.4 viruses. The virus obtained new PB2 and NP segments, and we detected 2 different PA segments in H5N8 viruses in the Netherlands. We found no correlation between PA segment and bird species between PA segment and geographic location (online Technical Appendix 2 Figure 1 [cluster C]).

Molecular dating suggests that these reassortment events were completed in August 2016 and thus most likely occurred in wild birds in Russia–Mongolia. A recent genetic analysis of 2 wild bird and several poultry H5N8 viruses in Germany also identified the NP and PA reassortments (22). In addition, we identified PB2 as a reassortment on the basis of molecular dating studies and its similarity to PB2 in LPAI viruses. The PA II gene segment was not observed in H5N8 viruses in Germany or other countries in Europe, based on the analysis of sequences that are currently available. Furthermore, 2 genetically distinct H5N5 viruses have been found in the Netherlands. An analysis of the outbreak in Italy (23), published after submission of this manuscript, also showed multiple independent introductions of H5N8 and H5N5 viruses. Those findings provide evidence for rapid and continuing reassortment of the H5 clade 2.3.4.4 viruses, which allow the virus to change its genetic architecture very quickly and might increase the ability of the virus to infect poultry or humans in the future. Hence, extensive surveillance of wild bird populations in the border area of Russia and Mongolia and in common breeding grounds in northern Siberia appears essential to enable early warning of novel reassortants and sequence mutations of H5 clade 2.3.4.4 viruses.

Acknowledgments

The authors are grateful to Patrick Dekker for construction of the ViralProfiler-Workflow and for his great support. We thank Jose Gonzales for the maps, Sylvia Pritz-Verschuren for technical assistance, and Armin Elbers for helpful discussion. We acknowledge the Netherlands Food and Consumer Product Safety Authority (Nederlandse Voedsel en Warenautoriteit [NVWA]) and Animal Health Service (Gezondheidsdienst voor Dieren [GD]) for excellent cooperation during the outbreak, and the dispatching service unit and diagnostic unit for handling and testing of all samples. We acknowledge the authors and submitting laboratories of the sequences from the GISAID EpiFlu Database.

This work was funded by the Dutch Ministry of Economic Affairs.

Dr. Beerens is a senior scientist and head of the National Reference Laboratory for Avian Influenza and Newcastle Disease in the Netherlands. Her research interests focus on molecular virology, genetics, and virus evolution.

References

- Xu X, Subbarao, Cox NJ, Guo Y. Genetic characterization of the pathogenic influenza A/Goose/Guangdong/1/96 (H5N1) virus: similarity of its hemagglutinin gene to those of H5N1 viruses from the 1997 outbreaks in Hong Kong. *Virology*. 1999;261:15–9. <http://dx.doi.org/10.1006/viro.1999.9820>
- Ellis TM, Bousfield RB, Bissett LA, Dyrting KC, Luk GS, Tsim ST, et al. Investigation of outbreaks of highly pathogenic H5N1 avian influenza in waterfowl and wild birds in Hong Kong in late 2002. *Avian Pathol*. 2004;33:492–505. <http://dx.doi.org/10.1080/03079450400003601>
- Olsen B, Munster VJ, Wallensten A, Waldenström J, Osterhaus AD, Fouchier RA. Global patterns of influenza A virus in wild birds. *Science*. 2006;312:384–8. <http://dx.doi.org/10.1126/science.1122438>
- Kilpatrick AM, Chmura AA, Gibbons DW, Fleischer RC, Marra PP, Daszak P. Predicting the global spread of H5N1 avian influenza. *Proc Natl Acad Sci U S A*. 2006;103:19368–73. <http://dx.doi.org/10.1073/pnas.0609227103>
- Reid SM, Shell WM, Barboi G, Onita I, Turcitu M, Cioranu R, et al. First reported incursion of highly pathogenic notifiable avian influenza A H5N1 viruses from clade 2.3.2 into European poultry. *Transbound Emerg Dis*. 2011;58:76–8. <http://dx.doi.org/10.1111/j.1865-1682.2010.01175.x>
- Lee DH, Torchetti MK, Winker K, Ip HS, Song CS, Swayne DE. Intercontinental spread of Asian-origin H5N8 to North America through Beringia by migratory birds. *J Virol*. 2015;89:6521–4. <http://dx.doi.org/10.1128/JVI.00728-15>
- Global Consortium for H5N8 and Related Influenza Viruses. Role for migratory wild birds in the global spread of avian influenza H5N8. *Science*. 2016;354:213–7. <http://dx.doi.org/10.1126/science.aaf8852>
- Bouwstra R, Heutink R, Bossers A, Harders F, Koch G, Elbers A. Full-genome sequence of influenza A(H5N8) virus in poultry linked to sequences of strains from Asia, the Netherlands, 2014. *Emerg Infect Dis*. 2015;21:872–4. <http://dx.doi.org/10.3201/eid2105.141839>
- Bouwstra RJ, Koch G, Heutink R, Harders F, van der Spek A, Elbers AR, et al. Phylogenetic analysis of highly pathogenic avian influenza A(H5N8) virus outbreak strains provides evidence for four separate introductions and one between-poultry farm transmission in the Netherlands, November 2014. *Euro Surveill*. 2015;20:21174. <http://dx.doi.org/10.2807/1560-7917.ES2015.20.26.21174>
- Lee DH, Sharshov K, Swayne DE, Kurskaya O, Sobolev I, Kabilov M, et al. Novel reassortant clade 2.3.4.4 avian influenza A(H5N8) virus in wild aquatic birds, Russia, 2016. *Emerg Infect Dis*. 2017;23:359–60. <http://dx.doi.org/10.3201/eid2302.161252>
- Slomka MJ, Pavlidis T, Banks J, Shell W, McNally A, Essen S, et al. Validated H5 Eurasian real-time reverse transcriptase-polymerase chain reaction and its application in H5N1 outbreaks in 2005–2006. *Avian Dis*. 2007;51(Suppl):373–7. <http://dx.doi.org/10.1637/7664-060906R1.1>
- Jonges M, Welkers MR, Jeeninga RE, Meijer A, Schneeberger P, Fouchier RA, et al. Emergence of the virulence-associated PB2 E627K substitution in a fatal human case of highly pathogenic avian influenza virus A(H7N7) infection as determined by Illumina ultra-deep sequencing. *J Virol*. 2014;88:1694–702. <http://dx.doi.org/10.1128/JVI.02044-13>
- Li W, Godzik A. Cd-hit: a fast program for clustering and comparing large sets of protein or nucleotide sequences. *Bioinformatics*. 2006;22:1658–9. <http://dx.doi.org/10.1093/bioinformatics/btl158>
- Tamura K, Stecher G, Peterson D, Filipski A, Kumar S. MEGA6: Molecular Evolutionary Genetics Analysis version 6.0. *Mol Biol Evol*. 2013;30:2725–9. <http://dx.doi.org/10.1093/molbev/mst197>
- Bataille A, van der Meer F, Stegeman A, Koch G. Evolutionary analysis of inter-farm transmission dynamics in a highly pathogenic avian influenza epidemic. *PLoS Pathog*. 2011;7:e1002094. <http://dx.doi.org/10.1371/journal.ppat.1002094>
- Hasegawa M, Kishino H, Yano T. Dating of the human-ape splitting by a molecular clock of mitochondrial DNA. *J Mol Evol*. 1985;22:160–74. <http://dx.doi.org/10.1007/BF02101694>
- Drummond AJ, Nicholls GK, Rodrigo AG, Solomon W. Estimating mutation parameters, population history and genealogy simultaneously from temporally spaced sequence data. *Genetics*. 2002;161:1307–20.
- Drummond AJ, Suchard MA, Xie D, Rambaut A. Bayesian phylogenetics with BEAUti and the BEAST 1.7. *Mol Biol Evol*. 2012;29:1969–73. <http://dx.doi.org/10.1093/molbev/mss075>
- Rambaut A. FigTree. 201. v.1.4.2: tree drawing tool [cited 2016 10 4] <http://tree.bio.ed.ac.uk/software/figtree>
- Letunic I, Bork P. Interactive tree of life (iTOL) v3: an online tool for the display and annotation of phylogenetic and other trees. *Nucleic Acids Res*. 2016;44(W1):W242–5. <http://dx.doi.org/10.1093/nar/gkw290>
- Kleyheeg E, Slaters R, Bodewes R, Rijks JM, Spierenburg M, Beerens N, et al. Deaths among wild birds during highly pathogenic avian influenza A(H5N8) virus outbreak, the Netherlands. *Emerg Infect Dis*. 2017;23:2050–4.
- Pohlmann A, Starick E, Harder T, Grund C, Höper D, Globig A, et al. Outbreaks among wild birds and domestic poultry caused by reassorted influenza A(H5N8) clade 2.3.4.4 viruses, Germany, 2016. *Emerg Infect Dis*. 2017;23:633–6. <http://dx.doi.org/10.3201/eid2304.161949>
- Fusaro A, Monne I, Mulatti P, Zecchin B, Bonfanti L, Ormelli S, et al. Genetic diversity of highly pathogenic avian influenza A(H5N8/H5N5) viruses in Italy, 2016–17. *Emerg Infect Dis*. 2017;23:1543–7. <http://dx.doi.org/10.3201/eid2309.170539>

Address for correspondence: Nancy Beerens, Wageningen Bioveterinary Research, Division of Virology, PO Box 65, 8200 AB, Lelystad, the Netherlands; email: nancy.beerens@wur.nl

Experimental Infection of Common Eider Ducklings with Wellfleet Bay Virus, a Newly Characterized Orthomyxovirus

Valerie Shearn-Bochsler, Hon Sang Ip, Anne Ballmann, Jeffrey S. Hall, Andrew B. Allison, Jennifer Ballard, Julie C. Ellis, Robert Cook, Samantha E.J. Gibbs, Chris Dwyer

Wellfleet Bay virus (WFBV), a novel orthomyxovirus in the genus *Quaranjavirus*, was first isolated in 2006 from carcasses of common eider (*Somateria mollissima*) during a mortality event in Wellfleet Bay (Barnstable County, Massachusetts, USA) and has since been repeatedly isolated during recurrent mortality events in this location. Hepatic, pancreatic, splenic, and intestinal necrosis was observed in dead eiders. We inoculated 6-week-old common eider ducklings with WFBV in an attempt to recreate the naturally occurring disease. Approximately 25% of inoculated eiders had onset of clinical disease and required euthanasia; an additional 18.75% were adversely affected based on net weight loss during the trial. Control ducklings did not become infected and did not have clinical disease. Infected ducklings with clinical disease had pathologic lesions consistent with those observed during natural mortality events. WFBV was reisolated from 37.5% of the inoculated ducklings. Ducklings surviving to 5 days postinoculation developed serum antibody titers to WFBV.

The common eider (*Somateria mollissima*) is a large sea duck with a circumpolar distribution. Eiders nest in dense colonies, have generally low reproductive rates but high annual survival rates, and feed on filter-feeding bivalves, sea urchins, starfish, and crabs (1). The American race (subspecies *S. m. dresseri*) breeds on islands from the south central coast of Labrador, Canada, south to Massachusetts, USA, with greatest numbers breeding in the Gulf of St. Lawrence, St. Lawrence estuary, New Brunswick,

and Nova Scotia (2). These birds typically overwinter from Newfoundland, Canada, south to New York, USA, with large rafts of $\geq 100,000$ eiders congregating annually in the open waters off Cape Cod, Massachusetts (1).

The earliest record of death affecting a large number of eiders off Cape Cod occurred during September 1956–March 1957 (3). The next reports were not until the mid-1980s and early 1990s, when ≈ 100 birds (predominantly eiders) died in 2 separate events occurring in midwinter and late spring. Death in both events was primarily attributed to emaciation, although acanthocephaliasis (infestation with intestinal thorny-headed worms) was also present (4). Since 1998, however, die-offs of common eiders have been reported with increasing frequency on Cape Cod, such that they have become an almost annual (or biannual) occurrence since 2006. This increase in reports likely coincides with the initiation of active beach surveillance at several locations around the cape, which began after the isolation of a novel virus from eiders during the fall 2006 mass mortality event at Great Island in Wellfleet Bay, Massachusetts, USA (41.9048°N, 70.0687°W) (5). Most eiders were found dead, but a few live birds displayed nonspecific clinical signs, including incoordination, lethargy, and respiratory distress. Four common eider carcasses recovered from Great Island were submitted to the US Geological Survey's National Wildlife Health Center (NWHC; Madison, WI, USA) for cause-of-death determination. Acute hepatic necrosis and variable pancreatic, splenic, and intestinal necrosis were diagnosed in all 4 of the submitted eiders, and a novel enveloped RNA virus, since named Wellfleet Bay virus (WFBV), was isolated from the liver of 2 of the 4 birds. Genetic analysis of WFBV demonstrated that it is most closely related to members of the *Quaranjavirus* genus within the family *Orthomyxoviridae* (6). Since 2006, the NWHC has diagnosed hepatic necrosis and variable splenic, intestinal, and pancreatic necrosis in common eiders from which WFBV was isolated during 4 separate mass mortality events occurring at Wellfleet Bay during September 2007–October

Author affiliations: US Geological Survey National Wildlife Health Center, Madison, Wisconsin, USA (V. Shearn-Bochsler, H.S. Ip, A. Ballmann, J.S. Hall); Cornell University, Ithaca, New York, USA (A.B. Allison); Arkansas Game and Fish Commission, Little Rock, Arkansas, USA (J. Ballard); Tufts University, North Grafton, Massachusetts, USA (J.C. Ellis); National Park Service, Wellfleet, Massachusetts, USA (R. Cook); US Fish and Wildlife Service, Fort Collins, Colorado, USA (S.E.J. Gibbs); US Fish and Wildlife Service, Hadley, Massachusetts, USA (C. Dwyer)

DOI: <https://doi.org/10.3201/eid2312.160366>

2011. We aimed to determine the pathogenicity of WFBV by experimentally inoculating common eider ducklings and observing clinical progression and pathologic changes after challenge.

Materials and Methods

Animals

We obtained the 22 common eiders used for this study by collecting eggs from wild breeding colonies in Maine, USA. We hatched and raised the ducklings to 4–5 weeks of age in a quarantined facility (Livingston Ripley Waterfowl Conservancy, Litchfield, CT, USA). We then transported the ducklings in an air-conditioned vehicle to the NWHC, where the infection trial was carried out. We acclimated the ducklings at the NWHC Biosafety Level 3 research facility for 7 days. We inoculated 16 ducklings with WFBV, housed 1 sham-inoculated duckling with the inoculated ducklings to act as a contact transmission control, and housed 5 sham-inoculated ducklings together in a separate room as controls. The NWHC–Animal Care and Use Committee approved animal use and protocols for this study (tracking no. EP100316).

We administered inoculations on day 0 of the infection trial. We randomly selected 6 inoculated ducklings (3 groups of 2) at the beginning of the study for euthanasia and necropsy on days 2, 4, and 7 postinoculation to determine pathologic changes and pathogenesis of the infection; we similarly chose 2 control ducklings and euthanized 1 on day 2 and 1 on day 4. We obtained health scores twice daily for all birds, and we weighed each eider daily. Health scores ranged 0–3, with 0 indicating normal, 1 indicating mild to moderate clinical abnormalities, 2 indicating severe clinical abnormalities, and 3 indicating death. We also euthanized any eiders not randomly scheduled for euthanasia before the end of the trial that reached a predetermined humane endpoint during the trial. We defined the humane endpoint as weight loss >30%, anorexia, lethargy, or other major illness lasting for at most 24 hours. We performed euthanasia by using CO₂ inhalation followed by cervical dislocation. We concluded the trial at 10 days postinoculation (DPI), at which time we euthanized all remaining eiders.

Virus

WFBV was first isolated from common eiders with hepatic necrosis in 2006, when it was isolated from liver homogenate inoculated onto Muscovy duck embryonic fibroblasts (7) and propagated in embryonating chicken eggs. The virus used for the inoculum in this trial was from a fourth-passage stock grown up in Muscovy cells originally derived from an eider carcass (NWHC case no. 22565, accession no. 002) collected in May 2009 during a mass

mortality event near Wellfleet Bay. Because the natural route of infection (i.e., ingestion, inhalation, or vectorborne transmission) of WFBV is not known, we used an adaptation of the standard World Organisation for Animal Health (OIE) procedure for the determination of pathogenicity of avian influenza virus in poultry (8). We inoculated each of sixteen 6–7-week-old eider ducklings with WFBV by 3 routes simultaneously (intravenous, intratracheal, and oral). We administered a volume of 0.1 mL of inocula (3×10^6 50% egg infective dose/mL) by each route, for total virus amounts of 1×10^6 50% egg infective dose per bird. We inoculated the 5 control eiders housed separately from the exposed birds and the 1 contact transmission bird with a sham solution in a similar manner.

Biologic Sample Collection and Analysis

We obtained daily oral and cloacal swabs before inoculation (0 DPI) through 10 DPI; placed them in a solution of viral isolation media (Eagle minimum essential medium, 10% fetal bovine serum, and 4% antibiotic–antimycotic solution, all from Sigma-Aldrich, St. Louis, MO, USA); and froze them at -80°C . We also obtained 1 mL of venous blood from all eider ducklings before inoculation, at 5 DPI, and again at 10 DPI. We placed blood into serum tubes (Becton Dickinson, Franklin Lakes, NJ, USA) and separated the serum from the cellular fraction before storage at -30°C . We obtained oral and cloacal swabs daily and placed them into virus transport media. We collected 1 mL of venous blood from all eiders at 5 DPI and again at 10 DPI, collected the samples into serum tubes, and separated the serum. For eiders euthanized before 10 DPI, we collected serum before euthanasia. We performed antibody detection by using a modified β microneutralization assay (9). The antigen was a fourth-passage WFBV strain diluted to 50% tissue culture infective doses of $10^3/25 \mu\text{L}$ in Eagle minimum essential medium. We serially diluted serum samples from 1:4 to 1:256 and tested them in quadruplicate. We used Vero M cells as the biologic indicator.

We performed postmortem examination on each eider after euthanasia, aseptically collecting cloacal and oropharyngeal swabs as well as tissue samples, including esophagus, intestine, liver, kidney, and spleen tissue from each bird and placing them into 1 mL of virus isolation media. We collected tissue samples (lungs, trachea, heart, brain, liver, kidneys, spleen, crop, proventriculus, gizzard, small and large intestine, pancreas, thymus, bursa of Fabricius, adrenal glands, and gonads) from each bird, fixed the samples in neutral-buffered 10% formalin solution, and processed them by standard methods for histopathologic examination. We examined slides by light microscopy and stained for WFBV any slides showing lesions by using immunohistochemistry as previously described

Table 1. Wellfleet Bay virus serum antibody titers and virus isolation results in common eider (*Somateria mollissima*) ducklings experimentally infected with Wellfleet Bay virus, by specimen or tissue type, day of trial, and band number of duckling*

Day of trial and band no.	Serum Ab titer	Specimen or tissue type						
		OP swab	CL swab	Esophagus	Intestine	Kidney	Liver	Spleen
Day 2								
27	Neg	0	0	0	2.00×10^3	3.40×10^4	2.00×10^4	2.00×10^4
32	NT	9.28×10^2	0	NT	NT	NT	NT	NT
52	Neg	0	0	9.28×10^2	6.32×10^2	6.32×10^2	6.23×10^2	9.28×10^4
Day 4								
16†	1:160	0	6.23×10	9.28×10^2	0	0	0	0
25	Neg	0	0	0	0	0	0	0
37†	1:320	0	0	0	0	0	0	0
42	1:160	0	0	0	0	0	0	0
Day 5								
22	1:160	0	0	NT	NT	NT	NT	NT
29	1:160	0	0	NT	NT	NT	NT	NT
30	1:320	0	0	NT	NT	NT	NT	NT
32	1:160	0	0	NT	NT	NT	NT	NT
34	1:160	0	0	NT	NT	NT	NT	NT
43	1:320	0	0	NT	NT	NT	NT	NT
48	1:320	0	0	NT	NT	NT	NT	NT
50	1:320	0	0	NT	NT	NT	NT	NT
59	1:160	0	0	NT	NT	NT	NT	NT
60	>1:20, <1:160	0	0	NT	NT	NT	NT	NT
11‡	Neg	0	0	NT	NT	NT	NT	NT
Day 7								
22†	1:160	0	0	0	0	0	0	0
29†	1:160	0	0	0	0	0	0	0
48	1:320	0	0	0	0	4.31×10^2	0	0
Day 10								
30	>1:640	0	0	0	0	0	0	0
32	1:160	0	0	0	0	0	0	0
34	>1:640	0	0	0	6.32×10^3	0	0	0
43	1:80	0	0	0	0	0	0	0
50	1:160	0	0	0	0	0	0	0
59	>1:640	0	0	0	0	0	0	0
60	>1:640	0	0	0	0	0	0	0
11‡	Neg	0	0	0	0	0	0	0

*Virus isolate results are expressed as PFU/mL. Negative serum Ab titer result defined as titer <1:5. Ab, antibody; CL, cloacal; NT, not tested; Neg, negative; OP, oropharyngeal.

†Euthanized because of illness.

‡Contact transmission control.

(i.e., anti-WFBV polyclonal antibody mouse hyperimmune ascites fluid) (6).

Results

Weight Changes

All control eiders gained weight during the trial. Weight gains ranged from 105% to 130% (10-day average 118%). We euthanized 4 (25%) of the 16 inoculated eiders because of clinical deterioration during the 10-day trial period. These 4 eiders (band nos. 16, 22, 29, and 37) all lost weight steadily from the time of inoculation to the time of euthanasia; weight loss ranged from 7% to 20%. Of the remaining inoculated birds, 3 had net weight loss at the time of scheduled euthanasia. The remaining 9 virus-inoculated birds had all gained weight at the time of euthanasia (range 101%–137%, average 120%). Thus, of the 16 inoculated eider ducklings, 43.75% had a net decrease in weight during the trial. The single contact transmission

control eider had a net gain in weight (16%) over the course of the trial.

Disease

Control ducklings remained clinically healthy throughout the trial, whereas 25% of virus-inoculated eiders had onset of severe clinical signs and were euthanized. We began to observe clinical signs in several inoculated birds by 3 DPI. Two eider ducklings (band nos. 16 and 59) were lethargic, ataxic, and frequently had their eyes closed. At 4 DPI, we euthanized 1 of these eiders (band no. 16) and 1 additional eider (band no. 37) because of clinical deterioration (e.g., weak, not moving, and having pale mucous membranes); the second affected eider from 3 DPI (band no. 59) appeared to be recovering. At 5 DPI, an additional inoculated eider (band no. 22) developed an irregular gait; by 7 DPI, this bird was stumbling, reluctant to move, and had pale mucous membranes and was euthanized. Also at 7 DPI, another eider (band no. 29) became weak, pale, and reluctant to move and was euthanized. All remaining

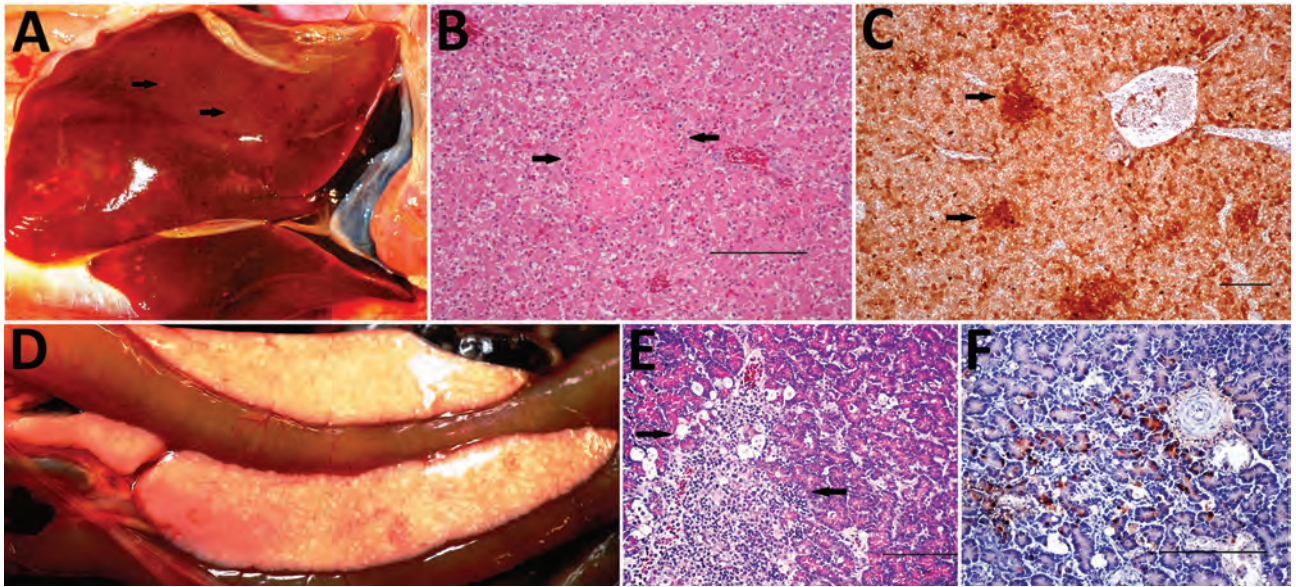


Figure 1. Gross, histopathologic, and immunohistochemical (IHC) findings in common eider (*Somateria mollissima*) ducklings experimentally infected with Wellfleet Bay virus (2 days postinoculation). A) Liver, enlarged, showing multifocal pinpoint areas of necrosis (arrows). B) Hematoxylin and eosin stain of liver tissue, showing focal hepatocellular necrosis (arrows). C) IHC stain of liver tissue, showing positive immunolabeling for Wellfleet Bay virus with multifocal staining of hepatocytes (arrows). D) Pancreas showing multifocal to coalescing acute necrosis. E) Hematoxylin and eosin stain of pancreas tissue, showing focally extensive necrosis of exocrine cells (arrows). F) IHC stain of pancreas tissue, showing positive immunolabeling for Wellfleet Bay virus in exocrine cells. Scale bars in panels B, C, E, and F indicate 100 μ m.

inoculated birds and the 1 contact transmission control were clinically normal throughout the trial.

Virus Isolation

We detected shedding of WFBV by oropharyngeal swab (band no. 32) at 2 DPI and by cloacal swab (band no. 16) at 4 DPI. We isolated virus from multiple tissues (kidney, liver, spleen, esophagus, intestine) of 2 eiders (band nos. 27 and 52) that were euthanized at 2 DPI. After 2 DPI, virus isolation was confined to single tissues from 3 separate birds, at 4 DPI (band no. 16, esophagus), 7 DPI (band no. 48, kidney), and 10 DPI (band no. 34, intestine) (Table 1). We did not detect virus on swabs or tissues taken from control birds housed separately from inoculated birds or from the contact transmission control bird.

Serum Antibody Detection

All virus-inoculated eiders developed serum antibodies to WFBV by 5 DPI. Antibodies persisted and remained stable or increased in all but 2 of the eiders that survived to the end of the trial (Table 1). Separately housed control eiders and the single contact transmission control eider did not develop detectable antibodies to WFBV.

Pathologic Changes

We observed severe gross and histopathologic abnormalities in both of the eiders euthanized at 2 DPI, before

clinical signs were observed in any of the virus-inoculated eiders. This finding suggests that viremia (we isolated virus from multiple tissues in both of these birds) and tissue damage occur very early in the course of infection. Pathologic abnormalities in these 2 eiders and in eiders showing signs of clinical illness later in the trial were consistent with those observed in adult common eiders from naturally occurring mass mortality events, including multifocal hepatic necrosis that progressed to hepatitis and pancreatic necrosis that progressed to pancreatitis. Immunohistochemical staining confirmed the presence of virus associated with these lesions (Figure 1). We scored the severity of hepatic lesions by histopathologic assessment of the number and extent of necrotic foci within sections of liver, with marked hepatic necrosis/hepatitis defined as affecting >30% of the hepatic parenchyma, moderate necrosis/hepatitis defined as affecting 20%–30%, and mild necrosis/hepatitis defined as affecting >0% to <20% (Table 2). Acute, marked thymic lymphocytic apoptosis, splenic necrosis, and lymphoid depletion in the bursa of Fabricius were also present in both birds; immunohistochemical staining for WFBV was positive in the thymus and spleen but not in the bursa of Fabricius. We observed no abnormalities in the control bird euthanized at 2 DPI, and both the thymus and bursa of Fabricius of this bird were robustly populated with lymphocytes (Figure 2).

Table 2. Necropsy findings in common eider (*Somateria mollissima*) ducklings experimentally infected with Wellfleet Bay virus and control ducklings, by control or inoculated status and band number of duckling*

Status and band no.	DPI	Weight change, %†	Health score‡	Virus isolated	Liver necrosis	Lymphoid depletion	Aspergillosis	Malaria	Muscle parasite
Control									
23	2	+4.76	0	No	–	–	+	–	–
36	4	+22.06	0	No	–	–	+	++	++
21	10	+20.63	0	No	–	–	+	++	++
28	10	+19.29	0	No	–	–	–	–	–
33	10	+14.02	0	No	–	–	–	++	+
Inoculated									
27	2	+2.88	0	Yes	+++	+++	++	–	–
52	2	–5.08	0	Yes	+++	+++	+	–	–
16§	4	–6.52	2	Yes	++	+++	+	+++	++
25	4	–13.60	0	No	++	+++	–	+	++
37§	4	–13.97	2	No	++	+++	–	–	++
42	4	–14.02	0	No	++	+++	+	–	–
22§	7	–20.14	2	No	++	+++	–	++	+++
29§	7	–17.87	2	No	++	+++	–	–	+
48	7	+1.03	0	Yes	–	++	+	++	+++
30	10	+13.25	0	No	++	+	+++	–	–
32	10	+17.20	0	No	–	+	++	–	–
34	10	+36.97	0	Yes	+	+	+	+	++
43	10	+17.45	0	No	+	+	+	+	+++
50	10	+29.27	0	No	–	–	++	++	+
59	10	+27.13	0	No	–	–	++	++	+
60	10	+0.55	0	No	–	+	+++	–	–
Contact transmission control									
11	10	+15.66	0	N	–	–	+++	++	+

*DPI, days postinoculation; +, mild; ++, moderate; +++, marked; –, negative.

†From day 0 to date of euthanasia.

‡Health scores ranged 0–3, with 0 indicating normal, 1 indicating mild to moderate clinical abnormalities, 2 indicating severe clinical abnormalities, and 3 indicating death.

§Euthanized because of illness.

Lymphoid depletion was a major finding in virus-inoculated eiders but was not present in the controls; all 5 control eiders had robust lymphoid organs at the time of scheduled euthanasia (at 2, 4, and 10 DPI). In contrast, inoculated birds that were euthanized at 2 DPI (2 birds) or 4 DPI (4 birds) and 2 of 3 birds euthanized at 7 DPI had marked lymphoid depletion in spleen, thymus, and bursa of Fabricius. Immunohistochemical stains confirmed the presence of WFBV in thymus and spleen but not in the bursa of Fabricius (Figure 2). The severity of lymphoid depletion was scored as marked if spleen, thymus, and bursa of Fabricius all showed an estimated $\geq 75\%$ decrease in expected numbers of lymphocytes, moderate if severity of depletion varied between lymphoid organs but was estimated as a $\geq 50\%$ decrease in lymphocytes, and mild if some lymphoid organs showed very little depletion whereas others showed moderate depletion (Table 2). The 2 birds euthanized at 7 DPI that had marked lymphoid depletion showed clinical signs, including at the time of euthanasia; the third bird had only mild to moderate lymphoid depletion and was clinically normal. By 10 DPI, all remaining virus-inoculated birds were clinically normal and had no or only mild lymphoid depletion.

Co-infections

The presence of 3 unanticipated pathogens in virus-inoculated, control, and contact transmission control eiders

complicated the interpretation of pathologic findings in some of the eiders euthanized after 2 DPI. Avian malaria (caused by infestation with *Plasmodium* sp. protozoa), aspergillosis (infection with *Aspergillus fumigatus*), and an unidentified skeletal muscle protozoan were variably present in control and inoculated ducklings. The skeletal muscle protozoan was present as degenerating, often calcified cysts invaded by macrophages and lymphocytes. We rated the severity of protozoal infection in the following manner: we removed a $2 \times 1 \times 1$ cm section of muscle from the cranioventral flexor carpi ulnaris muscle, where the parasites were most commonly observed on gross examination, and placed it in formalin. We performed histopathologic examinations on 3 cross-sections of this tissue from each bird and counted the number of discrete protozoal cysts present. Marked infestations were diagnosed as ≥ 50 total cysts or mineralized cyst remains with associated granulomatous inflammation, moderate as 20–50, and mild as 1–20. The contact transmission control eider and 4 of the 5 separately housed control ducklings had ≥ 1 co-infection, but all gained weight and remained clinically healthy throughout the trial. Two of the 4 virus-inoculated eiders that had clinical signs of illness had 1 co-infection of similar severity to those observed in controls; the other 2 had multiple co-infections. Co-infections in WFBV-inoculated eiders were more severe overall than those in

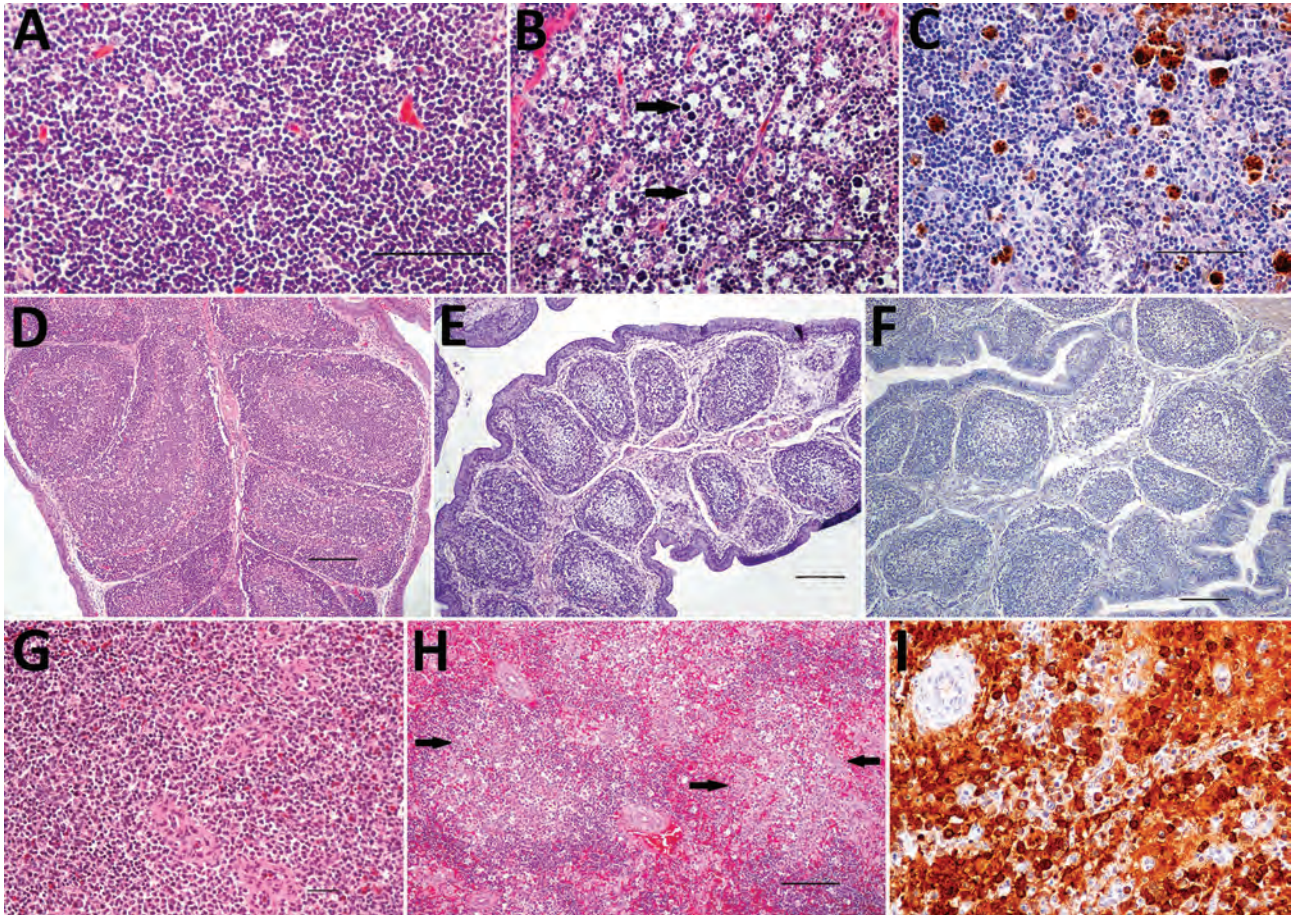


Figure 2. Histopathologic and immunohistochemical (IHC) findings in lymphoid organs of control and infected common eider (*Somateria mollissima*) ducklings experimentally infected with Wellfleet Bay virus (WFBV) (2 days postinoculation). A) Hematoxylin and eosin (H&E) stain of thymic cortex tissue from a control duckling. B) H&E stain of thymic cortex tissue from an infected duckling, showing marked multifocal acute apoptosis of lymphocytes (arrows). C) IHC stain of thymus tissue from an infected duckling, showing positive immunolabeling for WFBV in thymocytes. D) H&E stain of bursa of Fabricius tissue from a control duckling. E) H&E stain of bursa of Fabricius tissue from an infected duckling, showing marked diffuse lymphoid depletion. F) IHC stain of bursa of Fabricius tissue from an infected duckling showing negative immunolabeling for WFBV. G) H&E stain of spleen tissue from a control duckling. H) H&E stain of spleen tissue from an infected duckling, showing multifocal to coalescing acute necrosis (arrows). I) IHC stain of spleen tissue, showing positive immunolabeling for WFBV. I, original magnification $\times 200$. Scale bars in panels A, B, and C indicate 50 μm and in panels D, E, F, G, and H indicate 100 μm .

control eiders on the basis of numbers of parasites present (avian malaria and muscle protozoa) as well as severity and extent of associated tissue damage (Table 2). Pathologic abnormalities typical of natural WFBV disease were also present in eiders with major co-infections, and immunohistochemical staining confirmed the presence of virus associated with these lesions.

Discussion

This study determined the pathogenicity of WFBV, a novel orthomyxovirus in the genus *Quarantjavirus*, in common eiders by observing clinical progression and pathologic changes in experimentally inoculated eider ducklings over a 10-day period. We were able to determine that WFBV causes a unique, characteristic, and reproducible disease in this host.

Virus shedding occurred in only 2 infected eider ducklings very early in the course of infection with WFBV. This finding has practical implications; the diagnosis might easily be missed in naturally occurring infections if testing is confined to virus detection from oropharyngeal or cloacal swabs of dead or sick birds. Ducklings in this study did, however, develop serum antibody titers to WFBV by 5 DPI, and titers persisted through 10 DPI, when the experiment ended. Serologic testing would therefore be a useful tool for diagnosis of WFBV infection during a mass mortality event and for field surveillance.

Results of this study suggest that immune suppression might play an important role in the pathogenesis of WFBV disease in eiders. All eider ducklings that had onset of clinical disease had histopathologic evidence of marked

lymphoid depletion in the spleen, thymus, and bursa of Fabricius. In contrast, inoculated ducklings that remained clinically healthy until 7 DPI or 10 DPI had no or only mild lymphoid depletion. None of the control eiders (those housed separately plus the contact transmission control) demonstrated lymphoid depletion despite concurrent parasitic or fungal infections. Immune suppression induced by WFBV infection might lead to a greater risk for disease under conditions of increased stress or through the exacerbation of preexisting conditions. Co-infections in eiders with disease tended to be more severe than in eiders that remained asymptomatic during the trial (Table 2), although 1 eider (band no. 29) had only a mild muscle protozoan infestation. We hypothesize that under natural conditions, eiders affected by some combination of malnutrition, migration, concurrent disease, or other stressors might develop disease when infected with WFBV at a higher rate than birds without additional stressors.

In 2010 in Australia, an orthomyxovirus with genetic and antigenic properties similar to WFBV (designated as Cygnet River virus [CyRV]) was isolated during an outbreak of salmonellosis (*Salmonella enterica* serovar Typhimurium) in Muscovy ducks (*Cairina moschata*) on Kangaroo Island, South Australia (10). Genetic and antigenic comparisons between WFBV and CyRV indicate that they might be genetic variants of the same virus (6). It has not yet been determined what, if any, role CyRV played in the Muscovy duck deaths, given that salmonellosis alone is capable of causing a mortality event in waterfowl (11); however, we suggest that the high death rate observed in ducks with salmonellosis (97%) indicates that co-infection with CyRV might have contributed to the severity of this mortality event.

WFBV is the first *Quaranjavirus* to be definitively shown to cause major disease in its host species. In addition to CyRV, other members of the genus include Quarafil, Johnston Atoll, and Lake Chad viruses, all of which have been associated with colonial nesting avian species and their associated ticks (12). Quarafil virus is particularly interesting from a public health standpoint. This virus was named for the village in Egypt from which it was first isolated in *Argas arboreus* ticks associated with a nesting colony of egrets (*Bubulcus ibis ibis*). Quarafil virus was subsequently isolated from the blood of 2 young children with mild febrile illnesses (13). The children recovered without incident. Although these findings do not prove that illness in the children was caused by the Quarafil virus, they do indicate that at least 1 virus in the *Quaranjavirus* genus can infect humans. This fact highlights the importance of surveillance for and diagnosis of emerging diseases in wildlife as a means of detecting new pathogens with the potential to cause disease in humans and in nonhuman species.

The potential importance of WFBV to common eider populations is not yet clear. A recent article reported that another cyclically occurring infectious disease, avian cholera (caused by the bacterium *Pasteurella multocida*), is likely to have a substantial negative effect on the breeding population of common eiders on Southampton Island, Nunavut, Canada (14). This observation might also prove to be true of WFBV; however, much remains to be determined regarding the prevalence and sublethal effects of this virus during the breeding season.

Based on the results of our study, WFBV infection seems most likely to cause illness and death in eiders that are already physiologically stressed by migration or other natural phenomena or that contract what would otherwise be nonlethal co-infections. Further monitoring and surveillance of disease outbreaks associated with WFBV and research into its mode of transmission will increase our understanding of this virus and its potential for population-level effects.

Acknowledgments

We thank Bridget Cummings for daily assistance with care and handling of experimental eiders and Renee Long for processing virology samples. We also thank Brad Allen for continued support and assistance in obtaining eider eggs under state and federal scientific collecting permits from which this work was completed. We thank Susan Shaeffer and Ian Gereg for collecting and captive raising of the ducklings. We also thank Randall M. Mickley and volunteers with the Seabird Ecological Assessment Network for field assistance in the detection and collection of eider carcasses that formed the basis of this investigation.

This work was funded by the US Fish and Wildlife Service's Avian Health and Disease Program. The findings and conclusions in this article are those of the authors and do not necessarily represent the views of the US Fish and Wildlife Service.

Dr. Shearn-Bochsler is a veterinary pathologist at the US Department of the Interior's US Geological Survey National Wildlife Health Center, Madison, WI. She specializes in diseases of wild birds and endangered mammals.

References

- Goudie RI, Robertson GJ, Reed A. Common eider (*Somateria mollissima*). In: Poole A, Gill F, editors. The birds of North America. No. 546. Philadelphia: Academy of Natural Sciences; 2000. p. 32.
- Baldassarre GA. Ducks, geese and swans of North America. Baltimore: Johns Hopkins University Press; 2014. p. 1027.
- Clark GM, O'Meara D, Van Weelden JW. An epizootic among eider ducks involving an acanthocephalid worm. *J Wildl Manage.* 1958;22:204–5. <http://dx.doi.org/10.2307/3797332>
- U.S. Geological Survey, National Wildlife Health Center. Wildlife Health Information Sharing Partnership event reporting system (WHISPers) online database [cited 2015 Jun 22]. <https://www.nwhc.usgs.gov/whispers>

5. Ellis J, Courchesne S, Shearn-Bochsler V, Stantial M. Cyclic mass mortality of common eiders at Cape Cod, MA: an ongoing puzzle. In: Abstracts of the 37th Pacific Seabird Group Annual Meeting. Long Beach (CA): Pacific Seabird Group; 2010. p. 17–8.
6. Allison AB, Ballard JR, Tesh RB, Brown JD, Ruder MG, Keel MK, et al. Cyclic avian mass mortality in the northeastern United States is associated with a novel orthomyxovirus. *J Virol*. 2015;89:1389–403. <http://dx.doi.org/10.1128/JVI.02019-14>
7. Docherty DE, Slota PG. Use of Muscovy duck embryo fibroblasts for the isolation of viruses from wild birds. *J Tissue Cult Methods*. 1988;11:165–70. <http://dx.doi.org/10.1007/BF01404270>
8. World Organisation for Animal Health (OIE). Avian influenza. In: Manual of diagnostic tests and vaccines for terrestrial animals. Paris: The Organisation; 2005. p. 1–23.
9. National Veterinary Services Laboratories. Serologic microtitration techniques. Ames (IA): The Laboratories; 1981.
10. Kessell A, Hyatt A, Lehmann D, Shan S, Crameri S, Holmes C, et al. Cygnet River virus, a novel orthomyxovirus from ducks, Australia. *Emerg Infect Dis*. 2012;18:2044–6. <http://dx.doi.org/10.3201/eid1812.120500>
11. Friend M. Salmonellosis. In: Friend M, Franson JC, editors. Field manual of wildlife diseases. Washington: US Geological Survey; 1999. p. 99.
12. Presti RM, Zhao G, Beatty WL, Mihindukulasuriya KA, da Rosa AP, Popov VL, et al. Quarantil, Johnston Atoll, and Lake Chad viruses are novel members of the family Orthomyxoviridae. *J Virol*. 2009;83:11599–606. <http://dx.doi.org/10.1128/JVI.00677-09>
13. Taylor RM, Hurlbut HS, Work TH, Kingston JR, Hoogstraal H. Arboviruses isolated from Argas ticks in Egypt: Quarantil, Chenuda, and Nyamanini. *Am J Trop Med Hyg*. 1966;15:76–86. <http://dx.doi.org/10.4269/ajtmh.1966.15.76>
14. Descamps S, Jenouvrier S, Gilchrist HG, Forbes MR. Avian cholera, a threat to the viability of an Arctic seabird colony? *PLoS One*. 2012;7:e29659. <http://dx.doi.org/10.1371/journal.pone.0029659>

Address for correspondence: Valerie Shearn-Bochsler, US Geological Survey National Wildlife Health Center, 6006 Schroeder Rd, Madison, WI 53711, USA; email: vbochsler@usgs.gov

September 2017: Zoonoses

- *Candidatus* *Dirofilaria hongkongensis* as Causative Agent of Human Ocular Filariasis after Travel to India
- Mucus-Activatable Shiga Toxin Genotype *stx2d* in *Escherichia coli* O157:H7
- Acute Encephalitis Syndrome and Scrub Typhus in India
- Hematophagous Endeavors, Fact and Fancy

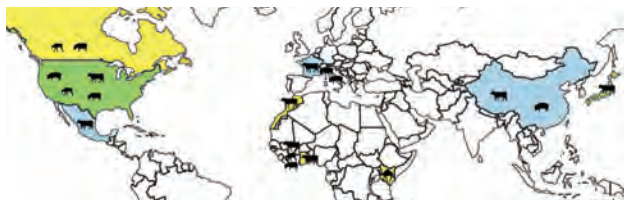


- Processes Underlying Rabies Virus Incursions across US–Canada Border as Revealed by Whole-Genome Phylogeography
- Real-Time Whole-Genome Sequencing for Surveillance of *Listeria monocytogenes*, France
- Role of Food Insecurity in Outbreak of Anthrax Infections among Humans and Hippopotamuses Living in a Game Reserve Area, Rural Zambia
- Bioinformatic Analyses of Whole-Genome Sequence Data in a Public Health Laboratory
- Serologic Evidence of Powassan Virus Infection in Patients with Suspected Lyme Disease
- Influenza D Virus in Animal Species in Guangdong Province, Southern China

- Seroprevalence of *Baylisascaris procyonis* Infection among Humans, Santa Barbara County, California, USA, 2014–2016



- Opiate Injection–Associated Skin, Soft Tissue, and Vascular Infections, England, UK, 1997–2016
- Detection of *Elizabethkingia* spp. in *Culicoides* Biting Midges, Australia
- Early Evidence for Zika Virus Circulation among *Aedes aegypti* Mosquitoes, Rio de Janeiro, Brazil
- Scrub Typhus Outbreak in a Remote Primary School, Bhutan, 2014
- Scrub Typhus as a Cause of Acute Encephalitis Syndrome, Gorakhpur, Uttar Pradesh, India
- Human Infection with *Burkholderia thailandensis*, China, 2013
- *mcr-1* and *bla*_{KPC-3} in *Escherichia coli* Sequence Type 744 after Meropenem and Colistin Therapy, Portugal



Group B *Streptococcus* Infections Caused by Improper Sourcing and Handling of Fish for Raw Consumption, Singapore, 2015–2016

Man L. Chau,¹ Swaine L. Chen,¹ Min Yap, Sri H.P. Hartantyo, Paul K.T. Chiew, Charlene J. Fernandez, Wai K. Wong, Rockey K. Fong, Wei L. Tan, Brian Z.Y. Tan, Youming Ng, Kyaw T. Aung, Kurosh S. Mehershahi, Christopher Goh, Joanne S.L. Kang, Timothy Barkham, Adeline O.K. Leong, Ramona A. Gutiérrez, Lee C. Ng



JOINTLY ACCREDITED PROVIDER*
INTERPROFESSIONAL CONTINUING EDUCATION

Medscape EDUCATION ACTIVITY

In support of improving patient care, this activity has been planned and implemented by Medscape, LLC and Emerging Infectious Diseases. Medscape, LLC is jointly accredited by the Accreditation Council for Continuing Medical Education (ACCME), the Accreditation Council for Pharmacy Education (ACPE), and the American Nurses Credentialing Center (ANCC), to provide continuing education for the healthcare team.

Medscape, LLC designates this Journal-based CME activity for a maximum of 1.00 **AMA PRA Category 1 Credit(s)**[™]. Physicians should claim only the credit commensurate with the extent of their participation in the activity.

All other clinicians completing this activity will be issued a certificate of participation. To participate in this journal CME activity: (1) review the learning objectives and author disclosures; (2) study the education content; (3) take the post-test with a 75% minimum passing score and complete the evaluation at <http://www.medscape.org/journal/eid>; and (4) view/print certificate. For CME questions, see page 2134.

Release date: November 15, 2017; Expiration date: November 15, 2018

Learning Objectives

Upon completion of this activity, participants will be able to:

- Evaluate clinical and epidemiological findings of a human group B *Streptococcus* outbreak in Singapore based on a microbial study of raw fish and human samples
- Determine the pathogenic potential of fish and human samples after a human group B *Streptococcus* outbreak in Singapore, based on a microbial study of these samples
- Assess the public health implications of a human group B *Streptococcus* outbreak in Singapore, based on a microbial study of raw fish and human samples.

CME Editor

Thomas J. Gryczan, MS, Technical Writer/Editor, Emerging Infectious Diseases. *Disclosure: Thomas J. Gryczan, MS, has disclosed no relevant financial relationships.*

CME Author

Laurie Barclay, MD, freelance writer and reviewer, Medscape, LLC. *Disclosure: Laurie Barclay, MD, has disclosed the following relevant financial relationships: owns stock, stock options, or bonds from Alnylam; Biogen; Pfizer.*

Authors

Disclosures: Man Ling Chau, BSc; Swaine L. Chen, MD, PhD; Min Yap, BSc; Sri Harminda Pahm Hartantyo, PhD; Paul King Tiong Chiew, DVM, MVP; Charlene Judith Fernandez, BS, DVM, MPH, CPH; Wai Kwan Wong, BSc; Rockey Kwonghung Fong, BVSc; Wei Ling Tan, BSc; Brian Zi Yan Tan, PhD; Youming Ng, BSc; Kyaw Thu Aung, MBBS, MSc, PGDip; Kurosh S. Mehershahi, PhD; Christopher Goh, MSc; Joanne Su Lin Kang, PhD; Timothy Barkham, MBBS, MSc, FRCPath; Adeline Oi Kheng Leong, MSc; Ramona Alikiteaga Gutiérrez, DVM, PhD; and Lee Ching Ng, PhD, have disclosed no relevant financial relationships.

Author affiliations: National Environment Agency, Singapore (M.L. Chau, M. Yap, S.H.P. Hartantyo, Y. Ng, K.T. Aung, C. Goh, J.S.L. Kang, A.O.K. Leong, R.A. Gutiérrez, L.C. Ng); Genome Institute of Singapore, Singapore (S.L. Chen); National University of Singapore, Singapore (S.L. Chen, K.S. Mehershahi); Agri-Food and Veterinary Authority of Singapore, Singapore (P.K.T. Chiew,

C.J. Fernandez, W.K. Wong, R.K. Fong, W.L. Tan, B.Z.Y. Tan); Nanyang Technological University, Singapore (P.K.T. Chiew, L.C. Ng); Tan Tock Seng Hospital, Singapore (T. Barkham)

DOI: <https://doi.org/10.3201/eid2312.170596>

¹These authors contributed equally to this article.

We assessed microbial safety and quality of raw fish sold in Singapore during 2015–2016 to complement epidemiologic findings for an outbreak of infection with group B *Streptococcus* serotype III sequence type (ST) 283 associated with raw fish consumption. Fish-associated group B *Streptococcus* ST283 strains included strains nearly identical (0–2 single-nucleotide polymorphisms) with the human outbreak strain, as well as strains in another distinct ST283 clade (57–71 single-nucleotide polymorphisms). Our investigations highlight the risk for contamination of freshwater fish (which are handled and distributed separately from saltwater fish sold as sashimi) and the need for improved hygienic handling of all fish for raw consumption. These results have led to updated policy and guidelines regarding the sale of ready-to-eat raw fish dishes in Singapore.

A major outbreak of group B *Streptococcus* (GBS) infection associated with consumption of a Chinese-style raw fish dish (*yusheng*) occurred in Singapore during 2015 and involved 238 persons during the first half of the year (1). The *yusheng* was typically made from sliced Asian bighead carp (*Hypophthalmichthys nobilis*) and snakehead (*Channa* spp.) and served as a side dish with porridge by food stalls within larger eating establishments. Persons with severe clinical cases had meningoencephalitis, bacteremia, and septic arthritis (2–4). GBS, or *Streptococcus agalactiae*, was identified as the causative agent (2,3).

GBS is found in ≈30% of healthy adults (5) and is a member of the human commensal gastrointestinal and genitourinary flora (4). GBS is a common cause of neonatal sepsis, is acquired by newborns from the vaginal flora of the mother, and is an increasingly common pathogen among vulnerable populations (6). The incidence of invasive disease in adults, particularly older adults, has been increasing (7,8). GBS is also a fish and bovine pathogen (9). Although GBS has been shown to colonize the gastrointestinal tract of humans linked to fish consumption (9), foodborne transmission leading to invasive disease has not been reported. Local epidemiologic investigations conducted separately (2,3) identified a single strain of GBS serotype III sequence type (ST) 283 as the causative agent of the outbreak in Singapore during 2015. GBS ST283 had previously been isolated from tilapia in Thailand (10) and in adult human cases in Hong Kong (11). However, GBS ST283 has not been reported to colonize the human gastrointestinal tract, although to date only 1 study of fish mongers and fish handlers has specifically looked for colonization by this strain (12).

We investigated microbial safety and quality of fish sold in the Singapore market during and after the outbreak during 2015 to trace the source of GBS ST283 and provide risk assessment data to support outbreak control and prevention measures. Shortly after identification of GBS ST283 as the cause of the outbreak, these data supported implementing a ban on the sale of ready-to-eat (RTE)

dishes containing raw freshwater fish, as well as imposing additional requirements for sale of RTE raw fish dishes made with saltwater fish (13). We report the results of our analysis, which might assist the review of guidelines for handling of fish meant for raw consumption in Singapore and other countries. This report offers unique food and environmental insights into the investigation of this outbreak and complements published epidemiologic findings (2,3).

Materials and Methods

Collection of Fish and Fish Tank Water Samples

We collected samples of fish commonly used for raw consumption (n = 997) and fish tank water for holding live freshwater fish (n = 102) along the supply chain in Singapore during August 2015–January 2016 (online Technical Appendix Table 1, <https://wwwnc.cdc.gov/EID/article/23/12/17-0596-Techapp1.pdf>). We tested samples for GBS, *Aeromonas* spp., *Listeria monocytogenes*, *Salmonella* spp., *Vibrio cholerae*, and *V. parahaemolyticus*, and determined *Escherichia coli* counts, *Staphylococcus aureus* counts, and standard plate counts (SPCs) (online Technical Appendix). We characterized selected species to determine their virulence potential (online Technical Appendix).

Statistical Analysis

We evaluated significant differences ($p < 0.05$) between bacterial counts (\log_{10} CFU/g) and presence of specific foodborne bacteria by using Kruskal-Wallis, Mann-Whitney, χ^2 , and Fisher exact tests as appropriate. We performed analysis by using SPSS version 24.0 software (IBM, Armonk, NY, USA).

Results

Raw Fish Samples from Food Stalls and Restaurants/Snack Bars

Although raw freshwater and saltwater fish were served as RTE food at food stalls, only raw saltwater fish were reportedly served at restaurants/snack bars. PCR positivity rates were 43.5% (20/46) for GBS and 23.9% (11/46) for GBS serotype III in sliced fish samples from food stalls. Fish sampled from restaurants/snack bars had significantly lower rates ($p < 0.05$) of 9.2% (26/282) for GBS and 0.7% (2/282) for GBS serotype III (Table). Among the 20 GBS PCR-positive samples from food stalls, 5 yielded isolates; these isolates were of serotype II ST652, serotype III ST283, serotype III ST335, and serotype V ST1 (online Technical Appendix Table 3). The GBS ST283 isolated was from a RTE sliced fish sample sold as grass carp collected from a food stall linked to a human case, as described (12). We did not detect GBS ST283 in samples from restaurant/snack

bars; however, we did find a range of other GBS, including serotypes Ia ST7, Ia ST103, Ia ST485, III ST651, III ST861, V ST1, V ST24, VI ST167, and VII ST1.

We found *Salmonella* serogroup B ST29 (serovar Stanley) (n = 2); *V. parahaemolyticus* (negative for *tdh*, *trh1*, and *trh2* genes) (n = 1); and non-O1 *V. cholerae* (n = 1) in freshwater fish samples from food stalls. We also isolated *V. cholerae* from saltwater fish samples, 1 from a food stall and 1 from a restaurant. We detected *L. monocytogenes* in 5 samples from restaurants/snack bars.

SPCs of most RTE raw freshwater (71.4%, 5/7) and saltwater (85.7%, 18/21) fish samples from food stalls exceeded the regulatory limit for RTE food (5 log₁₀ CFU/g) in Singapore (14). We observed no difference in SPCs for fish slices intended for raw consumption and cooking purposes (Figure 1). We also found that 24.8% (70/282) of saltwater fish samples from restaurants/snack bars did not comply with regulatory limits for SPCs, *E. coli* counts (1.3 log₁₀ CFU/g), or both (14). These results showed the poor quality of RTE raw freshwater and saltwater fish sold at food stalls in comparison to those sold at restaurants and snack bars.

Comparison of Freshwater and Saltwater Fish Samples from Fresh Produce Markets

Fish sold at food stalls were typically procured from local fresh produce markets. For the 62 samples of whole fish and fish parts we collected from these markets, we detected GBS ST283 in 28.2% (11/39) of the freshwater fish (Table), which included fish sold as tilapia, Asian bighead carp, grass carp, snakehead-haruan, snakehead-toman, and silver carp (online Technical Appendix Table 3). However, we did not detect GBS ST283 in saltwater fish. Other GBS strains detected among these fish include serotypes Ia ST7, Ia ST23, Ia ST24, and II ST28 (online Technical Appendix Table 3).

We detected *Aeromonas* spp. (48.4%, 30/62), *S. aureus* (27.4%, 17/62), non-O1 *V. cholerae* (12.9%, 8/62) and *V. parahaemolyticus* (negative for *tdh*, *trh1*, and *trh2* genes) (6.4%, 4/62) in fish samples from fresh produce markets. There was no difference in positivity rates of these organisms between freshwater and saltwater fish. We did not detect *L. monocytogenes* or *Salmonella* spp. in any fish samples collected from fresh produce markets.

Approximately 42% (15/36) of freshwater fish muscle samples had SPCs or *E. coli* counts, or both, exceeding regulatory limits for RTE food in Singapore (14). Positivity rates for GBS, GBS serotype III, and *E. coli*, as well as SPCs for saltwater fish, were significantly lower (p<0.05) (Figure 1; Table). *E. coli* and *S. aureus* counts for freshwater fish surfaces were significantly higher (p<0.05) than those for saltwater fish (Figure 2).

We collected 4 fish tank water samples from wet markets and supermarkets. One water sample and the live

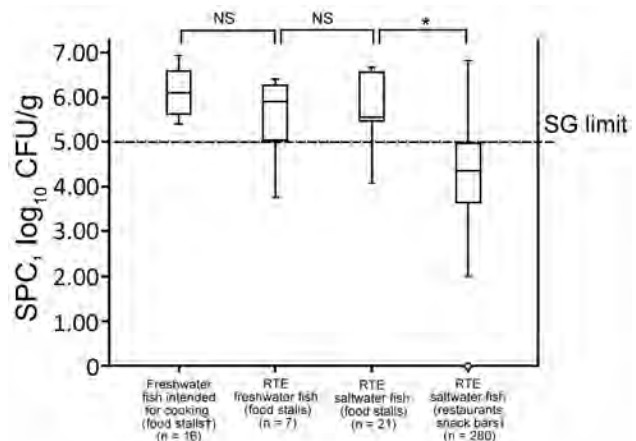


Figure 1. SPCs for sliced fish samples collected from various eating establishments during investigation of group B *Streptococcus* infections, Singapore, 2015–2016. Dashed horizontal line indicates regulatory limit of Singapore for SPCs for ready-to-eat foods (<5 log₁₀ CFU/g) (14). Top and bottom of boxes in plots indicate 25th and 75th percentiles, horizontal lines indicate medians, and whiskers indicate minimum and maximum values. *p<0.05. †Food stalls housed within larger eating establishments that include hawker centers, coffee shops, and eating houses. Open circle indicates an outlier. NS, not significant (p>0.05); RTE, ready to eat; SG, Singapore government; SPCs, standard plate counts.

freshwater fish the tank contained were positive for GBS by PCR and non-O1 *V. cholerae* by culture; the associated fish was positive for GBS ST283 by culture. Two other fish tank water samples and the live fish the tanks contained were positive for *E. coli*, *S. aureus*, or both. The level of *E. coli* detected in each positive fish tank water sample was 1.3 log₁₀ CFU/500 mL, which was greater than the 1 log₁₀ CFU/500 mL coliform (which includes *E. coli*) limit set by the British Columbia Centre for Disease Control (15).

Whole Freshwater Fish and Fish Tank Water from Ports

We tested for GBS only in whole fish and fish tank water samples collected from ports. We detected GBS ST283 in 1% (6/586) of freshwater fish samples; positive samples were from Asian bighead carps imported from and farmed in Malaysia. For 98 fish tank water samples collected from ports, 55.1% (54/98) were positive for GBS, and 6.1% (6/98) were positive for GBS ST283. Three of the GBS ST283–positive fish were kept in fish tank water that was also positive for GBS ST283.

Comparison of Saltwater Fish from Fresh Produce Markets and Sashimi Suppliers

Our data indicate the risk for contamination of fish sold at local fresh produce markets, although saltwater fish samples from fresh produce markets had lower rates of

Table. Positivity rates for GBS and other foodborne bacteria in fish samples, Singapore, 2015–2016*

Characteristic	Targeted bacteria, no. positive samples/no. tested (%)									
	All GBS	GBS serotype III	GBS serotype III ST283	<i>Aeromonas</i> spp.†	<i>E. coli</i>	<i>S. aureus</i>	<i>V. c.</i>	<i>V. p.</i>	<i>L. m.</i>	<i>Salmonella</i> spp.
Detection method	PCR	PCR	Culture, PCR	Culture	Culture	Culture	Culture	Culture	Culture	Culture
Ports										
Freshwater fish, n = 586	27/586 (4.6)	12/586 (2.0)	6/586 (1.0)	NT	NT	NT	NT	NT	NT	NT
Fresh produce markets‡										
Freshwater fish, n = 39	30/39 (76.9) ^a	14/39 (35.9) ^b	11/39 (28.2)	16/39 (41.0)	32/39 (82.0) ^c	11/39 (28.2)	6/39 (15.4)	2/39 (5.1)	0/39	0/39
Saltwater fish, n = 23	5/23 (21.7) ^a	2/23 (8.7) ^b	0/23	14/23 (60.9)	8/23 (34.8) ^c	6/23 (26.1)	2/23 (8.7)	2/23 (8.7)	0/23	0/23
Sashimi suppliers§										
Saltwater fish, n = 21	0/21	0/21	0/21	10/21 (47.6)	1/21 (4.7) ^f	0/21	0/21	0/21	1/21 (4.7)	0/21
Food stalls¶										
RTE freshwater fish, n = 7	5/7 (71.4)	4/7 (57.1)	1/7 (14.3)	NT	0/7	0/7 (0)	0/7	0/7	0/7	1/7 (14.3)
Freshwater fish for cooking, n = 18	8/18 (44.4)	4/18 (22.2)	0/18	NT	2/18 (11.1)	0/18	1/18 (5.6)	1/18 (5.6)	0/18	1/18 (5.6)
RTE saltwater fish, n = 21	7/21 (33.3) ^d	3/21 (14.3) ^e	0/21	NT	0/21	0/21	1/21 (5.0)	0/21	0/21	0/21
Restaurants, snack bars										
RTE saltwater fish, n = 282	26/282 (9.2) ^d	2/282 (0.7) ^e	0/282	NT	0/282	0/282	1/282 (0.4)	0/282	5/282 (1.8)	0/282

*A sample was considered positive when a specific organism was detected in ≥ 1 subsamples (surface, muscle, or organs) of a fish sample. Superscript letters a–e indicate a significant difference ($p < 0.05$) in positivity rates of targeted bacteria between fish types. *E. coli*, *Escherichia coli*; GBS, group B *Streptococcus*; *L. m.*, *Listeria monocytogenes*; NT, not tested; RTE, ready to eat; *S. aureus*, *Staphylococcus aureus*; ST283, sequence type 283; *V. c.*, *Vibrio cholerae*; *V. p.*, *V. parahaemolyticus*.

†*Aeromonas caviae*, *A. hydrophila*, and *A. sobria*.

‡Fish stalls at ports and wet markets, and fresh produce sections of supermarkets, excluding sashimi and sushi counters of supermarkets.

§Companies that supplied sashimi-grade fish to restaurants and snack bars.

¶Within larger eating establishments that include hawker centers, coffee shops, and eating houses.

contamination than freshwater fish samples. The SPCs and the positivity rates for *E. coli* in saltwater fish samples from sashimi suppliers were significantly lower ($p < 0.05$) than those for saltwater fish samples from fresh produce markets (Figure 3; Table), which suggested that the microbial quality of fish could be managed by improvements in handling throughout distribution channels. None of the saltwater fish muscle samples from sashimi suppliers exceeded the Singapore SPC ($5 \log_{10}$ CFU/g) and *E. coli* ($1.3 \log_{10}$ CFU/g) limits for RTE food (14). We did not detect GBS, *S. aureus*, *V. cholerae*, and *V. parahaemolyticus* in any fish samples collected from sashimi suppliers. However, we detected *L. monocytogenes* in 1 salmon sample.

Characterization of GBS Isolates

We detected 6 GBS serotypes (Ia, II, III, V, VI, and VII) and 13 STs (1, 7, 23, 24, 28, 103, 167, 283, 335, 485, 651, 652, and 861) in fish (online Technical Appendix Table 3). Although most strains were within clonal complexes (1, 10, 17, 19, and 23) associated with human carriage and diseases (16), a total of 20 isolates from 7 sashimi samples (SGEHI2015-IV45, SGEHI2015-IV72, SGEHI2015-IV74, SGEHI2015-IV89, SGEHI2015-IV100, SGEHI2015-IV211,

and SGEHI2015-IV232) did not belong to these clonal complexes. These strains had few closely related strains in the public genomic databases, and the closely related strains are mostly from animals (online Technical Appendix Figure 2).

We found GBS ST283 only among freshwater fish and water for holding freshwater fish. Genomic analyses indicated that GBS ST283 isolated from fish clustered in 2 clades (Figure 4). The first clade included 12 isolates from 6 fish from a food stall, a fresh produce market and a port, and 4 fish tank water samples from a port. Genome sequencing showed that these 12 isolates were nearly identical (0–2 SNPs and 0, 1, and 12 indels all in homopolymeric runs of >4 nt) compared with the 2.1-Mbp genome of the reference human outbreak strain, SG-M1, isolated from a meningitis patient during the GBS outbreak in Singapore during 2015 (12,17). Isolates that clustered into the second clade were 20 isolates from 12 fish and 2 fish tank water samples and did not include any human isolates either from this outbreak or from previous reports of human GBS infecting isolates. Sequences of these isolates showed higher intraclade diversity (57–71 SNPs and 11–33 indels) when compared with the SG-M1 genome (Figure 4).

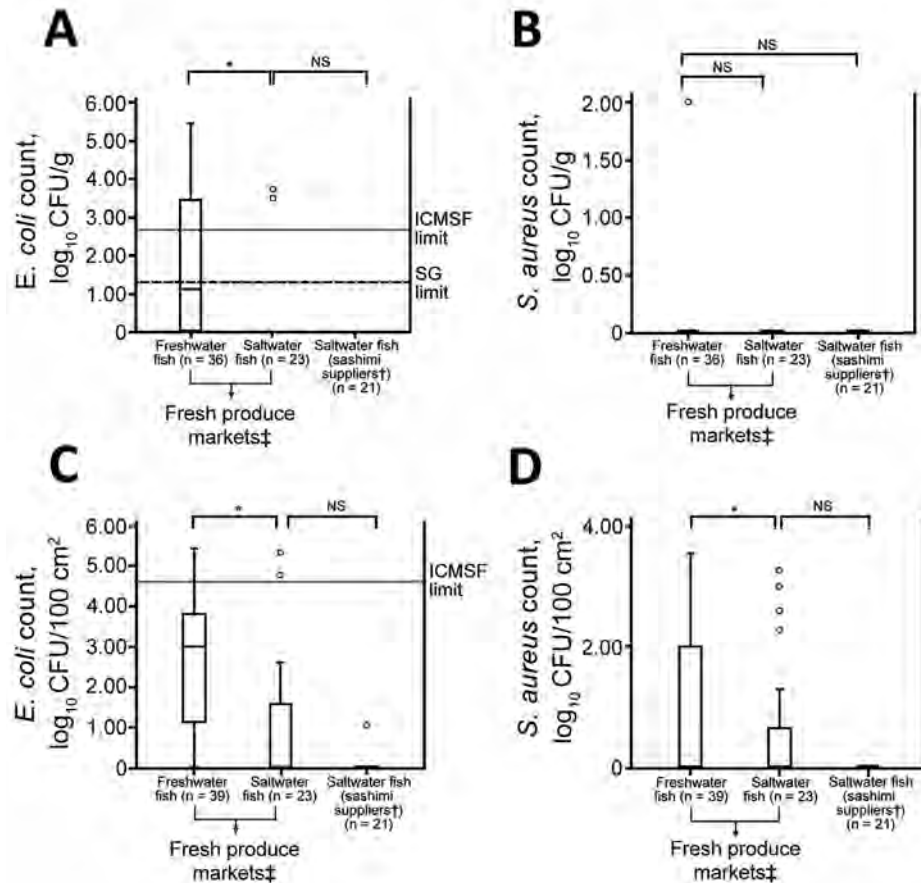


Figure 2. *Escherichia coli* (A and C) and *Staphylococcus aureus* (B and D) counts in fish muscle (muscle and surface swabs) collected from fresh produce markets during investigation of group B *Streptococcus* infections, Singapore, 2015–2016. Solid horizontal lines indicate ICMSF limit for *E. coli* count in fresh fish intended for cooking ($<2.7 \log_{10}$ CFU/g or $<4.7 \log_{10}$ CFU/100 cm²) (23). Dashed horizontal line indicates Singapore regulatory limit for *E. coli* count in ready-to-eat foods ($<1.3 \log_{10}$ CFU/g) (14). Top and bottom of boxes in plots indicate 25th and 75th percentiles, horizontal lines indicate medians, and whiskers indicate minimum and maximum values. Open circles indicate outliers. * $p < 0.05$. †Companies that supplied sashimi grade fish to restaurants and snack bars. ‡Fish stalls at ports and wet markets, as well as fresh produce sections of supermarkets, excluding sashimi and sushi counters of supermarkets. ICMSF, International Commission on Microbiological Specifications of Foods; NS, not significant ($p > 0.05$); SG, Singapore government; SPCs, standard plate counts.

Characterization of *S. aureus*, *V. cholerae*, and *V. parahaemolyticus* Isolates

We characterized 18 *S. aureus* isolates from 17 fish. All except 1 were obtained from fish surfaces. We detected >1 enterotoxin gene in two thirds of these isolates and the *sec* gene in 55.6% (10/18) of the isolates. Other enterotoxin genes (*sea*, *seg*, *seh*, *sei*, and *sel*) were detected at much lower rates (5.6% [1/18] to 11.1% [2/18]). We detected 4 enterotoxin genes (*sec*, *seg*, *sei*, and *sel*) in a *S. aureus* isolate obtained from the surface of a wolf herring sample collected from a port. We did not detect virulence genes (*ctxA*, *ctxB*, and *tcpA*) in any of the 16 non-O1 *V. cholerae* isolates from 9 fish and 1 fish tank water samples and did not detect virulence genes (*tdh*, *trh1*, and *trh2*) in any of the 6 *V. parahaemolyticus* isolates from 5 fish samples.

Discussion

We found GBS ST283, the causative strain of a severe foodborne outbreak in Singapore, in the local freshwater fish supply chain that stretches from food stalls to local fresh produce markets and back to ports. Patients with GBS ST283 infections during this outbreak were more likely to show development of meningoencephalitis, septic arthritis, and spinal infection than were persons with non-GBS

ST283 infections (12). Although this study suggested Malaysia as a source of the strain, the finding of the same ST in Hong Kong and Thailand (10,11) suggested that GBS ST283 is generally prevalent throughout the region.

Our analysis shows that there are at least 2 clades of GBS ST283 strains among fish in local markets. Fish and water strains from 1 clade were nearly identical to clinical strains from this outbreak (Figure 4). The small variability of 0–2 SNPs and 0–12 indels between fish and water strains and the reference human outbreak strain (SG-M1) is equivalent to variability observed in 131 clinical strains from the same outbreak reported elsewhere (0–5 SNPs from the SG-M1 reference) (12). Strains from a second clade of GBS ST283 had a difference of 57–71 SNPs and 11–33 indels when compared with the SG-M1 genome. Other GBS ST283 isolates, many collected in Hong Kong ≤ 17 years before this outbreak (11) are also different from the SG-M1 strain (≤ 129 SNPs) (Figure 4). We found no human-infecting isolate from Singapore or elsewhere within the second fish-associated GBS ST283 clade.

A major issue is whether all GBS ST283 strains are capable of causing invasive human disease by the foodborne route. If strains from the fish-associated clade are not pathogenic to humans, they could be used as effective controls for identifying the genetic basis of pathogenicity

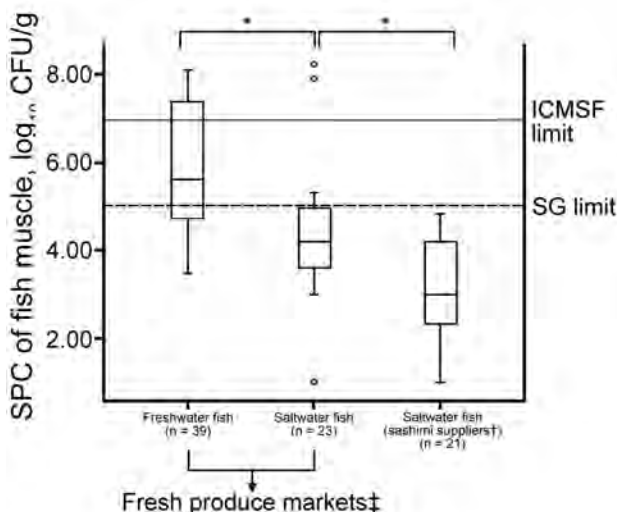


Figure 3. SPCs for fish samples (muscle) collected from fresh produce markets during investigation of group B *Streptococcus* infections, Singapore, 2015–2016. Solid horizontal line indicates ICMSF limit for SPCs in fresh fish intended for cooking ($<7 \log_{10}$ CFU/g) (23). Dashed horizontal line indicates Singapore regulatory limit for SPCs for ready-to-eat foods ($<5 \log_{10}$ CFU/g) (14). Top and bottom of boxes in plots indicate 25th and 75th percentiles, horizontal lines indicate medians, and whiskers indicate minimum and maximum values. Open circles indicate outliers. * $p < 0.05$. †Companies that supplied sashimi grade fish to restaurants and snack bars. ‡Fish stalls at ports and wet markets, as well as fresh produce sections of supermarkets, excluding sashimi and sushi counters of supermarkets. ICMSF, International Commission on Microbiological Specifications of Foods; SG, Singapore government; SPCs, standard plate counts.

of the first clade and the cause of its emergence, which resulted in outbreak in Singapore in 2015. If these strains are pathogenic to humans, then broader tracking of the prevalence of GBS ST283 would be warranted.

In contrast to GBS strains that are known to cause disease outbreaks in fish (10,18), the live and whole fish from which GBS ST283 was recovered in this study did not have defects, such as corneal opacity and exophthalmia (18), which suggests that this ST might not be pathogenic for freshwater fish. The closest GBS fish pathogens with published genomes, GD201008–001 (19) and HN016 (20), are serotype Ia ST7 strains that are distant ($>4,000$ SNPs) from all ST283 strains that our group and others have identified (12).

Detection of 6 GBS serotypes and 13 STs showed the diversity of GBS strains in fish. Although the sample size in this study was small and our results might not represent the distribution of GBS in all fish species, our findings provide valuable data for characterizing the public health risk from consuming raw fish. No baseline information on GBS in fish was publicly available before this outbreak because fish were not a recognized source or a recognized route of transmission of GBS. Further work on GBS STs

other than ST283 is underway to investigate the role of fish as a source of GBS disease in humans.

Several GBS strains from sashimi had relatively few closely related strains in the public genomic databases (online Technical Appendix Figure 2), which suggests that the GBS population associated with saltwater fish could be different from that associated with freshwater fish and humans. Another reason for this observation is that GBS from food and environmental sources are relatively undersampled in the genomic databases than those from humans.

We detected GBS serotypes Ia ST23 and Ia ST7, which are associated with human carriage (10), in fish samples. Although GBS ST7 has been described as a fish pathogen, the presence of GBS serotype Ia ST23 has not been reported in fish (10). GBS serotypes Ia ST23, and Ia ST7 and *E. coli*, which are all associated with human gut flora, suggest possible contamination of fish by effluent water.

The intentional introduction of animal feces into fish ponds as part of integrated farming (21,22) might further contribute to the complex flow of pathogens between animals and humans. Such findings point to areas for research to clarify the diversity and role of GBS strains in affecting animal and human health. For instance, GBS ST861, which was isolated from salmon in this study (online Technical Appendix Table 3), was also isolated from a clinical case in the same year in Singapore on the basis of metadata available in the PubMLST *S. agalactiae* database (<http://pubmlst.org/sagalactiae/>).

In addition to the finding of GBS ST283 in freshwater fish, detection of high SPCs and *E. coli* and *S. aureus* counts indicates the hazard of using such fish for preparing raw RTE dishes. Because *E. coli* is not part of the intestinal flora of cold-blooded animals (23), its presence suggests contamination from polluted water, unhygienic handling, or temperature abuse after harvesting. Similarly, because *S. aureus* is not part of usual fish flora, its presence on fish surfaces suggests possible transfer of human skin flora caused by unhygienic handling (24). We detected *V. parahaemolyticus*, an organism known to grow well in seawater but lyse rapidly in freshwater (24), in freshwater fish samples from fresh produce markets (5.1%, 2/39). This finding was not surprising because freshwater and saltwater fish are typically sold, handled, stored, and degutted within the same confined areas in fresh produce markets. Thus, despite lower SPCs and positive rates for *E. coli* in saltwater fish than in freshwater fish from fresh produce markets, saltwater fish procured from such environments are prone to cross-contamination.

Fish used by food stalls were generally obtained from such markets. Moreover, microbial counts for sliced fish samples from eating establishments indicated that most food stalls were not able to prepare RTE raw fish dishes of acceptable hygiene quality. Poor practices observed included

use of common chopping boards, knives, or slicers for preparing fish slices meant for raw consumption and cooking. If fish slices are contaminated, rinsing with water cannot improve their quality (online Technical Appendix).

In contrast to the quality of saltwater fish samples from fresh produce markets, all saltwater fish samples from

sashimi suppliers complied with local SPCs ($5 \log_{10}$ CFU/g) and *E. coli* ($1.3 \log_{10}$ CFU/g) limits for ready-to-eat food (14); all samples were negative for GBS, *S. aureus*, *Salmonella* spp., and *V. parahaemolyticus*. The compliance rate among restaurants/snack bars was higher because such premises are more likely to procure fish from

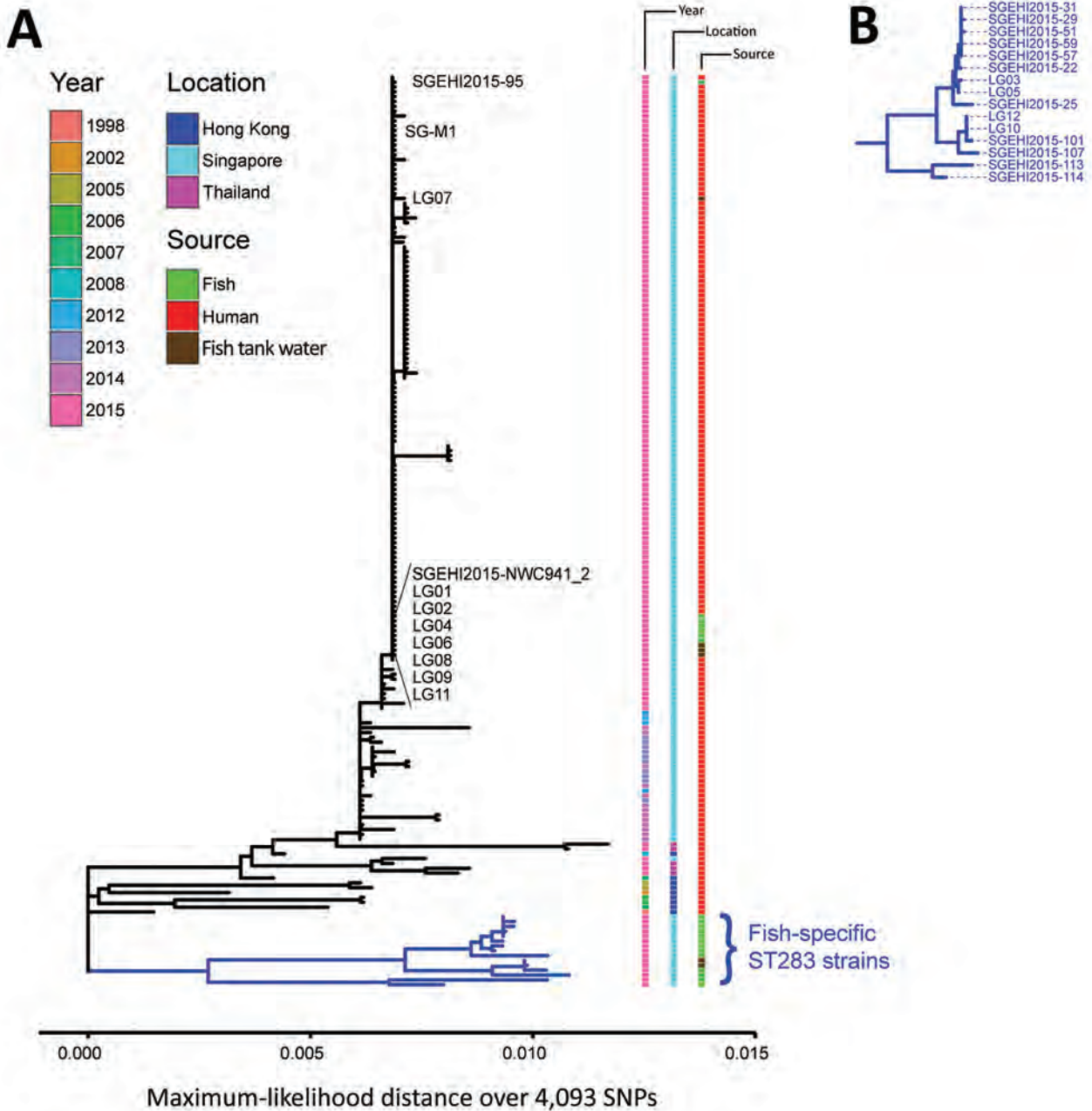


Figure 4. Phylogenetic analysis of group B *Streptococcus* (GBS) infections caused by improper sourcing and handling of raw fish for raw consumption, Singapore, 2015–2016. A) Maximum-likelihood single-nucleotide polymorphism (SNP)–based tree for GBS ST283 strains relative to the SG-M1 reference human outbreak strain. Year, location, and source (human or fish) for isolates are indicated. Twelve strains from 6 fish (SGEHI2015-NWC941, SGEHI2015–95, LG01, LG02, LG04, and LG06) and 4 fish tank water samples (LG07, LG08, LG09, and LG11) were nearly identical to the local reference outbreak strain SG-M1 (no SNP, 0 and 12 indels, respectively). Scale bar indicates distance over 4,093 total SNPs. B) Enlargement of blue subtree from bottom of tree in panel A showing fish GBS ST283 isolates that were different (57–71 SNPs and 11–33 indels) from the human outbreak strain. ST, sequence type.

sashimi suppliers that harvest fish from cleaner waters and adhere to stricter cold chain management practices. However, some saltwater fish samples from sashimi suppliers and restaurants were found to contain *Aeromonas* spp. (47.6%, 10/21) and *L. monocytogenes* (2.0%, 6/303), whose psychrotrophic nature has posed a challenge to the fish industry. *L. monocytogenes* is also a concern in chilled RTE food because of its ubiquity and persistence in food-processing environments (25).

Food and environmental findings of our study were consistent with epidemiologic findings for this outbreak (2,3). Multivariate analyses of a case–control study showed that persons who had consumed *yusheng* were more likely to acquire GBS ST283 infections than those who had not consumed *yusheng* (2). However, there was no strong association between GBS ST283 infections and consumption of sashimi and sushi (2).

Findings of this study have led to implementation of new policies in Singapore. These new policies included banning the use of freshwater fish in RTE dishes and requiring procurement of saltwater fish from suppliers for raw fish approved by the Agri-Food and Veterinary Authority of Singapore. Food stalls and food establishments providing catering services were required to stop selling RTE raw fish dishes until they complied with practices required for preparing RTE raw saltwater fish dishes.

The number of RTE fish samples collected from food stalls was limited because eating establishments were advised to stop the sale of RTE raw fish dishes containing Asian bighead carp and snakehead during July 24–December 5, 2015, while the outbreak investigation was underway (1). Sampling was not random because it was part of an outbreak investigation, but it was biased toward fish species and food stalls implicated in the outbreak. Thus, contamination rates might not reflect contamination rates of all fish species sold for raw consumption in the market. Similarly, testing of samples from ports and retail outlets was performed by using different protocols, which limited comparisons that could be made.

In conclusion, we detected GBS ST283, which caused a severe foodborne outbreak in Singapore in 2015, in freshwater fish, not only in food stalls and fish markets, but also in ports from which fish are imported. Comparison of human and fish isolates showed as few as 0–2 SNPs between human and fish isolates of GBS ST283 on a background of a diversity of GBS and other bacteria in freshwater fish. These data indicate the risk for contamination of raw freshwater fish and underscore the need for proper sourcing and handling of all fish for raw consumption. To control the outbreak, a ban on the sale of RTE raw freshwater fish dishes was implemented, and additional requirements were imposed for the sale of RTE raw fish dishes made with saltwater fish (13). Our

study complements the epidemiologic findings for this outbreak (2,3) and illustrates the need for public health authorities and industries to remain vigilant regarding emerging pathogens.

Acknowledgments

We thank the Agri-Food and Veterinary Authority of Singapore, the National Environment Agency, and the Ministry of Health of Singapore for providing operational support and Lyn Gilbert and Fanrong Kong for providing the GBS serotype VIII reference strain.

Analyses of fish and fish tank water samples was supported by the National Environment Agency and the Agri-Food and Veterinary Authority of Singapore. Whole-genome sequencing and analysis was supported by the Genome Institute of Singapore, the Agency for Science, Technology, and Research, and the Singapore Ministry of Health National Medical Research Council (NMRC/CIRG/1357/2013).

Ms. Chau is research group leader of the Applied Food Hygiene Epidemiology Group, Food and Environmental Hygiene Research Program, Environmental Health Institute, National Environment Agency, Singapore. Her research interests include microbiology, food hygiene and safety, and foodborne diseases.

References

1. Joint news release between the Ministry of Health Singapore (MOH) and the Agri-Food and Veterinary Authority of Singapore (AVA) and the National Environment Agency (NEA). Update on investigation into group B *Streptococcus* cases. July 24, 2015 [cited 2016 Aug 10]. <http://www.nea.gov.sg/corporate-functions/newsroom/news-releases/year/2015/month/7/category/food-hygiene/update-on-investigation-into-group-b-streptococcus-cases>
2. Tan S, Lin Y, Foo K, Koh HF, Tow C, Zhang Y, et al. Group B *Streptococcus* serotype III sequence type 283 bacteremia associated with consumption of raw fish, Singapore. *Emerg Infect Dis.* 2016;22:1970–3. <http://dx.doi.org/10.3201/eid2211.160210>
3. Rajendram P, Mar Kyaw W, Leo YS, Ho H, Chen WK, Lin R, et al. Group B *Streptococcus* sequence type 283 disease linked to consumption of raw fish, Singapore. *Emerg Infect Dis.* 2016; 22:1974–7. <http://dx.doi.org/10.3201/eid2211.160252>
4. Tan K, Wijaya L, Chiew HJ, Sitoh YY, Shafi H, Chen RC, et al. Diffusion-weighted MRI abnormalities in an outbreak of *Streptococcus agalactiae* serotype III, multilocus sequence type 283 meningitis. *J Magn Reson Imaging.* 2017;45:507–14. <http://dx.doi.org/10.1002/jmri.25373>
5. Manning SD, Neighbors K, Tallman PA, Gillespie B, Marrs CF, Borchardt SM, et al. Prevalence of group B *Streptococcus* colonization and potential for transmission by casual contact in healthy young men and women. *Clin Infect Dis.* 2004;39:380–8. <http://dx.doi.org/10.1086/422321>
6. Public Health Agency of Canada. *Streptococcus agalactiae*: pathogen safety data sheet—contaminated substances. April 30, 2012 [cited 2016 Aug 10]. <http://www.phac-aspc.gc.ca/lab-bio/res/psds-ftss/streptococcus-agalactiae-eng.php>
7. Ballard MS, Schönheyder HC, Knudsen JD, Lyytikäinen O, Dryden M, Kennedy KJ, et al.; International Bacteremia Surveillance Collaborative. The changing epidemiology of group B *Streptococcus* bloodstream infection: a multi-national population-

- based assessment. *Infect Dis (Lond)*. 2016;48:386–91. <http://dx.doi.org/10.3109/23744235.2015.1131330>
8. Phares CR, Lynfield R, Farley MM, Mohle-Boetani J, Harrison LH, Petit S, et al.; Active Bacterial Core surveillance/Emerging Infections Program Network. Epidemiology of invasive group B streptococcal disease in the United States, 1999–2005. *JAMA*. 2008;299:2056–65. <http://dx.doi.org/10.1001/jama.299.17.2056>
 9. Foxman B, Gillespie BW, Manning SD, Marrs CF. Risk factors for group B streptococcal colonization: potential for different transmission systems by capsular type. *Ann Epidemiol*. 2007;17:854–62. <http://dx.doi.org/10.1016/j.annepidem.2007.05.014>
 10. Delannoy CM, Crumlish M, Fontaine MC, Pollock J, Foster G, Dagleish MP, et al. Human *Streptococcus agalactiae* strains in aquatic mammals and fish. *BMC Microbiol*. 2013;13:41. <http://dx.doi.org/10.1186/1471-2180-13-41>
 11. Ip M, Cheuk ES, Tsui MH, Kong F, Leung TN, Gilbert GL. Identification of a *Streptococcus agalactiae* serotype III subtype 4 clone in association with adult invasive disease in Hong Kong. *J Clin Microbiol*. 2006;44:4252–4. <http://dx.doi.org/10.1128/JCM.01533-06>
 12. Kalimuddin S, Chen SL, Lim CTK, Koh TH, Tan TY, Kam M, et al.; Singapore Group B Streptococcus Consortium. 2015 epidemic of severe *Streptococcus agalactiae* ST283 infections in Singapore associated with the consumption of raw freshwater fish: a detailed analysis of clinical, epidemiological and bacterial sequencing data. *Clin Infect Dis*. 2017;64(Suppl_2):S145–52. <http://dx.doi.org/10.1093/cid/cix021>
 13. Joint news release between the Agri-Food and Veterinary Authority of Singapore (AVA) and the Ministry of Health Singapore (MOH) and the National Environment Agency (NEA). Freshwater fish banned from ready-to-eat raw fish dishes. December 5, 2015 [cited 2016 Aug 10]. <http://www.nea.gov.sg/corporate-functions/newsroom/news-releases/freshwater-fish-banned-from-ready-to-eat-raw-fish-dishes>
 14. Agri-Food and Veterinary Authority of Singapore. Sale of food act, chapter 283, section 56 (1), food regulations. December 20, 2016 [cited 2017 Jan 9]. <http://www.ava.gov.sg/legislation>
 15. British Columbia Centre for Disease Control. Food processing plants: guideline for live retail fish holding system. November 2013 [cited 2016 Aug 17]. http://www.bccdc.ca/resource-gallery/Documents/Educational%20Materials/EH/FPS/Food/RetailFishHoldingTankGuidelines_Nov2013trs.pdf
 16. Da Cunha V, Davies MR, Douarre PE, Rosinski-Chupin I, Margarit I, Spinali S, et al.; DEVANI Consortium. *Streptococcus agalactiae* clones infecting humans were selected and fixed through the extensive use of tetracycline. *Nat Commun*. 2014;5:4544. <http://dx.doi.org/10.1038/ncomms5544>
 17. Mehershahi KS, Hsu LY, Koh TH, Chen SL. Complete genome sequence of *Streptococcus agalactiae* serotype III, multilocus sequence type 283 strain SG-M1. *Genome Announc*. 2015;3:e01188–15.
 18. Abuseliana AF, Daud HH, Aziz SA, Bejo SK, Alsaïd M. Pathogenicity of *Streptococcus agalactiae* isolated from a fish farm in Selangor to juvenile red tilapia (*Oreochromis* sp.). *Journal of Animal and Veterinary Advances*. 2011;10:914–9. <http://dx.doi.org/10.3923/javaa.2011.914.919>
 19. Liu G, Zhang W, Lu C. Complete genome sequence of *Streptococcus agalactiae* GD201008-001, isolated in China from tilapia with meningoencephalitis. *J Bacteriol*. 2012;194:6653. <http://dx.doi.org/10.1128/JB.01788-12>
 20. Wang R, Li L, Huang Y, Luo F, Liang W, Gan X, et al. Comparative genome analysis identifies two large deletions in the genome of highly-passaged attenuated *Streptococcus agalactiae* strain YM001 compared to the parental pathogenic strain HN016. *BMC Genomics*. 2015;16:897. <http://dx.doi.org/10.1186/s12864-015-2026-y>
 21. Martins C, Eding EH, Verdegem MC, Heinsbroek LT, Schneider O, Blancheton J-P, et al. New developments in recirculating aquaculture systems in Europe: a perspective on environmental sustainability. *Aquacultural Engineering*. 2010;43:83–93. <http://dx.doi.org/10.1016/j.aquaeng.2010.09.002>
 22. Little D, Edwards P. Integrated livestock-fish farming systems. Rome: Food and Agriculture Organization of the United Nations; 2003 [cited 2017 Aug 15]. <http://www.fao.org/docrep/006/y5098e/y5098e00.htm>
 23. International Commission on Microbiological Specifications for Foods. Micro-organisms in foods 2: sampling for microbiological analysis; principles and specific applications. 2nd ed. 1986 [cited 2016 Aug 11]. <http://www.icmsf.org/pdf/icmsf2.pdf>
 24. Food and Drug Administration. Bad bug book: foodborne pathogenic microorganisms and natural toxins. 2nd ed. Silver Spring (MD): The Administration; 2012.
 25. Chau ML, Aung KT, Hapuarachchi HC, Lee PSV, Lim PY, Kang JSL, et al. Microbial survey of ready-to-eat salad ingredients sold at retail reveals the occurrence and the persistence of *Listeria monocytogenes* sequence types 2 and 87 in pre-packed smoked salmon. *BMC Microbiol*. 2017;17:46. <http://dx.doi.org/10.1186/s12866-017-0956-z>

Address for correspondence: Lee C. Ng, Environmental Health Institute, National Environment Agency, 11 Biopolis Way, #06-05/08, Helios Block, Singapore 138667, Singapore; email: Ng_Lee_Ching@nea.gov.sg

Distribution of Usutu Virus in Germany and Its Effect on Breeding Bird Populations

Renke Lühken, Hanna Jöst, Daniel Cadar, Stephanie Margarete Thomas, Stefan Bosch, Egbert Tannich, Norbert Becker, Ute Ziegler, Lars Lachmann, Jonas Schmidt-Chanasit

Usutu virus (USUV) is an emerging mosquito-borne flavivirus with an increasing number of reports from several countries in Europe, where USUV infection has caused high avian mortality rates. However, 20 years after the first observed outbreak of USUV in Europe, there is still no reliable assessment of the large-scale impact of USUV outbreaks on bird populations. In this study, we identified the areas suitable for USUV circulation in Germany and analyzed the effects of USUV on breeding bird populations. We calculated the USUV-associated additional decline of common blackbird (*Turdus merula*) populations as 15.7% inside USUV-suitable areas but found no significant effect for the other 14 common bird species investigated. Our results show that the emergence of USUV is a further threat for birds in Europe and that the large-scale impact on population levels, at least for common blackbirds, must be considered.

Usutu virus (USUV) is a mosquito-borne flavivirus that, together with West Nile virus (WNV), belongs to the Japanese encephalitis antigenic complex (1). Both viruses share a similar enzootic transmission cycle, with birds as amplifying hosts and ornithophilic mosquitoes as vectors (2). Mammals, including bats, horses, and humans, are considered incidental or dead-end hosts (3–6).

The clinical picture of human USUV infection includes fever, rash, jaundice, headache, nuchal rigidity,

Author affiliations: Bernhard Nocht Institute for Tropical Medicine, World Health Organization Collaborating Centre for Arbovirus and Hemorrhagic Fever Reference and Research, Hamburg, Germany (R. Lühken, H. Jöst, D. Cadar, E. Tannich, J. Schmidt-Chanasit); German Centre for Infection Research (DZIF), partner site Hamburg-Luebeck-Borstel, Hamburg (H. Jöst, E. Tannich, J. Schmidt-Chanasit); University of Bayreuth, Bayreuth, Germany (S.M. Thomas); Nature and Biodiversity Conservation Union (NABU), Stuttgart, Germany (S. Bosch); Institute for Dipterology, Speyer, Germany (N. Becker); University of Heidelberg, Heidelberg, Germany (N. Becker); Friedrich-Loeffler-Institut, Greifswald-Insel Riems, Germany (U. Ziegler); Nature and Biodiversity Conservation Union (NABU), Berlin, Germany (L. Lachmann)

DOI: <https://doi.org/10.3201/eid2312.171257>

hand tremor, and hyperreflexia (7). It has been generally assumed that the incidence of human USUV infections is very low compared with the incidence of WNV infections. However, this assumption is probably strongly biased by the comparatively low capacity to correctly identify USUV infection in humans (2,8). Recent data from Italy indicate that human USUV infections may not be a sporadic event and can even be more frequent than WNV infections in areas where both viruses co-circulate (9).

The most common recent ancestor of the USUV strains circulating in Europe emerged in Africa at least 500 years ago (10). In 1996, the first recognized USUV outbreak outside Africa caused a massive die-off among common blackbirds (*Turdus merula*) in the Tuscany region of Italy (11). During the next 2 decades, USUV was observed in several countries in Europe as responsible for periodic small epizootic outbreaks affecting birds (2,12). In Germany, the earliest observation of USUV was in 2010 in mosquitoes (13) and resulted in mass deaths of common blackbirds (12,14) and at least 2 human USUV infections (4,6).

Mosquito-borne pathogens such as WNV (15) or avian malaria (16) could have substantial negative effects on bird populations, such as the size of affected populations (15) or composition of species communities (16). Several bird taxa of different taxonomic orders were found to be susceptible to USUV infections (2); during the USUV outbreaks in Europe, common blackbirds accounted for the largest proportion of observed dead birds (2). The effect of USUV on the populations of this species is discussed in different studies, which gave different estimates for population declines. Savini et al. (17) estimated 1,000 deaths for blackbirds in Veneto, Italy, in 2008–2009. During the USUV outbreak in Vienna, Austria, and surrounding areas in 2003–2005, Steiner and Holzer (18) observed a population decline of ≈90%. Furthermore, Rubel et al. (19) estimated that only 0.2% of all dead blackbirds were detected by the national USUV monitoring program in Austria (20), and therefore, ≈50,000 birds died during the outbreak. Using the same method of estimation, ≈40,000 common blackbirds died in the earliest known outbreak

(2011–2012) in Germany (21). Further studies in Germany estimated 220,000–420,000 dead common blackbirds (22) and a local population reduction of >50% (23).

The existing studies lack 2 conditions: an explicit spatial distinction between areas in which USUV circulates and those in which it does not; and the analysis of long-term bird population data, which are necessary to test the hypotheses that USUV caused substantial population declines in birds. Therefore, 20 years after the first observed outbreak of USUV in Europe (11), a reliable assessment of the large-scale impact of USUV outbreaks on bird populations is missing. Identifying the population-level effects of the disease is challenging, because they must be distinguished from natural population fluctuations driven by environmental factors such as climate (15) or land use change (24). Thus, the analyses require long-term bird abundance data that extend before and after the emergence of the disease and that cover areas with and without circulation of the pathogen. Hence, the aims of this study were the identification of areas suitable for USUV circulation in Germany using a distribution modeling approach based on dead bird surveillance data and the comparative analysis of USUV effects on the breeding bird populations in USUV-suitable areas.

Materials and Methods

Distribution Modeling Data

The USUV data in Germany were collected as part of a dead bird surveillance program (12,14,25,26). After the description of a USUV outbreak in wild birds in Germany in 2011, we requested, by press releases and media dissemination, that citizens send dead birds for USUV screening at national reference laboratories. We necropsied the bird specimens and screened them for USUV-specific RNA. During August 2011–November 2015, a total of 230 specimens of 15 species (85.7% common blackbirds) from 132 different sites tested positive for USUV. We used European Land Surface Temperature (EuroLST) dataset maps with 9 bioclimatic variables at 250-m resolution as explanatory variables for the distribution modeling of USUV (27). Bioclimatic variables are derived from monthly temperature and rainfall values. These biologically meaningful variables represent annual trends, seasonality, and extreme or limiting environmental factors.

USUV Distribution Modeling

We applied an ensemble boosted regression tree (BRT) approach using R software (<https://www.r-project.org>) with the packages raster, dismo, and ecospat and visualized with ggplot2, which was successfully applied to other mosquito-borne viruses in the past (e.g., Zika virus) (28). We calibrated BRT models with presence-only data

and 10,000 random background points selected from the entire area of Germany. To account for the biased bird collection due to the unsystematic dead bird surveillance program and to increase the robustness of model predictions and quantify model uncertainty, we selected 300 random subsamples of the presence data with replacement. Due to locality uncertainties in the presence data (e.g., mobility of the birds and imprecise reporting by the volunteer senders), we applied a random point selection within the corresponding German postal code areas (0.31–891.68 km², mean size 32.00 km²) for all presence points (i.e., sites with birds testing positive for USUV) in each subsample. In addition, we selected a new set of 10,000 random background points for each model. We weighted background points and occurrence points equally in each of the 300 BRT models, which we averaged for the final USUV distribution map. We converted the continuous distribution map for USUV to a binary map with areas that are suitable or unsuitable for USUV. Following Pigott et al. (29), we selected a threshold that included 90% of the USUV occurrence points. We chose a threshold cutoff of 90% instead of 100% to account for potential spatial inaccuracies of the occurrence point dataset.

We validated the models with a 10-fold cross-validation approach. We produced a total of 300 random split sampling datasets with 10 subsets for training datasets (comprising 10% of the presence and background observations) and 10 subsets for test datasets (comprising 90% of the presence and background observations) each. We used the training datasets to assess the ability of the models to predict the test dataset with the area under the curve (AUC) statistic. We averaged the AUC values of the models across the 10 models of each split sampling dataset and finally across the 300 average AUC values. Furthermore, we applied a pairwise distance sampling procedure to avoid AUC inflation due to spatial sorting bias, which is considered to give a more realistic quantification of the model performance especially regarding its transferability (30).

Bird Population Data

Bird abundance data were collected within the citizen science program Stunde der Gartenvögel (Hour of the Garden Birds) in Germany. This program is organized by the German BirdLife partner Naturschutzbund Deutschland (Nature and Biodiversity Conservation Union) and its counterpart Landesbund für Vogelschutz in Bayern (Bavarian Society for the Protection of Birds). During the second weekend of May each year, German citizens were requested to count the maximum number of specimens per bird species observed in their gardens in a time frame of 1 hour. We used the data for the 15 most commonly detected bird species, with at least 247,000 observed specimens each during 2006–2016, for further analyses: Eurasian

blue tit (*Cyanistes caeruleus*), common chaffinch (*Fringilla coelebs*), Eurasian magpie (*Pica pica*), European greenfinch (*Chloris chloris*), black redstart (*Phoenicurus ochruros*), great tit (*Parus major*), common blackbird, house sparrow (*Passer domesticus*), Eurasian tree sparrow (*Passer montanus*), common swift (*Apus apus*), common house martin (*Delichon urbicum*), carrion crow (*Corvus corone*), common wood pigeon (*Columba palumbus*), European robin (*Erithacus rubecula*), and common starling (*Sturnus vulgaris*). The dataset consisted of 317,533 unique observation datasets with anonymized sampling locations at the level of postal code regions in Germany, each giving information on the number of specimens per bird species and sampling site.

Bird Population Modeling

We applied a generalized additive model approach to analyze the population development of each of the 15 bird species. This statistical approach was first developed by Fewster et al. (31) to describe population trends in breeding birds and later successfully used to model bird and bat populations (32,33). We used the GAM framework to fit a single smoothed curve to the trend of the number of bird specimens in the USUV-positive areas and USUV-negative areas per year. In addition, to allow for differences in relative abundances between sites, we included a site term in the models. Following the suggestion by Fewster et al. (31), we set the selection of the degree of smoothing in the GAM to 0.3 times the number of years of the survey data ($df = 3$).

We avoided the problems of temporal autocorrelation within the abundance data (31) and overdispersion (34) by using a bootstrap approach. We produced CIs around the smoothed trends with a total of 300 bootstrap samples by resampling with replacement observations from the original dataset for each bird species. We classified each sampling site of the bird population data to be located in the USUV-positive or USUV-negative area on the basis of site coordinates and the USUV binary map. Spatial information of the bird observation sites was available only at the level of postal code regions; therefore, for each bootstrap sample, we took the mean of observed specimens per species within each region and then randomly assigned it within its postal code region to classify it as within the USUV-suitable or USUV-unsuitable area.

We set 2011 as the baseline year (index = 100); this year was the last time bird abundance data were collected before the first epizootic outbreak of USUV in Germany (14). Nonoverlapping 95% bootstrap CIs with index = 100 and nonoverlapping 95% bootstrap CIs between the USUV-suitable areas and USUV-unsuitable areas in 2016 were interpreted as a statistically significant difference ($p < 0.05$).

Results

The mean of the ensemble of 300 BRTs indicated the highest probability for USUV circulation in southwestern Germany (Figures 1, 2; online Technical Appendix Figure 1, <https://wwwnc.cdc.gov/EID/article/23/12/17-1257-Techapp1.pdf>). Environmentally suitable areas extended from southwestern Germany at the border with France along the valley of the Upper Rhine toward western Germany. The area represented 9,510 km² of the country (2.7%). The EuroLST bioclimatic variable with the strongest influence on USUV risk was the annual mean temperature, contributing 71.4% to the variation in the ensemble of models. The next most influential variables were mean temperature of the coldest quarter of the year (8.9%), temperature seasonality (7.2%), and minimum temperature of the coldest month (5.2%). The other 5 variables had <5.0% effect each on USUV risk: mean temperature of the warmest quarter (2.8%), mean diurnal range (1.6%), temperature annual range (1.3%), maximum temperature of the warmest month (1.2%), and isothermality (0.4%) (online Technical Appendix Figure 2). With an AUC value of 0.89 (± 0.08 SD), 10-fold cross-validation indicated high predictive power of the BRT ensemble map.

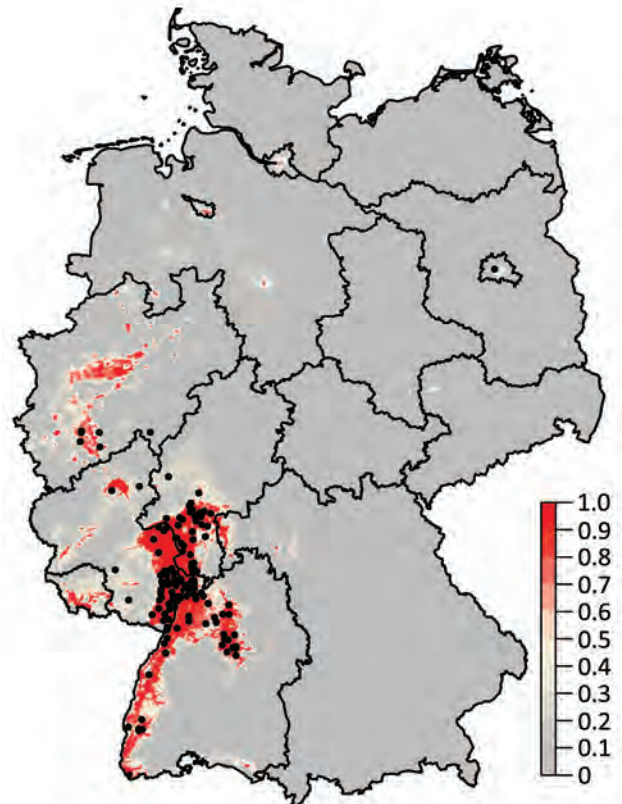


Figure 1. Probability of Usutu virus (USUV) occurrence in Germany derived from 300 boosted regression tree models. Black dots denote sites with dead birds that tested positive for USUV. The color intensity indicates the probability of occurrence of USUV.

Eleven of 15 bird species analyzed did not show a statistically significant difference in the population development between the areas suitable and unsuitable for USUV since 2011. We determined overlapping 95% bootstrap CIs between USUV-suitable and USUV-unsuitable areas for 2016 (Table; online Technical Appendix Figure 3). Only 4 species had nonoverlapping CIs in 2016 (Table; Figure 3), that is, statistically significant different population indices between both areas. However, the great tit and house sparrow showed higher population indices in the USUV-suitable areas, indicating no negative population impact of USUV. The Eurasian tree sparrow had a statistically significant lower population index in the USUV-suitable area, but the species' populations showed a very sharp positive development in both areas compared with the baseline year 2011. Thus, with a difference of $\approx 15.7\%$ between the means of population indices in 2016, only the common blackbird showed both a statistically significant lower population index compared with the baseline year (CIs < 100) and a statistically significant lower population index in the USUV-suitable area compared with the USUV-unsuitable area (nonoverlapping CIs between both areas).

Discussion

During the past 2 decades, an ongoing spread of USUV and a continuous circulation of the virus after initial establishment have been observed in different countries in Europe (2,10), highlighting the demand to understand the distribution of USUV and its ecosystem effects in the outbreak areas. Due to the enzootic transmission cycle of USUV with birds as amplifying hosts, the question regarding the effect of the virus on avian populations in particular was open. In this study, we compared the population dynamics of 15 common bird species between regions in Germany identified as USUV-suitable and USUV-unsuitable. Previous assessments were particularly limited by the missing explicit spatial distinction between areas with and without circulation of USUV. In addition, these studies did not distinguish population-level impacts of the disease from the natural fluctuations; that is, they did not use long-term bird abundance data that extend before and after the emergence of the first USUV outbreak.

Therefore, in a first step, we applied a distribution modeling approach to identify areas with and without potential circulation of USUV in Germany. The applied modeling approach was previously shown to be suitable to map the distribution of mosquito-borne viruses like dengue virus (35) or Zika virus (28). Potential outbreak areas for USUV were predominantly located in southwestern Germany, where the annual mean temperature was the most influential variable explaining the observed distribution (i.e., the virus showed an increasing probability of occurrence

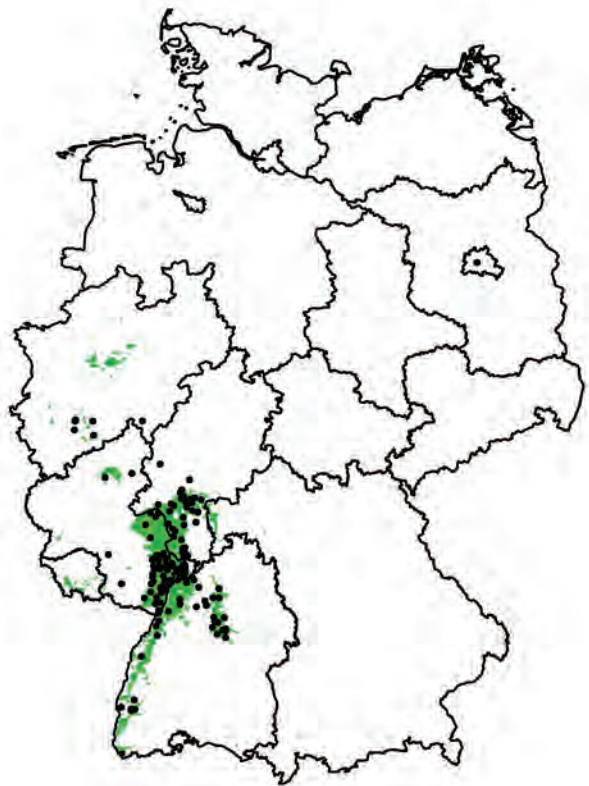


Figure 2. Areas suitable (green) and unsuitable (white) for Usutu virus (USUV) in Germany derived from 300 boosted regression tree models. Black dots denote sites with dead birds detected positive for USUV.

with increasing annual mean temperatures). Although the main transmission parameters of USUV are unknown (e.g., extrinsic incubation period), temperature is probably one of the most important drivers of USUV circulation, because the mosquito vectors are exothermic and the replication rate of the viruses increases as temperature increases. For example, laboratory experiments demonstrated that higher temperatures resulted in higher USUV infection rate of *Culex pipiens* mosquitoes (36). Nevertheless, although the ensemble of boosted regression tree models had a high performance in the differentiation of areas suitable and unsuitable for USUV in Germany, it should be kept in mind that this estimation has some degree of uncertainty. A high probability of occurrence for USUV does not necessarily mean that the virus ultimately arrives and establishes itself (28). In addition to environmental suitability, different additional parameters influence the spread and circulation of arboviruses, including vector/host mobility or herd immunity (19,37).

Furthermore, the annual dynamics of USUV highly depend on the temporal temperature profile within the course of the year. The high activity of USUV in the late summer and beginning of autumn 2016, for example, was

Table. Bird population indices by species differentiated USUV-suitable and USUV-unsuitable areas, Germany, 2016*

Species	Mean population index, % (95% CI)		Difference in mean change between areas, %†
	USUV-suitable area	USUV-unsuitable area	
Eurasian blue tit (<i>Cyanistes caeruleus</i>)	115.0 (108.3–120.8)	107.5 (105.8–108.8)	7.5
Common chaffinch (<i>Fringilla coelebs</i>)	98.5 (93.0–104.4)	93.6 (91.8–95.4)	4.9
Eurasian magpie (<i>Pica pica</i>)	104.1 (98.4–109.9)	97.0 (95.5–98.4)	7.0
Eurasian tree sparrow (<i>Passer montanus</i>)	560.8 (428.4–760.6)	2,318.7 (2,097.0–2,511.5)	–1,757.8
European greenfinch (<i>Chloris chloris</i>)	78.2 (72.5–83.6)	76.1 (74.6–77.4)	2.1
Black redstart (<i>Phoenicurus ochruros</i>)	49.8 (46.0–53.2)	50.4 (49.5–51.3)	0.6
Common blackbird (<i>Turdus merula</i>)	79.7 (77.1–82.3)	95.4 (94.6–96.2)	–15.7
House sparrow (<i>Passer domesticus</i>)	100.8 (94.0–106.8)	88.7 (87.2–90.2)	12.1
Great tit (<i>Parus major</i>)	114.5 (108.6–120.2)	105.5 (104.1–106.8)	9.0
Common swift (<i>Apus apus</i>)	67.7 (59.6–76.7)	73.2 (70.9–75.9)	–5.6
Common house martin (<i>Delichon urbicum</i>)	74.8 (66.8–83.1)	73.9 (71.4–76.5)	0.9
Carrion crow (<i>Corvus corone</i>)	129.8 (107.4–155.2)	119.3 (113.8–123.6)	10.5
Common wood pigeon (<i>Columba palumbus</i>)	191.4 (172.2–212.6)	175.0 (170.6–180.0)	16.5
European robin (<i>Erithacus rubecula</i>)	101.1 (94.5–108.0)	97.8 (95.9–99.5)	3.3
Common starling (<i>Sturnus vulgaris</i>)	106.9 (98.9–115.1)	115.8 (112.8–118.9)	–8.8

*USUV, Usutu virus.

†The difference in the mean change shows the magnitude and direction of divergence between the USUV-suitable and USUV-unsuitable area, i.e., a negative value indicates a lower population index for the USUV-suitable compared to the USUV-unsuitable area.

linked to temperature anomalies in September; significant positive deviation from the 30-year mean temperatures will have shortened the extrinsic incubation period and, at the same time, potentially caused increased vector abundance and associated vector-host contact rate (12,19).

We observed a statistically significant stronger decline of the population in the USUV outbreak areas compared with the USUV-unsuitable area was observed only for the common blackbird and not for any other analyzed bird taxa, including species regularly tested positive for USUV in Europe (e.g., house sparrow and common starling) (2). This finding is in contrast to other mosquito-borne avian viruses, which often show negative effects on the populations of several bird species at the same time; WNV in North America negatively affected the populations of ≥7 bird species, leading to population reduction of up to 45% (15), and avian malaria parasites potentially caused the extinction of several bird taxa in Hawaii, USA (16). One possible explanation might be that population declines of some species are masked by natural population dynamics or spatial-temporal variability of the population fluctuations (15), such as those caused by largely neglected bird pathogens like polyomaviruses (38). Nevertheless, although USUV can infect >30 bird taxa, blackbirds are generally by far the most frequently affected species, comprising >60% of all bird specimens testing positive for USUV in Europe (2). The underlying causes of a remarkably higher frequency of USUV-positive common blackbirds compared with other bird species are unknown, but some factors may include the wide distribution and abundance of the species (39), its conspicuous size and color, and its close association with humans (40), all of which might contribute to the high recovery rate of blackbird bodies. Potential reasons for a higher sensitivity to USUV might be a higher virus susceptibility (41), behavioral traits (42),

or different spatial-temporal distribution in relation to the vector/virus distribution (43).

During the USUV outbreak in Germany, the common blackbird population decreased by an additional 15.7% in the USUV-suitable area compared with the USUV-unsuitable area. Thus, assuming a mean density of 111.93 birds/km² (8 million breeding pairs each having approximately 3 fledglings per year [44] and a USUV-suitable area of 9,510 km²), ≥167,119 birds died due to USUV since 2011; this estimate does not include other population effects like immigration compensating a part of the USUV-related population decline. The estimate is substantially higher than the one determined in the study by Bosch et al. (21), assuming 40,000 common blackbird deaths in the USUV outbreak in Germany in 2011–2012, which did not account for persistent USUV-related deaths. At the same time, the overall population decline of the common blackbird is considerably smaller than 50%–90% (22,23), which might reflect only the short-term population declines. Nevertheless, several studies reported local extinction of common blackbirds probably caused by the USUV outbreak (18,21,22), which can be explained by local high virus transmission (e.g., favorable distribution of vectors and hosts). A relatively large spatial heterogeneity of the impact of mosquito-borne viruses on bird populations was also observed for WNV in North America (15); that rate is potentially related to the connection between the local vector and the bird community and influenced by land use and climate parameters (43).

USUV activity after the first outbreak in Germany in 2011–2012 was remarkably lower in the following years, as reflected in the detection of fewer USUV-positive dead birds (25,26). However, the common blackbird population in the USUV-suitable areas continued to decline after the initial outbreak. A similar observation was made for WNV

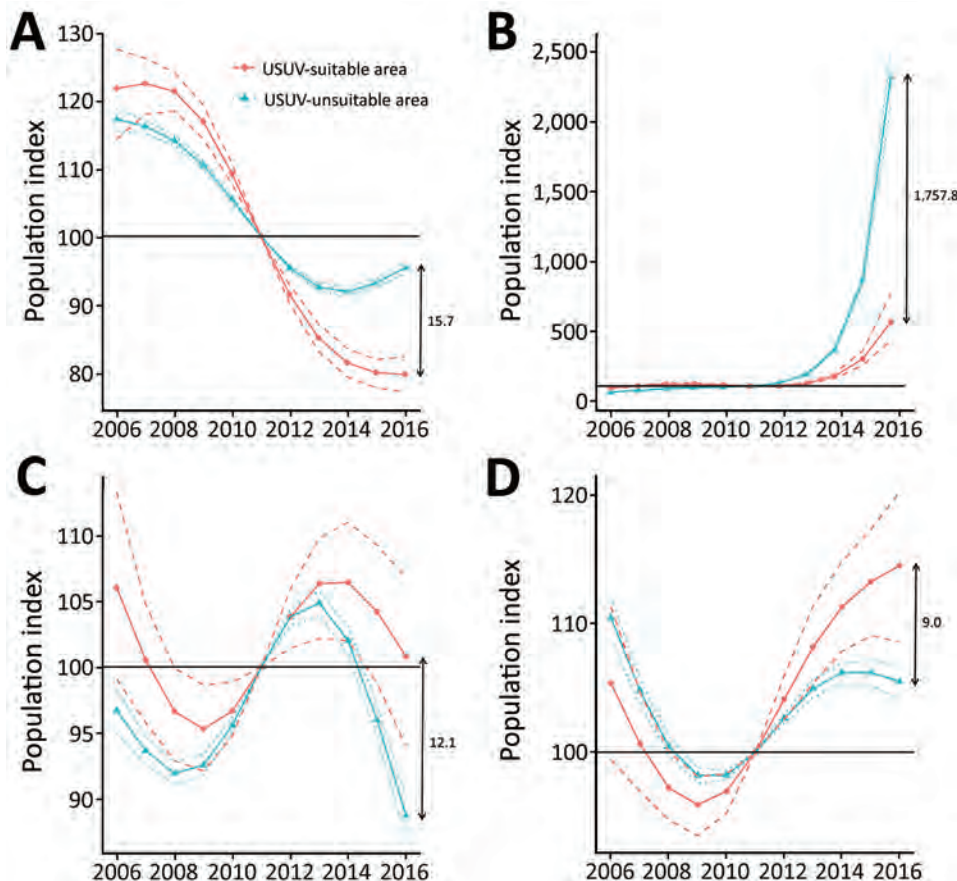


Figure 3. Index curves of the generalized additive model (GAM) approach with 300 bootstraps for breeding bird survey data of 4 bird species for Usutu virus (USUV)–suitable and USUV-unsuitable areas in Germany, 2016. A) Common blackbird; B) Eurasian tree sparrow; C) house sparrow; D) great tit. Solid lines indicate the mean indices from a GAM with 3 df; dashed/dotted lines represent nonoverlapping 95% bootstrap CIs. The horizontal line indicates the baseline year 2011 (index = 100), which is the last time point when bird abundance data were collected before the first known epizootic outbreak of USUV in Germany. Double arrows indicate the difference between the mean index curves for 2016.

in North America, which has a persistent impact for different bird species resulting in a lower survival rate without signs of recovery after the first outbreak of the virus (45). Therefore, due to the ongoing and widespread circulation of USUV in Central Europe (12), we must expect a long-term decline of common blackbird populations in areas with USUV occurrence, leading to a substantial alteration of the bird communities in the European USUV outbreak areas.

We still lack comprehensive data on the interaction between USUV and its vectors, hosts, and environmental parameters. We need data on the avian hosts to clarify the epidemiology of USUV and investigation into ecologic consequences, especially if they increase the risk of infection for humans. For example, the high mortality rate among common blackbirds might increase the chance of USUV spillover to humans, because the dead hosts are not present as immune or dead-end hosts (15,43,46,47). In addition, although no USUV effect was found for bird species classified as threatened (e.g., common starling) (48), a wide variety of bird species may be susceptible to USUV infections (2). Therefore, further studies should also focus on bird species not covered by the bird abundance dataset used here, such as wetland birds, which occupy areas that generally harbor high numbers of mosquitoes (49).

In summary, USUV had a statistically significant negative impact on the population of common blackbirds in suitable areas in Germany: a lower population index compared with the baseline year (CIs <100) and a statistically significant lower population index in the USUV-suitable area compared with the USUV-unsuitable area (nonoverlapping CIs between both areas). We observed no significant effect for the other 14 bird species included in the study. Five years after the first detection of USUV in southwest Germany, the circulation of the virus resulted in an additional decline of $\approx 15.7\%$ in the common blackbird populations compared with the development of populations not affected by USUV. Avian populations are under different threats, including changes of land use and climate change (15,24). The emergence of USUV in Europe is a further threat that can cause substantial changes in ecosystem services provided by birds, such as seed dispersal (50). The recent outbreak of USUV in 4 Central European countries (Germany, Netherlands, Belgium, and France) underlines the large-scale distribution of USUV spanning from southern to central Europe (2,12). In conclusion, USUV could affect bird populations, at least common blackbirds, across Europe.

Acknowledgments

We thank Heike Baum and Alexandra Bialonski for assistance in the laboratory work.

This work was financially supported by the German Federal Ministry of Food and Agriculture (BMEL) through the Federal Office for Agriculture and Food (BLE), grant no. 2819104315.

Dr. Lühken is a researcher at the Bernhard Nocht Institute for Tropical Medicine, World Health Organization Collaborating Centre for Arbovirus and Hemorrhagic Fever Reference and Research, Hamburg, Germany. His main research focus is the spatiotemporal distribution of vectors and associated pathogens.

References

- De Madrid AT, Porterfield JS. The flaviviruses (group B arboviruses): a cross-neutralization study. *J Gen Virol.* 1974; 23:91–6. <http://dx.doi.org/10.1099/0022-1317-23-1-91>
- Nikolay B. A review of West Nile and Usutu virus co-circulation in Europe: how much do transmission cycles overlap? *Trans R Soc Trop Med Hyg.* 2015;109:609–18. <http://dx.doi.org/10.1093/trstmh/trv066>
- Barbic L, Vilibic-Cavlek T, Listes E, Stevanovic V, Gjenero-Margan I, Ljubin-Sternak S, et al. Demonstration of Usutu virus antibodies in horses, Croatia. *Vector Borne Zoonotic Dis.* 2013;13:772–4. <http://dx.doi.org/10.1089/vbz.2012.1236>
- Cadar D, Maier P, Müller S, Kress J, Chudy M, Bialonski A, et al. Blood donor screening for West Nile virus (WNV) revealed acute Usutu virus (USUV) infection, Germany, September 2016. *Euro Surveill.* 2017;22:30501. <http://dx.doi.org/10.2807/1560-7917.ES.2017.22.14.30501>
- Cadar D, Becker N, Campos RM, Börstler J, Jöst H, Schmidt-Chanasit J. Usutu virus in bats, Germany, 2013. *Emerg Infect Dis.* 2014;20:1771–3. <http://dx.doi.org/10.3201/eid2010.140909>
- Allering L, Jöst H, Emmerich P, Günther S, Lattwein E, Schmidt M, et al. Detection of Usutu virus infection in a healthy blood donor from south-west Germany, 2012. *Euro Surveill.* 2012;17:20341.
- Vilibic-Cavlek T, Kaic B, Barbic L, Pem-Novosel I, Slavic-Vrzic V, Lesnikar V, et al. First evidence of simultaneous occurrence of West Nile virus and Usutu virus neuroinvasive disease in humans in Croatia during the 2013 outbreak. *Infection.* 2014;42:689–95. <http://dx.doi.org/10.1007/s15010-014-0625-1>
- Calzolari M, Bonilauri P, Bellini R, Albieri A, Defilippo F, Maioli G, et al. Evidence of simultaneous circulation of West Nile and Usutu viruses in mosquitoes sampled in Emilia-Romagna region (Italy) in 2009. *PLoS One.* 2010;5:e14324. <http://dx.doi.org/10.1371/journal.pone.0014324>
- Grottola A, Maracchi M, Tagliazucchi S, Gennari W, Di Gennaro A, Orsini M, et al. Usutu virus infections in humans: a retrospective analysis in the municipality of Modena, Italy. *Clin Microbiol Infect.* 2017;23:33–7. <http://dx.doi.org/10.1016/j.cmi.2016.09.019>
- Engel D, Jöst H, Wink M, Börstler J, Bosch S, Garigliani M-M, et al. Reconstruction of the Evolutionary history and dispersal of Usutu virus, a neglected emerging arbovirus in Europe and Africa. *MBio.* 2016;7:e01938–15. <http://dx.doi.org/10.1128/mBio.01938-15>
- Weissenböck H, Bakonyi T, Rossi G, Mani P, Nowotny N. Usutu virus, Italy, 1996. *Emerg Infect Dis.* 2013;19:274–7. <http://dx.doi.org/10.3201/eid1902.121191>
- Cadar D, Lühken R, van der Jeugd H, Garigliani M, Ziegler U, Keller M, et al. Widespread activity of multiple lineages of Usutu virus, western Europe, 2016. *Euro Surveill.* 2017;22:30452. <http://dx.doi.org/10.2807/1560-7917.ES.2017.22.4.30452>
- Jöst H, Bialonski A, Maus D, Sambri V, Eiden M, Groschup MH, et al. Isolation of Usutu virus in Germany. *Am J Trop Med Hyg.* 2011;85:551–3. <http://dx.doi.org/10.4269/ajtmh.2011.11-0248>
- Becker N, Jöst H, Ziegler U, Eiden M, Höper D, Emmerich P, et al. Epizootic emergence of Usutu virus in wild and captive birds in Germany. *PLoS One.* 2012;7:e32604. <http://dx.doi.org/10.1371/journal.pone.0032604>
- LaDeau SL, Kilpatrick AM, Marra PP. West Nile virus emergence and large-scale declines of North American bird populations. *Nature.* 2007;447:710–3. <http://dx.doi.org/10.1038/nature05829>
- van Riper C III, van Riper SG, Goff ML, Laird M. The epizootiology and ecological significance of malaria in Hawaiian land birds. *Ecol Monogr.* 1986;56:327–44. <http://dx.doi.org/10.2307/1942550>
- Savini G, Monaco F, Terregino C, Di Gennaro A, Bano L, Pinoni C, et al. Usutu virus in Italy: an emergence or a silent infection? *Vet Microbiol.* 2011;151:264–74. <http://dx.doi.org/10.1016/j.vetmic.2011.03.036>
- Steiner HM, Holzer T. Small-scaled differences in the period and extent of population decline in Viennese common blackbirds (*Turdus merula* L.) after the emergence of Usutu virus [in German]. *Vogelwarte.* 2008;46:25–35.
- Rubel F, Brugger K, Hantel M, Chvala-Mannsberger S, Bakonyi T, Weissenböck H, et al. Explaining Usutu virus dynamics in Austria: model development and calibration. *Prev Vet Med.* 2008;85:166–86. <http://dx.doi.org/10.1016/j.prevetmed.2008.01.006>
- Chvala S, Bakonyi T, Bukovsky C, Meister T, Brugger K, Rubel F, et al. Monitoring of Usutu virus activity and spread by using dead bird surveillance in Austria, 2003–2005. *Vet Microbiol.* 2007;122:237–45. <http://dx.doi.org/10.1016/j.vetmic.2007.01.029>
- Bosch S, Schmidt-Chanasit J, Fiedler W. Usutu virus as cause of mass mortality in blackbirds *Turdus merula* and other bird species in Europe: experiences from five outbreaks between 2001 and 2011 [in German]. *Vogelwarte.* 2012;50:109–22.
- Konrad A. Usutu virus associated population decline of common blackbirds in the northern Upper Rhine Plain in the summer 2011 [in German]. *Avifauna-Nordbad.* 2011;42.
- Tietze D, Lachmann L, Wink M. Does the Hour of the Garden Birds capture recent trends? [in German]. *Vogelwarte.* 2014;52:258–9.
- Sauerbrei R, Aue B, Krippes C, Diehl E, Wolters V. Bioenergy and biodiversity: Intensified biomass extraction from hedges impairs habitat conditions for birds. *J Environ Manage.* 2017;187:311–9. <http://dx.doi.org/10.1016/j.jenvman.2016.11.052>
- Ziegler U, Jöst H, Müller K, Fischer D, Rinder M, Tietze DT, et al. Epidemic spread of Usutu virus in southwest Germany in 2011 to 2013 and monitoring of wild birds for Usutu and West Nile viruses. *Vector Borne Zoonotic Dis.* 2015;15:481–8. <http://dx.doi.org/10.1089/vbz.2014.1746>
- Ziegler U, Fast C, Eiden M, Bock S, Schulze C, Hoepfer D, et al. Evidence for an independent third Usutu virus introduction into Germany. *Vet Microbiol.* 2016;192:60–6. <http://dx.doi.org/10.1016/j.vetmic.2016.06.007>
- Metz M, Rocchini D, Neteler M. Surface temperatures at the continental scale: tracking changes with remote sensing at unprecedented detail. *Remote Sens.* 2014;6:3822–40. <http://dx.doi.org/10.3390/rs6053822>
- Messina JP, Kraemer MU, Brady OJ, Pigott DM, Shearer FM, Weiss DJ, et al. Mapping global environmental suitability for Zika virus. *eLife.* 2016;5:e15272. <http://dx.doi.org/10.7554/eLife.15272>
- Pigott DM, Golding N, Mylne A, Huang Z, Henry AJ, Weiss DJ, et al. Mapping the zoonotic niche of Ebola virus disease in Africa. *eLife.* 2014;3:e04395. <http://dx.doi.org/10.7554/eLife.04395>

30. Wenger SJ, Olden JD. Assessing transferability of ecological models: an underappreciated aspect of statistical validation. *Methods Ecol Evol.* 2012;3:260–7. <http://dx.doi.org/10.1111/j.2041-210X.2011.00170.x>
31. Fewster RM, Buckland ST, Siriwardena GM, Baillie SR, Wilson JD. Analysis of population trends for farmland birds using generalized additive models. *Ecology.* 2000;81:1970–84. [http://dx.doi.org/10.1890/0012-9658\(2000\)081\[1970:AOPTFF\]2.0.CO;2](http://dx.doi.org/10.1890/0012-9658(2000)081[1970:AOPTFF]2.0.CO;2)
32. Barlow KE, Briggs PA, Haysom KA, Hutson AM, Lechiara NL, Racey PA, et al. Citizen science reveals trends in bat populations: the National Bat Monitoring Programme in Great Britain. *Biol Conserv.* 2015;182:14–26. <http://dx.doi.org/10.1016/j.biocon.2014.11.022>
33. Roche N, Langton S, Aughney T, Russ JM, Marnell F, Lynn D, et al. A car-based monitoring method reveals new information on bat populations and distributions in Ireland. *Anim Conserv.* 2011;14:642–51. <http://dx.doi.org/10.1111/j.1469-1795.2011.00470.x>
34. Zuur AF, Ieno EN, Walker N, Saveliev AA, Smith GM. *Mixed effects models and extensions in ecology with R.* 1st ed. New York: Springer; 2009.
35. Bhatt S, Gething PW, Brady OJ, Messina JP, Farlow AW, Moyes CL, et al. The global distribution and burden of dengue. *Nature.* 2013;496:504–7. <http://dx.doi.org/10.1038/nature12060>
36. Fros JJ, Miesen P, Vogels CB, Gaibani P, Sambri V, Martina BE, et al. Comparative Usutu and West Nile virus transmission potential by local *Culex pipiens* mosquitoes in north-western Europe. *One Health.* 2015;1:31–6. <http://dx.doi.org/10.1016/j.onehlt.2015.08.002>
37. Stoddard ST, Forshey BM, Morrison AC, Paz-Soldan VA, Vazquez-Prokopec GM, Astete H, et al. House-to-house human movement drives dengue virus transmission. *Proc Natl Acad Sci U S A.* 2013;110:994–9. <http://dx.doi.org/10.1073/pnas.1213349110>
38. Bert E, Tomassone L, Peccati C, Navarrete MG, Sola SC. Detection of beak and feather disease virus (BFDV) and avian polyomavirus (APV) DNA in psittacine birds in Italy. *J Vet Med B Infect Dis Vet Public Health.* 2005;52:64–8. <http://dx.doi.org/10.1111/j.1439-0450.2005.00823.x>
39. Hagemeyer WJM, Blair MJ, editors. *The EBCC atlas of European breeding birds—their distribution and abundance.* London: T & A D Poyser; 1997.
40. Glutz von Blotzheim UN, Bauer KM. *Handbook of the birds of Central Europe [in German].* Wiesbaden: Aula-Verlag; 1988.
41. Pérez-Ramírez E, Llorente F, Jiménez-Clavero MÁ. Experimental infections of wild birds with West Nile virus. *Viruses.* 2014;6:752–81. <http://dx.doi.org/10.3390/v6020752>
42. Ward MP, Raim A, Yaremych-Hamer S, Lampman R, Novak RJ. Does the roosting behavior of birds affect transmission dynamics of West Nile virus? *Am J Trop Med Hyg.* 2006;75:350–5.
43. Kilpatrick AM, Kramer LD, Jones MJ, Marra PP, Daszak P. West Nile virus epidemics in North America are driven by shifts in mosquito feeding behavior. *PLoS Biol.* 2006;4:e82. <http://dx.doi.org/10.1371/journal.pbio.0040082>
44. Gedeon K, Grüneberg A, Mitschke A, Sudfeldt C, Eickhorst W, Fischer S, et al. *Atlas Deutscher Brutvogelarten—atlas of German breeding birds [in German with English summaries].* Muenster (Germany): Dachverband Deutscher Avifaunisten; 2014.
45. George TL, Harrigan RJ, LaManna JA, DeSante DF, Saracco JF, Smith TB. Persistent impacts of West Nile virus on North American bird populations. *Proc Natl Acad Sci U S A.* 2015;112:14290–4. <http://dx.doi.org/10.1073/pnas.1507747112>
46. Kilpatrick AM, Kramer LD, Campbell SR, Alleyne EO, Dobson AP, Daszak P. West Nile virus risk assessment and the bridge vector paradigm. *Emerg Infect Dis.* 2005;11:425–9. <http://dx.doi.org/10.3201/eid1103.040364>
47. Molaei G, Andreadis TG, Armstrong PM, Anderson JF, Vossbrinck CR. Host feeding patterns of *Culex* mosquitoes and West Nile virus transmission, northeastern United States. *Emerg Infect Dis.* 2006;12:468–74. <http://dx.doi.org/10.3201/eid1203.051004>
48. Grüneberg C, Bauer H-G, Haupt H, Hüppop O, Ryslavy T, Südbeck P. Red list of breeding birds in Germany, 5 version, 30 November 2015 [in German]. *Berichte Zum Vogelschutz.* 2015;52:19–67.
49. Johnson BJ, Munafo K, Shappell L, Tsipoura N, Robson M, Ehrenfeld J, et al. The roles of mosquito and bird communities on the prevalence of West Nile virus in urban wetland and residential habitats. *Urban Ecosyst.* 2012;15:513–31. <http://dx.doi.org/10.1007/s11252-012-0248-1>
50. Whelan CJ, Wenny DG, Marquis RJ. Ecosystem services provided by birds. *Ann N Y Acad Sci.* 2008;1134:25–60. <http://dx.doi.org/10.1196/annals.1439.003>

Address for correspondence: Renke Lühken, Bernhard Nocht Institute for Tropical Medicine, Bernhard-Nocht-Str. 74, 20359 Hamburg, Germany; email: renkeluhken@gmail.com

PubMed Central

PubMed



Find *Emerging Infectious Diseases* content in the digital archives of the National Library of Medicine

www.pubmedcentral.nih.gov

Outbreaks of Neuroinvasive Astrovirus Associated with Encephalomyelitis, Weakness, and Paralysis among Weaned Pigs, Hungary

Ákos Boros, Mihály Albert, Péter Pankovics, Hunor Bíró, Patricia A. Pesavento, Tung Gia Phan, Eric Delwart, Gábor Reuter

A large, highly prolific swine farm in Hungary had a 2-year history of neurologic disease among newly weaned (25- to 35-day-old) pigs, with clinical signs of posterior paraplegia and a high mortality rate. Affected pigs that were necropsied had encephalomyelitis and neural necrosis. Porcine astrovirus type 3 was identified by reverse transcription PCR and in situ hybridization in brain and spinal cord samples in 6 animals from this farm. Among tissues tested by quantitative RT-PCR, the highest viral loads were detected in brain stem and spinal cord. Similar porcine astrovirus type 3 was also detected in archived brain and spinal cord samples from another 2 geographically distant farms. Viral RNA was predominantly restricted to neurons, particularly in the brain stem, cerebellum (Purkinje cells), and cervical spinal cord. Astrovirus was generally undetectable in feces but present in respiratory samples, indicating a possible respiratory infection. Astrovirus could cause common, neuroinvasive epidemic disease.

Astroviruses are small, nonenveloped viruses with single-stranded 6.2–7.8 kb RNA genome of positive polarity (1,2). The family *Astroviridae* is currently divided into 2 genera: the genus *Mamastrovirus* of mammal-infecting viruses and the genus *Avastrovirus* of avian viruses (3,4). The genetically heterogenic astroviruses that are widespread among mammals and birds are generally associated with gastroenteritis, less commonly with respiratory disease, and rarely encephalitis or disseminated infections (2,5–19). Astrovirus infections with central

nervous system (CNS) involvement were reported recently in mink, human, bovine, ovine, and swine hosts (the latter in certain cases of AII type congenital tremors) (5,6,12–14). Most neuroinvasive astroviruses belong to the Virginia/Human-Mink-Ovine (VA/HMO) phylogenetic clade and cluster with enteric astroviruses identified from asymptomatic or diarrheic humans and animals (15,16). Recent research shows that pigs harbor one of the highest astrovirus diversities among mammals examined (3,15,20). Porcine astroviruses (PoAstVs) were identified mainly from diarrheic fecal specimens, less commonly from respiratory specimens, although the etiologic role of astrovirus infection in gastroenteritis or in other diseases among swine is not settled (3,9,20–23). We report the detection of neuroinvasive porcine astrovirus type 3 (Ni-PoAstV-3) by reverse transcription PCR (RT-PCR) and in situ hybridization (ISH) in recent and archived CNS samples of newly weaned paraplegic pigs from 3 highly prolific swine farms in Hungary.

Materials and Methods

Sample Collection and Handling

During November 2015–July 2017, we collected multiple tissue samples from 5 paraplegic and 5 asymptomatic pigs at the index farm located in Hungary (GD; specific location redacted) (Table 1). We also tested nasal and anal swab pairs collected by using polyester-tipped swabs from another 5 paraplegic and 13 healthy animals. We washed tissue samples twice in 10 mmol/L phosphate buffered saline (PBS) to remove excess blood and held them at –80°C until total RNA extraction. For formalin-fixed, paraffin-embedded (FFPE) blocks, we fixed the dissected samples (Table 2) with buffered 8% formaldehyde, dehydrated and embedded into paraffin.

We also analyzed archived FFPE specimens from paraplegic pigs from earlier outbreaks of posterior paraplegia

Author affiliations: ÁNTSZ Regional Institute of State Public Health Service, Pécs, Hungary (A. Boros, P. Pankovics, G. Reuter); University of Pécs, Pécs (A. Boros, P. Pankovics, G. Reuter); Ceva Phylaxia Ltd., Budapest, Hungary (M. Albert); SHP Ltd., Kaposvár, Hungary (H. Bíró); University of California, Davis, California, USA (P.A. Pesavento); Blood Systems Research Institute, San Francisco, California, USA (T.G. Phan, E. Delwart); University of California, San Francisco (E. Delwart)

DOI: <https://doi.org/10.3201/eid2312.170804>

Table 1. Data on 5 symptomatic and 5 control newly weaned pigs from a farm in Hungary and results of PoAstV-3 screening by nested RT-PCR of samples collected during 2015–2017*

Data	Symptomatic animals†					Asymptomatic control animals‡				
	GD-1	GD-2	GD-3	GD-4	GD-5	GD-6	GD-7	GD-8	GD-9	GD-10
Collection month	2016	2016	2016	2016	2015	2016	2017	2017	2017	2017
	Mar	Mar	Jul	Jul	Nov	Jul	Jun	Jun	Jun	Jun
Age, d	25	25	25	25	35	35	25	25	25	35
Clinical signs (disease stage)	PP (1)	PP (1)	PP (3)	PP (3)	PP (3)	None	None	None	None	None
Brain stem	+	+	+	+	+	– (–)	– (–)	– (–)	– (–)	– (–)
Spinal cord										
Cervical	NA	NA	+	+	NA	NA	– (–)	– (–)	NA	NA
Thoracic	NA	NA	+	+	NA	NA	– (–)	– (–)	NA	NA
Lumbar	+	NA	+	+	+	– (–)	– (–)	– (–)	NA	NA
Nasal mucosa	– (+)‡	+‡	+	+	NA	– (–)	– (–)‡	– (–)‡	– (–)‡	– (–)‡
Lung	NA	NA	+	+	NA	NA	NA	NA	NA	NA
Tonsils	NA	– (–)	+	+	+	– (–)	NA	NA	NA	NA
Salivary glands	NA	NA	– (+)	+	NA	NA	NA	NA	NA	NA
Myocardium	NA	+	NA	NA	+	NA	NA	NA	NA	NA
Feces	– (–)	NA	– (+)	– (+)	NA	NA	– (–)	– (–)	– (–)	– (–)
Ileum	NA	NA	– (–)	– (+)	– (–)	– (–)	NA	NA	NA	NA
Lymph nodes										
Mesenteric	NA	– (–)	– (–)	– (–)	NA	– (–)	NA	NA	NA	NA
Submandibular	NA	NA	– (+)	+	NA	NA	NA	NA	NA	NA
Urine	NA	NA	– (–)	– (–)	NA	NA	NA	NA	NA	NA
Kidney	NA	NA	– (–)	– (–)	NA	NA	NA	NA	NA	NA
Liver	NA	NA	– (+)	– (+)	NA	NA	NA	NA	NA	NA
Spleen	NA	NA	– (–)	– (–)	NA	NA	NA	NA	NA	NA
Serum	NA	NA	+	+	NA	NA	NA	NA	NA	NA

*We collected tissues from 5 affected pigs with encephalomyelitis and PP and 5 asymptomatic control animals from the index farm. The screening nested RT-PCR primers are designed to the RNA-dependent RNA polymerase region of PoAstV-3. NA, no available sample; PoAstV-3, porcine astrovirus type 3; PP, posterior paraplegia; RT-PCR, reverse transcription PCR; +, positive; –, negative.

‡Symbols indicate results from first PCR reactions; symbols in parentheses indicate results from second (nested) RT-PCR reactions.

‡Nasal swab sample.

in Tázlár in 2011 and in Balmazújváros in 2014 (Table 2). The 3 swine farms are located in the central and eastern parts of Hungary, »100 km from each other, without known connection.

Previous Laboratory Diagnostics

CNS homogenates from the index farm tested negative by PCR for the following pathogens (families in parentheses): porcine reproductive and respiratory syndrome virus (*Arteriviridae*); porcine circovirus 2 (*Circoviridae*); hemagglutinating encephalitis virus (*Coronaviridae*); and porcine parvovirus 1, 2, 4, and porcine bocavirus (*Parvoviridae*). Immunohistochemical detection of *Toxoplasma gondii* and West Nile virus and bacterial cultivation attempts from the CNS samples were also negative. Virus isolation attempts using brain homogenates of affected animals in swine kidney (PK-15) and Caucasian colon adenocarcinoma (Caco-2) cell lines were not successful (no cytopathic effects were visible). We detected no PoAsV type 3 (PoAstV-3) in the cell culture supernatants by nested RT-PCR with RNA-dependent RNA polymerase (RdRp) primer pairs.

Total RNA Extraction and RT-PCR Screening

Treatment of FFPE samples included the deparaffination and rehydration steps, proteinase K digestion, and total RNA extraction. We used the same treatment protocols and

the same reaction conditions and reagents used in the RT-PCR and nested RT-PCR reactions as are described previously, with minor modifications (24–26) (online Technical Appendix, <https://wwwnc.cdc.gov/EID/article/23/13/17-0804-Techapp1.pdf>). For the RT-PCR screening of CNS samples for the presence of pestiviruses (*Flaviviridae*) and swine picornaviruses (*Picornaviridae*), including teschovirus, enterovirus, sapelovirus, Seneca Valley virus, pasivirus, kobuvirus and encephalomyocarditis, we used virus-specific primer pairs as well as the outer and inner primer pairs targeting the RdRp or the capsid regions of PoAstV-3 (Figure 1; online Technical Appendix Tables 1, 2).

Absolute Quantification Using Quantitative RT-PCR

For the absolute quantification of viral RNA present in different tissue, urine, and fecal samples, we used the SYBR Green–based quantitative RT-PCR (RT-qPCR) method (Maxima SYBR Green qPCR Master Mix; Thermo Scientific, Waltham, MA, USA). For the generation of standard curve, we used 10-fold dilution series of purified and spectrophotometrically quantified RNA transcripts in the reactions. The RT-qPCR assays contained 3 technical repeats of all samples and standards. The slope of the standard curve was –3.4228 and the calculated PCR efficiency was 99.96%. The detailed protocol is provided in the online Technical Appendix.

Table 2. Results of PoAstV-3 detection, histology, and ISH analyses using formalin-fixed, paraffin-embedded blocks of samples from 3 symptomatic newly weaned pigs from a farm in Hungary and samples from 2 other farms with symptomatic pigs*

Farm ID	Collection year	Animal ID	FFPE block ID	Nested RT-PCR†		Tissue samples	ISH‡		
				RdRp	Capsid				
GD	2016	GD-1	GD-1A	– (+)	– (+)	Spinal cord	+		
						Brainstem	+		
							Cerebellum	+	
							Medulla oblongata	–	
							Lymph node	–	
		2015	GD-2	GD-2A	– (–)	– (–)	Tonsil	–	
						Myocardium	–		
								Spleen	–
								Thymus	–
								Brainstem	+
					Cerebellum	+			
Tázlár	2011	TAZ-1	TAZ-1A	– (+)	– (+)	Hippocampus	–		
						Brainstem	+		
						Spinal cord	+		
Balmazújváros	2014	BAM-1	BAM-1A	– (–)	– (–)	Spinal cord	–		
						Brainstem	+		
						Cerebellum	+		

*The screening RT-PCR primers are designed to either the RdRp or the capsid region of PoAstV-3. GD, index farm; ID, identification; ISH, in situ hybridization; PoAstV-3, porcine astrovirus type 3; RdRp: RNA-dependent RNA polymerase; RT-PCR, reverse transcription PCR; +, positive; –, negative.

†Symbols indicate the results of the first screening PCRs; symbols in parentheses indicate the results of the second (nested) RT-PCR. The results of nested RT-PCR refer to a mixture of tissues embedded into the total of 7 paraffin blocks.

‡Indicates results for neuroinvasive PoAstV-3.

§FFPE samples were the only specimens taken from this animal.

Long-range Amplification, 5'/3' RACE-PCR, and Sanger Sequencing

For the complete genome (or complete 3' open reading frame [ORF] 1b–ORF2–3' untranslated region [UTR]) acquisitions of the PoAstVs, we used different long-range and 5'/3' rapid amplification of cDNA ends RT-PCRs according to previously described protocols (26,27). We designed the sequence-specific primers used for the amplification of overlapping genome fragments based on the genome of PoAstV-3 strain US-MO123 (GenBank accession no. JX556691) and closely related sequences downloaded from the GenBank database (online Technical Appendix Table 3). We sequenced PCR products directly with the BigDye Terminator v1.1 Cycle Sequencing Ready Reaction Kit (Applied Biosystems, Stafford, TX, USA) using the primer-walking method with an automated sequencer (ABI Prism 310 Genetic Analyzer; Applied Biosystems). We have submitted the nucleotide sequences of study astrovirus strains to GenBank under accession nos. KY073229–32.

Sequence and Phylogenetic Analyses

We aligned astrovirus sequences by using the MUSCLE web tool of EMBL-EBI (28) and performed pairwise nucleotide and amino acid identity calculations of the aligned sequences with GeneDoc version 2.7 (<http://iubio.bio.indiana.edu/soft/molbio/ibmpc/genedoc-readme.html>). We constructed phylogenetic trees of deduced amino acid sequence alignments by using MEGA version 6.06 software (29) and the neighbor-joining method with the Jones–Taylor–Thornton matrix-based model. Bootstrap values were set to 1,000 replicates, and only likelihood percentages of $\geq 50\%$ were indicated.

Histology and In Situ Hybridization

We performed chromogenic (with 3,3'-diaminobenzidine/DAB) in situ hybridization in FFPE slides (RNAScope 2.0, Brown Kit; Advanced Cell Diagnostics, Newark, CA, USA) according to the manufacturer's instructions for viral RNA detection of Ni-PoAstV-3. We used 30 probe pairs generated at Advanced Cell Diagnostics designed to hybridize native viral Ni-PoAstV-3 RNA. Negative controls included Dap-B (dihydrodipicolinate reductase gene from *Escherichia coli* probe); an unrelated viral probe; and normal porcine brain region-matched sections.

Results

Clinical Observations

There are $\approx 2,000$ sows and their offspring in the investigated highly prolific index farm (GD). Episodes of neurologic disease of unknown etiology have persisted in the past 2 years. The syndrome affects an average of 30–40 weaned pigs monthly (1.5%–2% of total), although the number of monthly cases infrequently rose to ≈ 80 pigs (4%) in the autumn–winter seasons. The clinical signs of posterior leg weakness or paraplegia and pitching (stage 1); later paralysis of both legs and skin pain (stage 2); or loss of consciousness, paresis, and serious flaccid paralysis of muscles (stage 3) typically appear among weaned pigs 25–35 days old, 1 week after the weaning procedure (Video). We did not observe gastroenteric symptoms. All of the affected pigs in stage 3 of the disease were unable to eat or drink; they died due to exsiccosis (dehydration) or were euthanized. Signs persisted typically for 1 week before death or euthanasia. Postmortem examination

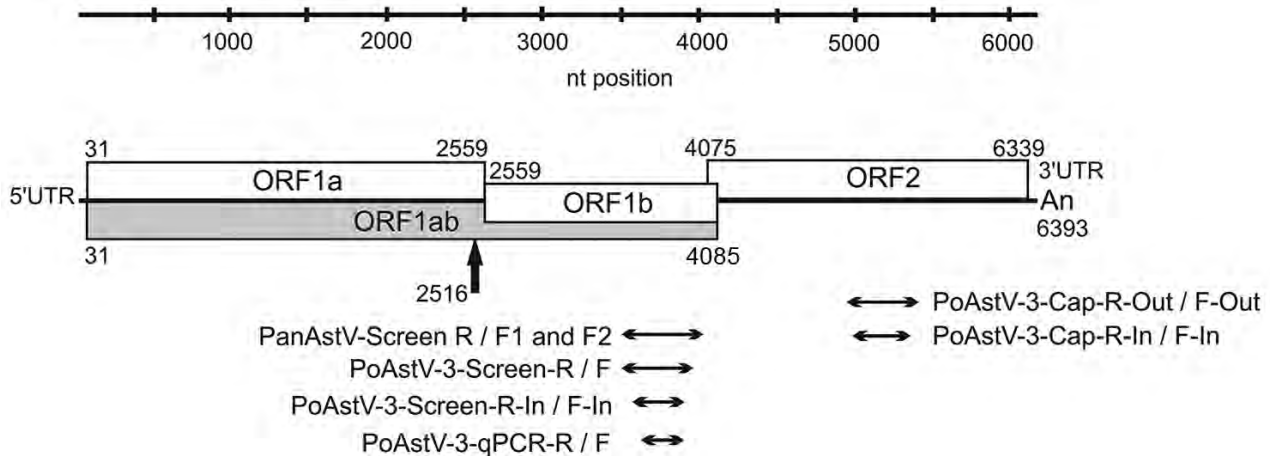


Figure 1. Genome map of the neuroinvasive PoAstV-3 strain NI-Brain/9-2016a/HUN (GenBank accession no. KY073229) from a symptomatic newly weaned pig from a farm in Hungary together with the location of RT-PCR products used for different astrovirus screening reactions and quantitative RT-PCR analyses. The black arrow indicates the possible localization of a ribosomal frame-shift during the synthesis of ORF1ab peptide. The first and last nucleotide positions of the ORFs are marked with numbers at the top and bottom of each box. ORF, open reading frame; PanAstV, panastrovirus; PoAstV-3, porcine astrovirus type 3; RT-PCR, reverse transcription PCR; UTR, untranslated region.

results showed no signs of mechanical damage (fractures, abscesses, or hemivertebrae). Pigs are vaccinated against porcine circovirus 2, *Mycoplasma hyopneumoniae*, and *Actinobacillus pleuropneumoniae*. Preventive amoxicillin treatment of the piglets was done routinely at weaning. Due to the preventive measures in effect as of spring 2017, which included extensive decontamination of the piggeries and the physical separation of the newly weaned pigs from different litters, the number of encephalomyelitis cases among weaned pigs decreased with only 1–2 cases/month observed on the index farm.

The 2 additionally examined swine farms located in Tázlár and Balmazújváros each held approximately 500 sows and their offspring. Similar symptoms of staggering and paralysis appeared among pigs 3–5 weeks old in outbreaks in 2011 (Tázlár) and 2014 (Balmazújváros).

Detection and Analysis of Astroviruses from CNS Samples of Affected Animals

In March 2016, we collected brain stem, spinal cord, nasal swab, and fecal samples from a newly weaned pig from index farm GD (GD-1, index animal) that showed signs of encephalomyelitis and posterior paraplegia (stage 1). The brain stem and spinal cord samples tested negative by RT-PCR for pestivirus (family *Flaviviridae*) and several swine-infecting picornaviruses (family *Picornaviridae*) (online Technical Appendix Table 1). On the basis of the increasing evidence of the pathogenic role of neurotropic astroviruses among humans and farm animals (5,6,14,17,30) we investigated the presence of astrovirus using panastrovirus PCR primers (online Technical Appendix Table 1) (31). The brain stem and spinal cord

samples showed strong RT-PCR positivity. The panastrovirus PCR products were sequenced using panastrovirus PCR primers (online Technical Appendix Table 1) and compared to each other and to the available astroviruses using blastn (<https://blast.ncbi.nlm.nih.gov/Blast.cgi>). The 397-nt sequences of brain stem and spinal cord were identical and showed 89% nt identity to PoAstV-3 isolate US-MO123 (GenBank accession no. JX556691) as the closest match (32).

We sequenced 2 samples from the index animal: the full-length genome of the neuroinvasive astrovirus strain NI-Brain/9-2016a/HUN (GenBank accession no. KY073229) from the brain stem sample and the complete capsid-encoding ORF2 from the spinal cord sample NI-SC/9-2016a/HUN (GenBank accession no. KY073230). The 6393-nt (without the poly[A] tail) complete genome showed the typical astrovirus genome organization with 3 putative ORFs, 2529 nt (ORF1a), 1527 nt (ORF1b), and 2265 nt (ORF2), flanked by short 5' and 3' UTRs (Figure 1). We identified the conserved proteolytic cleavage site ($V_{561}HQ^{-}TNT$) of serine protease (ORF1a) and the conserved $Y_{358}GDD$ motif of the RdRp (ORF1b) (33). The nonstructural proteins of ORF1a (842 aa) and ORF1b (508 aa) and the capsid protein of ORF2 (754 aa) showed 93%, 95%, and 93% aa identity, respectively, to the corresponding genome parts of the closest known relative PoAstV-3 strain, US-MO123. All of the conserved genomic features of mamastroviruses were present in strain NI-Brain/9-2016a/HUN: the conserved C_1CAA pentamer at the 5' end of the genome; the frame-shift heptamer motif ($A_{2511}AAAAAC$) followed by a stem-loop structure at the 3' end of ORF1a; the conserved sgRNA

promoter sequence motif of U₄₀₄₈UUGGAGgGGaGGAC-CaAAN₈AUGgC (variable nts are in lowercase, start codon of ORF2 is underlined) at the junction of ORF1b/ORF2; and the stem loop II-like motif (s2m) in the 3' end of the genome between nt position=s 6322 and 6353. The 3' UTR of NI-Brain/9-2016a/HUN is 27 nt shorter and did not contain the short sequence repeat found at the 3' end of strain US-MO123 (G_{6381/6392}AUUUCUUUNA). Based on the high sequence identity and the similar genomic features, the NI-Brain/9-2016a/HUN strain most likely belongs to the PoAstV-3 genotype. The ORF2 of NI-Brain/9-2016a/HUN shares 99% nt/aa identity with the corresponding capsid gene of NI-SC/9-2016a/HUN from the spinal cord of the same animal, suggesting that the same virus was present in both regions of the CNS.

We detected Ni-PoAstV-3 using RT-PCR in all CNS samples collected from another 4 affected newly weaned pigs held in the index farm (Table 1). All of the samples from the asymptomatic control animals were Ni-PoAstV-3 negative.

We determined the complete genomes of 2 Ni-PoAstV-3 strains (NI-Brain/173-2016a/HUN, GenBank accession no. KY073231; and NI-Brain/386-2015/HUN, accession no. KY073232) that originated from 2 affected animals (GD-3 and GD-5) in stage 3 of the disease, chosen at different times (July 2016 and November 2015) of the outbreak (Table 1). These isolates showed 99.5%, 100%, and 98.7%–99.2% aa identities, respectively, to NI-Brain/9-2016a/HUN in the ORF1a, ORF1b, and ORF2 (capsid) regions.

Most of the aa differences between the Ni-PoAstV-3 study strains and the other enteric PoAstV-3 strains are located in the N-terminal part of ORF1a and in the C-terminal part of ORF2 (Table 3). Phylogenetic analysis showed a close relationship between the identified Ni-PoAstV-3 sequences and the known PoAstV-3 strains located within the same larger clade containing most other mamastroviruses with known neurotropic potential (Figure 2).

Detection of Ni-PoAstV-3 in Non-CNS Samples

We detected Ni-PoAstV-3 in multiple non-CNS samples from the respiratory system, lymphoid system, circulatory system, and salivary glands of affected animals (Table 1). We detected virus only in the second PCR round in 1 ileum sample and in 2 of the 3 analyzed fecal samples using nested RT-PCR (Table 1). Samples from internal organs (spleen and kidney) and urine samples tested negative by nested RT-PCR (Table 1).

We determined the copy number of Ni-PoAstV-3 using SYBR Green-based -qPCR. All of the samples that showed nested RT-PCR positivity only in the second (nested) PCR round had negative test results by RT-qPCR, indicating low copy number (<100 copies/μg total RNA) of the virus in that tissue sample. The highest copy number was detected in the brain stem, followed by the spinal cord (Figure 3). Of note, we detected relatively high copy numbers in the tonsil and nasal mucosa samples (Figure 3). The serum of animal GD-3 contained 2.07 ×

Table 3. Amino acid differences between neuroinvasive PoAstV-3 strains from 3 symptomatic newly weaned pigs from a farm in Hungary and reference enteric PoAstV-3 strains detected from fecal samples*

Category	Genomic region									
	ORF1a	ORF1a	ORF1a	ORF1a	ORF1b	ORF1b	ORF2	ORF2	ORF2	ORF2
Amino acid position	1–400	1–400	401–844	401–844	1–508	1–508	1–415	1–415	416–754	416–754
PoAstV-3 type	Ni	Ent	Ni	Ent	Ni	Ent	Ni	Ent	Ni	Ent
Amino acid changes	M25	S/L	F408	L	N54	D	R29N	KT[I/A/V]	L439	H[P/V]
	Y41	F	I434	V	D106G	[A/E]D	S34	R	S453	D
	R117	K	S481	P	A181	S	R38	Y	F457	Y
	T120	S/L	S576	T/V	I206	V	V55	T	Y559	F
	T122	S/L	G608	N	R213	K	T57R	SK	A570[P]	N
	K151G	RC	N646	H	Y293	H/N	T61	A	N572[Y]	D
	L170	M	E679	D	E343	D			D581	N
	L179	M			K375	R			I601	V
	M185	L			I378	T			S617	N
	D208	E/N			N382	D			T628	S
	D202S[P/Q]	NPTDG			I415	A/T			S678	T
	P217A	TT							I696	V
	T220[V/A]	IS								
	P224	H/R								
	I299	V								
	E332	D								
	V338	L/I								
	L346	F								
	I369	V								

*We identified 3 PoAstV-3 isolates: NI-Brain/9-2016a/HUN (GenBank accession no. KY073230); NI-Brain/173-2016a/HUN (accession no. KY073231); and NI-Brain/386-2015/HUN (accession no. KY073232). We compared these with enteric strains from GenBank (accession nos. JX556691, LC201595-7, and LC201599). AD, presumed particle assembly domain; Ent, enteric; Ni, neuroinvasive; ORF, open reading frame; PoAstV-3, porcine astrovirus type 3; RID, presumed receptor-interaction domain.

10⁶ virus copies/mL and of animal GD-4 1.64 × 10³ virus copies/mL.

To validate the general presence of Ni-PoAstV-3 in the respiratory system and the absence of the virus in the feces during the acute phase of the illness, we collected additional

nasal and anal swab pairs from 5 affected pigs and 13 clinically healthy pigs of the same age (≈25–35 days) from the index farm. Four (80%) of the 5 nasal swab samples from affected animals tested positive but all of the anal swab samples tested negative using nested RT-PCR with primers

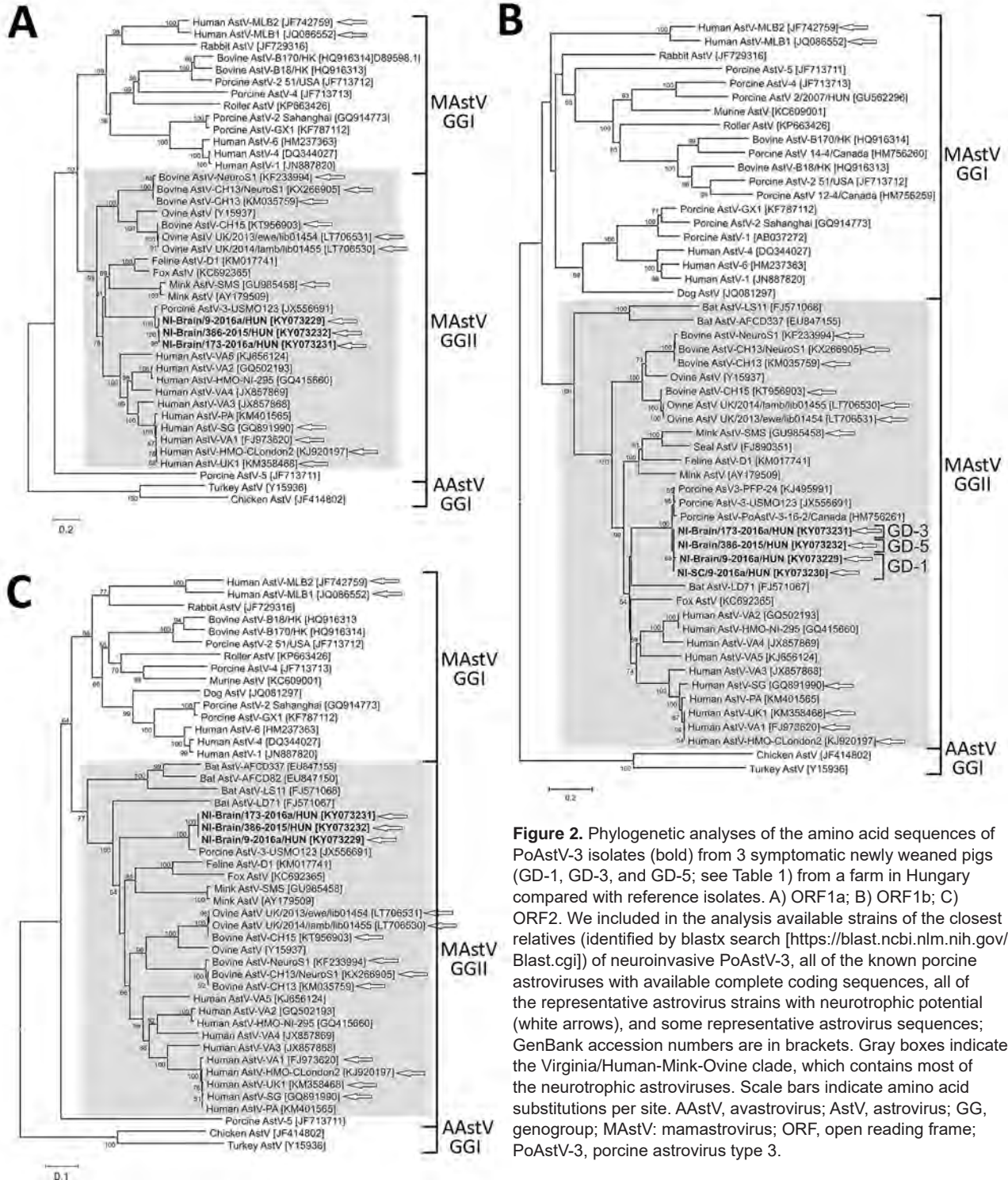


Figure 2. Phylogenetic analyses of the amino acid sequences of PoAstV-3 isolates (bold) from 3 symptomatic newly weaned pigs (GD-1, GD-3, and GD-5; see Table 1) from a farm in Hungary compared with reference isolates. A) ORF1a; B) ORF1b; C) ORF2. We included in the analysis available strains of the closest relatives (identified by blastx search [https://blast.ncbi.nlm.nih.gov/Blast.cgi]) of neuroinvasive PoAstV-3, all of the known porcine astroviruses with available complete coding sequences, all of the representative astrovirus strains with neurotrophic potential (white arrows), and some representative astrovirus sequences; GenBank accession numbers are in brackets. Gray boxes indicate the Virginia/Human-Mink-Ovine clade, which contains most of the neurotrophic astroviruses. Scale bars indicate amino acid substitutions per site. AAstV, avastrovirus; AstV, astrovirus; GG, genogroup; MAstV, mamastrovirus; ORF, open reading frame; PoAstV-3, porcine astrovirus type 3.

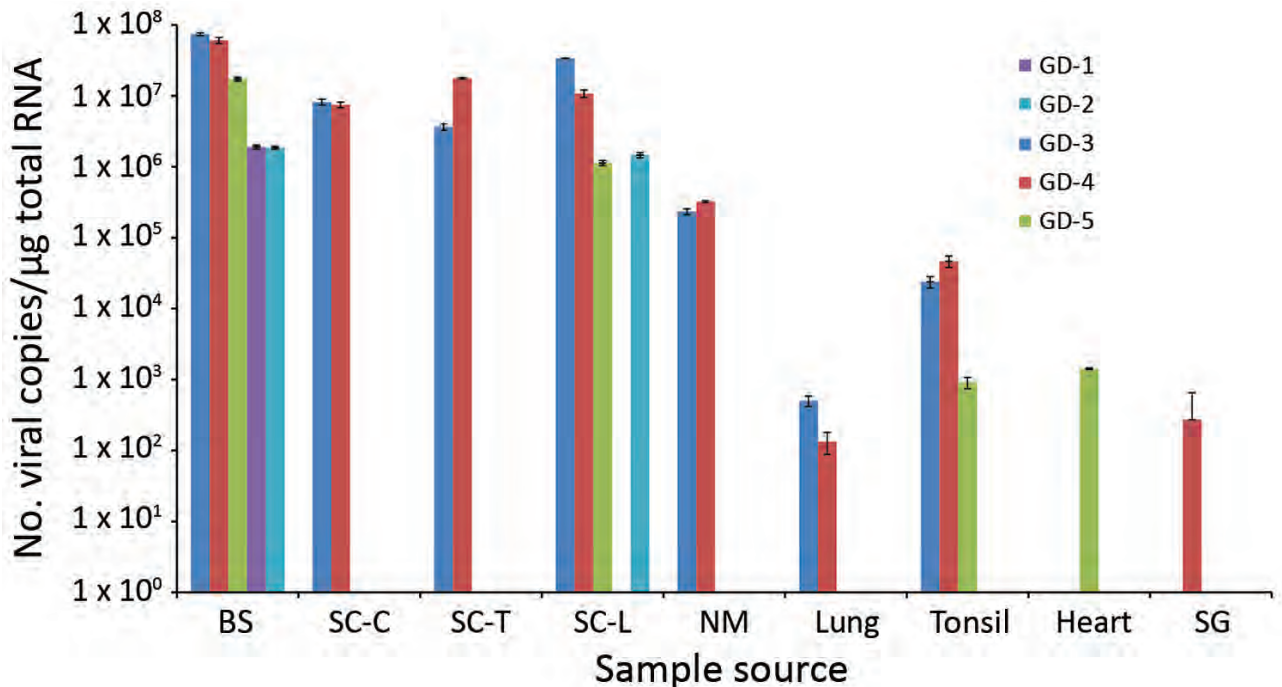


Figure 3. Logarithmic graph of the viral copy numbers of porcine astrovirus type 3 (PoAstV-3) in different organs determined by SYBR Green–based quantitative reverse transcription PCR (RT-qPCR) of samples from 5 symptomatic newly weaned pigs (GD-1–5; see Table 1) from a farm in Hungary. All the samples, which were positive for PoAstV-3 only by nested RT-PCR, were found negative by quantitative RT-PCR. BS, brain stem; CNS, central nervous system; NM, nasal mucosa; SC-C/T/L, cervical, thoracic, or lumbar spinal cord; SG, salivary gland.

targeting the RdRp region of Ni-PoAstV-3. The nasal and anal swab samples of the asymptomatic animals were all negative by nested RT-PCR. Because we collected varying amounts of samples by polyester-tipped swabs, we did not perform absolute quantification of Ni-PoAstV-3 by RT-qPCR.

Detection of Ni-PoAstV-3 in Archived FFPE Samples

All but 1 archived FFPE samples from Tázlár and Balmazújváros were positive by nested RT-PCR for Ni-PoAstV-3 using 2 sets of primer pairs targeting the RdRp and capsid genes of Ni-PoAstV-3 (Table 2; Figure 1; online Technical Appendix Table 2). The spinal cord FFPE sample from Balmazújváros had a negative result using both nested RT-PCR primer sets. The nested RT-PCR positive samples had positive results by ISH (data not shown).

Histology and ISH

Histologically, shared CNS lesions among the animals examined were moderate to marked lymphohistiocytic cell perivascular cuffing with marked vasculitis and neuronal degeneration, necrosis, and neurophagia with multifocal microgliosis and satellitosis (Figure 4). The neuronal necrosis was especially evident in the dorsal and ventral

horns of the cervical spinal cord gray matter, although it was also detected in neurons of the Purkinje layer (cerebellum), the medulla oblongata, cerebellar peduncles, and midbrain (Figure 5). Necrotic neurons were variously swollen and hypereosinophilic or shrunken with tinctorial changes including faded, amphophilic, or eosinophilic cytoplasm (Figure 5). Nuclei of affected neurons are pyknotic, karyorrhectic, or losing border definition within the cytoplasm. We performed ISH on 5 affected animals (Table 2). Ni-PoAstV-3 hybridization was predominantly restricted to neurons, including those with visible necrosis and, in the cerebellum in particular, some that were histologically unaffected, although some regions of gliosis (presumed inflammation after neuronal necrosis) also contained viral RNA (Figure 5, panel M). Hybridization was distinct, with punctate to diffuse cytoplasmic staining throughout the cytoplasm. The unique microarchitecture of the Purkinje layer of the cerebellum offered the clear demonstration that viral nucleic acid was present within dendritic processes coursing through the molecular layer (Figure 5, panels G, J). We found no pathologic lesions in other samples from kidneys, liver, gastrointestinal tract, or immune system (data not shown). The samples from the immune system were also negative by Ni-PoAstV-3 ISH (Table 2).

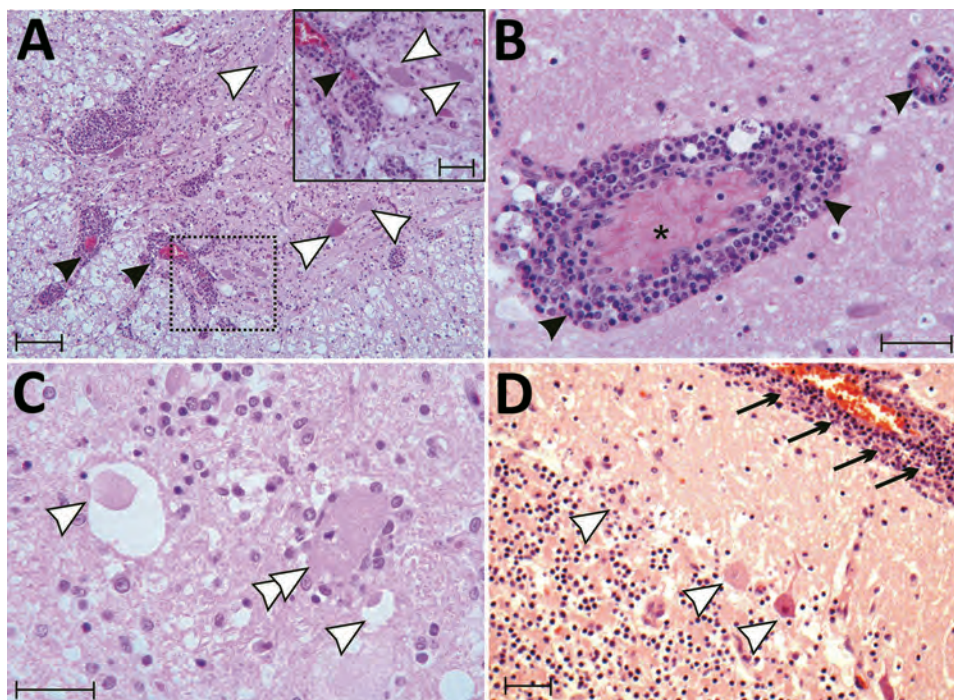


Figure 4. Tissue sections of cervical spinal cord (A), brain stem (B, C) and cerebellum (D) stained with hematoxylin and eosin from a symptomatic newly weaned pig from a farm in Hungary show the signs of stage 3 encephalomyelitis. Mononuclear perivascular cuffs with vasculitis (black arrowheads), neuronal necrosis (white arrowheads), neurophagia (white double arrowheads), multifocal microgliosis, and signs of meningitis (black arrows) are shown. Asterisk (*) indicates blood vessel. Scale bars indicate 50 μ m (panels A, D) or 20 μ m (panel A inset; panels B, C).

Discussion

We detected astrovirus RNA in multiple tissues collected during 2015–2017 from newly weaned pigs with encephalomyelitis and posterior paraplegia of unknown origin, with the highest viral load detected in brain stem and spinal cord samples. We detected the same virus in archived brain and spinal cord FFPE samples from similarly affected animals from 2 additional swine herds collected in 2011 and 2014. These data indicate that a genetically similar, neurovirulent astrovirus is circulating in multiple swine farms since 2011 or earlier in Hungary.

According to the refined classification for the assessment of causation (34), the Ni-PoAstV-3 and the observed encephalitis and paraplegia are in a probable causal relationship (Level 2). Paraplegia associated with astrovirus neuroinfection is not unprecedented; minks had astrovirus-induced “shaking mink syndrome” and were reported paraplegic at the final stage of the disease (12,35).

Neurologic signs were observable mainly among newly weaned pigs (Video, <https://wwwnc.cdc.gov/EID/article/23/12/17-0804-V1.htm>). The time of weaning, which involves nutritional (from milk to solid feed), social (mixing with different litters without the sow), and environmental (moving to a new pen) changes, is known to be the most stressful period in a pig’s lifetime and is associated with dysfunction of the immune system (36). Furthermore, the inadequate quantity and quality of colostrum intake of sucking piglets, and therefore the presumably low level of specific maternal antibodies due to highly prolific sows with large litters in the index farm,

might also contribute to the emergence of the clinical disease. Decreased immune status was frequently present with extraintestinal dissemination of astroviruses in humans and in mice (5,37–41).

Our sequence analyses indicate that the identified astrovirus strains belong to the PoAstV-3 genotype, which clusters within the VA/HMO phylogenetic clade (Figure 2), as do most mammalian strains with known neurotropic potential (6,14,19). However, other canonical human astroviruses outside of the VA/HMO clade could also be associated with CNS disease (41). At the molecular level, the most conspicuous difference between the genomes of neuroinvasive virus and the enteric PoAstV-3 strain U.S.-MO123 is the 27 nt deletions found in the 3’ UTR of the CNS-associated astroviruses. The possible impact of this 3’ UTR deletion on viral tropism is unknown, although neuroinvasive bovine astroviruses also possess 3’ UTR architecture that differs from the diarrhea-associated astroviruses (42).

At the amino acid level, one of the most divergent regions between the neuroinvasive and other PoAstV-3 strains was found at the receptor-interaction domain of ORF2 (Table 3), which contains potential receptor binding sites (43,44). This finding could indicate an altered receptor spectrum and therefore altered tissue tropism of neuroinvasive and enteric PoAstV-3 strains.

PoAstV-3 strains were previously detected only from fecal samples of healthy or diarrheic piglets worldwide (20,22,45). We found that Ni-PoAstV-3 was either undetectable or detected only at low viral loads in the

analyzed fecal samples, whereas the virus was generally detectable in the respiratory system of paraplegic pigs.

This finding may indicate that CNS infection and replication occur later than enteric replication or that initial

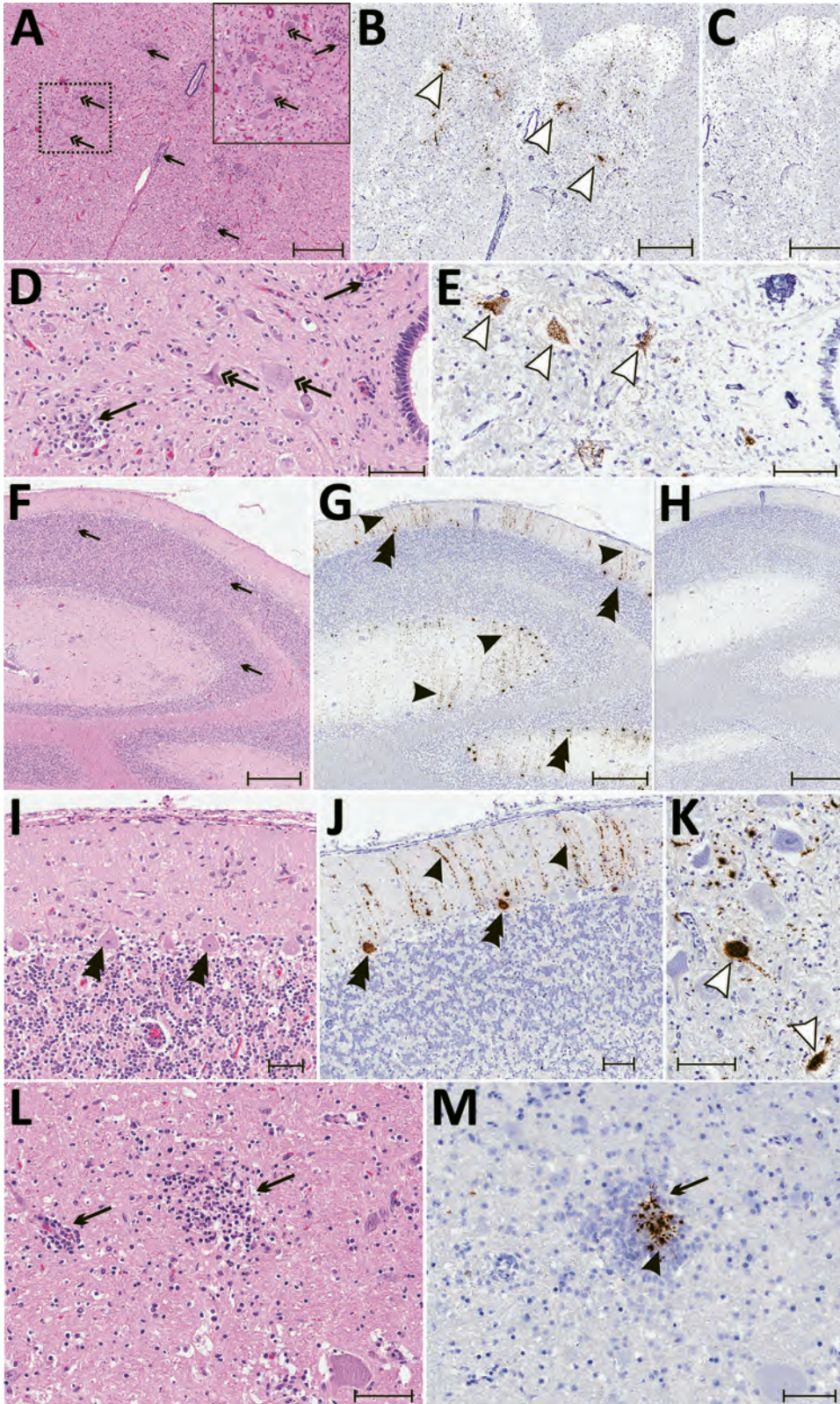


Figure 5. Results of histopathologic testing of central nervous system tissues from 2 symptomatic newly weaned pigs from a farm in Hungary. Sections of the cervical spinal cord (A–E), cerebellum (F–J), and cortex (L, M) from the index animal (GD-1) and the brain stem (K) from an additional affected stage 1 animal (GD-11). A, D, F, I, L) Hematoxylin and eosin stain. Gliosis (black arrows) is multifocal within the gray matter (panels A, D) and in the molecular layers (panels F, I, L, and M). Neuronal degeneration and necrosis are evident by hypereosinophilia, angular degeneration, and vacuolation (double arrows in panels A, D). Some Purkinje neurons are slightly angular with mild vacuolation (double arrowheads in panel I). B, E, G, J, K, M) In situ hybridization of neuroinvasive porcine astrovirus. Hybridization of the neuroinvasive porcine astrovirus probe is restricted to neurons (white arrowheads in panels B, E, K) or limited to Purkinje neurons (double black arrowheads in panels G, J) with extension into dendritic processes that course through the molecular layer (black arrowheads in panels G, J). Hybridization of the neuroinvasive porcine astrovirus type 3 probe (black arrowhead in panel M) is present in the gliosis (black arrows in panels L, M). C, H) Using a control probe on a serial section, no hybridization is detectable. In situ hybridization. Scale bars indicate 500 μ m (panels A–C, F–H) or 50 μ m (panels D, E, I–M).

replication occurs extraintestinally (e.g., in the respiratory tract). Multiple types of astroviruses were recently identified from nasopharyngeal swabs or lung tissue samples from swine, bovines, and humans with respiratory symptoms including the neurotropic human VA1 strain from a patient with febrile acute respiratory disease (9–11,23), although neither the respiratory tropism nor the airborne transmission of astroviruses has been experimentally confirmed. Therefore, testing of only fecal samples from sick animals may result in underestimation of the incidence of astrovirus in pigs.

We measured the highest viral loads of Ni-PoAstV-3 in brain and spinal cord samples, similar to those found in diseased ovine and human patients with astrovirus-associated encephalitis (5,14). Ni-PoAstV-3 was also detectable in serum specimens and multiple organs of the respiratory, lymphoid, and cardiovascular systems of diseased swine. These results indicate that Ni-PoAstV-3 can result in viremia and disseminated infection involving the brain, spinal cord, and multiple organs during the acute phase of encephalomyelitis and posterior paraplegia. Astroviruses seem to play a role in a common and severe disease (encephalomyelitis and paralysis) in pigs.

The observable histopathologic changes, as well as the neuronal localizations of Ni-PoAstV-3 RNA in CNS samples of paraplegic pigs, are comparable to astrovirus-associated encephalitic cases of minks, humans, and cattle. Similar neuronal degeneration or necrosis with microgliosis in the brain or cerebellum, as well as inflammation of gray matter of the spinal cord, were previously described in cattle with astrovirus-associated nonsuppurative encephalitis (6,35,46,47), which suggests the general course of an astrovirus neuroinfection.

While some astroviruses are known to cause outbreaks of gastroenteritis, astrovirus-associated encephalitis cases have been reported only sporadically among humans, cattle, and sheep (6,14–16,47). The constant presence with recurrent increases of neurologic disease cases in swine farms indicates that natural neuroinvasive astrovirus infections may cause common, severe, persistent epidemics among domestic pigs and constitute an economically important agent threatening livestock and even humans, considering the possible zoonotic and recombinant potential of astroviruses (48).

Our results must be interpreted in the light of some potential limitations, which are currently true for other astrovirus-associated encephalitis studies: the absence of experimental evidence such as in vivo inoculation experiments, which could clarify the true causality between the astrovirus neuroinfection and the manifested CNS symptoms; and the roles of presumed respiratory replication and decreased immune state. Therefore, despite a growing body of scientific data regarding the presence of astroviruses in CNS in

different animals, the direct association of astrovirus neuroinfection and encephalomyelitis should be treated with caution. Newly weaned pigs could potentially provide an in vivo animal model to study and clarify this association.

Acknowledgments

We thank Peter Engelmann for help in the cloning experiments.

This work was supported by grants from the Hungarian Scientific Research Fund (OTKA/NKFIH K111615) and Blood System Research Institute. Á.B. and P.P. were supported by the János Bolyai Research Scholarship of the Hungarian Academy of Sciences.

Dr. Boros is a molecular virologist at the Regional Laboratory of Virology, ÁNTSZ Regional Institute of State Public Health Service, Pécs, Hungary. His research interests include virus discovery and viral infectious diseases.

References

- Méndez E, Murillo A, Velázquez R, Burnham A, Arias CF. Replication cycle of astroviruses. In: Schultz-Cherry S, editor. *Astrovirus research: essential ideas, everyday impacts, future directions*. New York: Springer Science + Business Media; 2013. p. 19–47.
- Bosch A, Pintó RM, Guix S. Human astroviruses. *Clin Microbiol Rev*. 2014;27:1048–74. <http://dx.doi.org/10.1128/CMR.00013-14>
- Guix S, Bosch A, Pintó RM. Astrovirus taxonomy. In: Schultz-Cherry S, editor. *Astrovirus research: essential ideas, everyday impacts, future directions*. New York: Springer Science + Business Media; 2013. p. 97–119.
- Bosch A, Guix S, Krishna NK, Méndez E, Monroe SS, Pantin-Jackwood M, et al. *Astroviridae*. In: King AMQ, Adams MJ, Carstens EB, Lefkowitz EJ, editors. *Virus taxonomy: classification and nomenclature of viruses: ninth report of the International Committee on Taxonomy of Viruses*. San Diego: Elsevier; 2012. p. 953–9.
- Quan PL, Wagner TA, Briese T, Torgerson TR, Hornig M, Tashmukhamedova A, et al. Astrovirus encephalitis in boy with X-linked agammaglobulinemia. *Emerg Infect Dis*. 2010;16:918–25. <http://dx.doi.org/10.3201/eid1606.091536>
- Li L, Diab S, McGraw S, Barr B, Traslavina R, Higgins R, et al. Divergent astrovirus associated with neurologic disease in cattle. *Emerg Infect Dis*. 2013;19:1385–92. <http://dx.doi.org/10.3201/eid1909.130682>
- Meliopoulos V, Schultz-Cherry S. Astrovirus pathogenesis. In: Schultz-Cherry S, editor. *Astrovirus research: essential ideas, everyday impacts, future directions*. New York: Springer Science + Business Media; 2013. p. 97–119.
- Cordey S, Vu DL, Schibler M, L'Huillier AG, Brito F, Docquier M, et al. Astrovirus MLB2, a new gastroenteric virus associated with meningitis and disseminated infection. *Emerg Infect Dis*. 2016;22:846–53. <http://dx.doi.org/10.3201/eid2205.151807>
- Padmanabhan A, Hause BM. Detection and characterization of a novel genotype of porcine astrovirus 4 from nasal swabs from pigs with acute respiratory disease. *Arch Virol*. 2016;161:2575–9. <http://dx.doi.org/10.1007/s00705-016-2937-1>
- Cordey S, Brito F, Vu DL, Turin L, Kilowoko M, Kyungu E, et al. Astrovirus VA1 identified by next-generation sequencing in a nasopharyngeal specimen of a febrile Tanzanian child with acute respiratory disease of unknown etiology. *Emerg Microbes Infect*. 2016;5:e67. <http://dx.doi.org/10.1038/emi.2016.67>

11. Ng TFF, Kondov NO, Deng X, Van Eenennaam A, Neiberghs HL, Delwart E. A metagenomics and case-control study to identify viruses associated with bovine respiratory disease. *J Virol*. 2015;89:5340–9. <http://dx.doi.org/10.1128/JVI.00064-15>
12. Blomström AL, Widén F, Hammer AS, Belák S, Berg M. Detection of a novel astrovirus in brain tissue of mink suffering from shaking mink syndrome by use of viral metagenomics. *J Clin Microbiol*. 2010;48:4392–6. <http://dx.doi.org/10.1128/JCM.01040-10>
13. Blomström, AL, Ley C, Jacobson M. Astrovirus as a possible cause of congenital tremor type AII in piglets? *Acta Vet Scand*. 2014;56:82.
14. Pfaff F, Schlottau K, Scholes S, Courtenay A, Hoffmann B, Höper D, et al. A novel astrovirus associated with encephalitis and ganglionitis in domestic sheep. *Transbound Emerg Dis*. 2017;64:677–82. <http://dx.doi.org/10.1111/tbed.12623>
15. Vu DL, Bosch A, Pintó RM, Guix S. Epidemiology of classic and novel human astrovirus: gastroenteritis and beyond. *Viruses*. 2017;9:33. <http://dx.doi.org/10.3390/v9020033>
16. Vu DL, Cordey S, Brito F, Kaiser L. Novel human astroviruses: novel human diseases? *J Clin Virol*. 2016;82:56–63. <http://dx.doi.org/10.1016/j.jcv.2016.07.004>
17. Sato M, Kuroda M, Kasai M, Matsui H, Fukuyama T, Katano H, et al. Acute encephalopathy in an immunocompromised boy with astrovirus-MLB1 infection detected by next generation sequencing. *J Clin Virol*. 2016;78:66–70. <http://dx.doi.org/10.1016/j.jcv.2016.03.010>
18. Lum SH, Turner A, Guiver M, Bonney D, Martland T, Davies E, et al. An emerging opportunistic infection: fatal astrovirus (VA1/HMO-C) encephalitis in a pediatric stem cell transplant recipient. *Transpl Infect Dis*. 2016;18:960–4. <http://dx.doi.org/10.1111/tid.12607>
19. Brown JR, Morfopoulos S, Hubb J, Emmett WA, Ip W, Shah D, et al. Astrovirus VA1/HMO-C: an increasingly recognized neurotropic pathogen in immunocompromised patients. *Clin Infect Dis*. 2015;60:881–8. <http://dx.doi.org/10.1093/cid/ciu940>
20. Shan T, Li L, Simmonds P, Wang C, Moeser A, Delwart E. The fecal virome of pigs on a high-density farm. *J Virol*. 2011;85:11697–708. <http://dx.doi.org/10.1128/JVI.05217-11>
21. Reuter G, Knowles NJ. Porcine astroviruses. In: Zimmerman JJ, Karriker LA, Ramirez A, Schwartz KJ, Stevenson GW, editors. *Diseases of swine*, 10th ed. Hoboken (NJ): John Wiley & Sons; 2012. p. 487–9.
22. Xiao CT, Giménez-Lirola LG, Gerber PF, Jiang YH, Halbur PG, Opriessnig T. Identification and characterization of novel porcine astroviruses (PAstVs) with high prevalence and frequent co-infection of individual pigs with multiple PAstV types. *J Gen Virol*. 2013;94:570–82. <http://dx.doi.org/10.1099/vir.0.048744-00>
23. Xiao CT, Luo Z, Lv SL, Opriessnig T, Li RC, Yu XL. Identification and characterization of multiple porcine astrovirus genotypes in Hunan province, China. *Arch Virol*. 2017;162:943–52. <http://dx.doi.org/10.1007/s00705-016-3185-0>
24. Ma Z, Lui WO, Fire A, Dadrás SS. Profiling and discovery of novel miRNAs from formalin-fixed, paraffin-embedded melanoma and nodal specimens. *J Mol Diagn*. 2009;11:420–9. <http://dx.doi.org/10.2353/jmoldx.2009.090041>
25. Ma Z. Total RNA extraction from formalin-fixed, paraffin-embedded (FFPE) blocks. *Bio-protocol*. 2012;2:e161 [cited 2017 Sep 20]. <http://www.bio-protocol.org/e161>
26. Boros Á, Pankovics P, Simmonds P, Reuter G. Novel positive-sense, single-stranded RNA (+ssRNA) virus with di-cistronic genome from intestinal content of freshwater carp (*Cyprinus carpio*). *PLoS One*. 2011;6:e29145. <http://dx.doi.org/10.1371/journal.pone.0029145>
27. Boros A, Pankovics P, Knowles NJ, Reuter G. Natural interspecies recombinant bovine/porcine enterovirus in sheep. *J Gen Virol*. 2012;93:1941–51. <http://dx.doi.org/10.1099/vir.0.041335-0>
28. Edgar RC. MUSCLE: multiple sequence alignment with high accuracy and high throughput. *Nucleic Acids Res*. 2004;32:1792–7. <http://dx.doi.org/10.1093/nar/gkh340>
29. Tamura K, Stecher G, Peterson D, Filipiński A, Kumar S. MEGA6: Molecular Evolutionary Genetics Analysis version 6.0. *Mol Biol Evol*. 2013;30:2725–9. <http://dx.doi.org/10.1093/molbev/mst197>
30. Bouzalas IG, Wüthrich D, Walland J, Drögemüller C, Zurbriggen A, Vandeveldde M, et al. Neurotropic astrovirus in cattle with nonsuppurative encephalitis in Europe. *J Clin Microbiol*. 2014;52:3318–24. <http://dx.doi.org/10.1128/JCM.01195-14>
31. Chu DKW, Poon LLM, Guan Y, Peiris JSM. Novel astroviruses in insectivorous bats. *J Virol*. 2008;82:9107–14. <http://dx.doi.org/10.1128/JVI.00857-08>
32. Xiao CT, Halbur PG, Opriessnig T. Complete genome sequence of a newly identified porcine astrovirus genotype 3 strain US-MO123. *J Virol*. 2012;86:13126. <http://dx.doi.org/10.1128/JVI.02426-12>
33. Kapoor A, Li L, Victoria J, Oderinde B, Mason C, Pandey P, et al. Multiple novel astrovirus species in human stool. *J Gen Virol*. 2009;90:2965–72. <http://dx.doi.org/10.1099/vir.0.014449-0>
34. Lipkin WI, Anthony SJ. Virus hunting. *Virology*. 2015;479-480:194–9. <http://dx.doi.org/10.1016/j.virol.2015.02.006>
35. Gavier-Widén D, Bröjer C, Dietz HH, Englund L, Hammer AS, Hedlund KO, et al. Investigations into shaking mink syndrome: an encephalomyelitis of unknown cause in farmed mink (*Mustela vison*) kits in Scandinavia. *J Vet Diagn Invest*. 2004;16:305–12. <http://dx.doi.org/10.1177/104063870401600408>
36. Campbell JM, Crenshaw JD, Polo J. The biological stress of early weaned piglets. *J Anim Sci Biotechnol*. 2013;4:19. <http://dx.doi.org/10.1186/2049-1891-4-19>
37. Yokoyama CC, Loh J, Zhao G, Stappenbeck TS, Wang D, Huang HV, et al. Adaptively immunity restricts replication of novel murine astroviruses. *J Virol*. 2012;86:12262–70. <http://dx.doi.org/10.1128/JVI.02018-12>
38. Ng TFF, Kondov NO, Hayashimoto N, Uchida R, Cha Y, Beyer AI, et al. Identification of an astrovirus commonly infecting laboratory mice in the US and Japan. *PLoS One*. 2013;8:e66937. <http://dx.doi.org/10.1371/journal.pone.0066937>
39. Farkas T, Fey B, Keller G, Martella V, Egyed L. Molecular detection of novel astroviruses in wild and laboratory mice. *Virus Genes*. 2012;45:518–25. <http://dx.doi.org/10.1007/s11262-012-0803-0>
40. Marvin SA, Huerta CT, Sharp B, Freiden P, Cline TD, Schultz-Cherry S. Type I interferon response limits astrovirus replication and protects against increased barrier permeability in vitro and in vivo. *J Virol*. 2016;90:1988–96. <http://dx.doi.org/10.1128/JVI.02367-15>
41. Wunderli W, Meerbach A, Güngör T, Berger C, Greiner O, Caduff R, et al. Astrovirus infection in hospitalized infants with severe combined immunodeficiency after allogeneic hematopoietic stem cell transplantation. *PLoS One*. 2011;6:e27483. <http://dx.doi.org/10.1371/journal.pone.0027483>
42. Bouzalas IG, Wüthrich D, Selimovic-Hamza S, Drögemüller C, Bruggmann R, Seuberlich T. Full-genome based molecular characterization of encephalitis-associated bovine astroviruses. *Infect Genet Evol*. 2016;44:162–8. <http://dx.doi.org/10.1016/j.meegid.2016.06.052>
43. Dong J, Dong L, Méndez E, Tao Y. Crystal structure of the human astrovirus capsid spike. *Proc Natl Acad Sci U S A*. 2011;108:12681–6. <http://dx.doi.org/10.1073/pnas.1104834108>
44. Krishna NK. Identification of structural domains involved in astrovirus capsid biology. *Viral Immunol*. 2005;18:17–26. <http://dx.doi.org/10.1089/vim.2005.18.17>
45. Ito M, Kuroda M, Masuda T, Akagami M, Haga K, Tsuchiaka S, et al. Whole genome analysis of porcine astroviruses detected in

- Japanese pigs reveals genetic diversity and possible intra-genotypic recombination. *Infect Genet Evol.* 2017;50:38–48. <http://dx.doi.org/10.1016/j.meegid.2017.02.008>
46. Frémond ML, Pérot P, Muth E, Cros G, Dumarest M, Mahlaoui N, et al. Next-generation sequencing for diagnosis and tailored therapy: a case report of astrovirus-associated progressive encephalitis. *J Pediatric Infect Dis Soc.* 2015;4:e53–7. <http://dx.doi.org/10.1093/jpids/piv040>
47. Selimovic-Hamza S, Boujon CL, Hilbe M, Oevermann A, Seuberlich T. Frequency and pathological phenotype of bovine astrovirus CH13/NeuroS1 infection in neurologically-diseased cattle: towards assessment of causality. *Viruses.* 2017;9:12. <http://dx.doi.org/10.3390/v9010012>
48. Ulloa JC, Gutiérrez MF. Genomic analysis of two ORF2 segments of new porcine astrovirus isolates and their close relationship with human astroviruses. *Can J Microbiol.* 2010; 56:569–77. <http://dx.doi.org/10.1139/W10-042>

Address for correspondence: Gábor Reuter, Department of Medical Microbiology and Immunology, University of Pécs, Szigeti út 12, H-7624 Pécs, Hungary; email: reuter.gabor@gmail.com

December 2012: Zoonotic Infections

- Farm Animal Contact as Risk Factor for Transmission of Bovine-associated *Salmonella* Subtypes
- Reservoir Competence of Wildlife Host Species for *Babesia microti*



- Variant Rabbit Hemorrhagic Disease Virus in Young Rabbits, Spain
- Reservoir Competence of Vertebrate Hosts for *Anaplasma phagocytophilum*
- MRSA Variant in Companion Animals
- Arctic-like Rabies Virus, Bangladesh
- No Evidence of Prolonged Hendra Virus Shedding by 2 Patients, Australia
- Differentiation of Prions from L-type BSE versus Sporadic Creutzfeldt-Jakob Disease
- Hepatitis E Virus Outbreak in Monkey Facility, Japan
- Porcine Reproductive and Respiratory Syndrome Virus, Thailand, 2010–2011
- Cygnet River Virus, a Novel Orthomyxovirus from Ducks, Australia
- West Nile Virus Neurologic Disease in Humans, South Africa
- Outbreak of Influenza A(H3N2) Variant Virus Infection among Attendees of an Agricultural Fair, Pennsylvania, USA, 2011
- Group 2 Vaccinia Virus, Brazil
- Diagnostic Assays for Crimean-Congo Hemorrhagic Fever
- High Diversity of RNA Viruses in Rodents, Ethiopia
- *Borrelia*, *Rickettsia*, and *Ehrlichia* spp. in Bat Ticks, France, 2010
- Subclinical Influenza Virus A Infections in Pigs Exhibited at Agricultural Fairs, Ohio, 2009–2011
- Nonprimate Hepaciviruses in Domestic Horses, United Kingdom
- Transmission Routes for Nipah Virus from Malaysia and Bangladesh
- Virulent Avian Infectious Bronchitis Virus, People's Republic of China
- Enterovirus 71-associated Hand, Foot, and Mouth Disease, Southern Vietnam, 2011
- Epizootic Spread of Schmallenberg Virus among Wild Cervids, Belgium, Fall 2011



**EMERGING
INFECTIOUS DISEASES**

<https://wwwnc.cdc.gov/eid/articles/issue/18/12/table-of-contents>

Characterization of *Streptococcus pyogenes* from Animal Clinical Specimens, Spain

Ana Isabel Vela, Pilar Villalón, Juan Antonio Sáez-Nieto, Gema Chacón,
Lucas Domínguez, José Francisco Fernández-Garayzábal

Streptococcus pyogenes appears to be almost exclusively restricted to humans, with few reports on isolation from animals. We provide a detailed characterization (*emm* typing, pulsed-field gel electrophoresis [PFGE], and multilocus sequence typing [MLST]) of 15 *S. pyogenes* isolates from animals associated with different clinical backgrounds. We also investigated erythromycin resistance mechanisms and phenotypes and virulence genes. We observed 2 *emm* types: *emm12* (11 isolates) and *emm77* (4 isolates). Similarly, we observed 2 genetic lineages, sequence type (ST) 26 and ST63. Most isolates exhibited the M macrolide resistance phenotype and the *mefA/ermB* genotype. Isolates were grouped into 2 clones on the basis of *emm*-MLST-PFGE-virulence gene profile combinations: clone 1, characterized by the combined genotype *emm12*-ST36-pulsotype A-*speG*; and clone 2, characterized by the genotype *emm77*-ST63-pulsotype B-*speC*. Our results do not show conclusively that animals may represent a new reservoir of *S. pyogenes* but indicate the ability of human-derived *S. pyogenes* isolates to colonize and infect animals.

Streptococcus pyogenes (group A *Streptococcus*) is a Gram-positive bacterium that causes several diseases in humans. *S. pyogenes* usually colonizes the throat or skin epithelial surfaces and causes a wide variety of clinical manifestations, such as noninvasive pharyngitis, dermatitis, and scarlet fever (1,2). However, this pathogen is also responsible for deadly invasive systemic infections such as necrotizing fasciitis and streptococcal toxic shock syndrome (3). The ecologic niche of *S. pyogenes* appears to be quite narrow, with humans being the almost exclusive biologic host (4) and no animal or environmental reservoir of known importance contributing to its life cycle (2). Reports of isolation of *S. pyogenes* from sources other than humans are rare. *S. pyogenes* has recently been associated with an

infection in a free-living European hedgehog (*Erinaceus europaeus*) (5). *S. pyogenes* has also been recovered from the feces of a dog with possible antibiotic-associated colitis (6) and from the eye discharge of a dog with conjunctivitis (7). We know of no other reports of isolation of this microorganism from animals.

We conducted a study to provide a detailed characterization of animal *S. pyogenes* isolates using *emm* typing, pulsed-field gel electrophoresis (PFGE), and multilocus sequence typing (MLST). We also investigated erythromycin resistance mechanisms and phenotypes, as well as virulence genes.

Materials and Methods

Origin and Identification of Bacterial Isolates

We analyzed 15 isolates of *S. pyogenes* obtained from rabbits (n = 14) and sheep (n = 1) in Spain during 2006–2014 (Table 1). Most rabbit isolates were from unrelated animals, located in different commercial farms (n = 14) and locations throughout Spain. Links between rabbit farms were not identified. The sheep included in this study was from a farm that had no rabbits. Human contact with animals was restricted to the personnel working in the rabbit farms and sheep flocks.

We recovered isolates from different clinical backgrounds: 8 from skin infections, 4 from genital tract infections, and 1 each from respiratory infections, mastitis, and otitis. We collected samples from skin and ear infections with sterile cotton swabs and collected the milk sample from the mastitis case aseptically in a sterile tube. Rabbits with genital tract or lung infections were euthanized, at farms or laboratories, and necropsied under aseptic conditions; clinical specimens were collected with forceps and scissors scrubbed in 70% ethanol. Samples taken at farms were transported to the laboratory in refrigerated polyethylene bags and processed within 24 hours after sampling.

Clinical specimens were sampled onto blood agar plates that were incubated at 37°C for 24–48 hours. Identification of isolates as *S. pyogenes* was based on colony morphology, β -hemolysis, and biochemical characteristics using the commercial identification system rapid

Author affiliations: Complutense University, Madrid, Spain (A.I. Vela, L. Domínguez, J.F. Fernández-Garayzábal); Instituto de Salud Carlos III, Majadahonda, Madrid (P. Villalón, J.A. Sáez-Nieto); Laboratorio Exopol San Mateo, Zaragoza, Spain (G. Chacón)

DOI: <https://doi.org/10.3201/eid2312.151146>

Table 1. Features and disease manifestations of 15 animals from which *Streptococcus pyogenes* isolates were collected, Spain, 2006–2014

Isolate*	Animal	Clinical background	Specimen	Geographic region	Isolation date†
M50163	Rabbit	Metritis	Uterus	Valencia	2006 Jan
M79144	Rabbit	Abscesses and dermatitis	Skin	Valladolid	2013 Mar
M78761	Rabbit	Dermatitis	Skin	Valladolid	2013 Feb
M75791	Rabbit	Abscesses	Skin	Valencia	2012 Apr
M75539	Sheep	Abscesses	Skin	Zaragoza	2012 Mar
M75533	Rabbit	Otitis	Ear	Valencia	2012 Mar
M75123	Rabbit	Metritis	Uterus	Castellón	2012 Feb
M73512	Rabbit	Abortion	Uterus	Zaragoza	2011 Aug
M72636	Rabbit	Metritis	Uterus	Zaragoza	2011 May
M72193	Rabbit	Abscesses	Skin	Valencia	2011 Apr
83639	Rabbit	Abscesses and dermatitis	Skin	Valladolid	2014 Mar
83553	Rabbit	Pneumonia	Lung	Zaragoza	2014 Mar
M82209	Rabbit	Abscesses	Skin	Valladolid	2013 Dec
M75768	Rabbit	Mastitis	Milk	Zaragoza	2012 Mar
85374	Rabbit	Skin infection	Skin	Valladolid	2014 Aug

*Isolates M50163 and M73512 were recovered in pure culture. The remaining isolates were recovered together with *Staphylococcus aureus*.

†Except for isolates M79144 and M78761, which were isolated in the same farm but at different times, all other isolates were recovered from animals at different farms.

ID 32 STREP (BioMerieux, Marcy L'Étoile, France). Biochemical identification was also confirmed by sequencing the 16S rRNA gene (8).

Antimicrobial Drug Susceptibility Tests

We performed drug susceptibility testing using the Clinical and Laboratory Standards Institute broth microdilution method (9) in Mueller–Hinton broth supplemented with 5% lysed horse blood. We determined the susceptibilities of the isolates with a commercially available susceptibility test (CMV3AGPF Sensititer standard panel; Trek Diagnostics, West Essex, UK) performed according to the manufacturer's instructions. The agents we tested were penicillin (0.25–16 µg/mL), erythromycin (0.25–8 µg/mL), vancomycin (0.25–32 µg/mL), daptomycin (0.25–16 µg/mL), chloramphenicol (2–32 µg/mL), linezolid (0.5–8 µg/mL), tetracycline (1–32 µg/mL), quinupristin (0.5–32 µg/mL), tigecycline (0.05–0.5 µg/mL), streptomycin (512–2048 µg/mL), kanamycin (128–1024 µg/mL), lincomycin (1–8 µg/mL), and gentamicin (128–1024 µg/mL). In addition, we determined MICs of clindamycin, erythromycin, and tetracycline by Etest (AB Biodisk, Solna, Sweden). We interpreted the results using the Clinical and Laboratory Standards Institute breakpoints for streptococci (9) for penicillin, erythromycin, vancomycin, daptomycin, chloramphenicol, tetracycline, and quinupristin; the European Committee on Antimicrobial Susceptibility Testing breakpoints for tigecycline and linezolid (http://www.eucast.org/clinical_breakpoints); and the Comité de l'Antibiogramme de la Société Française de Microbiologie breakpoints (10) for streptomycin, kanamycin, lincomycin, and gentamicin.

Macrolide Resistance Phenotype

To identify macrolide resistance phenotypes, we used a double-disk diffusion test (D-zone test) using erythromycin (15 µg) and clindamycin (2 µg) disks, as described

by Hasenbein et al. (11). Isolates with blunting of the clindamycin inhibition zone around the disk adjacent to the erythromycin disk were considered to have an iMLS_B phenotype (erythromycin resistant and clindamycin inducible). Clindamycin-susceptible isolates without blunting indicated an M phenotype (erythromycin resistant and clindamycin susceptible). Isolates that were resistant to both antimicrobial drugs were considered to have a cMLS_B phenotype (constitutive erythromycin and clindamycin resistant).

Detection of Macrolides and Tetracycline Resistance Genes

We extracted DNA according to the protocol in the US Centers for Disease Control and Prevention (CDC) *S. pyogenes* sequence database (<http://www.cdc.gov/ncidod/biotech/strep/protocols.htm>). We screened all erythromycin-resistant isolates by PCR for the erythromycin resistance genes *ermB* (12), *ermA* (13), *mefA* (14), and *msrD* (15). We tested tetracycline-resistant isolates for the tetracycline resistance genes *tetM* and *tetO* (14).

Detection of Virulence Genes

We tested the *S. pyogenes* isolates for the presence of the virulence genes *speA*, *speB*, *speC*, *speF*, *speG*, *speH*, *speJ*, *speM*, *ssa*, and *smeZ* by PCR. We used primers and conditions described previously (16,17).

PFGE Analysis, MLST, and *emm* Typing

For PFGE analysis, genomic DNAs of the *S. pyogenes* isolates were prepared and digested with *Sma*I restriction enzyme (MBI Fermentas, Vilnius, Lithuania) following a previously published protocol (18). We performed MLST following the method established by Enright et al. (19) and assigned the allele and sequence type (ST) according to the PubMLST website (<http://pubmlst.org/spyogenes>). We amplified and sequenced the *emm* gene according to the

protocol of the CDC International Streptococcal Reference Laboratory (<http://www.cdc.gov/streplab/protocol-emm-type.html>). We compared the sequences of the *emm* genes with those in the CDC database using BLAST analysis (<http://www.cdc.gov/ncidod/biotech/strep/strepblast.htm>) for type assignment.

Results

We observed 2 *emm* types (Table 2): *emm12* was the most frequent (11 isolates), followed by *emm77* (4 isolates). Two pulsotypes (A and B) were generated after typing the isolates by PFGE with the restriction enzyme *Sma*I; 11 isolates were pulsotype A and 4 isolates pulsotype B (Figure). Similarly, we observed 2 genetic lineages (ST26 and ST63) after MLST analysis.

All 15 *S. pyogenes* isolates were susceptible to penicillin (MIC ≤ 0.25 mg/L), vancomycin (MICs ≤ 0.25 to 0.5 mg/L), daptomycin (MIC ≤ 0.25 mg/L), chloramphenicol (MICs ≤ 2 to 4 mg/L), tigecycline (MICs ≤ 0.015 to 0.12 mg/L), and gentamicin (MIC ≤ 128 mg/L). Additionally, all isolates but 1 were susceptible to kanamycin (MIC ≤ 128 mg/L), and 12 isolates showed susceptibility to linezolid (MICs < 2 mg/L), streptomycin (MICs $\geq 2,048$ mg/L), and lincomycin (≥ 8 mg/L). On the other hand, all isolates were resistant to tetracycline, with MICs ranging from 24 to 96 mg/L using Etest (Table 2). Eleven isolates showed tetracycline-resistant genotype *tetM/tetO*, 2 isolates *tetO*, and 1 isolate *tetM* (Table 2).

Most isolates (7/15) exhibited the M phenotype, 2 isolates the phenotype cMLS_B, and 1 the phenotype iMLS_B (Table 2). The macrolide-resistant genotype *mefA/ermB* was the most frequently observed, seen in all isolates but 1 with the M phenotype and in the isolate with phenotype cMLS_B. The genotype *ermB* was observed alone in 1 isolate of each phenotype. No isolate carried the *msrD* or *ermA* macrolide-resistant determinants.

We detected the chromosomal-encoded *speB* and *speF* genes in all isolates. We observed 2 different virulence

gene profiles based on the presence/absence of the *speG* and *speC* genes. We detected the genotype *speG* in 11 isolates and the genotype *speC* in 4 isolates (Table 2).

We grouped the 15 *S. pyogenes* isolates into 2 different clones on the basis of *emm*-MLST-PFGE-virulence genes profile combinations. Clone 1 grouped isolates characterized by the combined genotype *emm12*-ST36-pulsotype A-*speB/speF/speG*, whereas isolates of clone 2 were characterized by the genotype *emm77*-ST63-pulsotype B-*speB/speF/speC* (Table 2). In addition, isolates of clone 1 were erythromycin resistant, mainly exhibiting an M phenotype, and isolates of clone 2 were erythromycin susceptible.

Discussion

S. pyogenes is a human pathogen that has rarely been isolated from animals. It has been isolated from abscesses in cervical and mesenteric lymph nodes and liver of a free-living European hedgehog (*E. europaeus*) and from 2 dogs with severe colonic disease and conjunctivitis (5–7). Here we describe the detailed characterization of animal *S. pyogenes* isolates from different clinical specimens obtained from rabbits (n = 14) and sheep (n = 1) in Spain during 2006–2014. This pathogen was recovered mainly from noninvasive cases, with skin infections being the most common clinical presentation (n = 6), followed by genital tract infections (n = 4) (Table 1). *S. pyogenes* was isolated from all skin clinical samples together with *Staphylococcus aureus*, a well-recognized pathogen associated with different skin diseases in animals (20). These results indicate that although *S. pyogenes* should be able to colonize the skin of animals, it is difficult to ascertain its etiologic significance in skin infections. However, *S. pyogenes* was isolated in pure culture from clinical specimens of the genital tract, ears, mammary glands, and lungs in rabbits, indicating the potential role of *S. pyogenes* in these infections.

Most of the *S. pyogenes* isolates we tested (n = 11) exhibited the genotype *emm12*-ST36, which has been isolated

Table 2. Testing results for the 15 isolates characterized in study of *Streptococcus pyogenes* from animal specimens, Spain*

Isolate	<i>emm</i> type	PFGE profile	MLST type	MIC, mg/L			Macrolide resistance		TET resistance genes	Virulence genes
				ERY	CLIN	TET	Phenotype	Genotype		
M50163	12	A	ST36	>256	32	96	cMLS _B	<i>mefA/ermB</i>	<i>tetM/tetO</i>	<i>speB/speF/speG</i>
M79144	12	A	ST36	>256	0.75	48	M	<i>mefA/ermB</i>	<i>tetM/tetO</i>	<i>speB/speF/speG</i>
M78761	12	A	ST36	>256	0.75	32	M	<i>mefA/ermB</i>	<i>tetM/tetO</i>	<i>speB/speF/speG</i>
M75791	12	A	ST36	6	0.09	32	M	<i>mefA/ermB</i>	<i>tetM/tetO</i>	<i>speB/speF/speG</i>
M75539	12	A	ST36	8	0.19	24	M	<i>mefA/ermB</i>	<i>tetM/tetO</i>	<i>speB/speF/speG</i>
M75533	12	A	ST36	16	0.19	32	M	<i>mefA/ermB</i>	<i>tetM/tetO</i>	<i>speB/speF/speG</i>
M75123	12	A	ST36	12	0.19	48	M	<i>ermB</i>	<i>tetM/tetO</i>	<i>speB/speF/speG</i>
M73512	12	A	ST36	0.25	0.12	32			<i>tetM/tetO</i>	<i>speB/speF/speG</i>
M72636	12	A	ST36	>256	>256	48	cMLS _B	<i>ermB</i>	<i>tetM/tetO</i>	<i>speB/speF/speG</i>
M72193	12	A	ST36	>256	1.5	96	iMLS _B	<i>ermB</i>	<i>tetM/tetO</i>	<i>speB/speF/speG</i>
83639	12	A	ST36	>256	0.38	48	M	<i>ermB</i>	<i>tetM</i>	<i>speB/speF/speG</i>
83553	77	B	ST63	0.19	0.12	64				<i>speB/speF/spec</i>
85374	77	B	ST63	0.12	0.09	64			<i>tetO</i>	<i>speB/speF/spec</i>
M75768	77	B	ST63	0.12	0.09	32			<i>tetM/tetO</i>	<i>speB/speF/speC</i>
M82209	77	B	ST63	0.19	0.12	64			<i>tetO</i>	<i>speB/speF/speC</i>

*ERY, erythromycin; CLIN, clindamycin; MLST, multilocus sequence typing; PFGE, pulsed-field gel electrophoresis; ST, sequence type; TET, tetracycline.

repeatedly from humans in different countries (21–27), including Spain (28–30). This genotype can exhibit an M phenotype (31) and has been associated with skin and soft tissue infections (32), data that fit with our results, as more than half of the isolates with this genotype were isolated from abscesses and dermatitis (Table 2). The genotype *emm77*-ST63 that we identified in 4 animal isolates has also been detected in human *S. pyogenes* isolates (21,25,33), but unlike human isolates, the isolates in our study were erythromycin and clindamycin susceptible (Table 2).

All 11 isolates in clone 1 (pulsotype A) exhibited PFGE profiles that were indistinguishable from each other, and all 4 isolates in clone 2 also exhibited PFGE profiles that were indistinguishable from each other (pulsotype B; Figure). Isolates of *S. pyogenes* usually exhibit high levels of genetic diversity (4). Thus, the fact that we identified only 2 clones in different isolates collected over a period of 8 years was unexpected. The possibility of a common source of infection is very unlikely because all isolates were recovered at different times from different animals in farms located at geographically distant locations spread throughout Spain, without any epidemiologic relationship (Table 1). In addition, clinical specimens were processed independently in the same laboratory by highly qualified and trained personnel, which makes the possibility of a cross-contamination in the laboratory unlikely.

Under these conditions, multiple human-to-animal transmission events should be the most likely origin of these genotypes in sheep and rabbits. Another possible explanation could be that genotypes ST36 and ST63, although originating from humans, represent genetic lineages

with a specific host tropism, mainly for rabbits, which contributed to their successful dissemination in these animals, as observed with other streptococci (34). Cases of *S. pyogenes* infection were not recorded among the personnel working in the rabbit farms and sheep flock from which *S. pyogenes* was isolated. Asymptomatic human carriers have a key role in *S. pyogenes* transmission (35). For these reasons and even though screenings to identify asymptomatic *S. pyogenes* carriers were not carried out, we can speculate that asymptomatic employees were the most probable source of *S. pyogenes* in the animals included in the study. Although we cannot infer from the results of this study that animals, mainly rabbits, may represent a new reservoir of *S. pyogenes*, the results clearly indicate the ability of human-derived *S. pyogenes* isolates to colonize and infect animals, which could be more frequent than has been recognized until now.

Isolates with the genotype *mefA/ermB* usually correlate with the cMLS_B phenotype, but 5 of the 6 *S. pyogenes* isolates with the *mefA/ermB* genotype in our study exhibited M phenotype (Table 2), which agrees with previous observations (29). The *erm* gene usually confers co-resistance to macrolides, lincosamides, and streptogramins. Curiously, all M phenotype isolates in our study showed susceptibility to clindamycin and were positive for the *ermB* gene. This result, although unusual, has also been observed previously in *S. pyogenes* isolates from different countries (26,36–38). A possible explanation could be that the *ermB* gene was nonfunctional in the isolates with clindamycin-susceptible phenotypes. The isolate M72193 exhibited the iMLS_B phenotype but was *ermA*-negative (Table 2). This result, although infrequent, has also been observed in previous studies (39). Isolates with the iMLS_B phenotype have been further subdivided into 3 distinct types: type A, associated with the presence of the *ermB* gene; and types B and C, associated with the presence of the *ermA* gene (40,41). This isolate carried the *ermB* gene (Table 2), suggesting therefore an iMLS_B-A phenotype.

Unlike most human *S. pyogenes* isolates, which usually carry either *tetM* or *tetO* genes, most of the isolates in this study (n = 11) carried both genes (Table 2). Human isolates with the combination of *tetM* and *tetO* tetracycline-resistance genes have been identified previously in Spain (29). Another uncommon result was the identification of 1 isolate (83553) that was resistant to tetracycline (MIC 64 mg/L) but lacked resistance *tetM* and *tetO* genes (Table 2) commonly associated with tetracycline resistance in *S. pyogenes* (42). However, tetracycline-resistant strains and negativity to these genes have also been reported (43). Further studies will be necessary to elucidate the precise mechanism of resistance to tetracycline in this strain.

In summary, this study provides a detailed characterization of animal *S. pyogenes* isolates associated with

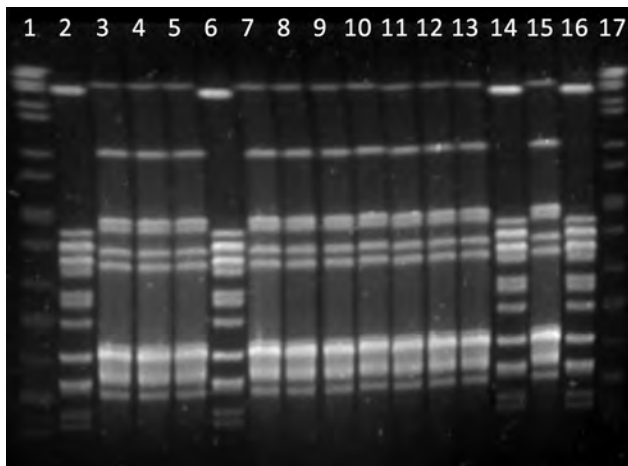


Figure. Pulsed-field gel electrophoresis patterns of *Smal*-digested DNA of clinical isolates of *Streptococcus pyogenes* from animal specimens, Spain, 2006–2014. Lanes 1 and 17, DNA molecular size marker; lanes 3, 4, 5, 7, 8, 9, 10, 11, 12, 13, 15, and 16, isolates M50163, M79144, M78761, M75791, M75539, M75533, M75123, M73512, M72636, M72193, and M83639, respectively (pulsotype A); lanes 2, 6, 14, and 16, isolates 83553, 85374, M75768, and M82209, respectively (pulsotype B).

different clinical backgrounds. This pathogen should be considered by veterinary microbiologists when processing clinical material from animals.

Dr. Vela is an associate professor at the Animal Health Department, Veterinary Faculty, Complutense University, Madrid, Spain. Her research focuses on the characterization of relevant animal bacterial pathogens.

References

- Bisno AL, Stevens D. *Streptococcus pyogenes* (including streptococcal toxic shock syndrome and necrotizing fasciitis). In: Mandell GL, Douglas RG, Dolin R, editors. Principles and practice of infectious diseases, 5th ed., vol. 2. Philadelphia: Churchill Livingstone; 2000. p. 2101–17.
- Ralph AP, Carapetis JR. Group A streptococcal diseases and their global burden. *Curr Top Microbiol Immunol*. 2013;368:1–27.
- Walker MJ, Barnett TC, McArthur JD, Cole JN, Gillen CM, Henningham A, et al. Disease manifestations and pathogenic mechanisms of group A *Streptococcus*. *Clin Microbiol Rev*. 2014;27:264–301. <http://dx.doi.org/10.1128/CMR.00101-13>
- Bessen DE. Population biology of the human restricted pathogen, *Streptococcus pyogenes*. *Infect Genet Evol*. 2009;9:581–93. <http://dx.doi.org/10.1016/j.meegid.2009.03.002>
- Franklin LH, Efstratiou A, Macgregor SK, John SK, Hopkins T, Cunningham AA, et al. *Streptococcus pyogenes* infection in a free-living European hedgehog (*Erinaceus europaeus*). *EcoHealth*. 2015;12:689–92. <http://dx.doi.org/10.1007/s10393-015-1051-2>
- Willard MD, Berridge B, Braniecki A, Bouley D. Possible antibiotic-associated colitis in a dog. *J Am Vet Med Assoc*. 1998; 213:1775–9, 1753–4.
- Sprot H, Efstratiou A, Hubble M, Morgan M. Man's best friend?—first report of prosthetic joint infection with *Streptococcus pyogenes* from a canine source. *J Infect*. 2012;64:625–7. <http://dx.doi.org/10.1016/j.jinf.2012.02.006>
- Vela AI, Fernández E, Lawson PA, Latre MV, Falsen E, Domínguez L, et al. *Streptococcus entericus* sp. nov., isolated from cattle intestine. *Int J Syst Evol Microbiol*. 2002;52:665–9. <http://dx.doi.org/10.1099/00207713-52-2-665>
- Clinical and Laboratory Standards Institute. Performance standards for antimicrobial susceptibility testing; twenty-second informational supplement (M100–S22). Wayne (PA): The Institute; 2012.
- Comité de l'antibiogramme de la Société Française de Microbiologie. Recommandations 2012. Paris: Société Française de Microbiologie; 2012 [cited 2015 Jul 8]. <http://www.sfm-microbiologie.org/>
- Hasenbein ME, Warner JE, Lambert KG, Cole SE, Onderdonk AB, McAdam AJ. Detection of multiple macrolide- and lincosamide-resistant strains of *Streptococcus pyogenes* from patients in the Boston area. *J Clin Microbiol*. 2004;42:1559–63. <http://dx.doi.org/10.1128/JCM.42.4.1559-1563.2004>
- Sutcliffe J, Grebe T, Tait-Kamradt A, Wondrack L. Detection of erythromycin-resistant determinants by PCR. *Antimicrob Agents Chemother*. 1996;40:2562–6.
- Seppälä H, Skurnik M, Soini H, Roberts MC, Huovinen P. A novel erythromycin resistance methylase gene (*ermTR*) in *Streptococcus pyogenes*. *Antimicrob Agents Chemother*. 1998;42:257–62.
- Malhotra-Kumar S, Lammens C, Piessens J, Goossens H. Multiplex PCR for simultaneous detection of macrolide and tetracycline resistance determinants in streptococci. *Antimicrob Agents Chemother*. 2005;49:4798–800. <http://dx.doi.org/10.1128/AAC.49.11.4798-4800.2005>
- Lüthje P, Schwarz S. Molecular basis of resistance to macrolides and lincosamides among staphylococci and streptococci from various animal sources collected in the resistance monitoring program BfT-GermVet. *Int J Antimicrob Agents*. 2007;29:528–35. <http://dx.doi.org/10.1016/j.ijantimicag.2006.12.016>
- Commons R, Rogers S, Gooding T, Danchin M, Carapetis J, Robins-Browne R, et al. Superantigen genes in group A streptococcal isolates and their relationship with *emm* types. *J Med Microbiol*. 2008;57:1238–46. <http://dx.doi.org/10.1099/jmm.0.2008/001156-0>
- Rivera A, Rebollo M, Miró E, Mateo M, Navarro F, Gurguí M, et al. Superantigen gene profile, *emm* type and antibiotic resistance genes among group A streptococcal isolates from Barcelona, Spain. *J Med Microbiol*. 2006;55:1115–23. <http://dx.doi.org/10.1099/jmm.0.46481-0>
- Stanley J, Linton D, Desai M, Efstratiou A, George R. Molecular subtyping of prevalent M serotypes of *Streptococcus pyogenes* causing invasive disease. *J Clin Microbiol*. 1995;33:2850–5.
- Enright MC, Spratt BG, Kalia A, Cross JH, Bessen DE. Multilocus sequence typing of *Streptococcus pyogenes* and the relationships between *emm* type and clone. *Infect Immun*. 2001;69:2416–27. <http://dx.doi.org/10.1128/IAI.69.4.2416-2427.2001>
- Foster AP. Staphylococcal skin disease in livestock. *Vet Dermatol*. 2012;23:342–51, e63. <http://dx.doi.org/10.1111/j.1365-3164.2012.01093.x>
- Enright MC, Spratt BG, Kalia A, Cross JH, Bessen DE. Multilocus sequence typing of *Streptococcus pyogenes* and the relationships between *emm* type and clone. *Infect Immun*. 2001;69:2416–27. <http://dx.doi.org/10.1128/IAI.69.4.2416-2427.2001>
- Steer AC, Law I, Matatolu L, Beall BW, Carapetis JR. Global *emm* type distribution of group A streptococci: systematic review and implications for vaccine development. *Lancet Infect Dis*. 2009;9:611–6. [http://dx.doi.org/10.1016/S1473-3099\(09\)70178-1](http://dx.doi.org/10.1016/S1473-3099(09)70178-1)
- Luca-Harari B, Ekelund K, van der Linden M, Staum-Kaltoft M, Hammerum AM, Jasir A. Clinical and epidemiological aspects of invasive *Streptococcus pyogenes* infections in Denmark during 2003 and 2004. *J Clin Microbiol*. 2008;46:79–86. <http://dx.doi.org/10.1128/JCM.01626-07>
- Silva-Costa C, Pinto FR, Ramírez M, Melo-Cristino J; Portuguese Surveillance Group for the Study of Respiratory Pathogens. Decrease in macrolide resistance and clonal instability among *Streptococcus pyogenes* in Portugal. *Clin Microbiol Infect*. 2008;14:1152–9. <http://dx.doi.org/10.1111/j.1469-0691.2008.02104.x>
- McGregor KF, Spratt BG. Identity and prevalence of multilocus sequence typing-defined clones of group A streptococci within a hospital setting. *J Clin Microbiol*. 2005;43:1963–7. <http://dx.doi.org/10.1128/JCM.43.4.1963-1967.2005>
- Reinert RR, Lütticken R, Sutcliffe JA, Tait-Kamradt A, Cil MY, Schorn HM, et al. Clonal relatedness of erythromycin-resistant *Streptococcus pyogenes* isolates in Germany. *Antimicrob Agents Chemother*. 2004;48:1369–73. <http://dx.doi.org/10.1128/AAC.48.4.1369-1373.2004>
- Szczyca K, Sadowy E, Izdebski R, Hryniewicz W. A rapid increase in macrolide resistance in *Streptococcus pyogenes* isolated in Poland during 1996–2002. *J Antimicrob Chemother*. 2004;54:828–31. <http://dx.doi.org/10.1093/jac/dkh420>
- Ardanuy C, Domenech A, Rolo D, Calatayud L, Tubau F, Ayats J, et al. Molecular characterization of macrolide- and multidrug-resistant *Streptococcus pyogenes* isolated from adult patients in Barcelona, Spain (1993–2008). *J Antimicrob Chemother*. 2010;65:634–43. <http://dx.doi.org/10.1093/jac/dkq006>
- Rubio-López V, Valdezate S, Alvarez D, Villalón P, Medina MJ, Salcedo C, et al. Molecular epidemiology, antimicrobial susceptibilities and resistance mechanisms of *Streptococcus pyogenes* isolates resistant to erythromycin and tetracycline in Spain (1994–2006). *BMC Microbiol*. 2012;12:215. <http://dx.doi.org/10.1186/1471-2180-12-215>
- Rivera A, Rebollo M, Miró E, Mateo M, Navarro F, Gurguí M, et al. Superantigen gene profile, *emm* type and antibiotic resistance genes among group A streptococcal isolates from Barcelona, Spain.

- J Med Microbiol. 2006;55:1115–23. <http://dx.doi.org/10.1099/jmm.0.46481-0>
31. Opavski N, Gajic I, Borek AL, Obszańska K, Stanojevic M, Lazarevic I, et al. Molecular characterization of macrolide resistant *Streptococcus pyogenes* isolates from pharyngitis patients in Serbia. *Infect Genet Evol.* 2015;33:246–52. <http://dx.doi.org/10.1016/j.meegid.2015.05.011>
 32. Lin JN, Chang LL, Lai CH, Lin HH, Chen YH. Clinical and molecular characteristics of invasive and noninvasive skin and soft tissue infections caused by group A *Streptococcus*. *J Clin Microbiol.* 2011;49:3632–7. <http://dx.doi.org/10.1128/JCM.00531-11>
 33. Pérez-Trallero E, Montes M, Orden B, Tamayo E, García-Arenzana JM, Marimón JM. Phenotypic and genotypic characterization of *Streptococcus pyogenes* isolates displaying the MLSB phenotype of macrolide resistance in Spain, 1999 to 2005. *Antimicrob Agents Chemother.* 2007;51:1228–33. <http://dx.doi.org/10.1128/AAC.01054-06>
 34. Sørensen UB, Poulsen K, Ghezso C, Margarit I, Kilian M. Emergence and global dissemination of host-specific *Streptococcus agalactiae* clones. *MBiol.* 2010;1:e00178–10. <http://dx.doi.org/10.1128/mBio.00178-10>
 35. Jordan HT, Richards CL Jr, Burton DC, Thigpen MC, Van Beneden CA. Group A streptococcal disease in long-term care facilities: descriptive epidemiology and potential control measures. *Clin Infect Dis.* 2007;45:742–52. <http://dx.doi.org/10.1086/520992>
 36. Acikgoz ZC, Gocer S, Tuncer S. Macrolide resistance determinants of group A streptococci in Ankara, Turkey. *J Antimicrob Chemother.* 2003;52:110–2. <http://dx.doi.org/10.1093/jac/dkg300>
 37. Szczypa K, Sadowy E, Izdebski R, Hryniewicz W. A rapid increase in macrolide resistance in *Streptococcus pyogenes* isolated in Poland during 1996–2002. *J Antimicrob Chemother.* 2004;54:828–31. <http://dx.doi.org/10.1093/jac/dkh420>
 38. Richter SS, Heilmann KP, Beekmann SE, Miller NJ, Miller AL, Rice CL, et al. Macrolide-resistant *Streptococcus pyogenes* in the United States, 2002–2003. *Clin Infect Dis.* 2005;41:599–608. <http://dx.doi.org/10.1086/432473>
 39. Pavlovic L, Grego E, Sipetic-Grujicic S. Prevalence of macrolide resistance in *Streptococcus pyogenes* collected in Serbia. *Jpn J Infect Dis.* 2010;63:275–6.
 40. Brenciani A, Bacciaglia A, Vecchi M, Vitali LA, Varaldo PE, Giovanetti E. Genetic elements carrying *erm(B)* in *Streptococcus pyogenes* and association with *tet(M)* tetracycline resistance gene. *Antimicrob Agents Chemother.* 2007;51:1209–16. <http://dx.doi.org/10.1128/AAC.01484-06>
 41. Giovanetti E, Montanari MP, Mingoaia M, Varaldo PE. Phenotypes and genotypes of erythromycin-resistant *Streptococcus pyogenes* strains in Italy and heterogeneity of inducibly resistant strains. *Antimicrob Agents Chemother.* 1999;43:1935–40.
 42. Giovanetti E, Brenciani A, Lupidi R, Roberts MC, Varaldo PE. Presence of the *tet(O)* gene in erythromycin- and tetracycline-resistant strains of *Streptococcus pyogenes* and linkage with either the *mef(A)* or the *erm(A)* gene. *Antimicrob Agents Chemother.* 2003;47:2844–9. <http://dx.doi.org/10.1128/AAC.47.9.2844-2849.2003>
 43. Dunder D, Sayan M, Tamer GS. Macrolide and tetracycline resistance and *emm* type distribution of *Streptococcus pyogenes* isolates recovered from Turkish patients. *Microb Drug Resist.* 2010;16:279–84.

Address for correspondence: Jose F. Fernández-Garayzábal, Universidad Complutense de Madrid, Ftad. de Veterinaria–Patología Animal I (Sanidad Animal), Avda. Puerta de Hierro s/n n/a, Madrid, Madrid 28040 Spain; email: jffernandez@vet.ucm.es

July 2016: Zoonoses



- Senecavirus A in Pigs, United States, 2015
- Two Linked Enteroinvasive *Escherichia coli* Outbreaks, Nottingham, United Kingdom, June 2014
- Porcine Bocavirus Infection Associated with Encephalomyelitis in a Pig, Germany
- African Swine Fever Epidemic, Poland, 2014–2015
- Hepatitis E Virus in Dromedaries, North and East Africa, United Arab Emirates and Pakistan, 1983–2015
- Turtle-Associated Salmonellosis, United States, 2006–2014
- Pregnancy, Labor, and Delivery after Ebola Virus Disease and Implications for Infection Control in Obstetric Services, United States, 2015
- Response to Middle East Respiratory Syndrome Coronavirus, Abu Dhabi, United Arab Emirates, 2013–2014
- Current Guidelines, Common Clinical Pitfalls, and Future Directions for Laboratory Diagnosis of Lyme Disease, United States
- *Tropheryma whipplei* as a Cause of Epidemic Fever, Senegal, 2010–2012



- Heatwave-Associated Vibriosis, Sweden and Finland, 2014
- Vesicular Disease in 9-Week-Old Pigs Experimentally Infected with Senecavirus A
- High Incidence of Chikungunya Virus and Frequency of Viremic Blood Donations during Epidemic, Puerto Rico, USA, 2014
- A Literature Review of Zika Virus

<https://wwwnc.cdc.gov/eid/articles/issue/22/7/table-of-contents>

EMERGING INFECTIOUS DISEASES

Bourbon Virus in Field-Collected Ticks, Missouri, USA

Harry M. Savage, Kristen L. Burkhalter, Marvin S. Godsey, Jr., Nicholas A. Panella, David C. Ashley, William L. Nicholson, Amy J. Lambert

Bourbon virus (BRBV) was first isolated in 2014 from a resident of Bourbon County, Kansas, USA, who died of the infection. In 2015, an ill Payne County, Oklahoma, resident tested positive for antibodies to BRBV, before fully recovering. We retrospectively tested for BRBV in 39,096 ticks from northwestern Missouri, located 240 km from Bourbon County, Kansas. We detected BRBV in 3 pools of *Amblyomma americanum* (L.) ticks: 1 pool of male adults and 2 pools of nymphs. Detection of BRBV in *A. americanum*, a species that is aggressive, feeds on humans, and is abundant in Kansas and Oklahoma, supports the premise that *A. americanum* is a vector of BRBV to humans. BRBV has not been detected in nonhuman vertebrates, and its natural history remains largely unknown.

Bourbon virus (BRBV) was first isolated from blood samples from a hospitalized male resident of Bourbon County, Kansas, USA (1). He was >50 years of age and previously healthy. Several days before becoming ill in late spring 2014, he reported several tick bites and an engorged tick on his shoulder. Initial symptoms included nausea, weakness, and diarrhea (1). On day 2 after symptom onset, he had experienced fever, anorexia, chills, headache, myalgia, and arthralgia. On day 4 after onset, he was hospitalized. Physical examination found a papular rash on his trunk. The patient had a temperature of 37.3°C and laboratory findings of leukopenia, lymphopenia, thrombocytopenia, hyponatremia, and increased levels of aspartate aminotransferase and alanine aminotransferase. He was treated with intravenous fluids and doxycycline for possible tickborne illness. Serologic assays for the causative agents of Rocky Mountain spotted fever, tularemia, brucellosis, babesiosis, and Q fever were negative, as were molecular tests for *Ehrlichia* spp. and *Anaplasma phagocytophilum* and blood smears for *Babesia* (1). The patient died 11 days after symptom onset.

Author affiliations: Centers for Disease Control and Prevention, Fort Collins, Colorado, USA (H.M. Savage, K.L. Burkhalter, M.S. Godsey, Jr., N.A. Panella, A.J. Lambert); Missouri Western State University, St. Joseph, Missouri, USA (D.C. Ashley); Centers for Disease Control and Prevention, Atlanta, Georgia, USA (W.L. Nicholson)

DOI: <https://doi.org/10.3201/eid2312.170532>

Virologic tests on EDTA-treated blood and separated serum collected from the patient on day 9 after symptom onset were negative for Heartland virus (HRTV; family *Bunyaviridae*, genus *Phlebovirus*) (1), a recently described tickborne virus (2,3). However, during plaque reduction neutralization tests for HRTV antibody, heterologous (non-HRTV) viral plaques were observed. Subsequently, plaque assay results revealed distinct plaques 3 days after inoculation within wells inoculated with blood and serum (1). Electron microscopy of virus particles demonstrated filamentous and spherical particles consistent with the morphology of the family *Orthomyxoviridae*. Full-length sequencing and phylogenetic analysis demonstrated that the virus was new, most closely but distantly related to the Old World virus Dhori virus, and a member of the genus *Thogotovirus* (1,4). This new virus was named Bourbon virus after the county of residence of the patient. BRBV is the first human pathogen of the genus *Thogotovirus* to be identified in the New World (4).

In May 2015, the Centers for Disease Control and Prevention (CDC) and the Oklahoma State Department of Health reported that a Payne County, Oklahoma, USA, resident became ill and tested positive for antibodies to BRBV by plaque reduction neutralization tests (E. Staples, O. Kosoy, CDC, pers. comm., 2016 Dec 5). The patient recovered fully.

In response to the report of the fatal BRBV case from eastern Kansas in 2014, we retrospectively tested ticks for BRBV that were collected during spring and summer 2013 from 6 sites in northwestern Missouri, ≈240 km from Bourbon County (Figure 1). We had originally collected, identified, pooled, and processed these tick samples as part of an ongoing HRTV surveillance program (5). The goals of our retrospective analysis were to determine whether BRBV was present in the neighboring state of Missouri, to incriminate possible vector species, and to determine which life history stages are involved in virus transmission to humans.

Materials and Methods

Tick Collections

We collected ticks at 6 sites in 3 counties of northwestern Missouri: Andrew, Gentry, and Nodaway (Figure 1). Five sites were properties owned by HRTV patients (sites 1, 2a, and 25–27), and 1 site (13b) was state recreational land,

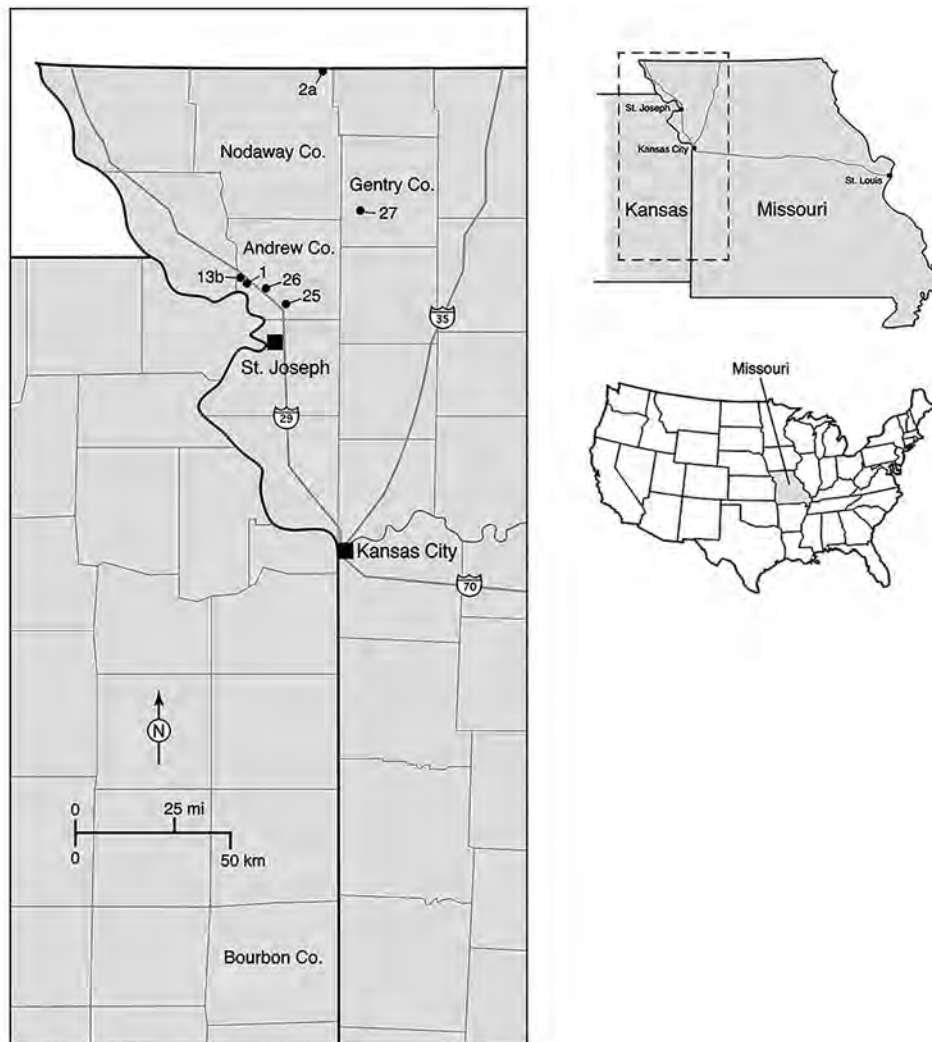


Figure 1. Locations of 6 tick sampling sites surveyed in northwestern Missouri, USA, during 2013 (indicated by site numbers), showing proximity of site to Bourbon County, Kansas (bottom center of map). Inset maps show location of area in main map (top, dashed box) and location of state of Missouri in the United States (bottom, gray shading). Co., County.

Honey Creek Conservation Area (5). Ticks were collected during three 1-week-long field trips in 2013; tick collections occurred on April 22–25, June 10–13, and July 22–25. We collected ticks primarily by flagging and secondarily by use of carbon dioxide–baited tick traps as described previously (3,5). We then froze the ticks on dry ice and shipped them to CDC (Fort Collins, CO, USA) for processing and testing.

Tick Processing, RNA Extraction, and Virus Detection

We identified ticks to species, sex, and life history stage using microscopes on refrigerated tables and standard taxonomic references (5) and grouped them into pools by site, collection date, collection type, species, sex, and stage. We homogenized tick pools in 1 mL chilled bovine albumin-1 (BA-1) in glass TenBroeck grinders (Fischer Scientific, Pittsburgh, PA, USA) as described previously (3,5). After centrifugation, we removed a 125- μ L aliquot of supernatant from each tick pool homogenate and placed the aliquot into an identically numbered tube for RNA extraction. The

remaining homogenates were held at -80°C for future confirmatory testing.

We extracted RNA from a 100- μ L sample removed from each aliquot tube using the QIAmp Virus BioRobot 9604 kit on a BioRobot Universal platform (both from QIAGEN, Valencia CA, USA) according to the manufacturer's protocol. Sequence and reporter information for BRBV primer/probe sets nucleoprotein (NP) 1 and polymerase basic (PB) 1, which we used for virus detection and confirmation, respectively, are as previously described (4). We screened all samples for BRBV by using primer/probe set NP1 in a real-time reverse transcription PCR (rRT-PCR) as described for HRTV (5). Pools positive in the screening assay were confirmed by reextracting RNA from the original tick homogenate and performing the quantitative rRT-PCR with 2 primer/probe sets, primer/probe sets NP1 and PB1. We considered pools BRBV positive if crossing threshold scores for both primer/probe sets were ≤ 37 .

To estimate the detection limit associated with a crossing threshold of 37, we spiked tick pools of specimens from an *A. americanum* colony with serial dilutions of BRBV, original strain (1,4). Pools comprised either 5 adult females or 25 nymphs and were ground in 1 mL BA-1. We tested 14 pools of adults and 14 pools of nymphs with each primer set.

Plaque Assays to Detect Viable Virus

We tested tick homogenates from rRT-PCR-positive samples for viable virus with 2-step cell culture assay using human hepatoma cell line 7 (HuH-7) following a published protocol (5). Initially, we inoculated a 200- μ L sample of tick homogenate into HuH-7 cells in separate T-25 flasks, monitored the flasks daily for cytopathic effect, and harvested on day 5 or 6. We then used this first viral harvest (V1) to inoculate HuH-7 cells in 6-well plates and counted plaques to estimate titer (5).

High-Throughput Sequencing and Phylogenetic Analysis

We extracted and purified BRBV RNA from HuH-7 V1 harvest from 2 pools that were rRT-PCR positive as previously described (1,4). We then conducted high-throughput sequencing on an Ion Torrent PGM sequencer (Life Technologies, Grand Island, NY, USA) and analyzed sequence data from repeated runs using the CLC Genomics Workbench 7.5.1 (CLCbio, Cambridge, MA, USA) and NGen 4 (DNASTar, Madison, WI, USA) software program as previously described (4). The total approximated average genome coverage across all genomic segments was 1,000 \times . We determined open reading frames using the EditSeq function of the Lasergene 9 package (DNASTar) and conducted phylogenetic analysis on nucleotide and amino acid sequences using MEGA5 software (6).

Results

Detection of BRBV in Ticks and Infection Rates

Based on spiked tick pools comprising 5 *A. americanum* adult females or 25 nymphs, ground in 1 mL BA-1, the cut-off crossing threshold of 37 corresponded to a detection limit of 10^{2.6} PFU/mL or pool (95% CI 10^{2.5}–10^{2.7}) for primer set NP1. The crossing threshold of 37 corresponded to a detection limit of 10^{1.4} PFU per mL or pool (95% CI 10^{1.3}–10^{1.5})

for primer set PB1. Results from adult and nymphal pools were not statistically different.

We tested 39,096 ticks representing 5 species collected from 6 sites in northwestern Missouri (Figure 1; Table 1). However, 2 species, *A. americanum* (L.) (97.6%) and *Dermacentor variabilis* (Say) (2.3%), accounted for 99.9% of ticks collected.

We tested an aliquot from all 3,073 tick pools from Missouri collections from 2013 by rRT-PCR using the screening primer/probe set NP1. Three pools were positive in the screening assay. Reextraction and testing of the original tick homogenates using both primer/probe sets NP1 and PB1 confirmed BRBV RNA in all 3 pools. All 3 tick pools yielded viable virus in cell culture. All 3 positive pools comprised *A. americanum* ticks (Table 2). One pool comprised 4 male adult ticks collected at site 2a on June 12; the other 2 pools each comprised 25 nymphs collected at site 27 on July 24.

The maximum-likelihood estimate (7) of the infection prevalence per 1,000 ticks, for nymphs of *A. americanum* from site 27 on July 24, 2013, the only day that this site was sampled, was 0.31 (95% CI 0.06–1.01), or \approx 1 infected nymph per 3,226 collected nymphs. The infection prevalence for *A. americanum* nymphs from all sites combined during the entire 2013 season was 0.07 (95% CI 0.01–0.22), or \approx 1 infected nymph per 14,286 collected nymphs.

The infection prevalence for adult male *A. americanum* ticks from site 2a on June 12, 2013, was 19.11 (95% CI 1.13–90.06); for adult male *A. americanum* ticks from site 2a during the entire 2013 season it was 7.35 (95% CI 0.42–35.19); and for all adult male *A. americanum* ticks from all sites combined during the 2013 season it was 0.32 (95% CI 0.02–1.53). The 95% CI for difference of proportions (7) between the infection prevalence for male adults and nymphs from all sites combined during the 2013 season includes zero (95% CI –1.46 to 0.13), indicating that infection prevalence for male adults and nymphs did not significantly differ.

Phylogenetic Analyses

To confirm the molecular identification of BRBV, we selected 2 pools, MO-2013-1246 of male adults and MO-2013-2499 of nymphs, for high-throughput sequencing and phylogenetic analysis. We deposited partial genomic sequence data in GenBank (accession nos. KY825740–KY825741). Analyses

Table 1. Characteristics of a retrospective study of Bourbon virus in field-collected ticks, Missouri, USA, 2013

Site	<i>Amblyomma americanum</i>			<i>Dermacentor variabilis</i>			<i>Haemaphysalis</i>	<i>Ixodes dentatus</i>		Total
	Adults	Nymphs	Larvae	Adults	Nymphs	Larvae	<i>leporispalustris</i> nymphs	Adults	Nymphs	
1	2,473	7,534	100	162	27			2	8	10,306
2a	267	2,822		141	14	28	1	1	4	3,278
13b	2,811	8,847	944	396	6	2	1	3	9	13,020*
25				6						6
26	389	4,528	696	91	4					5,708
27	252	6,478	11	36					1	6,778
Total	6,192	30,209	1,751	832	51	30	2	6	22	39,096*

*Includes 1 *I. scapularis* nymph collected at site 13b on June 11, 2013.

Table 2. Bourbon virus confirmed by real-time reverse transcription PCR in pools of *Amblyomma americanum* ticks, Missouri, USA, 2013

Pool no.	County	Site	Collection date	Stage	Sex*	No. specimens
MO-2013-1246	Nodaway	2a	Jun 12	Adult	M	4
MO-2013-2499	Gentry	27	Jul 24	Nymph	–	25
MO-2013-2530	Gentry	27	Jul 24	Nymph	–	25

*–, nymphs cannot be sexed.

revealed 6 RNA segments for strain MO-2013-1246, as previously reported for the BRBV human strain (4). We conducted phylogenetic analysis on a 152-aa sequence of PB2 subunit of the polymerase protein (Figure 2) to assess relationships with the BRBV strain from the fatal human case and other selected members of the *Orthomyxoviridae*. The 3 BRBV strains form a lineage with 100% bootstrap support. The BRBV lineage is a sister group to, and mostly closely related to, Dhori virus. The BRBV-Dhori lineage appears as a sister group to a lineage of 4 tick-associated viruses and distantly related to the influenza viruses and Quarantil virus.

The human BRBV strain from Kansas and tick pool MO-2013-1246 comprising male adult *A. amblyomma* ticks were very similar for the PB2 gene segment analyzed, sharing >99.0% sequence at the amino acid level and 95.0% identity at the RNA sequence level. Furthermore, the human BRBV strain from Kansas and tick pool MO-2013-2499 (nymphs) were very similar for the PB2 gene segment analyzed, sharing 99.0% sequence identity at the amino acid and RNA sequence levels.

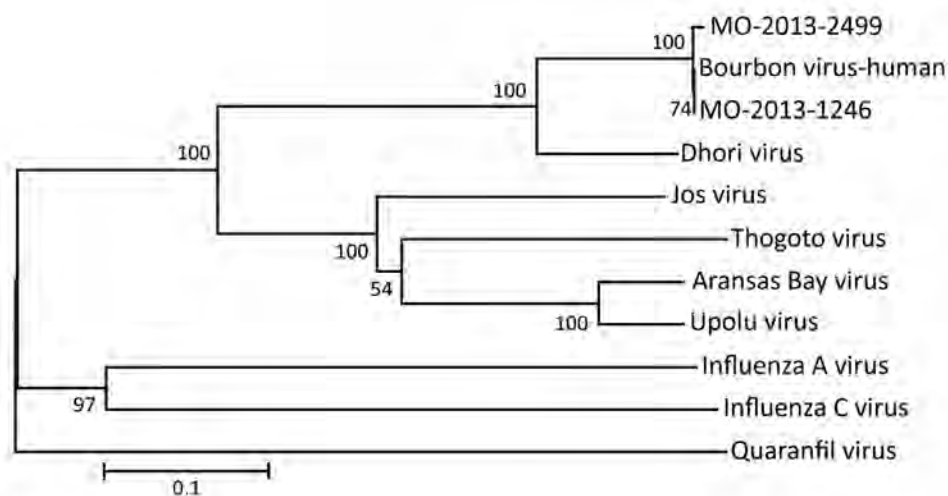
Discussion

We isolated BRBV from 3 pools of *A. americanum* ticks collected in northwestern Missouri: 1 pool of male adults and 2 pools of nymphs. The first detection of BRBV was from a fatal case in a man from nearby Bourbon County, Kansas (1); this

man reported tick exposure and an engorged tick on his shoulder shortly before he became ill. Tick exposure combined with laboratory findings of leukopenia and thrombocytopenia suggested that BRBV might be transmitted to humans by ticks. Detection of BRBV in field-collected *A. americanum* ticks from Missouri supports the premise that *A. americanum*, a species that is aggressive, feeds on humans (8), and is abundant in Kansas and Oklahoma (9), the states where the 2 persons with BRBV infection resided, is a vector of BRBV to humans.

Tick transmission of BRBV also is consistent with our knowledge of the vector status and phylogenetic relationships within the genus *Thogotovirus* and related viruses in the family *Orthomyxoviridae* (Figure 2). Viruses that have been placed in the genus *Thogotovirus* include BRBV (1), Thogoto virus (10,11), Araguari virus (10,12), Dhori virus (10,11), Jos virus (10,13), and Upolu virus (13,14). To our knowledge, the closely related Aransas Bay virus (14) has not been placed in genus *Thogotovirus*. All of these viruses, except Araguari virus, which has been isolated only from vertebrates, are believed to be transmitted by a variety of hard and soft tick species (15–22). Of these tick-transmitted viruses (Figure 2), only Thogoto virus, Dhori virus, and BRBV have been associated with human disease (1,18), and only BRBV and Aransas Bay virus are known to occur in North America. Aransas Bay virus has been isolated from the soft tick *Ornithodoros capensis*, a parasite of seabirds (19,23).

Figure 2. Phylogenetic analyses of partial polymerase basic 2 sequences of selected orthomyxoviruses. Bourbon virus sequences from 2 pools of *Amblyomma americanum* ticks (male adults, MO-2013-1246; nymphs, MO-2013-2499) collected in Missouri, USA, during 2013 grouped with the sequence of the original Bourbon virus isolated from a man who died in Bourbon County, Kansas, USA, during 2014. The evolutionary history was inferred using the neighbor-joining method with 2,000 replicates for bootstrap testing. The tree is drawn to scale, with branch lengths in the same units as those of the evolutionary distances used to infer the phylogenetic tree. The evolutionary distances were computed using the Poisson correction method. Scale bar indicates number of amino acid substitutions per site.



Dhori virus, the virus most closely related to BRBV (4), is an Old World virus known from Europe, North Africa, and western and central Asia. Dhori virus has been isolated primarily from metastriate ticks (hard ticks other than genus *Ixodes*), including *Hyalomma dromedarii*, *H. marginatum* (reported as *H. plumbeum plumbeum* in the former Soviet Union), *H. scupense*, and *Dermacentor marginatus* (16,18,20,24). On rare occasions, Dhori virus also has been isolated from mosquitoes, including *Anopheles hyrcanus* (24), and from 1 mixed pool of *Aedes caspius caspius* and *Culex hortensis* mosquitoes collected near the Naryn River in Kyrgyzstan (20). Human disease associated with Dhori virus infection is characterized by acute illness with severe fever, headache, general weakness, and retrobulbar pain; encephalitis occurs in $\approx 40\%$ of patients, and convalescence is long (2 months) (18). In addition, 5 laboratory infections resulting from aerosol exposure, 2 of which were characterized by encephalitis, have been reported (25).

Infection prevalence for BRBV in field-collected *A. americanum* ticks varied. The infection prevalence for nymphs, the stage with the largest sample size, was 0.31/1,000 or 1/3,226 nymphs at site 27. Nymphs collected at other sites were virus negative, resulting in a very low infection prevalence of 0.07/1,000 when all nymphal collections were combined for the 2013 season. For comparison, HRTV was detected in nymphs collected at 4 of the 6 sampled sites, and the infection prevalence for HRTV in nymphs from all sites during the 2013 season was 1.79/1,000, or 1 infected nymph of 559 nymphs tested (5).

The BRBV infection prevalence for adult male *A. americanum* ticks from site 2a on June 12, 2013, was very high (19.11/1,000), whereas the infection prevalence for adult male *A. americanum* ticks from site 2a during the entire 2013 season was 7.35/1,000, or 1 infected male adult among every 136 tested. However, the infection prevalence for all adult male *A. americanum* ticks from all sites combined during the 2013 season was 0.32/1,000, or 1 of 3,125 adult male ticks tested. Infection prevalence for adult male ticks appears higher than for nymphs; however, BRBV infection prevalence for male adults and nymphs from all sites combined during the 2013 season did not differ significantly.

Infection prevalence for BRBV in potential vectors remains poorly known; our interpretations are preliminary and await additional field studies. However, the very low infection prevalence for nymphs and varying rates for male adults suggest the possibility that other transmission cycles for BRBV might exist and that *A. americanum* ticks, although most likely an important vector to humans because of their aggressive host-seeking behavior and preference for medium and large mammals, might not be an important enzootic vector of BRBV. We hypothesize that *A. americanum* ticks acquire BRBV from occasional blood meals from ≥ 1 vertebrate hosts; that the virus successfully replicates and is

transstadially transmitted in *A. americanum* ticks; and that *A. americanum* ticks transmit the virus to incidental hosts, such as humans. The pool of male adult *A. americanum* ticks, MO-2013-1246, also was positive for HRTV (5), suggesting some overlap in the transmission cycles of HRTV and BRBV. BRBV and antibodies to BRBV have not been detected in vertebrates, other than the 2 humans, and the natural history of the virus remains unknown.

Acknowledgments

We thank Jason Velez for HuH-7 cell production, formulation of media, and advice on use of this cell system. We are grateful to Michael Levin for providing colony *A. americanum* ticks used to generate experimental pools and to Mark Delorey for statistical analysis of the titer associated with crossing threshold cutoffs.

Dr. Savage is a research entomologist at the Arboviral Diseases Branch, Division of Vector-Borne Diseases, National Center for Emerging and Zoonotic Infectious Diseases, Centers for Disease Control and Prevention, Fort Collins, Colorado. His research interests include the transmission dynamics of viruses vectored by mosquitoes and ticks.

References

1. Kosoy OI, Lambert AJ, Hawkinson DJ, Pastula DM, Goldsmith CS, Hunt DC, et al. Novel *Thogotovirus* associated with febrile illness and death, United States, 2014. *Emerg Infect Dis*. 2015;21:760–4. <http://dx.doi.org/10.3201/eid2105.150150>
2. McMullan LK, Folk SM, Kelly AJ, MacNeil A, Goldsmith CS, Metcalfe MG, et al. A new phlebovirus associated with severe febrile illness in Missouri. *N Engl J Med*. 2012;367:834–41. <http://dx.doi.org/10.1056/NEJMoa1203378>
3. Savage HM, Godsey MS Jr, Lambert A, Panella NA, Burkhalter KL, Harmon JR, et al. First detection of Heartland virus (*Bunyaviridae: Phlebovirus*) from field collected arthropods. *Am J Trop Med Hyg*. 2013;89:445–52. <http://dx.doi.org/10.4269/ajtmh.13-0209>
4. Lambert AJ, Velez JO, Brault AC, Calvert AE, Bell-Sakyl L, Bosco-Lauth AM, et al. Molecular, serological and in vitro culture-based characterization of Bourbon virus, a newly described human pathogen of the genus *Thogotovirus*. *J Clin Virol*. 2015;73:127–32. <http://dx.doi.org/10.1016/j.jcv.2015.10.021>
5. Savage HM, Godsey MS Jr, Panella NA, Burkhalter KL, Ashley DC, Lash RR, et al. Surveillance for Heartland virus (*Bunyaviridae: Phlebovirus*) in Missouri during 2013: first detection of virus in adults of *Amblyomma americanum* (Acari: Ixodidae). *J Med Entomol*. 2016;53:607–12. <http://dx.doi.org/10.1093/jme/tjw028>
6. Tamura K, Peterson D, Peterson N, Stecher G, Nei M, Kumar S. MEGA5: molecular evolutionary genetics analysis using maximum likelihood, evolutionary distance, and maximum parsimony methods. *Mol Biol Evol*. 2011;28:2731–9. <http://dx.doi.org/10.1093/molbev/msr121>
7. Biggerstaff BJ. PooledInfRate, version 4.0: a Microsoft Office add-in to compute prevalence estimates from pooled samples. Fort Collins (CO): Centers for Disease Control and Prevention; 2009.
8. Goddard J, Varela-Stokes AS. Role of the lone star tick, *Amblyomma americanum* (L.), in human and animal diseases. *Vet Parasitol*. 2009;160:1–12. <http://dx.doi.org/10.1016/j.vetpar.2008.10.089>
9. Springer YP, Eisen L, Beati L, James AM, Eisen RJ. Spatial distribution of counties in the continental United States with records of occurrence of *Amblyomma americanum* (Ixodida:

- Ixodidae). *J Med Entomol.* 2014;51:342–51. <http://dx.doi.org/10.1603/ME13115>
10. Bussetti AV, Palacios G, Travassos da Rosa A, Savji N, Jain K, Guzman H, et al. Genomic and antigenic characterization of Jos virus. *J Gen Virol.* 2012;93:293–8. <http://dx.doi.org/10.1099/vir.0.035121-0>
 11. King AMQ, Adams MJ, Carstens EB, Lefkowitz EJ, editors. *Virus taxonomy. Ninth report of the International Committee on Taxonomy of Viruses.* San Diego (CA): Elsevier Academic Press; 2012.
 12. Da Silva EV, Da Rosa AP, Nunes MRT, Diniz JA, Tesh RB, Cruz AC, et al. Araguari virus, a new member of the family *Orthomyxoviridae*: serologic, ultrastructural, and molecular characterization. *Am J Trop Med Hyg.* 2005;73:1050–8.
 13. Temmam S, Monteil-Bouchard S, Robert C, Baudoin J-P, Sambou M, Aubadie-Ladrix M, et al. Characterization of viral communities of biting midges and identification of novel *Thogotovirus* species and *Rhabdovirus* genus. *Viruses.* 2016;8:77. <http://dx.doi.org/10.3390/v8030077>
 14. Briese T, Chowdhary R, Travassos da Rosa A, Hutchison SK, Popov V, Street C, et al. Upolu virus and Aransas Bay virus, two presumptive bunyaviruses, are novel members of the family *Orthomyxoviridae*. *J Virol.* 2014;88:5298–309. <http://dx.doi.org/10.1128/JVI.03391-13>
 15. Albanese M, Bruno-Smiraglia C, Di Cuonzo G, Lavagnino A, Sarihongse S. Investigation on arboviruses in western Sicily: insect collection and virus isolation. *Ann Sclavo.* 1971;13:1–8.
 16. Anderson CR, Casals J. Dhori virus, a new agent isolated from *Hyalomma dromedarii* in India. *Indian J Med Res.* 1973;61:1416–20.
 17. Haig DA, Woodall JP, Danskin D. Thogoto virus: a hitherto undescribed agent isolated from ticks in Kenya. *J Gen Microbiol.* 1965;38:389–94. <http://dx.doi.org/10.1099/00221287-38-3-389>
 18. Hubálek Z, Rudolf I. Tick-borne viruses in Europe. *Parasitol Res.* 2012;111:9–36. <http://dx.doi.org/10.1007/s00436-012-2910-1>
 19. Keirans JE, Hutcheson HJ, Oliver JH Jr. *Ornithodoros (Alectorobius) capensis* Neumann (Acari: Ixodoidea: Argasidae), a parasite of seabirds, established along the southeastern seacoast of the United States. *J Med Entomol.* 1992;29:371–3. <http://dx.doi.org/10.1093/jmedent/29.2.371>
 20. Lvov DK, Karas FR, Tsyarkin YM, Vargina SG, Timofeev EM, Osipova NZ, et al. Batken virus, a new arbovirus isolated from ticks and mosquitoes in Kirghiz S.S.R. *Arch Gesamte Virusforsch.* 1974;44:70–3. <http://dx.doi.org/10.1007/BF01242183>
 21. Wood OL, Lee VH, Ash JS, Casals J. Crimean-Congo hemorrhagic fever, Thogoto, Dugbe, and Jos viruses isolated from ixodid ticks in Ethiopia. *Am J Trop Med Hyg.* 1978;27:600–4. <http://dx.doi.org/10.4269/ajtmh.1978.27.600>
 22. Yoshii K, Okamoto N, Nakao R, Klaus Hofstetter R, Yabu T, Masumoto H, et al. Isolation of the Thogoto virus from a *Haemaphysalis longicornis* in Kyoto City, Japan. *J Gen Virol.* 2015;96:2099–103. <http://dx.doi.org/10.1099/vir.0.000177>
 23. Yunker CE, Clifford CM, Keirans JE, Thomas LA, Rice RCA. Aransas Bay virus, a new arbovirus on the Upolu serogroup from *Ornithodoros capensis* (Acari: Argasidae) in coastal Texas. *J Med Entomol.* 1979;16:453–60. <http://dx.doi.org/10.1093/jmedent/16.6.453>
 24. Butenko AM, Chumakov MP. Isolation of Astra arbovirus, new to the USSR, from *Hyalomma marginatum* ticks and *Anopheles hyrcanus* mosquitoes in Astrakhan Region [in Russian]. *Vopr Med Virusol.* 1971;2:111–2.
 25. Butenko AM, Leshchinskaia EV, Semashko IV, Donets MA, Mart'ianova LI. Dhori virus—a causative agent of human disease. 5 cases of laboratory infection [in Russian]. *Vopr Virusol.* 1987;32:724–9.

Address for correspondence: Harry M. Savage, Centers for Disease Control and Prevention, PO Box 2087, Fort Collins, CO 80522, USA; email: hms1@cdc.gov

EID SPOTLIGHT TOPIC



Ticks

Ticks transmit a variety of different pathogens including bacteria, protozoa, and viruses that can produce serious and even fatal disease in humans and animals. Tens of thousands of cases of tickborne disease are reported each year, including Lyme disease. See the EID Lyme Disease Spotlight. Lyme disease is the most well-known tickborne disease. However, other tickborne illnesses such as Rocky Mountain spotted fever, tularemia, babesiosis, and ehrlichiosis also contribute to severe morbidity and more mortality each year.

Symptoms of tickborne disease are highly variable, but most include sudden onset of fever, headache, malaise, and sometimes rash. If left untreated, some of these diseases can be rapidly fatal.



<https://wwwnc.cdc.gov/eid/page/tick-spotlight>

**EMERGING
INFECTIOUS DISEASES®**

High Rate of MCR-1–Producing *Escherichia coli* and *Klebsiella pneumoniae* among Pigs, Portugal

Nicolas Kieffer, Marta Aires-de-Sousa, Patrice Nordmann, Laurent Poirel

The *mcr-1* (mobile colistin resistance 1) gene, which encodes phosphoethanolamine transferase, has been recently identified as a source of acquired resistance to polymyxins in *Escherichia coli*. Using the SuperPolymyxin selective medium, we prospectively screened 100 pigs at 2 farms in Portugal for polymyxin-resistant *Enterobacteriaceae* and recovered 98 plasmid-mediated MCR-1–producing isolates. Most isolates corresponded to nonclonally related *E. coli* belonging to many sequence types; we also found 2 *Klebsiella pneumoniae* sequence types. The *mcr-1* gene was carried on IncHI2 or IncP plasmid backbones. Our finding of a high rate of MCR-1 producers on 2 pig farms in Portugal highlights the diffusion of that colistin-resistance determinant at the farm level. The fact that the pigs received colistin as metaphylaxis in their feed during the 6 weeks before sampling suggests selective pressure.

The progressive global increase of antimicrobial drug resistance in *Enterobacteriaceae* is worrisome, and adding to the concern is the recent discovery of the plasmid-mediated mobile colistin resistance (MCR) genes *mcr-1* and *mcr-2* (1,2). These genes encode phosphoethanolamine transferases, which add a phosphoethanolamine group to the lipid A of the lipopolysaccharide, leading to gram-negative bacteria resistance to polymyxins (3). Since its discovery, the *mcr-1* gene has been identified almost worldwide, mostly in animal and environmental samples (3) and to a lesser extent in human clinical samples (4). The *mcr-1* gene has often been identified from *Escherichia coli* strains recovered from pigs (3,5–8). More recently, the *mcr-2* gene, which shares 76.8% nt identity with *mcr-1*, has been identified from a single *E. coli* isolate recovered from a pig in Belgium (2). The genetic element related to the *mcr-2* gene and possibly involved in its acquisition is insertion sequence (IS) ISEc69.

Author affiliations: Université de Fribourg, Fribourg, Switzerland (N. Kieffer, P. Nordmann, L. Poirel); Escola Superior de Saúde da Cruz Vermelha Portuguesa, Lisbon, Portugal (M. Aires-de-Sousa); University of Lausanne and University Hospital Centre, Lausanne, Switzerland (P. Nordmann)

DOI: <https://doi.org/10.3201/eid2312.170883>

The *mcr-1* gene has been identified on a large variety of plasmids, such as IncI2, IncX4, IncHI2, IncP, IncFI, IncFII, IncFIB, and IncY (3,9,10). The genetic context of the *mcr-1* gene always includes the *mcr-1* cassette, as previously described (11,12). In addition, IS*AplI* is often found upstream of the *mcr-1* gene. It has been recently shown that a second copy of IS*AplI* may be found downstream of the *mcr-1* gene, therefore bracketing the 2.6-kb *mcr-1* cassette and forming the composite transposon Tn6330, demonstrated to be functional and responsible for the transposition of *mcr-1* (13,14).

We speculate that the emergence and further dissemination of the *mcr-1* and -2 genes occurred from pigs and that IS*AplI* and ISEc69, respectively, were the main genetic elements involved in that process. We recently demonstrated that *Moraxella* spp. are sources of *mcr*-like encoding genes (15); *M. pluranimalium* has been identified as the progenitor of the *mcr-2* gene (16). Of note, all *Moraxella* spp. are widespread in pigs (17), thus allowing speculation that the whole genetic process that originally led to the emergence of the *mcr*-like genes occurred in those animals.

Worldwide, colistin is widely used in veterinary medicine for different purposes, including treatment of enteric infections, prophylaxis or metaphylaxis (18), and as growth promoter in several countries (19). Despite this selective pressure, studies reporting identification of colistin-resistant *Enterobacteriaceae* in veterinary medicine remain scarce, although an overall low prevalence of those resistant strains was noticed in Europe (8,10,20,21).

To evaluate the prevalence and genetic characterization of colistin-resistant *Enterobacteriaceae* on pig farms, we performed a prospective epidemiologic survey. The study was conducted in Portugal (the fifth largest polymyxin consumer in Europe), where colistin is heavily used in veterinary medicine (22).

Materials and Methods

Isolates and Susceptibility Testing

On 1 day in June 2016, we collected 100 rectal swab samples from pigs on 2 pig farms in Portugal, 30 km apart. These farms, harboring ≈3,000 pigs each, are production

holdings, where piglets are born and fattened before being delivered to slaughterhouses (23). All pigs sampled were 10–11 weeks of age. When the pigs were 5–10 weeks of age, their feed included colistin (0.5%), amoxicillin (0.5%), and zinc oxide (0.15%). The weekly dose of colistin in the regimen was ≈ 0.06 g/kg. Overall, all pigs received ≈ 5.5 g colistin for metaphylaxis over 6 weeks.

We incubated rectal swab samples overnight at 37°C in Luria-Bertani broth supplemented with 1 $\mu\text{g}/\text{mL}$ colistin. The next day, to select for colistin-resistant gram-negative isolates, we inoculated each enrichment tube onto SuperPolymyxin selective agar medium that contained 3.5 $\mu\text{g}/\text{mL}$ colistin and 10 $\mu\text{g}/\text{mL}$ daptomycin (ELITech-Group, Signes, France) (24). We identified colistin-resistant isolates recovered from SuperPolymyxin plates with API 20E (bioMérieux, La Balme les Grottes, France). We performed antimicrobial drug susceptibility testing by using the disk-diffusion method according to Clinical and Laboratory Standards Institute recommendations, on Muller-Hinton agar plates, except for colistin, for which we evaluated MICs for colistin by broth microdilution in cation-adjusted Muller-Hinton broth (Bio-Rad, Cressier, Switzerland), as recommended by the Clinical and Laboratory Standards Institute (25).

Molecular Analyses

Acquired colistin-resistance genes *mcr-1* and *mcr-2* were identified by PCR, with use of specific primers as reported (14), and amplicons were further sequenced by Microsynth (Balgach, Switzerland). We identified extended-spectrum β -lactamase (ESBL)-encoding genes by using primers specific for detection of *bla*_{TEM}, *bla*_{SHV}, and *bla*_{CTX-M} genes (26,27). The plasmidborne chloramphenicol gene *floR* was sought by using specific primers (28) among isolates exhibiting resistance to chloramphenicol. The clonal relationship of the colistin-resistant isolates was evaluated by pulsed-field gel electrophoresis, as described previously (29), and multilocus sequence typing was performed for a representative strain of each pulsotype. We assigned sequence types (STs) by using the multilocus sequence typing databases for *E. coli* (<http://mlst.warwick.ac.uk/mlst/dbs/Ecoli>) and *K. pneumoniae* (<http://bigsd.b.pasteur.fr/klebsiella/klebsiella.html>). The phylogenetic group of *E. coli* isolates was determined with the PCR-based Clermont method as described previously (30).

Conjugation Experiments and Plasmid Analyses

We performed conjugation assays on filters with azide-resistant *E. coli* J53 as the recipient strain. MCR-1 producers and the J53 isolate were cultured overnight in Luria-Bertani broth. To reach the logarithmic phase, the donor and recipient strains were subcultured in fresh Luria-Bertani broth for 3 h. We subsequently mixed the samples at a ratio of

10:1 and deposited 100 μL of this mix onto 22- μm filters, which we then incubated for 5 h at 37°C on Luria-Bertani agar plates. After the incubation, filters were resuspended in 0.85% NaCl, and we plated 250 μL of this mixture onto selective Luria-Bertani plates containing azide (100 $\mu\text{g}/\text{mL}$) and colistin (1 $\mu\text{g}/\text{mL}$). PCR was used to check all *E. coli* transconjugants for the *mcr-1* gene.

We typed plasmids carrying the *mcr-1* gene from *E. coli* transconjugants by using the PCR-based replicon typing method (31). The size of the plasmid was obtained after Kieser extraction (32) and agarose gel electrophoresis; we used as a reference *E. coli* 50192 isolate containing 4 characterized plasmids (154 kb, 66 kb, 48 kb, and 7 kb).

Results

From the 100 rectal swab samples collected, we recovered 108 colistin-resistant isolates from the SuperPolymyxin agar plates and identified 90 as *E. coli*, 17 as *K. pneumoniae*, and 1 as *Proteus mirabilis*. Of the 108 colistin-resistant isolates, 98 were positive for the *mcr-1* gene. Colistin MICs for all MCR-1-producing isolates ranged from 4 to 32 $\mu\text{g}/\text{mL}$ (Table). Among these positive isolates, 10 showed an ESBL phenotype. Sequencing revealed that all *mcr*-positive isolates possessed a gene that was 100% identical to *mcr-1*. All MCR-1-producing isolates possessed the *bla*_{TEM-1} gene, and all ESBL producers possessed the *bla*_{CTX-M-2} gene. All MCR-1-producing isolates were resistant to penicillins and tetracycline, 97.9% were resistant to sulfamethoxazole/trimethoprim, 96% were resistant to tobramycin, and 84.7% were resistant to chloramphenicol. Among the chloramphenicol-resistant isolates, 56% were positive for the *floR* resistance gene. No *mcr-2*-positive isolate was identified in our samples.

Pulsed-field gel electrophoresis identified 19 distinct *E. coli* clones from the first farm sampled and 18 from the second (Table). The isolates belonged to 15 STs (ST10, ST23, ST38, ST46, ST101, ST156, ST6453, and 8 new STs); only 2 (ST10 and ST101) were detected on both farms. Phylogenetic typing showed that each *E. coli* isolate belonged to 1 of the phylogroups A, B1, C, D, E, or F. No extraintestinal and virulent B2 phylogroup was detected among all *E. coli* isolates. In addition, we identified 2 *K. pneumoniae* STs (1 clone per farm), ST45 and ST1563.

Conjugation followed by PCR-based replicon typing analysis showed that the *mcr-1* gene was carried on different plasmids (Table). The *mcr-1* gene was identified on IncHI2 (54%), IncP (38%), and IncX4 (8%) plasmids. Conjugation experiments showed that resistance to sulfamethoxazole/trimethoprim and sulfonamides was systematically co-transferred along with the *mcr-1* gene when carried by IncHI2 plasmids and that resistance to tetracycline, tobramycin, chloramphenicol, and amoxicillin was also most often co-transferred by IncP plasmids (Table). Conversely, the *mcr-1*

Table. Genetic features associated with MCR-1–producing *Escherichia coli* and *Klebsiella pneumoniae* isolates from pigs, Portugal*

Strain	Species	No. pigs	ST†	Resistance genes	Colistin MIC, µg/mL	Incompatibility group (kb) of <i>mcr-1</i> plasmids	Resistance phenotype‡	Genetic context of <i>mcr-1</i> §
Farm 1								
P13	<i>E. coli</i>	6	ST101	<i>bla</i> _{CTX-M-2} , <i>bla</i> _{TEM-1} , <i>mcr-1</i>	4	IncHI2 (~250)	<u>SXT/TET/NAL/AMX/CTX/TMN/SUL</u>	II
P8	<i>E. coli</i>	1	ST101	<i>bla</i> _{CTX-M-2} , <i>bla</i> _{TEM-1} , <i>mcr-1</i> , <i>floR</i>	4	IncHI2 (~250)	<u>SXT/TET/AMX/CTX/TMN/SUL</u>	II
P28	<i>E. coli</i>	4	New ST ₁	<i>bla</i> _{TEM-1} , <i>mcr-1</i> , <i>floR</i>	8	IncHI2 (~250)	<u>SXT/TET/CHL/AMX/TMN/GMN/SUL</u>	II
P11	<i>E. coli</i>	1	New ST ₂	<i>bla</i> _{TEM-1} , <i>mcr-1</i> , <i>floR</i>	16	IncHI2 (~250)	<u>SXT/TET/CHL/AMX/TMN/SUL</u>	III
P4	<i>E. coli</i>	3	New ST ₁	<i>bla</i> _{TEM-1} , <i>mcr-1</i>	16	IncP (~60)	<u>TET/CHL/AMX/TMN/SUL</u>	II
P9	<i>E. coli</i>	1	New ST ₂	<i>bla</i> _{TEM-1} , <i>mcr-1</i>	16	IncP (~60)	<u>TET/CHL/AMX/TMN/SUL</u>	II
P27	<i>E. coli</i>	1	ST6453	<i>bla</i> _{TEM-1} , <i>mcr-1</i>	16	IncP (~60)	<u>TET/CHL/AMX/TMN/SUL</u>	I
P7	<i>E. coli</i>	1	New ST ₂	<i>bla</i> _{TEM-1} , <i>mcr-1</i>	16	IncP (~60)	<u>TET/CHL/AMX/TMN/SUL</u>	II
P43	<i>E. coli</i>	1	New ST ₄	<i>bla</i> _{TEM-1} , <i>mcr-1</i>	16	IncP (~60)	<u>TET/CHL/AMX/TMN/GMN</u>	III
P10	<i>E. coli</i>	1	ST10	<i>bla</i> _{TEM-1} , <i>mcr-1</i>	16	IncHI2 (~250)	<u>TET/CHL/AMX/TMN/SUL</u>	II
P5	<i>E. coli</i>	1	New ST ₄	<i>bla</i> _{TEM-1} , <i>mcr-1</i>	8	IncP (~60)	<u>TET/CHL/AMX/TMN/SUL</u>	II
P1	<i>E. coli</i>	1	New ST ₃	<i>bla</i> _{TEM-1} , <i>mcr-1</i>	8	IncP (~60)	<u>TET/CHL/AMX/TMN/SUL</u>	II
P2	<i>E. coli</i>	1	New ST ₂	<i>bla</i> _{TEM-1} , <i>mcr-1</i>	8	IncP (~60)	<u>SXT/TET/CHL/AMX/TMN/SUL</u>	II
P16	<i>E. coli</i>	1	ST10	<i>bla</i> _{TEM-1} , <i>mcr-1</i>	8	IncX4 (~30)	<u>SXT/TET/AMX/TMN/SUL</u>	III
P3	<i>E. coli</i>	5	ST156	<i>bla</i> _{TEM-1} , <i>mcr-1</i>	8	IncHI2 (~250)	<u>SXT/TET/NAL/CIP/AMX/TMN/SUL</u>	I
P20	<i>E. coli</i>	1	New ST ₂	<i>bla</i> _{TEM-1} , <i>mcr-1</i>	4	IncHI2 (~250)	<u>SXT/TET/AMX/TMN/SUL</u>	III
P22	<i>E. coli</i>	13	ST6453	<i>bla</i> _{TEM-1} , <i>mcr-1</i>	4	IncP (~60)	<u>TET/AMX/TMN/SUL</u>	I
P19	<i>E. coli</i>	1	New ST ₄	<i>bla</i> _{TEM-1} , <i>mcr-1</i>	4	IncP (~60)	<u>SXT/TET/CHL/NAL/AMX/TMN/SUL</u>	II
P37	<i>E. coli</i>	1	ST38	<i>bla</i> _{TEM-1} , <i>mcr-1</i>	4	IncP (~60)	<u>SXT/TET/AMX/TMN/SUL</u>	I
P6K	<i>K. pneumoniae</i>	6	ST45	<i>bla</i> _{TEM-1} , <i>mcr-1</i>	32	IncP (~60)	<u>TET/AMX/TMN/SUL</u>	II
Farm 2								
B21	<i>E. coli</i>	1	ST10	<i>bla</i> _{TEM-1} , <i>mcr-1</i> , <i>floR</i>	16	IncHI2 (~250)	<u>SXT/CHL/TET/NAL/CIP/AMX/TMN/SUL</u>	III
B12	<i>E. coli</i>	8	ST10	<i>bla</i> _{TEM-1} , <i>mcr-1</i> , <i>floR</i>	16	IncHI2 (~250)	<u>SXT/CHL/TET/NAL/CIP/AMX/TMN/SUL</u>	III
B30	<i>E. coli</i>	10	ST10	<i>bla</i> _{TEM-1} , <i>mcr-1</i> , <i>floR</i>	16	IncHI2 (~250)	<u>SXT/CHL/TET/NAL/CIP/AMX/TMN/SUL</u>	III
B3	<i>E. coli</i>	1	New ST ₆	<i>bla</i> _{TEM-1} , <i>mcr-1</i> , <i>floR</i>	16	IncHI2 (~250)	<u>SXT/CHL/TET/NAL/AMX/TMN/SUL</u>	I
B27	<i>E. coli</i>	1	New ST ₇	<i>bla</i> _{TEM-1} , <i>mcr-1</i> , <i>floR</i>	16	IncHI2 (~250)	<u>CHL/TET/NAL/CIP/AMX/TMN/SUL</u>	I
B47	<i>E. coli</i>	1	New ST ₇	<i>bla</i> _{TEM-1} , <i>mcr-1</i> , <i>floR</i>	16	IncHI2 (~250)	<u>SXT/CHL/TET/AMX/TMN/SUL</u>	III
B18	<i>E. coli</i>	2	New ST ₈	<i>bla</i> _{TEM-1} , <i>mcr-1</i> , <i>floR</i>	16	IncX4 (~30)	<u>SXT/CHL/TET/AMX/TMN/SUL</u>	III
B22	<i>E. coli</i>	5	New ST ₈	<i>bla</i> _{TEM-1} , <i>mcr-1</i> , <i>floR</i>	16	IncHI2 (~250)	<u>SXT/CHL/TET/AMX/TMN/SUL</u>	II
B4	<i>E. coli</i>	1	New ST ₇	<i>bla</i> _{TEM-1} , <i>mcr-1</i> , <i>floR</i>	16	IncHI2 (~250)	<u>SXT/CHL/TET/AMX/TMN/SUL</u>	III
B15	<i>E. coli</i>	1	ST46	<i>bla</i> _{TEM-1} , <i>mcr-1</i> , <i>floR</i>	8	IncHI2 (~250)	<u>SXT/CHL/TET/AMX/TMN/SUL</u>	III
B6	<i>E. coli</i>	2	ST101	<i>bla</i> _{TEM-1} , <i>mcr-1</i> , <i>floR</i>	8	IncHI2 (~250)	<u>SXT/CHL/TET/AMX/TMN/SUL</u>	III
B8	<i>E. coli</i>	1	New ST ₆	<i>bla</i> _{TEM-1} , <i>mcr-1</i> , <i>floR</i>	8	IncX4 (~30)	<u>SXT/CHL/TET/NAL/AMX/TMN/SUL</u>	III
B1	<i>E. coli</i>	1	New ST ₆	<i>bla</i> _{TEM-1} , <i>mcr-1</i> , <i>floR</i>	8	IncHI2 (~250)	<u>SXT/CHL/TET/AMX/TMN/SUL</u>	III
B11	<i>E. coli</i>	1	New ST ₇	<i>bla</i> _{TEM-1} , <i>mcr-1</i> , <i>floR</i>	8	IncHI2 (~250)	<u>CHL/TET/NAL/AMX/TMN/SUL</u>	IV
B9	<i>E. coli</i>	9	ST23	<i>bla</i> _{TEM-1} , <i>mcr-1</i> , <i>floR</i>	4	IncP (~60)	<u>SXT/CHL/TET/NAL/AMX/TMN/SUL</u>	II
B5	<i>E. coli</i>	1	New ST ₈	<i>bla</i> _{TEM-1} , <i>mcr-1</i> , <i>floR</i>	4	IncP (~60)	<u>SXT/CHL/TET/NAL/AMX/TMN/SUL</u>	III
B27K	<i>K. pneumoniae</i>	2	ST1563	<i>bla</i> _{TEM-1} , <i>mcr-1</i> , <i>floR</i>	32	IncHI2 (~250)	<u>SXT/CHL/TET/AMX/TMN/SUL</u>	I

*Only strains representative of each pulsed-field gel electrophoresis clonal lineage are listed. AMX, amoxicillin; CIP, ciprofloxacin; CHL, chloramphenicol; CTX, cefotaxime; NAL, nalidixic acid; ND, not determined; ST, sequence type; SUL, sulfonamides; SXT, sulfamethoxazole/trimethoprim; TET, tetracycline; TMN, tobramycin.

†STs were identified with the Warwick University database (<http://mlst.warwick.ac.uk/mlst/dbs/Ecoli>). Because this database accepts only whole-genome sequencing data to submit new STs, all new STs found were notified as New ST_x.

‡Underlining indicates co-resistances provided by the plasmid carrying *mcr-1*.

§Different genetic environments detected by PCR, as shown in the Figure.

gene was the only resistance determinant when located on IncX4 plasmids. Of note, IncP-type plasmids carrying *mcr-1* were predominant on the first farm, whereas IncHI2 plasmids were predominant on the second farm.

By PCR mapping using previously published primers (12,13), in all isolates we identified the ≈2.6-kb *mcr-1* cassette in association with 0, 1, or 2 copies of insertion sequence IS*Apl1*, depending on the isolates tested (Table; Figure). In addition, we found a genetic structure not previously reported in 1 isolate that consisted of a truncated IS*Apl1* element upstream of the *mcr-1* cassette. That structure, inserted into a kinase gene onto an IncHI2 plasmid, corresponded to a truncated version of transposon Tn6330 previously reported, with a 2-bp AG direct repeat bracketing the Δ IS*Apl1*-*mcr-1* structure, suggesting a former insertion event through a transposition mechanism (Figure).

Discussion

Prevalence of MCR-1-producing *Enterobacteriaceae* isolates, mainly *E. coli*, from 2 pig farms in Portugal was high. So far, the *mcr-1* gene has been identified mainly in animal samples, rarely in environmental and human samples (3,4,33–36). Previous studies describe the occurrence of MCR-1 producers in swine; prevalence in Europe ranged from 0.5% to 13.5% (6,8,36,37) and in China up to 20.6% (1). In our study, we detected an extremely high rate of MCR-1-producing *Enterobacteriaceae*, finding the *mcr-1* gene in isolates from 98% of pigs tested. We identified an MCR-1-producing *K. pneumoniae* among the pigs, which is noteworthy considering the infrequent recovery of *K. pneumoniae* from animals. Nevertheless, most of the *mcr-1*-positive isolates identified here were *E. coli*, as is reported in most epidemiologic studies (3). For the same pigs that had been screened (by nasal swabs) for methicillin-resistant *Staphylococcus aureus*, the rate of colonization was very high (99%); 2 main *spa* types of clone ST398 were identified (23).

Our study was performed with samples from pigs, and it would be of interest to conduct similar studies of humans. In France, a survey performed in a hospital during February–May 2016 (38) showed a high rate (23%) of fecal carriage with intrinsic colistin-resistant gram-negative isolates but a low rate (1.4%) of acquired polymyxin resistance; no *mcr-1* or *mcr-2* genes were identified. A retrospective study focusing on *Salmonella* isolates was previously performed in Portugal, and MCR-1 producers were reportedly found in humans and pork (39). No MCR-2-producing isolate was identified in our study, although this gene was also identified in pigs (2).

We used the newly developed SuperPolymyxin medium for our prospective epidemiologic study. The fact that no colistin-susceptible strain was recovered during the screening further highlights the excellent specificity of this medium.

Unexpectedly, we found that the studied collection of MCR-1 producers was highly diverse; we identified many STs and genetic features associated with *mcr-1*. The rate of *mcr-1* in our study was very high and caused by the dissemination of neither a single clone nor a plasmid. This high diversity could be explained by 2 key elements. First, considering that the selective pre-enrichment with Luria-Bertani broth supplemented with 1 μ g/mL of colistin and subsequent culturing on the Superpolymyxin medium exhibits a high sensitivity, such a prospective survey may detect higher rates of colistin-resistant isolates than would previous studies. Second, the presence of colistin in the pig food on the 2 farms studied probably represents an efficient selective pressure for MCR-1 acquisition. Findings of similar and comparative studies performed in countries that do not use polymyxins in animals, such as Norway or Finland, would be of interest.

Several STs of *E. coli* identified in this study were similar to those of other MCR-1-producing isolates reported from other studies. As an example, ST10 *E. coli* producing

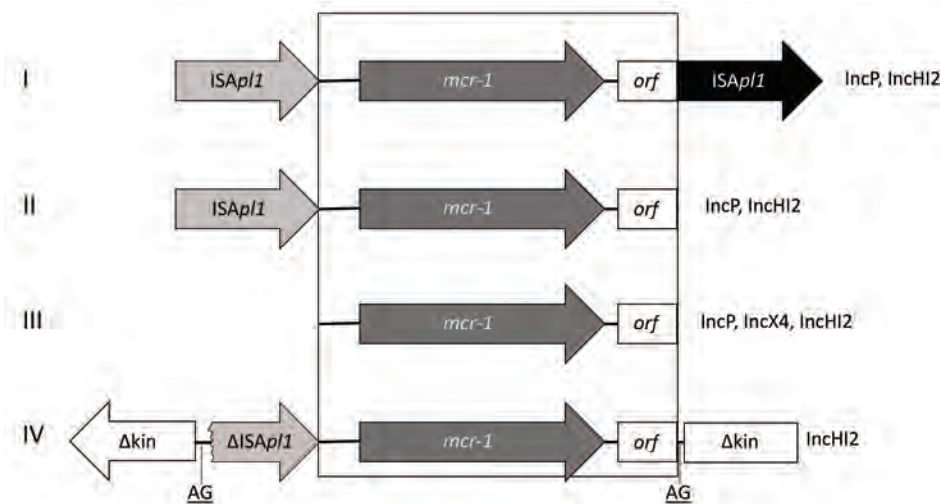


Figure. Genetic environments associated with the *mcr-1* (mobile colistin resistance 1) gene detected in select *Enterobacteriaceae* isolates from pigs, Portugal, by PCR. I) 1 copy of IS*Apl1* associated with *mcr-1* in 5' region; II) 2 copies of IS*Apl1* in 5' and 3' regions of *mcr-1*; III) no copy of IS*Apl1* associated with *mcr-1*; IV) truncated copy of IS*Apl1* associated with *mcr-1* in 5' region inserted in a kinase gene. IS, insertion sequence; orf, open reading frame.

MCR-1 was recovered from swine farms in Germany and in clinical samples in India and South Africa (6,11,40). In South Africa, ST101 *E. coli* was identified from a patient with a urinary tract infection (11). ST156 *E. coli* was identified at a hospital in China and in a muscovy duck in China, where it was co-producing MCR-1 and NDM (New Delhi metallo- β -lactamase)-5 carbapenemase (41,42). We showed that all *E. coli* isolates belonged to a commensal population and not to extraintestinal pathogenic strains, which is consistent with findings of other studies (3) and in line with the design of our study, which was analyzing the colonizing gut flora.

We showed that the *mcr-1* gene was carried by a diversity of plasmids. However, most plasmids recovered from the first farm were \approx 60-kb IncP plasmids, whereas those from the second farm were \approx 250-kb IncHI2 plasmids. Only 3 STs possessed a \approx 30-kb IncX4 plasmid carrying the *mcr-1* gene, which contrasts with other studies that have shown this type of plasmid to be predominant (43). In accordance with what has been observed with other characterized IncX4 plasmids, we found no other resistant determinant associated with *mcr-1* on that plasmid type. IncP and IncHI2 plasmids carried other resistance determinants associated with *mcr-1*. Remarkably, we found no IncI2-type plasmid carrying *mcr-1* in those isolates, although they have often been reported in the literature (1,3).

Analysis of the genetic features associated with the *mcr-1* gene further highlights that it was probably originally acquired by a transposition mechanism and that IS*AplI* played a major role; further truncations or rearrangements led to the stabilization of this structure, as suggested by Snestrud et al. (44). We also identified the entire composite transposon Tn6330 comprising 2 copies of IS*AplI* bracketing the *mcr-1* cassette (13). Because this entire transposon was detected in some isolates of this collection in addition to other defective versions of it, we can speculate that this structure may still be mobilizable and continue to disseminate between different genetic locations.

In summary, the rate of pig colonization with MCR-1-producing *Enterobacteriaceae* was high at the 2 farms we sampled, showing substantial diversity of species, clonality, and genetic aspects. Even if these results suggest that colistin constitutes a major driving force for selecting plasmids carrying the *mcr-1* gene, the occurrence of the *bla*_{TEM-1} gene on the same plasmid indicates that β -lactams might also be co-selecting for colistin resistance through the acquisition of such plasmids. In addition, this study showed that SuperPolymyxin is an efficient medium for screening colistin-resistant isolates from animal samples and performing such epidemiologic surveys. Last, considering that a recent report from Germany identified pig farms as potential sources of environmental contamination for

MCR-1-producing *E. coli* (6), our data strongly indicate the need for screening farm environments in Portugal, to evaluate the extent to which the spread of those resistant bacteria has already occurred and, therefore, to better measure the risk to human health.

Acknowledgments

We are grateful to S. Kumar-Malhotra for the gift of the MCR-2-producing *E. coli* strain.

This work has been funded by the University of Fribourg; by grants from the Animal Health and Welfare ERA-Net project, Switzerland; by the Office Fédéral de la Santé Publique, Bern, Switzerland (grant no. 16009294); by project PTDC/DTP-EPI/0842/2014 from Fundação para a Ciência e a Tecnologia, Portugal; and by the Novartis Foundation for Medical-Biological Research.

An international patent form has been filed on behalf of the University of Fribourg (Switzerland) corresponding to the SuperPolymyxin selective medium.

Mr. Kieffer is a PhD student in microbiology at the University of Fribourg, Switzerland. His main activities are related to the identification of acquired polymyxin and carbapenem resistance mechanisms in gram-negative bacteria, with a focus on the genetics of resistance gene acquisition.

References

- Liu YY, Wang Y, Walsh TR, Yi LX, Zhang R, Spencer J, et al. Emergence of plasmid-mediated colistin resistance mechanism MCR-1 in animals and human beings in China: a microbiological and molecular biological study. *Lancet Infect Dis*. 2016;16:161–8. [http://dx.doi.org/10.1016/S1473-3099\(15\)00424-7](http://dx.doi.org/10.1016/S1473-3099(15)00424-7)
- Xavier BB, Lammens C, Ruhel R, Kumar-Singh S, Butaye P, Goossens H, et al. Identification of a novel plasmid-mediated colistin-resistance gene, *mcr-2*, in *Escherichia coli*, Belgium, June 2016. *Euro Surveill*. 2016;21:30280. <http://dx.doi.org/10.2807/1560-7917.ES.2016.21.27.30280>
- Poirel L, Jayol A, Nordmann P. Polymyxins: antibacterial activity, susceptibility testing, and resistance mechanisms encoded by plasmids or chromosomes. *Clin Microbiol Rev*. 2017;30:557–96. <http://dx.doi.org/10.1128/CMR.00064-16>
- Liassine N, Assouvie L, Descombes MC, Tendon VD, Kieffer N, Poirel L, et al. Very low prevalence of MCR-1/MCR-2 plasmid-mediated colistin resistance in urinary tract *Enterobacteriaceae* in Switzerland. *Int J Infect Dis*. 2016;51:4–5. <http://dx.doi.org/10.1016/j.ijid.2016.08.008>
- Irrgang A, Roschanski N, Tenhagen BA, Grobbel M, Skladnikiewicz-Ziemer T, Thomas K, et al. Prevalence of *mcr-1* in *E. coli* from livestock and food in Germany, 2010–2015. *PLoS One*. 2016;11:e0159863. <http://dx.doi.org/10.1371/journal.pone.0159863>
- Guenther S, Falgenhauer L, Semmler T, Imirzalioglu C, Chakraborty T, Roesler U, et al. Environmental emission of multiresistant *Escherichia coli* carrying the colistin resistance gene *mcr-1* from German swine farms. *J Antimicrob Chemother*. 2017;72:1289–92.
- Huang X, Yu L, Chen X, Zhi C, Yao X, Liu Y, et al. High prevalence of colistin resistance and *mcr-1* gene in *Escherichia coli*

- isolated from food animals in China. *Front Microbiol.* 2017;8:562. <http://dx.doi.org/10.3389/fmicb.2017.00562>
8. Perrin-Guyomard A, Bruneau M, Houée P, Deleurme K, Legrandois P, Poirier C, et al. Prevalence of *mcr-1* in commensal *Escherichia coli* from French livestock, 2007 to 2014. *Euro Surveill.* 2016;21:30135. <http://dx.doi.org/10.2807/1560-7917.ES.2016.21.6.30135>
 9. Zhang C, Feng Y, Liu F, Jiang H, Qu Z, Lei M, et al. A phage-like IncY plasmid carrying the *mcr-1* gene in *Escherichia coli* from a pig farm in China. *Antimicrob Agents Chemother.* 2017;61:e02035-16. <http://dx.doi.org/10.1128/AAC.02035-16>
 10. Xavier BB, Lammens C, Butaye P, Goossens H, Malhotra-Kumar S. Complete sequence of an IncFII plasmid harbouring the colistin resistance gene *mcr-1* isolated from Belgian pig farms. *J Antimicrob Chemother.* 2016;71:2342-4. <http://dx.doi.org/10.1093/jac/dkw191>
 11. Poirel L, Kieffer N, Brink A, Coetze J, Jayol A, Nordmann P. Genetic features of MCR-1-producing colistin-resistant *Escherichia coli* isolates in South Africa. *Antimicrob Agents Chemother.* 2016;60:4394-7. <http://dx.doi.org/10.1128/AAC.00444-16>
 12. Zurfluh K, Kieffer N, Poirel L, Nordmann P, Stephan R. Features of the *mcr-1* cassette related to colistin resistance. *Antimicrob Agents Chemother.* 2016;60:6438-9. <http://dx.doi.org/10.1128/AAC.01519-16>
 13. Poirel L, Kieffer N, Nordmann P. In-vitro study of IS*ApII*-mediated mobilization of the colistin resistance gene *mcr-1*. *Antimicrob Agents Chemother.* 2017;61:e00127-17. <http://dx.doi.org/10.1128/AAC.00127-17>
 14. Zurfluh K, Klumpp J, Nüesch-Inderbinen M, Stephan R. Full-length nucleotide sequences of *mcr-1*-harboring plasmids isolated from extended-spectrum- β -lactamase-producing *Escherichia coli* isolates of different origins. *Antimicrob Agents Chemother.* 2016;60:5589-91. <http://dx.doi.org/10.1128/AAC.00935-16>
 15. Kieffer N, Nordmann P, Poirel L. *Moraxella* species as potential sources of MCR-like polymyxin-resistance determinants. *Antimicrob Agents Chemother.* 2017;61:e00129-17. <http://dx.doi.org/10.1128/AAC.00129-17>
 16. Poirel L, Kieffer N, Fernandez-Garayzabal JF, Vela AI, Larpin Y, Nordmann P. MCR-2-mediated plasmid-borne polymyxin resistance most likely originates from *Moraxella pluranimalium*. *J Antimicrob Chemother.* In press; 2017.
 17. Vela AI, Sánchez-Porro C, Aragón V, Olvera A, Domínguez L, Ventosa A, et al. *Moraxella porci* sp. nov., isolated from pigs. *Int J Syst Evol Microbiol.* 2010;60:2446-50. <http://dx.doi.org/10.1099/ijs.0.016626-0>
 18. Rhouma M, Beaudry F, Thériault W, Letellier A. Colistin in pig production: chemistry, mechanism of antibacterial action, microbial resistance emergence, and One Health perspectives. *Front Microbiol.* 2016;7:1789. <http://dx.doi.org/10.3389/fmicb.2016.01789>
 19. Katsunuma Y, Hanazumi M, Fujisaki H, Minato H, Hashimoto Y, Yonemochi C. Associations between the use of antimicrobial agents for growth promotion and the occurrence of antimicrobial-resistant *Escherichia coli* and enterococci in the feces of livestock and livestock farmers in Japan. *J Gen Appl Microbiol.* 2007;53:273-9. <http://dx.doi.org/10.2323/jgam.53.273>
 20. Quesada A, Ugarte-Ruiz M, Iglesias MR, Porrero MC, Martínez R, Florez-Cuadrado D, et al. Detection of plasmid mediated colistin resistance (MCR-1) in *Escherichia coli* and *Salmonella enterica* isolated from poultry and swine in Spain. *Res Vet Sci.* 2016;105:134-5. <http://dx.doi.org/10.1016/j.rvsc.2016.02.003>
 21. Falgenhauer L, Waezsada SE, Yao Y, Imirzalioglu C, Käsbohrer A, Roesler U, et al.; RESET Consortium. Colistin resistance gene *mcr-1* in extended-spectrum β -lactamase-producing and carbapenemase-producing Gram-negative bacteria in Germany. *Lancet Infect Dis.* 2016;16:282-3. [http://dx.doi.org/10.1016/S1473-3099\(16\)00009-8](http://dx.doi.org/10.1016/S1473-3099(16)00009-8)
 22. Catry B, Cavaleri M, Baptiste K, Grave K, Grein K, Holm A, et al. Use of colistin-containing products within the European Union and European Economic Area (EU/EEA): development of resistance in animals and possible impact on human and animal health. *Int J Antimicrob Agents.* 2015;46:297-306. <http://dx.doi.org/10.1016/j.ijantimicag.2015.06.005>
 23. Conceição T, de Lencastre H, Aires-de-Sousa M. Frequent isolation of methicillin resistant *Staphylococcus aureus* (MRSA) ST398 among healthy pigs in Portugal. *PLoS One.* 2017;12:e0175340. <http://dx.doi.org/10.1371/journal.pone.0175340>
 24. Nordmann P, Jayol A, Poirel L. A universal culture medium for screening polymyxin-resistant Gram-negative isolates. *J Clin Microbiol.* 2016;54:1395-9. <http://dx.doi.org/10.1128/JCM.00446-16>
 25. Clinical and Laboratory Standards Institute. Performance standards for antimicrobial susceptibility testing; 26th informational supplement (M100-S26). Wayne (PA): The Institute; 2016.
 26. Lartigue MF, Poirel L, Nordmann P. Diversity of genetic environment of *bla*_{CTX-M} genes. *FEMS Microbiol Lett.* 2004;234:201-7. <http://dx.doi.org/10.1111/j.1574-6968.2004.tb09534.x>
 27. Kim J, Lim YM. Prevalence of derepressed *ampC* mutants and extended-spectrum β -lactamase producers among clinical isolates of *Citrobacter freundii*, *Enterobacter* spp., and *Serratia marcescens* in Korea: dissemination of CTX-M-3, TEM-52, and SHV-12. *J Clin Microbiol.* 2005;43:2452-5. <http://dx.doi.org/10.1128/JCM.43.5.2452-2455.2005>
 28. Poirel L, Kieffer N, Liassine N, Thanh D, Nordmann P. Plasmid-mediated carbapenem and colistin resistance in a clinical isolate of *Escherichia coli*. *Lancet Infect Dis.* 2016;16:281. [http://dx.doi.org/10.1016/S1473-3099\(16\)00006-2](http://dx.doi.org/10.1016/S1473-3099(16)00006-2)
 29. Kieffer N, Nordmann P, Aires-de-Sousa M, Poirel L. High prevalence of carbapenemase-producing *Enterobacteriaceae* among hospitalized children in Luanda, Angola. *Antimicrob Agents Chemother.* 2016;60:6189-92. <http://dx.doi.org/10.1128/AAC.01201-16>
 30. Clermont O, Christenson JK, Denamur E, Gordon DM. The Clermont *Escherichia coli* phylo-typing method revisited: improvement of specificity and detection of new phylo-groups. *Environ Microbiol Rep.* 2013;5:58-65. <http://dx.doi.org/10.1111/1758-2229.12019>
 31. Carattoli A, Bertini A, Villa L, Falbo V, Hopkins KL, Threlfall EJ. Identification of plasmids by PCR-based replicon typing. *J Microbiol Methods.* 2005;63:219-28. <http://dx.doi.org/10.1016/j.mimet.2005.03.018>
 32. Kieser T. Factors affecting the isolation of CCC DNA from *Streptomyces lividans* and *Escherichia coli*. *Plasmid.* 1984;12:19-36. [http://dx.doi.org/10.1016/0147-619X\(84\)90063-5](http://dx.doi.org/10.1016/0147-619X(84)90063-5)
 33. Nordmann P, Assouvie L, Prod'Hom G, Poirel L, Greub G. Screening of plasmid-mediated MCR-1 colistin-resistance from bacteremia. *Eur J Clin Microbiol Infect Dis.* 2016;35:1891-2. <http://dx.doi.org/10.1007/s10096-016-2739-0>
 34. Jiang X, Poirel L, Nordmann P. Lack of polymyxin resistance among carbapenemase-producing *Enterobacteriaceae* in a university hospital in China. *Infect Dis (Lond).* 2017;49:556-7. <http://dx.doi.org/10.1080/23744235.2017.1292543>
 35. Buess S, Nüesch-Inderbinen M, Stephan R, Zurfluh K. Assessment of animals as a reservoir for colistin resistance: no MCR-1/MCR-2-producing *Enterobacteriaceae* detected in Swiss livestock. *J Glob Antimicrob Resist.* 2017;8:33-4. <http://dx.doi.org/10.1016/j.jgar.2016.11.001>
 36. Malhotra-Kumar S, Xavier BB, Das AJ, Lammens C, Butaye P, Goossens H. Colistin resistance gene *mcr-1* harboured on a multidrug resistant plasmid. *Lancet Infect Dis.* 2016;16:283-4. [http://dx.doi.org/10.1016/S1473-3099\(16\)00012-8](http://dx.doi.org/10.1016/S1473-3099(16)00012-8)

37. Falgenhauer L, Waezsada SE, Gwozdziński K, Ghosh H, Doijad S, Bunk B, et al. Chromosomal locations of *mcr-1* and *bla*_{CTX-M-15} in fluoroquinolone-resistant *Escherichia coli* ST410. *Emerg Infect Dis*. 2016;22:1689–91. <http://dx.doi.org/10.3201/eid2209.160692>
38. Saly M, Jayol A, Poirel L, Mégraud F, Nordmann P, Dubois V. Prevalence of faecal carriage of colistin-resistant Gram-negative rods in a university hospital in western France, 2016. *J Med Microbiol*. 2017;66:842–3. <http://dx.doi.org/10.1099/jmm.0.000497>
39. Campos J, Cristino L, Peixe L, Antunes P. MCR-1 in multidrug-resistant and copper-tolerant clinically relevant *Salmonella* 1,4,[5],12:i:- and *S. Rissen* clones in Portugal, 2011 to 2015. *Euro Surveill*. 2016;21:30270. <http://dx.doi.org/10.2807/1560-7917.ES.2016.21.26.30270>
40. Bernasconi OJ, Kuenzli E, Pires J, Tinguely R, Carattoli A, Hatz C, et al. Travelers can import colistin-resistant *Enterobacteriaceae*, including those possessing the plasmid-mediated *mcr-1* gene. *Antimicrob Agents Chemother*. 2016;60:5080–4. <http://dx.doi.org/10.1128/AAC.00731-16>
41. Yang RS, Feng Y, Lv XY, Duan JH, Chen J, Fang LX, et al. Emergence of NDM-5- and MCR-1-producing *Escherichia coli* clones ST648 and ST156 from a single muscovy duck (*Cairina moschata*). *Antimicrob Agents Chemother*. 2016;60:6899–902. <http://dx.doi.org/10.1128/AAC.01365-16>
42. He QW, Xu XH, Lan FJ, Zhao ZC, Wu ZY, Cao YP, et al. Molecular characteristic of *mcr-1* producing *Escherichia coli* in a Chinese university hospital. *Ann Clin Microbiol Antimicrob*. 2017;16:32. <http://dx.doi.org/10.1186/s12941-017-0207-z>
43. Sun J, Fang LX, Wu Z, Deng H, Yang RS, Li XP, et al. Genetic analysis of the IncX4 plasmids: implications for a unique pattern in the *mcr-1* acquisition. *Sci Rep*. 2017;7:424. <http://dx.doi.org/10.1038/s41598-017-00095-x>
44. Snesrud E, He S, Chandler M, Dekker JP, Hickman AB, McGann P, et al. A model for transposition of the colistin resistance gene *mcr-1* by IS*ApI1*. *Antimicrob Agents Chemother*. 2016;60:6973–6. <http://dx.doi.org/10.1128/AAC.01457-16>

Address for correspondence: Laurent Poirel, Medical and Molecular Microbiology Unit, Department of Medicine, Faculty of Science, University of Fribourg, rue Albert Gockel 3, CH-1700 Fribourg, Switzerland; email: laurent.poirel@unifr.ch

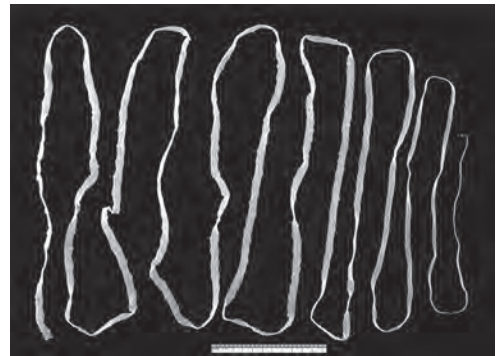
etymologia

Taenia saginata [te'ne-ə saɪ'e-na'ta]

Ronnie Henry

Johann Goeze is credited with the first correct description of *Taenia* [Latin, “flat band” or “ribbon”] *saginata* [Latin, “fed”], commonly known as the beef tapeworm, in 1782. Historically, *Taenia* tapeworms were believed to have infected humans no more than 10,000 years ago, around the time of domestication of cows and pigs.

However, more recent phylogenetic evidence suggests that ancestors of modern humans, living on the savannahs of Africa and preying on antelope and other bovids, became colonized with *Taenia* >3 million years ago. Parasite definitive hosts switched from large carnivores (probably hyenas) to hominids through their common prey, and this process triggered the evolution of human-infecting species of *Taenia*. Humans later spread these parasites to domestic animals.



Adult *Taenia saginata* tapeworm. Photo CDC/1986.

Sources

1. Despommier DD, Gwadz RW, Hotez PJ. *Taenia saginata* (Goeze 1782). In: *Parasitic Diseases*. 3rd ed. New York: Springer; 1995. p.76–80.
2. Hoberg EP, Alkire NL, de Queiroz A, Jones A. Out of Africa: origins of the *Taenia* tapeworms in humans. *Proc Biol Sci*. 2001;268:781–7. <http://dx.doi.org/10.1098/rspb.2000.1579>
3. Terefe Y, Hailemariam Z, Menkir S, Nakao M, Lavikainen A, Haukialmi V, et al. Phylogenetic characterisation of *Taenia* tapeworms in spotted hyenas and reconsideration of the “Out of Africa” hypothesis of *Taenia* in humans. *Int J Parasitol*. 2014;44:533–41. <http://dx.doi.org/10.1016/j.ijpara.2014.03.013>
4. Zarlenga DS, Hoberg E, Rosenthal B, Mattiucci S, Nascetti G. Anthropogenics: human influence on global and genetic homogenization of parasite populations. *J Parasitol*. 2014;100:756–72. <http://dx.doi.org/10.1645/14-622.1>

Address for correspondence: Ronnie Henry, Centers for Disease Control and Prevention, 1600 Clifton Rd NE, Mailstop E28, Atlanta, GA 30329-4027, USA; email: boq3@cdc.gov

DOI: <https://doi.org/10.3201/eid2312.ET2312>

History of *Taenia saginata* Tapeworms in Northern Russia

Sergey V. Konyaev, Minoru Nakao, Akira Ito, Antti Lavikainen

Taenia saginata is the most common species of tapeworm infecting humans. Infection is acquired by eating cysticercus larvae in undercooked beef. A closely related species, *T. asiatica*, is found in eastern and southeastern Asia. The larvae of *T. asiatica* develop in viscera of pigs. In northern Russia, there is a third member of this morphologically indistinguishable group. Cysticerci of so-called northern *T. saginata* are found in cerebral meninges of reindeer, and the unique life cycle is dependent on a native custom of eating raw reindeer brain. We report the winding history of this mysterious tapeworm from the first reports to the present time. In addition, we confirm the position of this parasite as a strain of *T. saginata* by analyzing a mitochondrial DNA sequence of an archival specimen. The origin of this strain might date back to reindeer domestication and contacts between cattle-herding and reindeer-herding peoples in Asia.

Taeniasis is among the oldest known human helminthiasis; written descriptions of the disease and history of the name taenia reach into antiquity. *Taenia* spp. infections are common in many countries; there are tens of millions of human carriers worldwide (1). The best-known etiologic agents, *Taenia saginata* Goeze 1782 and *T. solium* Linnaeus 1758, were described as 2 different tapeworm species >2 centuries ago, and both have many synonyms in the literature (2). Conversely, a third species of *Taenia* infecting humans, *T. asiatica* Eom et Rim 1993, is one of the most recently described taeniid species. This species was known to be a special form of *T. saginata* (3).

Similar to other taeniid tapeworms, human-infecting *Taenia* spp. require 2 mammalian hosts in an obligate predator-prey life cycle. Adult tapeworm stages develop in the human intestine. Gravid proglottids, which are full of eggs, are excreted in feces into the environment. Alternatively, for *T. asiatica* and *T. saginata*, proglottids can actively crawl out of the anus and cause irritation and discomfort (1-3). The infection is otherwise usually asymptomatic. Eggs scattered in the environment are then ingested by intermediate hosts, cattle and other bovids (for *T. saginata*)

or pigs (for *T. asiatica* and *T. solium*). Cysticercal larvae typically develop in muscles (*T. saginata* and *T. solium*) or visceral organs (*T. asiatica*) of the intermediate host. Humans can become infected by eating raw or undercooked meat or organs infected with cysticerci.

Unlike the other 2 species, *T. solium* commonly forms cysticerci in tissues of various atypical intermediate hosts, including rabbits, camels, dogs, cats, and humans (2,4). Another major feature distinguishing *T. solium* from the other 2 species is a double crown of rostellar hooks, which can be easily observed by microscopy in adult and larval stages; these hooks are absent in *T. asiatica* and *T. saginata*.

T. saginata is the most common and widely spread *Taenia* species infecting humans. This tapeworm is found in all continents and is endemic to eastern Europe, Southeast Asia, Africa, and Latin America (1,5). However, in addition to the classic strain of this parasite found in southern regions, which is associated with cattle raising, there is a lesser-known form of *T. saginata* in northern regions. Its present distribution is limited, perhaps including only some parts of northern Russia. This northern form or strain of *T. saginata* uses reindeer (*Rangifer tarandus*) instead of bovids as the intermediate host. The aim of this article is to provide information on the history and unique life cycle of this enigmatic human parasite in northern Russia and to resolve its taxonomic position on the basis of unpublished DNA data.

Early Records of *T. saginata* Infections in Reindeer and Reindeer-Herding Human Populations

The northern strain of *T. saginata* has been found in northern Siberia in Russia and the Far East Region of Russia (Figure 1). Krotov (6,7) reported that the northern strain of *T. saginata* was observed in 1872 by Dobrotvorsky, who reported taeniasis in the native population of Sakhalin Island. At that time, cattle had not yet been brought to the island. This finding was supported by observations of Krotov on taeniasis in reindeer herders on Sakhalin Island in 1955 (7). Researchers considered reindeer to be the most likely intermediate host, although larval stages were not found (7). Unfortunately, we could not analyze details of this study because we did not have access to the original data of Krotov, which were published in his academic

Author affiliations: Siberian Branch of the Russian Academy of Sciences, Novosibirsk, Russia (S.V. Konyaev); Asahikawa Medical University, Asahikawa, Japan (M. Nakao, A. Ito); University of Helsinki, Helsinki, Finland (A. Lavikainen)

DOI: <https://doi.org/10.3201/eid2312.162101>

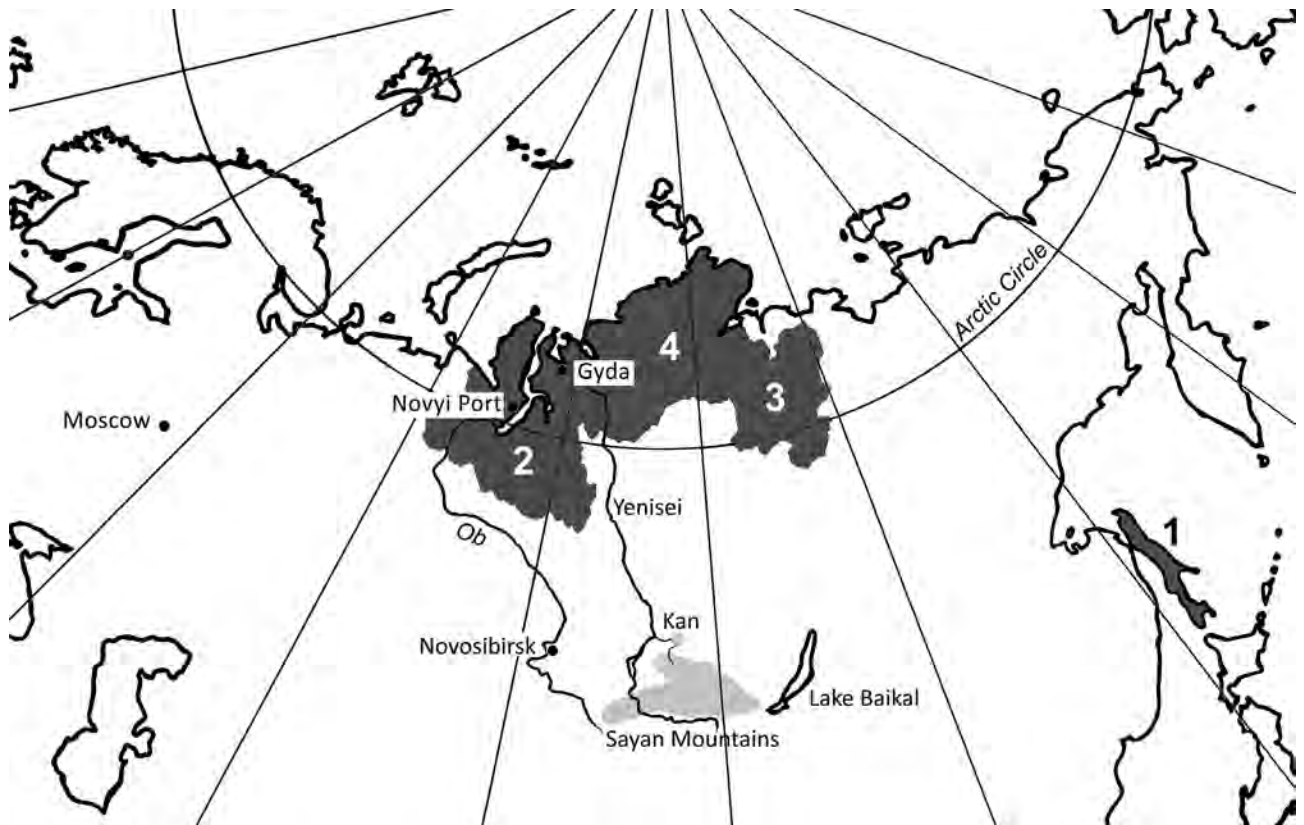


Figure 1. Regions where infections with the northern strain of *Taenia saginata* tapeworms in Siberia and the Far East region of Russia were detected (dark gray shading). 1, Sakhalin Island in 1872 and 1955; 2, Yamalo-Nenets Autonomous Okrug, since the 19th century to the present time; 3, Olenyoksky District, Yakutia, 1958; 4, Taymyr Autonomous Okrug, 1977. The probable cradle of reindeer herding in Asia and site of the host switch from cattle to reindeer (the Sayan Mountains) is indicated by light gray shading. The light gray dot indicates the Kan River archaeological site where taeniid eggs were found from human remains buried 3,000–4,000 years ago.

dissertation in 1955. After the observations of Krotov, taeniasis on Sakhalin Island did not attract further attention.

The suggestion that cases of taeniasis on Sakhalin Island represent the first report of the northern strain of *T. saginata* cannot be verified. The current population of Sakhalin Island has essentially abandoned reindeer herding. Reindeer are still used, but their number, as well as the size of the indigenous human population, is small. Large-scale reindeer husbandry on Sakhalin Island began in the Val collective farm (8), where Krotov (7) later detected possible human taeniasis. The reindeer population was initially 414 animals in 1930 and increased to 8,415 by 1967 (8). However, by 1998, after the collapse of the Soviet Union, the number of reindeer had decreased to 2,900. The present population is probably 150–200 animals.

Only the indigenous Ulta, which have a population of <350 persons (8), maintain the reindeer herding tradition on Sakhalin Island. Given the sharp decrease in the number of intermediate and final hosts, the northern strain of *T. saginata* has probably not survived on Sakhalin Island. In addition, a return to small-scale reindeer herding indicates that domestic reindeer are used primarily as

mount or pack animals, and wild reindeer are consumed as food. According to a state report of human parasitoses on Sakhalin Island, no cases of taeniasis have been found there in recent years (9).

In 1956, taeniasis in an indigenous person in the Krasnoselkup Region in the Yamalo-Nenets Autonomous Okrug (YaNAO) caused concern about spread of *T. saginata* in northern Siberia (10). The index patient was a Selkup reindeer herder. Anthelmintic treatment for 32 tapeworm carriers identified 11 cases of taeniasis among reindeer herders. Diphyllbothriasis and taeniasis were distinguished, but morphologic data for tapeworms were not provided in detail. It was concluded that the source of infection was probably reindeer meat, which was (and still is) the staple food in that region (10). Subsequently, taeniasis in humans was confirmed across the YaNAO (including the basins of the Ob, Nadym, Pur, and Taz Rivers and the Yamal and Gydan Peninsulas), in Khanty-Mansiysk (the capital of the Khanty-Mansi Autonomous Okrug); and in the Taymyr Autonomous Okrug (11–17). The highest prevalence (14%) in the local population was reported in the Yamal and Gydan Peninsulas (14). A recent archaeological

finding of taeniid eggs in a burial site from the 19th century (18) showed that taeniasis occurred in the Nenets population in the Taz tundra, which was contemporary with the first observation on Sakhalin Island (7).

In 1958, possible cysticerci of *T. saginata* were found in reindeer carcasses and organs in the Oleneksky District, Yakutia, but a specific diagnosis was not confirmed by microscopy (19). A survey identified tapeworm infection in 59 of 200 local schoolchildren (19). The local population consumed reindeer meat and fish. Nevertheless, infection with *Diphyllobothrium latum* tapeworms was not considered a possible differential diagnosis. At that time, beef was not consumed in the Oleneksky District (19). However, cattle were raised in other parts of Yakutia south of the Oleneksky District. Overall, the presence of reindeer-dependent *T. saginata* in Yakutia cannot be reliably confirmed. Recent records (20) showed that all recent cases of taeniasis reported in Yakutia were associated with beef consumption. Despite extensive meat inspection, cysticerci of *T. saginata* have not been currently reported in reindeer in Yakutia.

In a monograph on taeniid taxonomy and biology, Abuladze (2) summarized data on *Taenia* spp. circulating in northern Russia. He speculated that a special species of the genus *Taeniarhynchus* (in his classification, *Taenia* spp. without rostellar armature were considered a distinct genus) might be involved. However, this suggestion did not lead to a description of the full morphology or individual segments of the putative new species (2).

Experimental Infections

The first study to resolve the life history and host specificity of the northern strain of *T. saginata* was conducted in 1975 by Mozgovoy et al. at the Biological Institute (currently the Institute of Systematics and Ecology of Animals) of the Academy of Sciences, Novosibirsk (16) (Figure 2). A limited number of reindeer and cattle calves were infected with the southern and northern strains of *T. saginata* (online Technical Appendix Table 1, <https://wwwnc.cdc.gov/EID/article/23/12/16-2101-Techapp1.pdf>). Necropsies were performed on the animals after various postinfection periods. The southern strain was obtained from a patient in Barnaul (Altay Krai), and the northern strain was obtained from a patient in Gyda (a remote village in YaNAO).

Many fibrotic nodules, but no *T. saginata* cysticerci, were observed in muscles of 5 reindeer calves. One reindeer died because of a heavy infection with the northern strain. Numerous cysticerci were found in muscles, heart, diaphragm, and brain of this calf. Infectivity of larvae for humans was not tested, but $\approx 60\%$ of muscle cysticerci were dead (necrotic). In a reindeer infected with the southern form, cysticerci were found only in muscles. However, the experiment was subject to environmental contamination because animals were not isolated from the herd. Armed



Figure 2. Vera I. Shakhmatova, one of the pioneers of infection experiments with the northern strain of *Taenia saginata* tapeworms, examining parasitologic specimens during a field expedition in northern Siberia, Russia, 1975. Photograph courtesy of the Institute of Systematics and Ecology of Animals, Siberian Branch of the Russian Academy of Sciences.

(containing rostellar hooks) cysticerci of *Taenia* spp. transmitted by dogs (e.g., *Taenia parenchymatosa* tapeworms) were found in 6 reindeer, which indicated contamination of the pasture. This finding indicated that all experimental animals could also have had access to eggs of the northern strain of *T. saginata* excreted by herdsmen.

Infected cattle calves were kept in isolation in Altay Krai (Figure 3). Cysticerci of northern and southern strains developed in muscles (Figure 4). However, 55%–90% of cysticerci of the northern strain were found dead. Viability of larvae was confirmed by self-infection. One of the authors (not identified) of the study of Mozgovoy et al. (16) ate 4 cysticerci of the northern strain and shed *T. saginata* proglottids 80 days postinfection (online Technical Appendix Table 2).

These experiments yielded 2 conclusions. First, larvae of the northern strain can develop not only in muscles but also in the brain of reindeer. Second, the northern strain is capable of developing in cattle, although viability seems to be drastically reduced. However, this pioneering work went unnoticed by the Soviet scientific community, and researchers in Moscow later conducted similar experiments.



Figure 3. Researcher Anatoly M. Serdyukov with a calf experimentally infected with *Taenia saginata* tapeworms, Sovkhoz Rossia, Altai Krai, western Siberia, Russia, 1975. Photograph courtesy of the Institute of Systematics and Ecology of Animals, Siberian Branch of the Russian Academy of Sciences.

A research group from the K.I. Skrjabin Institute of Helminthology in Moscow conducted a series of experiments during the 1980s (17,21,22) that essentially duplicated the previous study conducted by Mozgovoy et al. (16). Eggs of the northern strain were obtained from 2 Nenets children from a small settlement (Novyi Port) on the Yamal Peninsula (17,21). The only meat the 2 children consumed was reindeer meat, and the children never left the territory. Comparative specimens for the southern strain were obtained from Moscow and Uzbekistan. Results confirmed the previous findings of Mozgovoy et al. (16). On the basis of a slightly higher number of experimental animals (online Technical Appendix Table 1), the affinity of the northern strain for reindeer brain was demonstrated. Low viability in cattle was also shown. In addition, 3 naturally infected reindeer were found among 413 carcasses examined in Novyi Port (17). All infected reindeer were >2 years of age (this group included 201 animals), and 1 or 2 cysticerci of *T. saginata* per animal were found (all in the brain). This finding was probably the only confirmed observation of natural infections in reindeer.

During an initial experiment, Kirichek et al. reported that “two reindeer died 14 and 28 days after infection without visible clinical signs of cysticercosis” (17). However, there was a dramatic story behind this laconic sentence. Reindeer used for experiments were born and reared isolated from natural herds in a vivarium in Salekhard (17). According to an anonymous eyewitness, the infected reindeer (2 adults and 1 calf) were transported to Moscow for observation. Just after arrival, both adult reindeer escaped. One soon died in a car accident, but the other one ran away and spent 2 weeks in parks in Moscow, until it was found and killed. These reindeer were unlikely to have been exposed

to additional *T. saginata* eggs during their escape. More than 1,000 degenerating cysticerci were found in their bodies. However, heads of these animals were not examined, possibly because of unscheduled dissections (17).

In 1986, successful self-infection was performed by Kirichek et al. with cysticerci from the brain of an experimentally infected reindeer (21) (online Technical Appendix Table 2). Cysticerci, collected 115 days postinfection were infective. The clinical course, including the prepatent period (97 days), signs (periodic diarrhea, light meteorism [rapid accumulation of gas in the intestine], anal irritation caused by actively moving proglottids, pyrosis, vomiting, and lack of appetite), and excretion of proglottids (21), corresponded to that of taeniasis caused by *T. asiatica* or the beef-derived southern strains of *T. saginata* (1–3).

Cerebral Cysticerci and Morphologic Characterization of Adult Tapeworms

Histopathologic analysis of northern strain cysticerci was performed by parasitologists from the Soviet Union and Czechoslovakia (22) for specimens from the experimental studies of the K.I. Skrjabin Institute (17,21). Viable cysticerci in reindeer were located in the subarachnoid space but were not found in brain tissue or spinal cord (22). Larval structure and tissue reactions corresponded to those of the southern strain in cattle muscle (22). The infection typically caused a nonpurulent meningoencephalitis with neurologic symptoms (e.g., reeling and walking in circles) (17). Cysticerci in reindeer muscles and heart died at an early developmental stage, possibly because of nutritional deficiency and immunologic response, and were fully resorbed within 3 months (17,22). It was assumed that immunologic responses appear later in the brain than in other tissues or are less effective (22).

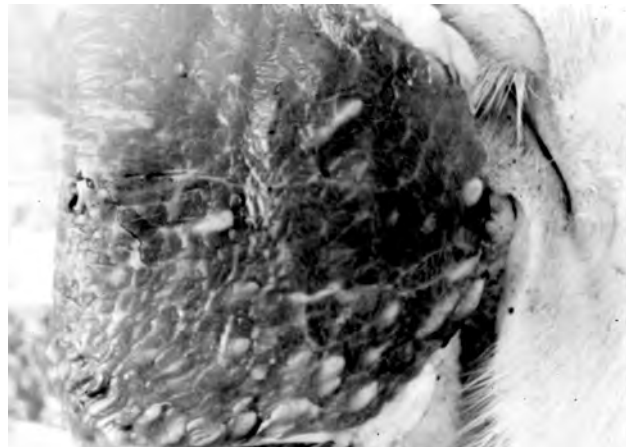


Figure 4. Muscle cysticerci of the northern strain of *Taenia saginata* tapeworms in an experimentally infected calf, western Siberia, Russia. Photograph courtesy of the Institute of Systematics and Ecology of Animals, Siberian Branch of the Russian Academy of Sciences.

Cerebral localization of cysticerci explained the unsuccessful attempts of previous researchers to find larvae of *T. saginata* in reindeer carcasses. The nonindigenous population in northern Siberia eagerly consumes venison, often undercooked. However, raw brain is consumed only by the native population. Given the extremely limited natural resources in northern Siberia, raw brain and other tissues have traditionally been a common source of nutrition for many indigenous peoples in this region (Figure 5).

Morphologic studies of northern *T. saginata* adult stages are limited. The literature does not provide data describing detected cestodes but refers only to their specific identification. It seems logical that expelled fragments were identified after diagnostic deworming, but criteria were not provided. We must assume that diagnoses were primarily based on 2 widely used attributes: lack of hooks in the scolex and number of uterine branches in mature proglottids (Figure 6, panels A, B).

A complete morphologic description of the northern strain was reported (23) (original illustrations in Figure 6). Serdyukov (23) also reported a detailed comparison



Figure 5. A Khanty mother and her child eating raw reindeer meat in the Yamal Peninsula (Yamalo-Nenets Autonomous Okrug), northern Siberia, Russia, 1991. Photograph courtesy of Marianna Flinkenberg-Gluschkoff.

between northern and southern strains by using specimens from patients in Gyda (8 specimens) and Novosibirsk (4 specimens). This study was conducted simultaneously with the experimental work of his colleagues (16). Only a few minor differences were detected (e.g., the cirrus sac was longer and the average number of uterine branches was slightly higher in the southern strain). Given the poorly understood natural phenotypic variation, the role of these differences remains unclear. If one considers the nearly complete congruence of morphologic characteristics, specimens of the northern strain were clearly related to *T. saginata* (and *T. asiatica*) and could not represent any other known species or group of *Taenia* tapeworms.

Identification by DNA Barcoding

In the Soviet Union and later in Russia, the northern strain of *T. saginata* was considered a form or isolate confined to an atypical intermediate host, the reindeer. This definition has not been subjected to further questioning, beyond the unsupported contention that it might represent a distinct species (2). Since the description of *T. asiatica*, a species closely related to *T. saginata*, a taxonomic reconsideration of the northern strain has become relevant. Nonbovid intermediate hosts and distinctly different predilection sites for cysticerci differentiate *T. asiatica* and northern *T. saginata* from classic *T. saginata*. Because *T. asiatica* was not known by parasitologists of the Soviet era, host switching from pigs to reindeer was not considered, and cysticercosis in pigs was not investigated in disease-endemic areas. Pigs are commonly reared for food production in villages in northern Russia because they are much easier to keep than cattle during the cold season.

A major question is the relationship between the northern strain and other unarmed (no rostellar hooks) *Taenia* spp. Could it represent an independent lineage, or could it be related to *T. asiatica* instead of classic *T. saginata*? On the basis of available descriptions (23–25), all 3 forms are virtually morphologically indistinguishable. Thus, molecular genetic characterization was required to confirm the identity of the northern strain.

To resolve this question, we analyzed a formalin-preserved archival specimen of the northern strain from the collection of the Institute of Systematics and Ecology of Animals in Novosibirsk. A fully developed tapeworm was expelled from a 7-year-old Nenets child in Gyda in 1974. The patient had never consumed beef or pork. Morphology of the specimen was reported (23). In addition, we attempted to extract DNA by using cysticerci (all specimens were preserved in formalin) from reindeer obtained during the experiments of Mosgovoy et al. (16), but PCR amplifications were unsuccessful.

The specimen from Gyda was characterized on the basis of a region of the mitochondrial cytochrome c oxidase

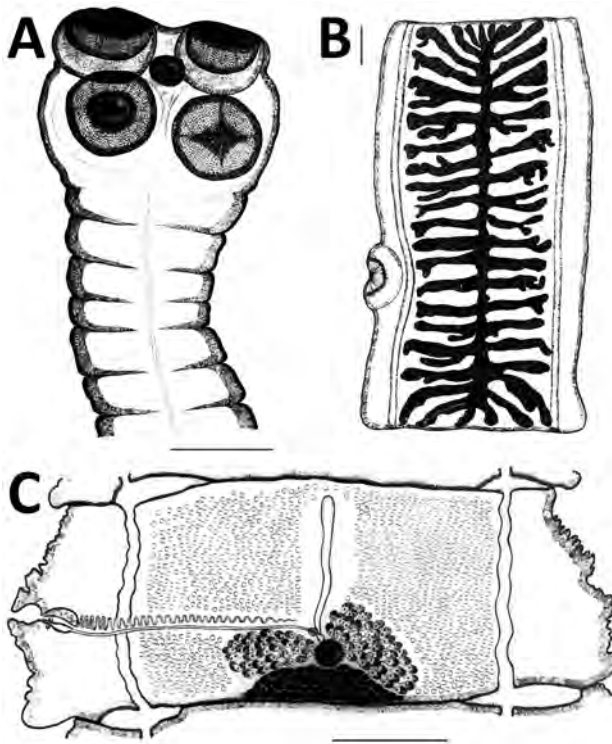


Figure 6. Original drawings of the northern strain of *Taenia saginata* tapeworms from Gyda, Yamalo-Nenets Autonomous Okrug, northern Siberia, Russia, by Serdyukov (23). A) Scolex showing the lack of a rostellar hook crown in the middle of the scolex, which is a synapomorphy in *T. saginata* and *T. asiatica* tapeworms. B) Gravid proglottid showing the number of uterine branches, which is a commonly used character in species identification. C) Mature proglottid. Scale bars indicate 1 mm. Image courtesy of the Institute of Systematics and Ecology of Animals, Siberian Branch of the Russian Academy of Sciences.

subunit 1 (*cox1*) gene of *T. saginata* (mitochondrial genome DDBJ/EMBL/GenBank accession no. NC_009938), which has been used for >20 years in barcoding of taeniids. We isolated genomic DNA from a tapeworm proglottid by using the DNeasy Tissue Kit (QIAGEN, Hilden, Germany). Because the DNA was fragmented and damaged by prolonged preservation in formalin, we generated short overlapping amplicons (≈ 200 bp each) by using specific primer pairs (online Technical Appendix Table 3). We performed PCR with 40 thermal cycles (94°C for 30 s, 50°C for 30 s, and 72°C for 30 s) and cloned amplicons by using the pGEM-T Vector System (Promega, Madison, WI, USA). Procedures for PCR, cloning, and sequencing have been reported (26). Overlapping *cox1* sequences obtained were assembled into a single contiguous sequence (426 nt, DDBJ/EMBL/GenBank accession no. LC063349). The resultant sequence was phylogenetically compared with those of *T. saginata*, *T. asiatica*, and *T. crocutae* (an outgroup). We used MEGA6 software (27)

for alignment, distance calculation, substitution model search, and maximum-likelihood estimation.

The sequence of *cox1* suggested that the specimen of the northern strain represents *T. saginata* (Figure 7). The *cox1* fragment differed only by 3 nt from the corresponding reference sequence of *T. saginata*. Nevertheless, no sequences identical to the Gydan specimen were found in DNA databases. The difference was within the variation that can be detected for sequences of *T. saginata* in these databases (DDBJ/EMBL/GenBank). Unfortunately, a short sequence from 1 specimen does not enable estimation of phylogeographic relationships of the northern strain.

Taenia asiatica and *T. saginata* are considered distinct species mainly because of differences in life history, localization in the intermediate host, and phylogenetic data indicating a sister species relationship (24,28,29). However, genetic studies have shown recent hybridization of these parasites, which clearly indicates that the reproductive barrier between them is not complete and is consistent with a relatively shallow time frame for divergence (30). This finding makes the validity of *T. asiatica* as a separate species questionable. Genetic distance between *T. asiatica* and *T. saginata* is much higher than between the northern and southern strains of *T. saginata* (Kimura 2-parameter distance 0.039 vs. 0.007, respectively). The northern strain of *T. saginata* is partially adapted (by unknown mechanisms) to the reindeer intermediate host (17,22). Evidence suggests a recent origin of the human–reindeer cycle in this geographically restricted area. Therefore, we conclude that strain is the most suitable definition for this parasite, as well as the basically equal form, which was used by parasitologists in the Soviet Union. The term isolate, which has also been used in Russia for *T. saginata* from northern regions, today refers most often to a particular taeniid specimen or materials derived from it.

Origin and Current Situation

The earliest archaeological evidence of reindeer domestication comes from the Sayan Mountains on the border of Siberia and Mongolia and dates from >2,000 years ago (31,32) (Figure 1). Reindeer domestication was not an isolated process, but in relation to other domesticated animals, including cattle (31,32), domestications provided an interface for host switching of *T. saginata*. A recent archaeoparasitologic study in the region of the Kan River, which runs northward from the Sayans Mountains, reported that human-infecting *Taenia* tapeworms might have established a wildlife-dependent cycle in Siberia before reindeer domestication (33). Three taeniid eggs were found in remains of a human buried 3,000–4,000 years ago, but animal bone findings at archaeological sites showed that diet during that period was based mainly on cervids other than reindeer (33). *T. saginata* is not known to have a life cycle involving wild cervids.

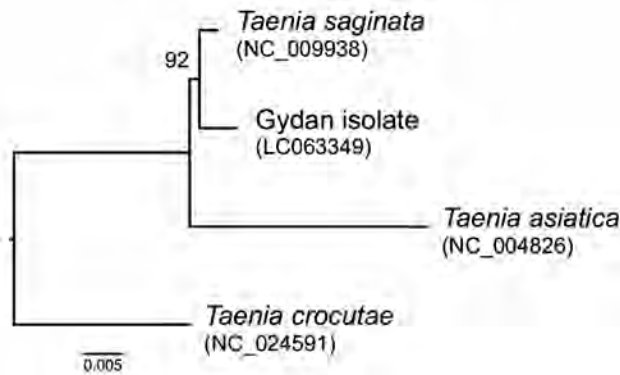


Figure 7. Maximum-likelihood tree of *Taenia saginata* tapeworm strains and *T. asiatica* tapeworms inferred from short fragments (426 nt) of the cytochrome c oxidase subunit 1 gene. The northern strain of *T. saginata* tapeworm is represented by the Gydan isolate from northern Siberia, Russia. *T. crocutae* tapeworm was used as an outgroup. Number along branch indicates a bootstrap percentage. GenBank accession numbers of original sequences are shown in parentheses. Scale bar indicates nucleotide substitutions per site.

Reindeer herding (and probably related parasites) spread widely across Siberia. Dominating cultures have later repressed old food habits. For example, in Yakutia, the Yakuts, who came relatively recently from the south, do not consume raw brain, but the Evenki, who are descendants of the first reindeer herders who migrated north and northeast from the region of Lake Baikal (32), still continue to locally maintain old dietary practices.

Genetic evidence indicates that reindeer were domesticated independently in Fennoscandia (northern Europe) (34). The indigenous reindeer-herding Sámi people do not eat raw reindeer tissues and have not done so in recent centuries (35,36). In Finland, for example, the traditional Sámi diet included reindeer brain in cooked brain cakes; only blood was occasionally consumed raw to provide health benefits (36). These findings indicate that there was no ecological niche for a brain-associated parasite in the western part of the reindeer husbandry area of Eurasia, or it became extinct a long time ago.

Today, YaNAO appears to be the only region to which the northern strain of *T. saginata* is endemic. Epidemiologic studies have shown that 10–25 cases are reported annually in YaNAO; virtually all cases are linked to raw reindeer brain consumption (37,38). Most of these cases were identified in the native population, which is deeply committed to traditions. Tapeworm carriers are typically nomadic reindeer herders.

Approximately 50,000–60,000 reindeer are slaughtered annually in YaNAO (37–39). Reindeer heads are not used for commercial food production or otherwise by industry. Thus, reindeer brains are not routinely inspected

for *T. saginata* cysticerci. According to the regional government of YaNAO, the reindeer population of the district is 730,000 animals, which is the largest herd in the world (39,40). More than 16,000 persons are involved in reindeer herding and migrate on the tundra. These persons have traditional nomadic lifestyles, food habits, and minimal access to healthcare. These facts, together with the long life span of the parasite, ensure that the northern strain of *T. saginata* will survive in this region for many years. Nevertheless, the modern world (globalization, oil drilling, and climate change) casts a dark shadow over the parasite life cycle, which is dependent on fragile traditional cultures of native populations in these regions.

Acknowledgments

We thank Marianna Flinckenberg-Gluschkoff for providing a photograph for publication and Derek Ho for language editing.

This study was supported by the Russian Federal Fundamental Scientific Research Programme for 2017–2019 (grant VI.51.1.4 to S.V.K.), the Grant-in-Aid for Scientific Research Program from the Japan Society for the Promotion of Science (grant 24406011 to A.I. and grant 26460503 to M.N.), and the Special Cooperation Fund for Promoting Science and Technology, Ministry of Education, Japan (to A.I.).

Dr. Konyaev is a veterinary parasitologist at the Institute of Systematics and Ecology of Animals, Siberian Branch of the Russian Academy of Sciences, Novosibirsk, Russia. His research interests focus on zoonotic helminthiases.

References

- Craig P, Ito A. Intestinal cestodes. *Curr Opin Infect Dis*. 2007;20:524–32. <http://dx.doi.org/10.1097/QCO.0b013e3282ef579e>
- Abuladze KI. Taeniata of animals and man and diseases caused by them. In: Skrjabin KI, editor. *Essentials of cestodology*, vol. IV. Jerusalem (Israel): Israel Program for Scientific Translations; 1970. p. 62–7.
- Fan PC. Taiwan *Taenia* and taeniasis. *Parasitol Today*. 1988;4:86–8. [http://dx.doi.org/10.1016/0169-4758\(88\)90204-9](http://dx.doi.org/10.1016/0169-4758(88)90204-9)
- Ito A, Putra MI, Subahar R, Sato MO, Okamoto M, Sako Y, et al. Dogs as alternative intermediate hosts of *Taenia solium* in Papua (Irian Jaya), Indonesia confirmed by highly specific ELISA and immunoblot using native and recombinant antigens and mitochondrial DNA analysis. *J Helminthol*. 2002;76:311–4. <http://dx.doi.org/10.1079/JOH2002128>
- Murrell KD, Dorny P, Flisser A, Geerts S, Kyvsgaard NC, McManus D, et al., editors. *WHO/FAO/OIE guidelines for the surveillance, prevention and control of taeniosis/cysticercosis*. Paris: World Health Organization; 2005.
- Krotov AI. Investigation of parasitic human and animal helminths in Sakhalin [in Russian]. *Med Parazitol (Mosk)*. 1954;23:368–9.
- Krotov AI. On the epidemiology of *Taeniarhynchus* infection [in Russian]. *Med Parazitol (Mosk)*. 1961;30:98–9.
- Missonova L. Reindeer husbandry and identity of the Uilta in Sakhalin (Soviet and post-Soviet periods) [in Russian]. *Acta Slavica Iaponica*. 2009;27:177–99.
- Darizhapov BB, Samarskiy SS. State report on the status of sanitary and epidemiological welfare of the population in the

- Sakhalin region in 2014 [in Russian]. Yuzhno-Sakhalinsk, Russia: Sakhalin regional office of the federal service for surveillance on consumer rights protection and human well being; 2015 [cited 2016 Nov 17]. http://www.65.rospotrebnadzor.ru/documents/ros/doclad/Shpil'Ko_VN_Helminths_in_the_population_of_the_river_Taz_basin [in Russian]. *Med Parazitol (Mosk)*. 1959;28:418–21.
11. Fedorov VG, Smirnova KS. Helminths of children in the Khanty-Mansiysk Autonomous Okrug [in Russian]. *Trudy Omskogo Meditsinskogo Instituta*. 1963;47:187–91.
 12. Zerchaninov LK, Klebanovskiy VA, Minakov LM, Troshkov VA. Helminth fauna of the population in the Nadym raion of the Yamalo-Nenets Okrug [in Russian]. In: Zerchaninov LK, Zubov NA, Klebanovskiy VA, editors. *Materials of a scientific conference on medical parasitology. Tyumen (USSR): Regional Printing House of the Tyumen Regional Executive Committee's Press Department; 1964. p. 92–5.*
 13. Shpil'ko VN. Some biohelminthoses of humans in Yamalo-Nenets Autonomous Okrug [dissertation] [in Russian]. Omsk (USSR): Omsk State Medical Institute; 1968.
 14. Klebanovskiy VA, Klimishin AA, Shpil'ko VN. Spreading of taeniarhynchosis in the Yamal peninsula [in Russian]. In: Kuzovlev AP, editor. *Regional questions of infection pathology [in Russian]. Tyumen (USSR): Ministry of Health of the Russian Soviet Federative Socialist Republic; 1974. p. 172–4.*
 15. Klebanovskiy VA, Smirnov PL, Klebanovskaya IA, Obgol'ts AA. Helminthiasis in population of Taymyr [in Russian]. In: Kornilova GV, editor. *Epidemiologic and prophylactic problems of nature-borne diseases in the Arctic. Omsk (USSR): Omskaya Pravda; 1977. p. 144–64.*
 16. Mozgovoy AA, Koval'chuk ES, Gosteev AK, Shakhmatova VI. Study of some population characteristics of *Taenia saginata* in western Siberia [in Russian]. *Proceedings of the Biological Institute of the Siberian Branch of the Academy of Sciences*. 1979;38:190–205.
 17. Kirichek VS, Belousov MN, Nikitin AS. New data on the epidemiology of taeniarhynchiasis in regions of the Far North in the USSR (based on observational data in the Yamal-Nenets Autonomous Okrug) [in Russian]. *Med Parazitol (Mosk)*. 1984;Nov–Dec:27–33.
 18. Slepchenko SM, Ivanov SN, Nikolaevich BA, Alekseevich TA, Sergeevich SV. Traditional living habits of the Taz Tundra population: a paleoparasitological study. *Korean J Parasitol*. 2016;54:617–23. <http://dx.doi.org/10.3347/kjp.2016.54.5.617>
 19. Safronov MG. Helminths in reindeer in the Tomponskiy and Lenekskiy Districts of the Yakut ASSR [in Russian]. *Proceedings the Yakut Scientific Research Institute of Agriculture*. 1960;3:103–6.
 20. Samoylova IY, Grigor'eva VI, Kornilova MV, Prugova EM, Kolesova EA, Budatsyrenova LB, et al., editors. *State report on the status of sanitary and epidemiological welfare of the population in the Sakha Republic (Yakutia) in 2012 [in Russian]. Yakutsk (Russia): Sakha Republic (Yakutia) Regional Office of the Federal Service for Surveillance on Consumer Rights Protection and Human Well Being; 2013 [cited 2016 Dec 20]. <http://14.rospotrebnadzor.ru/275>*
 21. Kirichek VS, Nikitin AS, Frolova AA, Iarotskii LS. Various features of the biology of a northern isolate of *Taeniarhynchus saginatus* Coeze, 1782 [in Russian]. *Med Parazitol (Mosk)*. 1986;Nov–Dec:37–9.
 22. Blažek K, Kirichek VS, Schramlová J. Pathology of experimental *Cysticercus bovis* infection in the reindeer (*Rangifer tarandus* Linné, 1758). *Folia Parasitol (Praha)*. 1986;33:39–44.
 23. Serdyukov, AM. On the species identity of taeniids of man in north of west Siberia [in Russian]. *Proceedings of the Biological Institute of the Siberian Branch of the Academy of Sciences*. 1979;38:206–20.
 24. Eom KS, Rim H-J. Morphologic descriptions of *Taenia asiatica* sp. n. *Korean J Parasitol*. 1993;31:1–6. <http://dx.doi.org/10.3347/kjp.1993.31.1.1>
 25. Fan PC, Lin CY, Chen CC, Chung WC. Morphological description of *Taenia saginata asiatica* (Cyclophyllidae: Taeniidae) from man in Asia. *J Helminthol*. 1995;69:299–303. <http://dx.doi.org/10.1017/S0022149X00014863>
 26. Knapp J, Nakao M, Yanagida T, Okamoto M, Saarma U, Lavikainen A, et al. Phylogenetic relationships within *Echinococcus* and *Taenia* tapeworms (Cestoda: Taeniidae): an inference from nuclear protein-coding genes. *Mol Phylogenet Evol*. 2011;61:628–38. <http://dx.doi.org/10.1016/j.ympev.2011.07.022>
 27. Tamura K, Stecher G, Peterson D, Filipiński A, Kumar S. MEGA6: Molecular Evolutionary Genetics Analysis Version 6.0. *Mol Biol Evol*. 2013;30:2725–9. <http://dx.doi.org/10.1093/molbev/mst197>
 28. Hoberg EP. Phylogeny of *Taenia*: species definitions and origins of human parasites. *Parasitol Int*. 2006;55(Suppl):S23–30. <http://dx.doi.org/10.1016/j.parint.2005.11.049>
 29. Hoberg EP, Alkire NL, de Queiroz A, Jones A. Out of Africa: origins of the *Taenia* tapeworms in humans. *Proc Biol Sci*. 2001;268:781–7. <http://dx.doi.org/10.1098/rspb.2000.1579>
 30. Yamane K, Suzuki Y, Tachi E, Li T, Chen X, Nakao M, et al. Recent hybridization between *Taenia asiatica* and *Taenia saginata*. *Parasitol Int*. 2012;61:351–5. <http://dx.doi.org/10.1016/j.parint.2012.01.005>
 31. Vitebsky P. *The reindeer people: living with animals and spirits in Siberia*. London: HarperCollins; 2006.
 32. Zgusta R. *The peoples of northeast Asia through time: precolonial ethnic and cultural processes along the coast between Hokkaido and the Bering Strait*. Leiden (the Netherlands): Brill; 2015.
 33. Slepchenko SM, Ivanov SN, Vybornov AV, Alekseevich TA, Sergeevich SV, Lysenko DN, et al. *Taenia* sp. in human burial from Kan River, East Siberia. *Mem Inst Oswaldo Cruz*. 2017;112:387–90. <http://dx.doi.org/10.1590/0074-02760160442>
 34. Røed KH, Flagstad O, Nieminen M, Holand O, Dwyer MJ, Røvn N, et al. Genetic analyses reveal independent domestication origins of Eurasian reindeer. *Proc Biol Sci*. 2008;275:1849–55. <http://dx.doi.org/10.1098/rspb.2008.0332>
 35. von Linné C. *Lapponian expedition in 1732 [in Finnish]. Hämeenlinna (Finland): Karisto; 1969.*
 36. Itkonen TI. *Laplanders in Finland until the year 1945 [in Finnish]. Part 1. Porvoo (Finland). Helsinki: WSOY; 1948.*
 37. Yamalo-Nenets Autonomous Okrug Regional Office of the Federal Service for Surveillance on Consumer Rights Protection and Human Well Being. *State report on the status of sanitary and epidemiological welfare of the population in the Yamalo-Nenets Autonomous Okrug in 2012 [in Russian]. Salekhard (Russia); 2013 [cited 2016 Dec 21]. <http://89.rospotrebnadzor.ru/s/89/files/documents/regional/95102.zip>*
 38. Yamalo-Nenets Autonomous Okrug Regional Office of the Federal Service for Surveillance on Consumer Rights Protection and Human Well Being. *State report on the status of sanitary and epidemiological welfare of the population in the Yamalo-Nenets Autonomous Okrug in 2014 [in Russian]. Salekhard (Russia); 2015 [cited 2016 Dec 21]. <http://89.rospotrebnadzor.ru/s/89/files/documents/regional/128829.pdf>*
 39. Gertyck O. Yamal trims back reindeer cull to 100,000 as herders fear future of nomadic lifestyle. *Siberian Times*, October 7, 2016 [cited 2016 Dec 21]. <http://siberiantimes.com/other/others/features/f0260-yamal-trims-back-reindeer-cull-to-100000-as-herders-fear-future-of-nomadic-lifestyle/?nf=Features>
 40. Official Website of the Government of YaNAO. *Successful reindeer calving in Yamal: the herd has increased by 110 thousand*, June 17, 2015 [cited 2016 Dec 21]. http://правительство.янао.рф/news/lenta/agroindustrial/detail/82484/?sphrase_id=136367

Address for correspondence: Antti Lavikainen, Department of Bacteriology and Immunology, Faculty of Medicine, University of Helsinki, PO Box 21, Haartmaninkatu 3, FI-00014, Helsinki, Finland; email: antti.lavikainen@helsinki.fi

Outbreak of Yellow Fever among Nonhuman Primates, Espírito Santo, Brazil, 2017

Natália Coelho Couto de Azevedo Fernandes, Mariana Sequetin Cunha, Juliana Mariotti Guerra, Rodrigo Albergaria Réssio, Cinthya dos Santos Cirqueira, Sílvia D'Andretta Iglezias, Júlia de Carvalho, Emerson L.L. Araujo, José Luiz Catão-Dias, Josué Díaz-Delgado

In January 2017, a yellow fever outbreak occurred in Espírito Santo, Brazil, where human immunization coverage is low. Histologic, immunohistologic, and PCR examinations were performed for 22 deceased nonhuman New World primates; typical yellow fever features were found in 21. Diagnosis in nonhuman primates prompted early public health response.

Yellow fever is a reemerging, zoonotic, noncontagious viral hemorrhagic disease endemic to Africa and South America; outbreaks occasionally occur among human and nonhuman primates (1). It is caused by the yellow fever virus (family *Flaviviridae*, genus *Flavivirus*), which is carried by the vector mosquitoes *Haemagogus* and *Sabethes* (sylvatic cycle) and *Aedes aegypti* (urban cycle) (2).

Presumptive first reports of infection with yellow fever virus occurred ≈500 years ago (San Domingo, 1498; western Africa, 1585), and the first epidemics were recorded in the 17th century (Barbados, Cuba, and Mexico) (3–5). By the 18th century, epidemics were already deemed a threat for public health in the Old and New Worlds; transoceanic migrations played a major role in virus spread (3,6). After entering Brazil by the coast in the 17th century, the virus was gradually displaced to northwestern and midwestern areas. Since the 19th century, yellow fever outbreaks occurred in many cities in Brazil, until 1942, when the urban cycle was eradicated. By the late 1900s through the first decade of the 21st century, beginning in 1997, intense virus circulation extended from the Amazon region to the contiguous states of Goiás and Mato Grosso do Sul (central Brazil). During 2008–2009, a new outbreak was registered and the virus reached southern and southeast regions of the country (1). In 2017, an epizootic occurred in Espírito

Santo state, Brazil, where yellow fever virus has not circulated in the past 50 years and human vaccination coverage is low. We performed diagnostics on a small cohort of New World nonhuman primates in this state.

The Study

In January 2017, an outbreak involving deaths of humans and New World nonhuman primates (hereafter nonhuman primates [NHPs]) spread from Minas Gerais state to Espírito Santo state. Espírito Santo is located in a forest along the Atlantic coast of southeastern Brazil and borders Minas Gerais, Rio de Janeiro, and Bahia states. The virus advanced through Atlantic forest fragments (7), areas previously considered not at risk for yellow fever virus transmission. We performed histopathologic analyses, immunohistochemical analyses (IHC), and PCRs on 22 NHPs that died early in the Espírito Santo outbreak (Figure 1).

Veterinarians trained by health authorities performed standardized necropsies under the yellow fever national surveillance program (8). Of 22 NHPs found dead, 2 were howler monkeys (*Alouatta* spp.) and 20 were NHPs not further identified. Liver, spleen, kidney, heart, and lung samples were collected and fixed in 10% neutral buffered formalin and processed for routine histopathology and in liquid nitrogen for RNA real-time reverse transcription quantitative PCR.

Histologic examination indicated the following for all animals: zonal bridging (largely midzonal and centrilobular) or massive liver necrosis with Councilman bodies, varying degrees of macrovacuolar and microvacuolar steatosis, and pleocellular (mainly lymphohistiocytic) inflammatory infiltrates, accompanied by hemorrhage and hemosiderosis (Figure 2, panels A, B; online Technical Appendix Table 1, <https://wwwnc.cdc.gov/EID/article/23/12/17-0685-Techapp1.pdf>). Additional liver lesions were microabscesses (6), endothelial necrosis (5), oval cell hyperplasia (2), massive macrovacuolar steatosis with rare midzonal to random single-cell necrosis (1) (Figure 2, panel C), and fibrin microthrombi in sinusoids (1). Other consistent findings were splenic lymphoid depletion and follicular necrosis/lymphocytolysis (19), acute renal tubular necrosis with protein casts and hemoglobin casts (6), and multisystemic hemorrhage, more prominent in lungs (6).

For IHC, we tested liver tissue sections with an in-house primary polyclonal anti-yellow fever virus antibody (1:40,000, derived from hyperimmune mouse serum); signal amplification was achieved with a HiDef Detection

Author affiliations: Instituto Adolfo Lutz, São Paulo, Brazil (N.C.C.A. Fernandes, M.S. Cunha, J.M. Guerra, R.A. Réssio, C.S. Cirqueira, S. D'Andretta Iglezias, J. de Carvalho, J. Díaz-Delgado); Ministério da Saúde, Brasília, Brazil (E.L.L. Araujo); Universidade de São Paulo, São Paulo (J.L. Catão-Dias, J. Díaz-Delgado)

DOI: <https://doi.org/10.3201/eid2312.170685>

HRP Polymer System (Cell Marque/Sigma-Aldrich, Rocklin, CA, USA) and visualization with diaminobenzidine (D-5637; Sigma-Aldrich, St. Louis, MO, USA). We included human and nonhuman primate positive and negative control tissues with omitted first-layer antibody. Tissue from all animals showed positive granular cytoplasmic hepatocyte immunolabeling, with varying percentages of involvement and immunolabeling intensity (online Technical Appendix Table 2). Immunopositivity was more intense in degenerating and remaining hepatocytes, most often encompassing periportal cord segments and terminal plates (Figure 2, panel D). Necrotic hepatocytes consistently lacked immunoreactivity.

For PCRs, we extracted viral RNA from whole blood ($n = 6$); serum ($n = 1$); and liver, kidney, and spleen ($n = 4$) tissue samples by using a QIAamp RNA Blood Mini Kit (QIAGEN, Valencia, CA, USA), following the manufacturer's instructions. We amplified virus fragment by using the protocol designed by Drosten et al. (9), which targets the 5' noncoding region (112-bp long) of the genome. All samples were positive; cycle thresholds were 11–26 (cutoff value 38; online Technical Appendix Table 2).

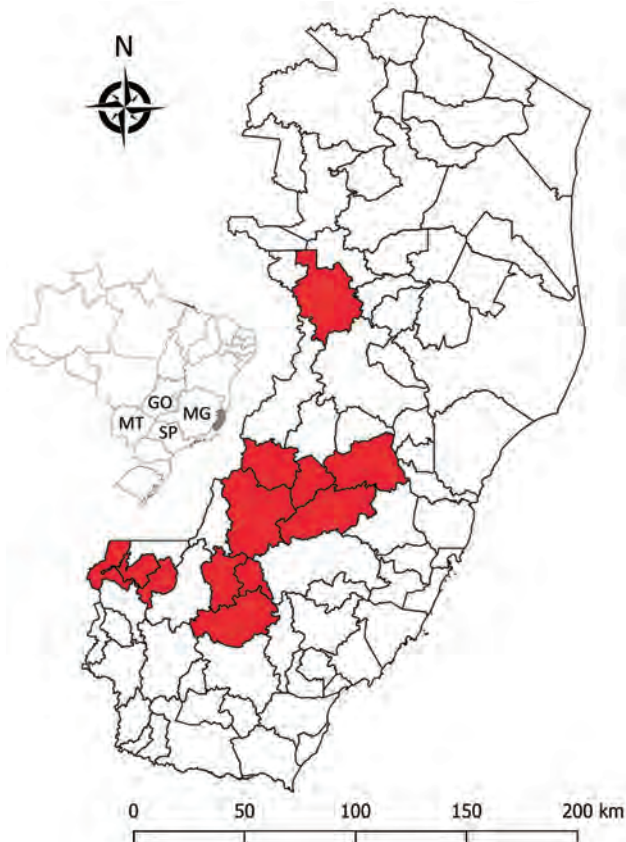


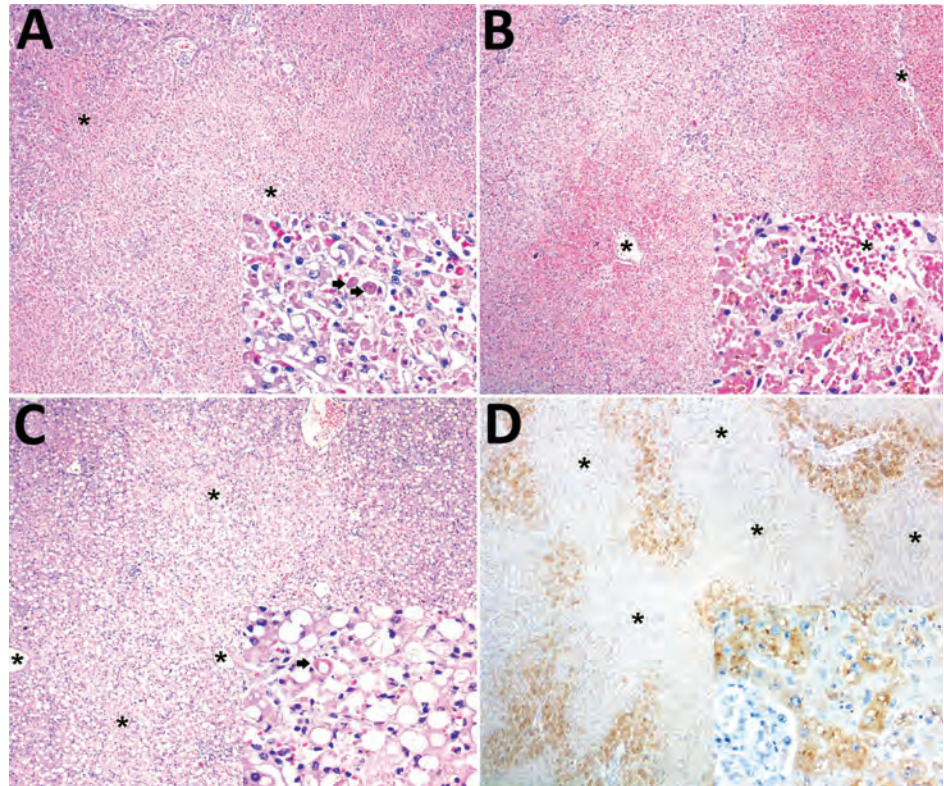
Figure 1. Locations (red shading) of nonhuman primates that died of yellow fever, Espirito Santo, Brazil, January 2017. Inset shows location of Espirito Santo (light gray shading) and 4 other states within Brazil. GO, Goiás; MG, Minas Gerais; MT, Mato Grosso do Sul; SP, São Paulo.

Brazil has an established yellow fever national surveillance program (e.g., postmortem NHP studies, vector analyses) focused on early detection of virus circulation, which enables prompt implementation of vaccination and vector control (8). Yellow fever diagnosis under this program is achieved by histopathologic, IHC, and PCR results from liver samples of NHPs, performed by reference laboratories (e.g., Adolfo Lutz Institute, São Paulo, Brazil). A multidisciplinary work team and combination of laboratory techniques are essential for a quick, high-quality response that initiates field actions (e.g., vaccination, vector control).

We observed classic histopathologic commonalities with yellow fever–associated disease in humans (midzonal lytic necrosis, apoptotic bodies, steatosis, and scarce paucicellular inflammation) (10,11). The severity and extent of these lesions probably accounted for severe hepatic failure and death of the animals. The knowledge of naturally occurring yellow fever–associated disease in NHPs gained since the early 1900s is fragmentary (12) and mainly limited to *Alouatta* spp. and *Callithrix* spp. NHPs (6,11). *Alouatta* spp. monkeys are very susceptible to yellow fever; fatal disease has supported a sentinel role for yellow fever virus circulation since the 1930s (11). Hepatic lesions of several NHP species, experimentally or naturally infected, are similar to those in humans (11). In this study, 1 animal had atypical liver histopathologic features, characterized by massive steatosis with rare midzonal to random single-cell necrosis/apoptosis. Additional liver findings were multifocal microabscesses, probably the result of acute bacterial ascending (intestinal) infection or concomitant septicemia; endothelial necrosis; and attempted hepatic regeneration as suggested by oval cell hyperplasia. The pathologic signature of yellow fever–associated disease in NHPs (≈ 150 species) is not fully resolved. Ongoing comparisons between yellow fever–associated disease in humans and NHPs may help elucidate convergent and divergent pathogenetic mechanisms and characterize typical and atypical features, thus delineating the pathologic signature in NHPs.

Before the advent of PCR, the method of choice for diagnosing yellow fever was IHC, which remains a highly reliable diagnostic tool (13), even in the presence of some autolysis (14). In our study and the ongoing outbreak, histopathologic analyses and IHC were vital for successful diagnosis, enabling detection of atypical presentation, paralleling the sensitivity and specificity of PCRs. In a public health context, IHC will greatly aid in yellow fever diagnosis when molecular analysis is not an option, as occurred for 11 of 22 cases in this study. Although RNA extraction from paraffin-embedded tissues is possible, it is not extensively applied and the degradation of RNA may lead to false-negative results.

Figure 2. Histopathologic and immunohistochemical findings in the livers of neotropical nonhuman primates that died of yellow fever, Espirito Santo, Brazil, January 2017. Asterisks (*) indicate centrilobular veins. A) Midzonal and centrilobular bridging hepatocellular lytic necrosis. Original magnification $\times 40$; hematoxylin and eosin (H&E) staining. Inset shows lytic hepatocellular necrosis with multiple Councilman-Rocha Lima (apoptotic) bodies (arrows). Original magnification $\times 400$; H&E staining. B) Massive (diffuse) hepatocellular lytic necrosis with severe centrilobular and midzonal hemorrhage. Original magnification $\times 40$; H&E staining. Inset shows prominent hepatocellular necrosis and dropout, and erythrocytes replace the hepatic cords (there is some artifactual formalin pigment [acid hematin] in necrotic hepatocytes). Original magnification $\times 400$; H&E staining. C) Massive macrovacuolar steatosis. Inset shows massive macrovacuolar steatosis mingled with single-cell hepatocellular necrosis (arrow). Original magnification $\times 400$; H&E staining. D) Positive immunolabeling confined to remaining periportal hepatocytes and terminal plate. Original magnification $\times 40$; immunohistochemical staining for yellow fever virus. Inset shows positive granular, cytoplasmic immunolabeling for yellow fever virus antigen in periportal hepatocytes and terminal plate. Original magnification $\times 400$; immunohistochemical staining for yellow fever virus.



Conclusions

During January–July 2017, yellow fever was diagnosed for 150 of 1,000 tested NHPs (15% occurrence) from southern states of Brazil. NHPs were effective yellow fever sentinels and enabled rapid government response (8,15). Although the Espirito Santo outbreak had damaging socioeconomic and environmental consequences, adequate case conduction and diagnosis may have prevented further human deaths and diminished disease expansion. In contrast, the effects of yellow fever virus spreading among NHPs in the Atlantic forest are expected to be devastating.

Acknowledgments

We thank Sônia Maria Pereira de Oliveira, Cristina Kanamura, Silvana de Mello Pereira da Silva, Rosângela Araújo, Sandra Lúcia Diogo, Seura de Almeida, Mariane Ingara, Thais de Souza Lima, Cleusa de Jesus, Magda Montalvão, Thalita Fabiana do Nascimento, Jéssica Astrath Petruzzi, and Paloma Martins do Nascimento for help with sample processing. The staff from ‘Núcleo de Gerenciamento de Amostras Biológicas’ at the Adolfo Lutz Institute and Ormi Francisca Dobrovosky are also greatly acknowledged for logistics help and sample submission, respectively.

J.D.D. received a postdoctoral fellowship by the São Paulo Research Foundation (grant no. 2017/02223-8). He greatly appreciates the authorization to conduct this work under PR no. 05/2012.

Dr. Fernandes is the leading veterinary pathologist responsible for yellow fever diagnosis in NHPs at the Adolfo Lutz Institute. Her research focuses on wildlife pathology and arbovirus disease mechanisms, specifically in comparative pathology of human and NHP yellow fever–associated disease, and seeks to characterize species-specific pathogenic mechanisms and factors modulating yellow fever–endemic cycles and triggering outbreaks among humans and NHPs in the Americas.

References

1. Monath TP, Vasconcelos PF. Yellow fever. *J Clin Virol*. 2015;64:160–73. <http://dx.doi.org/10.1016/j.jcv.2014.08.030>
2. Barrett AD, Monath TP. Epidemiology and ecology of yellow fever virus. *Adv Virus Res*. 2003;61:291–315. [http://dx.doi.org/10.1016/S0065-3527\(03\)61007-9](http://dx.doi.org/10.1016/S0065-3527(03)61007-9)
3. Cornet JP, Huard M, Camicas JL, Hervé JP, Germain M. Experimental transmission of the yellow fever virus by the tick *Amblyomma variegatum* (F.) [in French]. *Bull Soc Pathol Exot Filiales*. 1982;75:136–40.

4. de Souza RP, Foster PG, Sallum MAM, Coimbra TL, Maeda AY, Silveira VR, et al. Detection of a new yellow fever virus lineage within the South American genotype I in Brazil. *J Med Virol*. 2010;82:175–85. <http://dx.doi.org/10.1002/jmv.21606>
5. Gardner CL, Ryman KD. Yellow fever: a reemerging threat. *Clin Lab Med*. 2010;30:237–60. <http://dx.doi.org/10.1016/j.cll.2010.01.001>
6. Leal SG, Romano APM, Monteiro RV, Melo CBD, Vasconcelos PFDC, Castro MBD. Frequency of histopathological changes in Howler monkeys (*Alouatta* sp.) naturally infected with yellow fever virus in Brazil. *Rev Soc Bras Med Trop*. 2016;49:29–33. <http://dx.doi.org/10.1590/0037-8682-0363-2015>
7. World Health Organization. Yellow fever—Brazil (4 April 2017). Disease outbreak news [cited 2017 Apr 4]. <http://www.who.int/csr/don/04-april-2017-yellow-fever-brazil/en/>
8. Ministério da Saúde do Brasil, Secretaria de Vigilância em Saúde, Departamento de Vigilância das Doenças Transmissíveis. Guia de vigilância de epizootias em primatas não humanos e entomologia aplicada à vigilância da febre amarela. 2nd ed. Brasília (Brazil); 2017.
9. Drosten C, Götting S, Schilling S, Asper M, Panning M, Schmitz H, et al. Rapid detection and quantification of RNA of Ebola and Marburg viruses, Lassa virus, Crimean-Congo hemorrhagic fever virus, Rift Valley fever virus, dengue virus, and yellow fever virus by real-time reverse transcription-PCR. *J Clin Microbiol*. 2002;40:2323–30. <http://dx.doi.org/10.1128/JCM.40.7.2323-2330.2002>
10. Vieira WT, Gayotto LC, de Lima CP, de Brito T. Histopathology of the human liver in yellow fever with special emphasis on the diagnostic role of the Councilman body. *Histopathology*. 1983;7:195–208. <http://dx.doi.org/10.1111/j.1365-2559.1983.tb02235.x>
11. Strode GK. Yellow fever. New York: McGraw-Hill; 1951.
12. Martins-Romano AP. Febre Amarela. In: Cubas ZS, Silva JCR, Catão-Dias JL, editors. *Tratado de Animais Selvagens*. São Paulo (Brazil): Editora Roca; 2014. p. 1263–81.
13. Ezyaguire EJ, Walker DH, Zaki SR. Immunohistology of infectious diseases. In: Dabbs DJ, editor. *Diagnostic immunohistochemistry*. Philadelphia: Saunders, Elsevier Health Sciences; 2013. p. 58–82.
14. Hall WC, Crowell TP, Watts DM, Barros VL, Kruger H, Pinheiro F, et al. Demonstration of yellow fever and dengue antigens in formalin-fixed paraffin-embedded human liver by immunohistochemical analysis. *Am J Trop Med Hyg*. 1991;45:408–17. <http://dx.doi.org/10.4269/ajtmh.1991.45.408>
15. Almeida MA, Cardoso JC, Dos Santos E, da Fonseca DF, Cruz LL, Faraco FJ, et al. Surveillance for yellow fever virus in non-human primates in southern Brazil, 2001–2011: a tool for prioritizing human populations for vaccination. *PLoS Negl Trop Dis*. 2014;8:e2741. <http://dx.doi.org/10.1371/journal.pntd.0002741>

Address for correspondence: Natália Coelho Couto de Azevedo Fernandes, Instituto Adolfo Lutz, Centro de Patologia, Av. Dr. Arnaldo, 351–7º, Andar, Sala 706, Pacaembú São Paulo 01246-000, Brazil; email: nccaferlandes@yahoo.com.br

Now on Exhibit David J. Sencer CDC Museum

EBOLA

OPEN THROUGH MAY 25, 2018

People + Public Health + Political Will

EBOLA: People + Public Health + Political Will is an investigation of the historic 2014–16 Ebola Fever Virus epidemic in West Africa, the United States, and around the world. As the crisis unfolded in Guinea, Liberia, and Sierra Leone in 2014, it evolved into both a health and humanitarian crisis. When it became clear that Ebola could potentially spread exponentially, threatening global health security, there was a coordinated, massive response.

Hours

Monday: 9 a.m.–5 p.m.
 Tuesday: 9 a.m.–5 p.m.
 Wednesday: 9 a.m.–5 p.m.
 Thursday: 9 a.m.–7 p.m.
 Friday: 9 a.m.–5 p.m.
 Closed weekends and federal holidays

Location

1600 Clifton Road NE
 Atlanta, GA 30329
 Phone 404-639-0830
 Admission and parking free
 Government-issued photo ID required
 for adults over the age of 18

Free admission

Mycobacterium ulcerans DNA in Bandicoot Excreta in Buruli Ulcer–Endemic Area, Northern Queensland, Australia

Katharina Röltgen, Gerd Pluschke,
Paul D.R. Johnson, Janet Fyfe

To identify potential reservoirs/vectors of *Mycobacterium ulcerans* in northern Queensland, Australia, we analyzed environmental samples collected from the Daintree River catchment area, to which Buruli ulcer is endemic, and adjacent coastal lowlands by species-specific PCR. We detected *M. ulcerans* DNA in soil, mosquitoes, and excreta of bandicoots, which are small terrestrial marsupials.

Mycobacterium ulcerans infections, which cause the chronic, necrotizing skin disease Buruli ulcer (BU), occur mainly in focalized areas in West Africa but have also been reported in Australia, Asia, and the Americas (1). Much of the pathology of this debilitating disease is caused by mycolactone, a macrolide toxin (2) unique for members of the species *M. ulcerans*, which are also referred to as mycolactone-producing mycobacteria (3).

Although the definite route of infection with *M. ulcerans* remains obscure, in Victoria, Australia, small arboreal marsupials (possums) have been implicated as reservoirs of the pathogen, and mosquitoes have been implicated as vectors of the pathogen (4,5). In a second BU-endemic area of Australia, in Far North Queensland (6), a similar animal reservoir has not been identified. In this region, outbreaks of BU occur in waves, separated by several years, and are believed to be associated with environmental changes caused by heavy rainfall.

The major region in Far North Queensland to which BU is endemic is a rim of valleys and lowlands surrounding the Dagmar Range and extending from Daintree and Forest Creek in the northern region to Mossman in the southern region (6). In this area, a BU outbreak with 64 reported cases occurred in 2011 after the exceptionally long and wet

rainy season during 2010–2011, which led to flooding of the Daintree River basin (7). An additional 23 cases were identified in 2012, but numbers subsequently reported have been sporadic.

Although proximity to stagnant water bodies and hydromorphologic alterations are well-established risk factors for emergence of *M. ulcerans* infection foci (8), definite ecologic factors leading to focal emergence of BU in humans have not been determined. The aim of this study was to identify potential reservoirs and vectors of *M. ulcerans* in the BU-endemic area of Far North Queensland by analyzing environmental samples for the presence of species-specific DNA sequences.

The Study

We collected 102 environmental samples (55 from soil/mud/vegetation, 35 from insects or small insect pools, and 12 from animal excreta) in September 2013 from different locations within the Daintree River basin, in which BU cases were reported during the outbreak in 2011. Global positioning system coordinates were recorded for all sampling locations (Figure 1). Specimens were collected in sterile plastic containers and shipped to the Victorian Infectious Disease Reference Laboratory (Melbourne, Victoria, Australia) for PCR analysis.

We extracted DNA by using the FastPrep Instrument (MP Biomedicals, Solon, OH, USA) as described (4). We used the FastDNA Kit (MP Biomedicals) for insect samples and the FastDNA Spin Kit (MP Biomedicals) for soil, mud, vegetation, and feces samples. We analyzed DNA extracts by using semiquantitative real-time PCRs optimized for detection of *M. ulcerans* in environmental samples (9). We first screened all extracted DNA samples for *M. ulcerans* insertion sequence element IS2404. Subsequently, we analyzed IS2404-positive samples in a second real-time PCR to detect 2 additional regions in the genome of *M. ulcerans*: IS2606 and a sequence encoding the ketoreductase B domain of the mycolactone polyketide synthase genes.

Of the 102 samples, 5 (1 soil specimen, 2 bandicoot [*Isodon macrourus*] feces samples, 1 sample of an individual mosquito, and 1 pool of 2 mosquitoes) were positive for IS2404. Although 3 of the 5 specimens did not contain sufficient amounts of DNA to identify IS2606 and the ketoreductase B domain of the mycolactone polyketide

Author affiliations: Swiss Tropical and Public Health Institute, Basel, Switzerland (K. Röltgen, G. Pluschke); University of Basel, Basel (K. Röltgen, G. Pluschke); Austin Health, Heidelberg, Victoria, Australia (P.D.R. Johnson); University of Melbourne, Parkville, Victoria, Australia (P.D.R. Johnson); World Health Organization Collaborating Centre for *Mycobacterium ulcerans*, Melbourne, Victoria, Australia (P.D.R. Johnson, J. Fyfe); Doherty Institute, Melbourne (J. Fyfe)

DOI: <https://doi.org/10.3201/eid2312.170780>



Figure 1. Sample collection for detection of *Mycobacterium ulcerans* DNA in Buruli ulcer–endemic area, northern Queensland, Australia. Environmental samples were collected in the Daintree River basin during September (yellow) and October (green) 2013. Red indicates locations where Bandicoot feces and mosquito pool samples with positive results by real-time PCR for all 3 *M. ulcerans* targets were collected. Inset shows specimens from bandicoots and mosquitoes. Map created by using Google Earth (<https://www.google.com/earth/>).

synthase genes, as indicated by the high cycle threshold (C_t) values for multicopy IS2404 (Table), these markers were detectable in the other 2 samples (bandicoot feces and the pool of 2 mosquitoes) (Figure 1). The IS2404–positive soil sample and the 2 bandicoot feces specimens were collected at the same location (Figure 1), close to a small pond (Figure 2, panel A), and 2 positive mosquito samples were collected at Wonga Beach (Figure 1).

As reported (9), analysis of difference in real-time PCR cycle thresholds between IS2606 and IS2404 (ΔC_t [IS2606 – IS2404]) enables differentiation between strains of *M. ulcerans* known to cause BU in humans and other mycolactone-producing mycobacteria strains that contain IS2404 but have fewer copy numbers of IS2606 and are not known to cause disease in endotherms. Thus, DNA in bandicoot feces could be attributed to the *M. ulcerans* genotype known to cause BU (Table). Conversely, the mosquito pool contained DNA of a closely related *M. ulcerans* subspecies that had a low copy number for IS2606 (Table), which is usually not associated with disease in endotherms.

The location at which the bandicoot specimen containing *M. ulcerans* DNA was collected was situated in a nature refuge. In October 2013, we performed a follow-up environmental study that focused on environmental samples, predominantly animal excreta, collected in this refuge. Of 18 soil/mud/vegetation specimens, 12 insects/insect pools, and 74 animal excreta samples collected, only 1 sample, a bandicoot feces specimen found at almost the same location as the *M. ulcerans*–positive bandicoot feces specimens collected during the first sampling (Figure 1), was also positive for all *M. ulcerans* DNA markers tested (Table).

Conclusions

Motivated by increased evidence for the role of *M. ulcerans*–infected possums in the ecology of human BU in southeastern Australia (4,5), we searched for a similar animal reservoir of *M. ulcerans* in a BU-endemic area of northern Queensland. Detection of *M. ulcerans* DNA in bandicoot feces at 2 sampling time points separated by 4 weeks suggests that small mammals might be a potential

Table. Molecular genetic analysis of environmental samples for *Mycobacterium ulcerans* DNA in Buruli ulcer–endemic area, northern Queensland, Australia*

Sample	Real-time PCR analysis			
	IS2404	IS2606	IS2606–IS2404	KR
Bandicoot feces 1†	37.3	ND	ND	ND
Bandicoot feces 2†	27.8	29.1	1.3	28.9
Soil	36.3	ND	ND	ND
Mosquito	39.2	ND	ND	ND
Mosquito pool	31.0	38.6	7.6	31.9
Bandicoot feces‡	31.4	33.9	2.5	33.9

*Values are mean cycle thresholds of duplicate tests. IS, insertion sequence; KR, ketoreductase B domain of mycolactone polyketide synthase genes; ND, not detected.

†Collected in September 2013.

‡Collected in October 2013.

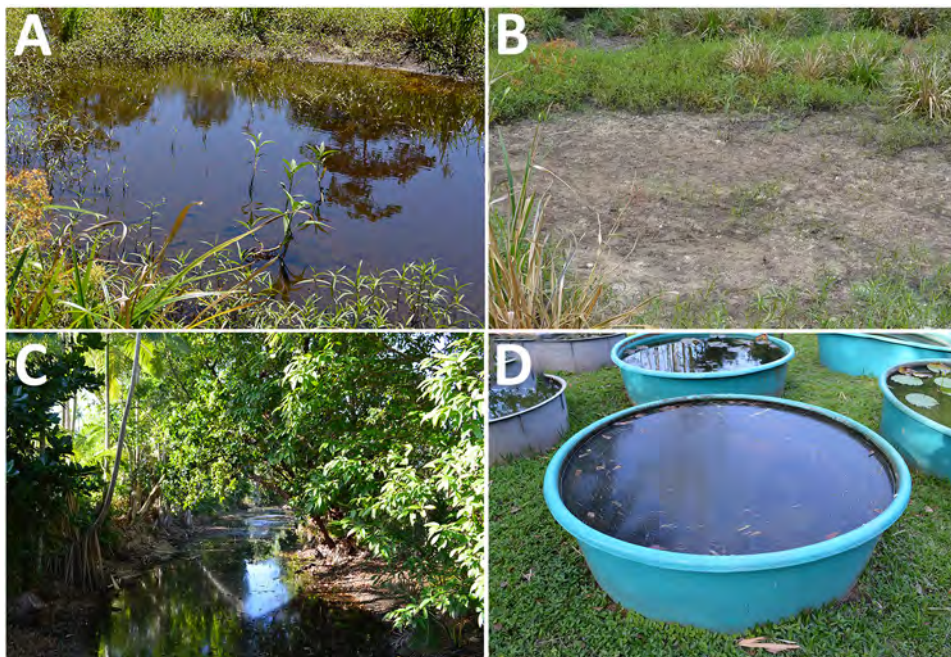


Figure 2. Sample locations for detection of *Mycobacterium ulcerans* DNA in Buruli ulcer-endemic area, northern Queensland, Australia. A) Pond where IS2404-positive soil sample was collected at first sampling time in September 2013; B) same location dried out at the end of the dry season in October. C, D) Other water bodies suspected to be linked to *M. ulcerans* infections, such as creeks (C) or water surfaces near houses (D), showed negative results for IS2404. IS, insertion sequence.

reservoir for this pathogen. Our data provide a basis for future investigations, which should include a survey of the local animal population for lesions of BU. Similar studies have not identified a mammalian animal reservoir in BU-endemic regions of West Africa (10). Therefore, investigations should be conducted to determine whether at least some marsupial species are more susceptible to *M. ulcerans* infection than other mammals.

In Far North Queensland, the Daintree River obtains its waters from the mountainous rainforest region northwest of the small town of Mossman and flows into the sea at Cape Tribulation. The wet season is November/December–April, and the dry season is May–October/November. We encountered different environmental conditions at the 2 sampling time points. In September, water bodies, including creeks, small lakes, and swamps, were filled with water (Figure 2, panel A). However, water levels were comparatively low at the end of the dry season in October; some water bodies had even dried up (Figure 2, panel B). Samples from other water bodies, such as creeks (Figure 2, panel C) or biotopes near houses (Figure 2, panel D) in which the presence of *M. ulcerans* was suspected, all showed negative results for IS2404.

Because outbreaks of BU in Far North Queensland were historically related to heavy rainfalls and flooding, future studies in this region should be performed during or shortly after the rainy season. Although mosquitoes seem to be involved in the ecology of BU in Victoria (5,11,12), the mosquito sample positive for *M. ulcerans* in this study did not have a bacterial genotype that is known to commonly cause disease in endotherms.

Acknowledgments

We thank Hendrik John Weimar, Barbara Maslen, and Allen Sheather for facilitating collection of environmental samples and Samuel Yaw Aboagye for assisting with testing of collected samples.

Dr. Röltgen is a scientist at the Swiss Tropical and Public Health Institute, Basel, Switzerland. Her research interests are molecular and seroepidemiologic aspects of *M. ulcerans* infection and development of point-of-care diagnostics for Buruli ulcer.

References

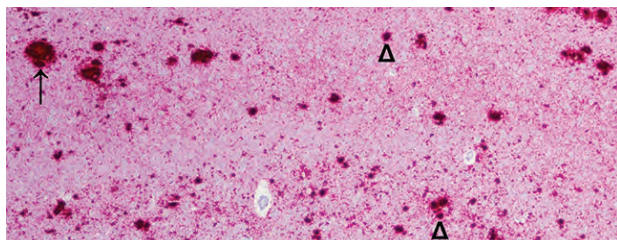
- Röltgen K, Pluschke G. Epidemiology and disease burden of Buruli ulcer: a review. *Research and Reports in Tropical Medicine*. 2015;2015:59–73.
- Hong H, Coutanceau E, Leclerc M, Caleechurn L, Leadlay PF, Demangel C. Mycolactone diffuses from *Mycobacterium ulcerans*-infected tissues and targets mononuclear cells in peripheral blood and lymphoid organs. *PLoS Negl Trop Dis*. 2008;2:e325. <http://dx.doi.org/10.1371/journal.pntd.0000325>
- Pidot SJ, Asiedu K, Käser M, Fyfe JA, Stinear TP. *Mycobacterium ulcerans* and other mycolactone-producing mycobacteria should be considered a single species. *PLoS Negl Trop Dis*. 2010;4:e663. <http://dx.doi.org/10.1371/journal.pntd.0000663>
- Fyfe JA, Lavender CJ, Handasyde KA, Legione AR, O'Brien CR, Stinear TP, et al. A major role for mammals in the ecology of *Mycobacterium ulcerans*. *PLoS Negl Trop Dis*. 2010;4:e791. <http://dx.doi.org/10.1371/journal.pntd.0000791>
- Johnson PD, Lavender CJ. Correlation between Buruli ulcer and vector-borne notifiable diseases, Victoria, Australia. *Emerg Infect Dis*. 2009;15:614–5. <http://dx.doi.org/10.3201/eid1504.081162>
- Steffen CM, Smith M, McBride WJ. *Mycobacterium ulcerans* infection in North Queensland: the 'Daintree ulcer'. *ANZ J Surg*. 2010;80:732–6. <http://dx.doi.org/10.1111/j.1445-2197.2010.05338.x>

7. Steffen CM, Freeborn H. *Mycobacterium ulcerans* in the Daintree 2009–2015 and the mini-epidemic of 2011. ANZ J Surg. 2016. <http://dx.doi.org/10.1111/ans.13817>
8. Merritt RW, Walker ED, Small PL, Wallace JR, Johnson PD, Benbow ME, et al. Ecology and transmission of Buruli ulcer disease: a systematic review. PLoS Negl Trop Dis. 2010;4:e911. <http://dx.doi.org/10.1371/journal.pntd.0000911>
9. Fyfe JA, Lavender CJ, Johnson PD, Globan M, Sievers A, Azuolas J, et al. Development and application of two multiplex real-time PCR assays for the detection of *Mycobacterium ulcerans* in clinical and environmental samples. Appl Environ Microbiol. 2007;73:4733–40. <http://dx.doi.org/10.1128/AEM.02971-06>
10. Röltgen K, Pluschke G. *Mycobacterium ulcerans* disease (Buruli ulcer): potential reservoirs and vectors. Current Clinical Microbiology Reports. 2015;2:35–43. <http://dx.doi.org/10.1007/s40588-015-0013-3>
11. Johnson PD, Azuolas J, Lavender CJ, Wishart E, Stinear TP, Hayman JA, et al. *Mycobacterium ulcerans* in mosquitoes captured during outbreak of Buruli ulcer, southeastern Australia. Emerg Infect Dis. 2007;13:1653–60. <http://dx.doi.org/10.3201/eid1311.061369>
12. Lavender CJ, Fyfe JA, Azuolas J, Brown K, Evans RN, Ray LR, et al. Risk of Buruli ulcer and detection of *Mycobacterium ulcerans* in mosquitoes in southeastern Australia. PLoS Negl Trop Dis. 2011;5:e1305. <http://dx.doi.org/10.1371/journal.pntd.0001305>

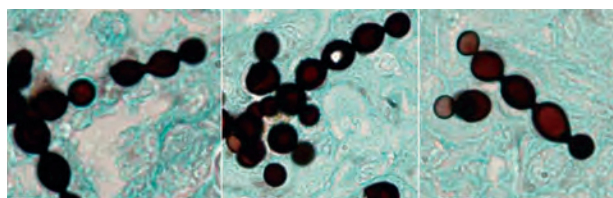
Address for correspondence: Katharina Röltgen, Unit of Molecular Immunology, Swiss Tropical and Public Health Institute, Socinstrasse 57, Basel 4002, Switzerland; email: katharina.roeltgen@unibas.ch

December 2016: Zoonotic Infections

- Investigation of and Response to 2 Plague Cases, Yosemite National Park, California, USA, 2015
- Anomalous High Rainfall and Soil Saturation as Combined Risk Indicator of Rift Valley Fever Outbreaks, South Africa, 2008–2011
- Cutaneous Granulomas in Dolphins Caused by Novel Uncultivated *Paracoccidioides brasiliensis*
- Vertebrate Host Susceptibility to Heartland Virus



- Whole-Genome Characterization and Strain Comparison of VT2f-Producing *Escherichia coli* Causing Hemolytic Uremic Syndrome
- African Horse Sickness Caused by Genome Reassortment and Reversion to Virulence of Live, Attenuated Vaccine Viruses, South Africa, 2004–2014
- *Streptococcus agalactiae* Serotype IV in Humans and Cattle, Northern Europe
- Effect of Live-Poultry Market Interventions on Influenza A(H7N9) Virus, Guangdong, China
- Infectious Dose of *Listeria monocytogenes* in Outbreak Linked to Ice Cream, United States, 2015
- *Baylisascaris procyonis* Roundworm Seroprevalence among Wildlife Rehabilitators, United States and Canada, 2012–2015



- Electrolyte and Metabolic Disturbances in Ebola Patients during a Clinical Trial, Guinea, 2015
- Genetically Different Highly Pathogenic Avian Influenza A(H5N1) Viruses in West Africa, 2015
- Highly Pathogenic Reassortant Avian Influenza A(H5N1) Virus Clade 2.3.2.1a in Poultry, Bhutan
- Horizontal Transmission of Chronic Wasting Disease in Reindeer
- Highly Divergent Dengue Virus Type 2 in Traveler Returning from Borneo to Australia
- Unusual Ebola Virus Chain of Transmission, Conakry, Guinea, 2014–2015
- Human Infection with Novel Spotted Fever Group Rickettsia Genotype, China, 2015
- Hepatitis E Virus in 3 Types of Laboratory Animals, China, 2012–2015
- Human Brucellosis in Febrile Patients Seeking Treatment at Remote Hospitals, Northeastern Kenya, 2014–2015
- Evaluating Healthcare Claims for Neurocysticercosis by Using All-Payer All-Claims Data, Oregon, USA, 2010–2013



**EMERGING
INFECTIOUS DISEASES**

<https://wwwnc.cdc.gov/eid/articles/issue/22/12/table-of-contents>

Avian Influenza A(H7N2) Virus in Human Exposed to Sick Cats, New York, USA, 2016

Atanaska Marinova-Petkova, Jen Laplante, Yunho Jang, Brian Lynch, Natosha Zanders, Marisela Rodriguez, Joyce Jones, Sharmi Thor, Erin Hodges, Juan A. De La Cruz, Jessica Belser, Hua Yang, Paul Carney, Bo Shu, LaShondra Berman, Thomas Stark, John Barnes, Fiona Havers, Patrick Yang, Susan C. Trock, Alicia Fry, Larisa Gubareva, Joseph S. Bresee, James Stevens, Demetre Daskalakis, Dakai Liu, Christopher T. Lee, Mia Kim Torchetti, Sandra Newbury, Francine Cigel, Kathy Toohey-Kurth, Kirsten St. George, David E. Wentworth, Stephen Lindstrom, C. Todd Davis

An outbreak of influenza A(H7N2) virus in cats in a shelter in New York, NY, USA, resulted in zoonotic transmission. Virus isolated from the infected human was closely related to virus isolated from a cat; both were related to low pathogenicity avian influenza A(H7N2) viruses detected in the United States during the early 2000s.

Avian influenza viruses occasionally cross the species barrier, infecting humans and other mammals after exposure to infected birds and contaminated environments. Unique among the avian influenza A subtypes, both low pathogenicity and highly pathogenic H7 viruses have demonstrated the ability to infect and cause disease in humans (1,2). In the eastern and northeastern United States, low pathogenicity avian influenza (LPAI) A(H7N2) viruses

circulated in live bird markets periodically during 1994–2006 (3) and caused poultry outbreaks in Virginia, West Virginia, and North Carolina in 2002 (4). During an outbreak in Virginia in 2002, human infection with H7N2 virus was serologically confirmed in a culler with respiratory symptoms (5). In 2003, another human case of H7N2 infection was reported in a New York resident (6); although the source of exposure remains unknown, the isolated virus was closely related to viruses detected in live bird markets in the region. Because of the sporadic nature of these and other zoonotic infections with influenza H7 viruses throughout the world, the World Health Organization (WHO) recommended development of several candidate vaccine viruses for pandemic preparedness purposes, including 2 vaccines derived from North American lineage LPAI viruses, A/turkey/Virginia/4529/2002 and A/New York/107/2003 (7).

The Study

On December 19, 2016, the New York City Department of Health and Mental Hygiene collected a respiratory specimen from a veterinarian experiencing influenza-like illness after exposure to sick domestic cats at an animal shelter in New York, NY, USA. The specimen tested positive for influenza A but could not be subtyped. Specimen aliquots were shipped to the Wadsworth Center, New York State Department of Health (Albany, NY, USA), and to the Centers for Disease Control and Prevention (CDC; Atlanta, GA, USA). Next-generation sequencing performed at the New York State Department of Health generated a partial genomic sequence (6 of 8 influenza A virus gene segments) that aligned most closely with North American lineage LPAI A(H7N2) viruses. North American lineage H7 real-time reverse transcription PCR (rRT-PCR) testing and diagnostic sequence analysis performed at CDC confirmed the sample to be positive for influenza A(H7N2) virus. Virus isolation was attempted by inoculating the sample in 10-day-old embryonated chicken eggs and MDCK CCL-34 and CRFK (Crandell-Rees Feline Kidney) cell lines (American Type Culture Collection). A/New York/108/2016 was successfully isolated from eggs but not from MDCK or CRFK cells. Codon complete sequencing of the egg-isolated virus (GISAID accession nos. EPI944622–9; <http://www.gisaid.org>) showed no nucleotide changes compared with the hemagglutinin (HA) and neuraminidase (NA) gene segments sequenced directly from the clinical specimen. The virus was nearly identical (99.9%) to a virus isolated

Author affiliations: Centers for Disease Control and Prevention, Atlanta, Georgia, USA (A. Marinova-Petkova, Y. Jang, B. Lynch, N. Zanders, M. Rodriguez, J. Jones, S. Thor, E. Hodges, J.A. De La Cruz, J. Belser, H. Yang, P. Carney, B. Shu, L. Berman, T. Stark, J. Barnes, F. Havers, P. Yang, S.C. Trock, A. Fry, L. Gubareva, J.S. Bresee, J. Stevens, D.E. Wentworth, S. Lindstrom, C.T. Davis); New York State Department of Health, Albany, New York, USA (J. Laplante, K. St. George); New York City Department of Health and Mental Hygiene, Long Island City, New York, USA (D. Daskalakis, D. Liu, C.T. Lee); US Department of Agriculture, Ames, Iowa, USA (M.K. Torchetti); University of Wisconsin, Madison, Wisconsin, USA (S. Newbury, F. Cigel, K. Toohey-Kurth)

DOI: <https://doi.org/10.3201/eid2312.170798>

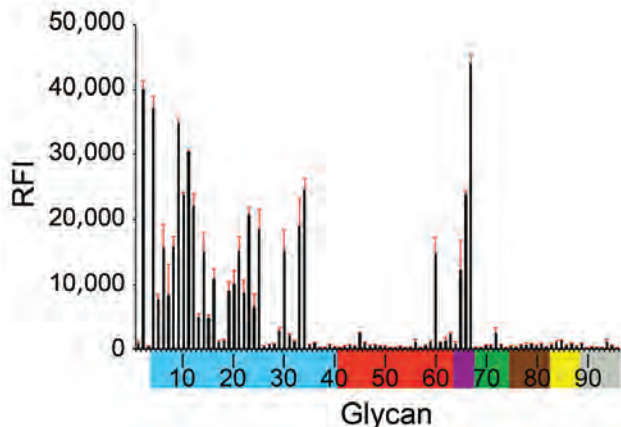


Figure 1. Receptor binding specificity of A/New York/108/2016 (H7N2) influenza virus isolated from a human who experienced influenza-like illness after exposure to sick domestic cats at an animal shelter in New York, NY, USA, 2016. Figure indicates glycan microarray analysis. Colored bars represent glycans that contain α -2,3 sialic acid (SA) (blue), α -2,6 SA (red), α -2,3/ α -2,6 mixed SA (purple), N-glycolyl SA (green), α -2,8 SA (brown), β -2,6 and 9-O-acetyl SA (yellow), and non-SA (gray). Error bars reflect SE in the signal for 6 independent replicates on the array. RFI, relative fluorescence intensity.

from a cat, A/feline/New York/16-040082-1/2016, from a New York shelter where the veterinarian had worked; the cat died of its illness. Phylogenetic analysis of the cat and human viruses showed that their genomes were closely related to LPAI A(H7N2) viruses that were circulating in the northeastern United States in the early 2000s (online Technical Appendix Figure, <https://wwwnc.cdc.gov/EID/article/23/12/17-0798-Techapp1.pdf>).

Analysis of the HA gene segments revealed that A/New York/108/2016 and A/feline/New York/16-040082-1/2016 were phylogenetically related to H7N2 viruses isolated from poultry in the eastern United States (New York, Virginia, Pennsylvania, North Carolina, Massachusetts) during 1996–2005, including 2 influenza A(H7N2) WHO-recommended candidate vaccine viruses. Although the internal protein coding gene segments (polybasic 1 and 2, polyacidic, nucleoprotein, matrix, nonstructural) were distant to sequences available in databases (average nucleotide identity to the closest genetic relative was 97.6%), analysis indicated that they were of LPAI virus origin and lacked known mammalian adaptive substitutions. The longer branch lengths of the internal protein coding gene segments highlighted the scarcity of sequence data available for contemporary H7N2 viruses in the United States.

Similar to well-characterized H7N2 viruses, such as A/turkey/Virginia/4529/2002 and A/New York/107/2003, A/New York/108/2016 had deletion of amino acids 212–219 in the mature HA protein (H7 numbering), known as the 220-loop of the HA receptor binding domain (8). Such deletion has been previously shown to enhance binding and

infectivity of H7 viruses to the mammalian respiratory tract and increase direct contact transmission between mammals (9). Glycan microarray analysis showed that A/New York/108/2016 bound preferentially to α -2,3 avian-like receptors but also showed binding to the α -2,6 glycan with internal sialoside (LSTb, glycan #60), as well as to glycans with mixed α -2,3/ α -2,6 receptors (Figure 1). Strong binding to the LSTb glycan has been previously reported for North America H7N2 viruses of avian origin (8,9) and 2013 human H7N9 viruses (10). The role of the LSTb glycan binding remains unknown; it has been identified only in human milk (11).

Additional molecular characterization of the HA1 protein showed 20 aa differences between A/New York/108/2016 and A/turkey/Virginia/4529/2002 (26 aa in both HA1 and HA2; Figure 2). The substitution A125S resulted in a gain of glycosylation in the HA protein of A/New York/108/2016, previously correlated with increased replication efficiency and wider tissue distribution of A/Netherlands/219/2003 (H7N7) (12). The substitution of T183I was shown in other avian influenza viruses (e.g., H5N1) to enhance binding to mammalian sialic acid receptors (13). Four of the 20 aa changes were in residues associated with antibody recognition at antigenic site B (E177G, S180N, T183I, and S188N) and antigenic site C (R269G).

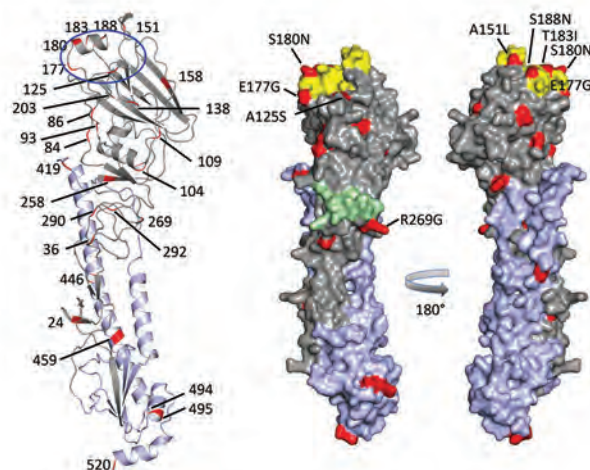


Figure 2. Receptor binding specificity of A/New York/108/2016 (H7N2) influenza virus isolated from a human who experienced influenza-like illness after exposure to sick domestic cats at an animal shelter in New York, NY, USA, 2016. Figure shows A/New York/108/2016 hemagglutinin (HA) monomer structure. HA1 is shown in gray, HA2 in light purple, amino acid changes in comparison with reference virus A/turkey/Virginia/4529/2002 (H7N2) in red. On the cartoon view (left), all amino acid changes in the HA protein are labeled. The location of the receptor binding site (blue circle) includes the 120-loop and the 180-helix. The 220-loop is missing due to deletion of amino acids 212–219 in the mature HA protein (H7 numbering). On the surface model (right), only amino acid substitutions adjacent to the antigenic sites and receptor binding site are labeled. Antigenic site B is yellow, antigenic site C green.

Table. Hemagglutination inhibition testing of influenza A(H7) virus isolated from cat and human in New York, NY, USA, 2016, and reference viruses*

Antigens	Subtype	Ferret antisera					Normal ferret serum
		α -Gs/NE	α -Tk/MN	α -Tk/VA	α -NY/107	α -NY/108	
Reference							
A/goose/Nebraska/17097-4/11	H7N9	160	80	160	80	<10	<10
A/turkey/Minnesota/0141354/09	H7N9	20	80	20	20	<10	<10
A/turkey/Virginia/4529/02	H7N2	40	10	160	640	10	<10
A/New York/107/03	H7N2	40	20	160	640	10	<10
A/New York/108/16†	H7N2	40	10	80	80	320	<10
Test							
A/feline/New York/16-040082-1/16	H7N2	40	10	80	80	320	<10

*Gray shading indicates homologous titers. α -, reference antiserum. Gs/NE, A/goose/Nebraska/17097-4/11; Tk/MN, A/turkey/Minnesota/0141354/09; Tk/VA, A/turkey/Virginia/4529/02; NY/107, A/New York/107/03; NY/108, A/New York/108/16.

†Virus isolated from human (veterinarian who experienced influenza-like illness after exposure to sick domestic cats at an animal shelter).

To determine the effect of these differences on antigenicity, we assessed the relationships in a 2-way hemagglutination inhibition assay, using a panel of ferret antisera raised to related H7 viruses (Table). The results showed that A/New York/108/2016 and A/feline/New York/16-040082-1/2016 reacted with α -A/turkey/Virginia/4529/2002 postinfection ferret antiserum (2-fold reduction of the hemagglutination inhibition titer compared with the A/turkey/Virginia/4529/2002 homologous titer) and α -A/New York/107/2003 antiserum (8-fold reduction compared with the A/New York/107/2003 homologous titer). These data suggest that the A/turkey/Virginia/4529/2002 candidate vaccine virus would provide cross protection if vaccination against the 2016 H7N2 viruses was needed. Both A/turkey/Virginia/4529/2002 and A/New York/107/2003, however, reacted poorly with the antiserum raised against A/New York/108/2016.

A 20-aa deletion in the NA stalk region, considered a genetic marker of poultry-adapted viruses (14), was also identified in the human and feline H7N2 viruses. No genetic markers known to reduce susceptibility to the NA inhibitor class of antiviral drugs were identified in the NA gene. Results of the NA inhibition assay indicated that the H7N2 viruses were susceptible to 4 NA inhibitors: oseltamivir, zanamivir, peramivir, and laninamivir (data not shown).

Conclusions

The circulation of an influenza A(H7N2) virus at the animal–human interface, especially among common companion animals such as domestic cats, is of public health concern. Moreover, from an epidemiologic perspective, it is essential to understand the current distribution of LPAI A(H7N2) viruses in both avian and feline hosts. The US Department of Agriculture and state departments of agriculture have conducted routine avian influenza surveillance in live bird markets; 132,000–212,000 tests for avian influenza were performed annually during 2007–2014 (15), but LPAI A(H7N2) viruses were not detected. The acquisition of many genetic changes throughout the genome of the human and cat H7N2 viruses we report, however, suggests

onward evolution of the virus since it was last detected in poultry and wild birds. We found that the human virus bound to α -2,6–linked sialic acid receptors, which are more common in mammals, yet retained α -2,3–linked sialic acid binding, indicating that it has dual receptor specificity; this information can be used in pandemic risk assessment of zoonotic viruses. Although human infections with LPAI A(H7N2) viruses have occurred previously, we know of no other reported instances of direct transmission from a cat to a human.

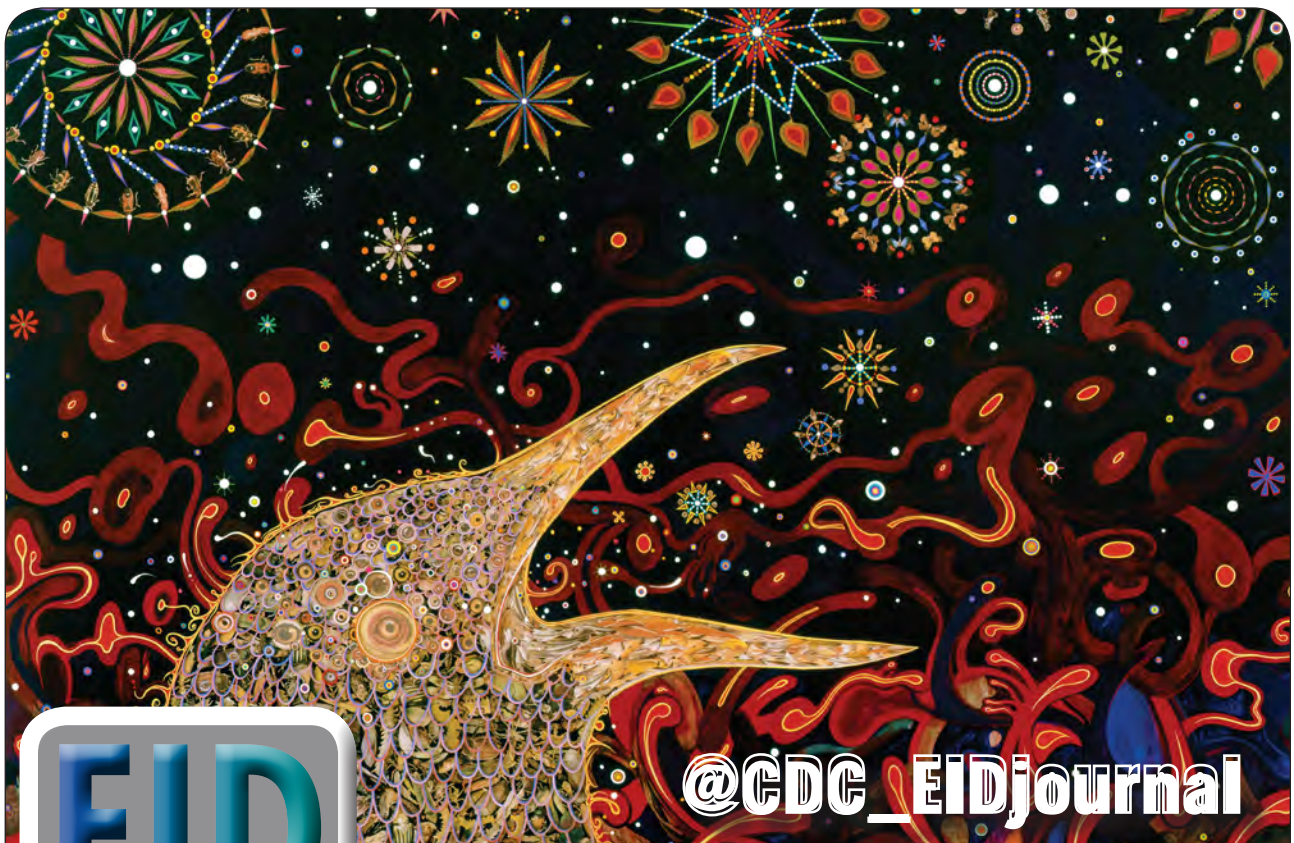
Dr. Marinova-Petkova is a microbiologist with the Influenza Division, National Center for Immunization and Respiratory Diseases, Centers for Disease Control and Prevention, Atlanta, Georgia, USA. Her research interests include studying influenza viruses at the animal–human interface, influenza virus evolution, and animal models for risk assessment of zoonotic pathogens.

References

1. Belser JA, Bridges CB, Katz JM, Tumpey TM. Past, present, and possible future human infection with influenza virus A subtype H7. *Emerg Infect Dis.* 2009;15:859–65. <http://dx.doi.org/10.3201/eid1506.090072>
2. World Health Organization. Influenza at the human-animal interface. 2016 [cited 2017 Feb 12]. http://www.who.int/influenza/human_animal_interface/Influenza_Summary_IRA_HA_interface_12_19_2016.pdf?ua=1
3. Senne DA, Pederson JC, Panigrahy B. Live-bird markets in the northeastern United States: a source of avian influenza in commercial poultry. In: Schrijver RS and Koch G, editors. *Proceedings of the Frontis Workshop on Avian Influenza: Prevention and Control.* Wageningen (the Netherlands): Springer; 2003. p. 19–24.
4. Senne DA, Holt TJ, Akey BL. An overview of the 2002 outbreak of low-pathogenic H7N2 avian influenza in Virginia, West Virginia and North Carolina. In: Schrijver RS and Koch G, editors. *Proceedings of the Frontis Workshop on Avian Influenza: Prevention and Control.* Wageningen (the Netherlands): Springer; 2003. p. 41–7.
5. Centers for Disease Control and Prevention (CDC). Update: influenza activity—United States, 2003–04 season. *MMWR Morb Mortal Wkly Rep.* 2004;53:284–7.
6. Ostrowsky B, Huang A, Terry W, Anton D, Brunagel B, Traynor L, et al. Low pathogenic avian influenza A (H7N2) virus infection in immunocompromised adult, New York, USA, 2003. *Emerg Infect Dis.* 2012;18:1128–31. <http://dx.doi.org/10.3201/eid1807.111913>

7. Pappas C, Matsuoka Y, Swayne DE, Donis RO. Development and evaluation of an influenza virus subtype H7N2 vaccine candidate for pandemic preparedness. *Clin Vaccine Immunol.* 2007;14:1425–32. <http://dx.doi.org/10.1128/CVI.00174-07>
8. Yang H, Chen L-M, Carney PJ, Donis RO, Stevens J. Structures of receptor complexes of a North American H7N2 influenza hemagglutinin with a loop deletion in the receptor binding site. *PLoS Pathog.* 2010;6:e1001081. <http://dx.doi.org/10.1371/journal.ppat.1001081>
9. Belser JA, Blixt O, Chen LM, Pappas C, Maines TR, Van Hoeven N, et al. Contemporary North American influenza H7 viruses possess human receptor specificity: implications for virus transmissibility. *Proc Natl Acad Sci U S A.* 2008;105:7558–63. <http://dx.doi.org/10.1073/pnas.0801259105>
10. Yang H, Carney PJ, Chang JC, Villanueva JM, Stevens J. Structural analysis of the hemagglutinin from the recent 2013 H7N9 influenza virus. *J Virol.* 2013;87:12433–46. <http://dx.doi.org/10.1128/JVI.01854-13>
11. Weinstein J, de Souza-e-Silva U, Paulson JC. Sialylation of glycoprotein oligosaccharides *N*-linked to asparagine. Enzymatic characterization of a Gal β 1 to 3(4)GlcNAc α 2 to 3 sialyltransferase and a Gal β 1 to 4GlcNAc α 2 to 6 sialyltransferase from rat liver. *J Biol Chem.* 1982;257:13845–53.
12. Fouchier RAM, Schneeberger PM, Rozendaal FW, Broekman JM, Kemink SAG, Munster V, et al. Avian influenza A virus (H7N7) associated with human conjunctivitis and a fatal case of acute respiratory distress syndrome. *Proc Natl Acad Sci U S A.* 2004;101:1356–61. <http://dx.doi.org/10.1073/pnas.0308352100>
13. Yang ZY, Wei CJ, Kong WP, Wu L, Xu L, Smith DF, et al. Immunization by avian H5 influenza hemagglutinin mutants with altered receptor binding specificity. *Science.* 2007;317:825–8. <http://dx.doi.org/10.1126/science.1135165>
14. Matrosovich M, Zhou N, Kawaoka Y, Webster R. The surface glycoproteins of H5 influenza viruses isolated from humans, chickens, and wild aquatic birds have distinguishable properties. *J Virol.* 1999;73:1146–55.
15. Myers TJ. Overview of avian influenza surveillance in the United States. US Department of Agriculture, Animal and Plant Health Inspection Service. 2015 [cited 2017 Feb 12]. https://www.aphis.usda.gov/animal_health/animal_dis_spec/poultry/downloads/mtg/presentations/we_3_myers_ai_surveillance_overview.pdf

Address for correspondence: C. Todd Davis, Centers for Disease Control and Prevention, 1600 Clifton Rd NE, Mailstop D30, Atlanta, GA 30329-4027, USA; email: ctdavis@cdc.gov



Follow the EID journal on Twitter and get the most current information from Emerging Infectious Diseases.

Deaths among Wild Birds during Highly Pathogenic Avian Influenza A(H5N8) Virus Outbreak, the Netherlands

Erik Kleyheeg,¹ Roy Slaterus, Rogier Bodewes, Jolianne M. Rijks, Marcel A.H. Spierenburg, Nancy Beerens, Leon Kelder, Marjolein J. Poen, Jan A. Stegeman, Ron A.M. Fouchier, Thijs Kuiken,² Henk P. van der Jeugd²

During autumn–winter 2016–2017, highly pathogenic avian influenza A(H5N8) viruses caused mass die-offs among wild birds in the Netherlands. Among the ≈13,600 birds reported dead, most were tufted ducks (*Aythya fuligula*) and Eurasian wigeons (*Anas penelope*). Recurrence of avian influenza outbreaks might alter wild bird population dynamics.

Since 1996, highly pathogenic avian influenza (HPAI) A viruses of the A/goose/Guangdong/1/96 lineage have caused major losses in the poultry industry worldwide and ≈800 confirmed human cases with a mortality rate of ≈50% (1,2). Wild waterbirds, the natural reservoir of low pathogenicity avian influenza viruses, are probably involved in long-distance spread of HPAI viruses (3,4).

In May–June 2016, a novel reassortant of HPAI virus subtype H5N8 clade 2.3.4.4a was detected in diseased waterbirds in China (5) and on the border between Russia and Mongolia (6). In October 2016, a similar H5N8 strain was found in a dead mute swan (*Cygnus olor*) in Hungary (7). H5N8 viruses then spread rapidly across Europe, causing widespread death among wild waterbirds (8).

The Study

Concurrent with first detections in Austria, Germany, and Denmark, an H5N8 outbreak started in the Netherlands in

Author affiliations: Dutch Center for Avian Migration and Demography, Wageningen, the Netherlands (E. Kleyheeg, H.P. van der Jeugd); Sovon, Dutch Center for Field Ornithology, Nijmegen, the Netherlands (R. Slaterus); Utrecht University, Utrecht, the Netherlands (R. Bodewes, J.A. Stegeman); Dutch Wildlife Health Center, Utrecht (J.M. Rijks); Netherlands Food and Consumer Product Safety Authority, Utrecht (M.A.H. Spierenburg); Wageningen Bioveterinary Research, Lelystad, the Netherlands (N. Beerens); Staatsbosbeheer, Amersfoort, the Netherlands (L. Kelder); Erasmus Medical Center, Rotterdam, the Netherlands (M.J. Poen, R.A.M. Fouchier, T. Kuiken)

DOI: <https://doi.org/10.3201/eid2312.171086>

early November 2016 (7). Unlike previous H5N8 outbreaks in the Netherlands during 2014–2015 (9,10), increased deaths among wild birds were observed this time.

To quantify deaths among species groups with known susceptibility (4,11) or that tested positive for H5N8 during the outbreak, we assembled daily mortality data from organizations gathering death reports or removing carcasses in the Netherlands during November 2016–January 2017 (online Technical Appendix 1 Table 1, <https://wwwnc.cdc.gov/EID/article/23/12/17-1086-Techapp1.xlsx>). This collection was facilitated by close cooperation between ornithologists, virologists, animal health organizations, and other organizations involved in managing the H5N8 outbreak. After potential double-counts were excluded as much as possible, ≈13,600 wild birds of 71 species were reported dead (Table); 49% of all carcasses were identified by species, most of which were tufted duck (*Aythya fuligula* [39%]) and Eurasian wigeon (*Anas penelope* [37%]). Unidentified waterbird carcasses probably also mostly represented these species. H5N8 infection was confirmed in 21 species and not detected among the low numbers of sampled birds representing 13 other species (online Technical Appendix 1 Table 2).

After the first H5N8 detection in diseased waterbirds on November 8, hundreds of carcasses were found at Gouwzee (52°27'09"N, 5°04'07"E) and Wolderwijd (52°20'51"N, 5°34'20"E). Deaths at these locations peaked within 10 days, with ≈5,300 carcasses reported by November 18 (Figure 1). An estimated 85% were tufted ducks. Other species found dead during this period included common pochard (*Aythya ferina* [6%]) and Eurasian coot (*Fulica atra* [4%]), in addition to great crested grebe (*Podiceps cristatus*), mute swan, greater scaup (*Aythya marila*), and several goose and gull species (each <1%).

Beginning in late November, outbreak hotspots moved from open water to water-rich agricultural areas (Figure 1; Video, <https://wwwnc.cdc.gov/EID/article/23/12/17-1086-V1.htm>). Deaths predominantly among Eurasian wigeon were reported from the island of Texel (≈883 birds) and the provinces Friesland (≈2,371), Noord-Holland

¹Current affiliation: Max Planck Institute for Ornithology, Radolfzell am Bodensee, Germany.

²These senior authors contributed equally to this article.

Table. Reported bird species, winter population size estimates, number of carcasses, and rRT-PCR test results per incident during outbreak of HPAI A(H5N8) virus, the Netherlands, November 2016–January 2017*

Avian family and species (common name)	Maximum estimated winter population, ×1,000†	No. carcasses	HPAI incidents tested‡
Anatidae (waterbirds)		7,326	51/134
<i>Anas penelope</i> (Eurasian wigeon)	680–920	2,511	18/18
<i>Aythya fuligula</i> (tufted duck)	190–230	2,633	8/11
Unidentified waterfowl		1,771	23/95
Podicipedidae (grebes)		31	3/5
Ardeidae (herons)§		165	0/13
Phalacrocoracidae (comorants)		50	1/2
Rallidae (rallids)		279	1/9
Scolopacidae (shorebirds)¶		103	0/2
Laridae (gulls)		698	12/28
<i>Larus marinus</i> (great black-backed gull)	7.4–13	78	5/5
Accipitridae (hawks)		119	4/17
Falconidae (falcons)		23	3/4
<i>Falco peregrinus</i> (peregrine falcon)	0.36–0.52	16	3/4
Corvidae (corvids)		88	3/10
Aves indet. (unidentified)		4,708	4/28
Total		13,590	84/255

*Incidents are defined as death reports of a species per site per day. HPAI, highly pathogenic avian influenza; rRT-PCR, real-time reverse transcription PCR.

†Population estimates represent the lowest and highest yearly maxima for the Netherlands during 2009–2014. Data from Sovon (Dutch Center for Field Ornithology, Nijmegen, the Netherlands).

‡Number of positive versus all tested incidents are presented (number positive/number tested), based on infection data from the Netherlands Food and Consumer Product Safety Authority, Dutch Wildlife Health Center, Wageningen Bioveterinary Research, and Erasmus Medical Center.

§H5N8 HPAI virus infection in grey heron (*Ardea cinerea*) was confirmed elsewhere in Europe (8).

¶Eurasian woodcocks (*Scolopax rusticola*) are more prone than other species to window collisions during nocturnal migration; thus, their deaths (54 carcasses reported) might not be related to HPAI.

(≈1,375), and Zuid-Holland (≈732). Reports of dead gulls, raptors and corvids, presumably infected after scavenging on carcasses, also increased.

Because these data are based on numbers of reported carcasses, they provide an underestimation of actual deaths. Although carcass detection rates during daily searches at Gouwzee and Wolderwijd were estimated to be 90%–95% (C. Oshaar, pers. comm., June 12, 2017), search efficiency was probably much lower at other outbreak hotspots. Collection rates of waterbird carcasses during typical avian botulism outbreaks are 10%–25% (12), suggesting that the number of carcasses reported during this H5N8 outbreak represented a limited proportion of total deaths.

We screened a relatively small proportion of carcasses for HPAI virus by real-time reverse transcription on tracheal and cloacal swab samples. We then determined pathogenicity and N-subtype by sequencing, as previously described (9,13). Testing confirmed H5N8 infection in a large proportion of sampled tufted ducks, Eurasian wigeons, gulls, raptors, and corvids (Table); another HPAI virus subtype was detected only twice (H5N5 in tufted duck and mute swan).

We used the public science database of Sovon (Dutch Center for Field Ornithology, Nijmegen, the Netherlands) to compare the number of deaths per species group during November 2016–January 2017 with those occurring in the same timeframe from 2010–2011 to 2015–2016 (Figure 2). Death counts among diving ducks (including tufted ducks) were >2,000 times higher than average during

November 2016–January 2017, and the relative prevalence of deaths substantially increased (4–177 times) for dabbling ducks, herons, geese, swans, and corvids. The same analysis based on another database (<http://www.waarneming.nl>) yielded similar results (online Technical Appendix 2 Figure, <https://wwwnc.cdc.gov/EID/article/23/12/17-1086-Techapp2.pdf>).

The elevated number of deaths among wild birds raises concern about potential population effects. After accounting for detection probability (12), we found that up to 5% of the wintering populations of tufted ducks and Eurasian wigeons in the Netherlands might have died. In addition, 2%–10% of the wintering population of great black-backed gulls (*Larus marinus*) and 11%–39% of the wintering population of peregrine falcons (*Falco peregrinus*) were similarly affected. Stronger effects were observed locally. At Gouwzee, ≈6,000 tufted ducks were counted in December after ≈2,000 of them had died in November. Assuming that no migration occurred, we estimate that up to 25% of the local population of tufted ducks might have died, which might affect population dynamics substantially. Additional studies are needed to evaluate long-term impacts on these populations and to elucidate why high numbers of birds survived or escaped infection.

The first H5N8 outbreak among poultry in the Netherlands occurred on November 25, two weeks after the first detection in wild waterbirds and coinciding with increasing death reports in Eurasian wigeons. This time lag might be related to the limited mobility of wintering *Aythya* ducks,

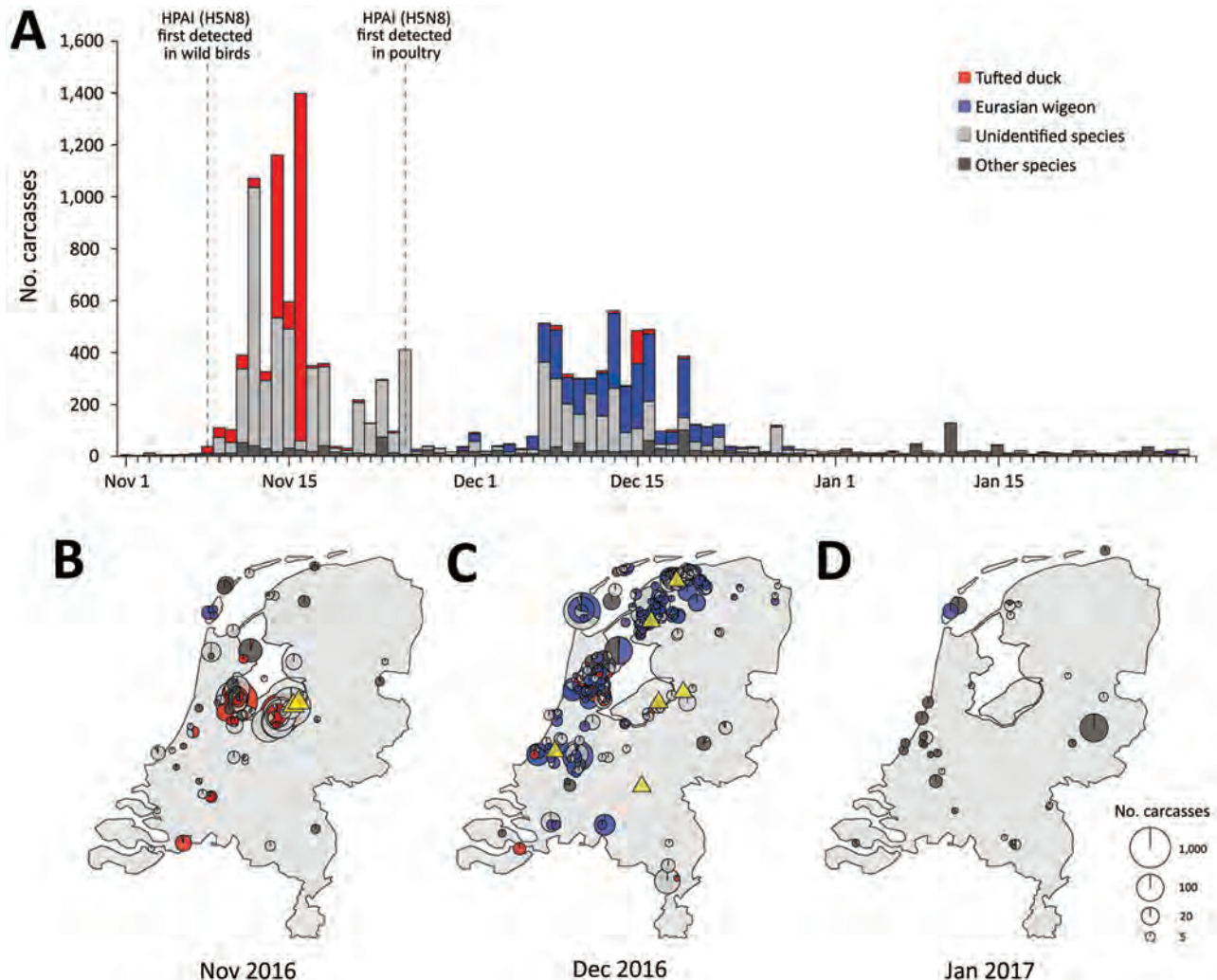


Figure 1. Spatiotemporal pattern of wild bird deaths during an outbreak of HPAI A(H5N8) virus, the Netherlands, November 2016–January 2017. A) Outbreak chronology in tufted duck (red); Eurasian wigeon (blue); unidentified carcasses (light gray), probably also mostly tufted duck and Eurasian wigeon; and all other species combined (dark gray). Dashed vertical lines depict the first detections in wild birds and in poultry in the Netherlands. B–D) Spatial overview of the reported cumulative number of deaths in November 2016 (B), December 2016 (C), and January 2017 (D). Each point on the maps is a pie chart giving the proportions of the respective species (groups) at that location and their size is scaled to the \log_{10} of the number of reported carcasses. Yellow triangles mark the locations of outbreaks in commercial poultry holdings. Only locations where ≥ 3 dead birds were reported are shown. HPAI, highly pathogenic avian influenza.

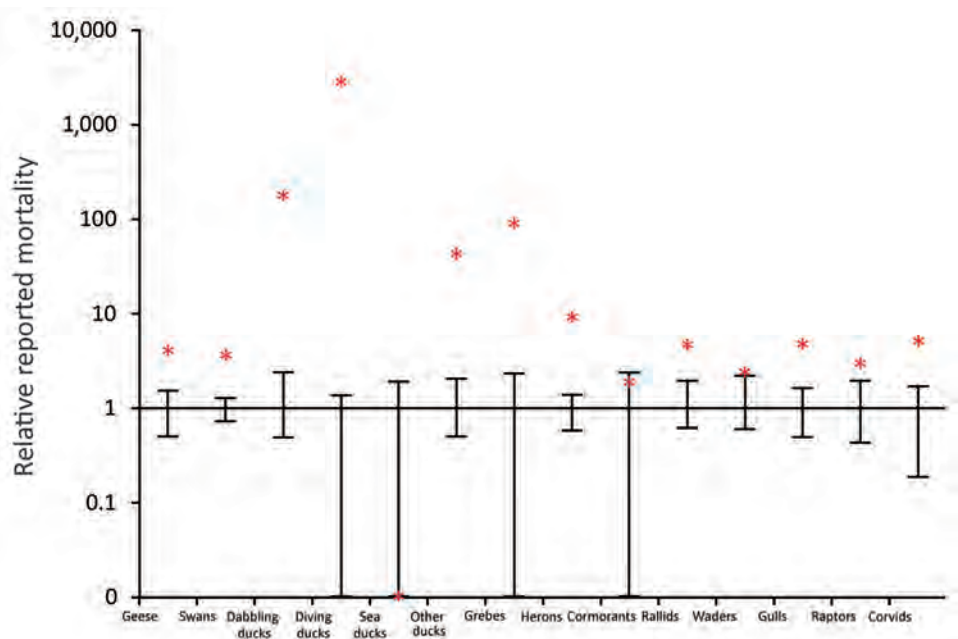
which, in contrast to Eurasian wigeons, rarely fly over land between foraging and roosting sites. Wild bird ecology might thus affect infection risk among poultry, which was further explored by researchers using network analyses of virus sequences obtained from wild birds and poultry during the same outbreak (14).

The quality of reporting of wild bird deaths during this H5N8 outbreak was vastly improved compared with earlier outbreaks, when species names, death rates, and spatiotemporal patterns of deaths were rarely recorded. However, documentation and management of future outbreaks in wild birds can be further improved. To contain outbreaks and minimize losses in the poultry sector, early HPAI virus

detection in wild birds is crucial. Monitoring of wild bird deaths can be optimized (e.g., by timely investigation at sites where migratory birds first arrive, especially when surrounding countries report outbreaks). Awareness of clinical signs in wild birds (online Technical Appendix 2) might facilitate this effort. Detailed, real-time, active and passive surveillance during outbreaks might help assess acute risk for infection in poultry. Such surveillance would require central coordination of information exchange during outbreaks, which would also facilitate evaluation afterward.

Readily available specific guidelines would help management of HPAI virus outbreaks in wild birds. National HPAI preparedness plans should include specific

Figure 2. Relative number of deaths among wild birds during an outbreak of highly pathogenic avian influenza A(H5N8) virus, the Netherlands, November 2016–January 2017. Number of reported deaths during November 2016–January 2017 (red asterisks) is shown relative to the normalized number of deaths reported over the same timeframe in the previous 5 years (average is 1, error bars indicate maximum and minimum from 2011–2012 to 2015–2016). The y-axis is on a log-scale (e.g., reported deaths among diving ducks during 2016–2017 was >2,000 times greater than the average reported in the previous 5 years). Within species groups, numbers of deaths are averaged over species. Data from Sovon (Dutch Center for Field Ornithology, Nijmegen, the Netherlands). A graph of the same analysis based on data from the Nature Information Foundation (<http://www.waarneming.nl>) was also plotted (online Technical Appendix 2, <https://wwwnc.cdc.gov/EID/article/23/12/17-1086-Techapp2.pdf>).



protocols about how to handle carcasses (e.g., biosafety and disposal instructions) and what to report (e.g., species, number of birds, demographic parameters, and presence of leg bands). Moreover, sufficient resources should be available for adequate sampling and testing of specimens to rule out other diseases and to track virus dynamics during an outbreak.

Conclusions

Our findings indicate that the 2016–2017 H5N8 outbreaks in the Netherlands were associated with unprecedented high HPAI-related mortality rates in a wide range of wild bird species. These latest H5N8 outbreaks have shifted the paradigm of wild birds as unaffected agents of HPAI viruses, with increasing concerns about potential effects on their populations. The Netherlands and other important staging areas for migratory waterbirds across Eurasia that have been affected by the 2016–2017 H5N8 outbreaks (3,15) are at risk for substantial numbers of bird deaths during future HPAI outbreaks. International responsibilities regarding migratory bird populations should stimulate national authorities to avert HPAI outbreaks not only in poultry and humans but also in wild birds.

Acknowledgments

We thank Menno Hornman, Jeroen Nienhuis, Natasha Buijs, Hanna Hesselink, Hisko de Vries, Eckard Boot, Cor Oshaar, Jan Regeling, Jan Roelsma, Geert Hamstra, Marko Cortel,

Rommert Cazemier, Hoogheemraadschap Hollands Noorderkwartier, Natuurmonumenten, Rijkswaterstaat, Staatsbosbeheer, and Wetterskip Fryslân for kindly sharing data on wild bird deaths.

Financial support for this study was provided by the Dutch Ministry of Economic Affairs and the US National Health Institute's National Institute of Allergy and Infectious Diseases (contract no. HHSN272201400008C).

Dr. Kleyheeg is a postdoctoral researcher at the Max Planck Institute for Ornithology, Radolfzell am Bodensee, Germany. His primary research interest is the relation between bird movement and the spread of pathogenic and nonpathogenic organisms.

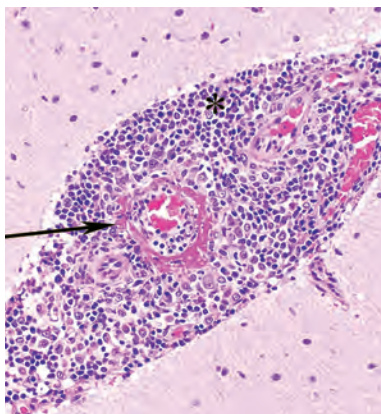
References

- Lai S, Qin Y, Cowling BJ, Ren X, Wardrop NA, Gilbert M, et al. Global epidemiology of avian influenza A H5N1 virus infection in humans, 1997–2015: a systematic review of individual case data. *Lancet Infect Dis.* 2016;16:e108–18. [http://dx.doi.org/10.1016/S1473-3099\(16\)00153-5](http://dx.doi.org/10.1016/S1473-3099(16)00153-5)
- World Health Organization. Cumulative number of confirmed human cases of avian influenza A(H5N1) reported to WHO [cited 2017 June 12]. http://www.who.int/influenza/human_animal_interface/H5N1_cumulative_table_archives
- Keawcharoen J, van Riel D, van Amerongen G, Bestebroer T, Beyer WE, van Lavieren R, et al. Wild ducks as long-distance vectors of highly pathogenic avian influenza virus (H5N1). *Emerg Infect Dis.* 2008;14:600–7. <http://dx.doi.org/10.3201/eid1404.071016>
- Lycett SJ, Bodewes R, Pohlmann A, Banks J, Bányai K, Boni MF, et al. Role for migratory wild birds in the global spread of avian

- influenza H5N8. *Science*. 2016;354:213–7. <http://dx.doi.org/10.1126/science.aaf8852>
5. Li M, Liu H, Bi Y, Sun J, Wong G, Liu D, et al. Highly pathogenic avian influenza A(H5N8) virus in wild migratory birds, Qinghai Lake, China. *Emerg Infect Dis*. 2017;23:637–41. <http://dx.doi.org/10.3201/eid2304.161866>
 6. Lee DH, Sharshov K, Swayne DE, Kurskaya O, Sobolev I, Kabilov M, et al. Novel Reassortant clade 2.3.4.4 avian influenza A(H5N8) virus in wild aquatic birds, Russia, 2016. *Emerg Infect Dis*. 2017;23:359–60. <http://dx.doi.org/10.3201/eid2302.161252>
 7. World Organisation for Animal Health (OIE). Avian influenza portal [cited 2017 May 29]. <http://www.oie.int/animal-health-in-the-world/update-on-avian-influenza>
 8. More S, Bicout D, Botner A, Butterworth A, Calistri A, et al. Urgent request on avian influenza. *EFSA J*. 2017;15:4687.
 9. Verhagen JH, van der Jeugd HP, Nolet BA, Slaterus R, Kharitonov SP, de Vries PP, et al. Wild bird surveillance around outbreaks of highly pathogenic avian influenza A(H5N8) virus in the Netherlands, 2014, within the context of global flyways. *Euro Surveill*. 2015;20:21069. <http://dx.doi.org/10.2807/1560-7917.ES2015.20.12.21069>
 10. Poen MJ, Verhagen JH, Manvell RJ, Brown I, Bestebroer TM, van der Vliet S, et al. Lack of virological and serological evidence for continued circulation of highly pathogenic avian influenza H5N8 virus in wild birds in the Netherlands, 14 November 2014 to 31 January 2016. *Euro Surveill*. 2016;21:30349. <http://dx.doi.org/10.2807/1560-7917.ES.2016.21.38.30349>
 11. Breed AC, Harris K, Hesterberg U, Gould G, Londt BZ, Brown IH, et al. Surveillance for avian influenza in wild birds in the European Union in 2007. *Avian Dis*. 2010;54(Suppl):399–404. <http://dx.doi.org/10.1637/8950-053109-Reg.1>
 12. Bollinger TK, Evelsizer DD, Dufour KW, Soos C, Clark RG, Wobeser G, et al. Ecology and management of avian botulism on the Canadian prairies [cited 2017 Jun 20]. http://www.phjv.ca/pdf/BotulismReport_FINAL_FullReport_Aug2011.pdf
 13. Bouwstra RJ, Koch G, Heutink R, Harders F, van der Spek A, Elbers ARW, et al. Phylogenetic analysis of highly pathogenic avian influenza A(H5N8) virus outbreak strains provides evidence for four separate introductions and one between-poultry farm transmission in the Netherlands, November 2014. *Euro Surveill*. 2015;20:21174. <http://dx.doi.org/10.2807/1560-7917.ES2015.20.26.21174>
 14. Beerens N, Heutink R, Bergervoet SA, Harders F, Bossers A, Koch G. Multiple reassorted viruses as cause of highly pathogenic avian influenza virus A(H5N8) epidemic, the Netherlands, 2016. *Emerg Infect Dis*. 2017;23:1974–81.
 15. Pohlmann A, Starick E, Harder T, Grund C, Höper D, Globig A, et al. Outbreaks among wild birds and domestic poultry caused by reassorted influenza A (H5N8) clade 2.3.4.4 viruses, Germany, 2016. *Emerg Infect Dis*. 2017;23:633–6. <http://dx.doi.org/10.3201/eid2304.161949>

Address for correspondence: Erik Kleyheeg, Max Planck Institute for Ornithology, Am Obstberg 1, 78315 Radolfzell am Bodensee, Germany; email: erikkleyheeg@gmail.com

December 2015: Zoonotic Infections



- Identifying and Reducing Remaining Stocks of Rinderpest Virus
- Opportunistic Pulmonary *Bordetella hinzii* Infection after Avian Exposure
- Zoonotic Leprosy in the Southeastern United States
- Influenza A(H6N1) Virus in Dogs, Taiwan

- Infection Risk for Persons Exposed to Highly Pathogenic Avian Influenza A H5 Virus–Infected Birds, United States, December 2014–2015
- High Prevalence of Intermediate *Leptospira* spp. DNA in Febrile Humans From Urban and Rural Ecuador
- Biological Warfare Plan in the 17th Century—the Siege of Candia, 1648–1669
- Methicillin-Resistant *Staphylococcus aureus* Prevalence among Captive Chimpanzees, Texas, USA, 2012
- Novel *Waddlia* Intracellular Bacterium in *Artibeus intermedius* Fruit Bats, Mexico



- Tembusu-Related Flavivirus in Ducks, Thailand
- Japanese Macaques (*Macaca fuscata*) as Natural Reservoir of *Bartonella quintana*
- *Onchocerca lupi* Nematode in a Cat, Europe
- Increased Number of Human Cases of Influenza Virus A(H5N1) Infection, Egypt, 2014–15
- Replication Capacity of Avian Influenza A(H9N2) Virus in Pet Birds, Chickens, and Mammals, Bangladesh

Pathogenic *Elizabethkingia miricola* Infection in Cultured Black-Spotted Frogs, China, 2016

Ruixue Hu, Junfa Yuan, Yin Meng,
Zhe Wang, Zemao Gu

Multiregional outbreaks of meningitis-like disease caused by *Elizabethkingia miricola* were confirmed in black-spotted frog farms in China in 2016. Whole-genome sequencing revealed that this amphibian *E. miricola* strain is closely related to human clinical isolates. Our findings indicate that *E. miricola* can be epizootic and may pose a threat to humans.

Elizabethkingia is a genus of gram-negative, nonmotile, non-spore-forming bacilli occasionally associated with human clinical infections (1–6). Although *E. meningoseptica* is the most commonly identified nosocomial pathogen of the genus (2), many descriptions of this species are misidentifications of *E. anophelis* and *E. miricola* (3–5). *E. anophelis*, initially isolated from the midgut of mosquitoes, caused a large outbreak centered in Wisconsin during 2015–2016 (5). *E. miricola* was found in 2003 in condensation water at the Mir space station (7). The first reported case of *E. miricola* infection was in a hematology patient in the United States in 2008 (8). Subsequently, *E. miricola* has been increasingly documented as causing bacteremia and sepsis in immunocompromised and immunocompetent patients, mostly in European countries (6). Until now, pathogenic *E. miricola* has seldom been isolated from Asia, and whether *E. miricola* can be pathogenic to animals is unknown.

The black-spotted frog, *Pelophylax nigromaculatus*, is a typical amphibian species, largely endemic to east Asia. Owing to the success of rearing it on an artificial diet, this frog has been widely farmed under special government approval as an edible animal in south-central China in recent years. In 2016, epidemic meningitis-like disease outbreaks in cultured black-spotted frogs occurred in separate farms. We identified *E. miricola* as the predominant pathogen and used whole-genome sequencing (WGS) to further characterize this Asian epizootic isolate and phylogenetically compare it with the available typical *Elizabethkingia* genomes.

Author affiliations: Huazhong Agricultural University, Wuhan, China (R. Hu, J. Yuan, Y. Meng, Z. Wang, Z. Gu); Hubei Engineering Research Center for Aquatic Animal Diseases Control and Prevention, Wuhan (R. Hu, J. Yuan, Z. Gu)

DOI: <https://doi.org/10.3201/eid2312.170942>

The Study

Since May 2016, many black-spotted frogs in farms in Hunan Province in south-central China have experienced an emerging, contagious disease characterized mainly by severe neurologic dysfunction. The first clinical sign is intermittent swimming in circles. Thereafter, the frogs develop signs of torticollis (Figure 1, panel A), disorientation (Video, <https://wwwnc.cdc.gov/EID/article/23/12/17-0942-V1.htm>), and anepithymia or meteorism (Figure 1, panel E). These signs are followed by cataracts (Figure 1, panel C); proptosis or hyperemia (Figure 1, panels B, D); agitation or lethargy; and, ultimately, death. The frogs are farmed in artificial ecologic wetlands or ponds with running water and shelter (online Technical Appendix Figure 1, <https://wwwnc.cdc.gov/EID/article/23/12/17-0942-Techapp1.pdf>). Most ponds in 1 farm, which share a common water supply, were infected sequentially within a short time. More than 60% of the frogs in the infected farms had signs of varying appearance, and 60%–90% of the diseased frogs died in the next few days or weeks. The disease continued until hibernation and returned the following spring.

During July–October 2016, we collected 213 abnormal frogs from 7 separate farms in Hunan Province, China (online Technical Appendix Figure 2). Histopathologic examination showed severe meningitis with denatured, incassate meninges. We observed inflammatory infiltrates, moderate multifocal gliosis, and perivascular cuffing in the cerebellum (online Technical Appendix Figure 3). Results of the diagnostic tests for *Batrachochytrium dendrobatidis* and ranaviruses were negative (Table 1). Although we observed Myxosporidia protozoa in the gallbladder and some protists in the intestine, they were not identified as the etiologic agents, considering the proportion of infection (online Technical Appendix Figure 4).

We confirmed bacterial infections in 190 (89.2%) of the 213 frogs; 90% were *E. miricola* according to the 16S rRNA gene sequence, which shared 99.36%–99.86% similarity with *E. miricola* DSM14571 (online Technical Appendix). We selected bacterial strain FL160902, isolated from frog no. 160, as the representative isolate and conducted experimental pathogenicity testing by various infection routes, including intramuscular injection, immersion infection, and cohabitation with infected frogs. All animal handling was done in compliance with the National Institutes of Health protocols (online Technical Appendix). After 2 weeks of observations

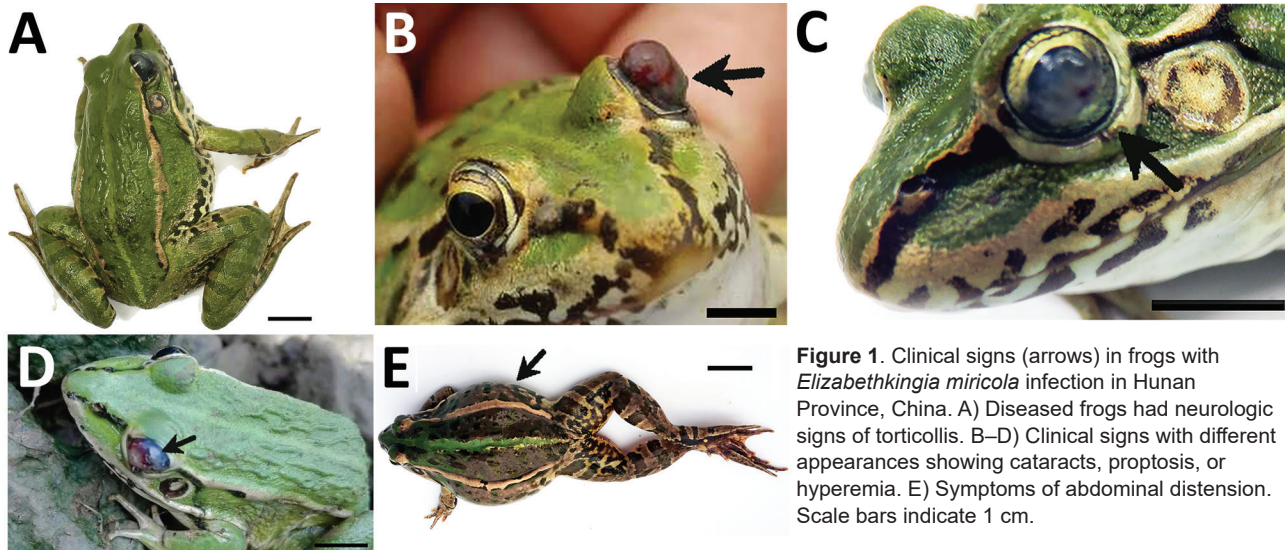


Figure 1. Clinical signs (arrows) in frogs with *Elizabethkingia miricola* infection in Hunan Province, China. A) Diseased frogs had neurologic signs of torticollis. B–D) Clinical signs with different appearances showing cataracts, proptosis, or hyperemia. E) Symptoms of abdominal distension. Scale bars indicate 1 cm.

(Table 2), we found that the cumulative mortality (10%–70%) increased with dose in the injection trial and that 100% of frogs exposed to *E. miricola* by immersion died. In the cohabitation studies, 30% mortality was recorded, indicating cross-infection. Koch's postulates were satisfied by identification of isolates from dead frogs as *E. miricola*, identical to FL160902.

To characterize *E. miricola* FL160902, we conducted WGS with the Illumina HiSeq 2500 platform (Illumina Inc., San Diego, CA, USA), producing 2×150 -bp paired-end reads. We assembled the trimmed reads using SOAPdenovo (<http://soap.genomics.org.cn/soapdenovo.html>). We

constructed a phylogenetic tree (Figure 2) of orthologous genes using RAXML (9) with 100 bootstrap replicates to examine the evolutionary relatedness between *E. miricola* FL160902 (GenBank accession no. NHPR00000000) and other *Elizabethkingia* genomes. The results showed that FL160902 was most closely related to CSID_3000517120, a clinical isolate of *E. miricola* from the United States sequenced by the Centers for Disease Control and Prevention (CDC) (10), revealing the potential of *E. miricola* FL160902 for pathogenicity in humans.

Before WGS was commonly used, *E. meningoseptica* (previously *Flavobacterium meningosepticum*) was

Table 1. Results from etiologic detection in 213 frogs collected in Hunan, China, July–October 2016*

Pathogen	Tested organ									No. positive
	Skin	Liver	Spleen	Kidney	Brain	Intestine	Muscle	Gallbladder	Heart	
Bacteria	NT	+	+	+	+	NT	NT	NT	NT	190†
Parasite‡	–	–	–	–	–	–	–	+	–	9
Fungus§	–	NT	NT	NT	NT	NT	NT	NT	NT	0
Ranaviruses	NT	NT	–	–	NT	NT	–	NT	NT	0

* NT, not tested; +, positive; –, negative.

†Predominant bacterial infection. The results were considered positive if any one of the tested organs was positive.

‡Class Myxosporia.

§*Batrachochytrium dendrobatidis*.

Table 2. Results of the experimental exposure of frogs to *Elizabethkingia miricola* isolate FL160902, China, 2016*

Route of infection	Concentration, CFU/mL	No. frogs per trial	Cumulative no. deaths, by days after exposure†							Mortality, %
			2	4	6	8	10	12	14	
Intramuscular injection‡	10^5	10	0	1	1	1	1	1	1	10
	10^6	10	0	0	1	1	5	5	5	50
	10^7	10	1	3	6	7	7	7	7	70
	SPSS§	10	0	0	0	0	0	0	0	0
Immersion inoculation¶	10^5	10	3	7	10	10	10	10	10	100
Cohabitation inoculation#	NA	10	0	0	1	3	3	3	3	30
Control	NA	10	0	0	0	0	0	0	0	0

*NA, not applicable.

†Deaths after 14 d were not included.

‡Injection volume 200 μ L.

§An equivalent volume injection of 0.70% stroke-physiologic saline solution.

¶Immersed for 30 min in *E. miricola* suspension.

#Frogs in this trial cohabited with frogs previously infected with *E. miricola*.

found to be separated into 2 main hybridization groups, UBI and UBII, that were ≈40%–55% interrelated; UBII could be further divided into 4 subgroups (11,12). However, because the isolates from different groups are phenotypically very similar, these genomic groups remain assigned at this time to *E. meningoseptica* (13). In our

phylogenetic tree, UBI group *E. meningoseptica* isolates did not group with the other *Elizabethkingia* spp. and were distantly related to UBII. Considering the low DNA–DNA relatedness (<70%) between the 2 groups and phylogenomic analysis based on WGS (3,11,12), we propose that UBII are not *E. meningoseptica*. The

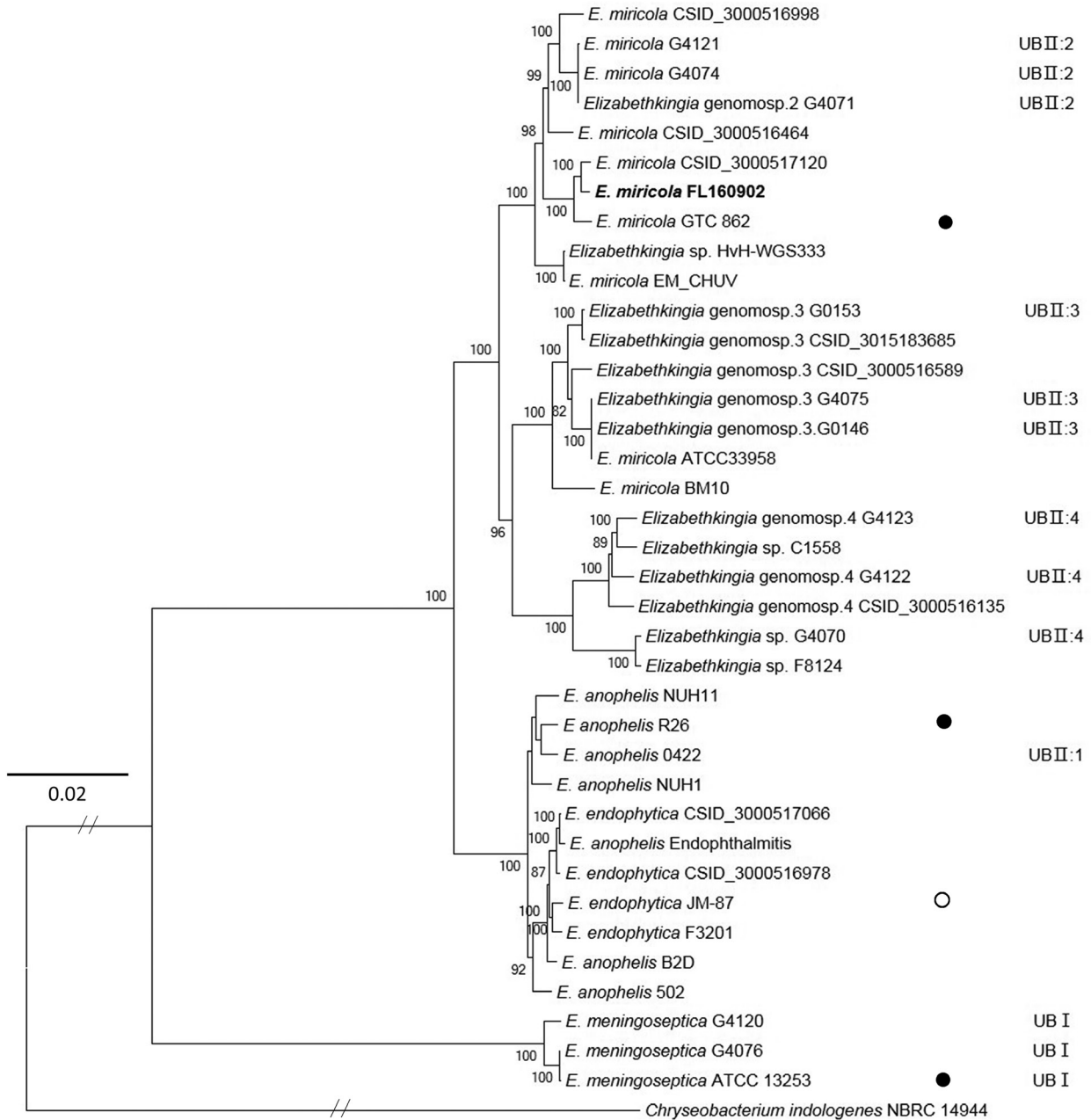


Figure 2. Maximum-likelihood phylogenetic tree of *Elizabethkingia miricola* FL160902 from an infected frog in Hunan Province, China, and reference genomes. The tree was constructed by using the single-copy orthologous genes of all the 38 genomes with 100 bootstrap replicates. Species identifications strictly followed the National Center for Biotechnology Information submitted names. Isolates assigned into UB groups and subgroups are according to Holmes et al. (12) and Bruun and Ursing (13). Solid circles indicate type strains; open circle indicates a former type strain. Bold indicates strain isolated in this study. Scale bar indicates nucleotide substitutions per site.

found to be separated into 2 main hybridization groups, UBI and UBII, that were ≈40%–55% interrelated; UBII could be further divided into 4 subgroups (11,12). However, because the isolates from different groups are phenotypically very similar, these genomic groups remain assigned at this time to *E. meningoseptica* (13). In our

phylogenetic tree, UBI group *E. meningoseptica* isolates did not group with the other *Elizabethkingia* spp. and were distantly related to UBII. Considering the low DNA–DNA relatedness (<70%) between the 2 groups and phylogenomic analysis based on WGS (3,11,12), we propose that UBII are not *E. meningoseptica*. The

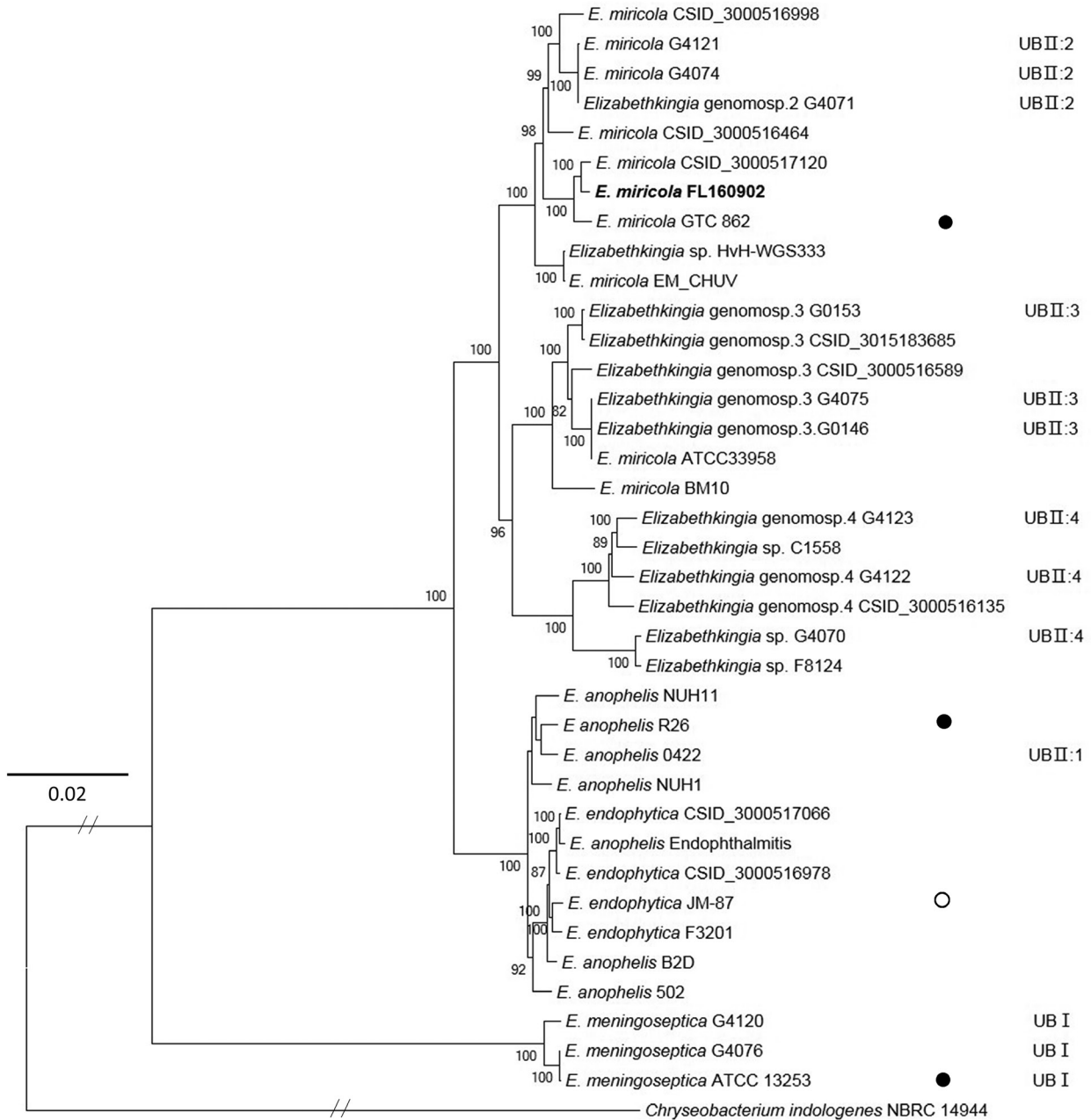


Figure 2. Maximum-likelihood phylogenetic tree of *Elizabethkingia miricola* FL160902 from an infected frog in Hunan Province, China, and reference genomes. The tree was constructed by using the single-copy orthologous genes of all the 38 genomes with 100 bootstrap replicates. Species identifications strictly followed the National Center for Biotechnology Information submitted names. Isolates assigned into UB groups and subgroups are according to Holmes et al. (12) and Bruun and Ursing (13). Solid circles indicate type strains; open circle indicates a former type strain. Bold indicates strain isolated in this study. Scale bar indicates nucleotide substitutions per site.

- indole-producing non-fermenters of CDC groups IIc, IIe, IIh and III, mostly from human clinical sources, and proposals of *Chryseobacterium bernardetii* sp. nov., *Chryseobacterium carnis* sp. nov., *Chryseobacterium lactis* sp. nov., *Chryseobacterium nakagawai* sp. nov. and *Chryseobacterium taklimakanense* comb. nov. *Int J Syst Evol Microbiol.* 2013;63:4639–62. <http://dx.doi.org/10.1099/ijss.0.054353-0>
13. Bruun B, Ursing J. Phenotypic characterization of *Flavobacterium meningosepticum* strains identified by DNA-DNA hybridization. *Acta Pathol Microbiol Immunol Scand B.* 1987;95:41–7.
14. Doijad S, Ghosh H, Glaeser S, Kämpfer P, Chakraborty T. Taxonomic reassessment of the genus *Elizabethkingia* using whole-genome sequencing: *Elizabethkingia endophytica* Kämpfer et al. 2015 is a later subjective synonym of *Elizabethkingia anophelis* Kämpfer et al. 2011. *Int J Syst Evol Microbiol.* 2016;66:4555–9. <http://dx.doi.org/10.1099/ijsem.0.001390>

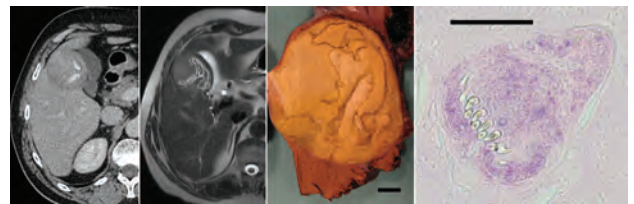
Address for correspondence: Zemao Gu, Huazhong Agricultural University–College of Fisheries, No. 1 Shizi Mountain St, Hongshan District Wuhan, Hubei 430070, China; email: guzemao@mail.hzau.edu.cn

December 2014: Zoonoses



- Variably Protease-Sensitive Prionopathy, a Unique Prion Variant with Inefficient Transmission Properties

- Geographic Divergence of Bovine and Human Shiga Toxin–Producing *Escherichia coli* O157:H7 Genotypes, New Zealand
- Bacterial Pathogens Associated with Hidradenitis Suppurativa, France
- Replication and Shedding of MERS-CoV in Upper Respiratory Tract of Inoculated Dromedary Camels
- Transmission Characteristics of Variably Protease-Sensitive Prionopathy
- Seroconversion for Infectious Pathogens among UK Military Personnel Deployed to Afghanistan, 2008–2011
- Circulation of Reassortant Influenza A(H7N9) Viruses in Poultry and Humans, Guangdong
- Molecular Evolution of Peste des Petits Ruminants Virus Province, China, 2013
- Effects of Knowledge, Attitudes, and Practices of Primary Care Providers on Antibiotic Selection, United States
- Accuracy of Herdsmen Reporting versus Serologic Testing for Estimating Foot-and-Mouth Disease Prevalence
- Residual Infestation and Recolonization during Urban *Triatoma infestans* Bug Control Campaign, Peru
- Two *Anaplasma phagocytophilum* Strains in *Ixodes scapularis* Ticks, Canada
- *Francisella tularensis* Bacteria Associated with Feline Tularemia in the United States
- Avian Bornavirus in Free-Ranging Psittacine Birds, Brazil
- Gouleako and Herbert Viruses in Pigs, Republic of Korea, 2013
- Human Infection with Influenza Virus A(H10N8) from Live Poultry Markets, China, 2014
- Molecular Epidemiology of Influenza A(H1N1)pdm09 Virus among Humans and Swine, Sri Lanka
- Novel Amdoparvovirus Infecting Farmed Raccoon Dogs and Arctic Foxes
- Novel Porcine Epidemic Diarrhea Virus Variant with Large Genomic Deletion, South Korea
- MERS Coronavirus Neutralizing Antibodies in Camels, Eastern Africa, 1983–1997
- Equine Influenza A(H3N8) Virus Infection in Cats
- *Echinococcus ortleppi* Infections in Humans and Cattle, France
- Human Hantavirus Infections in the Netherlands
- *Mycobacterium* Species Related to *M. leprae* and *M. lepromatosis* from Cows with Bovine Nodular Thelitis
- Human Metapneumovirus Infection in Chimpanzees, United States
- Putative New West Nile Virus Lineage in *Uranotaenia unguiculata* Mosquitoes, Austria, 2013
- Novel Bluetongue Virus in Goats, Corsica, France, 2014



West Nile Virus Lineage 2 in Horses and Other Animals with Neurologic Disease, South Africa, 2008–2015

**Marietjie Venter, Marthi Pretorius,
James A. Fuller, Elizabeth Botha,
Mpho Rakgotho, Voula Stivaktas,
Camilla Weyer, Marco Romito, June Williams**

During 2008–2015 in South Africa, we conducted West Nile virus surveillance in 1,407 animals with neurologic disease and identified mostly lineage 2 cases in horses (7.4%, 79/1,069), livestock (1.5%, 2/132), and wildlife (0.5%, 1/206); 35% were fatal. Geographic correlation of horse cases with seropositive veterinarians suggests disease in horses can predict risk in humans.

West Nile virus (WNV) circulates between ornithophilic mosquitoes and birds. Birds are used as WNV sentinels, but in Africa, birds rarely die of infections, probably because of genetic resistance (1). Therefore, another animal is needed to predict risk for WNV disease in Africa. Humans and horses are considered incidental dead-end hosts for WNV (2). Although $\approx 20\%$ of infections in these species are symptomatic, $\approx 1\%$ of human cases involve neurologic disease, with 1%–10% fatality rates (3), but 90% of horse cases involve neurologic disease, with 30%–40% fatality rates (4). Monitoring equine populations living near human populations might enable prediction of human outbreaks in Africa (5).

WNV is endemic to South Africa (1). The largest human outbreak occurred in 1974 in Karoo (1); during 1983–1984, a smaller epizootic outbreak occurred in Witwatersrand (Gauteng Province) (6). During 2010–2011, screening of the cerebrospinal fluid of patients in hospitals in Gauteng Province indicated WNV was present in 3.5% of unsolved cases of neurologic disease, suggesting severe WNV cases might be missed because of a lack of clinical awareness of the pathogenic potential of this virus (7).

Author affiliations: University of Pretoria Centre for Viral Zoonoses, Pretoria, South Africa (M. Venter, M. Pretorius, E. Botha, M. Rakgotho, V. Stivaktas, J. Williams); US Centers for Disease Control and Prevention, Global Disease Detection Centre, Pretoria (M. Venter, J.A. Fuller); National Health Laboratory Service, Tshwane, South Africa (M. Pretorius); University of Pretoria Equine Research Centre, Pretoria (C. Weyer); Onderstepoort Veterinary Research, Onderstepoort, South Africa (M. Romito)

DOI: <https://doi.org/10.3201/eid2312.162078>

WNV isolates are divided into 2 lineages (8): lineage 1, which predominates in the Northern Hemisphere and Australia, and lineage 2, which is endemic to southern Africa and Madagascar and started emerging in central Europe in 2008 (9). Lineage 2–associated encephalitis outbreaks have been occurring in Greece since 2010, causing hundreds of neurologic cases in humans (fatality rate 17%) and horses (3). Lineage 2 was first associated with severe neurologic disease in horses in South Africa in 2009 (8). Neurologic signs of infection in horses are similar for both lineages and include ataxia, weakness, recumbence, seizures, and muscle fasciculation (8,10). However, epidemiologic data are lacking.

South Africa conducts active surveillance for infectious pathogens in horses, such as African horse sickness virus (AHSV), to help the horse industry maintain disease-free status, as required by the World Organisation for Animal Health. Equine WNV is also a World Organisation for Animal Health–listed disease, enabling researchers to use horses for WNV surveillance internationally. To assist with predicting WNV human cases and managing outbreaks in susceptible animals, we sought to define the epidemiology of WNV in horses in South Africa.

The Study

We prospectively investigated horses and other animals with fever or neurologic signs during 2008–2015 and compared the geographic range of WNV-positive animals with that of WNV-seropositive veterinarians involved in equine, wildlife, and livestock disease management during 2011–2012 (11). A total of 210 veterinarians from all 9 South Africa provinces submitted blood, neurologic tissue, and visceral tissue specimens from horses (acquired during 2008–2015) and wildlife and livestock (acquired during 2010–2015) that displayed acute fever, neurologic disease, or other signs of acute infection, accompanied by their demographic and disease data, to the Centre for Viral Zoonoses, University of Pretoria (Pretoria, South Africa). A total of 1,407 samples (64% blood/serum, 25% tissue, 6% both blood/serum and tissue, 4% viral RNA) were received.

We tested all specimens for WNV, Shuni virus, alphaviruses, and equine encephalitis virus and submitted samples for rabies virus testing, if suspected, to Onderstepoort Veterinary Research, Onderstepoort, South Africa, as previously

Table 1. WNV infection, co-infection, disease, and death in horses, by year, South Africa, 2008–2015*

Category	No. (%) horses								
	2008	2009	2010	2011	2012	2013	2014	2015	Total
Total specimens	71	76	150	164	89	138	193	188	1,069
Confirmed WNV positive†	9 (12.7)	6 (7.9)	18 (12.0)	12 (7.3)	3 (3.4)	4 (2.9)	23 (11.9)	4 (2.1)	79 (7.4)
WNV PCR positive†	5 (7.0)	3 (3.9)	8 (5.3)	2 (1.2)	0 (0)	1 (0.7)	4 (2.1)	1 (0.5)	24 (2.2)
WNV IgM positive†	5 (7.0)	3 (3.9)	12 (8.0)	10 (6.1)	3 (3.4)	3 (2.2)	20 (10.4)	3 (1.6)	59 (5.5)
Deaths‡	5 (55.6)	3 (50.0)	8 (44.4)	3 (25.0)	1 (33.3)	1 (25.0)	5 (21.7)	1 (25.0)	27 (34.2)
Any neurologic signs‡	8 (88.9)	6 (100.0)	16 (88.9)	11 (91.7)	2 (66.7)	4 (100.0)	21 (91.3)	4 (100.0)	72 (91.1)
Fever‡	2 (22.2)	2 (33.3)	3 (16.7)	6 (50.0)	1 (33.3)	1 (25.0)	10 (43.5)	3 (75.0)	28 (35.4)
Co-infections‡ and co-infecting viruses	2 (22.2), 2 AHSV	2 (33.3), 2 SINV	1 (5.6), 1 SHUV	2 (16.7), 2 MIDV	2 (66.7), 1 AHSV, 1 SINV	0	4 (17.4), 2 MIDV, 1 SHUV, 1 EEV	1 (25.0), 1 SHUV	14 (17.7), 3 AHSV, 3 SINV, 3 SHUV, 4 MIDV, 1 EEV

*AHSV, African horse sickness virus; EEV, equine encephalitis virus; MIDV, Middleburg virus; SHUV, Shuni virus; SINV, Sindbis virus; WNV, West Nile virus.

†Percentage of total number of specimens tested.

‡Percentage of total number of confirmed WNV-positive cases. Confirmed cases were those that tested positive by PCR plus those that tested positive by WNV IgM Capture ELISA (IDEXX Laboratories, Montpellier, France) followed by neutralization assay.

described (12). All WNV-positive cases were tested for AHSV (13). We screened all equine serum and plasma specimens for WNV IgM (WNV IgM Capture ELISA Test; IDEXX Laboratories, Montpellier, France) and confirmed by neutralization assay (8). Reverse transcription PCR-positive cases were sequenced (GenBank accession nos. KY176717–36) and subjected to maximum likelihood analysis (online Technical Appendix Figure, <https://wwwnc.cdc.gov/EID/article/23/12/16-2078-Techapp1.pdf>). We compared WNV positivity with clinical signs in horses by logistic regression using crude odds ratios (ORs) and adjusted ORs (aORs) with 95% CIs (Stata 14; StataCorp LLC, College Station, Texas, USA) (online Technical Appendix Table).

Most clinical cases were in horses (76.0%, 1,069/1,407), followed by wildlife (14.6%, 206/1,407) and livestock (9.4%, 132/1,407). We detected most WNV cases in horses (7.3%, 79/1,069; $p < 0.001$), and 1 (0.5%) case in wildlife (imported North American white-tailed deer [*Odocoileus virginianus*]), and 2 in (1.5%) livestock

(locally bred Ayreshire cow [*Bos taurus*], boer goat [*Capra aegagrus hircus*]).

Real-time PCR results were positive for 24 cases; 20 isolates could be sequenced, and 18 clustered with lineage 2 (online Technical Appendix Figure). A mare and her miscarried fetus were the only animals infected with lineage 1 viruses (14). We detected 14 (17.7%) co-infections in WNV-infected horses (Table 1), with high fatality rates for most co-infecting viruses: MIDV (100%, 4/4); AHSV (66.7%, 2/3); SINV (100%, 3/3); Shuni virus (33.3%, 1/3); and equine encephalitis virus (0%, 0/1).

Most (77.2%) WNV cases occurred in Southern Hemisphere autumn (March–May) (Figure 1), 2–3 months after peak precipitation. The interannual detection rate among horses was 2.1–12.7% (Table 1). Most specimens came from Gauteng ($n = 400$) and Western Cape ($n = 296$) Provinces (Figure 2, panel A). Most WNV-positive cases were from Gauteng Province (7.3%, 29/400), but detection rates were highest in Northern Cape (10.2%) and Eastern Cape

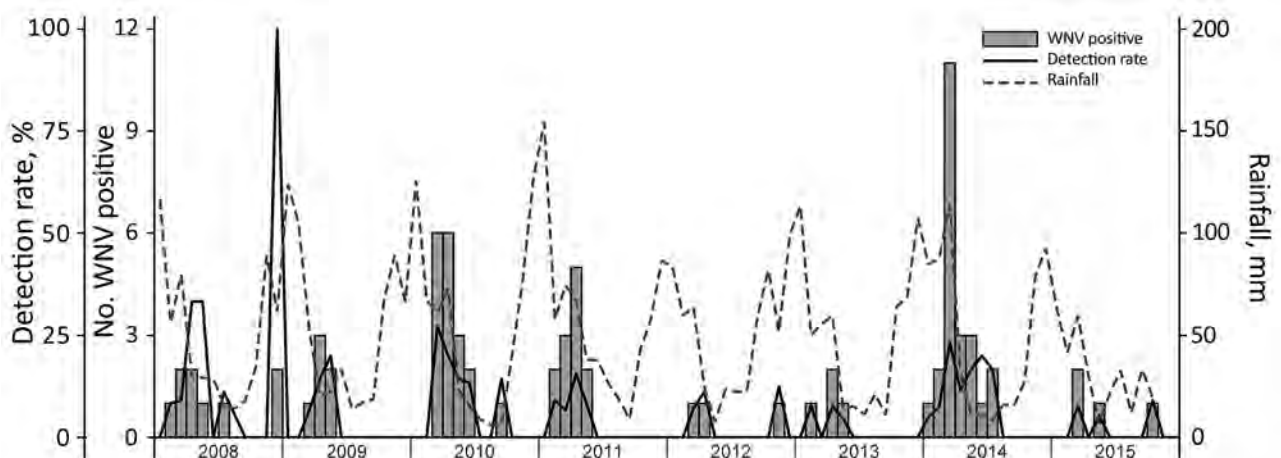


Figure 1. Seasonal occurrence of WNV in horses, South Africa, 2008–2015. Rainfall levels are indicated as a potential correlate for increases in the prevalence of the WNV mosquito vector *Culex univittatus*. WNV, West Nile virus.

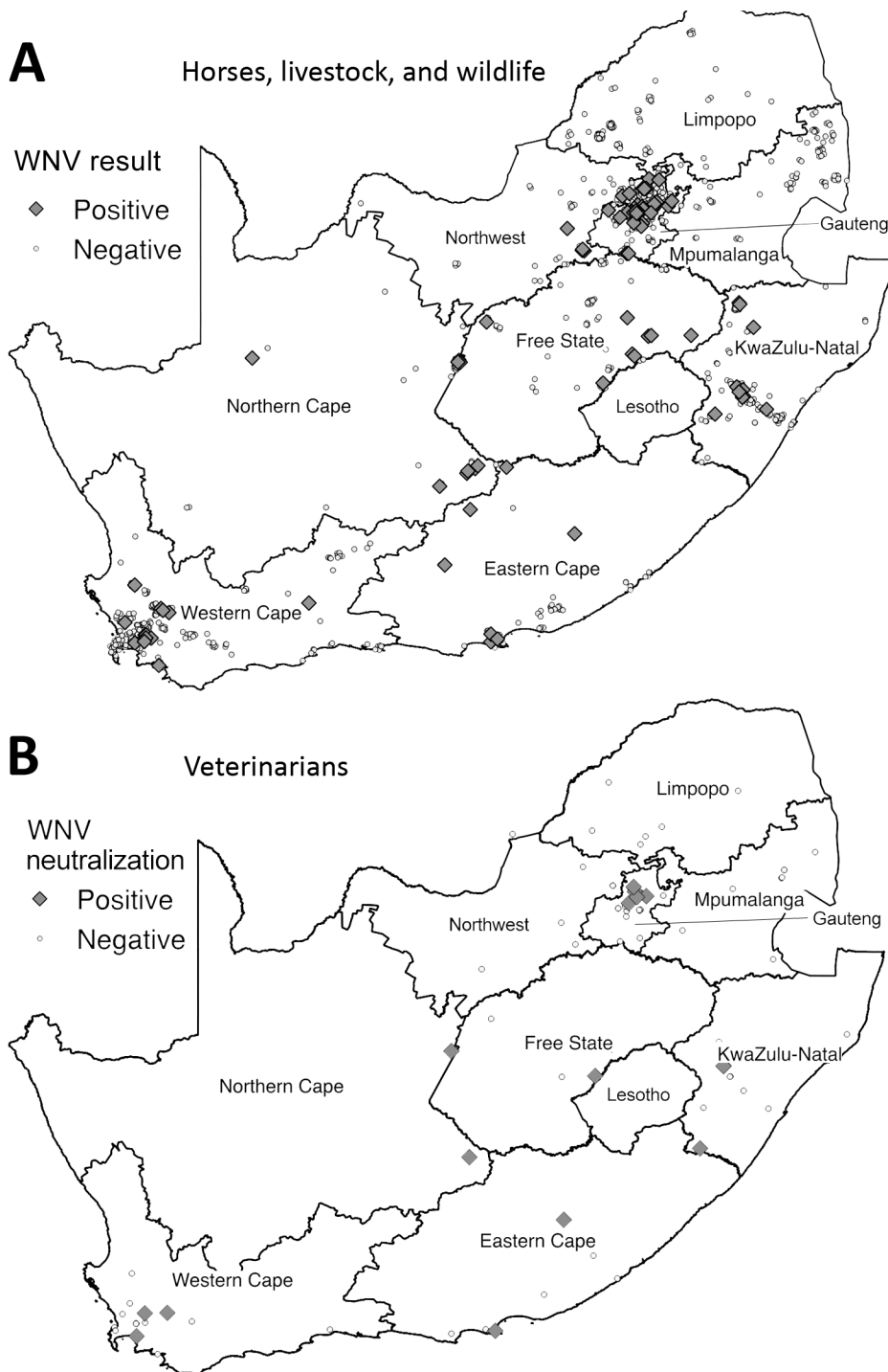


Figure 2. Distribution of WNV cases among horses, livestock animals, and wildlife species during 2008–2015 and of WNV neutralizing antibody–positive veterinarians involved in equine, wildlife, and livestock disease management during 2011–2012, South Africa. A) Samples were collected from horses during 2008–2015 and from livestock and wildlife 2010–2015. Samples were considered positive if they tested positive for WNV genome by PCR or for WNV IgM by WNV IgM Capture ELISA (IDEXX Laboratories, Montpellier, France) and WNV neutralizing antibody by neutralization assay. B) Distribution of veterinarians described in previous report (11). Human serum was considered positive if virus neutralization was observed at a titer of 1:10 and higher. WNV, West Nile virus.

(10.5%) Provinces. Of 152 samples from Limpopo and Mpumalanga Provinces, 99 of which came from wildlife species, none were WNV positive. The geographic distribution of WNV-seropositive veterinarians (11) was similar to that of WNV-positive horses (Figure 2 panel B).

Older horses (≥ 15 y) were least likely (4.9%, 3/61) and 1–4-year-old horses most likely (41.0%, 25/61) to test

WNV positive (Table 2); 35.4% of WNV-positive horses were febrile, 93.7% displayed neurologic signs, and 34.2% died. WNV-associated signs included ataxia, paralysis, paresis, seizures, and tongue paralysis. Multiple logistic regression models (online Technical Appendix Table) confirmed neurologic signs as a strong predictor (aOR 4.12, 95% CI 1.59–10.70) and fever a weak predictor (aOR 1.25,

Table 2. Characteristics of 1,069 horses positive and negative for WNV infection, South Africa, 2008–2015*

Variable	No./total (%)		Crude OR (95% CI)
	WNV negative, n = 990	WNV positive, n = 79	
Detection method and result			
PCR+ IgM–	NA	20/79 (25.3)	
PCR– IgM+	NA	55/79 (69.6)	
PCR+ IgM+	NA	4/79 (5.1)	
Age, y†			
<1	64/617 (10.4)	6/61 (9.8)	1.00 (Reference)
1–4	170/617 (27.6)	25/61 (41.0)	1.57 (0.62–4.00)
5–9	152/617 (24.6)	15/61 (24.6)	1.05 (0.39–2.84)
10–14	145/617 (23.5)	12/61 (19.7)	0.88 (0.32–2.46)
≥15	86/617 (13.9)	3/61 (4.9)‡	0.37 (0.09–1.54)
Died or euthanized§	240/976 (24.6)	27/79 (34.2)	1.59 (0.98–2.59)
Fever¶	389/981 (39.7)	28/79 (35.4)	0.84 (0.52–1.35)
Neurologic signs			
Any neurologic sign#	785/990 (79.3)	74/79 (93.7)	3.86 (1.54–9.68)
Ataxia¶	249/981 (25.4)	21/79 (26.6)	1.06 (0.63–1.79)
Paralysis¶	67/981 (6.8)	10/79 (12.7)	1.98 (0.97–4.01)
Paresis**	71/980 (7.2)	13/79 (16.5)	2.52 (1.33–4.79)
Recumbent¶	105/981 (10.7)	6/79 (7.6)	0.69 (0.29–1.62)
Seizure¶	35/981 (3.6)	4/79 (5.1)	1.44 (0.50–4.16)
Tongue paralysis¶	5/981 (0.5)	2/79 (2.5)	5.07 (0.97–26.56)
Other signs			
Anorexia¶	132/981 (13.5)	6/79 (7.6)	0.53 (0.23–1.24)
Icterus**	63/980 (6.4)	8/79 (10.1)	1.64 (0.76–3.56)
Rectal prolapse¶	6/981 (0.6)	2/79 (2.5)	4.22 (0.84–21.27)

*NA, not applicable; OR, odds ratio; WNV, West Nile virus; +, positive; –, negative.

†Data on age were missing for 391 of 1,069 horses. Test for trend $p = 0.036$.

‡ $p = 0.035$.

§Data on this disease characteristic were missing for 14 of 1,069 horses.

¶Data on this neurologic sign were missing for 9 of 1,069 horses.

#Defined as the presence of any specific neurologic sign or the clinician indicated that it was a neurologic case without indicating specific neurologic signs.

**Data on this neurologic sign were missing for 10 of 1,069 horses.

95% CI 0.75–2.06) of WNV positivity. Paresis (aOR 2.74, 95% CI 1.30–5.79) and tongue paralysis (aOR 7.73, 95% CI 1.27–47.18) were both predictive of WNV positivity.

Conclusions

This 8-year surveillance confirmed annual WNV outbreaks among horses in South Africa, most cases being lineage 2. The neurologic signs and fatality rate among WNV lineage 2–infected horses correlated with those described for lineage 1 in Europe and the United States (4). Locally bred and imported horses appeared similarly susceptible to WNV neurologic disease. Younger animals were more likely to be infected, although all age groups had fatalities. Generalized neurologic signs, such as paresis and paralysis with death, positively correlated with WNV infection in horses. Fatal WNV encephalitis was diagnosed in a giraffe at Onderstepoort Veterinary Research (M. Romito, unpub. data), suggesting certain wildlife species in Africa might be more susceptible; however, we did not detect WNV-positive local wildlife in our sample. WNV-induced fetal death was recorded only once, with lineage 1 infection, but should continue to be monitored.

The geographic distribution of WNV is mainly dependent on favorable ecology, rainfall, and competent vectors. The range of *Culex univittatus* mosquitoes, the

predominant WNV vector, correlated with the geographic distribution of equine cases in South Africa (6). The distribution of WNV exposure among horses correlated with that among humans (Figure 2, panels A, B), suggesting horses could serve as sentinels for human risk for WNV disease in South Africa. Horses have low WNV viremia, precluding them from transmitting infections and establishing epidemics in humans; however, those handling horse central nervous system tissue should do so with caution (15). Vaccination before the start of the rainy season could reduce the risk for WNV in horses.

In summary, surveillance for neurologic disease in animals across South Africa showed WNV lineage 2 as the primary cause of annual outbreaks, with high fatality rates in horses. Horses proved to be good sentinels for WNV in Africa and can be used to determine geographic and seasonal risk patterns for human WNV disease.

Acknowledgments

We thank all veterinarians and animal owners who submitted specimens for this study, as well as the staff members of the Equine Research Centre, University of Pretoria, and Onderstepoort Veterinary Institute; veterinary pathologists who collaborated with us to solve cases; and former research assistants and students.

The protocol was reviewed and approved by the Department of Agriculture Forestry and Fisheries in terms of Section 20 of the Animal Diseases Act (Act No. 35 of 1984) of South Africa and approved by the University of Pretoria Animal Ethics committee, IRB 0000 2235 IORG0001762. Funding was provided by cooperative agreement 1U19GH000571-01 with the Global Disease Detection Centre, US Centers for Disease Control and Prevention, Atlanta, Georgia, USA (2013–2015). Part of this work was funded by the National Research Foundation of South Africa and the National Health Laboratory Services (2008–2012).

Dr. Venter is a professor of medical virology at the Centre for Viral Zoonoses, University of Pretoria, where she heads the Emerging Arbo and Respiratory Virus research group. She specializes in molecular epidemiology and One Health research to investigate zoonotic viruses, particularly neurologic and respiratory viruses, in Africa.

References

- Jupp PG. The ecology of West Nile virus in South Africa and the occurrence of outbreaks in humans. *Ann NY Acad Sci.* 2001;951:143–52. <http://dx.doi.org/10.1111/j.1749-6632.2001.tb02692.x>
- Petersen LR, Roehrig JT. West Nile virus: a reemerging global pathogen. *Emerg Infect Dis.* 2001;7:611–4. <http://dx.doi.org/10.3201/eid0704.017401>
- Danis K, Papa A, Theocharopoulos G, Dougas G, Athanasiou M, Detsis M, et al. Outbreak of West Nile virus infection in Greece, 2010. *Emerg Infect Dis.* 2011;17:1868–72. <http://dx.doi.org/10.3201/eid1710.110525>
- Ward MP, Schuermann JA, Highfield LD, Murray KO. Characteristics of an outbreak of West Nile virus encephalomyelitis in a previously uninfected population of horses. *Vet Microbiol.* 2006;118:255–9. <http://dx.doi.org/10.1016/j.vetmic.2006.07.016>
- Ward MP, Scheuermann JA. The relationship between equine and human West Nile virus disease occurrence. *Vet Microbiol.* 2008;129:378–83. <http://dx.doi.org/10.1016/j.vetmic.2007.11.022>
- Burt FJ, Grobbelaar AA, Leman PA, Anthony FS, Gibson GV, Swanepoel R. Phylogenetic relationships of southern African West Nile virus isolates. *Emerg Infect Dis.* 2002;8:820–6. <http://dx.doi.org/10.3201/eid0808.020027>
- Zaayman D, Venter M. West Nile virus neurologic disease in humans, South Africa, September 2008–May 2009. *Emerg Infect Dis.* 2012;18:2051–4. <http://dx.doi.org/10.3201/eid1812.111208>
- Venter M, Human S, Zaayman D, Gerdes GH, Williams J, Steyl J, et al. Lineage 2 West Nile virus as cause of fatal neurologic disease in horses, South Africa. *Emerg Infect Dis.* 2009;15:877–84. <http://dx.doi.org/10.3201/eid1506.081515>
- Bakonyi T, Ivanics E, Erdélyi K, Ursu K, Ferenczi E, Weissenböck H, et al. Lineage 1 and 2 strains of encephalitic West Nile virus, central Europe. *Emerg Infect Dis.* 2006;12:618–23. <http://dx.doi.org/10.3201/eid1204.051379>
- Ward MP, Levy M, Thacker HL, Ash M, Norman SK, Moore GE, et al. Investigation of an outbreak of encephalomyelitis caused by West Nile virus in 136 horses. *J Am Vet Med Assoc.* 2004;225:84–9. <http://dx.doi.org/10.2460/javma.2004.225.84>
- van Eeden C, Swanepoel R, Venter M. Antibodies against West Nile and Shuni viruses in veterinarians, South Africa. *Emerg Infect Dis.* 2014;20:1409–11. <http://dx.doi.org/10.3201/eid2008.131724>
- van Niekerk S, Human S, Williams J, van Wilpe E, Pretorius M, Swanepoel R, et al. Sindbis and Middelburg old world alphaviruses associated with neurologic disease in horses, South Africa. *Emerg Infect Dis.* 2015;21:2225–9. <http://dx.doi.org/10.3201/eid2112.150132>
- Guthrie AJ, Maclachlan NJ, Joone C, Lourens CW, Weyer CT, Quan M, et al. Diagnostic accuracy of a duplex real-time reverse transcription quantitative PCR assay for detection of African horse sickness virus. *J Virol Methods.* 2013;189:30–5. <http://dx.doi.org/10.1016/j.jviromet.2012.12.014>
- Venter M, Human S, van Niekerk S, Williams J, van Eeden C, Freeman F. Fatal neurologic disease and abortion in mare infected with lineage 1 West Nile virus, South Africa. *Emerg Infect Dis.* 2011;17:1534–6.
- Venter M, Steyl J, Human S, Weyer J, Zaayman D, Blumberg L, et al. Transmission of West Nile virus during horse autopsy. *Emerg Infect Dis.* 2010;16:573–5. <http://dx.doi.org/10.3201/eid1603.091042>

Address for correspondence: Marietjie Venter, Centre for Viral Zoonoses, Department Medical Virology, University of Pretoria, PO Box 2034, Pretoria 0001, South Africa; email: marietjie.venter@up.ac.za

World AIDS Day, December 1



December 1 is World AIDS Day, an opportunity for people to work actively and collaboratively with partners around the world to raise awareness about HIV and help us move closer to the goal of an AIDS-free generation. This year's theme, "The Time to Act Is Now," calls us to act with urgency to implement the latest high-impact, evidence-based HIV prevention strategies.

<http://wwwnc.cdc.gov/eid/page/world-aids>

**EMERGING
INFECTIOUS DISEASES®**

Tick-Borne Encephalitis in Sheep, Romania

Jiri Salat, Andrei D. Mihalca, Marian Mihaiu,
David Modrý, Daniel Ruzek

Little is known about the occurrence of tick-borne encephalitis in Romania. Sheep are an infection source for humans and are useful sentinels for risk analysis. We demonstrate high antibody prevalence (15.02%) among sheep used as sentinels for this disease in 80% of the tested localities in 5 counties of northwestern Romania.

Tick-borne encephalitis (TBE) virus (family *Flaviviridae*, genus *Flavivirus*), is a zoonotic pathogen that causes severe neurologic disease in humans. In Europe, most cases of TBE are reported in Scandinavia and in countries in Central and Eastern Europe countries, but little is known about the current TBE epidemiologic situation in Romania.

The main tick vector for TBE virus, *Ixodes ricinus*, prefers leaf litter and the lower vegetation layers of temperate deciduous and mixed forests. In areas with high rainfall, *I. ricinus* ticks also occur in high densities in coniferous forests and in open areas such as grasslands (1). *I. ricinus* ticks are widely distributed in Romania (2) and are the most common ticks found on a variety of vertebrate hosts, including humans (3,4).

Large domestic animals such as goats, sheep, and cattle are potential hosts for *I. ricinus* ticks. These animals may also develop an antibody response after infection with TBE virus without showing clinical signs and thus are a source of TBE virus among humans who consume nonpasteurized milk and milk products, which makes them valuable sentinels for the identification of TBE risk areas (5).

Romania has the third largest sheep flock in the European Union (EU), after Great Britain and Spain, totaling ~9.5 million sheep, which accounts for 11% of the total EU flock. Most of the animals are used for milk and meat production. The purpose of this study was to determine the current TBE virus infection status in northwestern Romania by using sheep as sentinels for TBE virus circulation.

Author affiliations: Veterinary Research Institute, Brno, Czech Republic (J. Salat, D. Ruzek); University of Agricultural Sciences and Veterinary Medicine, Cluj-Napoca, Romania (A.D. Mihalca, M. Mihaiu); Faculty of Veterinary Medicine and CEITEC VFU, University of Veterinary and Pharmaceutical Sciences, Brno (D. Modrý); Institute of Parasitology, Biology Centre of the Czech Academy of Sciences, Ceske Budejovice, Czech Republic (D. Ruzek)

DOI: <https://doi.org/10.3201/eid2312.170166>

The Study

In September 2016, we randomly selected 519 serum aliquots from adult sheep from samples previously collected (July–August 2016) by the National Program for Surveillance, Prevention, Control and Eradication of Animal Diseases in 5 counties in northwestern Romania (Figure). The counties, number of samples, and number of sampling sites were Bihor, 119 samples, 12 locations; Bistrița-Năsăud, 100 samples, 10 locations; Cluj, 100 samples, 7 locations; Mureș, 100 samples, 11 locations; and Sălaj, 100 samples, 10 locations). We froze the aliquots at -20°C before processing. We used the IMMUNOZYM FSME (TBE) IgG All-Species kit (Progen GmbH, Heidelberg, Germany) ELISA to detect TBE virus antibodies. We retested samples exhibiting ≥ 25 Vienna units/mL by using virus neutralization test (VNT) as described previously (6).

We tested samples from 168 (32.37%) sheep with borderline or positive results from ELISA by using VNT, and this method identified 78 (15.02%) animals as positive for antibodies specifically neutralizing TBE virus (online Technical Appendix Table, <http://wwwnc.cdc.gov/EID/article/23/12/17-0166-Techapp1.pdf>). Positive results were distributed among the counties we investigated: the highest seroprevalence was identified in sheep in Bihor County (27.73%) and the lowest seroprevalence in Mureș County (2%) (Table; Figure). We found positive sheep samples in 40 (80%) of 50 examined locations.

Conclusions

TBE has been reported previously in Romania, but few studies confirmed the presence of the virus (7–10). However, in the past 3 decades, except for a few occasional records (11) and small-scale serologic surveys during clinical outbreaks, there have been large knowledge gaps in the studies on TBE in Romania, and the prevalence and distribution remain fairly unknown. We used sheep as sentinels for TBE virus distribution in northwestern Romania and identified the virus by VNT in 15.02% of sheep in 40 of 50 examined localities in 5 counties.

According to the latest technical report by the European Centre for Disease Control and Prevention (12), during 2008–2010, only 14 cases of TBE were reported among humans in Romania. All 14 cases originated in 5 counties in northwestern Romania; incidence was low ($<0.5/100,000$ inhabitants) in Bihor, Bistrița-Năsăud, Cluj, and Mureș and moderate ($0.5\text{--}4.0/100,000$ inhabitants) in Sălaj. In a recent survey done by collecting *I. ricinus* ticks from vegetation, livestock, and reptiles in central

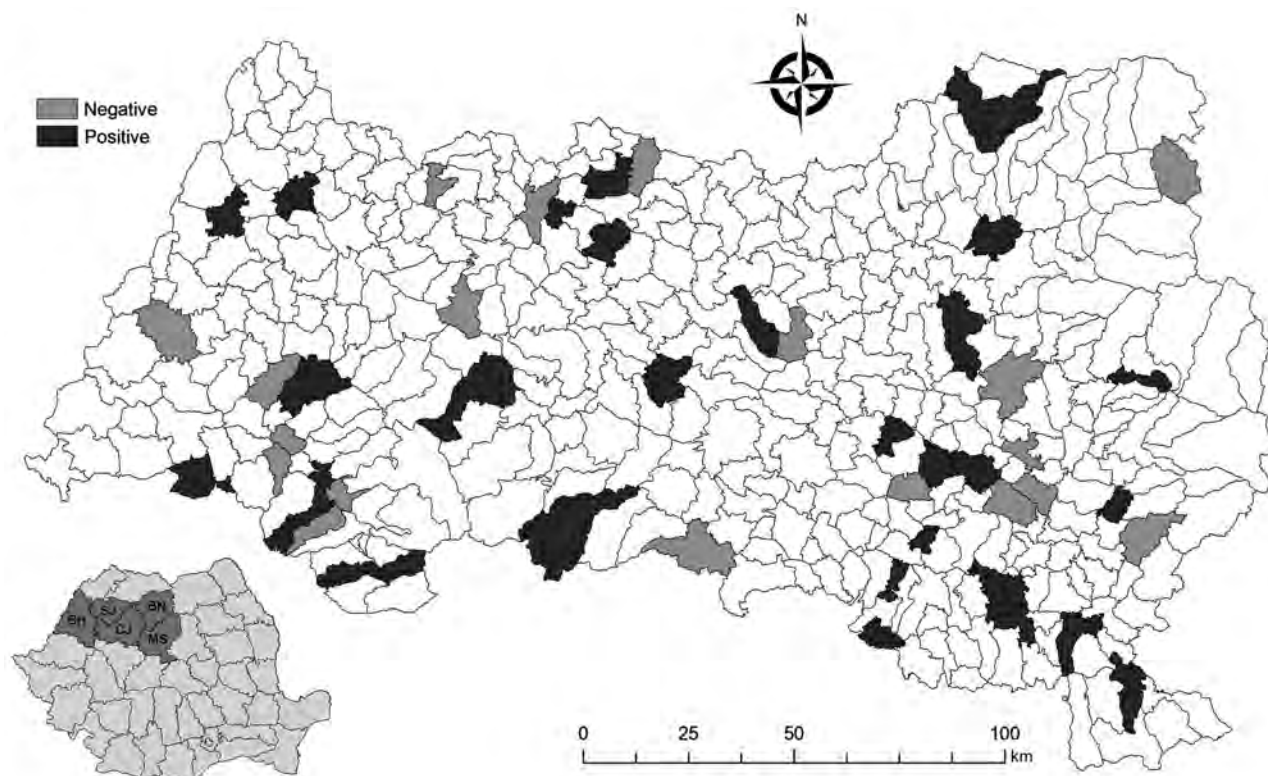


Figure. Locations in northwestern Romania where sheep were positive for tick-borne encephalitis virus–specific antibodies, determined by using virus neutralization test (6). BH, Bihor; BN, Bistrița-Năsăud; CJ, Cluj; MS, Mureș; SJ, Sălaj.

and southeastern Romania, the prevalence of the TBE virus estimated by using molecular methods was <1% (13). Coipan et al. evaluated the seropositivity for TBE in 51 patients who had neurologic signs and were admitted to a hospital in Sibiu County, Romania; specific TBE antibodies were found in samples from 38 (75%) patients (14). An outbreak of rural TBE was reported in the central Romania region of Transylvania, related to consumption of infected goat milk; specific serology in 41.5% of the patients was positive for TBE virus (15). Similar seroprevalence studies in other outbreaks found lower seropositivity values (5.8%–11.6%) in human patients (15); the same study randomly evaluated 1,669 human serum samples from Transylvania and reported a 0.5% seroprevalence for TBE. Taken together, these results suggest that clinical

cases of TBE in Romania are largely underreported, and many case-patients are misdiagnosed.

Our study confirms that TBE virus is endemic in northwestern Romania and should be considered a public health risk in this country. Considering the number of sheep and their almost ubiquitous presence in this country, their sentinel role in countrywide mapping of the TBE distribution should be evaluated.

This study was partially supported by the Czech Science Foundation (project No. 16-20054S) and by project LO1218 with financial support from the Ministry of Education, Youth and Sports of the Czech Republic under the NPU I program. J.S. was supported by project QJ1510104 of the Ministry of Agriculture of the Czech Republic. The work has been done under the frame of COST Action TD1303 “EurNegVec.”

Table. Seroprevalence of tick-borne encephalitis in sheep, northwestern Romania*

County	No. samples	No. locations	ELISA-positive samples,		VNT-positive samples,	
			%†	%	%	No. VNT-positive locations
Bihor	119	12	29.41	27.73		11
Bistrița-Năsăud	100	10	18.00	12.00		5
Cluj	100	7	67.00	11.00		5
Mureș	100	11	16.00	2.00		2
Sălaj	100	10	32.00	20.00		9
Total	519	50	32.37	15.2		32

*Testing locations were within communes subdivision of counties in Romania.

†Includes all positive and suggestive samples with antibody titer ≥ 25 Vienna units/mL.

Dr. Salat is a research scientist at the Veterinary Research Institute, Brno, Czech Republic. His research interests include tick-borne encephalitis and other zoonotic viral diseases.

References

1. Gray JS, Kahl O, Robertson JN, Daniel M, Estrada-Peña A, Gettinby G, et al. Lyme borreliosis habitat assessment. *Zentralbl Bakteriol.* 1998;287:211–28. [http://dx.doi.org/10.1016/S0934-8840\(98\)80123-0](http://dx.doi.org/10.1016/S0934-8840(98)80123-0)
2. Mihalca AD, Gherman CM, Magdaş C, Dumitrache MO, Györke A, Sándor AD, et al. *Ixodes ricinus* is the dominant questing tick in forest habitats in Romania: the results from a countrywide dragging campaign. *Exp Appl Acarol.* 2012;58:175–82. <http://dx.doi.org/10.1007/s10493-012-9568-3>
3. Mihalca AD, Dumitrache MO, Magdaş C, Gherman CM, Domşa C, Mircean V, et al. Synopsis of the hard ticks (*Acari: Ixodidae*) of Romania with update on host associations and geographical distribution. *Exp Appl Acarol.* 2012;58:183–206. <http://dx.doi.org/10.1007/s10493-012-9566-5>
4. Briciu VT, Titilincu A, Țăulescu DF, Cârștina D, Lefkaditis M, Mihalca AD. First survey on hard ticks (*Ixodidae*) collected from humans in Romania: possible risks for tick-borne diseases. *Exp Appl Acarol.* 2011;54:199–204. <http://dx.doi.org/10.1007/s10493-010-9418-0>
5. Klaus C, Beer M, Saier R, Schau U, Moog U, Hoffmann B, et al. Goats and sheep as sentinels for tick-borne encephalitis (TBE) virus—epidemiological studies in areas endemic and non-endemic for TBE virus in Germany. *Ticks Tick Borne Dis.* 2012;3:27–37. <http://dx.doi.org/10.1016/j.ttbdis.2011.09.011>
6. Širmarová J, Tichá L, Golovchenko M, Salát J, Grubhoffer L, Rudenko N, et al. Seroprevalence of *Borrelia burgdorferi* sensu lato and tick-borne encephalitis virus in zoo animal species in the Czech Republic. *Ticks Tick Borne Dis.* 2014;5:523–7. <http://dx.doi.org/10.1016/j.ttbdis.2014.03.008>
7. Drăgănescu N. Study of some current viral encephalitides in the Socialist Republic of Rumania [in Rumanian]. *Stud Cercet Inframicrobiol.* 1968;19:297–312.
8. Drăgănescu N, Gîrjabu E, Iftimovici R, Totescu E, Iacobescu V, Tudor G, et al. Investigations on the presence of antibodies to alphaviruses, flaviviruses, Bunyavirus and Kemerovo virus in humans and some domestic animals. *Virologie.* 1978;29:107–11.
9. Drăgănescu N. Study of arboviruses in Romania (1958–1978). Results obtained in the “Stefan S. Nicolau” Institute of Virology. *Virologie.* 1979;30:283–93.
10. Ardeleanu D, Ardeleanu A, Albeanu M, Pricunda G, Drăgănescu N. Some epidemiological aspects of infections caused by tick-borne encephalitis virus in the region of Gorj [in Romanian]. *Stud Cercet Inframicrobiol.* 1968;19:87–90.
11. Petrescu A, Copelovici Y, Drăgănescu N, Birnaure F, Gîrjabu E, Mihail A, et al. The evidence of circulation of some viruses in a great town of Romania during the first half of 1992. *Rev Roum Virol.* 1993;44:243–51.
12. European Centre for Disease Prevention and Control. Epidemiological situation of tick-borne encephalitis in the European Union and European Free Trade Association countries. Stockholm: The Centre; 2012 [cited 2017 Aug 31]. <https://ecdc.europa.eu/en/publications-data/epidemiological-situation-tick-borne-encephalitis-european-union-and-european>
13. Vladimirescu A, Dumitrescu G, Ionescu L, Neculescu M, Moraru V, Popescu D, et al. Real-Time PCR studies regarding the *Borrelia burgdorferi*, *Francisella tularensis*, tick borne encephalitis virus (TBEv) and Crimean Congo hemorrhagic fever virus (CCHFv) occurrence in the Romanian ticks. *Int J Infect Dis.* 2016;45S:193–4. <http://dx.doi.org/10.1016/j.ijid.2016.02.448>
14. Coipan EC, Alexse A, Vladimirescu AF, Nicolescu G. Seropositivity among human subjects for both TBEV and *Borrelia burgdorferi* s.l. during a TBE outbreak in Sibiu County, Romania. *Int J Infect Dis.* 2008;12(S1):e334. <http://dx.doi.org/10.1016/j.ijid.2008.05.892>
15. Molnár GB, Persecă T, Feder A, Păcuraru D, Marialaki E, Cojan A. Epidemiological assessment of morbidity and natural foci of TBE-CEE virus infection in Transylvania [in Romanian]. *Rev Med Chir Soc Med Nat Iasi.* 2008;112:471–7.

Address for correspondence: Andrei D. Mihalca, Faculty of Veterinary Medicine, University of Agricultural Sciences and Veterinary Medicine, Calea Manastur 3-5, Cluj-Napoca 400372, Romania; email: amihalca@usamvcluj.ro



Manage your email alerts so you only receive content of interest to you.

Sign up for an online subscription:
wwwnc.cdc.gov/eid/subscribe.htm

Newly Recognized Pediatric Cases of Typhus Group Rickettsiosis, Houston, Texas, USA

Medscape EDUCATION **ACTIVITY**



JOINTLY ACCREDITED PROVIDER™
INTERPROFESSIONAL CONTINUING EDUCATION

In support of improving patient care, this activity has been planned and implemented by Medscape, LLC and Emerging Infectious Diseases. Medscape, LLC is jointly accredited by the Accreditation Council for Continuing Medical Education (ACCME), the Accreditation Council for Pharmacy Education (ACPE), and the American Nurses Credentialing Center (ANCC), to provide continuing education for the healthcare team.

Medscape, LLC designates this Journal-based CME activity for a maximum of 1.00 **AMA PRA Category 1 Credit(s)**™. Physicians should claim only the credit commensurate with the extent of their participation in the activity.

All other clinicians completing this activity will be issued a certificate of participation. To participate in this journal CME activity: (1) review the learning objectives and author disclosures; (2) study the education content; (3) take the post-test with a 75% minimum passing score and complete the evaluation at <http://www.medscape.org/journal/eid>; and (4) view/print certificate. For CME questions, see page 2135.

Release date: November 16, 2017; Expiration date: November 16, 2018

Learning Objectives

Upon completion of this activity, participants will be able to:

- Evaluate clinical features of cases of typhus group rickettsiosis (TGR) at a large, Houston-area pediatric hospital between 2008 and 2016, based on a retrospective medical record review
- Compare epidemiological features of cases of TGR at a large, Houston-area pediatric hospital between 2008 and 2016, based on a retrospective medical record review
- Assess the public health implications of cases of TGR at a large, Houston-area pediatric hospital between 2008 and 2016, based on a retrospective medical record review

CME Editor

Dana C. Dolan, BS, Copyeditor, Emerging Infectious Diseases. *Disclosure: Dana C. Dolan, BS, has disclosed no relevant financial relationships.*

CME Author

Laurie Barclay, MD, freelance writer and reviewer, Medscape, LLC. *Disclosure: Laurie Barclay, MD, has disclosed the following relevant financial relationships: owns stock, stock options, or bonds from Alnylam; Biogen; Pfizer.*

Authors

Disclosures: Timothy Erickson, MSPH; Juliana da Silva, MD; Melissa S. Nolan, MPH, PhD; Flor M. Munoz, MD; and Kristy O. Murray, DVM, PhD, have disclosed no relevant financial relationships. Lucila Marquez, MD, MPH, has disclosed the following relevant financial relationship: received grants for clinical research from Cempra.

**Timothy Erickson, Juliana da Silva,
Melissa S. Nolan, Lucila Marquez,
Flor M. Munoz, Kristy O. Murray**

An increase in typhus group rickettsiosis and an expanding geographic range occurred in Texas, USA, over a decade. Because this illness commonly affects children, we retrospectively examined medical records from 2008–2016 at a large Houston-area pediatric hospital and identified 36 cases. The earliest known cases were diagnosed in 2011.

Author affiliations: The University of Texas Health Science Center, Houston, Texas, USA (T. Erickson); Baylor College of Medicine and Texas Children's Hospital, Houston (T. Erickson, J. da Silva, M.S. Nolan, L. Marquez, F.M. Munoz, K.O. Murray)

DOI: <https://doi.org/10.3201/eid2312.170631>

Typus group rickettsiosis (TGR) is a vectorborne zoonotic disease most commonly caused by the bacterium *Rickettsia typhi*, the etiologic agent of murine typhus. Since 2003, the annual incidence of TGR cases in Texas has increased and expanded geographically (1). Recently, a study conducted in Galveston County found that 7 of 18 persons with acute fever were positive for *R. typhi* (2). In the Houston/Harris County metropolitan area, which is adjacent to Galveston County, TGR was first reported to the Texas Department of State Health Services (TXD-SHS) in 2007 (1). By 2013, 27 cases had been reported to the state. Because the highest attack rate occurs in children 5–19 years of age, we became concerned that children with possible *R. typhi* infection were brought to Texas Children's Hospital (TCH), a large, 692-bed pediatric

Table. Demographic, social, and clinical characteristics of pediatric typhus group rickettsiosis case-patients, Houston, TX, USA, 2008–2016*

Characteristic	All cases, n = 36	Confirmed cases, n = 18	Probable cases, n = 13	Suspected cases, n = 5
Median age (range), y	11 (2–23)	9 (2–23)	9 (4–17)	16 (8–19)
Sex				
M	18 (50)	7 (39)	7 (54)	4 (80)
F	18 (50)	11 (61)	6 (46)	1 (20)
Race/ethnicity				
White	19 (53)	8 (44)	9 (69)	2 (40)
Hispanic	15 (42)	9 (50)	4 (31)	2 (40)
Other or unknown	2 (6)	1 (6)	0	1 (20)
Exposures				
Dogs	17 (47)	9 (50)	8 (62)	0
Cats	16 (44)	8 (44)	6 (46)	2 (40)
Opossums	2 (6)	1 (6)	0	1 (20)
Fleas	8 (22)	4 (22)	3 (23)	1 (20)
History of travel				
To endemic area of Texas	4 (11)	4 (22)	0	0
To endemic area outside United States	2 (6)	2 (11)	0	0
To area with no known <i>Rickettsia typhi</i>	4 (11)	3 (17)	1 (8)	0
Signs and symptoms				
Fever	35 (97)	17 (94)	13 (100)	5 (100)
Rash	26 (72)	13 (72)	10 (77)	3 (60)
Headache	14 (39)	8 (44)	3 (23)	3 (60)
Malaise	13 (36)	8 (44)	5 (39)	2 (40)
Vomiting	12 (33)	7 (39)	4 (31)	1 (20)
Anorexia	11 (31)	7 (39)	4 (31)	0
Classical triad†	11 (31)	5 (28)	3 (23)	3 (60)
Lymphadenopathy	10 (28)	4 (22)	4 (31)	2 (40)
Abdominal pain	10 (28)	5 (28)	4 (31)	1 (20)
Conjunctivitis	9 (25)	4 (22)	4 (31)	1 (20)
Clinical findings				
Hepatosplenomegaly	6 (19)	4 (22)	2 (15)	1 (20)
Altered mental status	3 (8)	3 (17)	0	0
Elevated aminotransaminases				
Aspartate aminotransaminase	31 (86)	16 (89)	11 (85)	4 (80)
Alanine aminotransaminase	32 (89)	17 (94)	11 (85)	4 (80)
Hypoalbuminemia	11 (31)	6 (33)	3 (23)	2 (40)
Thrombocytopenia	22 (61)	11 (61)	9 (69)	2 (40)
Median days hospitalized (range)	5 (0–14)	6 (1–14)	5 (0–10)	4 (0–5)
PICU admissions	7 (19)	5 (28)	2 (15)	0
Median titer for <i>R. typhi</i> (range)	1:1,024 (1:64–16,384)	1:2,048 (1:1,024–1:16,384)	1:256 (1:128–1:512)	1:64 (1:64)

*Values are no. (%) except as indicated. A confirmed case was defined by one of the following: 1) immunofluorescent antibody (IFA) assay titer $\geq 1:1,024$, and a titer for *R. typhi* ≥ 2 -fold greater than that for *R. rickettsii* to rule out cross-reactivity; 2) PCR positive; or 3) ≥ 4 -fold increase in titer between acute and convalescent specimens. A probable case was defined as 1) an IFA titer $\geq 1:128$, and a titer for *R. typhi* ≥ 2 -fold greater than *R. rickettsii* and 2) clinically compatible illness involving fever with rash. A suspected case was defined as 1) IFA titer $\geq 1:64$ and negative titer for *R. rickettsii* and 2) clinically compatible illness.

†Symptoms were fever, headache, and rash.

hospital system in Houston. To evaluate this recent emergence, we retrospectively searched the hospital diagnostic testing database to identify all TGR-positive patients.

The Study

We conducted a retrospective review to identify TGR patients seen at TCH from January 1, 2008, through December 31, 2016. We identified cases by searching all laboratory orders for rickettsial panel immunofluorescent antibody (IFA) testing. We determined these patients' case status by following guidance from TXDSHS (1). We defined a confirmed case as 1 of the following: 1) IFA assay titer $\geq 1:1024$ and a titer for *R. typhi* ≥ 2 -fold greater than that for *R. rickettsii*; 2) a positive PCR result; or 3) a ≥ 4 -fold

increase in titer between acute and convalescent specimens. We defined a probable case as IFA titer $\geq 1:128$ and a titer for *R. typhi* ≥ 2 -fold greater than that for *R. rickettsii*; and a clinically compatible illness involving fever with rash. We defined a suspected case as IFA titer $\geq 1:64$ and negative titer for *R. rickettsii*; and clinically compatible illness. We abstracted demographic and clinical data on all identified TGR case-patients.

When searching diagnostic laboratory orders for rickettsial IFA, we identified 425 test submissions. On the basis of diagnostic results and clinical compatibility, we identified 36 TGR cases: 18 confirmed, 13 probable, and 5 suspected cases. One case was additionally confirmed *R. typhi*-positive by PCR at the Centers for Disease Control

and Prevention (Atlanta, GA, USA). Only 3 case-patients had convalescent specimens collected, and each yielded ≥ 4 -fold increase in titer, thereby confirming infection.

The case population was predominantly non-Hispanic whites (53%) (Table), which were overrepresented when compared with the proportion of 31% from the Houston/Harris County US Census population for mid-2016 (3). Hispanics represented 42% of the patient population, which matched the known census population (42%) The black population was underrepresented (0% of patients vs. 20% Census population) (3).

Upon review of the medical records, nearly all case-patients (35/36; 97%) were febrile when they sought care (median temperature 103°F) (Table). Eleven (31%) case-patients had the classical triad for typhus of fever, rash, and headache. Other common symptoms included malaise, vomiting, anorexia, abdominal pain, lymphadenopathy, and conjunctivitis. Approximately one fifth had hepatosplenomegaly noted on physical exam. Most case-patients also had elevated transaminases (86%) and thrombocytopenia (61%). A median of 8 days elapsed between symptom onset and arrival at the hospital for medical care and 13 days from symptom onset to defervescence. Whereas the median time from symptom onset to initiation of treatment was 12 days, the median time from initiation of doxycycline treatment to defervescence was only 1 day.

Most case-patients (30/36; 83%) were admitted for hospitalization, with a median length of stay of 5 days. Of those, 7 (19%) required intensive care due to severity of illness. Hispanic patients were significantly more likely to be admitted to the pediatric intensive care unit (86% of these patients were Hispanic; odds ratio 12.7, 95% CI 1.2–612.3; $p = 0.027$ by 2-tailed Fisher exact test). No deaths occurred.

All but 2 case-patients had reported animal exposure, and 27 (75%) had reported exposure to either domestic

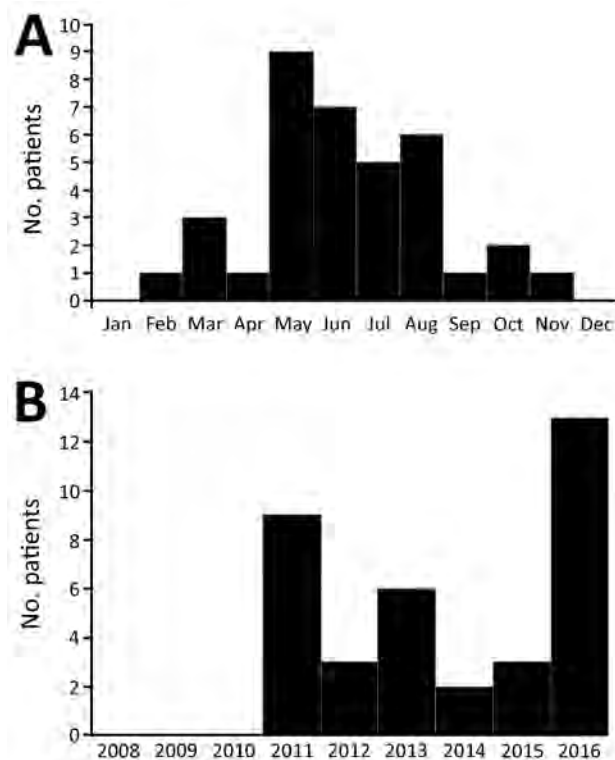


Figure 1. Temporal distribution of *Rickettsia typhi*-positive pediatric case-patients by time of symptom onset, Houston, Texas, USA, 2011–2016. A) By month of symptom onset. B) By year of symptom onset.

dogs or cats. Two case-patients reported contact with an opossum; 1 of these had no contact with domestic pets. Eight case-patients reported contact with fleas, and all 8 also reported animal contact. Most cases were reported during summer months when fleas are most prevalent (Figure 1, panel A). No TGR cases were diagnosed in

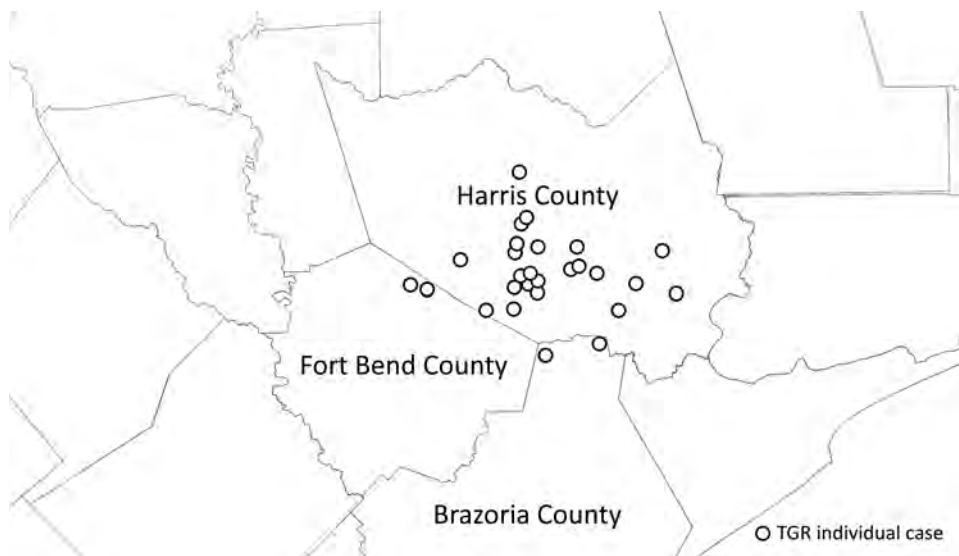


Figure 2. Spatial distribution of *Rickettsia typhi*-positive pediatric case-patients with no history of travel by location of residence around the Houston/Harris County, Texas, USA, metropolitan region.

2008–2010. The year with the highest number of cases was 2016 (Figure 1, panel B).

Thirty (83%) case-patients resided in the Houston metropolitan area; cases were geographically clustered in western Houston (Figure 2). Of these case-patients, 26 (72%) had no history of travel. Three cases were within 70 miles of the Louisiana border. In Louisiana, TGRs are not reportable diseases (4).

Recently, we demonstrated evidence of TGR re-emergence into new geographic areas of Texas, including Houston/Harris County, the third most populated county in the United States (1). Here we present the clinical findings of pediatric patients with TGRs in the Houston metropolitan area, starting in 2011. To track this evidence of emergence, it is critical to raise clinical awareness and encourage testing, diagnosis, and public health reporting of new cases.

Rickettsial infections are reportable in Texas, with cases passively reported by medical care providers. In working with TXDSHS, we cross-referenced our patient list with the public health surveillance database and found only 15 (48%) of the 31 confirmed or probable cases were reported, highlighting a critical gap in passive surveillance. Reporting did improve over time, with 71% (10/14) of 2015–2016 cases reported to TXDSHS, compared with only 29% (5/17) of 2011–2014 cases. Barriers to reporting could be related to low awareness of reporting requirements, complexity of patient care, and the inherent delays in receiving testing results, typically after discharge. Public health surveillance is critical for disease tracking, prevention, and control efforts; therefore, further work is needed to optimize public health reporting of rickettsial infections.

Approximately one third of the pediatric TGR cases we report exhibited the classic triad of fever, headache, and rash, which is considered the hallmark of *R. typhi* infection. Another pediatric study also reported similar findings (5). The severity of illness in our patients was remarkable, with 1 in 5 patients requiring intensive care. Early clinical suspicion, diagnosis, and appropriate treatment of suspected rickettsial infections is critical to shorten the duration of illness and prevent serious, life-threatening outcomes.

Our study documents the identification and clinical description of pediatric cases of TGRs in the Houston area. While we believe TGR is emerging locally, it is plausible that prior cases simply went undetected and undiagnosed. A study conducted in 2004 found that 10% of homeless persons in Houston tested seropositive for *R. typhi* (6). That study looked only at past exposure, however, so we do not know where those persons acquired the infection. Because studies are lacking in this region regarding the specific

reservoirs and vectors responsible for transmission, establishing research in this area is critical.

Conclusions

The recent emergence of TGRs in Houston poses a public health threat. Our report provides insight into the presentation and epidemiology of disease in a pediatric population. It is still unknown what factors put these children at risk for infection. The sylvatic and domestic transmission cycles of *R. typhi*, including vectors and mammalian reservoirs, require further investigation. Improved physician awareness through reporting of clinical studies and case series will assist in appropriate diagnosis and management of disease throughout Texas and the southern United States.

Acknowledgments

We thank Bonny Mayes for assisting with cross-referencing our cases with the state surveillance database.

This study was reviewed and approved by the Baylor College of Medicine Institutional Review Board (H-34878).

Mr. Erickson is a doctoral student in epidemiology at the University of Texas Health Science Center at Houston, School of Public Health. He received his MSPH in public health from Texas A&M University. His research interests include the epidemiology of infectious diseases, particularly rickettsial diseases.

References

1. Murray KO, Evert N, Mayes B, Fonken E, Erickson T, Garcia MN, et al. Typhus group rickettsiosis, Texas, USA, 2003–2013. *Emerg Infect Dis.* 2017;23:645–8. <http://dx.doi.org/10.3201/eid2304.160958>
2. Blanton LS, Vohra RF, Bouyer DH, Walker DH. Reemergence of murine typhus in Galveston, Texas, USA, 2013. *Emerg Infect Dis.* 2015;21:484–6. <http://dx.doi.org/10.3201/eid2103.140716>
3. US Census Bureau. Quick facts: Harris County, Texas. 2015 [cited 2016 Aug 1]. <http://www.census.gov/quickfacts/table/AGE275210/48201>
4. Louisiana Department of Health. Sanitary code—state of Louisiana. Part 2—the control of disease. 2016 [cited 2017 Sep 26] <http://new.dhh.louisiana.gov/assets/oph/Center-PHCH/Center-CH/infectious-epi/Surveillance/sanitarycode.pdf>.
5. Whiteford SF, Taylor JP, Dumler JS. Clinical, laboratory, and epidemiologic features of murine typhus in 97 Texas children. *Arch Pediatr Adolesc Med.* 2001;155:396–400. <http://dx.doi.org/10.1001/archpedi.155.3.396>
6. Reeves WK, Murray KO, Meyer TE, Bull LM, Pascua RF, Holmes KC, et al. Serological evidence of typhus group rickettsia in a homeless population in Houston, Texas. *J Vector Ecol.* 2008;33:205–7. [http://dx.doi.org/10.3376/1081-1710\(2008\)33\[205:SEOTGR\]2.0.CO;2](http://dx.doi.org/10.3376/1081-1710(2008)33[205:SEOTGR]2.0.CO;2)

Address for correspondence: Kristy O. Murray, Baylor College of Medicine, 1102 Bates Ave, Ste 550, Houston, TX 77030, USA; email: kmurray@bcm.edu

Identification of *Dermacentor reticulatus* Ticks Carrying *Rickettsia raoultii* on Migrating Jackal, Denmark

Kirstine Klitgaard, Mariann Chriél,
Anastasia Isbrand, Tim K. Jensen, René Bødker

From a migrating golden jackal (*Canis aureus*), we retrieved 21 live male *Dermacentor reticulatus* ticks, a species not previously reported from wildlife in Denmark. We identified *Rickettsia raoultii* from 18 (86%) of the ticks. This bacterium is associated with scalp eschar and neck lymphadenopathy after tick bite syndrome among humans.

Since 2012, Denmark has received a sudden and poorly understood wave of gray wolves (*Canis lupus*) and golden jackals (*C. aureus*) migrating long distances from their birthplaces in eastern and central Europe (1). These long-distance dispersals create a risk for introducing tick vectors and pathogens to new geographic areas. We report discovery of *Dermacentor reticulatus* ticks infected with *Rickettsia raoultii* from a wild golden jackal in Thorsminde, in the western region of Denmark.

The Study

In February 2017, the wildlife service delivered the body of a golden jackal from Western Jutland, >200 km north of the Denmark–Germany border, to the National Veterinary Institute (Lyngby, Denmark). During necropsy, we collected 21 male *Dermacentor reticulatus* ticks, a species that had not previously been reported among wildlife in Denmark. We screened the ticks and a blood sample from the jackal for tickborne pathogens by using a high-throughput real-time PCR (2). This assay enables simultaneous detection of 37 European tickborne pathogens, including the spotted fever group (SFG) *Rickettsia*, and specifically the species *R. conorii*, *R. slovaca*, *R. massiliae*, and *R. helvetica*, as well as confirmation of 4 tick species, including *D. reticulatus* (2). Tick DNA was extracted as previously described (3).

PCR confirmed the morphologic characterization: all the ticks collected from the jackal were *D. reticulatus*. One tick contained *Anaplasma phagocytophilum*, and 18 ticks contained SFG *Rickettsia* spp.; however, the specific *Rickettsia* species was not among the 4 species included in the PCR. To identify the species, we PCR amplified the *ompA*, *ompB*, and *gltA* genes for a subset of 4 samples and

sequenced them as previously described (4,5). For the remaining 14 samples, we sequenced the *ompA* gene. A BLAST search (<http://www.ncbi.nlm.nih.gov/BLAST/>) identified the *ompB* gene as 100% and the *ompA* and *gltA* genes as 99% identical to the genome sequence of the type strain of *Rickettsia raoultii* sp. nov. strain Khabarovsk^T (CSUR R3^T, ATCC VR-1596^T) (6). The specific primers used for gene amplification and sequencing of bacteria identified from *D. reticulatus* ticks by real-time PCR are provided in the Table. We deposited the sequences we obtained into GenBank (accession nos. MF166729–36 and MF166741–44).

The surge of large carnivores, reaching countries in northern Europe from breeding areas in central Europe, is a recent development that appears to be caused by reduced hunting resulting from effective wildlife protection (1,7). This migration may facilitate the spread of vectors and zoonotic pathogens into new regions. Even if these migrations do not result in the establishment of a new carnivore population, Denmark has high fox and deer densities in the forests, as well as farm animals grazing on pastures, that can support tick species such as *D. reticulatus* or *D. marginatus*.

D. reticulatus ticks are spreading rapidly through Europe, and changes in the environment, climate, or both seem to be favorable to the establishment of this tick in areas not previously supporting populations of the species (8). *D. reticulatus* ticks are established in the southern United Kingdom, and recently, also in the Netherlands. Both countries lack wolf and jackal populations (9). Therefore, it is the actual process of migration and not the establishment of the carnivores in Denmark that constitutes a risk.

However, for these migrations to result in the introduction of ticks, the migrations must first originate in *Dermacentor* tick–endemic areas, which are located several hundred kilometers south of the Danish border. Second, the migrations must be rapid enough for the ticks to remain attached to the migrating carnivores during the entire migration. Individual gray wolves are indeed capable of migrating distances of 800–1,200 km within a short period; the first wolf known to arrive in northern Jutland has been genetically traced to the border area between Germany, the Czech Republic, and Poland, >800 km away from Denmark (1).

The finding of 21 adult male *D. reticulatus* ticks on a jackal hunted in western Denmark strongly indicates that jackal migrations are also long enough to originate from

Author affiliations: National Veterinary Institute, Lyngby, Denmark

DOI: <https://doi.org/10.3201/eid2312.170919>

Table. Primers used for gene amplification and sequencing of *Rickettsia* spp. obtained from *Dermacentor reticulatus* ticks from a migrating jackal, Denmark

Primer name	Primer sequence, 5' → 3'	Target gene	Length, bp	Reference
120–2,788	AAACAATAATCAAGGTACTGT	<i>ompB</i>	765	(5)
120–3,599	TACTTCCGGTTACAGCAAAGT			
Rr 190.70p	ATGGCGAATATTTCTCCAAA	<i>ompA</i>	631	(4)
Rr190–701n	GTTCCGTTAATGGCAGCATCT			
RpCS877p	GGGGACCTGCTCACGGCGG	<i>gltA</i>	380	(4)
RpCS1258n	ATTGCAAAAAGTACAGTGAACA			

Dermacentor tick–endemic areas and fast enough to allow the ticks to complete the migration to Denmark. The origin of the jackal received at the National Veterinary Institute is unknown, but the nearest known breeding populations of golden jackals are in Austria and Hungary (7). Female ticks were absent on the jackal because they drop off after feeding, but each female *D. reticulatus* tick can lay up to 7,200 eggs (8), which would have been deposited somewhere between the endemic tick region and Denmark. Some of those eggs may have landed in a favorable environment.

The SFG *Rickettsia R. slovaca* and *R. raoultii*, which are exotic to Denmark, are the most consequential zoonotic pathogens carried by *D. reticulatus* ticks. These bacteria are a public health concern because they cause scalp eschar and neck lymphadenopathy after tick bite (SENLAT) syndrome (10,11). SENLAT is an emerging tickborne infection and among the most common tickborne rickettsiosis in Europe (8). The disease is defined as the association of a tick bite, an inoculation eschar on the scalp, and cervical adenopathies (10,11). The main signs and symptoms are a crustaceous lesion (early) or eschar (late) at the site of the tick's attachment and regional painful lymph nodes (10,11).

R. raoultii was only recently characterized and named from bacteria isolated from *Dermacentor* tick species collected in Russia and France (6). In 2016, *R. raoultii* was reported for the first time in Austria and the Czech Republic (12,13). A relatively high prevalence of *R. raoultii* has been reported in ticks from various regions of Europe, from 14.9% in Austria (12) to 58% in Hungary (14). In the case we report, the high prevalence (85.7%) of *R. raoultii*–infected ticks from the jackal may have been accentuated by co-feeding transmission between ticks on the same host (8).

We did not identify any rickettsiae from the blood of the jackal by PCR. However, because ticks are able to sustain rickettsial transmission cycles transovarially and transstadially, it is possible that there is, in fact, no host reservoir of *R. raoultii* (8). If the ticks serve as a reservoir of *R. raoultii*, the distribution of this bacterium will be identical to that of the tick's area of dispersal (15). *D. reticulatus* males remain on the host for 2–3 months and have an intermittent feeding behavior (8). This trait makes them vectors of pathogenic agents, and recent studies have also shown that male *D. reticulatus* ticks play a strategic role in the transmission of *R. slovaca* and *R. raoultii* to humans (8).

Although SENLAT is a milder rickettsiosis, physicians should be aware of the potential diagnosis of this emerging tickborne disease. A reason for concern is that the intracellular *Rickettsia* infections require treatment with different antimicrobial drugs than, for example, *Borrelia* infections.

Conclusions

The simultaneous finding of a new carnivore, a new tick vector, and a new zoonotic pathogen in Denmark demonstrates that the unexpected recent wave of large carnivores migrating over long distances into Denmark is more than a theoretical risk to human and animal health. *Ixodes ricinus* ticks are abundant in most forests in Denmark. However, forests cover only 14% of Denmark's area, and the preference of *D. reticulatus* ticks for more open areas could dramatically increase the area of Denmark and northern Europe with a risk for tick bites and tickborne infections.

Acknowledgments

Special thanks go to Hans Erik Swart and Jens Henrik Jakobsen for handling the jackal.

Necropsy was funded by the Danish Nature Agency project no. 2013/S080-135070. The tick and pathogen analysis was supported by the Danish Veterinary and Food Administration, Ministry of Environment and Food Denmark, and by the Scandtick Innovation project, EU Regional Development Programme InterReg OKS.

Dr. Klitgaard is a molecular biologist and senior researcher at the National Veterinary Institute, Technical University of Denmark. Her primary research interests are microbial ecology and the etiology of bacterial diseases.

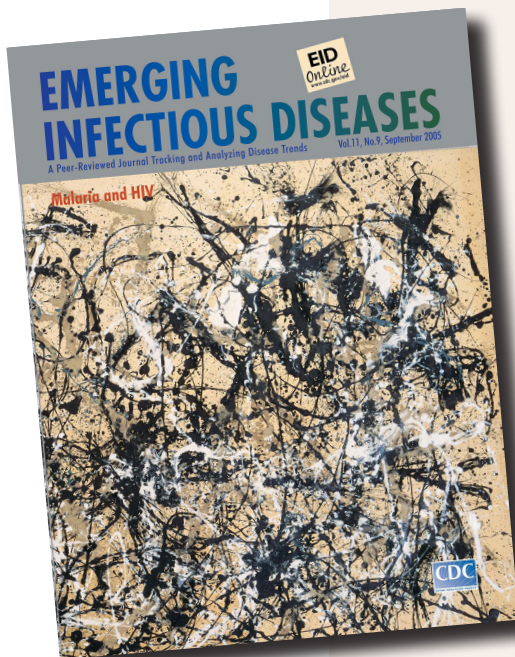
References

- Andersen LW, Harms V, Caniglia R, Czarnomska SD, Fabbri E, Jędrzejewska B, et al. Long-distance dispersal of a wolf, *Canis lupus*, in northwestern Europe. *Mammal Res.* 2015;60:163–8. <http://dx.doi.org/10.1007/s13364-015-0220-6>
- Michelet L, Delannoy S, Devillers E, Umhang G, Aspan A, Juremalm M, et al. High-throughput screening of tick-borne pathogens in Europe. *Front Cell Infect Microbiol.* 2014;4:103. <http://dx.doi.org/10.3389/fcimb.2014.00103>
- Jensen PM, Christoffersen CS, Moutailler S, Michelet L, Klitgaard K, Bødker R. Transmission differentials for multiple

- pathogens as inferred from their prevalence in larva, nymph and adult of *Ixodes ricinus* (Acari: Ixodidae). *Exp Appl Acarol*. 2017;71:171–82. <http://dx.doi.org/10.1007/s10493-017-0110-5>
4. Regnery RL, Spruill CL, Plikaytis BD. Genotypic identification of rickettsiae and estimation of intraspecies sequence divergence for portions of two rickettsial genes. *J Bacteriol*. 1991;173:1576–89. <http://dx.doi.org/10.1128/jb.173.5.1576-1589.1991>
 5. Roux V, Fournier PE, Raoult D. Differentiation of spotted fever group rickettsiae by sequencing and analysis of restriction fragment length polymorphism of PCR-amplified DNA of the gene encoding the protein rOmpA. *J Clin Microbiol*. 1996;34:2058–65.
 6. Mediannikov O, Matsumoto K, Samoilenko I, Drancourt M, Roux V, Rydkina E, et al. *Rickettsia raoultii* sp. nov., a spotted fever group rickettsia associated with *Dermacentor* ticks in Europe and Russia. *Int J Syst Evol Microbiol*. 2008;58:1635–9. <http://dx.doi.org/10.1099/ijs.0.64952-0>
 7. Trouwborst A, Krofel M, Linnell JDC. Legal implications of range expansions in a terrestrial carnivore: the case of the golden jackal (*Canis aureus*) in Europe. *Biodivers Conserv*. 2015;24:2593–610. <http://dx.doi.org/10.1007/s10531-015-0948-y>
 8. Földvári G, Široký P, Szekeres S, Majoros G, Sprong H. *Dermacentor reticulatus*: a vector on the rise. *Parasit Vectors*. 2016;9:314. <http://dx.doi.org/10.1186/s13071-016-1599-x>
 9. Jongejan F, Ringenier M, Putting M, Berger L, Burgers S, Kortekaas R, et al. Novel foci of *Dermacentor reticulatus* ticks infected with *Babesia canis* and *Babesia caballi* in the Netherlands and in Belgium. *Parasit Vectors*. 2015;8:232. <http://dx.doi.org/10.1186/s13071-015-0841-2>
 10. Angelakis E, Waton J, Imbert P, Socolovschi C, Edouard S, Dellamonica P. Scalp eschar and neck lymphadenopathy caused by *Bartonella henselae* after tick bite. 2010;50:549–51.
 11. Dubourg G, Socolovschi C, Del Giudice P, Fournier PE, Raoult D. Scalp eschar and neck lymphadenopathy after tick bite: an emerging syndrome with multiple causes. *Eur J Clin Microbiol Infect Dis*. 2014;33:1449–56. <http://dx.doi.org/10.1007/s10096-014-2090-2>
 12. Duscher GG, Hodžić A, Weiler M, Vaux AGC, Rudolf I, Sixl W, et al. First report of *Rickettsia raoultii* in field collected *Dermacentor reticulatus* ticks from Austria. *Ticks Tick Borne Dis*. 2016;7:720–2. <http://dx.doi.org/10.1016/j.ttbdis.2016.02.022>
 13. Rudolf I, Vencíková K, Blažejová H, Betášová L, Mendel J, Hubálek Z, et al. First report of *Rickettsia raoultii* and *Rickettsia helvetica* in *Dermacentor reticulatus* ticks from the Czech Republic. *Ticks Tick Borne Dis*. 2016;7:1222–4. <http://dx.doi.org/10.1016/j.ttbdis.2016.07.011>
 14. Szekeres S, Docters van Leeuwen A, Rigó K, Jablonszky M, Majoros G, Sprong H, et al. Prevalence and diversity of human pathogenic rickettsiae in urban versus rural habitats, Hungary. *Exp Appl Acarol*. 2016;68:223–6. <http://dx.doi.org/10.1007/s10493-015-9989-x>
 15. Socolovschi C, Mediannikov O, Raoult D, Parola P. Update on tick-borne bacterial diseases in Europe. *Parasite*. 2009;259–73. PubMed <http://dx.doi.org/10.1051/parasite/2009164259>

Address for correspondence: René Bødker, National Veterinary Institute (DTU), Kemitorget, Building 202, 2800 Kgs. Lyngby, Denmark; email: rebo@vet.dtu.dk

etymologia revisited



Rickettsia [rĭ-ket'se-ə]

Genus of gram-negative, rod-shaped or coccoid bacteria that are transmitted by lice, fleas, ticks, and mites. Named after American pathologist Howard Taylor Ricketts; despite the similar name, *Rickettsia* spp. do not cause rickets (from the Greek *rhakhis*, “spine”), a disorder of bone development caused by vitamin deficiency.

Source: Dorland’s illustrated medical dictionary. 30th ed. Philadelphia: Saunders; 2003.

Originally published September 2005

https://wwwnc.cdc.gov/eid/article/11/9/et-1109_article

Investigation of Acute Flaccid Paralysis Reported with La Crosse Virus Infection, Ohio, USA, 2008–2014

Morgan J. Hennessey, Daniel M. Pastula,
Kimberly Machesky, Marc Fischer,
Nicole P. Lindsey, Mary DiOrio,
J. Erin Staples, Sietske de Fijter

Infection with La Crosse virus can cause meningoencephalitis, but it is not known to cause acute flaccid paralysis (AFP). During 2008–2014, nine confirmed or probable La Crosse virus disease cases with possible AFP were reported in Ohio, USA. After an epidemiologic and clinical investigation, we determined no patients truly had AFP.

La Crosse virus is an *Orthobunyavirus* transmitted to humans primarily through the bite of *Aedes triseriatus* (eastern treehole) mosquitoes; the virus is endemic to the midwestern and Appalachian areas of the United States (1,2). Infection with La Crosse virus can result in severe disease, such as meningoencephalitis, which is primarily seen in children. Most infections do not usually result in permanent motor sequelae, but some have resulted in longer term learning difficulties and behavior changes (2). Although other mosquito-borne viral diseases (e.g., West Nile virus) have been associated with acute flaccid paralysis (AFP)—a clinical syndrome of rapidly progressive flaccid paralysis typically caused by dysfunction of the anterior horn cells, peripheral motor nerves or nerve roots, neuromuscular junction, or muscle—La Crosse virus has not been identified as a cause (3,4). During 2008–2014, nine of the total 148 confirmed or probable La Crosse virus disease cases in Ohio were reported as having AFP by local health departments, per the national arboviral case definition (5–7). We performed an investigation to describe the clinical features and outcomes for these cases and determine if the La Crosse virus infections were associated with AFP.

Author affiliations: Centers for Disease Control and Prevention, Atlanta, Georgia, USA (M.J. Hennessey, D.M. Pastula); Centers for Disease Control and Prevention, Fort Collins, Colorado, USA (M.J. Hennessey, D.M. Pastula, M. Fischer, N.P. Lindsey, J.E. Staples); Ohio Department of Health, Columbus, Ohio, USA (K. Machesky, M. DiOrio, S. de Fijter)

DOI: <https://doi.org/10.3201/eid2312.170944>

The Study

We reviewed medical records from all 9 case-patients' initial illnesses and abstracted data using a standard form. We contacted patients and, after obtaining consent, administered a questionnaire to assess any residual weakness in the patients and their current functional status according to the modified Rankin scale (a standardized measure of disability for persons with neurologic conditions, by which a score of 0 is normal and 5 denotes severe disability) (8). If the patient was <18 years of age at the time of the follow-up interview, we obtained permission from a parent or guardian and administered the questionnaire to the parents. For patients with unclear neurologic findings or diagnosis, a board-certified neurologist performed a follow-up neurologic examination. We obtained human ethics approval for this investigation from the Centers for Disease Control and Prevention Institutional Review Board.

We defined AFP as a clinical syndrome of rapid-onset extremity weakness, sometimes accompanied by weakness in a facial or respiratory muscle that is flaccid (i.e., without any upper motor neuron signs in the affected areas suggestive of central nervous system motor tract pathology) (4). Upper motor neuron signs included increased muscle tone or spasticity, increased deep-tendon reflexes, the presence of Babinski and Hoffmann signs, abnormally slow finger or toe taps out of proportion to weakness, or a clear upper motor neuron pattern of weakness (e.g., hemiparesis involving the face, arm, and leg). In addition, a brain lesion that corresponded to the patient's weakness identified by magnetic resonance imaging (MRI) or suggested by electroencephalography (EEG) provided corroborating evidence of an upper motor neuron or central nervous system motor tract pathology that would not be consistent with AFP. Finally, any residual weakness with a clear upper motor neuron pattern (e.g., hemiparesis involving the face, arm, and leg) or any residual upper motor neuron signs in the previously affected areas were also used to rule out AFP.

Of the 9 La Crosse virus disease case-patients with AFP, 8 had confirmed infections and 1 probable. At the time of disease diagnosis, the median age of the 9 case-patients was 12 years (range 4–78 years); 5 (56%) were male. Illness onset dates ranged from September 2008 to

September 2013, and case-patients were residents of 8 counties located throughout the state. During their acute illness, all patients experienced fever, altered mental status, and weakness (Table 1). Other common symptoms that patients reported were seizures (7, 78%), headache (7, 78%), and nausea or vomiting (6, 67%). After a median hospitalization of 17 days (range 5–28 days), 7 patients were discharged to their homes, 1 patient to an acute rehabilitation facility, and 1 to a skilled nursing facility.

Of the 9 case-patients, we reached 7 (78%) by telephone to determine their current clinical status; 1 patient could not be reached for follow-up, and the other patient had died (Table 2). The cause of death for this patient was unclear, but after we reviewed the medical and death records, we did not believe it was directly associated with La Crosse virus infection. Of the 7 patients we evaluated, 2 (29%) reported residual focal weakness related to their previous La Crosse virus disease, and 3 (47%) had a current modified Rankin scale score of ≥ 1 (median 1), indicating some sort of residual disability.

We saw in our review of case-patients' medical records that all 9 had rapid-onset focal muscle weakness during their illness. Seven patients had upper motor signs or a clear upper motor neuron pattern of weakness in the affected areas and were therefore determined not to have AFP. Furthermore, all 7 had evidence of a brain lesion that corresponded to their weakness pattern (5 by MRI, 1 by EEG, and 1 by both MRI and EEG). For the other 2 patients, we found insufficient evidence in the medical records to determine whether they had AFP and performed in-person neurologic exams. One patient had no residual weakness but had residual upper motor neuron signs in the previously

Table 1. Clinical symptoms reported at time of acute illness for 9 patients with La Crosse virus infection and reported acute flaccid paralysis, Ohio, USA, 2008–2014

Clinical sign/symptom	No. (%) patients
Fever	9 (100)
Altered mental status	9 (100)
Weakness	9 (100)
Seizure	7 (78)
Headache	7 (78)
Nausea/vomiting	6 (67)
Muscle pain/myalgia	1 (11)

affected areas. The other patient had both residual weakness and upper motor neuron signs in the affected areas. Therefore, none of the 9 cases were determined to have AFP by our definition.

Conclusions

Although all 9 La Crosse virus disease case-patients we investigated had acute weakness or paralysis, none met the definition for AFP. The most likely explanation for the initial AFP reports was difficulty in distinguishing flaccid or lower motor neuron weakness due to peripheral nervous system pathology (i.e., pathology at or distal to the anterior horn cells) from spastic or upper motor neuron weakness due to central nervous system pathology (i.e., pathology in the spinal cord or brain motor tracts). Thus, we found no evidence of AFP being associated with La Crosse virus infection.

To further assist in classifying cases as having AFP, we propose the following surveillance definition for AFP, based on a World Health Organization technical document: a clinical syndrome of rapid-onset extremity weakness, sometimes accompanied by facial or respiratory

Table 2. Clinical characteristics and follow-up for 9 patients with La Crosse virus infection and reported acute flaccid paralysis, Ohio, USA, 2008–2014*

Case-patient no.	At time of acute illness					At time of follow-up investigation			
	Age, y/sex	Upper motor neuron†		Brain lesions‡		Upper motor neuron†		Reported weakness	Modified Rankin score§
		Signs	Pattern	MRI	EEG	Signs	Pattern		
1	12/F	Yes	Yes	Yes	No	–¶	–	No	0
2	4/M	Yes	Yes	Yes	No	–	–	–	–
3	12/M	Yes	No	Yes	Yes	–	–	No	0
4	12/M	Yes	No	Yes	No	–	–	–	6#
5	78/F	Yes	No	Yes	–	–	–	Yes	3
6	8/M	No	Yes	Yes	–	–	–	No	0
7	13/M	No	Yes	–	Yes	–	–	No	0
8	7/F	No	No	–	–	Yes	No	No	1
9	12/F	No	No	–	–	Yes	Yes	Yes	1

*EEG, electroencephalography; MRI, magnetic resonance imaging.

†Upper motor neuron signs included increased tone, increased reflexes, Babinski sign, or abnormally slow finger or foot taps, and patterns of weakness included hemiparesis or weakness preferentially involving the distal extensor muscles.

‡A brain lesion identified by MRI or EEG consistent with the patient's pattern of weakness provided corroborating evidence of an upper motor neuron pathology.

§Modified Rankin score measures disability or dependence in daily activities for patients who have had a stroke or other neurologic disability. Scores range 0–6 as follows: 0, No symptoms; 1, No substantial disability and carries out all usual activities despite some symptoms; 2, Slight disability and able to look after own affairs without assistance but unable to carry out all previous activities; 3, Moderate disability requiring some help but able to walk unassisted; 4, Moderate disability requiring help with bodily needs and unable to walk unassisted; 5, Severe disability that requires constant nursing care; 6, Deceased.

¶Information was not available or not assessed.

#Patient had a primary immunodeficiency that required chronic steroid replacement. Several years after his acute La Crosse virus disease, the patient experienced acute gastroenteritis and subsequently died of an unknown etiology; no autopsy was performed.

muscle weakness, that is flaccid (i.e., without any upper motor neuron signs in the affected areas suggestive of central nervous system motor tract pathology) (4). AFP can include clinical syndromes caused by acute dysfunction of the anterior horn cells (e.g., acute flaccid myelitis), peripheral motor nerves or nerve roots (e.g., Guillain-Barré syndrome), neuromuscular junction (e.g., botulism or myasthenic crisis), or muscle (e.g., acute myopathies) (3,4). Rarely, a sudden-onset spinal cord injury or myelopathy can cause a temporary AFP referred to as spinal shock, although it is typical for upper motor neuron signs to develop eventually in these cases (4). The Centers for Disease Control and Prevention will continue to work with public health partners to adopt a standardized surveillance definition for AFP, which we hope will mitigate the risk of an incorrect association between certain infections, like La Crosse virus, and AFP.

Acknowledgments

We thank James J. Sejvar and Richard Gary for their help in drafting the protocol for this investigation.

Dr. Hennessey is an epidemiologist with the US Department of Agriculture, Animal and Plant Health Inspection Service, Veterinary Services, Center for Epidemiology and Animal Health. He served as an Epidemic Intelligence Service Officer with the Centers for Disease Control and Prevention during 2014–2016.

References

1. Haddow AD, Odoi A. The incidence risk, clustering, and clinical presentation of La Crosse virus infections in the eastern United States, 2003–2007. *PLoS One*. 2009;4:e6145. <http://dx.doi.org/10.1371/journal.pone.0006145>
2. Balfour HH Jr, Siem RA, Bauer H, Quie PG. California arbovirus (La Crosse) infections. I. Clinical and laboratory findings in 66 children with meningoencephalitis. *Pediatrics*. 1973;52:680–91.
3. Marx A, Glass JD, Sutter RW. Differential diagnosis of acute flaccid paralysis and its role in poliomyelitis surveillance. *Epidemiol Rev*. 2000;22:298–316. <http://dx.doi.org/10.1093/oxfordjournals.epirev.a018041>
4. World Health Organization. Acute onset flaccid paralysis (technical document). 1993 [cited 2017 May 8]. <http://www.who.int/iris/handle/10665/61626>
5. Centers for Disease Control and Prevention. La Crosse virus disease cases and deaths reported to CDC by year and clinical presentation, 2004–2013. 2016 [cited 2017 Aug 28]. https://www.cdc.gov/lac/resources/LACbyYear_2004-2013.pdf
6. United States Geological Survey. La Crosse virus, human, 2008–2014 [cited 2017 Aug 28]. <https://diseasemaps.usgs.gov/mapviewer/>
7. Centers for Disease Control and Prevention. National Notifiable Diseases Surveillance System (NNDSS): arboviral diseases, neuroinvasive and non-neuroinvasive. 2005 [cited 2017 Aug 28]. <https://wwwn.cdc.gov/nndss/conditions/arboviral-diseases-neuroinvasive-and-non-neuroinvasive/>
8. van Swieten JC, Koudstaal PJ, Visser MC, Schouten HJ, van Gijn J. Interobserver agreement for the assessment of handicap in stroke patients. *Stroke*. 1988;19:604–7. <http://dx.doi.org/10.1161/01.STR.19.5.604>

Address for correspondence: J. Erin Staples, Centers for Disease Control and Prevention, 3156 Rampart Rd, Fort Collins, CO 80521, USA; email: estaples@cdc.gov



Discover the world...

of Travel Health

www.cdc.gov/travel

Visit the CDC Travelers' Health website for up-to-date information on global disease activity and international travel health recommendations.

Department of Health and Human Services • Centers for Disease Control and Prevention

Phylogenetic Characterization of Crimean-Congo Hemorrhagic Fever Virus, Spain

Eva Ramírez de Arellano, Lourdes Hernández,
M. José Goyanes, Marta Arsuaga,
Ana Fernández Cruz, Anabel Negrodo,¹
María Paz Sánchez-Seco¹

Two cases of Crimean-Congo hemorrhagic fever were reported in Spain during 2016. We obtained the virus from a patient sample and characterized its full genomic sequence. Phylogenetic analysis indicated that the virus corresponds to the African genotype III, which includes viruses previously found in West and South Africa.

Crimean-Congo hemorrhagic fever (CCHF) is a severe disease transmitted to humans mainly by ticks, primarily of *Hyalomma* spp. This zoonotic disease is caused by CCHF virus (CCHFV), a nairovirus in the family *Bunyaviridae*, which was detected first in Crimea in 1944 and isolated 12 years later in the Democratic Republic of the Congo. Since the beginning of the 21st century, CCHFV has been spreading from disease-endemic areas to new regions previously considered free of the disease, particularly in areas where *Hyalomma* spp. ticks are present. In nature, CCHFV usually circulates between asymptomatic animals and ticks in an enzootic cycle.

CCHFV has a negative-sense and tripartite RNA genome (small [S], medium [M], and large [L] segments) with high genetic diversity. The sequences of the S segment, which is the most conserved at the nucleotide level, could be distributed in 6 lineages (1–6). Each genetic lineage has been linked to geographic regions in Africa, the Middle East, Asia, and Europe, where *Hyalomma* spp. ticks are present (7). Genotypes I, II, and III have been described in Africa; genotype IV in Asia; and genotypes V and VI in Europe. However, strains have moved between geographic regions; migrating birds, unregulated wildlife trade, livestock import and export, and a global movement of humans could have dispersed the virus or CCHFV-infected ticks (8).

In western Europe, the presence of the virus had only been detected indirectly by means of serologic methods in

the serum of 2 people from southern Portugal (9). However, genotype III CCHFV was detected in ticks from deer captured in western Spain in 2010 and ticks from birds migrating from Morocco in 2013 (10,11). No cases among humans in Spain had been reported until 2016, when 2 autochthonous cases were diagnosed (12). Here, we report the complete genomic sequence of the virus from 1 of these case-patients and show the phylogenetic relationships among the 3 segments.

The Study

We previously detected CCHFV in serum samples from the 2 patients in Spain with autochthonous CCHFV (12); the index case-patient died. For this study, we obtained viral RNA (3.6×10^7 copies/mL) from the secondary case-patient in a sample taken 4 days after onset of symptoms by using the QIAamp viral RNA Mini kit (QIAGEN, Hilden, Germany). We then amplified the virus in a single-step reverse-transcription PCR by using the SuperScript III One-Step RT-PCR system with the Platinum Taq High Fidelity DNA Polymerase kit (Invitrogen Life Technologies, Barcelona, Spain) with overlapping primers throughout the complete genome (Table). PCR conditions were amplification at 52.5°C for 30 min, 94°C for 2 min, and then 40 cycles at 94°C for 15 s, 48°C–55°C for 30 s, and 68°C for 1 min/kb, with a final extension cycle at 68°C for 5 min. We designed primers for each segment in most conserved regions after aligning available CCHFV sequences from all genotypes retrieved from GenBank (Table). We directly sequenced purified amplicons by using additional internal primers (data not shown). We assembled and analyzed the consensus sequence of each segment by using SeqMan Pro from the Lasergene Suite 12 (DNASTAR Inc., Madison, WI, USA). To get complete finished genomes, we used a hybrid-capture method as described by Blackley et al. (13) by using probes designed against the CCHFV sequences obtained from amplicon sequencing.

To characterize the complete CCHFV genome, we performed a phylogenetic analysis of the full S, M, and L segments (Figure, <https://wwwnc.cdc.gov/EID/article/23/12/17-1002-F1.htm>). The 3 segments were aligned by using ClustalW in MEGA 5.2 (<http://www.megasoftware.net>) and representative available CCHFV sequences from GenBank of all genotypes. We generated

Author affiliations: National Center of Microbiology Arbovirus and Imported Viral Diseases Laboratory, Madrid, Spain (E. Ramírez de Arellano, L. Hernández, A. Negrodo, M. Paz Sánchez-Seco); Gregorio Marañón Hospital, Madrid (M.J. Goyanes, A. Fernández Cruz); La Paz Hospital, IdiPaz, Madrid (M. Arsuaga)

DOI: <https://doi.org/10.3201/eid2312.171002>

¹These authors contributed equally to this article.

Table. RT-PCR primers used for generation of amplicons used for sequencing CCHFV full genome from strains isolated from patient samples in Spain, 2016*

Primer pair	5' → 3' sequence	5' → 3' position relative to reference strain AB1-2009	Amplified segment, kb	Temperature, °C†
CRCON+1	RWAAYGGRCTTTRTGGAYACYTTAC	123–147	S, 1.4	50.5
CRCON1R-S	TCTCAAAGATAYCGTTGCCGCAC	1,651–1,673		
CRCON1F-M	TCTCAAAGAAAATACTTGCGGC	1–22	M, 2.3	48
CRCON4R-M	GCATYTCAGCATCTATTGCATT	2,326–22,347		
CRCONF4F-M	TTGTAGAYCAAAGACTRGGCAG	1,775–1,796	M, 2.1	48
CRCON6R-M	GCCYGCTTCAATCAAGCTACA	3,829–3,849		
CRCON6F-M	TCAATTGAGGCACCATGGGG	3,280–3,299	M, 2.1	50
CRCON8R-M	TCTCAAAGATATAGTGGCGGCA	5,348–5,369		
CRCON1F-L	TCTCAAAGATATCAATCCGCC	1–22	L, 2.2	48
CRCON3R-L	AGTGTGCAAAAATGTRCAAATCTC	2,202–2224		
CRCON3F-L	CCTGAAAGTGACCTCACCCGC	1,562–1,582	L, 3.1	55
CRCON6R-L	TTGGCATGCTTGCCAGGGCTTAG	4,656–4,677		
CRCON7F-L	TGCTTGCCAGGGCTTAGTAGGCT	4,661–4,682	L, 2.3	50.5
CRCON9R-L	TCATGCATGCAACCACTGAAAT	6,948–6,969		
CCHF-L2F	GAAGAGCTATATGACATAAGGC	6,137–6,158	L, 1.6	48
CCHF-L1R	TTGGCACTATCTTTCATTGAC	7,752–7,773		
CRCON10F-L	GGTAGTTTCAAGATGATTACGCAA	7,616–7,638	L, 1.4	48
CRCON10R-L	CCTGTTAATTGTTGCCACAA	9,019–9,039		
CRCON7200F	ATGCAACAGGTTCTGAAAAATG	7,199–7,220	L, 3.5	48
CRCON11R-L	ATGCTCCTAGTGATGCCATAATG	10,743–10,765		
CRCON12F-L	TCTTTTGAAGGTGAAGCATCTTG	10,585–10,607	L, 1.6	48
CCHF-L2R	TCTCAAAGAAAATCGTTCCCCCAC	12,149–12,172		

*F, forward; L, large segment; M, medium segment; R, reverse; RT-PCR, reverse transcription PCR; S, small segment.

†Melting temperature used.

a phylogenetic tree by using neighbor-joining algorithms and analyzed 1,000 replicates for bootstrap testing. GenBank accession numbers for sequences used in this study are MF287636 for the S fragment, MF287637 for the M fragment, and MF287638 for the L fragment.

The nucleotide sequence of the different CCHFV segments from the infected patient we analyzed in this study showed 99% identity with the Sudan AB1–2009 CCHFV strain (5) in S, M, and L segments (GenBank accession nos. HQ378179.1, HQ378187.1, and HQ378183.1, respectively) (Figure) and were grouped within genotype III (Africa 3). CCHFV found in ticks from Spain in 2010 and from birds from Morocco in 2011 also clustered in this group (10,11). In addition, no reassortant segment has been found in the analysis of the full genome, even though reassortant strains have been described in this genotype (2).

Conclusions

The results of the sequence analysis we describe corroborate our previous results (12), obtained by analyzing a small fragment in the S segment, showing that CCHFV from genotype III (Africa III) is circulating in southwestern Europe. CCHFV circulating in Spain caused 2 autochthonous cases that resulted in the death of the index case-patient and a serious illness in the second case-patient, providing evidence of its pathogenicity. The risk for infection in Spain is considered low, but human infection caused by the bite of an infected tick has occurred 6 years after the virus was discovered in ticks (10).

Because the virus is circulating in Spain, additional studies will be required to establish the distribution of the virus in this country.

Acknowledgment

We thank Amir Gacem for reviewing the grammar.

This study was partially funded by ISCIII, Projects RD12/0018/0006 and RD16CIII/0003/0003, “Red de Enfermedades Tropicales,” Subprogram RETICS Plan Estatal de I+D+I 2013–2016, and co-funded by FEDER “Una manera de hacer Europa.” The finished genomes were obtained with support from the US Defense Biological Product Assurance Office.

Dr. Ramirez de Arellano is a postdoctoral researcher who has worked in the Arbovirus and Imported Viral Diseases Laboratory of the National Center of Microbiology (Madrid, Spain) since 2011. Her primary research interests are detection of emerging viruses that circulate in Spain, for which she has implemented molecular biology tools.

References

1. Chamberlain J, Cook N, Lloyd G, Mioulet V, Tolley H, Hewson R. Co-evolutionary patterns of variation in small and large RNA segments of Crimean-Congo hemorrhagic fever virus. *J Gen Virol.* 2005;86:3337–41. <http://dx.doi.org/10.1099/vir.0.81213-0>
2. Deyde VM, Khristova ML, Rollin PE, Ksiazek TG, Nichol ST. Crimean-Congo hemorrhagic fever virus genomics and global diversity. *J Virol.* 2006;80:8834–42. <http://dx.doi.org/10.1128/JVI.00752-06>
3. Anagnostou V, Papa A. Evolution of Crimean-Congo hemorrhagic fever virus. *Infect Genet Evol.* 2009;9:948–54. <http://dx.doi.org/10.1016/j.meegid.2009.06.018>

4. Carroll SA, Bird BH, Rollin PE, Nichol ST. Ancient common ancestry of Crimean-Congo hemorrhagic fever virus. *Mol Phylogenet Evol*. 2010;55:1103–10. <http://dx.doi.org/10.1016/j.ympev.2010.01.006>
5. Aradaib IE, Erickson BR, Karsany MS, Khristova ML, Elageb RM, Mohamed ME, et al. Multiple Crimean-Congo hemorrhagic fever virus strains are associated with disease outbreaks in Sudan, 2008–2009. *PLoS Negl Trop Dis*. 2011;5:e1159. <http://dx.doi.org/10.1371/journal.pntd.0001159>
6. Singh P, Chhabra M, Sharma P, Jaiswal R, Singh G, Mittal V, et al. Molecular epidemiology of Crimean-Congo haemorrhagic fever virus in India. *Epidemiol Infect*. 2016;15:1–4.
7. Hoogstraal H. The epidemiology of tick-borne Crimean-Congo hemorrhagic fever in Asia, Europe, and Africa. *J Med Entomol*. 1979;15:307–417. <http://dx.doi.org/10.1093/jmedent/15.4.307>
8. Bente DA, Forrester NL, Watts DM, McAuley AJ, Whitehouse CA, Bray M. Crimean-Congo hemorrhagic fever: history, epidemiology, pathogenesis, clinical syndrome and genetic diversity. *Antiviral Res*. 2013; 100:159–89. [PubMed http://dx.doi.org/10.1016/j.antiviral.2013.07.006](http://dx.doi.org/10.1016/j.antiviral.2013.07.006)
9. Filipe AR, Calisher CH, Laznick J. Antibodies to Congo-Crimean haemorrhagic fever, Dhori, Thogoto and Bhanja viruses in southern Portugal. *Acta Virol*. 1985;29:324–8. <http://dx.doi.org/10.1016/j.antiviral.2013.07.006>
10. Estrada-Peña A, Palomar AM, Santibáñez P, Sánchez N, Habela MA, Portillo A, et al. Crimean-Congo hemorrhagic fever virus in ticks, southwestern Europe, 2010. *Emerg Infect Dis*. 2012;18:179–80. <http://dx.doi.org/10.3201/eid1801.111040>
11. Palomar AM, Portillo A, Santibáñez P, Mazuelas D, Arizaga J, Crespo A, et al. Crimean-Congo hemorrhagic fever virus in ticks from migratory birds, Morocco. *Emerg Infect Dis*. 2013;19:260–3. [PubMed http://dx.doi.org/10.3201/eid1902.121193](http://dx.doi.org/10.3201/eid1902.121193)
12. Negrodo A, de la Calle-Prieto F, Palencia-Herrejón E, Mora-Rillo M, Astray-Mochales J, Sánchez-Seco MP, et al.; Crimean Congo Hemorrhagic Fever@Madrid Working Group. Autochthonous Crimean-Congo hemorrhagic fever in Spain. *N Engl J Med*. 2017;377:154–61. <http://dx.doi.org/10.1056/NEJMoa1615162>
13. Blackley DJ, Wiley MR, Ladner JT, Fallah M, Lo T, Gilbert ML, Gregory C, et al. Reduced evolutionary rate in reemerged Ebola virus transmission chains. *Sci Adv*. 2016;2:e1600378. <http://dx.doi.org/10.1126/sciadv.1600378>

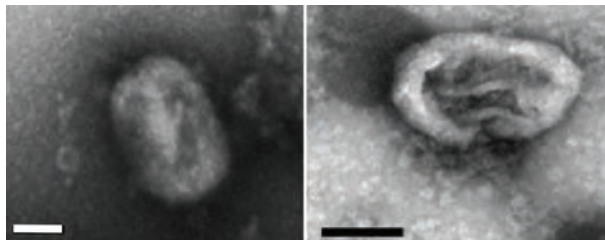
Address for correspondence: María Paz Sánchez-Seco, National Center of Microbiology, Arbovirus and Imported Viral Diseases Laboratory, Crta. Majadahonda-Pozuelo Km 2, 28220-Majadahonda, Madrid, Spain; email: paz.sanchez@isciii.es

December 2013: Zoonotic Infections



- Institute of Medicine and National Research Council Recommendations for One Health Initiative
- Epidemiologic Investigations into Outbreaks of Rift Valley Fever in Humans, South Africa, 2008–2011
- Potential Role of Deer Tick Virus in Powassan Encephalitis Cases in Lyme Disease–endemic Areas of New York, USA
- Twenty-Year Summary of Surveillance for Human Hantavirus Infections, United States
- Spontaneous Generation of Infectious Prion Disease in Transgenic Mice
- Zoonotic *Chlamydiaceae* Species Associated with Trachoma, Nepal
- Guillain-Barré Syndrome Surveillance during National Influenza Vaccination Campaign, New York, USA, 2009
- Antiviral Susceptibility of Highly Pathogenic Avian Influenza A(H5N1) Viruses Isolated from Poultry, Vietnam, 2009–2011
- Novel Reassortant Influenza A(H1N2) Virus Derived from A(H1N1)pdm09 Virus Isolated from Swine, Japan, 2012

- Myocarditis after Trimethoprim/Sulfamethoxazole Treatment for Ehrlichiosis
- Distinct Lineage of Vesiculovirus from Big Brown Bats, United States
- Acute *Toxoplasma gondii* Infection among Family Members in the United States
- Outbreak of Human Infection with *Sarcocystis nesbitti*, Malaysia, 2012
- Transmission of Brucellosis from Elk to Cattle and Bison, Greater Yellowstone Area, USA, 2002–2012
- Concomitant Human Infections with 2 Cowpox Virus Strains in Related Cases, France, 2011
- Zoonotic *Onchocerca lupi* infection in Dogs, Greece and Portugal, 2011–2012
- Novel Cause of Tuberculosis in Meerkats, South Africa
- Cerebellar Cysticercosis Caused by Larval *Taenia crassiceps* Tapeworm in Immunocompetent Woman, Germany



Lack of Secondary Transmission of Ebola Virus from Healthcare Worker to 238 Contacts, United Kingdom, December 2014

Paul Crook, Alison Smith-Palmer, Helen Maguire, Noel McCarthy, Hilary Kirkbride, Bruce Court, Sanch Kanagarajah, Deborah Turbitt, Syed Ahmed, Paul Cosford, Isabel Oliver

In December 2014, Ebola virus disease (EVD) was diagnosed in a healthcare worker in the United Kingdom after the worker returned from an Ebola treatment center in Sierra Leone. The worker flew on 2 flights during the early stages of disease. Follow-up of 238 contacts showed no evidence of secondary transmission of Ebola virus.

More than 28,000 cases of Ebola virus disease (EVD) were reported during the epidemic in West Africa in 2014–2015 (1). International healthcare workers (HCWs) responded, and a number subsequently became infected with EVD, including those given a diagnosis after their return travel (2). There is international guidance for follow-up of aircraft contacts of case-patients with EVD (3–5).

We report contact tracing after EVD was diagnosed in an HCW in the United Kingdom who had worked in an Ebola treatment center in Sierra Leone. This worker had become ill while traveling back to the United Kingdom via Morocco.

The Study

For this investigation, a multiagency incident control team and contact tracing teams were established with staff of Public Health England (PHE) and Health Protection Scotland. We undertook a risk assessment that included interviewing the case-patient about symptoms, travel, and contacts. We used preexisting guidance (6) to classify contacts according to their degree of exposure to the case-patient and to other persons with EVD on the basis of the degree of infectiousness and physical contact (Table). The degree of public health follow-up of contacts was formulated according to their exposure category (Table).

We asked airlines to provide passenger manifests; advanced passenger information (nationality, passport

Author affiliations: Public Health England, London, UK (P. Crook, H. Maguire, N. McCarthy, H. Kirkbride, B. Court, S. Kanagarajah, D. Turbitt, P. Cosford, I. Oliver); Health Protection Scotland, Glasgow, Scotland, UK (A. Smith-Palmer, S. Ahmed); University College London, London (H. Maguire)

DOI: <https://doi.org/10.3201/eid2312.171100>

numbers, date of birth); and contact details. If contact details were missing or incorrect, we sought additional information from Her Majesty's Passport Office, the UK Border Agency, PHE port entry screening and returning workers information, the National Health Service Patient Demographic Service, and online social networks. For contacts with UK addresses, we conducted a home visit if telephone contact was unsuccessful. For foreign national contacts, PHE also contacted the National Focal Point of the relevant country as per International Health Regulations. Public helplines were established to provide a contact point for those potentially affected. PHE provided public health advice to United Kingdom airline staff, and Moroccan authorities provided public health advice to Morocco airline staff. Moroccan authorities led contact tracing for the flight to Morocco, which is not reported in this article.

The case-patient was a UK national HCW (39-year-old woman) who had worked in an Ebola treatment center in Sierra Leone and had direct patient contact. On December 28, 2014, she flew from Sierra Leone to Glasgow on 3 flights and 2 aircraft of 2 airlines: from Freetown, Sierra Leone, to Casablanca, Morocco (3 h, 40 min); Casablanca to London, England (3 h, 30 min); and London to Glasgow, Scotland (1 h, 20 min).

During exit screening before boarding in Freetown and Casablanca, the case-patient was reported to have been afebrile. Symptoms of fever and malaise began during the Casablanca to London flight. At London Heathrow Airport, several readings of temperatures $<37.6^{\circ}\text{C}$ were made by screening staff before onward travel. In Glasgow, after the case-patient took a taxi home, her symptoms worsened, and she telephoned local health services. The case-patient did not report vomiting, diarrhea, or bleeding before diagnosis and admission. Contacts had not been exposed to body fluids.

The case-patient was admitted to a hospital in Glasgow and given a diagnosis of EVD on December 29, 2014. The patient was subsequently transferred by military plane to a specialist infectious diseases hospital in London on December 30, 2014. She survived her illness.

Aircraft passengers in the same seat row and 2 rows in front of and behind the case-patient were classified as category 2 contacts. All other passengers and crew were classified as category 1 contacts. Border Force staff, health

Table. Characteristics of 238 contacts of a healthcare worker with Ebola virus disease and summary of public health action, by category, United Kingdom, December 2014*

Characteristic	No. contacts by exposure category			Total
	1; No direct contact	2; Direct contact with low risk for exposure	3; Direct contact with high risk for exposure	
Exposure setting				
Casablanca–LHR passengers	109	23	0	132
Casablanca–LHR crew	13	0	0	13
LHR PHE screeners	4	0	0	4
LHR Border Force	7	0	0	7
LHR–Glasgow passengers	62	8	0	70
LHR–Glasgow crew	7†	0	0	7
Healthcare workers	4‡	0	0	4
Glasgow community	0	1	0	1
Total§	185	24	29¶	238
Summary of public health action	Risk assessment questionnaire completed; provided telephone advice on symptoms of EVD; action to take if they had fever or symptoms consistent with EVD in the 21 d after their most recent exposure; advised that there was no reason to stop their day-to-day activities during the surveillance period provided they remained well; advised that their family and household contacts were not at risk for EVD if contact remained asymptomatic	As for category 1 plus provided written advice and a temperature monitoring kit, advised to take their temperature twice a day and to contact the local public health team if they had a fever or symptoms consistent with EVD in the 21 d after their most recent exposure; advised to delay any nonessential healthcare treatment until after the 21-d period; local public health teams assessed the contact after 21 d and reported their completion of public health follow-up	As for category 2 plus required to contact the local public health team daily to report their temperature and advised not to undertake healthcare activity; if contact was not made, the local public health team contacted them	NA

*In England a home visit was attempted if no telephone contact was possible. EVD, Ebola virus disease; LHR, London Heathrow Airport; NA, not applicable; PHE, Public Health England.

†Includes 3 cabin staff and 4 land customer services staff.

‡Includes 2 doctors and 2 nurses who provided dedicated care to the patient while in the specialist infectious diseases unit.

§Reflects overall number of persons categorized according to their highest category, including those categorized because of their healthcare work contact in Sierra Leone. Numbers in each category do not represent a sum of a column.

¶29 contacts who flew Casablanca–LHR were classified as category 3 because of their healthcare-related activity in West Africa.

screeners, and HCWs were classified as category 1 contacts, and a community contact was classified as category 2 contact (Table).

A total of 238 persons, including 185 category 1 contacts and 24 category 2 contacts, were assessed as having sufficient exposure to the case-patient to warrant further public health follow-up (Table). Although no contacts were classified as being category 3 (direct contact with high exposure risk) because of exposure to the case-patient, 29 contacts were classified as category 3 because of other Ebola exposures, including healthcare work in Sierra Leone.

All 16 non-flight-related contacts were successfully followed up. Passengers on the Casablanca to London flight represented 17 nationalities, and 59 (45%) of 132 had non-UK passports. We successfully contacted all passengers on both flights, except for 3 category 1 passengers who had non-UK passports (199/202, 99%); a total of 162 (80%) passengers were contacted within 48 h of diagnosis for the case-patient.

We provided information for the 3 passengers we could not contact to their respective countries through their

National Focal Point. Two persons in the United Kingdom required home visits. All flight crew were contacted. No additional cases of EVD were identified among contacts.

Conclusions

We report no evidence of secondary transmission of Ebola virus to contacts of a case-patient who contracted EVD during the Ebola epidemic in West Africa in 2014–2015 and who was given a diagnosis in the United Kingdom. There have been few reports of symptomatic EVD case-patients traveling by commercial airline, and secondary transmission has not been documented (7–10). The case-patient we report was probably in the early stages of illness, and there was no evidence of high-risk exposure to body fluids on board the aircraft.

A precautionary approach was taken regarding classification of contacts on the aircraft. We used a wider definition for the closest contact category than that recommended by international guidance (1 seat in either direction of the case-patient) (3–5) but consistent with that used for the response to a case diagnosed in the United

States (10). The decision to contact all persons on the affected aircraft was taken to inform and reassure contacts, not just to prevent transmission.

The limited information on passengers initially available hampered the ability to make contact promptly and resulted in extensive efforts to trace persons. Furthermore, flight manifests included passengers who had not flown. Issues with flight information have arisen before in the United Kingdom related to contact tracing (11). The need for airlines to collect personal rather than agency contact details should be stressed. To ensure a rapid response, public health agencies need to work with airlines and other international organizations to ensure access to a minimum dataset that would support rapid notification of contacts. In the United Kingdom, the National Health Service Patient Demographic Service was essential for obtaining contact details and identifying whether contacts were likely to be UK residents. In addition, the Ebola port entry screening and returning workers scheme provided rapid information on 37 contacts whose journey originated in Ebola-affected countries.

Temperature screening while the case-patient transferred through Heathrow Airport did not confirm fever, and the patient was allowed to continue the journey. In the presence of exit screening, airport entry screening might not detect imported EVD (12,13). However, one purpose of this screening has been to ensure that persons receive information to enable them to seek care quickly and in a manner that helps prevent transmission. Advice provided during airport screening and healthcare deployments aims to ensure that when symptoms develop, exposed persons contact health services early and by telephone, enabling responders to take appropriate measures to reduce transmission. In this instance, early contact with health services resulted in only a small number of contacts outside the flights. An evaluation of EVD port entry screening and a scheme for returning workers in the United Kingdom is under way.

This study provides support for the conclusion that there is low risk for transmission of Ebola virus on aircraft from EVD case-patients in the early stages of disease. Providing information and advice to contacts can be a helpful public health intervention in minimizing virus transmission.

Acknowledgments

We thank the staff at the Royal Free London National Health Service Foundation Trust for case-patient interviewing; National Incident Control Team members, including Gina Radford and Jill Meara, and Health Protection Scotland staff; PHE Centre Health Protection teams, including Sara Atkin; PHE Field Epidemiology Service teams; the PHE Centre for Chemicals Radiation and Environmental Hazards; the PHE Centre for Infectious Disease Surveillance and Control, including Carol Chatt; the PHE International Health Regulations team, including

Jane Jones, Joanne Freedman, and Gemma Smith; and Public Health Wales, including Chris Williams, for coordination and support with contact tracing; the PHE Ebola Guidance Cell for advice on contact tracing; Keith Neal for liaison with screening teams; Piers Mook for database coordination; PHE Ebola screening and returning workers, including Mark Driver and Tanya Semple, for liaison with airlines; the PHE Emergency Response Department for coordination and establishing a help line; and Moroccan and other international public health authorities for support with airline staff and passenger contact tracing.

Dr. Crook is a consultant epidemiologist in the Field Epidemiology Service of Public Health England, London, UK. His research interests are outbreak response and epidemiology of sexually transmitted infections and HIV infections, including shigellosis in men who have sex with men.

References

1. World Health Organization. Ebola situation report, March 20, 2016 [cited 2017 Sep 14]. <http://apps.who.int/ebola/current-situation/ebola-situation-report-30-march-2016>
2. Petti S, Protano C, Messano GA, Scully C. Ebola virus infection among western healthcare workers unable to recall the transmission route. *Biomed Res Int*. 2016;2016:8054709. Epub 2016 Nov 27. <http://dx.doi.org/10.1155/2016/8054709>
3. Leitmeyer K. European risk assessment guidance for infectious diseases transmitted on aircraft—the RAGIDA project. *Euro Surveill*. 2011;16:19845.
4. Gilsdorf A, Morgan D, Leitmeyer K. Guidance for contact tracing of cases of Lassa fever, Ebola or Marburg haemorrhagic fever on an airplane: results of a European expert consultation. *BMC Public Health*. 2012;12:1014. <http://dx.doi.org/10.1186/1471-2458-12-1014>
5. World Health Organization. Travel and transport risk assessment: interim guidance for public health authorities and the transport sector, 2014 [cited 2017 Sep 14]. http://apps.who.int/iris/bitstream/10665/132168/1/WHO_EVD_Guidance_TravelTransportRisk_14.1_eng.pdf
6. Advisory Committee on Dangerous Pathogens Public Health England. Management of hazard group 4 viral haemorrhagic fevers and similar human infectious diseases of high consequence, November 2015 [cited 2017 Sep 14]. <http://www.nric.org.uk/node/54189>
7. Formenty P, Hatz C, Le Guenno B, Stoll A, Rogenmoser P, Widmer A. Human infection due to Ebola virus, subtype Côte d'Ivoire: clinical and biologic presentation. *J Infect Dis*. 1999;179(Suppl 1):S48–53. <http://dx.doi.org/10.1086/514285>
8. Shuaib F, Gunnala R, Musa EO, Mahoney FJ, Oguntimhin O, Nguku PM, et al.; Centers for Disease Control and Prevention (CDC). Ebola virus disease outbreak—Nigeria, July–September 2014. *MMWR Morb Mortal Wkly Rep*. 2014;63:867–72.
9. Fasina FO, Shittu A, Lazarus D, Tomori O, Simonsen L, Viboud C, et al. Transmission dynamics and control of Ebola virus disease outbreak in Nigeria, July to September 2014. *Euro Surveill*. 2014;19:20920. <http://dx.doi.org/10.2807/1560-7917.ES2014.19.40.20920>
10. Regan JJ, Jungerman R, Montiel SH, Newsome K, Objio T, Washburn F, et al.; Centers for Disease Control and Prevention (CDC). Public health response to commercial airline travel of a person with Ebola virus infection—United States, 2014. *MMWR Morb Mortal Wkly Rep*. 2015;64:63–6.
11. Parry-Ford F, Boddington N, Pebody R, Phin N, on behalf of the Incident Management C; Incident Management Team. Public

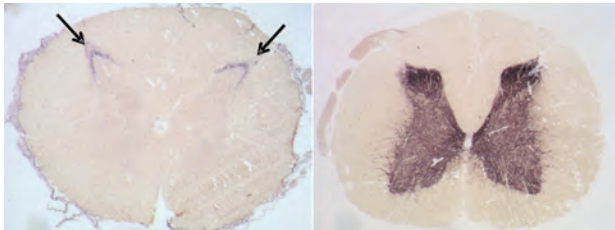
- health response to two incidents of confirmed MERS-CoV cases travelling on flights through London Heathrow Airport in 2014: lessons learnt. *Euro Surveill.* 2015;20:21114. <http://dx.doi.org/10.2807/1560-7917.ES2015.20.18.21114>
12. Mabey D, Flasche S, Edmunds WJ. Airport screening for Ebola. *BMJ.* 2014;349:g6202. <http://dx.doi.org/10.1136/bmj.g6202>

13. Cosford P. Advantages of airport screening for Ebola. *BMJ.* 2014;349:g6585. <http://dx.doi.org/10.1136/bmj.g6585>

Address for correspondence: Paul Crook, Field Epidemiology Service, Public Health England, Skipton House, 80 London Rd, London SE1 6LH, UK; email: paul.crook@phe.gov.uk

May 2013: Zoonoses

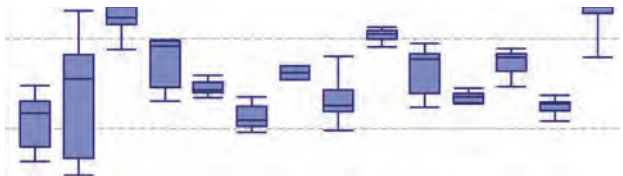
- Transmission of *Mycobacterium tuberculosis* Beijing Strains, Alberta, Canada, 1991–2007
- Foodborne Transmission of Bovine Spongiform Encephalopathy to Nonhuman Primates
- Populations at Risk for Alveolar Echinococcosis, France
- WHO International Standard to Harmonize Assays for Detection of Hepatitis E Virus RNA
- Full-Genome Deep Sequencing and Phylogenetic Analysis of Novel Human Betacoronavirus
- Targeting Surveillance for Zoonotic Virus Discovery
- Changes in Severity of Influenza A(H1N1)pdm09 Infection from Pandemic to First Postpandemic Season, Germany



- Severe Fever with Thrombocytopenia Syndrome Virus among Domesticated Animals, China
- *Campylobacter coli* Outbreak among Men Who Have Sex with Men, Quebec, Canada, 2010–2011
- Delayed Diagnosis of Chronic Q Fever and Cardiac Valve Surgery
- Treatment of Tularemia in Patient with Chronic Graft-versus-Host Disease
- Scrub Typhus Outbreak, Northern Thailand, 2006–2007
- *Rickettsia parkeri* Infection Detected from Eschar Swab Specimens
- Contaminated Ventilator Air Flow Sensor and *Bacillus cereus* Colonization of Newborns
- Mapping Environmental Suitability for Malaria Transmission, Greece



- Implications of Dengue Outbreaks for Blood Supply, Australia
- Novel Molecular Type of *Clostridium difficile* in Neonatal Pigs, Western Australia
- Novel Lyssavirus in Bat, Spain
- *Borrelia recurrentis* in Head Lice, Ethiopia
- Tuberculosis Exposure among Evacuees at a Shelter after Earthquake, Japan, 2011
- Primaquine Tolerance in Patient with Relapsing Vivax Malaria
- Tickborne Encephalitis Associated with Consumption of Raw Goat Milk, Slovenia, 2012
- Spread of Multidrug-Resistant *Acinetobacter baumannii* Clone, France
- *Plasmodium falciparum* with Multidrug Resistance 1 Gene Duplications, Senegal
- Atypical Erythema Migrans in PCR-Positive Lyme Disease
- Brucellosis in Guangdong Province, People's Republic of China, 2005–2010



Diagnostic Accuracy of Parameters for Zika and Dengue Virus Infections, Singapore

Hanley J. Ho, Joshua G.X. Wong, Win Mar Kyaw, David C. Lye, Yee Sin Leo, Angela Chow

Singapore experienced its first documented Zika virus outbreak in 2016. We identified clinical and laboratory parameters that increase the probability for Zika or dengue virus infection. Early during the illness, combinations of key parameters obtained through clinical assessment and hematologic tests can help distinguish between these infections.

Zika virus recently emerged as a clinically important arbovirus that can cause fetal complications in infected pregnant women and Guillain-Barré syndrome in adults (1–3). Since the first reported large Zika outbreak on Yap Island in 2007 (4), widespread community outbreaks have been reported in many other countries (4,5).

Dengue virus (DENV) threatens the 50% of the world's population who live in at-risk areas and causes ≈390 million infections annually (6). The frequency and magnitude of epidemic dengue have increased exponentially during the past 4 decades because of such factors as population growth and rising temperatures (7). Severe dengue can result in plasma leakage, systemic shock, multiorgan failure, and eventual death (8).

Zika and dengue have similar presenting symptoms (including fever, rash, arthralgia, myalgia, and headache) (4,9); incubation periods; and transmission routes through *Aedes* mosquitoes (5,6). Accurate and early diagnosis is essential to properly manage the unique complications of each disease.

In Singapore, a tropical island city-state in Southeast Asia, DENV is endemic. Dengue epidemics have been recorded every few years since the 1990s and now predominantly affect adults (8). In August 2016, Singapore experienced its first documented Zika outbreak (10). Before that outbreak, national surveillance of community-based patients (ongoing since 2014) had not detected any local Zika cases (11). The Zika outbreak occurred on the background of ongoing DENV circulation, and medical practitioners had to consider concurrent testing for both infections as part of clinical management.

Using the likelihood ratio approach, we identified clinical and laboratory parameters that increase the

likelihood of a laboratory-confirmed diagnosis of Zika virus or DENV infection at first presentation to clinical care. The clinical diagnostic process may lack sensitivity and specificity (12). A positive likelihood ratio (LR+) is calculated using the proportion of patients with the disease having a positive clinical or laboratory finding divided by the proportion of patients without the disease having that same finding (13). This information adds value to clinical diagnosis by refining the posttest probability of a disease. In the absence of confirmatory laboratory tests, a thorough assessment of such parameters may help distinguish between the 2 diseases.

The Study

We reviewed 2 prospectively recruited cohorts of patients with suspected Zika virus and DENV infections treated at Tan Tock Seng Hospital (Singapore), an adult tertiary care hospital. This hospital also houses the Communicable Disease Centre, the designated institution for centralized management of emerging infectious diseases in Singapore.

The Zika cohort comprised persons with suspected Zika virus infection recruited during August and September 2016. We followed the case definition used by the Singapore Ministry of Health (i.e., any person living, working, or studying in the outbreak area with fever and maculopapular rash plus ≥1 additional symptom of arthralgia, myalgia, headache, or conjunctivitis). Patients whose illness partially or fully met the case definition underwent confirmatory laboratory testing through detection of Zika virus RNA in serum and urine samples using real-time reverse transcription PCR (RT-PCR) (14). Confirmed cases were defined as a positive result for a Zika virus serum or urine test. We excluded patients with laboratory-confirmed dengue co-infection, using dengue NS1 antigen (Bio-Rad Laboratories, Marnes-la-Coquette, France) or RT-PCR (15).

The dengue cohort comprised persons with suspected DENV infection recruited during January 2010–September 2012. Persons in this cohort had fever (temperature ≥37.5°C), with or without additional signs or symptoms, and no alternative diagnosis at the time they sought care. Cases were defined as a serum-positive DENV NS1 antigen or RT-PCR.

To evaluate parameters during the early phase of each illness, for both cohorts, we limited participant recruitment to persons who sought care within 5 days after symptom onset. We obtained ethics approval from the National

Author affiliation: Tan Tock Seng Hospital, Singapore

DOI: <https://doi.org/10.3201/eid2312.171224>

Healthcare Group (NHG Domain Specific Review Board reference no. 2016/01027).

The Zika cohort comprised 281 persons with suspected Zika virus infection (online Technical Appendix Table 1, <https://wwwnc.cdc.gov/EID/article/23/12/17-1224-Techapp1.pdf>): 130 case-patients (without dengue co-infection) and 151 non-case-patients. The median age of case-patients (34 years [interquartile range (IQR) 26–49 years]) was similar to that of non-case-patients (31 years [IQR 24–38 years]). Sex distribution was similar between case-patients (60% male) and non-case-patients.

The DENV cohort comprised 310 persons with suspected DENV infection: 175 case-patients and 135 non-case-patients. Age groups were similar for case-patients (median age 36 years [IQR 29–43 years]) and non-case-patients (median age 32 years [IQR 27–42 years]), and both groups consisted primarily of male patients.

Zika virus infection case-patients most commonly had rash (94%), myalgia (41%), and documented fever (35%) (Figure 1); non-case-patients mainly had myalgia (62%), documented fever (42%), and rash (41%). Low proportions of both groups had marked thrombocytopenia (platelets $<100 \times 10^9/L$ [reference $170\text{--}420 \times 10^9/L$]), leukopenia, or lymphopenia.

DENV case-patients and non-case-patients most commonly had headache, myalgia, and nausea (Figure 2). Eighty-two percent of case-patients reported gastrointestinal symptoms and, compared with non-case-patients, case-patients reported much higher proportions of leukopenia (89% vs. 39%), lymphopenia (81% vs. 37%), and marked thrombocytopenia (53% vs. 31%).

For assessment of Zika virus infection, among individual parameters evaluated, presence of rash gave the highest LR+, sensitivity and negative predictive value, and lowest negative likelihood ratio (Table 1, <https://wwwnc.cdc.gov/EID/article/23/12/17-1224-T1.htm>). We obtained the highest LR+ using a combination of rash and conjunctivitis (LRT+ = 6.73, 95% CI 2.68–16.90).

For assessment of DENV infection, documented fever gave the highest individual LR+ of 3.13 (95% CI 2.48–3.94) (Table 2, <https://wwwnc.cdc.gov/EID/article/23/12/17-1224-T2.htm>). We obtained the highest LR+ using a combination of documented fever, lymphopenia, and thrombocytopenia (LR+ = 5.11, 95% CI 2.51–10.38).

Conclusions

Our study demonstrated some key differences between the 2 diseases. Presence of rash featured much more prominently in Zika virus infection than DENV infection during the first 5 days of illness. For dengue patients, rashes usually appear during the critical or recovery phases (typically around the fifth day of illness or thereafter) (9). Also, in contrast with dengue patients, relatively few Zika patients had hematologic abnormalities.

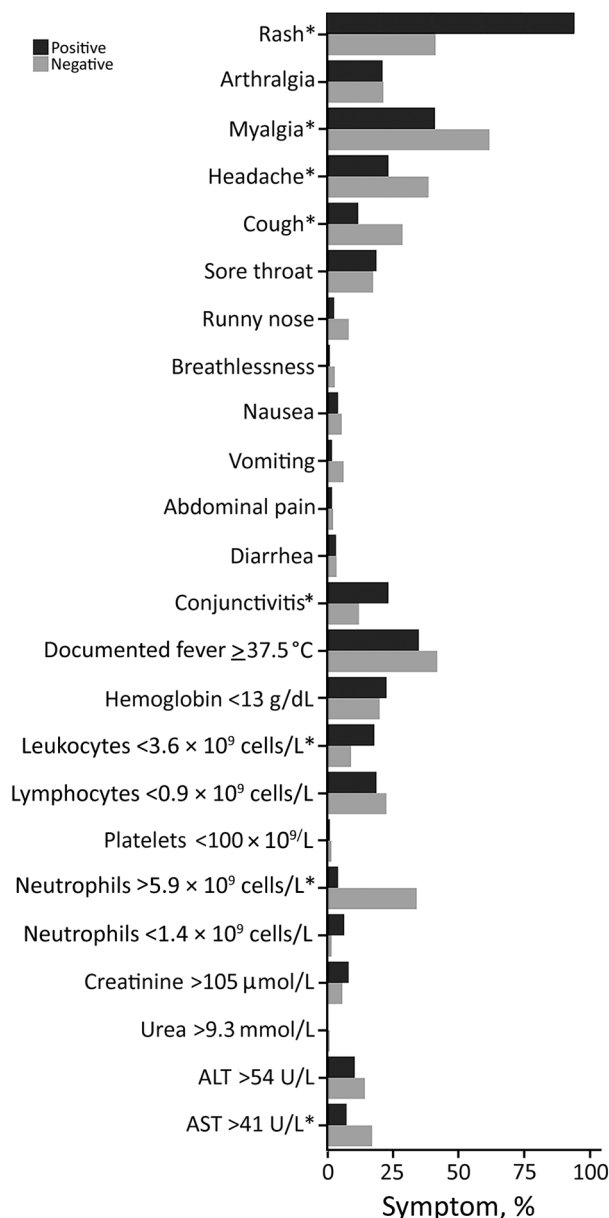


Figure 1. Clinical and laboratory parameters of Zika virus cohort, Singapore. *Statistically significant differences ($p < 0.05$).

Regardless of the patient's pretest probability for a disease, the change in posttest probability is approximated by a constant (13). In our study, presence of rash with conjunctivitis gave the highest increase in probability ($\approx 40\%$) of Zika virus infection, whereas a combination of documented fever, lymphopenia, and thrombocytopenia increased the probability for DENV infection by $\approx 30\%$ (online Technical Appendix Table 2). In contrast, absence of rash in a patient with suspected Zika or absence of lymphopenia in a patient with suspected dengue reduced the probability of the respective disease by 30%–45%. In countries where these

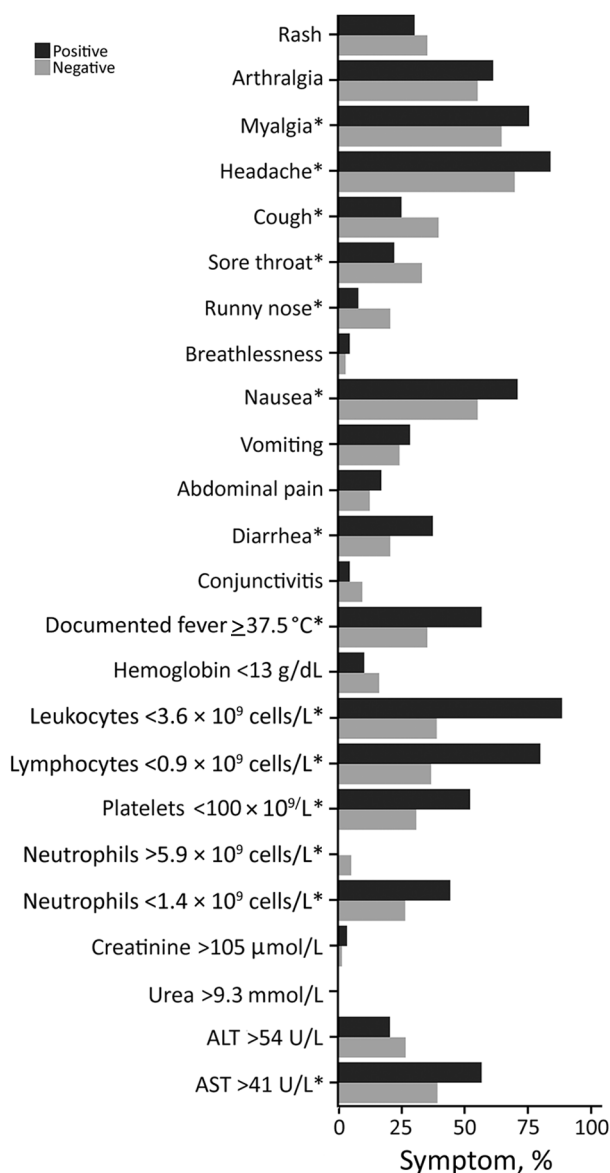


Figure 2. Clinical and laboratory parameters of dengue cohort, Singapore. *Statistically significant differences ($p < 0.05$).

viruses co-circulate, and where access to confirmatory laboratory testing is limited, these may be simple methods to help medical practitioners assess a patient suspected to have Zika or dengue.

The strengths of our study include the analysis of common parameters, standardized to ensure comparability across the 2 cohorts. Our analysis presents likelihood ratios, which are easy to interpret and aid clinical diagnosis by refining the posttest probability of a disease. The main study limitation is that our analysis compared 2 cohorts recruited at separate times and hence does not directly distinguish between the 2 infections. However, hospital workflows and clinical assessment methods

for patients largely did not change between these periods. In both cohorts, cases could have been misclassified as noncases because RT-PCR might have missed patients who sought care late. We reduced this risk by restricting recruitment to patients seeking care within 5 days after symptom onset. Our study demonstrates that a thorough assessment of clinical and hematologic parameters can aid the clinical diagnosis of Zika virus and DENV infections in the early stages.

Acknowledgments

We thank the staff of the Department of Clinical Epidemiology, Tan Tock Seng Hospital, who helped extract and collate data from the hospital databases for the study.

This work was supported by the STOP Dengue Translational Clinical Research program, funded by the National Research Foundation through the National Medical Research Council, Singapore (grant no. NMRC/TCR/005/2008).

Dr. Ho is a public health physician working in infectious disease epidemiology. His research interests include surveillance and control of emerging infectious diseases; implementation of preventive measures, such as adult vaccination programs; and outbreak investigation and management.

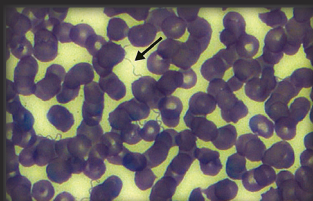
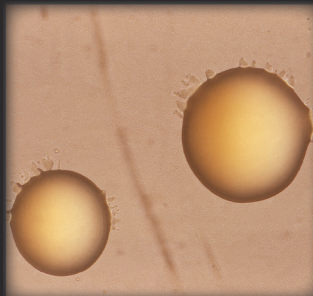
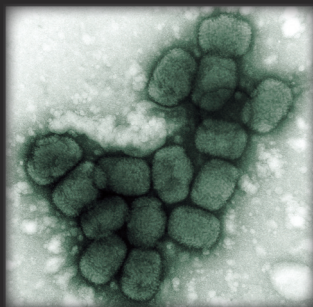
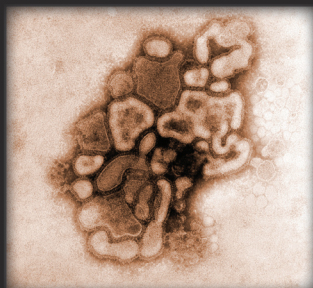
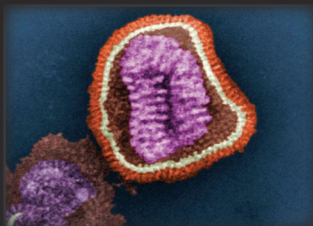
References

1. Kleber de Oliveira W, Cortez-Escalante J, De Oliveira WT, do Carmo GM, Henriques CM, Coelho GE, et al. Increase in reported prevalence of microcephaly in infants born to women living in areas with confirmed Zika virus transmission during the first trimester of pregnancy—Brazil, 2015. *MMWR Morb Mortal Wkly Rep.* 2016;65:242–7. <http://dx.doi.org/10.15585/mmwr.mm6509e2>
2. Rasmussen SA, Jamieson DJ, Honein MA, Petersen LR. Zika virus and birth defects—reviewing the evidence for causality. *N Engl J Med.* 2016;374:1981–7. <http://dx.doi.org/10.1056/NEJMs1604338>
3. Cao-Lormeau VM, Blake A, Mons S, Lastere S, Roche C, Vanhomwegen J, et al. Guillain-Barré syndrome outbreak associated with Zika virus infection in French Polynesia: a case-control study. *Lancet.* 2016;387:1531–9. [http://dx.doi.org/10.1016/S0140-6736\(16\)00562-6](http://dx.doi.org/10.1016/S0140-6736(16)00562-6)
4. Duffy MR, Chen TH, Hancock WT, Powers AM, Kool JL, Lanciotti RS, et al. Zika virus outbreak on Yap Island, Federated States of Micronesia. *N Engl J Med.* 2009;360:2536–43. <http://dx.doi.org/10.1056/NEJMoa0805715>
5. Paixão ES, Barreto F, Teixeira MG, Costa MC, Rodrigues LC. History, epidemiology, and clinical manifestations of Zika: a systematic review. *Am J Public Health.* 2016;106:606–12. <http://dx.doi.org/10.2105/AJPH.2016.303112>
6. Bhatt S, Gething PW, Brady OJ, Messina JP, Farlow AW, Moyes CL, et al. The global distribution and burden of dengue. *Nature.* 2013;496:504–7. <http://dx.doi.org/10.1038/nature12060>
7. Struchiner CJ, Rocklöv J, Wilder-Smith A, Massad E. Increasing dengue incidence in Singapore over the past 40 years: population growth, climate and mobility. *PLoS One.* 2015;10:e0136286. <http://dx.doi.org/10.1371/journal.pone.0136286>
8. Hapuarachchi HC, Koo C, Rajarethinam J, Chong CS, Lin C, Yap G, et al. Epidemic resurgence of dengue fever in Singapore in 2013–2014: a virological and entomological perspective. *BMC Infect Dis.* 2016;16:300. <http://dx.doi.org/10.1186/s12879-016-1606-z>

9. World Health Organization. Dengue guidelines for diagnosis, treatment, prevention and control: new edition 2009. 2017 [cited 2017 Jul 25]. <http://www.who.int/rpc/guidelines/9789241547871/en/>
10. Leo YS, Chow A. Zika virus has arrived in Singapore. *Lancet Infect Dis*. 2016;16:1317–9. [http://dx.doi.org/10.1016/S1473-3099\(16\)30448-0](http://dx.doi.org/10.1016/S1473-3099(16)30448-0)
11. The Straits Times. Singapore. Parliament: Singapore's Zika efforts started two years ago. 2016 Sep 14 [cited 2017 Jul 25]. <http://www.straitstimes.com/singapore/singapores-zika-efforts-started-two-years-ago>
12. Berner ES, Graber ML. Overconfidence as a cause of diagnostic error in medicine. *Am J Med*. 2008;121(Suppl):S2–23. <http://dx.doi.org/10.1016/j.amjmed.2008.01.001>
13. McGee S. Simplifying likelihood ratios. *J Gen Intern Med*. 2002;17:646–9. <http://dx.doi.org/10.1046/j.1525-1497.2002.10750.x>
14. Lanciotti RS, Kosoy OL, Laven JJ, Velez JO, Lambert AJ, Johnson AJ, et al. Genetic and serologic properties of Zika virus associated with an epidemic, Yap State, Micronesia, 2007. *Emerg Infect Dis*. 2008;14:1232–9. <http://dx.doi.org/10.3201/eid1408.080287>
15. Lai YL, Chung YK, Tan HC, Yap HF, Yap G, Ooi EE, et al. Cost-effective real-time reverse transcriptase PCR (RT-PCR) to screen for dengue virus followed by rapid single-tube multiplex RT-PCR for serotyping of the virus. *J Clin Microbiol*. 2007;45:935–41. <http://dx.doi.org/10.1128/JCM.01258-06>

Address for correspondence: Hanley J. Ho, Department of Clinical Epidemiology, Tan Tock Seng Hospital, 11 Jalan Tan Tock Seng, 308433, Singapore; email: hanleyho@gmail.com

The Public Health Image Library (PHIL)



The Public Health Image Library (PHIL), Centers for Disease Control and Prevention, contains thousands of public health-related images, including high-resolution (print quality) photographs, illustrations, and videos.

PHIL collections illustrate current events and articles, supply visual content for health promotion brochures, document the effects of disease, and enhance instructional media.

PHIL images, accessible to PC and Macintosh users, are in the public domain and available without charge.

Visit PHIL at:
<http://phil.cdc.gov/phil>

New Avian Hepadnavirus in Palaeognathous Bird, Germany

Wendy K. Jo,¹ Vanessa M. Pfankuche,¹ Henning Petersen, Samuel Frei, Maya Kummrow, Stephan Lorenzen, Martin Ludlow, Julia Metzger, Wolfgang Baumgärtner, Albert Osterhaus, Erhard van der Vries

Author affiliations: University of Veterinary Medicine Hannover, Foundation, Hannover, Germany (W.K. Jo, V.M. Pfankuche, H. Petersen, M. Ludlow, J. Metzger, W. Baumgärtner, A. Osterhaus, E. van der Vries); Center for Systems Neuroscience, Hannover (W.K. Jo, V.M. Pfankuche, W. Baumgärtner, A. Osterhaus); Wuppertal Zoo, Wuppertal, Germany (S. Frei, M. Kummrow); Bernhard Nocht Institute for Tropical Medicine, Hamburg (S. Lorenzen); Artemis One Health, Utrecht, the Netherlands (A. Osterhaus)

DOI: <https://doi.org/10.3201/eid2312.161634>

In 2015, we identified an avian hepatitis B virus associated with hepatitis in a group of captive elegant-crested tinamous (*Eudromia elegans*) in Germany. The full-length genome of this virus shares <76% sequence identity with other avihepadnaviruses. The virus may therefore be considered a new extant avian hepadnavirus.

Hepatitis B virus (HBV) belongs to the family *Hepadnaviridae*, members of which constitute 2 major extant genera: *Orthohepadnavirus*, which infect mammals, and *Avihepadnavirus*, which infect birds (1). Recently, evidence of a likely third genus was found with the discovery of a new fish hepadnavirus (2). In addition, HBV-derived endogenous viral elements have been reported in several neoavian birds (e.g., budgerigars and several finches) (3,4) and reptiles (e.g., turtles and crocodiles) (5).

Hepadnaviruses generally are characterized by their narrow host range and strong hepatotropism (1). They are enveloped, partially double-stranded DNA viruses with a small circular genome (≈3 kb) and at least 3 open reading frames (ORFs) (1). In orthohepadnaviruses, a fourth ORF encodes the X protein, which is associated with hepatocellular carcinoma in their respective host species. Avihepadnaviruses appear to have an X-like protein region; however, either a premature stop codon is present or no ORF is found in most cases (6). We describe a new avian HBV causing severe hepatitis in the elegant-crested tinamou (*Eudromia elegans*), a member of the ancient group of birds the Palaeognathae, which

includes emus (*Dromaius novaehollandiae*) and ostriches (*Struthio* spp.).

In 2015, a deceased adult elegant-crested tinamou kept at Wuppertal Zoo (Wuppertal, Germany) underwent necropsy at the University of Veterinary Medicine Hannover, Foundation (Hannover, Germany). Initial histologic examination revealed moderate, necrotizing hepatitis and inclusion body–like structures within the hepatocytes. To identify a putative causative agent, we isolated nucleic acids from the liver and prepared them for sequencing on an Illumina MiSeq system (Illumina, San Diego, CA, USA) (online Technical Appendix, <https://wwwnc.cdc.gov/EID/article/23/12/16-1634-Techapp1.pdf>). We compared obtained reads with sequences in GenBank using an in-house metagenomics pipeline. Approximately 78% of the reads aligned to existing avihepadnavirus sequences. A full genome (3,024 bp) of the putative elegant-crested tinamou HBV (ETHBV) was subsequently constructed by de novo assembly mapping >2 million reads (88.6%) to the virus genome (GenBank accession no. KY977506).

The newly identified ETHBV shared <76% nt sequence identity with other avian HBVs (online Technical Appendix Table 1). Phylogenetic analysis showed that ETHBV clustered within the genus *Avihepadnavirus*, forming a new clade (Figure, panel A). The organization of the ETHBV genome was similar to other avian HBVs because all 3 overlapping ORFs (polymerase, nucleocapsid [preC/C], and presurface [preS/S] antigen) and several essential sequence motifs (e.g., the epsilon element, TATA boxes, and direct repeat sites DR1 and DR2) were identified (online Technical Appendix Figure 1). We also found an X-like sequence. However, similar to duck HBV, ETHBV lacks a putative translation start site. It has been suggested that the X protein evolved later in mammalian hosts (5), which explains the absence of X-like ORF in the ETHBV genome. Comparison of pairwise amino acid identities between ETHBV and other avihepadnaviruses showed low homologies between their functional proteins (64%–69% similarity to the polymerase, 75%–80% to the preC/C, 52%–62% to the preS/S [online Technical Appendix Table 2]).

The identification of ETHBV prompted us to retrospectively screen the flock of 7 elegant-crested tinamous at Wuppertal Zoo and the 6 that had died within the past 4 years and had undergone necropsy at the University of Veterinary Medicine Hannover, Foundation (online Technical Appendix Table 4). For that purpose, we designed a set of degenerated primers targeting a short region of the polymerase–preC/C genome in all avihepadnaviruses (online Technical Appendix). All birds were found positive by PCR (online Technical Appendix Table 4), including liver tissue from embryonated eggs, implying that ETHBV is vertically transmitted (Figure, panel B). We then obtained a second ETHBV genome (GenBank accession

¹These authors contributed equally to this article.

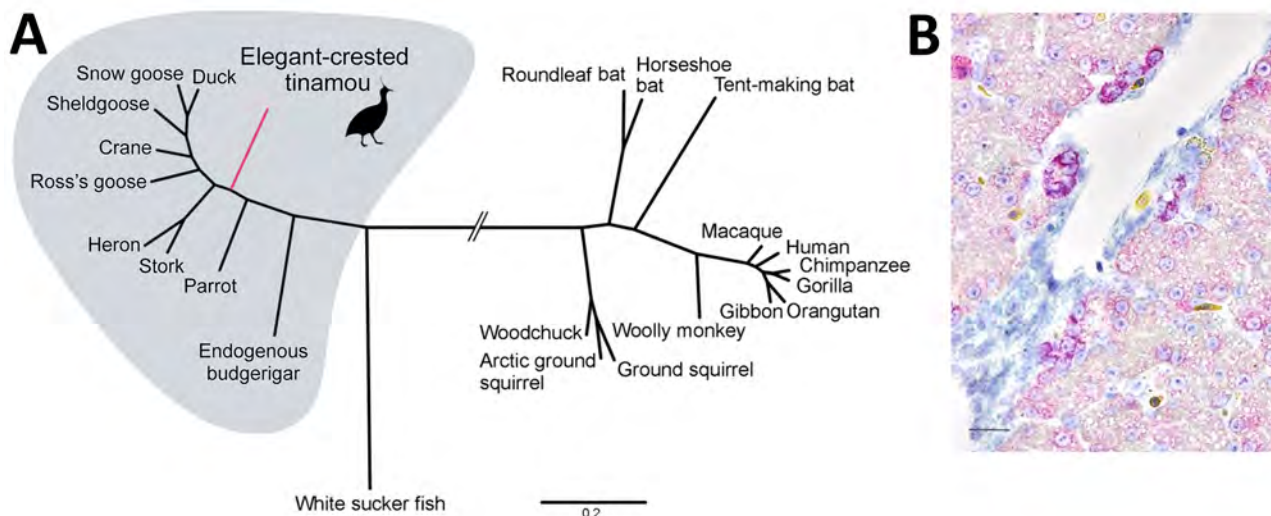


Figure. Phylogenetic and histopathologic analysis of probable new avian hepadnavirus, elegant-crested tinamou hepatitis B virus (ETHBV), Germany. A) Bayesian phylogeny of virus isolated from an elegant-crested tinamou (*Eudromia elegans*) compared with reference viruses. Tree was created on the basis of full-genome sequences from the family *Hepadnaviridae*. The analysis was run for 4 million generations and sampled every 100 steps, and the first 25% of samples were discarded as burn-in in MrBayes (7). Hasegawa-Kishino-Yano nucleotide substitution model was selected as best-fit model according to Bayesian information criteria. Posterior probabilities are shown in online Technical Appendix Figure 3 (<https://wwwnc.cdc.gov/EID/article/23/12/16-1634-Techapp1.pdf>). Branches were truncated for graphical reasons (interrupted lines). GenBank accession number for isolates, is available online (<http://wwwnc.cdc.gov/EID/article/23/16-1634-F1.htm>). Scale bar indicates nucleotide substitutions per site. B) ETHBV-specific RNA (in red; Fast Red) localized within hepatocytes of the liver tissue of an elegant-crested tinamou embryo by in situ hybridization (online Technical Appendix). Positive signal is enhanced in hepatocytes localized close to the vessels and negative in endothelial cells. Nonprobe incubation of the tinamou and liver tissue from a pheasant were used as negative controls. Scale bar indicates 40 μ m.

no. KY977507) from another tinamou from the same flock by deep sequencing; this genome showed 99.8% nt sequence identity with the initial ETHBV genome. Tinamou serum samples from another zoo were also screened but tested negative by PCR (online Technical Appendix Table 4).

To further characterize ETHBV, we confirmed infection in the liver using an in situ hybridization protocol (8) in an adult and embryo tinamou (Figure, panel B). In addition to ETHBV infection in the liver, we found some positive cells in kidney and testis tissue. Although hepadnaviruses generally are host restricted, exceptions have been reported (e.g., crane HBV) (9). We attempted to infect Pekin duck embryos through the allantoic cavity, as well as by intravenous infection routes, and were not able to demonstrate replication (data not shown).

ETHBV can be considered a new extant hepadnavirus associated with hepatitis in the elegant-crested tinamou. Whether ETHBV can infect other species within the Palaeognathae or whether it is host restricted within other tinamou species remains to be elucidated. The discovery of ETHBV suggests that other avian species may harbor as-yet undiscovered HBVs. The pathogenesis of avian hepadnavirus infections and the mechanisms of virus transmission in captive tinamou flocks warrant further investigation.

Acknowledgments

We thank Mareike Schubert, Kerstin Rohn, Danuta Waschke, Bettina Buck, Caroline Schütz, Kerstin Schöne, Heike Klippert-Hasberg, Mogens Drabert, Stefan Neander, and Jörn Wrede for excellent technical assistance. We also are grateful to Severin Dressen and Emile Prins for their collaboration in the project.

This study was in part supported by a grant from the Niedersachsen-Research Network on Neuroinfectiology from the Ministry of Science and Culture of Lower Saxony, Germany. This study also was in part supported by the COMPARE project and received funding from the European Union's Horizon 2020 research and innovation program COMPARE (grant agreement no. 643476).

Dr. Jo is a PhD candidate at the University of Veterinary Medicine Hannover Research Center for Emerging Infections and Zoonoses, Hannover, Germany. Her research interests include virus discovery, emerging and re-emerging infections, cross-species transmission, viral evolution, and host adaptation.

References

- Funk A, Mhamdi M, Will H, Sirma H. Avian hepatitis B viruses: molecular and cellular biology, phylogenesis, and host tropism. *World J Gastroenterol*. 2007;13:91–103. <http://dx.doi.org/10.3748/wjg.v13.i1.91>

2. Hahn CM, Iwanowicz LR, Cornman RS, Conway CM, Winton JR, Blazer VS. Characterization of a novel hepadnavirus in the white sucker (*Catostomus commersonii*) from the Great Lakes region of the United States. *J Virol*. 2015;89:11801–11. <http://dx.doi.org/10.1128/JVI.01278-15>
3. Liu W, Pan S, Yang H, Bai W, Shen Z, Liu J, et al. The first full-length endogenous hepadnaviruses: identification and analysis. *J Virol*. 2012;86:9510–3. <http://dx.doi.org/10.1128/JVI.01164-12>
4. Suh A, Brosius J, Schmitz J, Kriegs JO. The genome of a Mesozoic paleovirus reveals the evolution of hepatitis B viruses. *Nat Commun*. 2013;4:1791. <http://dx.doi.org/10.1038/ncomms2798>
5. Suh A, Weber CC, Kehlmaier C, Braun EL, Green RE, Fritz U, et al. Early mesozoic coexistence of amniotes and hepadnaviridae. *PLoS Genet*. 2014;10:e1004559. <http://dx.doi.org/10.1371/journal.pgen.1004559>
6. Chang SF, Netter HJ, Hildt E, Schuster R, Schaefer S, Hsu YC, et al. Duck hepatitis B virus expresses a regulatory HBx-like protein from a hidden open reading frame. *J Virol*. 2001;75:161–70. <http://dx.doi.org/10.1128/JVI.75.1.161-170.2001>
7. Huelsenbeck JP, Ronquist F. MRBAYES: Bayesian inference of phylogenetic trees. *Bioinformatics*. 2001;17:754–5. <http://dx.doi.org/10.1093/bioinformatics/17.8.754>
8. Pfankuche VM, Bodewes R, Hahn K, Puff C, Beineke A, Habierski A, et al. Porcine bocavirus infection associated with encephalomyelitis in a pig, Germany. *Emerg Infect Dis*. 2016;22:1310–2. <http://dx.doi.org/10.3201/eid2207.152049>
9. Prassolov A, Hohenberg H, Kalinina T, Schneider C, Cova L, Krone O, et al. New hepatitis B virus of cranes that has an unexpected broad host range. *J Virol*. 2003;77:1964–76. <http://dx.doi.org/10.1128/JVI.77.3.1964-1976.2003>

Address for correspondence: Erhard van der Vries, Department of Infectious Diseases & Immunology, Faculty of Veterinary Medicine, Section Virology, Utrecht University, Utrecht, the Netherlands; email: e.vandervries@uu.nl

Acute Myopericarditis Associated with Tickborne *Rickettsia sibirica mongolitimonae*

Pablo Revilla-Martí, Álvaro Cecilio-Irazola, Jara Gayán-Ordás, Isabel Sanjoaquin-Conde, Jose Antonio Linares-Vicente, José A. Oteo

Author affiliations: Hospital Clínico Universitario Lozano Blesa, Zaragoza, Spain (P. Revilla-Martí, A. Cecilio-Irazola, J. Gayán-Ordás, I. Sanjoaquin-Conde, J.A. Linares-Vicente); Centro de Investigación Biomédica de La Rioja, Logroño, Spain (J.A. Oteo)

DOI: <https://doi.org/10.3201/eid2312.170293>

We report an unusual case of myopericarditis caused by *Rickettsia sibirica mongolitimonae*. Because of increasing reports of *Rickettsia* spp. as etiologic agents of acute myopericarditis and the ease and success with which it was treated in the patient reported here, rickettsial infection should be included in the differential diagnosis for myopericarditis.

Myopericarditis is a primarily pericardial inflammatory syndrome occurring when clinical diagnostic criteria for pericarditis are satisfied and concurrent mild myocardial involvement is documented by elevated biomarkers of myocardial damage (i.e., increased troponins). Limited clinical data on the causes of myopericarditis suggest that viral infections are among the most common causes in developed countries, although the list of agents is increasing. We identified an unusual case of myopericarditis caused by *Rickettsia sibirica mongolitimonae*, an emerging pathogen in southern Europe with a broad clinical spectrum (1).

In September 2016, a 39-year-old man with no remarkable medical history sought care at an emergency department in Spain with acute-onset central chest pain and fever. The previous week, he had hunted in northeastern Spain. Physical examination revealed a systolic blood pressure of 115 mm Hg, heart rate 80 beats/min, peripheral pulse oximetry of 98%, and an axillary temperature of 38.7°C. No murmurs, rales, or gallops were detected on cardiac examination. A necrotic left gluteus eschar and multiple enlarged left inguinal lymph nodes were noted. He had neither lymphangitis nor widespread rash, and his mucous membranes appeared normal. He did not remember tick bites.

An electrocardiogram demonstrated a sinus rhythm with diffuse ST-segment elevation, and a transthoracic echocardiogram showed a normal biventricular ejection fraction with mild pericardial effusion. High-sensitive T troponin level was 575.3 ng/L (reference <14 ng/L), and blood cultures and serologic tests for common viruses were all negative. He was admitted to the hospital, and a cardiac magnetic resonance study performed 48 hours later confirmed the suspected diagnosis of myopericarditis.

Because of the eschar, tickborne-related rickettsiosis was suspected, and ibuprofen (1,800 mg/d) and doxycycline (100 mg every 12 h) were started. After the third day on medical therapy, the patient became afebrile, and the electrocardiographic changes gradually resolved. He was discharged after 12 days. Doxycycline was maintained for 14 days.

Acute-phase serologic tests yielded negative results for HIV; *Borrelia burgdorferi* sensu lato (chemiluminescence immunoassay, Liason, Diasorin, Spain); spotted fever group rickettsia (SFGR) (commercial [Focus Diagnostics, Cypress, CA, USA] and in-house tests); and *Francisella tularensis* (in-house microagglutination assay). An eschar swab sample and an eschar biopsy sample were removed under aseptic

Table. Characteristics of adults previously reported with myopericarditis associated with *Rickettsia* spp. infection*

Characteristic	Patient 1 (2)	Patient 2 (3)	Patient 3 (4)	Patient 4 (5)	Patient 5 (6)	Patient 6 (7)	Patient 7 (8)	Patient 8 (9)
Age, y/sex	28/M	52/F	74/F	35/M	25/F	54/M	Unk/unk	26/M
Country	Spain	Australia	South Africa	South Africa	United States	United States	Sri Lanka	United States
Signs and symptoms								
Fever	No	Yes	Yes	Yes	Yes	Yes	Yes	Yes
Rash	No	Yes	Yes	Yes	Yes	No	Unk	Yes
Adenopathy	Yes	No	Yes	No	Unk	Unk	Unk	Unk
Lymphangitis	Yes	No	Yes	Yes	Unk	Unk	Unk	Unk
Headache	Yes	Yes	Yes	No	Unk	Yes	Unk	Unk
Myalgia	No	Yes	No	No	Unk	Yes	Unk	Unk
Chest pain	Yes	Yes	Yes	Yes	Unk	Yes	Unk	Unk
Heart failure	No	Yes	Yes	No	Unk	No	Unk	Unk
Eschar	Yes; neck	No	Yes; unk	Yes;	Unk	Unk	No	No
				abdomen				
Organism	<i>R. slovaca</i>	<i>R. australis</i>	<i>R. africae</i>	<i>R. africae</i>	<i>R. rickettsii</i>	<i>R. rickettsii</i>	<i>R. conorii</i>	<i>R. rickettsii</i>
LVD	No	Yes	Unk	No	Yes	Yes	Unk	Yes
PE	No	No	Unk	No	Yes	No	Unk	No
Treatment	Doxycycline	Tigecycline, doxycycline	Doxycycline	Doxycycline	Unk	Doxycycline	Doxycycline	Doxycycline

*LVD, left ventricular dysfunction; PE, pericardial effusion; unk, unknown.

conditions and sent together with EDTA-treated blood and serum specimens to Spain's reference center for rickettsioses (Hospital San Pedro—Centro de Investigación Biomédica de La Rioja, Logroño, Spain) for molecular analysis. Samples were tested by PCR for the presence of *Rickettsia* spp. (*ompB*, *ompA*, and *sca 4* genes). Fragments of *ompB* rickettsial genes (285/285 bp) were amplified from the eschar biopsy and swab. The sequences obtained showed 99.8% identity to the corresponding sequences of *R. sibirica mongolitimonae* (GenBank accession no. AF123715).

A convalescent-phase serum specimen collected 7 weeks after hospital discharge was tested by indirect immunofluorescence assay for IgG against SFGR. Commercial (Focus Diagnostics) and in-house *R. conorii* and *R. slovaca* antibody testing showed an IgG of 1:1,024. In-house microagglutination assay results for *F. tularensis* were not reactive.

Myopericarditis, a rare complication of human rickettsiosis, usually occurs with acute infection caused by *R. rickettsii* or *R. conorii*. To our knowledge, there are few reports of a myopericarditis due to SFGR infections (Table) (2–9), and in PubMed, we found none attributed to *R. sibirica mongolitimonae*.

R. sibirica mongolitimonae is an intracellular bacterium that was first reported as a human pathogen in 1996; since then, several cases have been reported from France, Portugal, Greece, and Spain showing seasonal variations with predominance during spring and summer (1). Clinical manifestations include fever with or without rash, myalgia, and headache. A characteristic rope-like lymphangitis from the eschar to the draining lymph node is evident in one third of patients (1).

Rickettsiosis is commonly diagnosed on the basis of serologic testing, although use of molecular tools or cell culture on a skin biopsy specimen from an eschar is one of the best methods to identify *Rickettsia* spp. Swabbing an

eschar is painless, and its results are similar to skin biopsy samples by molecular tools. In the patient we reported, the swab sample from the eschar was useful for rickettsial diagnosis (10). Negative test results for other agents and the clinical response to doxycycline strongly supported the diagnosis of acute myopericarditis associated with *R. sibirica mongolitimonae*. Because of increasing reports of different species of *Rickettsia* involved as etiologic agents of acute myopericarditis and the ease and success with which this infection was treated, we strongly recommend including rickettsial infection in the differential diagnosis in the adequate epidemiology context.

Dr. Revilla-Martí is a cardiologist at Hospital Clínico Universitario Lozano Blesa in Zaragoza, Spain. His research interests include heart failure and myocardial diseases.

References

- Portillo A, Santibáñez S, García-Álvarez L, Palomar AM, Oteo JA. Rickettsioses in Europe. *Microbes Infect.* 2015;17:834–8. <http://dx.doi.org/10.1016/j.micinf.2015.09.009>
- Silva JT, López-Medrano F, Fernández-Ruiz M, Foz ER, Portillo A, Oteo JA, et al. Tickborne lymphadenopathy complicated by acute myopericarditis, Spain. *Emerg Infect Dis.* 2015;21:2240–2. <http://dx.doi.org/10.3201/eid2112.150672>
- Wilson PA, Tierney L, Lai K, Graves S. Queensland tick typhus: three cases with unusual clinical features. *Intern Med J.* 2013;43:823–5. <http://dx.doi.org/10.1111/imj.12184>
- Roch N, Epaulard O, Pelloux I, Pavese P, Brion JP, Raoult D, et al. African tick bite fever in elderly patients: 8 cases in French tourists returning from South Africa. *Clin Infect Dis.* 2008;47:e28–35. <http://dx.doi.org/10.1086/589868>
- Bellini C, Monti M, Potin M, Dalle Ave A, Bille J, Greub G. Cardiac involvement in a patient with clinical and serological evidence of African tick-bite fever. *BMC Infect Dis.* 2005;5:90–5. <http://dx.doi.org/10.1186/1471-2334-5-90>
- Nesbit RM, Horton JM, Littman L. Myocarditis, pericarditis and cardiac tamponade associated with Rocky Mountain spotted fever. *J Am Coll Cardiol.* 2011;57:2453.

7. Doyle A, Bhalla KS, Jones JM III, Ennis DM. Myocardial involvement in Rocky Mountain spotted fever: a case report and review. *Am J Med Sci*. 2006;332:208–10. <http://dx.doi.org/10.1097/0000441-200610000-00009>
8. Kularatne SA, Rajapakse RP, Wickramasinghe WM, Nanayakkara DM, Budagoda SS, Weerakoon KG, et al. Rickettsioses in the central hills of Sri Lanka: serological evidence of increasing burden of spotted fever group. *Int J Infect Dis*. 2013;17:e988–92. <http://dx.doi.org/10.1016/j.ijid.2013.05.014>
9. Kushawaha A, Brown M, Martin I, Evenhuis W. Hitch-hiker taken for a ride: an unusual case of myocarditis, septic shock and adult respiratory distress syndrome. *BMJ Case Rep*. 2013;2013. pii: bcr2012007155. <http://dx.doi.org/10.1136/bcr-2012-007155>
10. Solary J, Socolovschi C, Aubry C, Brouqui P, Raoult D, Parola P. Detection of *Rickettsia sibirica mongolitimonae* by using cutaneous swab samples and quantitative PCR. *Emerg Infect Dis*. 2014;20:716–8. <http://dx.doi.org/10.3201/eid2004.130575>

Address for correspondence: Pablo Revilla-Marti, Hospital Clinico Universitario Lozano Blesa, Avenida San Juan Bosco 15, Zaragoza 50009, Spain; email: pablorevillamarti@gmail.com

Enteropathogenic *Escherichia coli* O80:H2 in Young Calves with Diarrhea, Belgium

Damien Thiry, Marc Saulmont, Shino Takaki, Klara De Rauw, Jean-Noël Duprez, Atsushi Iguchi, Denis Piérard, Jacques G. Mainil

Author affiliations: University of Liège, Liège, Belgium (D. Thiry, S. Takaki, J.-N. Duprez, J.G. Mainil); Association Régionale de Santé et d'Identification Animales, Ciney, Belgium (M. Saulmont); Universitair Ziekenhuis Brussel, Brussels, Belgium (K. De Rauw, D. Piérard); University of Miyazaki, Miyazaki, Japan (S. Takaki, A. Iguchi)

DOI: <https://doi.org/10.3201/eid2312.170450>

Serogroup O80 was detected in 40% of 104 enteropathogenic *Escherichia coli* isolates from calves with diarrhea from 42 farms in Belgium during 2008–2015. These isolates harbored the *eae-ξ* and *fliC_{H2}* genes, similar to the O80 attaching-effacing Shigatoxigenic *E. coli* isolates found in humans in France. This strain might be emerging.

Enteropathogenic and attaching-effacing Shigatoxigenic *Escherichia coli* (EPEC and AE-STECS) cause bloody diarrhea in humans and young calves. For clarity,

we use the term AE-STECS instead of enterohemorrhagic *E. coli*, similar to a previous publication (1), to refer to STECS isolates from animals that produce attaching-effacing lesions. EPEC and AE-STECS that infect humans are diverse and comprise scores of serotypes (2); in contrast, most calf AE-STECS strains comprise a few serotypes, mostly O5:H-, O26:H11, O111:H-, and O118:H16 (3). The O26:H11 serotype is also the most common among calf EPEC. However, most serotypes that infect calves have not been identified (3). Therefore, during November 2008–June 2015, we conducted a study on 104 EPEC and 153 AE-STECS isolates collected from the feces or the intestinal contents of calves suffering diarrhea (1 isolate/calf) at the Association Régionale de Santé et d'Identification Animales in Ciney, Belgium. Isolates were screened by PCR for genes of the 10 most pathogenic and common calf and human O serogroups: O5, O26, O103, O104, O111, O118, O121, O145, O157, and O165. Confirming published results (3), 80% (122/153) of AE-STECS isolates and only 21% (22/104) of EPEC isolates tested positive for 1 of these (J.G. Mainil, unpub. data) (4). We sought to further characterize this collection of calf EPEC with unidentified O serogroups.

We submitted 9 calf EPECs with unidentified serogroups to the O-typing multiplex PCR platform (5); 6 of 9 EPEC isolates contained the O80 serogroup–encoding gene, and 3 belonged to 3 other O serogroups. We subsequently performed an O80 serogroup–specific PCR (5) of all 31 AE-STECS and 82 EPEC isolates with unidentified serogroups, along with one O80-positive *E. coli* strain and negative controls; 42 EPEC isolates and the O80-positive *E. coli* strain but no AE-STECS isolates or negative controls tested positive.

We further tested the calf EPEC isolates and 3 human Shiga toxin 2–encoding gene (*stx2*)–positive AE-STECS O80 isolates from the STECS National Reference Center (Brussels, Belgium) by PCR for *fliC_{H2}* and *eae-ξ* genes found in human AE-STECS O80 strains. For amplifying *eae-ξ*, we used previously published PCR conditions (6), and for amplifying *fliC_{H2}*, we used primers H2_F (5'-TGATCCGACATCTCCTGATG-3') and H2_R (5'-CCGTCATCACCAATCAACGC-3') and the following thermocycler conditions: initial denaturation at 94°C for 1 min; 30 cycles of denaturation for 30 s at 94°C, annealing for 30 s at 58°C, and elongation for 1 min at 72°C; and final elongation at 72°C for 2 min. All 42 calf EPEC and 3 human AE-STECS isolates tested positive by both PCRS.

Among the 104 calf EPEC isolates, O80:H2 was frequently found (40% were PCR positive) and, thus, could be considered emerging. Indeed, the EPEC O80 isolates were isolated from calves from 42 farms. The yearly EPEC O80:H2 isolation rate varied from 12% in 2009 to 40%–50% during 2010–2013 to as high as 73% for the

Table. Comparison of yearly isolation rates of EPEC O80:H2 and O26 from calves with diarrhea, Belgium, January 2009–June 2015*

Year	Total no.	EPEC	
		O80:H2, %	O26, %
2009	17	24	12
2010	19	47	5
2011	12	50	33
2012	9	33	22
2013	15	47	20
2014	20	25	25
2015	11	73	9
Total	104	41	16

*In 2008, only isolates collected in November and December were studied, and 1 EPEC was identified. EPEC, enteropathogenic *Escherichia coli*.

first 6 months of 2015 (Table). In comparison, the rate for EPEC O26 serotype was 5%–25%. Although prevalence data before 2009 are lacking, EPEC O80 isolates have been found infrequently in animals: 8 in dead poultry (7,8), 1 in a piglet with diarrhea (9), 1 in a healthy cow (9), and 5 in lambs with diarrhea (10). However, even fewer AE-STECS O80 isolates have been found: 2 in healthy cattle (6); 1 in a calf with diarrhea in January 1987 (J.G. Mainil, unpub. data); and 1 in raw cow's milk cheese (9). According to the literature, the O80:H2 serotype might be emerging in France, where human cases of AE-STECS O80:H2 have been reported (9).

Molecular virulotyping results indicate that our calf EPEC O80 isolates appeared to be more closely related to human AE-STECS (because they all harbored *eae*- ξ and *fliC*_{H26}) than to ovine and poultry EPEC O80 (which usually harbor *eae*- β and *fliC*_{H26}) (J.G. Mainil, unpub. data) (8,10). Further studies are needed to characterize these calf EPEC O80:H2 isolates, and the isolation rate of EPEC O80:H2 in calves with diarrhea must be tracked. Additional PCR virulotyping should be performed with our isolates to identify, if present, other EPEC-related virulence genes and extraintestinal *E. coli*-related virulence genes. Some genes could be located on plasmids, like those that were found in AE-STECS O80:H2 patients with bacteremia and internal organ infections (9), although the infected calves from which our isolates were taken did not show evidence of septicemia before or after necropsy. The relationship among calf EPEC O80:H2 isolates (which are all independent isolates, not constituting a single strain until proven otherwise) and between calf and human isolates needs to be further characterized with pulsed-field gel electrophoresis and whole-genome sequencing. The prevalence of O80:H2 EPEC and AE-STECS in healthy cattle at slaughterhouses and farms in Belgium should be examined. Finally, we need to determine whether these calf EPEC O80:H2 isolates are true EPEC, AE-STECS derivatives that have lost *stx* genes, or AE-STECS precursors that could acquire *stx* genes in the future. This work will aid in the detection, prevention, and control of this potentially emerging pathogen.

Acknowledgments

The authors thank Maika Furukawa for her efficient technical support and Melha Mellata for helpful discussions.

The University of Liège provided financial support (Fonds Spéciaux de la Recherche, 2016–2018). S.T. is a trainee veterinary student from the University of Miyazaki, Japan, under the Japan Public-Private Partnership Student Study Abroad Program of the Japan Student Services Organization.

Dr. Thiry is an assistant professor at the Bacteriology Laboratory at the Faculty of Veterinary Medicine of the University of Liège. His areas of research are the identification of enteropathogenic and Shiga toxin-producing *Escherichia coli* isolated from young diarrheic calves and bacteriophages as an alternative treatment for bacterial infections (*Escherichia coli* and *Staphylococcus aureus*) in cattle.

References

- Piérard D, De Greve H, Haesebrouck F, Mainil J. O157:H7 and O104:H4 vero/Shiga toxin-producing *Escherichia coli* outbreaks: respective role of cattle and humans. *Vet Res (Faisalabad)*. 2012;43:13. <http://dx.doi.org/10.1186/1297-9716-43-13>
- Tozzoli R, Scheutz F. Diarrhoeagenic *Escherichia coli* infections in humans. In: Morabito S, editor. *Pathogenic Escherichia coli: molecular and cellular microbiology*. Norwich (UK): Horizon Scientific Press and Caister Academic Press; 2014.
- Mainil JG, Fairbrother JM. Pathogenic *Escherichia coli* in domestic mammals and birds. In: Morabito S, editor. *Pathogenic Escherichia coli: molecular and cellular microbiology*. Norwich (UK): Horizon Scientific Press and Caister Academic Press; 2014.
- Fakih I, Thiry D, Duprez JN, Saulmont M, Iguchi A, Piérard D, et al. Identification of Shiga toxin-producing (STEC) and enteropathogenic (EPEC) *Escherichia coli* in diarrhoeic calves and comparative genomics of O5 bovine and human STEC. *Vet Microbiol*. 2017;202:16–22. <http://dx.doi.org/10.1016/j.vetmic.2016.02.017>
- Iguchi A, Iyoda S, Seto K, Morita-Ishihara T, Scheutz F, Ohnishi M; Pathogenic *E. coli* Working Group in Japan. *Escherichia coli* O-genotyping PCR: a comprehensive and practical platform for molecular O serogrouping. *J Clin Microbiol*. 2015;53:2427–32. <http://dx.doi.org/10.1128/JCM.00321-15>
- Blanco M, Blanco JE, Mora A, Dahbi G, Alonso MP, González EA, et al. Serotypes, virulence genes, and intimin types of Shiga toxin (verotoxin)-producing *Escherichia coli* isolates from cattle in Spain and identification of a new intimin variant gene (*eae*- ξ). *J Clin Microbiol*. 2004;42:645–51. <http://dx.doi.org/10.1128/JCM.42.2.645-651.2004>
- Schouler C, Schaeffer B, Brée A, Mora A, Dahbi G, Biet F, et al. Diagnostic strategy for identifying avian pathogenic *Escherichia coli* based on four patterns of virulence genes. *J Clin Microbiol*. 2012;50:1673–8. <http://dx.doi.org/10.1128/JCM.05057-11>
- Oh JY, Kang MS, An BK, Shin EG, Kim MJ, Kim YJ, et al. Prevalence and characteristics of intimin-producing *Escherichia coli* strains isolated from healthy chickens in Korea. *Poult Sci*. 2012;91:2438–43. <http://dx.doi.org/10.3382/ps.2012-02301>
- Soysal N, Mariani-Kurkdjian P, Smail Y, Liguori S, Gouali M, Loukiadis E, et al. Enterohemorrhagic *Escherichia coli* hybrid pathotype O80:H2 as a new therapeutic challenge. *Emerg Infect Dis*. 2016;22:1604–12. <http://dx.doi.org/10.3201/eid2209.160304>

10. Cid D, Ruiz-Santa-Quiteria JA, Marín I, Sanz R, Orden JA, Amils R, et al. Association between intimin (*eae*) and *espB* gene subtypes in attaching and effacing *Escherichia coli* strains isolated from diarrhoeic lambs and goat kids. *Microbiology*. 2001;147: 2341–53. <http://dx.doi.org/10.1099/00221287-147-8-2341>

Address for correspondence: Jacques G. Mainil, Bacteriology Laboratory, Department of Infectious Diseases, Faculty of Veterinary Medicine, Campus du Sart Tilman B43a, Quartier Vallée 2, Avenue de Cureghem 6, Université de Liège, 4000, Liège, Belgium; email: jg.mainil@uliege.be

Incentives for Bushmeat Consumption and Importation among West African Immigrants, Minnesota, USA

Emily Walz, David Wilson, Jacob C. Stauffer, Danushka Wanduragala, William M. Stauffer, Dominic A. Travis,¹ Jonathan D. Alpern¹

Author affiliations: University of Minnesota, Minneapolis, Minnesota, USA (E. Walz, W.M. Stauffer, D.A. Travis, J.D. Alpern); African Career, Education, and Resources, Inc., Brooklyn Park, Minnesota, USA (D. Wilson); Stillwater High School, Stillwater, Minnesota, USA (J.C. Stauffer); Minnesota Department of Health, St. Paul, Minnesota, USA (D. Wanduragala)

DOI: <https://doi.org/10.3201/eid2312.170563>

The knowledge, attitudes, and practices surrounding bushmeat consumption and importation in the United States are not well described. Focus groups of West African persons living in Minnesota, USA, found that perceived risks are low and unlikely to deter consumers. Incentives for importation and consumption were multifactorial in this community.

Bushmeat hunting and butchery are risk factors for zoonotic disease transmission (1–3). However, less is known about health risks to those who consume products that are already butchered when purchased. Bushmeat in this report refers to meat from wild African animals such as rodents, hooved animals, carnivores, primates, and bats (3).

Thousands of pounds of bushmeat are illegally imported into the United States annually (4), mostly from West

Africa (5). A previous study of bushmeat consumption by African immigrants in the United States described mixed perceptions regarding the risks and benefits of consuming bushmeat (5). Improved understanding of the complex social drivers of these practices is needed to better characterize risk and formulate communication strategies.

To identify the cultural perspectives and knowledge, attitudes, and practices surrounding bushmeat importation and consumption, we held focus groups with members of the Liberian community living in the Minneapolis–St. Paul area of Minnesota, USA. Minneapolis–St. Paul has the largest Liberia-born population in the United States, and ranks fifth in overall African populations in US metropolitan areas (6). Recognizing the history of stigmatization associated with increased risk for Ebola virus among persons from West Africa, we engaged a community-based organization to partner in the planning and execution of this study (7,8). Creating a comfortable environment where participants share personal experiences and insights freely is a key tenet of focus group methodology (9); this partnership was essential in gaining trust and maintaining cultural sensitivity.

Inclusion criteria for participant selection included: 1) minimum age 18 years, 2) self-identification as West African, and 3) willingness to discuss bushmeat in a group setting. The partner organization recruited community members by using a combination of purposeful sampling and social media advertisement and facilitated 3 focus groups (10–12 participants, each for 90 min) in January and February 2016; a designated research team member attended each session. A standard guide for questions was used for each session (online Technical Appendix, <https://wwwnc.cdc.gov/EID/article/23/12/17-0563-Techapp1.pdf>). The University of Minnesota Institutional Review Board approved this study.

Sessions were audio recorded and transcribed; participants were not identified. Nonverbal cues (i.e., gestures, emotions, points of hesitation, nods of agreement) and other participant interactions were added to the transcript by a notetaker. We analyzed the collected data by using a modified grounded theory method with inductive analysis as previously described (10). Two authors (E.W., J.D.A.) analyzed each transcript by using an open and selective coding approach. Subsequently, all transcripts were analyzed together by using axial coding further describing relationships among themes (Table); representative quotes from participants were selected to exemplify a relationship or common theme (9) (Table). We supported validity of findings by using member-checking, triangulation of findings with multiple sources, and peer debriefing (9). Many themes were repeated in all groups; however, this study was limited by inability to confirm that we had reached saturation of perspectives. According to Creswell, it is ideal

¹These senior authors contributed equally to this article.

Table. Representative quotations and associated themes discussed by Liberian immigrants in bushmeat focus groups, Minnesota, USA*

Theme	Key quotation
1. Nostalgia/cultural connection is a driver for consumption	"So it goes back to the cultural thing, like she said. The taste and that which you're used to. I mean it's how you're brought up, and all that stuff. It's just something like you go away to school and you just miss your mom's cooking. So that's just what it is."
2. Bushmeat is readily accessible and consumed when visiting friends/relatives in West Africa	Moderator: So for those that I hear, you know, about the regulations, about disease and all of that, do you think that if they were to go back home, would they still eat bushmeat ? "Oh yeah." "Yeah." (Many others nodding)
3. Skepticism over potential zoonoses from bushmeat	"I don't believe that monkey or bat is carrying this virus. But these beliefs come from my experience. When I was growing up, I would talk to my grand uncle and we used to walk in the forest, teaching me how to survive in the forest... And he taught me one thing, anything that can kill any animal can kill you. And anything an animal carries that can kill it... When you see the animal, you'll see it's sick and you see it dead. So anything that can kill me, the animal will not survive. So monkey cannot carry a virus that can kill me [and not look sick]. "
4. Cooking and proper food preparation can mitigate disease risk	"When you kill the bushmeat in Africa, before you even eat it, it goes over the fire, they dry the meat, and there it goes in the pot and we are cooking it in Africa—we are not cooking for five minutes. I don't care how the virus or bacteria is, when you put it in the fire it will not survive for a minute. When we start talking about Ebola, well, Ebola did not come from eating bushmeat, but the Ebola virus might have been on the meat, but when you put it on the fire, I don't think that the Ebola virus could survive. "
5. African bushmeat may be banned in the United States due to human health risks	"So if you tell somebody, you know someone who don't know anything about Africa or West Africa and you tell a person, 'I eat bushmeat,' right, and they think 'do you know how many animals over there... who have XYZ, difficult diseases?' So, from their perspective, I'm going to freak out, like, why are you bringing this into my country, where most likely, I don't know what it carries, or it could be transmitted and there'll be a big epidemic. "

*Bold text indicates emphasis of quotation.

to repeat focus group sessions with new participants until novel perspectives no longer arise (9).

Participants had resided in the United States from 6 months to 35 years; approximately half were female (online Technical Appendix Table 1). All had consumed bushmeat, either abroad or in the United States. The 2 fundamental drivers of consumption in the United States were to 1) strengthen connection with African roots or 2) share the social experience with friends or relatives (Table). Many participants also reported frequent consumption of bushmeat while visiting West Africa (Table).

Most participants reported preference for what they described as "dried bushmeat." "Drying" involved varying degrees of smoking, aging, and desiccation. Dried bushmeat, compared with raw or partially smoked products, was preferred for importation because its decreased odor is believed to reduce detection.

Concern about zoonotic or foodborne disease dissuaded few participants from obtaining or consuming bushmeat, despite heightened awareness that wildlife could harbor Ebola virus. Among those who acknowledged this potential, most believed careful preparation and thorough cooking mitigated risk. For instance, participants cited traditional Liberian cooking techniques (extensive boiling for long durations) as a protective factor (Table).

Some participants were knowledgeable of hunting and butchering techniques, but most participants purchased dried consumer products and had not participated in the processing of carcasses. Although there were consistent gaps in knowledge of import regulations, it was

commonly perceived that political, public health, or discriminatory (e.g., racist, xenophobic) justifications were factors (Table).

These focus groups yielded detailed and nuanced information on the knowledge, attitudes, and practices related to bushmeat use and consumption among Liberians and Liberian Americans in a US metro area. Although this study did not directly enumerate the volume and type of bushmeat imported into the United States, our results provide a description of sociocultural factors involved on the demand side of the supply chain, a common gap in most risk assessments, and give insight into potential education and risk management strategies. We found that engaging the community in a culturally appropriate manner encouraged open dialogue, creating opportunities for education regarding import regulations and risk mitigation strategies (e.g., careful preparation and thorough cooking).

Acknowledgments

We acknowledge African Career, Education, and Resources Inc. for assistance in planning, hosting, and conducting the focus groups. Particular thanks to Nelima Sitati Munene, Denise Butler, and Wynfred Russell for initial planning stages and contributions to wording of the question script and to Wokie Freeman for moderating the focus groups. We thank Arnold Vang for contributions in planning and information on local airport confiscations. Additional thanks to Jared Erdmann with the Minneapolis Health Department for providing collaborative training with partners.

This study was funded by the International Society of Travel Medicine (ISTM) 2014–2015 Research Award, as well as the Department of Veterinary Population Medicine, College of Veterinary Medicine, University of Minnesota.

Dr. Walz is a researcher in the Department of Veterinary and Biomedical Sciences, College of Veterinary Medicine, at the University of Minnesota. Her research focuses on risks for infectious diseases in animals and humans.

References

1. Paige SB, Frost SDW, Gibson MA, Jones JH, Shankar A, Switzer WM, et al. Beyond bushmeat: animal contact, injury, and zoonotic disease risk in western Uganda. *EcoHealth*. 2014;11:534–43. <http://dx.doi.org/10.1007/s10393-014-0942-y>
2. Subramanian M. Zoonotic disease risk and the bushmeat trade: assessing awareness among hunters and traders in Sierra Leone. *EcoHealth*. 2012;9:471–82. <http://dx.doi.org/10.1007/s10393-012-0807-1>
3. Friant S, Paige SB, Goldberg TL. Drivers of bushmeat hunting and perceptions of zoonoses in Nigerian hunting communities. Bausch DG, editor. *PLoS Negl Trop Dis*. 2015;9:e0003792. <https://doi.org/10.1371/journal.pntd.0003792>
4. US Fish and Wildlife Service. Bushmeat [cited 2016 Mar 25]. <http://www.fws.gov/international/wildlife-without-borders/global-program/bushmeat.html>
5. Bair-Brake H, Bell T, Higgins A, Bailey N, Duda M, Shapiro S, et al. Is that a rodent in your luggage? A mixed method approach to describe bushmeat importation into the United States. *Zoonoses Public Health*. 2014;61:97–104. <http://dx.doi.org/10.1111/zph.12050>
6. US Census Bureau. American Community Survey. 2015 [cited 2017 Apr 3]. <https://factfinder.census.gov/faces/tableservices/jsf/pages/productview.xhtml?src=bkmk>
7. Sell TK, Boddie C, McGinty EE, Pollack K, Smith KC, Burke TA, et al. Media messages and perception of risk for Ebola virus infection, United States. *Emerg Infect Dis*. 2017;23:108–11. <http://dx.doi.org/10.3201/eid2301.160589>
8. Sepic M. Minnesota's Liberian immigrants fear stigma from Ebola. NPR. 2014 Oct 10 [cited 2017 Mar 23]. <http://www.npr.org/2014/10/10/355187977/minnesotas-liberian-immigrants-fear-stigma-from-ebola>
9. Creswell JW. Research design: qualitative, quantitative, and mixed methods approaches. 4th ed. Los Angeles: SAGE Publications; 2009.
10. Betancourt TS, Abdi S, Ito BS, Lilienthal GM, Agalab N, Ellis H. We left one war and came to another: resource loss, acculturative stress, and caregiver-child relationships in Somali refugee families. *Cultur Divers Ethnic Minor Psychol*. 2015; 21:114–25. <http://dx.doi.org/10.1037/a0037538>

Address for correspondence: Emily Walz, University of Minnesota, 1971 Commonwealth Ave, St. Paul, MN 55108, USA; walz148@umn.edu

Porcine Astrovirus Type 3 in Central Nervous System of Swine with Polioencephalomyelitis

Bailey Arruda, Paulo Arruda, Melissa Hensch, Qi Chen, Ying Zheng, Chenghuai Yang, Igor Renan Honorato Gatto, Franco Matias Ferreyra, Phil Gauger, Kent Schwartz, Laura Bradner, Karen Harmon, Ben Hause, Ganwu Li

Author affiliations: Iowa State University, Ames, Iowa, USA (B. Arruda, Q. Chen, Y. Zheng, C. Yang, F.M. Ferreyra, P. Gauger, K. Schwartz, L. Bradner, K. Harmon, G. Li); Veterinary Resources Inc., Ames (P. Arruda); The Maschhoffs, Carlyle, Illinois, USA (M. Hensch); São Paulo State University (Unesp), Jaboticabal, Brazil (I.R.H. Gatto); Cambridge Technologies, Worthington, Minnesota, USA (B. Hause)

DOI: <https://doi.org/10.3201/eid2312.170703>

Using next-generation sequencing, we identified and genetically characterized a porcine astrovirus type 3 strain found in tissues from the central nervous system of 1 piglet and 3 sows with neurologic signs and nonsuppurative polioencephalomyelitis. Further studies are needed to understand the potential for cross-species transmission and clinical impact.

Astroviruses have been identified in a variety of mammals and birds; infection is often asymptomatic (1). Recently astroviruses have been implicated in cases of encephalomyelitis in humans, mink, cattle, and sheep (2–5). We describe the use of unbiased next-generation sequencing to identify and genetically characterize a porcine astrovirus type 3 (PoAstV-3) in central nervous system (CNS) tissues of a 5-week-old piglet and 3 sows with neurologic signs and histopathologic lesions compatible with a neurotropic viral infection.

A multisite swine production farm submitted swine neurologic cases on 3 different occasions over a 9-month period to the Iowa State Veterinary Diagnostic Laboratory (Ames, Iowa, USA); 1 submission (2 live piglets) represented a population of 4–12-week-old pigs and 2 submissions (submission 2, two live sows; submission 3, head and tissue of sow) representing sows. In all cases, affected swine exhibited clinical signs that ranged from hind limb weakness to quadriplegia and occasionally convulsions (Video, <https://wwwnc.cdc.gov/EID/article/23/12/17-0703-V1.htm>). The sow farm reported a case-fatality rate of 100%. The young pigs, which were farrowed from sows from the aforementioned sow farm, originated

from 2 commercial grow-out facilities that reported a case-fatality rate of 75%. Histologic lesions in the CNS were consistent with a viral etiology. The following viruses were not detected in CNS samples by PCR: porcine reproductive and respiratory syndrome virus types 1 and 2, porcine circovirus 2, suid alphaherpesvirus 1,

teschovirus A, sapelovirus A, or atypical porcine pestivirus. No pathogens were isolated by bacterial culture. Because of the persistence and severity of clinical signs, histologic lesions, and lack of detection of a viral etiology, two 5-week-old piglets and 4 sows with neurologic signs were submitted by a veterinarian for diagnostic

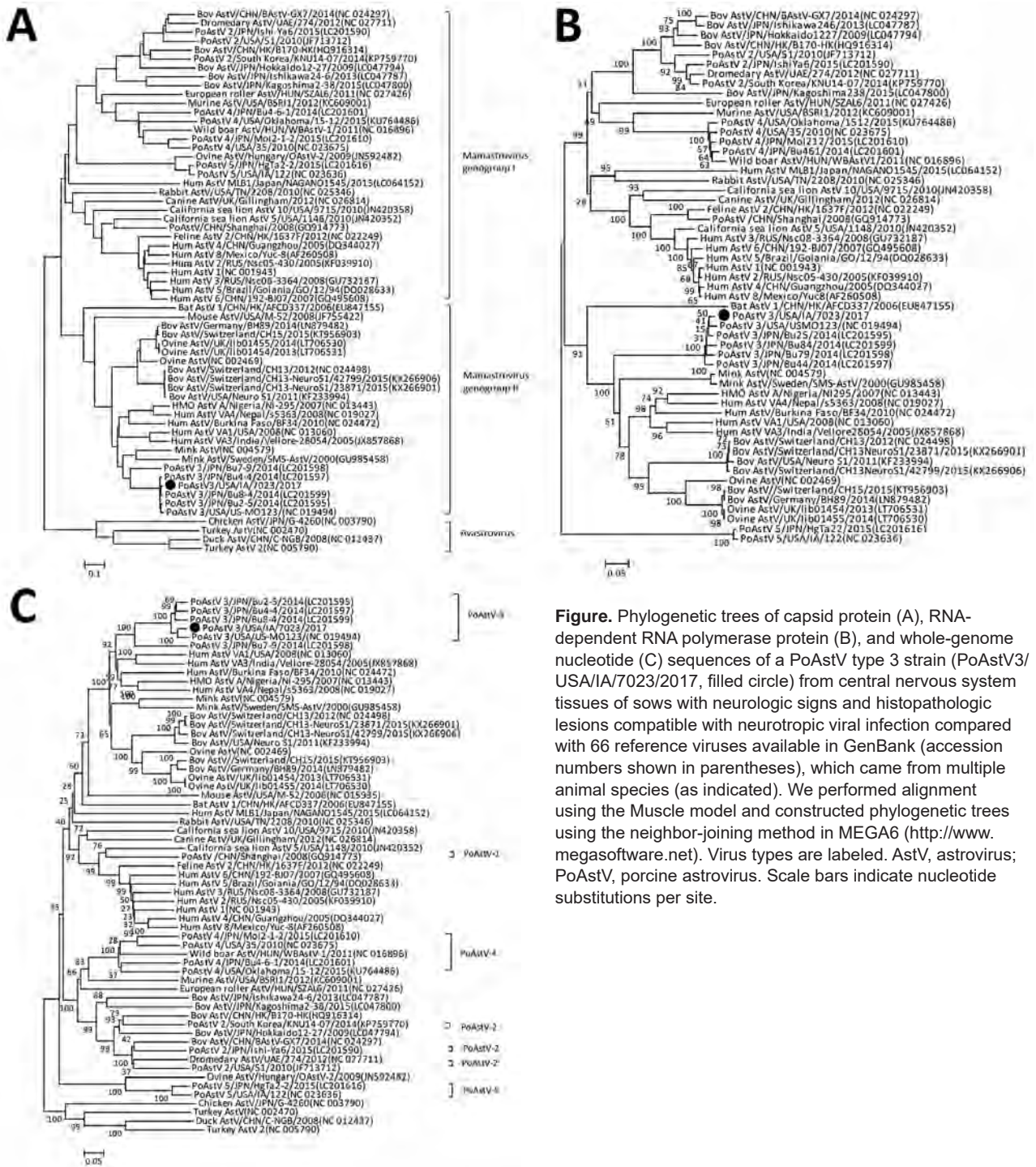


Figure. Phylogenetic trees of capsid protein (A), RNA-dependent RNA polymerase protein (B), and whole-genome nucleotide (C) sequences of a PoAstV type 3 strain (PoAstV/USA/IA/7023/2017, filled circle) from central nervous system tissues of sows with neurologic signs and histopathologic lesions compatible with neurotropic viral infection compared with 66 reference viruses available in GenBank (accession numbers shown in parentheses), which came from multiple animal species (as indicated). We performed alignment using the Muscle model and constructed phylogenetic trees using the neighbor-joining method in MEGA6 (<http://www.megasoftware.net>). Virus types are labeled. AstV, astrovirus; PoAstV, porcine astrovirus. Scale bars indicate nucleotide substitutions per site.

testing by histopathology and next-generation sequencing. Histologic examination revealed severe, nonsuppurative polioencephalomyelitis in 3 of 4 sows and 1 of 2 piglets (online Technical Appendix Figure, <https://wwwnc.cdc.gov/EID/article/23/12/17-0703-Techapp1.pdf>).

We performed metagenomic sequencing for each animal using pooled RNA extracted from the cerebrum, cerebellum, brain stem, and spinal cord as previously described (6,7). We analyzed the sequences obtained using the MiSeq System (Illumina, San Diego, CA, USA) by using Kraken, an ultrafast and highly accurate program for assigning taxonomic labels by examining the k-mers within a read and querying a standard Kraken database with those k-mers (8). We assembled reads de novo using CLC Genomics Workbench (QIAGEN, Valencia, CA, USA) and identified the contigs by blastn (<https://blast.ncbi.nlm.nih.gov/Blast.cgi>). The largest contig, encompassing $\approx 2,000$ reads, encoded a near-complete astrovirus genome of 6,461 nt and was designated PoAstV3/USA/IA/7023/2017 (GenBank accession no. KY940545). This sequence originated from a sow sample. A near-complete astrovirus genomic sequence was also obtained from the piglet (contig length 5,935 bp; E = 0) and had 100% nucleotide identity to PoAstV3/USA/IA/7023/2017. We also identified porcine endogenous retrovirus (contig lengths 1,865 bp and 1,317 bp; E = 0) in sow samples. When using a minimum contig length of 500 nt, we identified rotavirus (contig length 832 bp; 32 reads; E = 0; GenBank accession no. KU058672.1) in piglet samples.

Phylogenetic comparisons of the capsid protein sequence, RNA-dependent RNA polymerase protein sequence, and whole-genome nucleotide sequence placed PoAstV3/USA/IA/7023/2017 in the same cluster as other strains of PoAstV-3 (Figure, panels A–C). The isolate we identified was most closely related to PoAstV3/USA/US-MO123 (GenBank accession no. NC_019494.1; 94.1% amino acid identity; online Technical Appendix Table 1), which was detected in a swine fecal sample (9). On the basis of these phylogenetic analyses, PoAstV3/USA/IA/7023/2017 is more closely related to neurotropic astroviruses from humans, minks, cows, and sheep (2–5) than to PoAstV-1, PoAstV-2, PoAstV-4, and PoAstV-5.

We detected viral RNA by using a PoAstV-3 quantitative real-time PCR with previously fresh-frozen CNS tissues from animals with polioencephalomyelitis (online Technical Appendix Table 2). We did not detect viral RNA in serum, feces, lung, liver, kidney, or spleen samples of animals with histologic lesions or any sample from animals without histologic lesions (9).

We describe the identification and genetic characterization of PoAstV-3 in CNS tissue from a piglet and sows with neurologic signs and histologic lesions compatible with a neurotropic virus similar to those described in

neurotropic astrovirus cases in other species (2–5). In humans, disease is primarily associated with immunocompromised patients. In cows, the virus is not commonly detected in feces, and the disease does not appear to be associated with immunocompromised animals (4). In this case, PoAstV-3 was not detected in feces of affected animals, and evidence of immunosuppression was lacking. The overall PCR prevalence of PoAstV-3 in feces of pigs in North America is reported to be low (1.2%) (10).

The PoAstV-3 we identified had 92.2% nucleotide sequence similarity to PoAstV-3 identified from a survey that evaluated feces samples from pigs (9). The significance of this finding is unclear. Investigations are needed to clarify the ecology and epidemiology of PoAstV-3 and the pathophysiology of neurotropic astroviruses. Studies have demonstrated the potential for recombination between porcine and human astroviruses, suggesting zoonotic potential (9,10).

Dr. Arruda is an assistant professor and diagnostic pathologist at the Iowa State University Veterinary Diagnostic Laboratory. Her primary field of research is the infectious diseases of swine.

References

- De Benedictis P, Schultz-Cherry S, Burnham A, Cattoli G. Astrovirus infections in humans and animals - molecular biology, genetic diversity, and interspecies transmissions. *Infect Genet Evol*. 2011;11:1529–44. <http://dx.doi.org/10.1016/j.meegid.2011.07.024>
- Quan PL, Wagner TA, Briese T, Torgerson TR, Hornig M, Tashmukhamedova A, et al. Astrovirus encephalitis in boy with X-linked agammaglobulinemia. *Emerg Infect Dis*. 2010;16:918–25. <http://dx.doi.org/10.3201/eid1606.091536>
- Blomström AL, Widén F, Hammer AS, Belák S, Berg M. Detection of a novel astrovirus in brain tissue of mink suffering from shaking mink syndrome by use of viral metagenomics. *J Clin Microbiol*. 2010;48:4392–6. <http://dx.doi.org/10.1128/JCM.01040-10>
- Li L, Diab S, McGraw S, Barr B, Traslavina R, Higgins R, et al. Divergent astrovirus associated with neurologic disease in cattle. *Emerg Infect Dis*. 2013;19:1385–92. <http://dx.doi.org/10.3201/eid1909.130682>
- Pfaff F, Schlottau K, Scholes S, Courtenay A, Hoffmann B, Höper D, et al. A novel astrovirus associated with encephalitis and ganglionitis in domestic sheep. *Transbound Emerg Dis*. 2017;64:677–82. <http://dx.doi.org/10.1111/tbed.12623>
- Hause BM, Collin EA, Anderson J, Hesse RA, Anderson G. Bovine rhinitis viruses are common in US cattle with bovine respiratory disease. *PLoS One*. 2015;10:e0121998. <http://dx.doi.org/10.1371/journal.pone.0121998>
- Zhang J, Zheng Y, Xia XQ, Chen Q, Bade SA, Yoon KJ, et al. High-throughput whole genome sequencing of porcine reproductive and respiratory syndrome virus from cell culture materials and clinical specimens using next-generation sequencing technology. *J Vet Diagn Invest*. 2017;29:41–50. <http://dx.doi.org/10.1177/1040638716673404>
- Wood DE, Salzberg SL. Kraken: ultrafast metagenomic sequence classification using exact alignments. *Genome Biol*. 2014;15:R46. <http://dx.doi.org/10.1186/gb-2014-15-3-r46>
- Xiao CT, Halbur PG, Opriessnig T. Complete genome sequence of a newly identified porcine astrovirus genotype 3 strain US-MO123. *J Virol*. 2012;86:13126. <http://dx.doi.org/10.1128/JVI.02426-12>

10. Xiao CT, Giménez-Lirola LG, Gerber PF, Jiang YH, Halbur PG, Opriessnig T. Identification and characterization of novel porcine astroviruses (PAstVs) with high prevalence and frequent co-infection of individual pigs with multiple PAstV types. *J Gen Virol.* 2013;94:570–82. <http://dx.doi.org/10.1099/vir.0.048744-0>

Address for correspondence: Bailey Arruda, 1850 Christensen Dr, Department of Veterinary Diagnostic and Production Animal Medicine, Iowa State University, Ames, IA 50011, USA; email: wilberts@iastate.edu

Avian Influenza A(H7N9) Viruses Co-circulating among Chickens, Southern China

Nianchen Wang,¹ Minhua Sun,¹ Wenqing Wang,¹ Guowen Ouyang, Zuxian Chen, You Zhang, Bingbing Zhao, Siyu Wu, Gianni Huang, Hailiang Sun, Ming Liao, Peirong Jiao

Author affiliations: South China Agricultural University, Guangzhou, China (N. Wang, W. Wang, G. Ouyang, Z. Chen, Y. Zhang, B. Zhao, S. Wu, J. Huang, H. Sun, M. Liao, P. Jiao); Institute of Animal Health, Guangdong Academy of Agricultural Sciences, Guangdong, China (M. Sun)

DOI: <https://doi.org/10.3201/eid2312.170782>

During 2016–2017, three avian influenza A(H7N9) viruses were isolated from chickens in southern China. Each virus had different insertion points in the cleavage site of the hemagglutinin protein compared to the first identified H7N9 virus. We determined that these viruses were double or triple reassortant viruses.

Since its first documentation on March 30, 2013, through March 16, 2017, avian influenza A(H7N9) virus has caused 5 epidemic waves of infection among humans in China, resulting in 1,307 laboratory-confirmed clinical cases and 489 deaths (1). According to reports of H7N9 virus outbreaks among humans in China, the virus clustered into the Yangtze River Delta lineage and the Pearl River Delta lineage (2). As with most low-pathogenicity avian influenza viruses, the early H7N9 avian influenza virus produced mild symptoms in domestic poultry and was therefore generally only detected through active virologic surveillance (3,4).

In April 2017, H7N9 viruses (isolates A/chicken/Guangdong/Q1/2016, A/chicken/Guangdong/Q26/2017, and A/chicken/Guangdong/Q39/2017, hereafter Q1, Q26, and Q39) were identified from lung samples of chickens that were collected from Guangdong, China, in June 2016 and January 2017. We sequenced all 8 genes of these viruses to trace the origin and clarify the genetic properties. The nucleotide sequences are available from GenBank (accession nos. MF280181–204).

The H7 hemagglutinin (HA) gene of all 3 viruses belonged to the Yangtze River Delta lineage A (Figure). However, unlike the early H7N9 virus, the HA genes were 1,695 bp and coded 565 aa, and the isolates had 4 inserted amino acids at cleavage sites (KRTAR⁻G). In addition, Q26 and Q39 had 4 continuous basic amino acids at cleavage sites (KRRKRTAR⁻G), which is a characteristic of highly pathogenic avian influenza virus (Online Technical Appendix, Table 1, <https://wwwnc.cdc.gov/EID/article/23/12/17-0782-Techapp1.pdf>). Q1 had a mutation (Q226L) at the receptor binding site of the HA protein, indicating a higher binding affinity for sialic acid α 2,6, a characteristic of human cell-surface receptors (5).

Both Q1 and Q39 had an NA gene of Yangtze River Delta lineage A, whereas the NA gene of Q26 was of Pearl River Delta lineage (online Technical Appendix Table 1, Figure). A246T and R292K, which are related to drug resistance, had no substitution in the NA protein of the viruses we analyzed.

The polymerase basic (PB) 1 and 2, polymerase acidic, and nonstructural genes of Q1 and Q39 were all of Yangtze River Delta lineage A, and nucleoprotein genes were of Yangtze River Delta lineage B. The PB2 and nucleoprotein genes of Q26 were of Yangtze River Delta lineage A; PB1, polymerase acidic, and nonstructural genes of Q26 were clustered to the Pearl River Delta lineage (online Technical Appendix Table 1, Figure). E627K and D701N had no substitution in the PB2 protein of the viruses, which was thought to contribute to the adaptation, replication, and virulence of influenza viruses in humans and mice (6,7).

Of particular note, the matrix M gene of Q1 clustered into A/goose/Guangdong/1/96-lineage (H5N1) (GSGD96 lineage) and had a nucleotide of 94.8%. However, the matrix genes of Q26 and Q39 clustered into Yangtze River Delta lineage B of H7N9 virus (online Technical Appendix Table 1, Figure).

To clarify the pathogenicity and transmission of the virus, we inoculated 11 chickens with each isolate (10^6 50% egg infectious dose [EID₅₀] in 0.1 mL of phosphate-buffered saline) and 3 chickens with 0.1 mL phosphate-buffered saline as the control group. We observed all chickens for clinical symptoms for 14 days. The infected chickens exhibited anorexia and signs of depression at 2 days post-inoculation (DPI). The Q1 inoculated group died within 4 DPI, Q26 within 3 DPI, and Q39 within 2 DPI; contact

¹These authors contributed equally to this article.

groups of Q1, Q26, and Q39 died within 7 DPI, 4 DPI, and 5 DPI, respectively. These viruses replicated systemically in chickens of inoculated groups and were detected in all of the tested organs by 3 DPI. The mean virus titers in the

trachea, liver, spleen, kidney, brain, and lung were 4.92–8.42 log₁₀ EID₅₀/g/0.1 mL (online Technical Appendix Table 2). The Q1, Q26, and Q39 virus titers in lung samples for each contact group were 7.5–8.1 log₁₀ EID₅₀/g/0.1 mL.

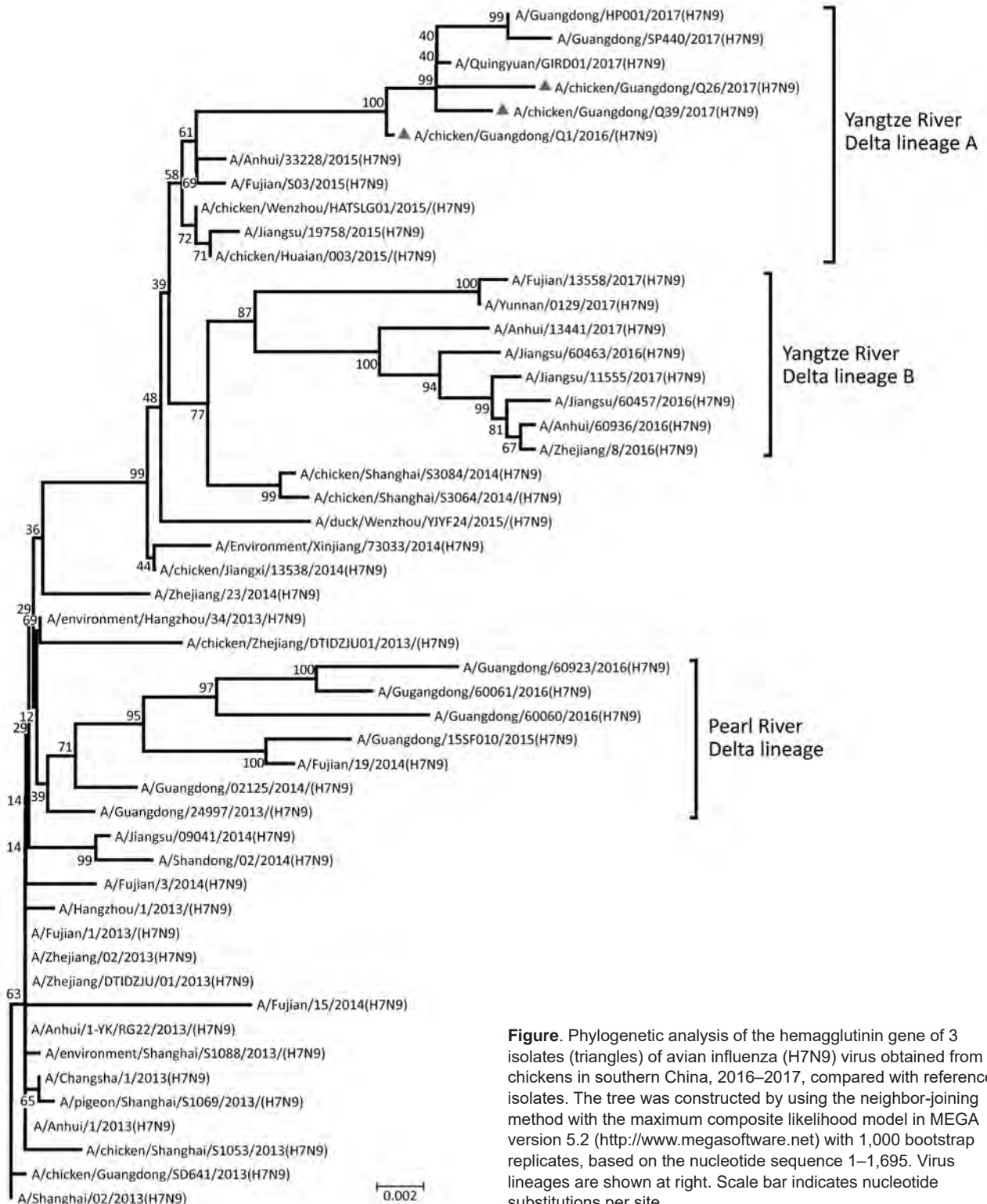


Figure. Phylogenetic analysis of the hemagglutinin gene of 3 isolates (triangles) of avian influenza (H7N9) virus obtained from chickens in southern China, 2016–2017, compared with reference isolates. The tree was constructed by using the neighbor-joining method with the maximum composite likelihood model in MEGA version 5.2 (<http://www.megasoftware.net>) with 1,000 bootstrap replicates, based on the nucleotide sequence 1–1,695. Virus lineages are shown at right. Scale bar indicates nucleotide substitutions per site.

Therefore, the new H7N9 viruses were highly pathogenic to chickens when compared with the early H7N9 virus and could transmit among chickens by contact.

The biological features of H7N9 virus and its pandemic potential have caused global concern (8). The early H7N9 viruses lacked the basic HA cleavage site, exhibited low pathogenicity, and caused mild or no disease in poultry (9). The cleavage site in HA protein of the isolates we analyzed were KGKRTAR[^]G or KRKRTAR[^]G. They had high pathogenicity and replication in chickens and could transmit among chickens by contact. Therefore, these new H7N9 viruses could cause a pandemic among poultry and humans in China.

Molecular evolution showed that Q1 was a triple reassortant virus (H5, H7, and H9 subtypes) consisting of Yangtze River Delta A and B lineages of H7N9 and GSGD96 lineage of H5N1. The Q26 and Q39 viruses were both double reassortant avian influenza viruses (H7 and H9 subtype), as was the early H7N9 virus (Figure; online Technical Appendix Table 1, Figure). Therefore, the 3 H7N9 viruses we isolated have 2 kinds of insertions in the cleavage sites and were likely derived from different lineages of H7N9 viruses, or even from different subtypes that were co-circulating in southern China during 2016–2017.

Acknowledgments

We thank the Key Laboratory of Zoonosis, Ministry of Agriculture; the National and Regional Joint Engineering Laboratory for Medicament of Zoonosis Prevention and Control; the Key Laboratory of Animal Vaccine Development, Ministry of Agriculture; and the Key Laboratory of Zoonoses Control and Prevention of Guangdong.

This work was supported by grants from the National Key Research and Development Program of China (2016YFD0500207), the National Natural Science Foundation of China (U1501212), the Natural Science Foundation of Guangdong Province (2016A030308001), and Basic Research (Discipline Layout) of Shenzhen (JCYJ20160323163102764).

Mr. Nianchen Wang is a student in the Master of Science program in the College of Veterinary Medicine, South China Agricultural University. His primary research interest is the epidemiology and pathogenesis of avian influenza viruses.

References

- World Health Organization. Update on monthly risk assessment summary [cited 2017 Apr 20]. http://www.who.int/influenza/human_animal_interface/Influenza_Summary_IRA_HA_interface_04_20_2017.pdf?ua=1
- Wang D, Yang L, Zhu W, Zhang Y, Zou S, Bo H, et al. Two outbreak sources of influenza A (H7N9) viruses have been established in China. *J Virol*. 2016;90:5561–73. <http://dx.doi.org/10.1128/JVI.03173-15>
- Kang M, He J, Song T, Rutherford S, Wu J, Lin J, et al. Environmental sampling for avian influenza A(H7N9) in live-poultry markets in Guangdong, China. *PLoS One*. 2015; 10:e0126335. <http://dx.doi.org/10.1371/journal.pone.0126335>
- Shi J, Deng G, Liu P, Zhou J, Guan L, Li W, et al. Isolation and characterization of H7N9 viruses from live poultry markets—implication of the source of current H7N9 infection in humans. *Chin Sci Bull*. 2013;58:1857–63. <https://doi.org/10.1007/s11434-013-5873-4>
- Ramos I, Krammer F, Hai R, Aguilera D, Bernal-Rubio D, Steel J, et al. H7N9 influenza viruses interact preferentially with α 2,3-linked sialic acids and bind weakly to α 2,6-linked sialic acids. *J Gen Virol*. 2013;94:2417–23. <http://dx.doi.org/10.1099/vir.0.056184-0>
- Li Z, Chen H, Jiao P, Deng G, Tian G, Li Y, et al. Molecular basis of replication of duck H5N1 influenza viruses in a mammalian mouse model. *J Virol*. 2005;79:12058–64. <http://dx.doi.org/10.1128/JVI.79.18.12058-12064.2005>
- Hatta M, Gao P, Halfmann P, Kawaoka Y. Molecular basis for high virulence of Hong Kong H5N1 influenza A viruses. *Science*. 2001;293:1840–2. <http://dx.doi.org/10.1126/science.1062882>
- Zhou J, Wang D, Gao R, Zhao B, Song J, Qi X, et al. Biological features of novel avian influenza A (H7N9) virus. *Nature*. 2013;499:500–3. <http://dx.doi.org/10.1038/nature12379>
- World Health Organization. Update on analysis of recent scientific information on avian influenza A (H7N9) virus [cited 2017 Feb 10]. http://www.who.int/influenza/human_animal_interface/avian_influenza/riskassessment_AH7N9_201702/en/

Address for correspondence: Peirong Jiao or Ming Liao, College of Veterinary Medicine, South China Agricultural University, 483 Wushan Rd, Guangzhou 510642, China; email: prjiao@scau.edu.cn or mliao@scau.edu.cn

Rabies and Distemper Outbreaks in Smallest Ethiopian Wolf Population

Jorgelina Marino, Claudio Sillero-Zubiri, Asefa Deressa, Eric Bedin, Alemayehu Bitewa, Fekadu Lema, Gebeyehu Rskay, Ashley Banyard, Anthony R. Fooks

Author affiliations: University of Oxford, Oxford, UK (J. Marino, C. Sillero-Zubiri, E. Bedin); International Union for Conservation of Nature Species Survival Commission Canid Specialist Group, Oxford (C. Sillero-Zubiri); Ethiopian Public Health Institute, Addis Ababa, Ethiopia (A. Deressa); Environmental, Forest, Wildlife Development and Protection Authority, Bahir Dar, Ethiopia (A. Bitewa); Ethiopian Wolf Conservation Programme, Bale Robe, Ethiopia (J. Marino); Ethiopian Wolf Conservation Programme, Bahir Dar (F. Lema, G. Rskay); Animal and Plant Health Agency, Weybridge, UK (A. Banyard, A.R. Fooks)

DOI: <https://doi.org/10.3201/eid2312.170893>

Widespread deaths recently devastated the smallest known population of Ethiopian wolves. Of 7 carcasses found, all 3 tested were positive for rabies. Two wolves were subsequently vaccinated for rabies; 1 of these later died from canine distemper. Only 2 of a known population of 13 wolves survived.

Canine diseases pose a growing threat to wildlife species of conservation concern worldwide. Although extensive oral vaccinations have eliminated rabies virus (RABV) from wild carnivore populations in some developed countries (1), elsewhere, the challenges to controlling diseases in endangered wildlife are many and persistent. Massive outbreaks of rabies and, more recently, canine distemper have repeatedly decimated populations of Ethiopian wolves (*Canis simensis*) in the Bale Mountains of Ethiopia, where more than half of a global population of ≈ 500 wolves live (2,3). Extensive efforts to control RABV in the reservoir population of sympatric domestic dogs have proved insufficient. Therefore, reactive vaccination of Ethiopian wolves, carried out in response to an outbreak in wolves, has been the primary mechanism to curtail mortality in the affected wolf populations in the Bale Mountains (4).

The fragile status of the Bale population highlights the conservation value of the other remaining, much smaller, wolf populations scattered throughout the highlands of Ethiopia. Models predict these small populations to be particularly vulnerable to disease outbreaks (5); however, no outbreaks had been detected outside Bale, either because they went unnoticed, because in small populations outbreaks die out before causing a major epizootic event, or both. We report consecutive rabies and canine distemper outbreaks among Ethiopian wolves in Delanta, in the Wollo highlands.

This group of wolves is the smallest extant wolf population; 13 wolves in 3 family packs lived in the remaining 20 km² of Afroalpine habitat in 2015. The first wolf carcass was detected in late June 2016; by early September, 7 deaths had been confirmed. RABV infection was identified as the cause of death in all 3 of the carcasses tested, as

well as in samples from 1 domestic dog concurrently found dead within wolf habitat (Table). A vaccination intervention was initiated in September 2016, when only 3 wolves were known to be alive; 1 adult male (>2 years of age) and 1 subadult female (1–2 years of age) were trapped (7) and parenterally inoculated with Nobivac Rabies (Merck Animal Health, Madison, NJ, USA) (4). In December 2016, the female wolf was found dead and tested positive for canine distemper virus (CDV) (Table); CDV was also detected in a dog carcass found concurrently in the vicinity of the wolf range. In late May, the vaccinated male was still alive and was observed until at least April 2017 with an unknown adult female.

Evidence indicates a first outbreak of rabies, overlapping or followed soon after by a canine distemper outbreak. Confirmation of disease in contemporarily recovered dog carcasses is consistent with a pattern of transmission from reservoir domestic dogs to their wild relatives (as observed in the Bale Mountains [8]), with disastrous consequences for the small Delanta population, which harbored <20 wolves before the epizootic events. Although the larger Bale wolf population has recovered from epizootic events in the past (2,9), smaller populations are expected to be less resilient, a factor exacerbated by their virtual isolation from other wolf populations. Modeling has predicted a high extinction risk if Ethiopian wolf populations are affected by consecutive epizootic events over a short period of time (5). The combined exacerbated effects of RABV and CDV infection were first described in 2010 in the Bale Mountains (3).

Although the loss of Afroalpine habitats is bound to determine the fate of Ethiopian wolf populations (2 extinctions were recorded in areas of a similar size to that of Delaware during 1999 and 2010) (2), incursions of infectious diseases can drive local extinctions. Preemptive vaccination, in combination with actions to protect the habitat of this specialized predator, could greatly reduce the risk of populations becoming extinct, even if a relatively low proportion of the wolves is successfully vaccinated (4). Recently, SAG2, an oral rabies vaccine, was successfully tested in Ethiopian wolves (10), and a CDV parenteral vaccination trial is ongoing, with positive

Table. Characteristics of and test results for Ethiopian wolf and domestic dog carcasses recovered in Delanta, Ethiopia, 2016*

Date found	Species	Age and sex	Postmortem	Tested for RABV†	Tested for CDV‡
Jun 26	Ethiopian wolf	Juvenile female	No	NA	NA
Jun 28	Ethiopian wolf	Juvenile male	Yes	No	No
Jul 07	Ethiopian wolf	Adult male	Yes	Positive	No
Jul 11	Ethiopian wolf	Juvenile female	Yes	Positive	No
Jul 18	Ethiopian wolf	Juvenile female	No	NA	NA
Aug 12	Ethiopian wolf	Adult male	No	NA	NA
Sep 01	Domestic dog	Adult male	Yes	Positive	Negative
Sep 07	Ethiopian wolf	Adult female	Yes	Positive	Negative
Nov 27	Domestic dog	Adult male	Yes	Negative	Positive
Dec 27	Ethiopian wolf	Adult female	Yes	Negative	Positive

*CDV, canine distemper virus; NA, not applicable; RABV, rabies virus.

†Rabies diagnostic reverse transcription PCR was performed as described previously (6).

‡CDV diagnostic reverse transcription PCR was performed as described previously (3).

preliminary results. We propose proactive vaccination of Ethiopian wolves across their distribution as an effective and urgently needed strategy to protect the species from extinction. This program should be part of an integrated disease control plan that also includes controlling disease in domestic dogs, limiting contact between dogs and wolves, and conducting policy and education interventions to reduce the size and roaming behavior of local dog populations (2).

Acknowledgments

We thank the Ethiopian Wildlife Conservation Authority and Environment and Forest and Wildlife Protection and Development Authority (Amhara National Regional State) for support and permission to work in Delanta. We thank Delanta and Gubalafu Waredas and Wolf Ambassadors, and Leigh Thorne and Daisy Jennings for excellent technical assistance.

The work was funded by the Born Free Foundation and the Wildlife Conservation Network. The work undertaken by Animal and Plant Health Agency is funded by a grant (SEV3500) from the UK Department for Environment, Food and Rural Affairs, Scottish and Welsh Governments.

The animal care and use protocols for the ethical handling of Ethiopian wolves were approved by the Ethiopian Wildlife Conservation Authority and the University of Oxford's Local Ethical Review Process (Zoology ERC; case no. ZERC040905) and adhere to the United Kingdom's ASPA regulations (1986).

Dr. Marino is a conservation ecologist with the University of Oxford's Wildlife Conservation Research Unit (WildCRU), Oxford, UK, and is science director of the Ethiopian Wolf Conservation Programme. She is interested in the ecology and conservation of threatened carnivores, and coordinates Ethiopian Wolf Conservation Programme monitoring efforts, looking at the demography of the rare and endangered Ethiopian wolf, interactions with free-ranging dogs, and the impact of viral diseases.

References

- Mähl P, Cliquet F, Guiot A-L, Niin E, Fournials E, Saint-Jean N, et al. Twenty year experience of the oral rabies vaccine SAG2 in wildlife: a global review. *Vet Res (Faisalabad)*. 2014;45:77. <http://dx.doi.org/10.1186/s13567-014-0077-8>
- Strategic planning for Ethiopian wolf conservation. Oxford (UK): International Union for the Conservation of Nature, Canid Specialist Group; 2011. p. 79 [cited 2017 May 25]. <https://portals.iucn.org/library/efiles/documents/2011-090.pdf>
- Gordon CH, Banyard AC, Hussein A, Laurenson MK, Malcolm JR, Marino J, et al. Canine distemper in endangered Ethiopian wolves. *Emerg Infect Dis*. 2015;21:824–32. <http://dx.doi.org/10.3201/eid2105.141920>
- Haydon DT, Randall DA, Matthews L, Knobel DL, Tallents LA, Gravenor MB, et al. Low-coverage vaccination strategies for the conservation of endangered species. *Nature*. 2006;443:692–5. <http://dx.doi.org/10.1038/nature05177>
- Haydon DT, Laurenson MK, Sillero-Zubiri C. Integrating epidemiology into population viability analysis: managing the risk posed by rabies and canine distemper to the Ethiopian wolf. *Conserv Biol*. 2002;16:1372–85. <http://dx.doi.org/10.1046/j.1523-1739.2002.00559.x>
- Johnson N, Mansfield KL, Marston DA, Wilson C, Goddard T, Selden D, et al. A new outbreak of rabies in rare Ethiopian wolves (*Canis simensis*). *Arch Virol*. 2010;155:1175–7. <http://dx.doi.org/10.1007/s00705-010-0689-x>
- Sillero-Zubiri C. Field immobilization of Ethiopian wolves (*Canis simensis*). *J Wildl Dis*. 1996;32:147–51. <http://dx.doi.org/10.7589/0090-3558-32.1.147>
- Laurenson K, Sillero-Zubiri C, Thompson H, Shiferaw F, Thirgood S, Malcolm J. Disease as a threat to endangered species: Ethiopian wolves, domestic dogs and canine pathogens. *Anim Conserv*. 1998;1:273–80. <http://dx.doi.org/10.1111/j.1469-1795.1998.tb00038.x>
- Marino J, Sillero-Zubiri C, Gottelli D, Johnson PJ, Macdonald DW. The fall and rise of Ethiopian wolves: lessons for conservation of long-lived, social predators. *Anim Conserv*. 2013;16:621–32. <http://dx.doi.org/10.1111/acv.12036>
- Sillero-Zubiri C, Marino J, Gordon CH, Bedin E, Hussein A, Regassa F, et al. Feasibility and efficacy of oral rabies vaccine SAG2 in endangered Ethiopian wolves. *Vaccine*. 2016;34:4792–8. <http://dx.doi.org/10.1016/j.vaccine.2016.08.021>

Address for correspondence: Jorgelina Marino, Wildlife Conservation Research Unit, University of Oxford, The Reanati-Kaplan Centre, Tubney House, Tubney, Oxford OX13 5QL, UK; email: jorgelina.marino@zoo.ox.ac.uk

High Abundance and Genetic Variability of Atypical Porcine Pestivirus in Pigs from Europe and Asia

Alexander Postel, Denise Meyer, Gökce Nur Cagatay, Francesco Feliziani, Gian Mario De Mia, Nicole Fischer, Adam Grundhoff, Vesna Milićević, Ming-Chung Deng, Chia-Yi Chang, Hua-Ji Qiu, Yuan Sun, Michael Wendt, Paul Becher

Author affiliations: University of Veterinary Medicine, Hannover, Germany (A. Postel, D. Meyer, G.N. Cagatay, M. Wendt, P. Becher); Istituto Zooprofilattico Sperimentale dell'Umbria e delle Marche, Perugia, Italy (F. Feliziani, G.M. De Mia); University Medical Center Hamburg-Eppendorf, Hamburg, Germany (N. Fischer); Heinrich Pette Institute, Hamburg (A. Grundhoff); Institute of Veterinary Medicine of Serbia, Belgrade, Republic of Serbia (V. Milićević); Animal Health Research Institute,

New Taipei City, Taiwan (M.-C. Deng, C.-Y. Chang); Harbin Veterinary Research Institute, Harbin, China (H.-J. Qiu, Y. Sun)

DOI: <https://doi.org/10.3201/eid2312.170951>

Atypical porcine pestivirus (APPV) was recently reported to be associated with neurologic disorders in newborn piglets. Investigations of 1,460 serum samples of apparently healthy pigs from different parts of Europe and Asia demonstrate a geographically wide distribution of genetically highly variable APPV and high APPV genome and antibody detection rates.

Pestiviruses are highly variable RNA viruses within the family *Flaviviridae*. The recently discovered atypical porcine pestivirus (APPV) is capable of inducing neurologic disorder in its host, like other pathogens of this family (e.g., tick-borne encephalitis virus, Zika virus). Several recently published reports demonstrate that APPV is a prominent cause of virus-induced congenital tremor in pigs (1–4). Serum samples from healthy but viremic animals can induce birth of clinically affected offspring when experimentally transferred to sows during gestation (1,2). So far, APPV presence has been reported from the United States, some countries within Europe, and China (2,4–7). The economic relevance of APPV-related losses in pig production remains to be determined, but estimation revealed a drop in reproductive performance of 10% in an affected farm (4). Early data from the United States and Germany suggested a relatively high abundance (2.4%–22%) of APPV genomes in apparently healthy pigs (3,6,8) that likely play an important epidemiologic role as virus carriers. We investigated APPV genome and antibody abundance in healthy pigs from different parts of Europe and Asia to provide insight into genetic diversity of this novel pathogen.

We tested 1,460 serum samples from Germany, Great Britain, Italy, Serbia, Switzerland, mainland China, and Taiwan by using an APPV-specific PCR and an indirect APPV ELISA, as previously described (3,9). The sample set comprised 369 serum samples from Germany that were previously screened for the presence of APPV genomes (3). For our study, serum samples were taken from apparently healthy pigs within the framework of national veterinary health management in concordance with national legal and ethical regulations.

For APPV genome detection, we conducted a PCR targeting the nonstructural protein (NS) 3 encoding region and confirmed specificity of amplification by gel electrophoresis (3). We detected APPV genomes in domestic pigs from all investigated regions. In total, 130 (8.9%) of the 1,460 tested samples were APPV genome positive (Figure). Genome detection rates ranged from 2.3% (2/86

samples from Great Britain) to 17.5% (35/200 samples from Italy). Moreover, we demonstrated that APPV was abundant in Asia; we detected the APPV genome in 11/219 samples (5%) from mainland China and 22/200 samples (11%) from Taiwan.

We used individual samples with high genome loads to generate amplicons in a seminested PCR and subsequently performed Sanger sequencing (FlexiRun, LGC Genomics, Berlin, Germany). We generated 20 different APPV NS3 sequences from apparently healthy pigs of all countries (sequences deposited into GenBank under accession nos. MF279213–32). Genetic differences reflect geographic origin to a low degree (Figure); genetic variability even within a country is remarkably high (e.g., Germany and Italy). Genetic analyses including sequence data obtained from samples of diseased piglets revealed no correlation of pathogenicity with certain genetic variants (Figure).

In addition to the NS3 fragments, we determined APPV complete coding sequences (CDS) from 1 sample from a healthy pig from China (deposited into GenBank under accession no. MF167292) and 2 samples (accession nos. MF167290 and MF167291) obtained from pigs during outbreaks of congenital tremors in Germany (3,9). We performed next-generation sequencing as previously described (3). The outbreak isolates from Germany were almost identical (0.2% genetic distance) and were similar to an isolate from northern Germany (accession no. LT594521). The APPV from China had a unique 93-nt deletion in the NS5A encoding region. A similar genome (97.9% identity) is lacking this deletion (Guangxi Province; accession no. KY652092). The biological relevance of the deletion remains elusive, but classical pestiviruses show a remarkable genetic tolerance in this genomic region (10). The sequence data we obtained reveal a high genetic variability (up to 21% genetic distance), which is comparable to that of classical swine fever virus (online Technical Appendix, <https://wwwnc.cdc.gov/EID/article/23/12/17-0951-Techapp1.pdf>).

We applied an indirect APPV E^{ms} antibody ELISA, as described (9), and classified the serologic status into low ($S/p \leq 0.5$), intermediate ($0.5 < S/p < 1.0$), or highly ($S/p \geq 1.0$) reactive. Due to the lack of reference material and a standard assay, we could not determine test parameters (e.g., sensitivity, specificity) at this stage. Nevertheless, the ELISA was a valuable tool for detecting seroconversion in infected pigs; $\geq 60\%$ of the animals showed intermediate to high reactivity in the antibody ELISA (Figure), which is in line with high APPV genome detection rates. We detected similar frequencies of APPV antibody-positive samples for each region, independent of the genome detection rates (Figure). We found most of the viral genomes ($\approx 86\%$) in samples with intermediate or low antibody status; few ($\approx 14\%$) of the highly antibody-positive animals were viremic at the same time. This

observation might indicate a degree of protection provided by the induced antibodies. Of the 40% of the pigs that were antibody negative, 10% were genome positive; possible explanations are that serum samples were taken either from acutely infected animals before induction of a detectable antibody response or from persistently infected

animals lacking a specific humoral immune response due to a specifically acquired immunotolerance, a well-known consequence of intrauterine pestivirus infections.

Our findings indicate that the recently discovered APPV is abundant on several continents. APPV must be regarded as a pig pathogen of likely worldwide relevance.

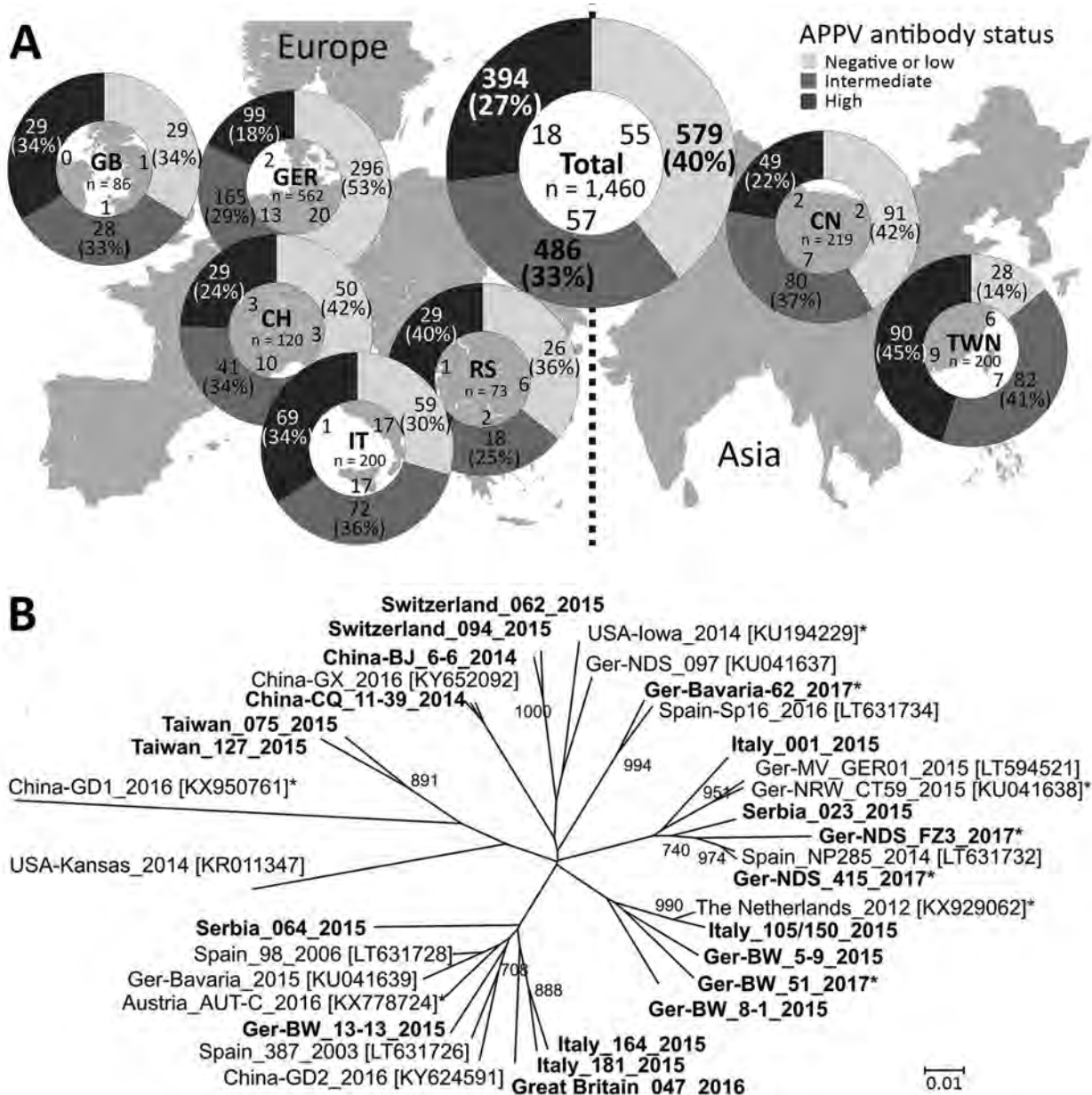


Figure. Detection rates of APPV genome and antibodies and genetic variability in Europe and Asia. A) APPV antibody status in pigs from parts of Europe and Asia. The region of origin, the number of investigated samples, and the absolute numbers of APPV genome-positive samples in dependence on the serologic category (low, intermediate, or high APPV antibody status) are shown in the central circle. B) Phylogenetic tree based on a 400-nt fragment in the nonstructural protein 3 encoding region. We calculated genetic distances using the Kimura 2-parameter model. We performed phylogenetic analysis by the neighbor-joining method including 1,000 iterations for bootstrap analysis. Only bootstrap values ≥ 700 are indicated. Bold indicates sequences generated in this study; asterisks indicate sequences from piglets with congenital tremor. Accession numbers for reference sequences from GenBank are shown in brackets. Scale bar indicates nucleotide substitutions per site. APPV, atypical porcine pestivirus; CH, Switzerland; CN, China; GB, Great Britain; GER, Germany; IT, Italy; RS, Serbia; TWN, Taiwan.

Acknowledgments

We thank Tanja Frey and Birgitta Polley; the serum bank of the Federal Food Safety and Veterinary Office, Bern, Switzerland; the Animal and Plant Health Agency, Weybridge, UK; and the animal health service, Baden-Württemberg, Germany, for providing serum samples. We thank Daniela Indenbirken and Malik Alawi for their support in library preparation and analysis of next-generation sequencing data, and Elena Gräf for her support in Sanger sequencing. This work in part was financially supported by Boehringer Ingelheim.

Dr. Postel is a veterinarian and the head of the Laboratory for Molecular Biology of the European Union and World Organisation for Animal Health Reference Laboratory for Classical Swine Fever at the Institute of Virology of the University of Veterinary Medicine in Hannover, Germany. Research interests are molecular evolution and pathogenesis of pestiviruses and related viruses, characterization of novel pestivirus isolates, and diagnosis and control of classical swine fever.

References

1. Arruda BL, Arruda PH, Magstadt DR, Schwartz KJ, Dohlman T, Schleining JA, et al. Identification of a divergent lineage porcine pestivirus in nursing piglets with congenital tremors and reproduction of disease following experimental inoculation. *PLoS One*. 2016;11:e0150104. <http://dx.doi.org/10.1371/journal.pone.0150104>
2. de Groof A, Deijs M, Guelen L, van Grinsven L, van Os-Galdos L, Vogels W, et al. Atypical porcine pestivirus: a possible cause of congenital tremor type A-II in newborn piglets. *Viruses*. 2016; 8:271. <http://dx.doi.org/10.3390/v8100271>
3. Postel A, Hansmann F, Baechlein C, Fischer N, Alawi M, Grundhoff A, et al. Presence of atypical porcine pestivirus (APPV) genomes in newborn piglets correlates with congenital tremor. *Sci Rep*. 2016;6:27735. <http://dx.doi.org/10.1038/srep27735>
4. Schwarz L, Riedel C, Högl S, Sinn LJ, Voglmayr T, Wöchtel B, et al. Congenital infection with atypical porcine pestivirus (APPV) is associated with disease and viral persistence. *Vet Res (Faisalabad)*. 2017;48:1. <http://dx.doi.org/10.1186/s13567-016-0406-1>
5. British Veterinary Association. Congenital tremor associated with atypical porcine pestivirus. *Vet Rec*. 2017;180:42–3. <http://dx.doi.org/10.1136/vr.j121>
6. Hause BM, Collin EA, Peddireddi L, Yuan F, Chen Z, Hesse RA, et al. Discovery of a novel putative atypical porcine pestivirus in pigs in the USA. *J Gen Virol*. 2015;96:2994–8. <http://dx.doi.org/10.1099/jgv.0.000251>
7. Yuan J, Han Z, Li J, Huang Y, Yang J, Ding H, et al. Atypical porcine pestivirus as a novel type of pestivirus in pigs in China. *Front Microbiol*. 2017;8:862. <http://dx.doi.org/10.3389/fmicb.2017.00862>
8. Beer M, Wernike K, Dräger C, Höper D, Pohlmann A, Bergemann C, et al. High prevalence of highly variable atypical porcine pestiviruses found in Germany. *Transbound Emerg Dis*. 2016. <http://dx.doi.org/10.1111/tbed.12532>
9. Postel A, Meyer D, Petrov A, Becher P. Recent emergence of a novel porcine pestivirus: interference with classical swine fever diagnosis? *Emerg Microbes Infect*. 2017;6:e19. <http://dx.doi.org/10.1038/emi.2017.5>
10. Isken O, Langerwisch U, Schönherr R, Lamp B, Schröder K, Duden R, et al. Functional characterization of bovine viral diarrhea virus nonstructural protein 5A by reverse genetic analysis and live cell imaging. *J Virol*. 2014;88:82–98. <http://dx.doi.org/10.1128/JVI.01957-13>

Address for correspondence: Paul Becher, EU and OIE Reference Laboratory for Classical Swine Fever, Institute for Virology, University of Veterinary Medicine Hannover, Buenteweg 17, 30559 Hannover, Germany; email: paul.becher@tiho-hannover.de

Human Case of *Streptococcus suis* Disease, Ontario, Canada

Jeisa Gomez-Torres, Asim Nimir, James Cluett, Anita Aggarwal, Sameer Elsayed, Deirdre Soares, Sarah Teatero, Yan Chen, Marcelo Gottschalk, Nahuel Fittipaldi

Author affiliations: Tillsonburg District Memorial Hospital, Tillsonburg, Ontario, Canada (J. Gomez-Torres, A. Nimir); Tillsonburg Family Physicians, Tillsonburg (J. Cluett); Woodstock General Hospital, Woodstock, Ontario, Canada (A. Aggarwal, S. Elsayed); Western University, London, Ontario, Canada (S. Elsayed); Public Health Ontario Laboratory, Toronto, Ontario, Canada (D. Soares, S. Teatero, Y. Chen, N. Fittipaldi); University of Montreal, St-Hyacinthe, Quebec, Canada (M. Gottschalk); University of Toronto, Toronto (N. Fittipaldi)

DOI: <https://doi.org/10.3201/eid2312.171005>

We report a case of *Streptococcus suis* human disease in Ontario, Canada, caused by a serotype 2 strain genotypically similar to those commonly isolated from pigs in North America. Initially, the isolate was misidentified as a viridans group *Streptococcus*. Human *S. suis* infections may be underdiagnosed in North America.

Streptococcus suis is a zoonotic agent responsible for both sporadic and outbreak human disease in several Asian countries (1–3). However, human *S. suis* infections are less frequent in Western countries, and particularly in North America (3,4). We describe a severe human *S. suis* infection in Ontario, Canada.

The patient, a 69-year-old male farmer, was brought to the emergency department of a rural community hospital in southwestern Ontario after being found unresponsive by his

wife. His medical history included congestive heart failure, moderate to severe mitral regurgitation, hypertension, microcytic anemia, and bilateral hearing loss. According to his wife, he had unintentionally lost 9 kg over the previous 2 months and had reported feeling cold the previous evening. He had not reported headache, sore throat, chest pain, cough, shortness of breath, abdominal pain, nausea, vomiting, or diarrhea, and he had not been in contact with persons who were ill.

The patient's vital signs were normal except for a temperature of 39.9°C. He was comatose and had a Glasgow Coma Scale score of 9. There was no evidence of trauma. Physical examination was unremarkable except for the presence of nystagmus. Hematologic studies showed a leukocyte count of 11.8×10^9 cells/L with 11% neutrophils; platelet count, creatinine, and liver enzymes were all within normal limits. Results of computed tomography of the brain were normal. A chest radiograph revealed moderate bilateral peribronchial thickening with increased interstitial markings. Empiric treatment with intravenous (IV) piperacillin/tazobactam for septic syndrome was initiated. The patient's neurologic status rapidly deteriorated (Glasgow Coma Scale score of 5), and he required intubation. He was transferred to a regional hospital, where empiric antibiotic drugs were changed to IV vancomycin and ceftriaxone. Blood cultures grew a gram-positive α -hemolytic organism, identified by using the Vitek II system as *Streptococcus thoraltensis*, a rare viridans group *Streptococcus*. Treatment was changed to IV penicillin G. After 48 hours, the patient improved, was extubated, and was transferred back to the rural hospital. Upon arrival, he remained confused, was transiently febrile, and had visual hallucinations. IV penicillin G was continued. The patient continued to improve. Repeat blood cultures were negative. Transthoracic 2-dimensional echocardiography did not identify lesions. The patient was discharged on day 10 to complete a 14-day course of IV ceftriaxone at home. He has since fully recovered.

As part of standard procedures, the patient isolate was sent to the Public Health Ontario Laboratory (Toronto, Ontario, Canada), where it was identified as *S. suis* by using matrix-assisted laser desorption/ionization time-of-flight mass spectrometry. The genome of the isolate was sequenced by using Illumina Technology (Illumina, San Diego, CA, USA); bioinformatics-based typing (5) assigned the isolate to serotype 2 and sequence type (ST) 25. Further phylogenetic analysis determined that the isolate belonged to ST25 clade NAV1 (Figure), which is common among diseased swine in Canada (6,7) but heretofore not associated with human disease. The isolate, confirmed as serotype 2 by using the coagglutination test (8), did not produce the virulence markers muramidase-released protein, extracellular factor, or the hemolysin sulilysin.

When questioned about swine contact, the patient reported raising $\approx 2,000$ pigs on his farm. There was no

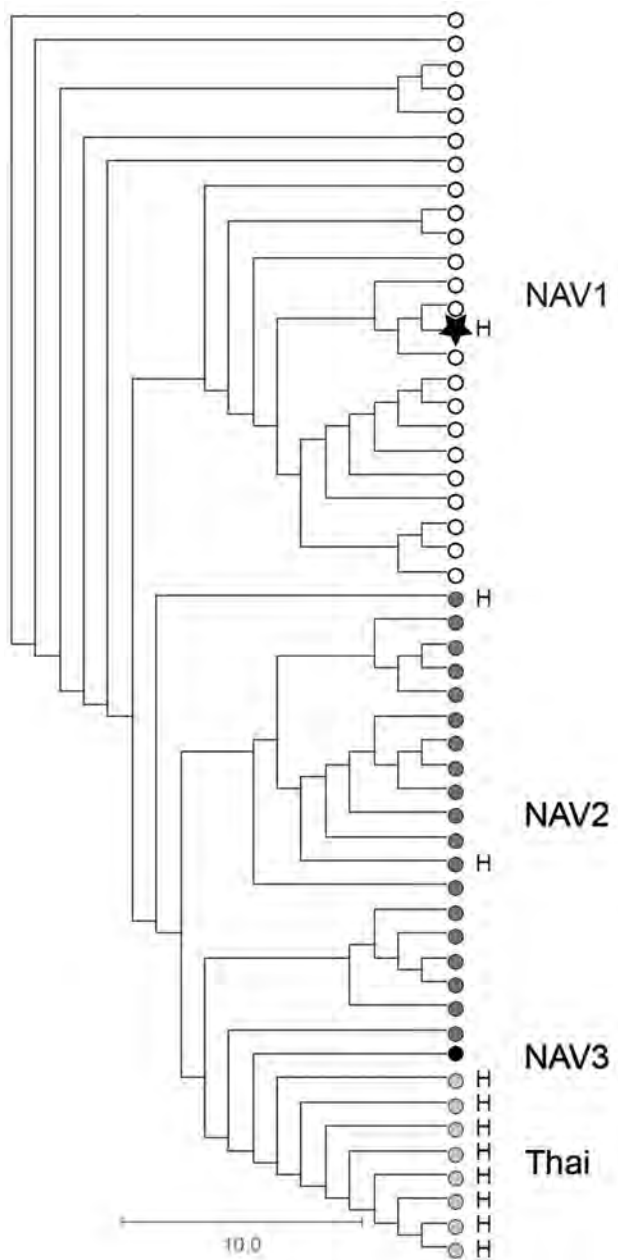


Figure. Phylogenetic relationships among *Streptococcus suis* serotype 2 sequence type (ST) 25 isolate from a patient in Ontario, Canada (star), and 51 previously described (6) porcine and human serotype 2 ST25 *S. suis* isolates. The cladogram is based on nonredundant single-nucleotide polymorphism loci identified in the genome of all isolates relative to the *S. suis* serotype 2 ST25 core genome, as defined by Athey et al. (6). The human isolate from Ontario is genetically more closely related to serotype 2 ST25 strains of clade NAV1 (open circles), which are commonly recovered from diseased pigs in North America and which have not previously been associated with human disease, than to other serotype 2 ST25 clades from North America (NAV2, dark gray circles, and NAV3, black circle) or serotype 2 ST25 organisms from Thailand (light gray circles). Scale bar indicates nucleotide substitutions per site. H, isolates recovered from human infections.

evidence of active disease among these animals. However, pigs in porcine farms not deemed of high-health status are regularly colonized by *S. suis* (3). Most cases of *S. suis* disease in humans have been linked to accidental inoculation through skin injuries (3). The patient reported that in the days before his hospitalization, a pig died unexpectedly, and he removed it from the pen without using protective equipment such as gloves or safety glasses. However, there was no indication that this animal had died of a *S. suis* infection. The patient also described transient worsening of his bilateral hearing loss during hospitalization. Hearing loss from *S. suis* infection occurs frequently (9).

S. suis zoonotic disease has emerged in Asia and occurs frequently in Europe among persons in close contact with pigs (3). In contrast, only 8 human *S. suis* cases have been reported in Canada and the United States, which together are the second largest swine producers worldwide (3). This lower number of cases may be related to the lower virulence of *S. suis* serotype 2 genotypes circulating in North America (ST25 and ST28) in comparison to serotype 2 genotypes circulating in Europe and Asia (ST1, ST7) (4,6,7). However, *S. suis* infections may be underdiagnosed in North America. Our data and previous reports (10) show that the organism is sometimes misidentified as other α -hemolytic streptococci by commercial identification systems. Here, the isolate was initially identified as viridans group *Streptococcus*, and only the use of matrix-assisted laser desorption/ionization time-of-flight mass spectrometry at the reference laboratory permitted correct identification. While proper identification was unlikely to have led to a different treatment course in this case, our report underscores the need to increase awareness of *S. suis* as a potential agent of human infections and serves as a reminder to routinely query patients about animal contact, particularly in areas with intensive pig farming operations.

Acknowledgments

We are grateful to the patient for consenting to publication of his clinical data. We thank Allison McGeer (Sinai Health System, Toronto) for critical reading of an earlier version of this manuscript. We also thank the staff of Public Health Ontario Genome Core for sequencing the genome of the *S. suis* isolate.

Dr. Gomez-Torres is an internist at Tillsonburg District Memorial Hospital. Her primary research interest is infectious diseases in hospital settings.

References

1. Fulde M, Valentin-Weigand P. Epidemiology and pathogenicity of zoonotic streptococci. *Curr Top Microbiol Immunol*. 2012; 368:49–81. http://dx.doi.org/10.1007/82_2012_277
2. Wertheim HF, Nghia HD, Taylor W, Schultz C. *Streptococcus suis*: an emerging human pathogen. *Clin Infect Dis*. 2009;48:617–25. <http://dx.doi.org/10.1086/596763>
3. Gottschalk M, Xu J, Calzas C, Segura M. *Streptococcus suis*: a new emerging or an old neglected zoonotic pathogen? *Future Microbiol*. 2010;5:371–91. <http://dx.doi.org/10.2217/fmb.10.2>
4. Goyette-Desjardins G, Auger JP, Xu J, Segura M, Gottschalk M. *Streptococcus suis*, an important pig pathogen and emerging zoonotic agent—an update on the worldwide distribution based on serotyping and sequence typing. *Emerg Microbes Infect*. 2014;3:e45. <http://dx.doi.org/10.1038/emi.2014.45>
5. Athey TB, Teatero S, Lacouture S, Takamatsu D, Gottschalk M, Fittipaldi N. Determining *Streptococcus suis* serotype from short-read whole-genome sequencing data. *BMC Microbiol*. 2016;16:162. <http://dx.doi.org/10.1186/s12866-016-0782-8>
6. Athey TB, Teatero S, Takamatsu D, Wasserscheid J, Dewar K, Gottschalk M, et al. Population structure and antimicrobial resistance profiles of *Streptococcus suis* serotype 2 sequence type 25 strains. *PLoS One*. 2016;11:e0150908. <http://dx.doi.org/10.1371/journal.pone.0150908>
7. Fittipaldi N, Xu J, Lacouture S, Tharavichitkul P, Osaki M, Sekizaki T, et al. Lineage and virulence of *Streptococcus suis* serotype 2 isolates from North America. *Emerg Infect Dis*. 2011;17:2239–44. <http://dx.doi.org/10.3201/eid1712.110609>
8. Gottschalk M, Higgins R, Boudreau M. Use of polyvalent coagglutination reagents for serotyping of *Streptococcus suis*. *J Clin Microbiol*. 1993;31:2192–4.
9. van Samkar A, Brouwer MC, Schultz C, van der Ende A, van de Beek D. *Streptococcus suis* meningitis: A systematic review and meta-analysis. *PLoS Negl Trop Dis*. 2015;9:e0004191. <http://dx.doi.org/10.1371/journal.pntd.0004191>
10. Fongcom A, Pruksakorn S, Netsirisawan P, Pongprasert R, Onsibud P. *Streptococcus suis* infection: a prospective study in northern Thailand. *Southeast Asian J Trop Med Public Health*. 2009;40:511–7.

Address for correspondence: Nahuel Fittipaldi, Public Health Ontario Laboratory, 661 University Ave, Ste 17-100, Toronto, ON M5G 1M1, Canada; email: nahuel.fittipaldi@oahpp.ca

Moku Virus in Invasive Asian Hornets, Belgium, 2016

Mutien Garigliany, Bernard Taminiau, Noémie El Agrebi, Daniel Cadar, Gautier Gilliaux, Marie Hue, Daniel Desmecht, Georges Daube, Annick Linden, Frédéric Farnir, Michel De Proft, Claude Saegerman

Author affiliations: Faculty of Veterinary Medicine, Liège, Belgium (M. Garigliany, B. Taminiau, N. El Agrebi, G. Gilliaux, M. Hue, D. Desmecht, G. Daube, A. Linden, F. Farnir, C. Saegerman); Bernhard Nocht Institute for Tropical Medicine, Hamburg, Germany (D. Cadar); Walloon Agricultural Research Centre, Gembloux, Belgium (M. De Proft)

DOI: <https://doi.org/10.3201/eid2312.171080>

We report the detection of Moku virus in invasive Asian hornets (*Vespa velutina nigrithorax*) in Belgium. This constitutes an unexpected report of this iflavirus outside Hawaii, USA, where it was recently described in social wasps. Although virulence of Moku virus is unknown, its potential spread raises concern for European honeybee populations.

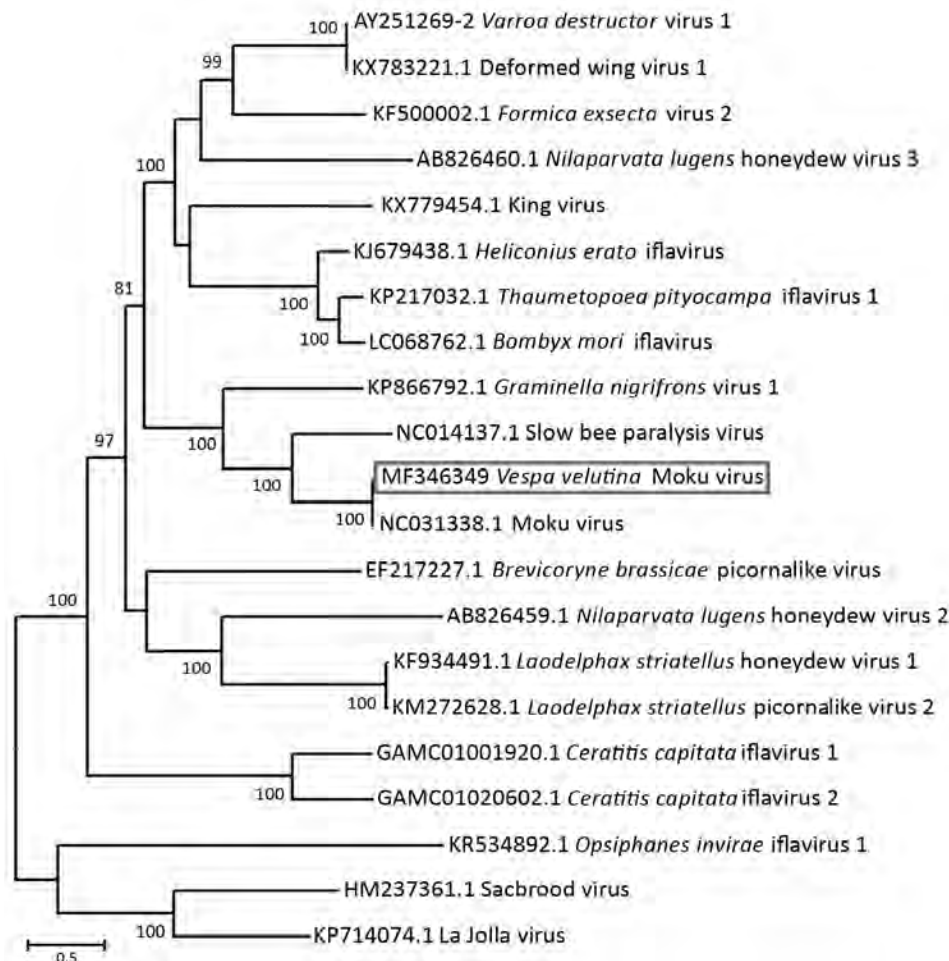
With their work estimated to have a global economic value of €153 billion, insects are critical pollinators of crops in agriculture, with the honeybee (*Apis mellifera*) being by far the major player in this process (1). Honeybee populations are decreasing dramatically worldwide, however, threatening food security. Environmental changes, pesticides, pathogens, and parasitic species are all recognized drivers of this decline (2). Among these, the Varroa mite (*Varroa destructor*) has been shown to have a critical effect on honeybee populations, both by its direct parasitic effects and through the transmission of pathogenic viruses such as deformed wing virus (2).

The Asian yellow-legged hornet (*Vespa velutina nigrithorax*), a natural predator of honeybees, has a native range spanning from India through China and as far as

Indonesia (3). It is a particularly efficient invader because of its distinctive biology and behavior (4,5). The hornet was accidentally introduced from China into Europe, with sightings in France in 2004, and has rapidly spread to neighboring countries, including Belgium, since 2011 (6). In invaded areas, hornets' feeding sites are primarily apiaries, which present an attractive, abundant, and defenseless prey source (5). *V. velutina nigrithorax* hornets not only contribute by hunting to the loss of honeybee colonies but also interact with the honeybees and can act as viral reservoirs, as *V. destructor* mites do, and infect the bees through spillover events (7,8). To explore the possibility of transmission of viruses from these hornets to honeybees, we performed a viral metagenomic analysis of Asian hornets collected in Belgium in 2016.

We submitted a pool of 5 female and 5 male adult *V. velutina nigrithorax* hornets collected in Belgium in November 2016 to a viral metagenomics analysis by next-generation sequencing (detailed methods in online Technical Appendix, <https://wwwnc.cdc.gov/EID/article/23/12/17-1080-Techapp1.pdf>). A blastx (<https://blast.ncbi.nlm.nih.gov/Blast.cgi>) alignment to GenBank viral sequences enabled the assignment of

Figure. Evolutionary relationships of Moku virus generated from a pool of 5 female and 5 male Asian hornets (*Vespa velutina*) collected in Belgium in 2016 (box) compared with representative members of the genus *Iflavirus*, based on the maximum-likelihood phylogeny of the polyprotein sequences. The phylogenetic analysis was performed using MEGA6 (10) and the LG substitution model, as determined by a model selection analysis. Bootstrap percentages >70% (from 500 resamplings) are indicated at each node. GenBank accession numbers are indicated for each species. Scale bar indicates amino acid substitutions per site.



most viral sequences to phages (not represented) and viruses of the *Partitiviridae* and *Parvoviridae* (*Densovirinae*) families (online Technical Appendix Figure 1); however, a few reads pointed to a member of the *Iflaviridae* family, which contains such notable bee pathogens as deformed wing virus and slow bee paralysis virus (9). blastn alignment showed a positive match to Moku virus (9). Template-based assembly using Moku virus (GenBank accession no. KU645789) (9) permitted a near-full genome reconstruction from 1,215 matching reads out of 4,587,801. We used primer walking PCR and Sanger sequencing to fill the gaps in the genome (online Technical Appendix Figure 2).

The full viral genome sequence we obtained is 10,032 nt in length (GenBank accession no. MF346349) and has a mean nucleotide identity of 96.0% to the Hawaiian Moku virus strain (accession no. KU645789) (9), with both viruses showing an open reading frame of the same length (9,153 nt) sharing an amino acid identity of 99.0%. We performed an alignment to the full translated polyprotein amino acid sequence of representative iflaviruses available in GenBank using the Muscle aligner implemented in Geneious version 8.1.8 (Biomatters, Auckland, New Zealand). A maximum-likelihood phylogenetic analysis performed on the full-length polyprotein sequence yielded comparable results to that obtained on a conserved region of the RNA-dependent RNA polymerase (9), confirming the high identity of the Moku virus we obtained from the *V. velutina nigrithorax* hornet pools with the Hawaiian isolate of Moku virus, as well as its proximity to slow bee paralysis virus (Figure).

Our results show a large diversity of viruses in invasive Asian hornets collected in Belgium in 2016. Among these, we detected an iflavirus with high identity to the recently described Moku virus found in social wasps (*Vespula pensylvanica*), honeybees, and Varroa mites in Hawaii (9). Such a high nucleotide identity unequivocally places both strains in a single species. The potential pathogenicity of Moku virus for honeybees is currently unknown, but its relatively close relationship with the highly virulent slow bee paralysis virus warrants further studies (9). There is an urgent need to assess the presence of Moku virus in honeybees and *Varroa* mites in areas of Europe where the Asian hornet has become endemic, such as several regions in France. As highlighted by Mordecai et al. (9), the carriage of Moku virus in *V. destructor* mites in Hawaii is of great concern given the role played by this mite in the maintenance and transmission of viruses, including the deformed wing iflavirus, to honeybees. Furthermore, although Moku virus was shown to be highly dominant among viral species infecting *V. pensylvanica* wasps (9), suggesting that this species is a likely reservoir of the virus, we could not establish the same relationship for the Asian hornet

V. velutina, in which *Partitiviridae* were much more abundant. It remains to be determined whether Moku virus is a virus of *Vesputidae* or, more likely given the relatively low number of reads detected, could have been picked up by these hornets from their prey, such as honeybees. Further studies are needed to establish the origin, host range, and transmission route of Moku virus; its virulence; and the risks it may represent for European honeybee populations.

Acknowledgments

We thank the Fundamental and Applied Research for Animal and Health Center, Liège, Belgium, for the access to its metagenomics platform, and the Walloon Agricultural Research Centre, Gembloux, Belgium, for the access to historical specimens of the Asian hornet *Vespa velutina*.

Dr. Garigliany is a professor of pathology at the Veterinary Faculty of the University of Liège, Belgium. His research activities focus on the biology of viruses and related host–pathogen interactions.

References

- Gallai N, Salles J-M, Settele J, Vaissière BE. Economic valuation of the vulnerability of world agriculture confronted with pollinator decline. *Ecol Econ*. 2009;68:810–21. <http://dx.doi.org/10.1016/j.ecolecon.2008.06.014>
- Brown MJF, Dicks LV, Paxton RJ, Baldock KCR, Barron AB, Chauzat M-P, et al. A horizon scan of future threats and opportunities for pollinators and pollination. *PeerJ*. 2016;4:e2249. <http://dx.doi.org/10.7717/peerj.2249>
- Franklin DN, Brown MA, Datta S, Cuthbertson AGS, Budge GE, Keeling MJ. Invasion dynamics of Asian hornet, *Vespa velutina* (Hymenoptera: Vespidae): a case study of a commune in south-west France. *Appl Entomol Zool (Jpn)*. 2017;52:221–9. <http://dx.doi.org/10.1007/s13355-016-0470-z>
- Arca M, Mougel F, Guillemaud T, Dupas S, Rome Q, Perrard A, et al. Reconstructing the invasion and the demographic history of the yellow-legged hornet, *Vespa velutina*, in Europe. *Biol Invasions*. 2015;17:2357–71. <http://dx.doi.org/10.1007/s10530-015-0880-9>
- Couto A, Monceau K, Bonnard O, Thiéry D, Sandoz J-C. Olfactory attraction of the hornet *Vespa velutina* to honeybee colony odors and pheromones. *PLoS One*. 2014;9:e115943. <http://dx.doi.org/10.1371/journal.pone.0115943>
- Monceau K, Thiéry D. *Vespa velutina* nest distribution at a local scale: an 8-year survey of the invasive honeybee predator. *Insect Sci*. 2017;24:663–74. <http://dx.doi.org/10.1111/1744-7917.12331>
- Wilfert L, Long G, Leggett HC, Schmid-Hempel P, Butlin R, Martin SJM, et al. Deformed wing virus is a recent global epidemic in honeybees driven by Varroa mites. *Science*. 2016;351:594–7. <http://dx.doi.org/10.1126/science.aac9976>
- Manley R, Boots M, Wilfert L. Condition-dependent virulence of slow bee paralysis virus in *Bombus terrestris*: are the impacts of honeybee viruses in wild pollinators underestimated? *Oecologia*. 2017;184:305–15. <http://dx.doi.org/10.1007/s00442-017-3851-2>
- Mordecai GJ, Brettell LE, Pachori P, Villalobos EM, Martin SJ, Jones IM, et al. Moku virus; a new iflavirus found in wasps, honey bees and Varroa. *Sci Rep*. 2016;6:34983. <http://dx.doi.org/10.1038/srep34983>

10. Tamura K, Stecher G, Peterson D, Filipiński A, Kumar S. MEGA6: Molecular Evolutionary Genetics Analysis version 6.0. *Mol Biol Evol*. 2013;30:2725–9. <http://dx.doi.org/10.1093/molbev/mst197>

Address for correspondence: Mutien Garigliany, University of Liege, Department of Pathology, Avenue de Cureghem 6, B43, Liège B-4000 Belgium; email: mmgarigliany@uliege.be

Angiostrongylus cantonensis DNA in Cerebrospinal Fluid of Persons with Eosinophilic Meningitis, Laos

Damien K.Y. Ming, Sayaphet Rattanavong, Tehmina Bharucha, Onanong Sengvilaipaseuth, Audrey Dubot-Pérès, Paul N. Newton, Matthew T. Robinson

Author affiliations: Imperial College London, London, UK (D.K.Y. Ming); Lao-Oxford-Mahosot Hospital Wellcome Trust Research Unit, Vientiane, Laos (D.K.Y. Ming, S. Rattanavong, T. Bharucha, O. Sengvilaipaseuth, A. Dubot-Pérès, P.N. Newton, M.T. Robinson); University College London, London (T. Bharucha); Aix-Marseille Université, Marseille, France (A. Dubot-Pérès); University of Oxford, Oxford, UK (P.N. Newton, M.T. Robinson)

DOI: <https://doi.org/10.3201/eid2312.171107>

Definitive identification of *Angiostrongylus cantonensis* parasites from clinical specimens is difficult. As a result, regional epidemiology and burden are poorly characterized. To ascertain presence of this parasite in patients in Laos with eosinophilic meningitis, we performed quantitative PCRs on 36 cerebrospinal fluid samples; 4 positive samples confirmed the parasite's presence.

Humans are incidental hosts of *Angiostrongylus cantonensis* nematodes; global distribution of these nematodes is being increasingly recognized (1). Ingestion of larvae from undercooked infected snails or food contaminated with mollusk secretions can result in the migration of *A. cantonensis* parasites through the human central nervous system (CNS) (2). The presence of the parasite and associated inflammation in the CNS can contribute to a meningoencephalitic syndrome, typified by a cerebrospinal fluid (CSF) eosinophilia constituting $\geq 10\%$ of total CSF leukocyte count.

Formal diagnosis of angiostrongyliasis is difficult because the parasite is typically present in low numbers within the CSF (3). Serologic methods are limited by cross-reactivity with other helminths (4), and antibody-based methods may lack sensitivity, especially during acute illness (5).

Host sampling studies have identified *A. cantonensis* parasites in some Mekong region countries but not in Lao People's Democratic Republic (Laos) (6). To ascertain the presence of this parasite in patients with eosinophilic meningitis in Laos, we tested samples from a cohort of 1,065 patients suspected of having CNS infection at Mahosot Hospital, Vientiane, Laos, during 2003–2013 by Giemsa staining and identified 54 CSF samples containing $\geq 10\%$ eosinophils. Of these, 36 samples from 35 patients were available for this study (1 patient underwent lumbar puncture twice) and were tested by conventional and quantitative PCR (cPCR and qPCR). From the same cohort, we also performed qPCR testing on another 50 CSF samples with 1%–9% eosinophils.

DNA was extracted from 200 μL of CSF by using a QIAamp DNA Mini Kit (QIAGEN, Hilden, Germany) and eluted in 30 μL buffer. We ran the extract in parallel with positive samples (*A. cantonensis* DNA from experimentally infected rats, University of Sydney, Sydney, Australia) and negative controls by using published cPCR (7) and qPCR (8) protocols. We used Platinum PCR SuperMix (Thermo Fisher, Waltham, MA, USA) and performed assays on a Bio-Rad CFX96 (Bio-Rad, Watford, UK).

Among patients with CSF eosinophilia $\geq 10\%$, male patients predominated, although sex of patients did not differ significantly among patients with or without CSF eosinophilia (Table). Of the 36 CSF samples that contained $\geq 10\%$ eosinophils, all were negative by cPCR, but 4 (11.1%) were positive for *A. cantonensis* DNA by qPCR; median quantification cycle was 35.9 (range 34.1–37.4). Sensitivity of qPCR was apparently higher than that of cPCR. The median duration of illness for patients with positive qPCR was 4 (range 0–10) days. Of 3 patients with a positive qPCR, 2 reported that they had eaten raw snails in the previous month.

Results from 2 CSF samples obtained from the same patient and tested by qPCR were discordant; CSF obtained after 7 days of illness was negative for *A. cantonensis* DNA, but a sample obtained on day 13 was positive (quantification cycle 34.1). This finding is consistent with previous observations (8), and it is plausible that during the acute stages of infection, insufficient nucleic material is present for detection. Although lumbar puncture is invasive, a high clinical suspicion of angiostrongyliasis in the context of a negative qPCR may therefore warrant a repeated lumbar puncture. All positive samples had CSF eosinophil proportions $>40\%$, and all samples containing a 1%–9% eosinophil proportion tested negative by qPCR, supporting the conventional cutoff of a CSF eosinophilia $\geq 10\%$ in the diagnosis of CNS angiostrongyliasis.

Table. Demographics and clinical characteristics of 35 patients with eosinophilic meningitis tested by qPCR for *Angiostrongylus cantonensis* parasites*

Characteristic	Positive, n = 4†	Negative, n = 31†
Median age, y (IQR)	25 (21–42)	25 (20–40)
Sex, no. (%)		
M	4/4 (100)	19/31 (61)
F	0	12/31 (39)
Median duration of illness, d (IQR)	4 (1–9)	4 (0–6.5)
Median eosinophil % of total leukocyte count (IQR)	65 (50–73)	33 (14–56)
Diet in past mo		
Raw fish	3/3	7/13
Raw shellfish	2/2	3/11
Raw snails	2/3	5/12
Raw crab	2/2	2/11
Fulfilled WHO criteria for meningitis at admission, no. (%)	3/4 (75)	9/28 (32)
Median CSF opening pressure, cm H ₂ O (IQR)	28 (22–35)	27 (17–40)
Median CSF leukocyte count, × 10 ⁶ cells/L (IQR)	583 (493–1,198)	125 (40–580)
Median CSF protein, g/L (IQR)	0.68 (0.31–1.08)	0.56 (0.31–1.00)
Median CSF glucose, mmol/L (IQR)	2.7 (2.4–4.2)	3.1 (2.4–4.9)

*CSF, cerebrospinal fluid; IQR, interquartile range; qPCR, quantitative PCR; WHO, World Health Organization.

†Denominators vary according to available data.

Our findings are consistent with those from studies demonstrating *A. cantonensis* parasites as a cause of eosinophilic meningitis in the region, although the proportion of *A. cantonensis*-positive cases in our cohort was lower than that from Vietnam (11.1% vs. 67.3%) (9). Results may be affected by factors such as geographic location, differences in healthcare access, and the contribution of other causes of eosinophilic meningitis, such as *Gnathostoma spinigerum* nematodes. In the absence of a reliable reference diagnostic standard, we were unable to estimate the proportion of false-negative results in this cohort or to correlate findings with other immunodiagnostic modalities. Further studies on eosinophilic meningitis from a wider geographic area and improved diagnostics would help establish the overall clinical burden of CNS angiostrongyliasis in Laos.

Diet (consumption of raw snails and food contaminated by snails) is considered a major risk factor for angiostrongyliasis, making an epidemiologic link and public health interventions a possibility. The exact host species responsible for transmission remains unclear, however, given that *A. cantonensis* parasites have apparently yet to be identified within snails in Laos.

Our identification of *A. cantonensis* DNA by qPCR of CSF samples from 4 (11%) of 35 patients with eosinophilic meningitis confirms the parasite's presence in Laos. Further regional characterization, coupled with dietary surveys, will be invaluable for stratifying the risk for human transmission and guiding public health interventions.

Acknowledgments

We are thankful for the support of the directors and staff of Mahosot Hospital, especially of the Adult Infectious Disease ward and the Microbiology Laboratory.

Funding was provided by the Wellcome Trust (London, UK) and L'Institut de Recherche pour le Développement (Marseille, France).

Dr. Ming is an academic clinical fellow in infectious diseases at Imperial College London. His research interests include tropical medicine and parasitology.

References

- Barratt J, Chan D, Sandaradura I, Malik R, Spielman D, Lee R, et al. *Angiostrongylus cantonensis*: a review of its distribution, molecular biology and clinical significance as a human pathogen. *Parasitology*. 2016;143:1087–118. <http://dx.doi.org/10.1017/S0031182016000652>
- Wang Q-PP, Lai D-HH, Zhu X-QQ, Chen X-GG, Lun Z-RR. Human angiostrongyliasis. *Lancet Infect Dis*. 2008;8:621–30. [http://dx.doi.org/10.1016/S1473-3099\(08\)70229-9](http://dx.doi.org/10.1016/S1473-3099(08)70229-9)
- Punyagupta S, Juttijudata P, Bunnag T. Eosinophilic meningitis in Thailand. Clinical studies of 484 typical cases probably caused by *Angiostrongylus cantonensis*. *Am J Trop Med Hyg*. 1975;24:921–31. <http://dx.doi.org/10.4269/ajtmh.1975.24.921>
- Morassutti AL, Rascoe LN, Handali S, DA Silva AJ, Wilkins PP, Graeff-Teixeira C. Cross-reactivity of the 31 kDa antigen of *Angiostrongylus cantonensis*—dealing with the immunodiagnosis of meningoencephalitis. *Parasitology*. 2017;144:459–63. <http://dx.doi.org/10.1017/S0031182016001918>
- Slom TJ, Cortese MM, Gerber SI, Jones RC, Holtz TH, Lopez AS, et al. An outbreak of eosinophilic meningitis caused by *Angiostrongylus cantonensis* in travelers returning from the Caribbean. *N Engl J Med*. 2002;346:668–75. <http://dx.doi.org/10.1056/NEJMoa012462>
- Rodpai R, Intapan PM, Thanchomngang T, Sanpool O, Sadaow L, Laymanivong S, et al. *Angiostrongylus cantonensis* and *A. malaysiensis* broadly overlap in Thailand, Lao PDR, Cambodia and Myanmar: a molecular survey of larvae in land snails. *PLoS One*. 2016;11:e0161128. <http://dx.doi.org/10.1371/journal.pone.0161128>
- Qvarnstrom Y, Sullivan JJ, Bishop HS, Hollingsworth R, da Silva AJ. PCR-based detection of *Angiostrongylus cantonensis* in tissue and mucus secretions from molluscan hosts. *Appl Environ Microbiol*. 2007;73:1415–9. <http://dx.doi.org/10.1128/AEM.01968-06>
- Qvarnstrom Y, Xayavong M, da Silva AC, Park SY, Whelen AC, Calimlim PS, et al. Real-time polymerase chain reaction detection of *Angiostrongylus cantonensis* DNA in cerebrospinal fluid from patients with eosinophilic meningitis. *Am J Trop Med Hyg*. 2016;94:176–81. <http://dx.doi.org/10.4269/ajtmh.15-0146>

9. McBride A, Chau TTH, Hong NTT, Mai NTH, Anh NT, Thanh TT, et al. *Angiostrongylus cantonensis* is an important cause of eosinophilic meningitis in southern Vietnam. *Clin Infect Dis*. 2017;64:1784–7. <http://dx.doi.org/10.1093/cid/cix118>

Address for correspondence: Damien K.Y. Ming, Imperial College London, The Section of Infectious Diseases and Immunity, Commonwealth Building, Hammersmith Campus, London SW7 2AZ, UK; email: damien.ming@doctors.org.uk

Tool for Eliminating Dog-Mediated Human Rabies through Mass Dog Vaccination Campaigns

Eduardo A. Undurraga,¹ Jesse D. Blanton, S.M. Thumbi, Athman Mwatondo, Mathew Muturi, Ryan M. Wallace

Author affiliations: Centers for Disease Control and Prevention, Atlanta, Georgia, USA (E.A. Undurraga, J.D. Blanton, R.M. Wallace); Kenya Medical Research Institute, Nairobi, Kenya (S.M. Thumbi); Washington State University, Pullman, Washington, USA (S.M. Thumbi); Kenya Ministry of Health, Nairobi (A. Mwatondo, M. Muturi)

DOI: <https://doi.org/10.3201/eid2312.171148>

The World Health Organization and collaborating agencies have set the goal of eliminating dog-mediated human rabies by 2030. Building on experience with rabies endemic countries, we constructed a user-friendly tool to help public health officials plan the resources needed to achieve this goal through mass vaccination of dogs.

Globally, rabies kills ≈60,000 persons annually; most (≈99%) cases are transmitted by domestic dogs (1–3). Controlling dog rabies through periodic mass vaccination campaigns substantially reduces human exposures (4). The elimination of dog rabies in most of the Western Hemisphere and countries in Asia has demonstrated the effectiveness and sustainability of vaccinating dogs (5,6) by combining massive dog rabies vaccination with coordinated efforts of the medical and veterinary sectors (One Health approach), including education about responsible

pet ownership, rabies awareness campaigns, and access to postexposure prophylaxis (5,6).

The World Health Organization recommends that at least 70% of the dog population be vaccinated to control and potentially eliminate dog rabies (3). In 2016, WHO and partner organizations set the goal of eliminating dog-mediated human rabies by 2030 (7). This goal could be achieved by massive, costly administration of preexposure and postexposure prophylaxis, mass vaccination of dogs, or both.

Countries to which rabies is endemic in dogs are at different stages in their rabies control efforts (5,8). Countries at early stages face barriers related to a limited understanding of the local epidemiology, logistic and operational challenges, competing priorities from other diseases, and lack of planning tools to reasonably project the resources needed. During 2016, we estimated the resources potentially required to eliminate dog rabies globally by 2030 (7). We combined multiple data sources to estimate 4 key factors that affect this goal: country development, cost of dog vaccination programs, potential demand for dog rabies vaccine, and estimated number of vaccinators. We aimed to realistically assess the global situation by highlighting the main challenges that might hamper elimination efforts. However, although these global estimates can inform an important discussion about global and regional strategic planning and resource mobilization, they are not necessarily useful to inform country-level decision-making. We addressed this limitation by providing a user-friendly tool that requires only limited country-specific data to help countries plan toward the goal of eliminating dog rabies through mass dog vaccination.

We designed the tool to plan for dog rabies elimination by 2030 (a 13-year framework). We assumed 13 years would be enough time for even the least developed rabies control programs to achieve elimination, provided the country was fully committed. The country's starting point within this time frame would depend on its current dog vaccination rate, and the given country would demonstrate incremental improvements in preparation for the vaccination campaign (e.g., training of workforce involved, dog population surveys) or in the proportion of the dog population vaccinated. The tool requires input of demographic data (human population, percentage urban, human-to-dog ratio); current dog vaccination coverage; logistic data for the campaigns (available vaccinators, dog vaccination rates, campaign duration); and an estimated cost per vaccinated dog. We constructed a worksheet to help users estimate the cost per vaccinated dog based on a pilot campaign. The tool (including assumptions, instructions, and data requirements) is available for public use (online Technical Appendix, <https://wwwnc.cdc.gov/EID/article/23/12/17-1148-Techapp1.xlsm>) and already has been used in Haiti and Guatemala as part of a rabies elimination workshop held at the Centers for Disease Control and

¹Current affiliation: Pontificia Universidad Católica de Chile, Santiago, Chile.

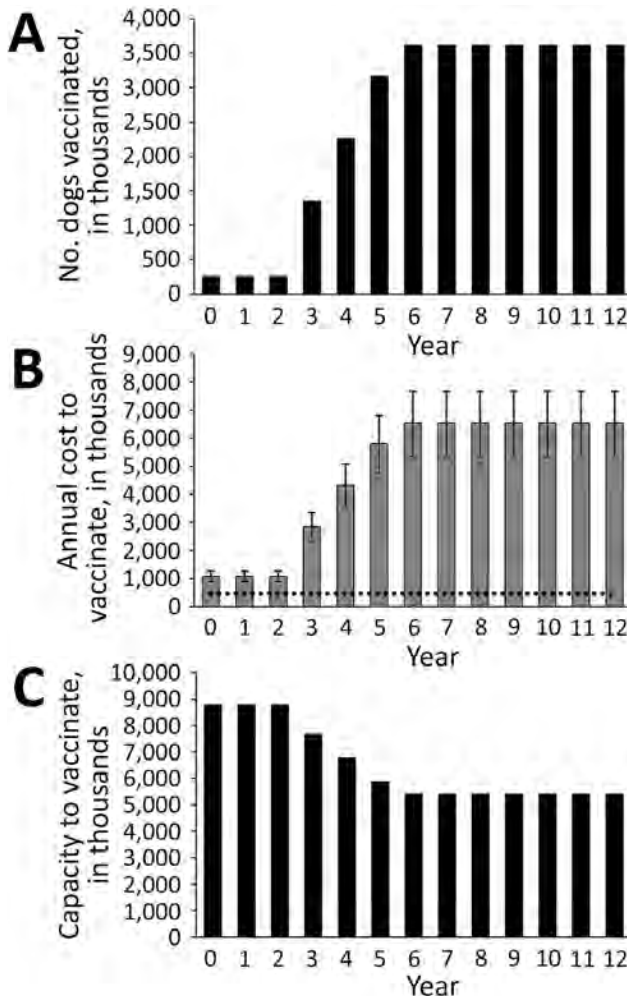


Figure. Illustrative results from the planning aid tool for controlling dog rabies through dog vaccination using input data, Kenya, 2016. A) Number of annual dog vaccinations required in accordance with World Health Organization recommendations. The tool assumes a threshold of 70% of dog vaccination during 7 years as a conservative estimate to eliminate dog-mediated rabies. The actual proportion of the dog population that needs to be vaccinated depends on local conditions of rabies transmission (10). Based on field data, Kenya estimates that 3 consecutive years of 70% coverage of dog vaccination would end dog–dog rabies transmission. The estimate by Hampson et al. (1) estimate of 523 annual deaths was based on active surveillance in eastern Kenya; current passive surveillance reports higher bite rates, so the estimate probably represents a lower bound of the number of deaths that could be avoided through mass dog vaccination. B) Total annual cost (US \$) of dog vaccination. Error bars indicate 95% CIs. Horizontal dotted line indicates current spending for dog vaccination. C) Net dog vaccination capacity (i.e., total number of dogs per year minus the number of dogs Kenya needs to vaccinate to achieve the dog vaccination coverage goal). If the number is positive, the country has enough capacity to vaccinate; if negative, the country needs more vaccinators, increased vaccination efficiency, or more campaign days. The estimated annual costs are based on the cost per dog vaccinated; excess vaccinator capacity is not included in the aggregate costs.

1Prevention (Atlanta, GA, USA). Users can account for uncertainty in point estimates by varying model parameters.

To show the utility of the planning tool, we input known information from 2 recent mass dog vaccination campaigns in western Kenya to project expected long-term costs and a timeline for rabies elimination. With a conservative estimate of 523 (95% CI 138–1,100) annual human rabies-associated deaths and substantial medical costs (1), Kenya is actively trying to eliminate human rabies by 2030 (9). We used the following values: 46,050,302 persons, of whom 26% live in urban areas; 7.4 and 21.2 humans per dog in rural and urban areas, respectively; 5% of the dog population vaccinated; 4,300 available vaccinators; 100 dogs vaccinated daily per vaccinator; a 21-day campaign in each region; an estimated cost per dog vaccinated of US \$1.81 (range US \$1.48–\$2.12); and 0% discount rate (Figure). Conditional on the availability of resources, the results suggest that Kenya can eliminate dog rabies during the next 13 years, in line with the 2030 global goal; vaccination campaigns would cost ≈US \$62.0 million (range US \$50.6 million–\$72.8 million), equivalent to ≈\$56.0 million additional aggregate spending over 13 years (not discounted). If the average vaccination rate was 100 dogs per vaccinator per day, Kenya would have enough capacity to conduct 21-day campaigns and reach the 70% dog vaccination goal.

The tool enables users to estimate the resources required to eliminate rabies using country-specific input values. We hope this tool will help stimulate and inform a necessary discussion on strategic planning, resource mobilization, and continuous execution of rabies elimination.

This work was funded by the Centers for Disease Control and Prevention.

Dr. Undurraga was a Steven M. Teutsch Prevention Effectiveness Fellow in the Division of Preparedness and Emerging Infections, National Center for Emerging and Zoonotic Infectious Diseases, Centers for Disease Control and Prevention, when this work was done. He is currently an assistant professor at the School of Government, Pontificia Universidad Católica de Chile, Santiago. His primary research interests include population health, health economics, and social policy.

References

- Hampson K, Coudeville L, Lembo T, Sambo M, Kieffer A, Atlan M, et al.; Global Alliance for Rabies Control Partners for Rabies Prevention. Estimating the global burden of endemic canine rabies. *PLoS Negl Trop Dis*. 2015;9:e0003709. Erratum in: *PLoS Negl Trop Dis*. 2015;9:e0003786. <http://dx.doi.org/10.1371/journal.pntd.0003709>
- Knobel DL, Cleaveland S, Coleman PG, Fèvre EM, Meltzer MI, Miranda MEG, et al. Re-evaluating the burden of rabies in Africa and Asia. *Bull World Health Organ*. 2005;83:360–8.

3. World Health Organization. WHO Expert Consultation on Rabies. Second report [cited 2016 Mar 30]. http://apps.who.int/iris/bitstream/10665/85346/1/9789240690943_eng.pdf
4. World Health Organization. Rabies vaccines: WHO position paper. *Wkly Epidemiol Rec.* 2010;85:309–20 [cited 2017 Oct 5]. <http://www.who.int/wer/2010/wer8532/en/>
5. Rupprecht CE, Hanlon CA, Hemachudha T. Rabies re-examined. *Lancet Infect Dis.* 2002;2:327–43. [http://dx.doi.org/10.1016/S1473-3099\(02\)00287-6](http://dx.doi.org/10.1016/S1473-3099(02)00287-6)
6. Vigilato MAN, Clavijo A, Knobl T, Silva HMT, Cosivi O, Schneider MC, et al. Progress towards eliminating canine rabies: policies and perspectives from Latin America and the Caribbean. *Philos Trans R Soc Lond B Biol Sci.* 2013;368:20120143. <http://dx.doi.org/10.1098/rstb.2012.0143>
7. Wallace RM, Undurraga EA, Blanton JD, Cleaton J, Franka R. Elimination of dog-mediated human rabies deaths by 2030: needs assessment and alternatives for progress based on dog vaccination. *Front Vet Sci.* 2017;4:9. <http://dx.doi.org/10.3389/fvets.2017.00009>
8. Lembo T, Hampson K, Kaare MT, Ernest E, Knobel D, Kazwala RR, et al. The feasibility of canine rabies elimination in Africa: dispelling doubts with data. *PLoS Negl Trop Dis.* 2010;4:e626. <http://dx.doi.org/10.1371/journal.pntd.0000626>
9. Republic of Kenya Ministry of Health and Ministry of Agriculture. Strategic plan for the elimination of human rabies in Kenya 2014–2030 [cited 2017 Jun 1]. <http://zdukenya.org/wp-content/uploads/2012/09/National-Rabies-Elimination-Strategy.pdf>
10. Zinsstag J, Dürr S, Penny MA, Mindekem R, Roth F, Menendez Gonzalez S, et al. Transmission dynamics and economics of rabies control in dogs and humans in an African city. *Proc Natl Acad Sci U S A.* 2009;106:14996–5001. <http://dx.doi.org/10.1073/pnas.0904740106>

Address for correspondence: Eduardo A. Undurraga, School of Government, Pontificia Universidad Católica de Chile, Vicuña Mackenna 4860, Macul CP 7820436, Región Metropolitana, Chile; email: eundurra@uc.cl

Unexpected Infection with *Armillifer* Parasites

Idzi Potters, Claude Desaiwe, Steven Van Den Broucke, Marjan Van Esbroeck, Lutgarde Lynen

Author affiliations: Institute of Tropical Medicine Antwerp, Antwerp, Belgium (I. Potters, S. Van Den Broucke, M. Van Esbroeck, L. Lynen); Central University Hospital of Liège, Liège, Belgium (C. Desaiwe)

DOI: <https://doi.org/10.3201/eid2312.171189>

Visceral pentastomiasis is usually found incidentally during surgery. We describe a case of visceral pentastomiasis discovered during inguinoscrotal hernia surgery for a man

from Benin, Africa. Because surgical removal of nymphs is needed for symptomatic patients only, this patient's asymptomatic pentastomiasis was not treated and he recovered from surgery uneventfully.

In November 2015, a surgeon from Belgium, working for Medics without Vacation in Bassila, Benin, Africa, incidentally discovered pentastomiasis in an adult man during surgery for a massive inguinoscrotal hernia (half a liter content). Other than the hernia, the patient had no health problems. During the procedure, the surgeon observed at least 10 coiled, larva-like structures on the patient's peritoneal tissue. He removed the hernial sac and sent a tissue specimen to the national reference laboratory for parasitology at the Institute of Tropical Medicine (Antwerp, Belgium) for identification of the parasite. Apart from the hernia symptoms, the patient was asymptomatic, so the parasites were not removed; the patient's surgical recovery was uneventful.

Macroscopic examination of the peritoneal tissue detected 8 distinct, typical larva-like structures with an average length of 1–2 cm (Figure, panel A). Because the structures were suspected to be pentastomes, they were compared with reference material from the Institute of Tropical Medicine Educational Department (Figure, panel B) and confirmed as *Armillifer* spp. nymphs. On the basis of the patient's residence in Benin, and the fact that the recovered nymphs consistently exhibited <22 annuli, the structures were presumptively identified as *A. armillatus* (1,2). Adults of this species are often found in the respiratory system of large snakes. Although no information was available regarding the patient's contact with snakes, the presence of this parasite in a resident of Benin is not surprising because snake consumption in that country is common practice. The patient's surgeon confirmed that dead snakes were indeed often sold for consumption along the streets near the hospital.

The Pentastomida are a peculiar group of gonochoric, vermiform endoparasites, currently classified as a unique phylum, related to branchiuran crustaceans (3). The main characteristics of this group of ancient parasitic arthropods are an often annulated elongate body and a mouth typically flanked by 2 pairs of hooks.

Human visceral pentastomiasis can be caused by several species of pentastomes: *Linguatula serrata* (worldwide, predominantly the Middle East), *A. armillatus* (West and Central Africa), *A. moniliformis* (Southeast Asia), *A. grandis* (Africa), *A. agkistrodontis* (China), *Porocephalus crotali* (worldwide, predominantly the Americas), and *P. taiwana* (China) (2,4,5). Reported cases of human visceral pentastomiasis were caused mainly by *A. armillatus* pentastomes (6) from infected snakes, which shed ova in excretions and respiratory secretions, thereby



Figure. *Armillifer armillatus* parasites. A) Typically coiled *Armillifer armillatus* nymphs, averaging 1–2 cm long and consistently showing <22 annuli. B) Adult female and numerous nymphs. Reference material from the Educational Department, Institute of Tropical Medicine, Antwerp, Belgium.

contaminating vegetation and water. Intermediate hosts are mainly rodents and small mammals. After oral uptake by the intermediate host, the ova hatch and free 4-legged primary larvae that migrate to the viscera, become encapsulated, and after several molts transform into legless nymphs (2,7). The cycle is complete when the intermediate host is in turn consumed by a snake of an appropriate species. Humans can become intermediate hosts through ingestion of environmental ova, by eating undercooked infected snake meat, or by oral uptake of ova when in close contact with snakes (1,2,6). Diagnosis of human visceral pentastomiasis is classically made by either identifying the nymphs during autopsy or surgery or by discovering typically crescentic or coiled opacities, representing calcified dead larvae, on abdominal or chest radiographs.

The finding of pentastomiasis in patients with inguinal hernia, as with the patient reported here, has been described for 2 patients in Ghana (8). The number of reported cases of human pentastomiasis from Africa is increasing (6,8); because infection with *Armillifer* parasites is usually asymptomatic, we assume that the incidence of this infection is underestimated. Autopsy studies have reported prevalence rates as high as 22% in the Democratic Republic of the Congo and 45% in Malaysia (9,10). As industrialized countries are increasingly receiving immigrants and refugees from Africa, it is conceivable that this disease will be more frequently encountered.

Because pentastomes are usually not mentioned in the helminth section of parasitology textbooks, laboratory technicians, clinicians, and surgeons who are unfamiliar with this parasite might be startled when incidentally discovering it. They should note that visceral pentastomiasis is usually asymptomatic and that surgical removal of the nymphs should be considered only for symptomatic patients with high parasite loads. No medical treatment is available.

Acknowledgments

We gratefully acknowledge the excellent laboratory assistance provided by Hilde Cox and Henk Vereecken.

Mr. Potters works at the national reference laboratory for parasitology at the Institute of Tropical Medicine, Antwerp, Belgium. His research interest is tropical parasitology. He regularly coordinates, organizes, and lectures at workshops on parasitology, including diagnostic techniques for parasitology.

References

1. Tappe D, Haeupler A, Schäfer H, Racz P, Cramer JP, Poppert S. *Armillifer armillatus* pentastomiasis in African immigrant, Germany. *Emerg Infect Dis.* 2013;19:507–8. <http://dx.doi.org/10.3201/eid1903.121508>
2. Tappe D, Büttner DW. Diagnosis of human visceral pentastomiasis. *PLoS Negl Trop Dis.* 2009;3:e320. <http://dx.doi.org/10.1371/journal.pntd.0000320>

3. Lavrov DV, Brown WM, Boore JL. Phylogenetic position of the Pentastomida and (pan)crustacean relationships. *Proc Biol Sci*. 2004;271:537–44. <http://dx.doi.org/10.1098/rspb.2003.2631>
4. Yao MH, Wu F, Tang LF. Human pentastomiasis in China: case report and literature review. *J Parasitol*. 2008;94:1295–8. <http://dx.doi.org/10.1645/GE-1597.1>
5. Latif B, Omar E, Heo CC, Othman N, Tappe D. Human pentastomiasis caused by *Armillifer moniliformis* in Malaysian Borneo. *Am J Trop Med Hyg*. 2011;85:878–81. <http://dx.doi.org/10.4269/ajtmh.2011.11-0404>
6. Tappe D, Meyer M, Oesterlein A, Jaye A, Frosch M, Schoen C, et al. Transmission of *Armillifer armillatus* ova at snake farm, The Gambia, West Africa. *Emerg Infect Dis*. 2011;17:251–4. <http://dx.doi.org/10.3201/eid1702.101118>
7. Meyers WM, Neafie RC, Connor DH. Pentastomiasis. In: Binford CH, Connor DH, editors. *Pathology of tropical and extraordinary diseases*. Washington (DC): Armed Forces Institute of Pathology; 1976. p. 546–50.
8. Dakubo JCB, Etwire VK. Human pentastomiasis in upper east region of Ghana: report of two cases. *Postgrad Med J Ghana*. 2014;3:56–60.
9. Mouchet R. Note sur *Porocephalus moniliformis*. *Bull Soc Path exot*. 1914;7:497–501.
10. Prathap K, Lau KS, Bolton JM. Pentastomiasis: a common finding at autopsy among Malaysian aborigines. *Am J Trop Med Hyg*. 1969;18:20–7. <http://dx.doi.org/10.4269/ajtmh.1969.18.20>

Address for correspondence: Idzi Potters, Department of Clinical Sciences, Institute of Tropical Medicine Antwerp, Kronenburgstraat 43/3, 2000 Antwerp, Belgium; email: ipotters@itg.be

Influenza A(H9N2) Virus, Burkina Faso

Bianca Zecchin,¹ Germaine Minoungou,¹ Alice Fusaro, Sidi Moctar, Anne Ouedraogo-Kaboré, Alessia Schivo, Annalisa Salviato, Sabrina Marciano, Isabella Monne

Author affiliations: Istituto Zooprofilattico Sperimentale delle Venezie, Legnaro, Padova, Italy (B. Zecchin, A. Fusaro, A. Schivo, A. Salviato, S. Marciano, I. Monne); Laboratoire National d'Élevage de Ouagadougou, Ouagadougou, Burkina Faso (G. Minoungou, S. Moctar, A. Ouedraogo-Kaboré)

DOI: <https://doi.org/10.3201/eid2312.171294>

We identified influenza A(H9N2) virus G1 lineage in poultry in Burkina Faso. Urgent actions are needed to raise awareness about the risk associated with spread of this zoonotic virus

¹These authors contributed equally to this article.

subtype in the area and to construct a strategy for effective prevention and control of influenza caused by this virus.

Since their detection in China in 1992, influenza A(H9N2) viruses have caused large economic losses to the poultry industry and have occasionally been transmitted to mammalian species, including humans. Three main genetic lineages were described among the Eurasian H9N2 subtype viruses: G1, Y280, and Y439 (Korean) lineage (1). In the past decade, the G1 lineage has spread mostly in gallinaceous birds across Asia, the Middle East, and eventually North Africa, where H9N2 outbreaks were reported in Libya (2006 and 2013) (2), Tunisia (2010–2012) (3), Egypt (2011–present), and Morocco (2016) (4).

The Veterinary Services of Ouagadougou, Burkina Faso, submitted 30 tracheal swab specimens and 10 organ samples collected in January 2017 in Burkina Faso to the World Organisation for Animal Health/Food and Agriculture Organization of the United Nations Reference Laboratory for Avian Influenza, Istituto Zooprofilattico Sperimentale delle Venezie (Legnaro, Padova, Italy). All samples were collected from a layer farm that was experiencing decreased egg production and respiratory signs among its flock; the animals were suspected to have infectious bronchitis virus (IBV).

Molecular analyses of the animal samples showed negative results for IBV and indicated that animals from the farm were infected with avian influenza A(H9N2) virus. The 8 gene segments were obtained for 1 representative virus by using a MiSeq Platform (Illumina, San Diego, CA, USA). Sequences were submitted to GenBank under accession numbers MF510849–56.

The maximum-likelihood phylogenetic tree of the hemagglutinin (HA) gene showed that the H9N2 subtype virus from Burkina Faso belonged to the G1 lineage, which has remarkable zoonotic potential. This virus clustered with H9N2 subtype viruses isolated in Morocco in 2016 (99.2% similarity) and with an H9N2 subtype virus identified in the United Arab Emirates in 2015 (A/chicken/Dubai/D2506.A/2015) (98.7% similarity) (online Technical Appendix Figure 1, <https://wwwnc.cdc.gov/EID/article/23/12/17-1294-Teachapp1.pdf>). Phylogenetic trees obtained for all other gene segments confirmed clustering with viruses from Morocco and the United Arab Emirates, similar to that observed for HA gene phylogeny.

Phylogeographic analysis (online Technical Appendix) identified multiple introductions of influenza A(H9N2) virus into North Africa from the Middle East and Pakistan. The H9N2 subtype virus identified in Burkina Faso seems to have originated from Morocco, although we cannot rule out the possibility that H9N2 subtype viruses were circulating in unsampled locations (online Technical Appendix Figure 2, Video, <https://wwwnc.cdc.gov/EID/article/23/12/17-1294-V1.htm>).

Analyses of the deep sequencing data showed that $\approx 50\%$ of the virus population in the tracheal swab specimen had leucine at position 226 (H3 numbering) of the HA receptor binding site (sequence coverage of 14,152 reads in the indicated position), which enables preferential binding to human-like $\alpha 2$ -6-linked sialic acid receptors (5). Furthermore, a potential additional glycosylation site (NLS), which had not previously been detected in the G1 lineage, was identified at positions 271–273 (H3 numbering). In the acidic polymerase protein, the H9N2 subtype virus from Burkina Faso had the mutation PA-S409N, which is considered a host specificity marker of human influenza virus (6). The same mutation was detected in related viruses from Morocco and Dubai.

Identification of H9N2 subtype virus in West Africa, where highly pathogenic H5 strains of the A/goose/Guangdong/1/1996 lineage (Gs/GD) have been widely circulating since the beginning of 2015, is a concern because of animal health implications, negative effects on local economies, and possible emergence of reassortant viruses with unknown biological properties. Reassortment events between H9N2 and highly pathogenic H5N1 subtype viruses were reported in China in 2005 and 2016 (7,8) and in Bangladesh in 2012 (9). In December 2013, an H5N1 subtype virus that had an H9N2 subtype polymerase basic 2 gene was reported in a patient in Canada who had returned from China (10). Moreover, H5N6 subtype reassortant viruses belonging to clade 2.3.4.4, which contain H9N2 subtype-like internal genes, were identified in China in 2015–2016 (8).

H5 strains belonging to clades 2.3.2.1c and 2.3.4.4 are currently circulating in West Africa. This finding, combined with detection of human-like receptor specificity and 2 mutations typical of human influenza viruses in the H9N2 subtype virus from Burkina Faso, might indicate emergence of a strain capable of infecting humans and warrants additional attention to the avian influenza situation in West Africa. Furthermore, identification of H9N2 subtype viruses in Morocco and Burkina Faso in chickens suggests that commercial poultry trade between North and West Africa might have played a key role in spread of the virus.

Involvement of wild birds in long-distance spread of H9N2 subtype G1 virus seems unlikely because this lineage is strongly adapted to poultry. These observations highlight the difficulty in tracing and containing circulating H9N2 subtype G1 virus and underline the need to review current approaches of disease reporting to understand spread and effects of this virus, which are probably underestimated. Thus, it is imperative to provide strategic guidance to countries in West Africa on technical and policy options for cost-effective surveillance and prevention and control of multiple cocirculating influenza virus strains.

Acknowledgments

We thank Silvia Ormelli and Francesca Ellero for providing excellent technical assistance and authors and originating and submitting laboratories for providing virus sequences from the GISAID EpiFlu Database (<https://platform.gisaid.org>; online Technical Appendix Table 2).

Dr. Zecchin is a biotechnologist at the Istituto Zooprofilattico Sperimentale delle Venezie, Padova, Italy. Her primary research interests include studying the molecular phylogeny and the evolutionary dynamics of viruses.

References

1. Peiris JS, Guan Y, Markwell D, Ghose P, Webster RG, Shortridge KF. Cocirculation of avian H9N2 and contemporary “human” H3N2 influenza A viruses in pigs in southeastern China: potential for genetic reassortment? *J Virol*. 2001;75:9679–86. <http://dx.doi.org/10.1128/JVI.75.20.9679-9686.2001>
2. Kammon A, Heidari A, Dayhum A, Eldaghayes I, Sharif M, Monne I, et al. Characterization of avian influenza and Newcastle disease viruses from poultry in Libya. *Avian Dis*. 2015;59:422–30. <http://dx.doi.org/10.1637/11068-032215-ResNote.1>
3. Tombari W, Ghram A. Production of a truncated recombinant HA1 for influenza A H9 subtype screening. *Biologicals*. 2016;44:546–55. <http://dx.doi.org/10.1016/j.biologicals.2016.07.006>
4. El Houadfi M, Fellahi S, Nassik S, Guérin JL, Ducatez MF. First outbreaks and phylogenetic analyses of avian influenza H9N2 viruses isolated from poultry flocks in Morocco. *Virol J*. 2016;13:140. <http://dx.doi.org/10.1186/s12985-016-0596-1>
5. Wan H, Perez DR. Amino acid 226 in the hemagglutinin of H9N2 influenza viruses determines cell tropism and replication in human airway epithelial cells. *J Virol*. 2007;81:5181–91. <http://dx.doi.org/10.1128/JVI.02827-06>
6. Chen GW, Chang SC, Mok CK, Lo YL, Kung YN, Huang JH, et al. Genomic signatures of human versus avian influenza A viruses. *Emerg Infect Dis*. 2006;12:1353–60. <http://dx.doi.org/10.3201/eid1209.060276>
7. Dong G, Xu C, Wang C, Wu B, Luo J, Zhang H, et al. Reassortant H9N2 influenza viruses containing H5N1-like PB1 genes isolated from black-billed magpies in southern China. *PLoS One*. 2011; 6:e25808. <http://dx.doi.org/10.1371/journal.pone.0025808>
8. Chen LJ, Lin XD, Tian JH, Liao Y, Ying XH, Shao JW, et al. Diversity, evolution and population dynamics of avian influenza viruses circulating in the live poultry markets in China. *Virology*. 2017;505:33–41. <http://dx.doi.org/10.1016/j.virol.2017.02.009>
9. Monne I, Yamage M, Dauphin G, Claes F, Ahmed G, Giasuddin M, et al. Reassortant avian influenza A(H5N1) viruses with H9N2-PB1 gene in poultry, Bangladesh. *Emerg Infect Dis*. 2013;19:1630–4. <http://dx.doi.org/10.3201/eid1910.130534>
10. Pabbaraju K, Tellier R, Wong S, Li Y, Bastien N, Tang JW, et al. Full-genome analysis of avian influenza A(H5N1) virus from a human, North America, 2013. *Emerg Infect Dis*. 2014;20:887–91. <http://dx.doi.org/10.3201/eid2005.140164>

Address for correspondence: Bianca Zecchin, Istituto Zooprofilattico Sperimentale delle Venezie, Division of Comparative Biomedical Sciences, Viale dell’Università 10, 35020 Legnaro, Padova, Italy; email: بزecchin@izsvenezie.it

Detection of Zika Virus in April 2013 Patient Samples, Rio de Janeiro, Brazil

Sonia R. Lambert Passos,
 Maria A. Borges dos Santos, José Cerbino-Neto,
 Sibelle N. Buonora, Thiago M.L. Souza,
 Raquel V.C. de Oliveira, Alexandre Vizzoni,
 Giselle Barbosa-Lima, Yasmine R. Vieira,
 Marcondes Silva de Lima, Yara H. M. Hökerberg

Author affiliations: Oswaldo Cruz Foundation, Rio de Janeiro, Brazil (S.R.L. Passos, T.M.L. Souza); Estácio de Sá University, Rio de Janeiro (S.R.L. Passos, Y.H.M. Hökerberg); Fundação Oswaldo Cruz Escola Nacional de Saúde Pública, Rio de Janeiro (M.A. Borges dos Santos); Evandro Chagas National Institute of Infectious Diseases, Rio de Janeiro (J. Cerbino-Neto, S.N. Buonora, R.V.C. de Oliveira, A. Vizzoni, G. Barbosa-Lima, Y.R. Vieira, M.S. de Lima, Y.H.M. Hökerberg); Universidade Federal do Rio de Janeiro, Rio de Janeiro (S.N. Buonora)

DOI: <https://doi.org/10.3201/eid2312.171375>

We tested 210 dengue virus–negative samples collected from febrile patients during a dengue virus type 4 outbreak in Rio de Janeiro in April 2013 and found 3 samples positive for Zika virus. Our findings support previously published entomological data suggesting Zika virus was introduced into Brazil during October 2012–May 2013.

In 2016, Brasil et al. (1), on the basis of a large number of suspected ($n = 364$) and laboratory-confirmed ($n = 119$) cases, reported the first Zika virus outbreak in Rio de Janeiro, with peak transmission in May 2015. Reports confirming Zika virus infection by reverse transcription PCR (RT-PCR) indicated the virus was present earlier in Rio Grande do Norte, Brazil, in October 2014 (2) and in Bahia, Brazil, in May 2015 (3). These cases were thought to be the first to occur in humans in Brazil and to correspond with the first occurrences of presumptive vectorborne transmission of Zika virus in the continental Americas.

By August 2015, Zika virus infection had been confirmed in 13 states of Brazil (Bahia, Rio Grande do Norte, São Paulo, Alagoas, Pará, Roraima, Rio de Janeiro, Maranhão, Pernambuco, Ceará, Paraíba, Paraná, and Piauí), some of which were located >2,500 miles apart (4). Because Zika virus circulation can occur simultaneously with dengue virus (DENV) in regions plagued by *Aedes aegypti* mosquitoes, we used frozen serum samples previously collected during a DENV type 4 (DENV-4) outbreak to investigate whether co-circulation might have been occurring before reported cases.

We evaluated 210 samples collected from patients (median age 36.6 years) with acute febrile syndrome who visited

an acute healthcare facility in Tijuca, a middle-class district in the northern zone of Rio de Janeiro, Brazil, during a DENV-4 outbreak occurring March–May 2013. All samples tested negative for DENV RNA by RT-PCR and DENV non-structural protein 1 by Platelia Dengue NS1 Ag ELISA (Bio-Rad Laboratories, Marnes-la-Coquette, France) (5).

In June 2017, we performed a molecular test to rapidly detect Zika virus in previously frozen acute-phase samples. We extracted viral RNA from 200- μ L samples by using the QIAamp Viral RNA Mini Kit (QIAGEN, Valencia, CA, USA) according to the manufacturer's instructions. We performed quantitative RT-PCR (qRT-PCR) with the QuantiNova Probe RT-PCR Kit (QIAGEN) in a Rotor-Gene Q Sequence Detection System (QIAGEN) using 25- μ L reaction mixtures containing 5 μ L of RNA template. We used primers, probes, and cycling conditions for Zika virus detection recommended by the Centers for Disease Control and Prevention (6). Samples suspected positive (defined as having a cycle threshold <38) were retested in triplicate, and consistently positive samples were confirmed by repeating RNA extraction and qRT-PCR in duplicate.

Of the 210 samples, 21 tested positive by qRT-PCR and were thus suspected positive for Zika virus; 4 of 21 tested positive for Zika virus RNA in triplicate qRT-PCR reactions.

Table. Distribution of clinical signs and symptoms among 3 patients retrospectively identified as having Zika virus infection, Rio de Janeiro, Brazil, 2013*

No. patients, sign or symptom	Patient A	Patient B	Patient C
3 patients			
Arthralgia†	Yes	Yes	Yes
Fever†, no. days	Yes, 1	Yes, 2	Yes, 1
Headache	Yes	Yes	Yes
Myalgia	Yes	Yes	Yes
Nausea	Yes	Yes	Yes
Prostration	Yes	Yes	Yes
Retroorbital pain	Yes	Yes	Yes
2 patients			
Adenomegaly	Yes	Yes	No
Chills	Yes	No	Yes
Dizziness	Yes	Yes	No
Low back pain	No	Yes	Yes
Taste alteration	Yes	Yes	No
Vomiting	Yes	No	Yes
1 patient			
Anorexia	No	No	Yes
Cold extremities	Yes	No	No
Cough	Yes	No	No
Dyspnea	No	Yes	No
Eye congestion	No	Yes	No
Eye redness perception†	No	Yes	No
Hemoconcentration	No	No	Yes
Hoarseness	No	Yes	No
Leukopenia	No	Yes	No
Oropharyngeal pain	Yes	No	No
Otalgia	No	Yes	No
Pruritus	No	Yes	No
Thready pulse	Yes	No	No

*No patients had exanthema.

†Signs and symptoms considered in Brazilian Ministry of Health's definition for suspected Zika virus infection

(<http://portalsaude.saude.gov.br/index.php/descricao-da-doenca-zika>).

However, 1 of the 4 also tested positive by Panbio Dengue IgM Capture ELISA (Standard Diagnostics Inc., Yongin, South Korea). We confirmed that the other 3 samples (2 from men and 1 from a woman) were positive for Zika virus genome after repetition of RNA extraction and qRT-PCR.

Zika virus–positive patients were young (18, 25, and 26 years of age), lived in Tijuca, had low-grade fever (1–2 days) during acute disease, and had no underlying conditions. Their travel histories were not available. All patients reported prostration, myalgia, arthralgia, headache, retro-orbital pain, and nausea (Table). None reported rash or hemorrhages. Hematocrit levels were 40%–45%, platelet counts $2.19\text{--}3.53 \times 10^5/\mu\text{L}$, and leukocyte counts $4.4\text{--}19.8 \times 10^3$ cells/ μL .

Zika virus dissemination beyond Asia and Africa occurred after the 2007 epidemic in Micronesia (6) and, in particular, after the 2013–2014 outbreak in French Polynesia, which involved a large number of symptomatic patients and patients with severe disease, with some having neurologic syndromes (7). Brasil et al. (1) stated that the phylogenetic analysis of cases in Rio de Janeiro supports the hypothesis that Zika virus was introduced into the city in August 2014, possibly during the International Va'a Federation World Sprint Championship canoe race, which included teams from 4 Zika virus–endemic countries of the Pacific region. Faria et al. (7) used viral genome analyses of the southeastern Asia and Pacific founder lineage to estimate that Zika virus was present in Brazil by February 2014; these authors also suggested that the northeast region of Brazil was the initial virus dissemination point. Massad et al. (8) used mathematical models and concluded that Zika virus was most likely introduced into Brazil by infected travelers arriving during October 2013–March 2014.

However, our findings suggest that Zika virus had already been circulating in Rio de Janeiro since April 2013, consistent with the report by Metsky et al. (9) stating that Zika virus had been circulating undetected in multiple regions for many months before the initial case reports. This view is also supported by entomological data from Ayllón et al. (10), who used a surveillance program involving field-trapped mosquitoes to perform genetic analyses of mosquito-borne viruses found in Rio de Janeiro during February 2014–June 2016. Their results suggest that Zika virus was probably already in circulation in Rio de Janeiro during May–November 2013, introduced multiple times from different in-country sources, and that the virus was introduced into the Americas via Brazil during October 2012–May 2013 (10).

This work was funded by Conselho Nacional de Desenvolvimento Científico e Tecnológico, Programa de Excelência em Pesquisa 402068/2012-2. S.R.L.P. was

supported by Conselho Nacional de Desenvolvimento Científico e Tecnológico grant 310765/2016-1 and Universidade Estácio de Sá Pesquisa Produtividade. Y.H.M.H. was supported by Universidade Estácio de Sá Pesquisa Produtividade and Fundação de Amparo à Pesquisa do Estado do Rio de Janeiro (E-26/110.188/2014). S.R.L.P., M.A.B.S., and J.C.N. are members of the Rede Nacional de Especialistas em Zika e Doenças Correlatas (the Brazilian National Zika Network).

Dr. Passos is a lead investigator at Evandro Chagas National Institute of Infectious Diseases in Rio de Janeiro, Brazil. Her research interests are clinical epidemiology of emerging infectious vectorborne diseases.

References

1. Brasil P, Calvet GA, Siqueira AM, Wakimoto M, de Sequeira PC, Nobre A, et al. Zika virus outbreak in Rio de Janeiro, Brazil: clinical characterization, epidemiological and virological aspects. *PLoS Negl Trop Dis*. 2016;10:e0004636. <http://dx.doi.org/10.1371/journal.pntd.0004636>
2. Zanluca C, Melo VC, Mosimann ALP, Santos GI, Santos CN, Luz K. First report of autochthonous transmission of Zika virus in Brazil. *Mem Inst Oswaldo Cruz*. 2015;110:569–72. <http://dx.doi.org/10.1590/0074-02760150192>
3. Campos GS, Bandeira AC, Sardi SI. Zika virus outbreak, Bahia, Brazil. *Emerg Infect Dis*. 2015;21:1885–6. <http://dx.doi.org/10.3201/eid2110.150847>
4. Freitas ARR, Angerami RN, von Zuben APB, Donalísio MR. Introduction and transmission of Zika virus in Brazil: new challenges for the Americas. *Rev Inst Med Trop Sao Paulo*. 2016;58:24. <http://dx.doi.org/10.1590/S1678-9946201658024>
5. Buonora SN, Passos SRL, do Carmo CN, Quintela FM, de Oliveira DN, dos Santos FB, et al. Accuracy of clinical criteria and an immunochromatographic strip test for dengue diagnosis in a DENV-4 epidemic. *BMC Infect Dis*. 2016;16:37. <http://dx.doi.org/10.1186/s12879-016-1368-7>
6. Lanciotti RS, Kosoy OL, Laven JJ, Velez JO, Lambert AJ, Johnson AJ, et al. Genetic and serologic properties of Zika virus associated with an epidemic, Yap State, Micronesia, 2007. *Emerg Infect Dis*. 2008;14:1232–9. <http://dx.doi.org/10.3201/eid1408.080287>
7. Faria NR, Quick J, Claro IM, Thézé J, de Jesus JG, Giovanetti M, et al. Establishment and cryptic transmission of Zika virus in Brazil and the Americas. *Nature*. 2017;546:406–10. <http://dx.doi.org/10.1038/nature22401>
8. Massad E, Burattini MN, Khan K, Struchiner CJ, Coutinho FAB, Wilder-Smith A. On the origin and timing of Zika virus introduction in Brazil. *Epidemiol Infect*. 2017;145:2303–12. <http://dx.doi.org/10.1017/S0950268817001200>
9. Metsky HC, Matranga CB, Wohl S, Schaffner SF, Freije CA, Winnicki SM, et al. Zika virus evolution and spread in the Americas. *Nature*. 2017;546:411–5. <http://dx.doi.org/10.1038/nature22402>
10. Ayllón T, Campos RM, Brasil P, Morone FC, Câmara DCP, Meira GLS, et al. Early evidence for Zika virus circulation among *Aedes aegypti* mosquitoes, Rio de Janeiro, Brazil. *Emerg Infect Dis*. 2017;23:1411–2. <http://dx.doi.org/10.3201/eid2308.162007>

Address for correspondence: Sonia R. Lambert Passos, Evandro Chagas National Institute of Infectious Diseases, Clinical Epidemiology Laboratory, Av Brasil 4036 sala 201 A, Manguinhos, Rio de Janeiro, RJ, CEP 210 40-361, Brazil; email: sonia.lambert@ini.fiocruz.br

Wildlife as Source of Human *Escherichia coli* O157 Infection

Brian Crook, Helena Senior

Author affiliation: Health and Safety Laboratory, Health and Safety Executive, Buxton, United Kingdom

DOI: <https://doi.org/10.3201/eid2312.171210>

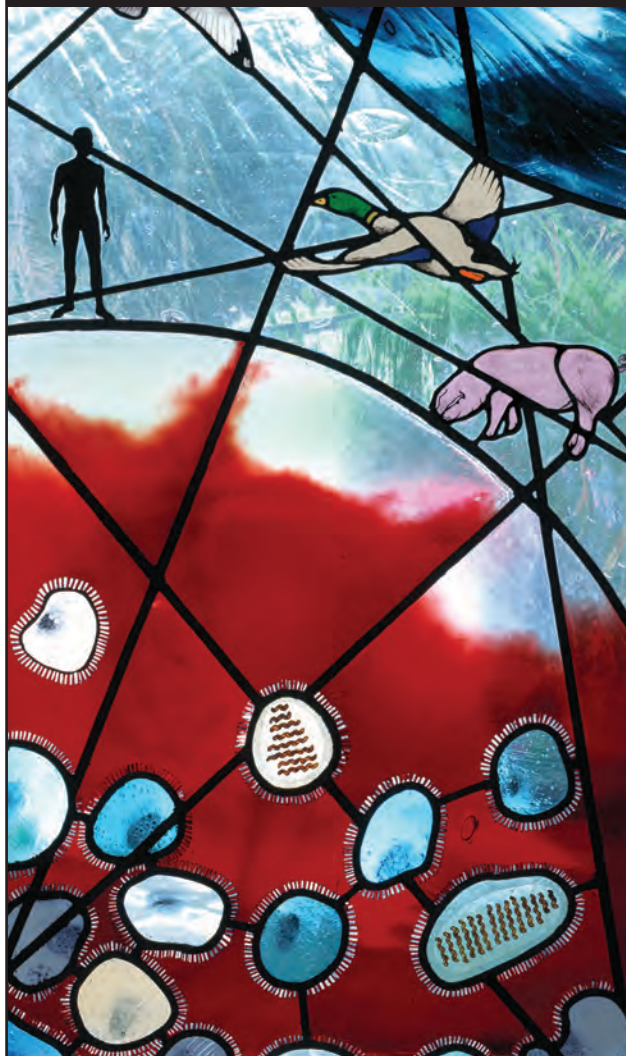
To the Editor: The article by Probert et al. (1) highlighted that wild animals (in this case, deer) can act as a reservoir of Shiga toxin–producing *Escherichia coli* (STEC) O157 infection. Our previous research (2) broadens this to include wild animals as STEC O157 carriers. In our study, an outbreak of STEC O157 infection in eastern England was epidemiologically linked to visiting a wildlife park. Unlike in petting zoos, the visitors had no direct contact with the animals. Transmission of infection was attributed to contact with the feces of wild rabbits (*Oryctolagus cuniculus*) in a play area; the rabbits had been in contact with STEC O157–positive cattle in an adjacent field (3). To prove this hypothesis, we identified rabbit populations living on farms with STEC O157–positive cattle. We trapped the rabbits humanely in cages, collected their feces during their confinement before release, and tested the feces for STEC O157 by culture and PCR. Of 97 samples collected in the summer, 8 (8.2%) were positive by culture; these samples came from 4 of 6 farms in the study. By PCR analysis, 20 of 97 (20.6%) samples were positive. None was positive during the winter, when cattle were housed indoors, suggesting a link between STEC O157 positivity in cattle and rabbits. In conclusion, when outbreaks of this serious human infection are linked to the rural environment, it is necessary to take wildlife into consideration, both as a reservoir of transmission and as carriers. Equally, persons should not underestimate the necessity of good hand hygiene if they have contact with wild animal feces.

References

1. Probert WS, Miller GM, Ledin KE. Contaminated stream water as source for *Escherichia coli* O157 illness in children. *Emerg Infect Dis*. 2017;23:1216–8. <http://dx.doi.org/10.3201/eid2307.170226>
2. Scaife HR, Cowan D, Finney J, Kinghorn-Perry SF, Crook B. Wild rabbits (*Oryctolagus cuniculus*) as potential carriers of verocytotoxin-producing *Escherichia coli*. *Vet Rec*. 2006;159:175–8. <http://dx.doi.org/10.1136/vr.159.6.175>
3. Bailey JR, Warner L, Pritchard GC, Williamson S, Carson T, Willshaw G, et al. Wild rabbits—a novel vector for Vero cytotoxigenic *Escherichia coli* (VTEC) O157. *Commun Dis Public Health*. 2002;5:74–5.

Address for correspondence: Brian Crook, Health and Safety Laboratory—Microbiology Team, Harpur Hill, Buxton SK17 9JN, UK; email: brian.crook@hsl.gsi.gov.uk

EID Podcast: Stained Glass and Flu



The work of art shown here depicts the interrelationship of human, animal, and environmental health.

Stained-glass windows have been appreciated for their utility and splendor for more than 1,000 years, and this engaging work of art by stained glass artist Jenny Hammond reminds us that influenza A viruses—which can be easily spread between animals and human, use various host species, and exist in many different environments—remain an enduring and global health concern.

Visit our website to listen:

**EMERGING
INFECTIOUS DISEASES**

<https://www2c.cdc.gov/podcasts/player.asp?f=8644950>

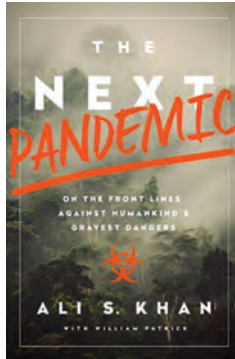
The Next Pandemic: On the Front Lines Against Humankind's Gravest Dangers

Ali S. Khan with William Patrick; PublicAffairs,
New York, NY, USA; ISBN-10: 1610395913; ISBN-13:
978-1610395915; Pages: 288; Price: \$26.99

Stalin notoriously remarked that one death was a tragedy, while a million were a statistic. An impressive feature of this book is that, while recounting a great many deaths, it maintains a human and humane perspective. Dr. Ali S. Khan is a former director of the Office of Public Health Preparedness and Response at the Centers for Disease Control and Prevention and has been close to the epicenter of almost all the potential pandemic threats of the last few decades. With William Patrick, an accomplished writer and editor in his own right, Khan has produced an accessible, fascinating book for the general reader that shares his experiences in the service of his country and the world.

The book describes so many outbreaks that its approach is inevitably a little scattershot, but 2 subjects stand out: the investigation of the anthrax mailings to Congress is covered as well as I have seen anywhere, and the sections dealing with the nightmare of Ebola in West Africa should be required reading for anyone looking to improve our response to infectious disease emergencies. As the authors note, maintaining high standards of data hygiene is difficult anywhere, but particularly so if we lack the will to prioritize public health even when resources are scarce.

Throughout, there is a subtle but steady bass line of anguish over the difficulty of translating the science we know into effective action. Khan argues that to keep our priorities straight we need to recognize how the



unscrupulous, from black marketeers to politicians, exploit outbreaks as opportunities for advancement; addressing that issue is an essential part of fighting the disease. In the words of Albert Camus, “It is up to us not to join forces with the pestilences.” We might not, but how can we stop others from doing so? Khan suggests the creation of a United Nations Undersecretary for Health Security, which sounds sensible, but it is not clear what policies that person might enact, and even less so how they would be enforced.

It is the personal stories here that are the most affecting, in the understanding that Khan extends to an Ebola-infected nurse who denies that she knows how she acquired the disease, or the prejudice faced by Khan himself as a Muslim American in the years following 9/11. These diseases infect humans, kill humans, and are battled by humans, with all the complicated consequences that entails.

There are a few missteps. The persistent nagging use of clichés like “disease detectives” can sound patronizing. An assertion that viruses are “collectively intelligent” will surely raise eyebrows, and the title is a little misleading, in that there is less focus than expected on genuine catastrophic pandemic threats. However, as another confessed “infectious disease nerd” I found it fascinating. It will be enjoyed by working epidemiologists; it should be a point of reference for policymakers; and I suspect it will inspire many future officers in the Epidemic Intelligence Service.

William P. Hanage

Author affiliation: Harvard T.H. Chan School of Public Health, Boston, Massachusetts, USA

DOI: <http://dx.doi.org/10.3201/eid2312.171137>

Address for correspondence: W.P. Hanage, Center for Communicable Disease Dynamics, Department of Epidemiology, Harvard T.H. Chan School of Public Health, 677 Huntington Ave, Boston, MA 02115, USA; email: whanage@hsph.harvard.edu.



Bindu Viswanathan, (b. 1971), *A Timeless Symbiosis*, 2017 (detail). Acrylic on canvas, with small mirror embellishments, 22 in × 28 in/56 cm × 71 cm. Digital image courtesy of the artist.

Everything within a Circle Is One Thing

Byron Breedlove

“Everything within a circle is one thing, which is encircled, enframed,” wrote 20th-century American mythologist and lecturer Joseph Campbell. This month’s cover art, *A Timeless Symbiosis*, uses the motif of circles to connect animals and humans. Bindu Viswanathan, the artist who created the painting, is also a lecturer and biostatistician at the University of Texas, Austin. Many of her

paintings inspire viewers to think about the fuller connection between animals and humans. According to Viswanathan, “Circles have no beginning and no end, much like the interdependence of humans and animals. They also represent the womb, the origin of life, and its continuum.” (All quotes from B. Viswanathan, pers. comm. Nov 3, 2017.)

Viswanathan incorporates elements from the Indian tribal art of the Warli, an indigenous people who live in the hills of western India, into *A Timeless Symbiosis*. For instance, Warli art, which has been practiced since at least

Author affiliation: Centers for Disease Control and Prevention, Atlanta, Georgia, USA

DOI: <https://doi.org/10.3201/eid2312.AC2312>

the 10th century ACE, often depicts the intertwined links of humans with both domestic and wild animals.

Viswanathan's meticulous interplay of geometric forms, vibrant colors, calculated symmetry, and traditional symbols is arrayed within concentric circles and draws the viewer deeper and deeper into the painting. The outer circular border comprises 122 Warli-style figures, linked hand in hand, keeping vigil. Within the next circle, against a dark blue background, ornamentally decorated pairs of pigs, cows, chickens, and rats—all animals associated with domestication—are interspersed among figures of humans, posed as though engaged in traditional agrarian tasks. The disproportionate size of the animals underscores their importance to and impact on the people.

More human figures are juxtaposed with bats and birds, wild animals many humans are likely to encounter and major sources of diverse zoonotic viruses throughout the world. The radiating central image contains what is perhaps best described as a viewer's choice, possibly a sun or essential life force, or maybe a virus or other microscopic organism.

Throughout each of the circles, the artist incorporates various geometric forms—stair-stepped pyramids, triangles, and circles—and then reuses those forms to create ornate, complex designs. Viswanathan notes that “I gravitate toward geometric designs and symmetry in my abstract art, which stems from the same source that is inspired by mathematics. As a biostatistician, I model complex relationships that exist in the natural world.”

Once a viewer is drawn to the center of the painting, the tendency is to move back through the circles to the edges of the fiery orange border and then reexamine the careful symmetry, much like the process of viewing a mandala. The artist portrays her theme of symbiosis on multiple levels and illustrates the complex relationships and connections between humans and animals.

Rudolph Virchow, one of the 19th century's principal leaders in medicine and pathology, stated that “Between

animal and human medicine, there is no dividing line—nor should there be.” Virchow stressed that diseases of humans and animals are interconnected and devised the term “zoonosis” to describe the links between infectious diseases in animal and human health. The ring of people forming the outer edge of *A Timeless Symbiosis* can serve to symbolize the modern One Health concept, an initiative that requires close collaboration among researchers in the animal, human, and environmental health sectors to protect and preserve life.

Bibliography

1. Belay ED, Kile JC, Hall AJ, Barton-Behravesh C, Parsons MB, Salyer S, et al. Zoonotic disease programs for enhancing global health security. *Emerg Infect Dis.* 2017;23(Suppl):S65–S70. <http://dx.doi.org/10.3201/eid2313.170544>
2. Campbell J, Moyers B. *The power of myth.* New York: Random House; 2011. p. 269.
3. Centers for Disease Control and Prevention. One Health. Zoonotic diseases [cited 2017 Nov 5] <https://www.cdc.gov/onehealth/basics/zoonotic-diseases.html>
4. Cooper JC. *An illustrated encyclopaedia of traditional symbols.* London: Thames and Hudson; 1978. p. 36–7; 103.
5. Garriock I. Telling stories and drawing life—Indian Warli community projects at the V&A Museum of Childhood. Victoria and Albert Museum [cited 2017 Nov 5]. <http://www.vam.ac.uk/blog/museum-of-childhood/warli-at-moc>
6. Klauder JV. Interrelations of human and veterinary medicine; discussion of some aspects of comparative dermatology. *N Engl J Med.* 1958;258:170–7. <http://dx.doi.org/10.1056/NEJM195801232580405>
7. Schultz MG. Photo quiz. Rudolf Virchow. *Emerg Infect Dis.* 2008;14:1480–1. <http://dx.doi.org/10.3201/eid1409.086672>
8. Sundberg JP, Schofield PN. One medicine, one pathology, and the One Health concept. *J Am Vet Med Assoc.* 2009;234:1530–1. <http://dx.doi.org/10.2460/javma.234.12.1530>
9. Warrior N. The tales of the folk from the west—Warli painting. Open art [cited 2017 Nov 5]. <https://www.openart.in/2016/09/tales-folk-west-warli-painting/>

Address for correspondence: Byron Breedlove, EID Journal, Centers for Disease Control and Prevention, 1600 Clifton Rd NE, Mailstop C19, Atlanta, GA 30329-4027, USA; email: wbb1@cdc.gov

REVIEWER APPRECIATION

EMERGING INFECTIOUS DISEASES™

A Peer-Reviewed Journal Tracking and Analyzing Disease Trends

Emerging Infectious Diseases thanks the following reviewers for their support through thoughtful, thorough, and timely reviews in 2017.

Please contact us if your name is missing from this list.

Emma Aarons	Carmen Ardanuy	Quique Bassat	Martin Blaser
Preben Aavitsland	Matthew Arduino	Nathalie Bastien	Lucas Blanton
Mustafa Ababneh	Paul Arguin	Antonio Battisti	Bradley Blitvich
Raquel Abad	Mary Ari	Lauren Bayliss	Evan Bloch
Celia Abolnik	Gregory Armstrong	Bernard Beall	David Blok
Jônatas Abrahão	Nichole Arrigo	Ben Beard	Sandra Blome
Joseph Abrams	Bailey Arruda	Cecile Bebear	Sharon Bloom
Masatoki Adachi	Ray Arthur	Christiane Bebear	Emily Blumberg
Laura Adams	Jean-Pierre Arzouni	Paul Becher	Patrick Boerlin
Toïdi Adékambi	Marise Asensi	Torben Becker	Andrea Boggild
Bishwa Adhikari	David Asher	Emily Beeler	John Bohnsack
Jennifer Adjemian	Kingsley Asiedu	Martin Beer	Abdoulie Bojang
Cornelia Adlhoch	M. A. Pérez-Jacoiste Asín	Richard Beigi	Remy Bonnin
Mavis Agbandje-McKenna	Edwin Asturias	Jessica Belser	James Bono
Rakesh Aggarwal	Barry Atkinson	David Bemis	Robert Bonomo
Patricia Aguilar	Houssam Attoui	Jeff Bender	Jeff Borchert
Vincent Akonkhai	Maite Aubry	Kaitlin Benedict	Matthias Borchert
Murat Akova	Sarah Auburn	John Bennett	Iara Borges
Manar Al-Lawama	Tatjana Avsic	Sarah Bennett	Andrew Borman
Cesar Albariño	Tracy Ayers	David Bennitz	Ray Borrow
Heather Alexander	Constância Ayres	Beatrice Bercot	Graham Bothamley
Margarete Alfonso	Andrew Azman	Nicholas Bergren	Teun Bouseman
Matthew Aliota	Tadash Baba	Ruth Berkelman	Michel Boussinesq
David Allen	Shawn Babiuk	James Berkley	Donald Bouyer
Robert Allison	Eran Bacharach	Kristen Bernard	Anna Bowen
Alzira Almeida	Laura Bachmann	Eric Bertherat	Michael Bowen
Daniel Altmann	Rodrigo Bacigalupe	Kateri Bertran	Richard Bowen
Francisco Alvarado-Ramy	John Baddley	Marianne Besnard	Richard Bradbury
Gerardo Alvarez	Edgar Badell	John Besser	Christopher Braden
Maria Alves	Karoun Bagamian	Amrita Bharat	John Branda
Katia Ambert-Balay	Brian Baker	Julu Bhatnagar	Paulo Brandão
Donne Ameme	Tamás Bakonyi	Tarun Bhatnagar	Mary Brandt
Lisa H. Amir	Amanda Balish	Philippe Biagini	Jonas Brant
Brian Amman	Kaushik Banerjee	Dominique Bicout	Aaron Brault
Benjamin Anderson	Gad Baneth	Martina Bielaszewska	Byron Breedlove
John Anderson	Ashley Banyard	Brad Biggerstaff	Andrea Brenciani
M. Anderson	Lisa Barco	Matthew Biggerstaff	Eric Brenner
Tim Anderson	Bridget Barker	Bridgette Jeanne Billioux	Benjamin Bristow
Theodore Andreadis	Christopher Barker	Brian Bird	William Brogdon
Antonia Andreu	Lawrence Barker	David Bishai	John Brooks
Nick Andrews	Celine Barnadas	Carolyn Black	Philippe Brouqui
Soa Fy Andriamandimby	John Barnes	William Black IV	Catherine Brown
Emmanouil Angelakis	Joel Barratt	Carina Blackmore	Corrie Brown
Nicholas Anstey	Alan Barrett	Stuart Blacksell	Kevin Brown
Gloria Anyalechi	Peter Barry	Carol Blair	Beau Bruce
Satoru Arai	Lytic Bartholomay	David Blair	Udo Buchholz
Maris Arcilla	Sridhar Basavaraju	David Blaney	Carmen Buchrieser

Philippe Buchy	Hee Kyoung Chun	Anindya De	Gregory Ebel
Alicia Budd	Rumi Chunara	Miranda de Graaf	Mark Eberhard
Christine Budke	Michael Ciancanelli	Cornelis de Haan	Hideki Ebihara
Silja Buehler	Holly Ciesielczuk	Henriette De Valk	Marcela Echavarria
Howard Burkom	Paul Cieslak	Emilio DeBess	Tim Eckmanns
Cara Burns	Alexander Ciota	Kevin DeCock	Paul Edelstein
Michael Busch	Cliff Clark	Victor del Rio Vilas	Srilatha Edupuganti
Karen Bush	Kerry Clark	Eric Delaporte	Kristine Edwards
Thomas Butler	Jean-Michel Claverie	Eric Delwart	Paul Effler
Leonard Calabrese	Jan Clement	Walter Demczuk	Androulla Efstratiou
Charles Calisher	Axel Cloeckaert	Henk den Bakker	Rebecca Eisen
Steven Callister	Frank Cobelens	Jeroen Den Boer	Tobias Eisenberg
Vitaliano Cama	Lark Coffey	Dan Denoon	Khalid El Karkouri
Nicholas Carbonetti	Susan Coffin	Shalini Desai	Elamin Elbasha
Gail Carson	Nicole Cohen	Philippe Desprès	Natalia Elguezabal
Edgar M. Carvalho	Robert Cohen	Ulrich Desselberger	Barbara Ellis
Kylie Carville	Ted Cohen	Gregor Devine	Evelyn Ellis-Grosse
Irene Casas	Matthew Coldiron	Brecht Devleesschauwer	Matthew Ellison
Cristina Cassetti	Michelle Cole	Anja Dewegheleire	Marc Eloit
Paolo Castiglia	Gail Sondermeyer Cooksey	Maureen Diaz	David Engelthaler
Luis Castilla-Guerra	Laura Cooley	Elizabeth Didier	J. A. Englund
Kenneth Castro	Jamaica Corker	Sabine Diedrich	Edward Epp
Antonino Catanzaro	Victor Corman	Daniel Diekema	Jonathan Epstein
Shana Cato	David Cornblath	Seydina Diene	Dean Erdman
Giovanni Cattoli	Sofia Cortes	Jo-Anne Dillon	Julia Ershova
Mike Catton	Galileu Costa	Gaston Djomand	Miguel Escobedo
Simon Cauchemez	Deborah Couldwell	Gerhard Dobler	Eric Esswein
Peter Cegielski	Robert Cowie	André Doi	Mary Estes
Catherine Cetre-Sossah	Ben Cowling	Yohei Doi	Agustin Estrada-Peña
Victoria Chalker	Paul Cox	Samuel Dominguez	Steen Ethelberg
Jocelyn Chan	Lisa Cranmer	Lu Dong	Jean-Louis Excler
Martin C.W. Chan	Matthew Crist	Paul Douglas	Christopher Fairley
Louisa Chapman	Curtis Croker	Richard Douglass	Joseph Falkinham
Rémi Charrel	Deborah Cromer	Scott Dowell	Luiza Falleiros Arlant
Luis Chaves	James Crooks	Michel Drancourt	Dennis Falzon
Nora Chea	Ian Crozier	Michael Drebot	Seamus Fanning
Liang Chen	Bart Currie	Jan Felix Drexler	Nicholas Feasey
Mark Chen	Sally Cutler	Dragana Drinkovic	Heinz Feldmann
Shaohong Chen	Juliana Da Silva	Amanda Driscoll	Leora Feldstein
Tai-Ho Chen	Cristina Da Silva Carias	Jan Drobeniuc	Peter Feng
James Cherry	Kevin Dalton	Christian Drosten	David Fidock
Harrell Chesson	Ádám Dán	Patrick Drury	Amy Parker Fiebelkorn
Francisco Chiaravalloti-Neto	David Dance	Simon Drysdale	Richard Fielding
Tom Chiller	Rachel Daniels	Zhaojun Duan	Thea Fischer
Chien-Shun Chiou	Richard Danila	Timothee Dub	Robert Fitzhenry
Charles Chiu	M. Carolina	Mariette Ducatez	Julia Fitzner
Mary Choi	Danovaro-Holliday	Nisha Duggal	Jason Folster
B.B. Chomel	Jessica Darenberg	Roger Dumke	Emanuela Foni
Terence Chorba	Virginia Dato	John Stephen Dumler	Anthony Fooks
Michael Chou	Victoria Davey	Angela Dunn	Pierre Formenty
Anuradha Chowdhary	Charles Davis	Myrielle Dupont-Rouzeyrol	Naomi Forrester
Henrik Christensen	Larry Davis	Edison Durigon	Michael Forstner
Rebecca Christofferson	Meghan Davis	Mark Dworkin	J. Fortenberry
Kaw Bing Chua	Michaela Day	Clare Dykewicz	Ron Fouchier

 REVIEWER APPRECIATION

Pierre-Edouard Fournier	Daniel Glikman	Eric Halsey	Peter Horby
Brian Foy	Cyrille Goarant	Scott Halstead	Taisuke Horimoto
Rennos Fragkoudis	Federico Gobbi	David Halvorson	Jennifer Horney
Monique Franca	Sylvain Godreuil	Xiang Han	Mady Hornig
Jose Franco	Richard Goering	William Hanage	M. Hossain
Carlos Franco-Paredes	David Goldsman	W. Hancock	Jennifer House
Richard Franka	Andrew Golnar	Jun Hang	J.W. Hovius
David Freedman	Yann Gomard	Nancy Hanson	Scott Huang
Eleanor Friedman	Isabel Gómez Villafañe	Stephan Harbarth	Xi Huang
Rachel Friedman	Camila Gonzales	Timm Harder	Martin Hugh-Jones
Alexander Friedrich	Aubree Gordon	Diane Harper	James Hughes
Lisa Frigati	Stephen Gordon	Aaron Harris	David S.C. Hui
Kai Frölich	Michael Gosciminski	Rainer Hartl	Georgina Humphreys
King-Wa Fu	Céline Gossner	Rodrigo Hasbun	Kevin Hung
Hans-Peter Fuehrer	Neela Goswami	Henrik Hasman	Elizabeth Hunsperger
Tsuguto Fujimoto	Magnus Gottfredsson	Douglas Hatch	James Hurley
Paula Fujiwara	Marcelo Gottschalk	Bill Hausdorff	A.C. Hurt
Isaac Chun-Hai Fung	Kevin Gough	Ben Hause	Muhammad Jami Husain
Jennifer Furin	Ernest Gould	Skerdi Haviari	Jimee Hwang
Simona Gabrielli	Frédérique Gouriet	Hal Hawkins	Alexandros Ikonomidis
Kenneth Gage	Nelesh Govender	William Hawley	Giuseppe Ippolito
Ohad Gal-Mor	Yonatan Grad	Frederick Hayden	James Irvine
Maria Teresa	Kathie Grant	John Hayman	Beth Isaac
Galán-Puchades	Nicholas Grassly	Mark Head	Michael Ison
John Galgiani	Stephen Graves	Claire Jane Heath	Tadashi Itagaki
Naomh Gallagher	Gregory Gray	Sonia Hegde	Megumi Itoh
Gale Galland	Michael Green	Albert Heim	Danielle Iuliano
Nadia Gallardo-Romero	Sharon Greene	Tom Hennessy	Louise Ivers
Mark Gallivan	Gilbert Greub	Ronnie Henry	Hidemasa Izumiya
Manoj Gambhir	Marie Griffin	Juan Hernandez Garcia	Brendan Jackson
Neel Gandhi	Ardath Grills	Barbara Herwaldt	Thomas Jaenisch
Hongjiang Gao	Jacques Grosset	Angela Hewlett	Seema Jain
Erika Garcia	Nathan Grubaugh	Roger Hewson	Varsha Jain
Ravindra Kumar Garg	Roland Grunow	Carole Hickman	Yunho Jang
Shikha Garg	Jeannette Guarner	Kaci Hickox	Julie Jarand
Philippe Gautret	Jonathan Gubbay	Susan Hills	Josef Järhult
Joel Gaydos	Duane Gubler	Joe Hinnebusch	Sophie Jarraud
Wondwossen Gebreyes	Humberto Guerra	Jun Hirai	Aurelie Jayol
Jay Gee	Alice Guh	Michele Hlavsa	Claire Jenkins
Irina Gelmanova	Jeanine Guidry	Charlotte Hobbs	Wei Jia
Rick Gelting	Sophie Guillot	Eric Hoberg	Shibo Jiang
Kathleen Gensheimer	Jesús Guinea	Robert Hoekstra	Reimar Johne
Christine George	Nicole Guiso	Karin Hoelzer	Nick Johnson
Patrick Gérardin	Christopher Gulvik	Mike Holbrook	Jeremy Jones
Sue Gerber	Marta Gwinn	David Holland	Lisa Jones-Engel
Dale Gerding	Andrew Haddow	Steven Holland	Heesoo Joo
Nancy Gerloff	Christos Hadjichristodoulou	F. Hollinger	Emily Kahn
Peter Gerner-Smidt	Stephen Hadler	Scott Holmberg	Adriana Kajon
Martin Gilbert	Marisa Haenni	Lori Holtz	Nassim Kamar
Suzanne Gilboa	Stefan Hagmann	Deborah Holtzman	Mary Kamb
John Gimnig	Stephen Hajduk	Stacy Holzbauer	Saleem Kamili
Christophe Ginevra	Aron Hall	Michael Hombach	Mark Kane
Guillaume Girault	Victoria Hall	Margaret Honein	Jon Kaplan
John Glasser	Otto Haller	Philip Hopewell	Amit Kapoor

Shanthi Kappagoda	K. Kostev	Juliana Leite	Jean-Yves Madec
Subhash Kapre	Camille Kotton	Nadine Lemaitre	Fabrizio Maggi
Adolf Karchmer	Andrew Kotze	Eyal Leshem	Shelley Magill
Erik Karlsson	Natalia Kozak-Muiznieks	Fernanda Lessa	Christopher Maher
Stephanie Karst	Colleen Kraft	Simon Lévesque	Taronna Maines
Vladimir Kartashev	Laura Kramer	Min Levine	Richard Malik
Midori Kato-Maeda	Peter Krause	Adrian Lewis	Vincent Mallet
Alan Katz	Scott Krauss	Yu Li	Tauqeer Mallhi
Louis Katz	Barry Kreiswirth	Yuan Li	Denis Malvy
Rebecca Katz	S. Krishna	Hai Liang	Lisa Manhart
Carol A. Kauffman	Chayakrit Krittanawong	Qiuyan Liao	Annette Mankertz
Daniel R. Kaul	Pavla Krizova	Direk Limmathurotsakul	Jean Manson
Ghazi Kayali	Erna Kroon	Jessica Lin	Nina Marano
Lara Keid	Detlev Kruger	Michael Lin	Tony Marfin
Paul Kellam	Thomas Ksiazek	Sally Lin	Atanaska Marinova-Petkova
Patrick Kelly	Roman Kuchta	Yusen Lin	Wanda Markotter
Joan Kenney	Matthew Kuehnert	Kimberly Lindblade	Suzanne Marks
Chris Kenyon	Jens Kuhn	William Lindsley	Natasha Markuson
Gil Kersh	Edward Kuijper	Susan Lipsett	Mariel Marlow
Siraj Khan	Thijs Kuiken	Margaret Littlejohn	Adriana Marques
Yury Khudyakov	Shu-Chen Kuo	Anastasia Litvintseva	Christina Marra
Nicolas Kieffer	Ekaterina Kurbatova	Jian-Hua Liu	Theodore Marras
James Kile	Ivan Kuzmin	Jinhua Liu	Jeanne Marrazzo
Andy Kilianski	Bernard La Scola	Spencer Lloyd	Tom Marrie
Gerry Killeen	Tinja Lääveri	Shawn Lockhart	Sonya Marshall-Gradisnik
A. Kilpatrick	Desiree LaBeaud	Ann Loeffler	Denise Marston
Dong-Min Kim	Marcelo Labruna	Vincent Lombardi	Douglas Marthaler
Mina Kim	Tamar Lachish	Guy Loneragan	Irene Martin
Linda Kimsey	Dominique Laffly	Shih Keng Loong	Jose Martin-Moreno
Luke Kingry	Tsan Yuk Lam	Adriana Lopez	Rosecelis Martinez
André Kipnis	Cristiane Lamas	Anna Lena Lopez	Andrea Marzi
Karin Kirchgatter	Amy Lambert	Rogelio Lopez-Velez	Brian Maskery
Robert Kirkcaldy	Patrick Lammie	Job Lopez	Joel Maslow
Hannah Kirking	Robert Lanciotti	Benjamin Lopman	Orietta Massidda
Peter Kirkland	Gabrielle Landolt	Jacob Lorenzo-Morales	Henry Masur
Uriel Kitron	Robert Lane	Alessio Lorusso	Amy Mathers
Anne Kjemtrup	Tatiana Lanzieri	Nicola Low	Joseph Matovu
Jeffrey Klausner	Simon Grandjean Lapierre	Matt Lozier	Yasufumi Matsumura
Terry Klein	Cornelia Lass-Floerl	Charles Lubelczyk	Rapeephan Maude
Jonas Klingstrom	Maria Latrofa	Jay Lucidarme	Max Maurin
Darryn Knobel	Eric Lau	Patrick Luedtke	Leonard Mayer
Marjolein Knoester	Susanna K.P. Lau	Yaniv Lustig	Jerry Mazurek
Mirjam Knol	Irwin Law	Joseph Lutgring	William McBride
Barbara Knust	Wayne Lawrence	Ulzii-Orshikh	Todd McCarty
Miwako Kobayashi	Helen Lazear	Luvsansharav	Andrea McCollum
Nobumichi Kobayashi	Kirsty Le Doare	Samantha Lycett	John McCormick
Katia Koelle	Karin Leder	Jennifer Lyons	Malcolm McCrae
Katrin Kohl	John Lednický	Louis Macareo	L. Clifford McDonald
Thomas Kohl	James LeDuc	Kimberly Mace	Chris McGowin
Nobuo Koizumi	Chang-Won Lee	Derek MacFadden	Catherine McLean
Florence Komurian-Pradel	Dong-Hun Lee	Elia Machado	Lucy McNamara
Qingzhong Kong	David Lefebvre	Ian Mackay	Jennifer McQuiston
Jeffrey Koplan	Florence	John Mackenzie	Dana Meaney-Delman
Anita Koshy	Legrand-Abravanel	Timothy Mackey	Rachel Mearkle

 REVIEWER APPRECIATION

Oleg Mediannikov	Atis Muehlenbachs	Shannon Novosad	Lucia Pawloski
Jean-Louis Mège	Lapo Mughini-Gras	Thomas Nutman	Gabriela Paz-Bailey
Adam Meijer	Miguel Mulders	Patricia Nuttall	Malik Peiris
Jacques F. Meis	Thomas Müller	Sheila O'Brien	L. Peixe
Roberto Melano	William Muller	David O'Callaghan	Mary-Louise Penrith
Analy Melo	Mark Mulligan	Annette O'Connor	Maurice Pensaert
Martin Meltzer	Michael Mulvey	Michael O'Hara	Pasi Penttinen
Daniel Menucci	Elizabeth Mumford	Wendy O'Meara	Dana Perella
Greg Mertz	Vincent Munster	Theresa Ochoa	Rashika Perera
Sharon Messenger	David Murdoch	Sophie Octavia	Sabine Pereyre
Dik Mevius	Manoj Murhekar	Welling Oei	Daniel Perez
Hermann Meyer	Jean-Luc Murk	John Oeltmann	Jose-Luis Perez Arellano
Susan Mikota	Frederick Murphy	Abiola Olaitan	José-Antonio Pérez-Molina
Lucimar Milagres	Georgina Murphy	L. Olarte	Steven Pergam
Elizabeth Miller	Trudy Murphy	Gene Olinger	Stanley Perlman
Michele Miller	Kris Murray	Kevin Olival	Vincent Perreten
Mathieu Million	Kristy Murray	Sara Oliver	Joseph F. Perz
Alexander Millman	Didier Musso	Sonja Olsen	Brett Petersen
James Mills	Tony Mutsaers	Donald Olson	Emily Petersen
Larissa Minicucci	David Myerson	Ken Olson	Jeannine Petersen
Arialdi Minino	Khin Myint	Victoria Olson	Giulia Pezzoni
Eric Mintz	Pierre Nabeth	Jerry Ongerth	Michael Pfaller
Paolo Miotto	Susan Nadin-Davis	Tanja Opriessnig	Martin Pfeiffer
Nischay Mishra	Osamu Nakagomi	Walter Orenstein	Yvonne Pfeifer
John Modlin	Ho Namkoong	Jennifer Orgle	Anne Piantadosi
Vittal Mogasale	Srinivas Nanduri	Hendrick Ormel	Martine Piarroux
Hamish Mohammed	Robin Nandy	Hitoshi Oshitani	Harry Pickering
Chris Mok	Oswaldo Jose Moreira	José A. Oteo	Allan Pillay
Igor Mokrousov	Nascimento	Domenico Otranto	Robert Pinner
Claudia Molins	Adoracion Navarro-Torne	Nao Otsuka	Benjamin Pinsky
Isabella Monne	Maria Negrón	Michael Otto	Amelia Pinto
Steve Monroe	Mark Nelder	Kwame Owusu-Edusei	Maria Pisu
Susan Montgomery	Christina Nelson	Christopher Paddock	John Pitman
Antonio Montresor	Eric Nelson	Kristen Page	Johann Pitout
Troy Moon	Gary Nelson	Frederic Pages	Laure Pittet
Patrick Moonan	Noele Nelson	Julia Painter	Paul Planet
Camille Moore	Nicole Nemeth	Gustavo Palacios	Maia Platt
Cynthia Moore	Jason Newland	Xiaoli Pang	Maurizio Pocchiari
Luke Moore	Alexandra Newman	Mary Pantin-Jackwood	Yuwana Podin
Stefano Morabito	Lisa Ng	Anna Papa	Laurent Poiré
Jacob Moran-Gilad	Terry Fei Fan Ng	Igor Paploski	Maria Politis
David Morens	Ann Nguyen	John Papp	Marjorie Pollack
Maria Moretti	Karamoko Niaré	Peter Pappas	Richard Pollack
Ethan Morgan	Ainsley Nicholson	Satya Parida	Leo Pomar
Marina Morgan	William Nicholson	Daniel Paris	Constança Pomba
Oliver Morgan	Matthias Niedrig	Won-Ju Park	Leo Poon
J. Glenn Morris	Eva Møller Nielsen	Philippe Parola	Spyros Pournaras
Sheldon Morris	Karin Nielsen	Gabriel Parra	Ann Powers
Lillian Morris-Manahan	Sandra Niendorf	Meelis Partel	Ian Pray
Stephen Morse	Hubert Niesters	Mohammed Parvez	Ranjan Premaratna
Irmgard Moser	Silda Nikaj	John Pasick	John Prescott
Eric Mossel	Eric Nilles	Daniel Pastula	Rebecca Prevots
Varvara Mouchtouri	Takeshi Nishijima	Payal Patel	Erin Price
Scott Moye-Rowley	Andreas Nitsche	Devi Patnayak	Núria Prim

Bobbi Pritt	Jason Rosch	David Scollard	Peter Spencer
Christine Prue	Felix Rosenberg	Thomas Scott	Jessica Spengler
Sebastien Puechmaille	Benjamin Rossi	Barbara Seaworth	Patrizia Spigaglia
Joanna Pulit-Penalosa	Shannan Rossi	Joaquim Segalés	Gianfranco Spiteri
Michael Purdy	Melinda Rostal	James Sejvar	Philip Spradling
Anne Purfield	Paul Rota	Zuzana Sekeyova	Armand Sprecher
Xiangguo Qiu	Camilla Rothe	D.C. Sellon	Padmini Srikantiah
Krista Queen	Laura Lester Rothfeldt	Torsten Seuberlich	Kirsten St. George
Yvonne Qvarnstrom	Caroline Rouard	Daniel Sexton	Judy St. Leger
Ingrid Rabe	Janell Routh	Wayne Shandera	Sylvie Stacy
Elida Rabelo	Steven Ruben	E.M. Shankar	Helen Stagg
Gowrisankar Rajam	Etienne Ruppé	Aditya Sharma	David Stallknecht
Andrew Ramey	Thomas Russo	Colin Sharp	Miles Stanford
M. Ramirez	Victor Rutten	Paul Sharp	J. Staples
Artur Ramos	Sadie Ryan	Tyler Sharp	Jeffrey Starke
Stéphane Ranque	Tove Ryman	Jeanne Sheffield	Juergen Stech
Didier Raoult	David Sack	Thomas Shelite	Robert Steffen
Brian Raphael	Claude Saegerman	Harsha Sheorey	Gail Stennies
Jason Rasgon	David Safronetz	Carmen Sheppard	Roger Stephan
Magnus Rasmussen	Dan Salkeld	Weifeng Shi	Dennis Stevens
Sonja Rasmussen	Oscar Salomon	Samuel Shillcutt	James Stevens
Mario Raviglione	Orjan Samuelsen	Anna Shore	O. Stine
Jonathan Rayner	Fabio Sanchez	Stanford Shulman	Jason Stout
Jennifer Read	Pablo Sanchez	Carol Sibley	Norval Strachan
Timothy Read	Susan Sanchez	Kassim Sidibe	Anne Straily
Adam Readhead	Elisabeth Sanders	Eva Sierra	Susan Stramer
John Redd	Dieudonne Sankara	Monica Sierra	Marc Strassburg
Joanna Regan	Gilberto Santiago	Lynn Silver	Daniel Streblov
Michael Reiskind	Carlos Santos	Graham Simmons	Ellen Stromdahl
Hilary Reno	Sarah Sapp	Les Sims	James Strong
Chantal Reusken	Jan Sargeant	Andreas Sing	Fiona Strouts
Mary Reynolds	Daniel Sauvard	Pallavi Singh	Jason Stull
Louis Rice	Harry Savage	Raj Singh	Anita Suijkerbuijk
Allen Richards	Hugo Sax	Animesh Sinha	Sheena Sullivan
Lauren Richey	Elaine Scallan	Tarja Sironen	Xiang-Jie Sun
Juergen Richt	Ilana Schafer	Daouda Sissoko	Rebecca Sunenshine
Rebeca Rico-Hesse	William Schaffner	Maria Sjölund-Karlsson	Leonardo Susta
Mark Riddle	Frieder Schaumburg	Krzysztof Smietanka	Gerd Sutter
Alison Ridpath	Aaron Scherer	Andrew Smith	Troy Sutton
Antoinette Righarts	Jarad Schiffer	Darci Smith	Erik Svensson
Laura Riley	Barbara Schimmer	David Smith	Mario Sviben
Thomas Riley	Axel Schmidt	Donald Smith	Robert Swanepoel
George Risi	Jonas Schmidt-Chanasit	Gavin Smith	David Swayne
Stephen Ritchie	Elizabeth Schnaubelt	Kirk Smith	William Switzer
Suelee Robbe-Austerman	Eileen Schneider	Kristine Smith	Monica Szymanska
Chrissy H. Roberts	Tony Schountz	Sarah Smith	Florian Tagini
Gemma Robertson	Angelica Schreiber	Tara Smith	Muhamed-Kheir Taha
Joan Robinson	Declan Schroeder	David Sniadack	Paula Tahtinen
Guenael Rodier	Amy Schuh	David Snyderman	Elizabeth Talbot
Jesús Rodríguez-Baño	Krysten Schuler	Heidi Soeters	Eldin Talundzic
Alfonso Rodríguez-Morales	Stacey Schultz-Cherry	Hojoon Sohn	Paul Tambyah
Louise Roer	Tom Schwan	Glenn Songer	Azaibi Tamin
Pierre Rollin	Martin Schwemmlé	Frank Sorvillo	Pranita Tamma
Axelle Ronsse	Jessica Schwind	Erica Spackman	Kathrine Tan

 REVIEWER APPRECIATION

Patrick Tang	Paul Turner	Duc Vugia	Paul-Louis Woerther
Phillip Tarr	Jane Turton	Dominique Vuitton	Tiffany Wolf
Jacqueline Tate	Kenneth Tyler	Debra Wadford	Cameron Wolfe
Pierre Tattevin	Venkatachalam	Jonathan Wadsworth	Nicole Wolter
Robert Tauxe	Udhayakumar	Jesse Waggoner	Katja Wolthers
Melanie Taylor	Rolando Ulloa-Gutierrez	Niteen Wairagkar	Frank Wong
Thomas Taylor, Jr.	Eduardo Undurraga	Ronald Waldman	Susan Wong
Richard Tedder	Elizabeth Unger	Henry Walke	Kimberly Workowski
Marcio Teixeira Nunes	James Ussher	David Walker	Gary Wormser
Sam Telford	Timothy Uyeki	Ryan Wallace	Danielle Wroblewski
Glenn Telling	Mieke Uyttendaele	Sandra Walser	Haibo Wu
Karen Terio	Ronald Valdiserri	Xiu-Feng Wan	Linwan Wu
Eyasu Teshale	Louis Valiquette	David Wang	Peng Wu
Janjira Thaipadungpanit	Snigdha Vallabhaneni	Ninglan Wang	Wenbo Xu
Elitza Theel	Chris Van Beneden	Susan Wang	Laith Yakob
Volker Thiel	Rafael Van den Bergh	Tina Wang	Hiroshi Yamasaki
Corinne Thompson	Andrew van den Hurk	Xi-Ling Wang	Bingyu Yan
George Thompson	Annemiek van der Eijk	Xin Wang	X. Frank Yang
William Thompson	Mark van der Linden	Yi-Chen Wang	Hui-Ling Yen
Sharmi Thor	Wim van der Poel	Ray Waters	Jingjing Yin
Cheleste Thorpe	Barbara Van Der Pol	Douglas Watts	Kevin Yin
John Threlfall	Marianne van der Sande	Scott Weaver	InKyu Yoon
Julie Thwing	H Rogier van Doorn	Richard Webby	Cristin Young
Aura Timen	Marjolein van Gent	J. Todd Weber	Hai Yu
Tejpratap Tiwari	Jakko van Ingen	Scott Weese	Hongjie Yu
James Tobias	Koen Vandelanoot	Michael Weigand	Xuejie Yu
James Todd	Olli Vapalahti	Peter Weina	Yun-Song Yu
Evelyn Toh	George Varghese	Robert Weinstein	Kwok-Yung Yuen
Kentaro Tohma	Jay Varma	Eric Weintraub	Hans Zaaijer
Rafael Toledo	Arvind Varsani	Louis Weiss	Sherif Zaki
Mia Torchetti	Pedro Vasconcelos	Thomas Weitzel	Lorenzo Zammarchi
Maija Toropainen	Gilberto Vaughan	Jim Wellehan	Aleksandra Zasada
Montserrat Torremorell	Lourdes Vaz-de-Lima	Zou Wen-Quan	Bianca Zecchin
Gregorio Torres	Everardo Vega	Guido Werner	Hervé Zeller
Pat Totten	Srinivasan Velusamy	Joel Wertheim	Jean-Pierre Zellweger
Sherry Towers	Rob M. Verdijk	Joseph L. Wheat	Jon Zelner
Jonathan Towner	Andrew Vernon	Anne Wheeler	Marcus Zervos
Indi Trehan	Nicolas Veziris	A. White	George Zhanel
François-William Tremblay	Dhanasekaran Vijaykrishna	Jennifer White	Sean Zhang
Susan Trock	Amy Vincent	Peter White	Xinyan Zhang
Darren Trott	Jan Vinjé	Hilary Whitham	Jiangqin Zhao
Raymond Tsang	Erika Vlieghe	Robert Whittaker	Fangjun Zhou
Sharon Tsay	Ulrich Vogel	Nathan Wiederhold	Haijian Zhou
Sung-Pin Tseng	Line Vold	Lynne Wilcox	Hong Zhou
Apichal Tuanyok	Sarah Volkman	Annelies Wilder-Smith	Lei Zhou
Lorena Tuchscher de	Michael von Fricken	John Williams	Hua Zhu
Hauschopp	Anne von Gottberg	Margaret Williams	Emily Zielinski-Gutierrez
David Tuller	C. Fordham von Reyn	Carla Winston	Danila Zimenkov
Felipe Tuon	Sirenda Vong	Anne-Luise Winter	James Zingesser
Christine Turenne	Neil Vora	Kevin Winthrop	Sarah Zohdy
Claire Turner	Wilna Vosloo	Carl Heinz Wirsing	Richard Zuckerman
Patricia Turner	David Vu	von Konig	

EMERGING INFECTIOUS DISEASES®

Upcoming Issue

- Increased Severity and Spread of *Mycobacterium ulcerans*, Southeastern Australia
- Japanese Encephalitis Virus Transmitted Via Blood Transfusion, Hong Kong, China
- Sensitivity and Specificity of a Suspected Case Definition Used during the West Africa Ebola Epidemic
- Dangers of Noncritical Use of Historical Plague Databases
- Mammalian Pathogenesis and Transmission of Avian Influenza A(H7N9) Viruses, Tennessee, USA, 2017
- Expected Duration of Adverse Pregnancy Outcomes after Zika Epidemic
- Rodent Abundance and Hantavirus Infection in Protected Area, East Central Argentina
- High Seroprevalence of Jamestown Canyon Virus among Deer and Humans, Nova Scotia, Canada
- Recognition of Azole-Resistant Aspergillosis by Physicians Specializing in Infectious Disease, United States
- Dengue Fever in Burkina Faso, 2016
- Yellow Fever Virus in Urine and Semen of Convalescent Patient, Brazil
- Challenges and Opportunities for Eliminating Canine-Mediated Human Rabies Deaths in Haiti
- Increasing Number of Scarlet Fever Cases, South Korea, 2011–2016
- Molecular Characterization of Autochthonous Chikungunya Cluster in Latium Region, Italy
- Estimation of Undiagnosed *Naegleria fowleri* Primary Amebic Meningoencephalitis, United States
- Whole Genome Analysis of Recurrent *Staphylococcus aureus* t571/ST398 Infection in an Iowa Farmer
- Visceral Leishmaniasis Caused by *Leishmania siamensis* acquired in Guyana
- Conjunctivitis Outbreak Costs Healthcare System 3.3 Million Euros, Réunion Island
- Investigation of Pneumonic Plague, Madagascar

Complete list of articles in the January issue at
<http://www.cdc.gov/eid/upcoming.htm>

Upcoming Infectious Disease Activities

February 1–3, 2018

8th Advances in Aspergillosis
Lisbon, Portugal
www.AAA2018.org

February 12–14, 2018

ASM Biothreats
Baltimore, MD
<https://www.asm.org/index.php/biothreats-2018>

March 1–4, 2018

18th International Congress
on Infectious Diseases (ICID)
Buenos Aires, Argentina
<http://www.isid.org/icid/>

March 7–9, 2018

ISIRV
2nd International Meeting on
Respiratory Pathogens
Singapore
<https://www.isirv.org/site/>

May 6–9, 2018

ASM Clinical Virology Symposium
West Palm Beach, FL
<https://www.asm.org/index.php/2018-clinical-virology-symposium>

June 7–11, 2018

ASM Microbe
Atlanta, GA
<https://www.asm.org/index.php/asm-microbe-2018>

August 26–29, 2018

ICEID
International Conference on
Emerging Infectious Diseases*
Atlanta, GA
<https://www.cdc.gov/iceid/index.html>

* The World Academy of Science, Engineering and Technology (WASET) is sponsoring a similarly named event in London in February 2018. Please note that CDC is not affiliated with this event.

Announcements

To submit an announcement, send an email message to EIDEditor (eideditor@cdc.gov). Include the date of the event, the location, the sponsoring organization(s), and a website that readers may visit or a telephone number or email address that readers may contact for more information.

Announcements may be posted on the journal Web page only, depending on the event date.

Earning CME Credit

To obtain credit, you should first read the journal article. After reading the article, you should be able to answer the following, related, multiple-choice questions. To complete the questions (with a minimum 75% passing score) and earn continuing medical education (CME) credit, please go to <http://www.medscape.org/journal/eid>. Credit cannot be obtained for tests completed on paper, although you may use the worksheet below to keep a record of your answers.

You must be a registered user on <http://www.medscape.org>. If you are not registered on <http://www.medscape.org>, please click on the “Register” link on the right hand side of the website.

Only one answer is correct for each question. Once you successfully answer all post-test questions, you will be able to view and/or print your certificate. For questions regarding this activity, contact the accredited provider, CME@medscape.net. For technical assistance, contact CME@medscape.net. American Medical Association’s Physician’s Recognition Award (AMA PRA) credits are accepted in the US as evidence of participation in CME activities. For further information on this award, please go to <https://www.ama-assn.org>. The AMA has determined that physicians not licensed in the US who participate in this CME activity are eligible for AMA PRA Category 1 Credits™. Through agreements that the AMA has made with agencies in some countries, AMA PRA credit may be acceptable as evidence of participation in CME activities. If you are not licensed in the US, please complete the questions online, print the AMA PRA CME credit certificate, and present it to your national medical association for review.

Article Title

Group B *Streptococcus* Infections Caused by Improper Sourcing and Handling of Fish for Raw Consumption, Singapore, 2015–2016

CME Questions

1. You are advising a public health department in Singapore regarding the potential for future human group B *Streptococcus* (GBS) outbreak. On the basis of the microbial study of raw fish and human samples by Chau and colleagues, which one of the following statements about the clinical and epidemiological findings of a human GBS outbreak in Singapore is correct?

- A. The outbreak was associated with consumption of raw saltwater fish
- B. The source of the outbreak was limited to restaurants
- C. The causative agent was *Streptococcus viridans*
- D. Severe clinical cases included meningoenzephalitis, bacteremia, spinal infection and septic arthritis

2. According to the microbial study of raw fish and human samples by Chau and colleagues, which one of the following statements about the pathogenic potential of fish and human samples after a human GBS outbreak in Singapore is correct?

- A. Fish-associated GBS ST283 strains included only strains nearly identical to the human outbreak strain
- B. The study proves that all GBS ST283 strains are capable of causing invasive human disease through the foodborne route

- C. The live and whole fish from which GBS ST283 was recovered did not show corneal opacity or exophthalmia, suggesting this strain may not be pathogenic to freshwater fish
- D. The human outbreak strain is highly similar to known GBS fish pathogens with published genomes

3. According to the microbial study of raw fish and human samples by Chau and colleagues, which one of the following statements about public health implications of a human GBS outbreak in Singapore is correct?

- A. Both saltwater and freshwater fish are suitable for raw consumption if proper sourcing and handling standards are followed
- B. To control the outbreak, the sale of ready-to-eat (RTE) raw freshwater fish dishes was banned, and additional requirements were imposed for sale of RTE raw fish dishes using saltwater fish
- C. GBS ST283 was the only hazard identified in freshwater fish used to prepare raw RTE dishes
- D. Most food stalls tested were able to prepare RTE raw fish dishes of acceptable hygiene quality

Earning CME Credit

To obtain credit, you should first read the journal article. After reading the article, you should be able to answer the following, related, multiple-choice questions. To complete the questions (with a minimum 75% passing score) and earn continuing medical education (CME) credit, please go to <http://www.medscape.org/journal/eid>. Credit cannot be obtained for tests completed on paper, although you may use the worksheet below to keep a record of your answers.

You must be a registered user on <http://www.medscape.org>. If you are not registered on <http://www.medscape.org>, please click on the "Register" link on the right hand side of the website.

Only one answer is correct for each question. Once you successfully answer all post-test questions, you will be able to view and/or print your certificate. For questions regarding this activity, contact the accredited provider, CME@medscape.net. For technical assistance, contact CME@medscape.net. American Medical Association's Physician's Recognition Award (AMA PRA) credits are accepted in the US as evidence of participation in CME activities. For further information on this award, please go to <https://www.ama-assn.org>. The AMA has determined that physicians not licensed in the US who participate in this CME activity are eligible for AMA PRA Category 1 Credits™. Through agreements that the AMA has made with agencies in some countries, AMA PRA credit may be acceptable as evidence of participation in CME activities. If you are not licensed in the US, please complete the questions online, print the AMA PRA CME credit certificate, and present it to your national medical association for review.

Article Title

Newly Recognized Pediatric Cases of Typhus Group Rickettsiosis, Houston, Texas, USA

CME Questions

1. Your patient is a 10-year-old boy with suspected typhus group rickettsiosis (TGR). On the basis of the retrospective medical record review by Erickson and colleagues, which one of the following statements about clinical features of cases of TGR at a large, Houston-area pediatric hospital between 2008 and 2016 is correct?

- A. About three quarters of patients had the "classical triad" of fever, rash, and headache
- B. Malaise, vomiting, anorexia, abdominal pain, lymphadenopathy, and conjunctivitis were other common symptoms
- C. Elevated transaminases and thrombocytopenia occurred in less than half of patients
- D. About 5% of patients required intensive care

2. According to the retrospective medical record review by Erickson and colleagues, which one of the following statements about epidemiological features of cases of TGR at a large, Houston-area pediatric hospital between 2008 and 2016 is correct?

- A. Half of case-patients had documented animal exposures
- B. The highest number of diagnosed cases occurred in 2012

- C. Most case-patients had a history of recent travel
- D. Most cases presented during summer months, when fleas are most prevalent

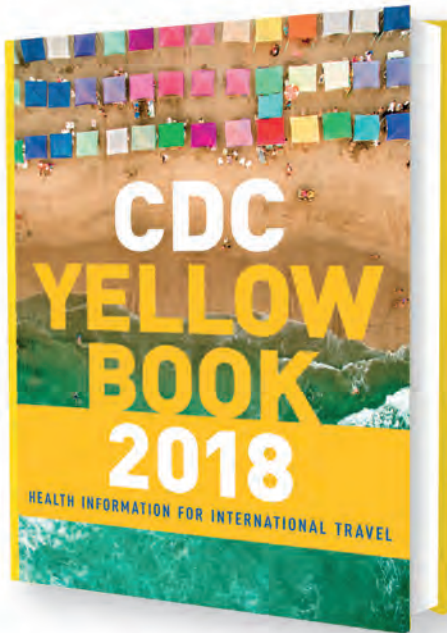
3. According to the retrospective medical record review by Erickson and colleagues, which one of the following statements about public health implications of cases of TGR at a large, Houston-area pediatric hospital between 2008 and 2016 is correct?

- A. The study proves that exposure to domestic pets puts children at risk for infection
- B. More than three quarters of confirmed or probable cases identified in this series were reported
- C. Barriers to reporting may include low awareness of reporting requirements, complexity of patient care, and delays in receiving test results, especially after discharge
- D. Suspicion for TGR need not be high if the classical triad of fever, rash, and headache is absent

CDC YELLOW BOOK

HEALTH INFORMATION FOR INTERNATIONAL TRAVEL

2018



Available Now - New for 2018

The fully revised and updated *CDC Yellow Book 2018: Health Information for International Travel* codifies the U.S. government's most current health guidelines and information for clinicians advising international travelers, including pretravel vaccine recommendations, destination-specific health advice, and easy-to-reference maps, tables, and charts.

ISBN: 9780190628611 | \$49.95 | May 2017 | Paperback | 704 pages

The 2018 Yellow Book includes important travel medicine updates:

- The latest information about emerging infectious disease threats such as Zika, Ebola, and sarcocystosis
- New cholera vaccine recommendations
- Updated guidance on the use of antibiotics in the treatment of travelers' diarrhea
- Special considerations for unique types of travel such as wilderness expeditions, work-related travel, and study abroad

IDSA members: log in via www.idsociety.org before purchasing this title to receive your **20% discount**

OXFORD
UNIVERSITY PRESS

Order your copy at:

www.oup.com/academic

Emerging Infectious Diseases is a peer-reviewed journal established expressly to promote the recognition of new and reemerging infectious diseases around the world and improve the understanding of factors involved in disease emergence, prevention, and elimination.

The journal is intended for professionals in infectious diseases and related sciences. We welcome contributions from infectious disease specialists in academia, industry, clinical practice, and public health, as well as from specialists in economics, social sciences, and other disciplines. Manuscripts in all categories should explain the contents in public health terms. For information on manuscript categories and suitability of proposed articles, see below and visit <http://wwwnc.cdc.gov/eid/pages/author-resource-center.htm>.

Summary of Authors' Instructions

Author's Instructions. For a complete list of EID's manuscript guidelines, see the author resource page: <http://wwwnc.cdc.gov/eid/page/author-resource-center>.

Manuscript Submission. To submit a manuscript, access Manuscript Central from the Emerging Infectious Diseases web page (www.cdc.gov/eid). Include a cover letter indicating the proposed category of the article (e.g., Research, Dispatch), verifying the word and reference counts, and confirming that the final manuscript has been seen and approved by all authors. Complete provided Authors Checklist.

Manuscript Preparation. For word processing, use MS Word. Set the document to show continuous line numbers. List the following information in this order: title page, article summary line, keywords, abstract, text, acknowledgments, biographical sketch, references, tables, and figure legends. Appendix materials and figures should be in separate files.

Title Page. Give complete information about each author (i.e., full name, graduate degree(s), affiliation, and the name of the institution in which the work was done). Clearly identify the corresponding author and provide that author's mailing address (include phone number, fax number, and email address). Include separate word counts for abstract and text.

Keywords. Use terms as listed in the National Library of Medicine Medical Subject Headings index (www.ncbi.nlm.nih.gov/mesh).

Text. Double-space everything, including the title page, abstract, references, tables, and figure legends. Indent paragraphs; leave no extra space between paragraphs. After a period, leave only one space before beginning the next sentence. Use 12-point Times New Roman font and format with ragged right margins (left align). Italicize (rather than underline) scientific names when needed.

Biographical Sketch. Include a short biographical sketch of the first author—both authors if only two. Include affiliations and the author's primary research interests.

References. Follow Uniform Requirements (www.icmje.org/index.html). Do not use endnotes for references. Place reference numbers in parentheses, not superscripts. Number citations in order of appearance (including in text, figures, and tables). Cite personal communications, unpublished data, and manuscripts in preparation or submitted for publication in parentheses in text. Consult List of Journals Indexed in Index Medicus for accepted journal abbreviations; if a journal is not listed, spell out the journal title. List the first six authors followed by "et al." Do not cite references in the abstract.

Tables. Provide tables within the manuscript file, not as separate files. Use the MS Word table tool, no columns, tabs, spaces, or other programs. Footnote any use of bold-face. Tables should be no wider than 17 cm. Condense or divide larger tables. Extensive tables may be made available online only.

Figures. Submit editable figures as separate files (e.g., Microsoft Excel, PowerPoint). Photographs should be submitted as high-resolution (600 dpi) .tif or .jpeg files. Do not embed figures in the manuscript file. Use Arial 10 pt. or 12 pt. font for lettering so that figures, symbols, lettering, and numbering can remain legible when reduced to print size. Place figure keys within the figure. Figure legends should be placed at the end of the manuscript file.

Videos. Submit as AVI, MOV, MPG, MPEG, or WMV. Videos should not exceed 5 minutes and should include an audio description and complete captioning. If audio is not available, provide a description of the action in the video as a separate Word file. Published or copyrighted material (e.g., music) is discouraged and must be accompanied by written release. If video is part of a manuscript, files must be uploaded with manuscript submission. When uploading, choose "Video" file. Include a brief video legend in the manuscript file.

Types of Articles

Perspectives. Articles should not exceed 3,500 words and 50 references. Use of subheadings in the main body of the text is recommended. Photographs and illustrations are encouraged. Provide a short abstract (150 words), 1-sentence summary, and biographical sketch. Articles should provide insightful analysis and commentary about new and reemerging infectious diseases and related issues. Perspectives may address factors known to influence the emergence of diseases, including microbial adaptation and change, human demographics and behavior, technology and industry, economic development and land use, international travel and commerce, and the breakdown of public health measures.

Synopses. Articles should not exceed 3,500 words in the main body of the text or include more than 50 references. Use of subheadings in the main body of the text is recommended. Photographs and illustrations are encouraged. Provide a short abstract (not to exceed 150 words), a 1-line summary of the conclusions, and a brief

biographical sketch of first author or of both authors if only 2 authors. This section comprises case series papers and concise reviews of infectious diseases or closely related topics. Preference is given to reviews of new and emerging diseases; however, timely updates of other diseases or topics are also welcome. If detailed methods are included, a separate section on experimental procedures should immediately follow the body of the text.

Research. Articles should not exceed 3,500 words and 50 references. Use of subheadings in the main body of the text is recommended. Photographs and illustrations are encouraged. Provide a short abstract (150 words), 1-sentence summary, and biographical sketch. Report laboratory and epidemiologic results within a public health perspective. Explain the value of the research in public health terms and place the findings in a larger perspective (i.e., "Here is what we found, and here is what the findings mean").

Policy and Historical Reviews. Articles should not exceed 3,500 words and 50 references. Use of subheadings in the main body of the text is recommended. Photographs and illustrations are encouraged. Provide a short abstract (150 words), 1-sentence summary, and biographical sketch. Articles in this section include public health policy or historical reports that are based on research and analysis of emerging disease issues.

Dispatches. Articles should be no more than 1,200 words and need not be divided into sections. If subheadings are used, they should be general, e.g., "The Study" and "Conclusions." Provide a brief abstract (50 words); references (not to exceed 15); figures or illustrations (not to exceed 2); tables (not to exceed 2); and biographical sketch. Dispatches are updates on infectious disease trends and research that include descriptions of new methods for detecting, characterizing, or subtyping new or reemerging pathogens. Developments in antimicrobial drugs, vaccines, or infectious disease prevention or elimination programs are appropriate. Case reports are also welcome.

Another Dimension. Thoughtful essays, short stories, or poems on philosophical issues related to science, medical practice, and human health. Topics may include science and the human condition, the unanticipated side of epidemic investigations, or how people perceive and cope with infection and illness. This section is intended to evoke compassion for human suffering and to expand the science reader's literary scope. Manuscripts are selected for publication as much for their content (the experiences they describe) as for their literary merit. Include biographical sketch.

Research Letters Reporting Cases, Outbreaks, or Original Research. EID publishes letters that report cases, outbreaks, or original research as Research Letters. Authors should provide a short abstract (50-word maximum), references (not to exceed 10), and a short biographical sketch. These letters should not exceed 800 words in the main body of the text and may include either 1 figure or 1 table. Do not divide Research Letters into sections.

Letters Commenting on Articles. Letters commenting on articles should contain a maximum of 300 words and 5 references; they are more likely to be published if submitted within 4 weeks of the original article's publication.

Commentaries. Thoughtful discussions (500–1,000 words) of current topics. Commentaries may contain references (not to exceed 15) but no abstract, figures, or tables. Include biographical sketch.

Books, Other Media. Reviews (250–500 words) of new books or other media on emerging disease issues are welcome. Title, author(s), publisher, number of pages, and other pertinent details should be included.

Conference Summaries. Summaries of emerging infectious disease conference activities (500–1,000 words) are published online only. They should be submitted no later than 6 months after the conference and focus on content rather than process. Provide illustrations, references, and links to full reports of conference activities.

Online Reports. Reports on consensus group meetings, workshops, and other activities in which suggestions for diagnostic, treatment, or reporting methods related to infectious disease topics are formulated may be published online only. These should not exceed 3,500 words and should be authored by the group. We do not publish official guidelines or policy recommendations.

Photo Quiz. The photo quiz (1,200 words) highlights a person who made notable contributions to public health and medicine. Provide a photo of the subject, a brief clue to the person's identity, and five possible answers, followed by an essay describing the person's life and his or her significance to public health, science, and infectious disease.

Etymologia. Etymologia (100 words, 5 references). We welcome thoroughly researched derivations of emerging disease terms. Historical and other context could be included.

Announcements. We welcome brief announcements of timely events of interest to our readers. Announcements may be posted online only, depending on the event date. Email to eideditor@cdc.gov.

In This Issue

Synopses

Fatal Outbreak in Tonkean Macaques Caused by Possibly Novel Orthopoxvirus, Italy, January 2015	1941
Spread of Canine Influenza A(H3N2) Virus, United States	1950

Research

Evolutionary Context of Non-Sorbitol-Fermenting Shiga Toxin-Producing <i>Escherichia coli</i> O55:H7	1958
Multiple Reassorted Viruses as Cause of a Highly Pathogenic Avian Influenza A(H5N8) Virus Epidemic, Netherlands, 2016	1966
Experimental Infection of Common Eider Ducklings with Wellfleet Bay Virus, a Newly Characterized Orthomyxovirus	1974
Group B <i>Streptococcus</i> Infections Caused by Improper Sourcing and Handling of Fish for Raw Consumption, Singapore, 2015–2016	1982
Distribution of Usutu Virus in Germany and its Effect on Breeding Bird Populations	1991
Outbreaks of Neuroinvasive Astrovirus Associated with Encephalomyelitis, Weakness, and Paralysis among Weaned Pigs, Hungary	1999
Characterization of <i>Streptococcus pyogenes</i> from Animal Clinical Specimens, Spain	2011
Bourbon Virus in Field-Collected Ticks, Missouri, USA	2017
High Rate of MCR-1-Producing <i>Escherichia coli</i> and <i>Klebsiella pneumoniae</i> among Pigs, Portugal	2023

Historical Review

History of <i>Taenia saginata</i> Tapeworms in Northern Russia	2030
--	------

Dispatches

Outbreak of Yellow Fever among Nonhuman Primates, Espirito Santo, Brazil, 2017	2038
<i>Mycobacterium ulcerans</i> DNA in Bandicoot Excreta in Buruli Ulcer-Endemic Area, Northern Queensland, Australia	2042
Avian Influenza A(H7N2) Virus in a Human Exposed to Sick Cats, New York, USA, 2016	2046
Deaths among Wild Birds During Highly Pathogenic Avian Influenza A(H5N8) Virus Outbreak, the Netherlands	2050
Pathogenic <i>Elizabethkingia miricola</i> Infection in Cultured Black-Spotted Frogs, China, 2016	2055
West Nile Virus Lineage 2 in Horses and Other Animals with Neurologic Disease, South Africa, 2008–2015	2060
Tick-Borne Encephalitis in Sheep, Romania	2065
Newly Recognized Pediatric Cases of Typhus Group Rickettsiosis, Houston, Texas, USA	2068
Identification of <i>Dermacentor reticulatus</i> Ticks Carrying <i>Rickettsia raoultii</i> on Migrating Jackal, Denmark	2072
Investigation of Acute Flaccid Paralysis Reported with La Crosse Virus Infection, Ohio, USA, 2008–2014	2075
Phylogenetic Characterization of Crimean-Congo Hemorrhagic Fever Virus, Spain	2078
Lack of Secondary Transmission of Ebola Virus from Healthcare Worker to 238 Contacts, United Kingdom, December 2014	2081
Diagnostic Accuracy of Parameters for Zika and Dengue Virus Infections, Singapore	2085